High Density Lipoprotein Composition and Function in Healthy Pregnancy and Preeclampsia

Patamat Patanapirunhakit, MD

This thesis is submitted in fulfilment of the requirements for the degree of Doctor of Philosophy (PhD)

School of Cardiovascular and Metabolic Health
College of Medical, Veterinary and Life Sciences

University of Glasgow

June 2022

Abstract

High density lipoprotein (HDL) is well-known for its ability to protect vascular function. It is hypothesised that HDL could be a protective factor for vascular function in healthy pregnancy that fails in preeclampsia resulting in endothelial dysfunction. The aims of this thesis were to determine HDL composition and function throughout healthy pregnancy and in preeclampsia. HDL protein and sphingolipid compositions were determined using proteomic and lipid analysis approaches in healthy pregnancy from pre-pregnancy to postpartum. There were 16 proteins changed in HDL throughout gestation. Higher HDL α-1-antitrypsin content was observed in the first trimester (median LFQ intensity $5.8x10^8$ at 8.4 weeks and 4.2 $x10^8$ pre-pregnancy, p=0.044) and may protect the reverse cholesterol transport (RCT) function of HDL. HDL content of sphingosine-1-phosphate (S1P) and ceramides increased in the third trimester (S1P 101.1±9.8, 108.0±19.8 and 128.8±15.6 ng/mL, C18:0 12.0±2.6, 16.9±6.8 and 20.2±6.2 ng/mL, C20:0 30.6±10.6, 40.32±13.0 and 52.6±17.5 ng/mL, C22:0 196.0±101.8, 266.9±119.6 and 362.7±164.2 ng/mL, C24:1 137.2±48.4, 151.8±54.8 and 201.4±60.4 ng/mL for 16, 25 and 35 weeks, respectively), suggesting improved anti-inflammatory, vasodilatory and RCT function of HDL. In preeclampsia, the third trimester HDL protein composition, both late and early onset, was compared to HDL from gestation-matched healthy pregnancy. ApoA-IV was lower in early-onset preeclampsia (median LFQ intensity $3.0x10^9$ and $3.9x10^9$ for early-onset preeclampsia and control, p=0.018), suggesting that HDL may be less efficient at inhibiting excessive inflammation in early-onset preeclampsia. The LFQ intensities of antithrombin-III ($9.3x10^7$ and $1.4x10^8$ for late-onset preeclampsia and control, p=0.045) and ß-2-glycoprotein 1 ($5.9x10^8$ and $9.0x10^8$ for late-onset preeclampsia and control, p=0.030) were lower in late-onset preeclampsia which might suggest both activating and inhibiting effects on the coagulation cascade. Next, assays to assess HDL function, including HDL effects on vascular reactivity using wire myography and the anti-clotting potential of HDL, were developed. The wire myography protocol was able to assess HDL effect on vasoconstriction responses of human pregnant visceral adipose tissue arteries, but not vasodilatory responses because vessels contracted to the maximum dose of noradrenaline did not maintain a stable contraction. An anti-thrombotic functional assay of HDL was developed by adapting an existing

thrombin generation assay protocol used for plasma. NaBr carried over from HDL isolation process inhibited thrombin production in the assay, leading to difficulty in standardizing thrombin generation activity measured in HDL samples. Finally, an isolation protocol for HDL was developed where potential extracellular vesicle (EV) contamination in HDL samples was removed using a combination of size-exclusion chromatography and sequential ultracentrifugation. ApoA-I recovery in HDL isolated by this protocol was 39.8%. Comparison of protein composition of EV and HDL (EV-free HDL) isolated by this protocol and HDL isolated by the gold standard method, sequential ultracentrifugation, suggested that the EV proteins that were removed from HDL by this isolation protocol were mostly immunoglobulins and complement proteins. Several essential HDL proteins were partially removed from the HDL particles during the isolation of EV-free HDL, for example, apoC-IV, apoA-IV and paroxonase-1. In conclusion, this thesis provided evidence of pregnancy and preeclampsia-associated changes of HDL protein, S1P and ceramide in a manner that may improve or decrease HDL function. HDL functional assays are needed to validate the relevance of these HDL composition findings.

Table of Contents

List of Tables

List of Figures

Conferences, Presentation and Publication

Conferences

2018, Glasgow Pregnancy Research Forum, Queen Elizabeth University Hospital, Glasgow

2018, 5th UK Congress on Obesity (UKCO), Newcastle University, Newcastle

2018, 44th Adipose Tissue Discussion group, University of Edinburgh, Edinburgh

2019, 26th European Congress on Obesity, Glasgow

Poster presentation

Pregnant, but not non-pregnant HDL reduces rat uterine artery constriction, Glasgow pregnancy research day, University of Glasgow, 2019

The HDL proteome changes throughout gestation in healthy pregnancy and differs between healthy pregnancy and preeclampsia in the third trimester, On-Air Joint Meeting of the European Society of Hypertension (ESH) and the International Society of Hypertension (ISH), 2021

The HDL proteome changes throughout gestation in healthy pregnancy and differs between healthy pregnancy and preeclampsia in the third trimester, HEART UK 34th Annual Medical & Scientific Virtual Conference, 2021

Oral presentation

The HDL proteome changes throughout gestation in healthy pregnancy and differs between healthy pregnancy and preeclampsia in the third trimester, Maternal Obesity and Preeclampsia: Common Pathway, Amsterdam, The Netherlands, 2019

Publications

Beazer JD, Patanapirunhakit P, Gill JMR, Graham D, Karlsson H, Ljunggren S, Mulder MT, Freeman DJ. High-density lipoprotein's vascular protective functions in metabolic and cardiovascular disease - could extracellular vesicles be at play? Clin Sci (Lond). 2020 Nov 27;134(22):2977-2986. doi: 10.1042/CS20200892. PMID: 33210708.

Patanapirunhakit P, Karlsson H, Mulder M, Ljunggren S, Graham D, Freeman D. Sphingolipids in HDL - Potential markers for adaptation to pregnancy? Biochem Biophys Acta Mol Cell Biol Lipids. 2021 Aug;1866(8):158955. doi: 10.1016/j.bbalip.2021.158955. Epub 2021 Apr 29. PMID: 33933650.

Acknowledgements

Firstly, I would like to express my deepest gratitude to my supervisors, Dr Dilys Freeman and Dr Delyth Graham, for offering me an amazing opportunity as a PhD student at University of Glasgow and supporting me through this PhD journey. I cannot thank you enough for being such kind and supportive supervisors, and also my inspirational role models. I have learnt a lot from both of you and I would not be able to complete this body of work without all the encouragements and supports you have given me, especially during the pandemic time. I would also like to thank Department of Physiology, Faculty of Medicine, Siriraj hospital for your generous funding and supports for me to carry out this work.

I would like to thank Dr Helen Karlsson, Dr Stefan Ljunggren and Dr Monique Mulder for giving me the opportunity to work and learn from your laboratories, and for your welcome and a wonderful experience during my time in Sweden and The Netherlands. I would also like to thank Dr Catherine Bagot and Dr Hiten Mistry for your support in conducting our collaborative research. Thank you to all of you for an inspiring experience in our collaborative group.

Thank you to all the staffs of maternity unit and biorepository unit, Queen Elizabeth University Hospital for helping me with the recruitment of the study participants, sample collection and preparation. Thank you also to all the lovely mothers who participated in this study. I would like to thank Elisabeth Beattie, Laura Haddow and John McAbney for teaching me the wire myography technique and helping me with improving the protocol. Thank you to Dr Vivienne Gibson, Dr Susan Mcniell and all the staffs at Department of Haematology, Glasgow Royal Infirmary, for teaching me the thrombin generation assay technique and helping me out with developing the protocol. Thank you to all of you for your kindness and supports.

My lab mates from the Freeman and Baillie labs, Amaal, Galvin, Jack, Ella, Bracy, Amy, Tara, Connor, Joyce, Alice, Chloe, Emma, Ellie and Tom, you were so welcoming and made my time in the lab so entertaining. I feel so lucky to be a part of this lab family. Special thanks to Galvin, Tara and Amy for your fabulous presence. I am so thankful for our friendship. You truly make me feel at home. Jack, thank you for happy days! you have created for everyone in the lab.

Another special thanks to my lab mum, Fiona Jordan, for teaching me all the laboratory skills, taking care of me and making me feel so welcome. Thank you to my Thai crew; P'Sang, P'Khea, P'Pun, P'Not, P'Gade, P'Gig, Pun, Pong and Fah, for being a family to me. Thank you to P'Khea, Fiona and Jack for managing my belongings when I unexpectedly left Glasgow.

Last but most not least, I am truly grateful for having all the supports from my wonderful family since the first day of my life. To my mum and dad, Sasithon and Nantawat Patanapirunhakit, and my lovely brothers, Pete and Pea, you are the happiness of my life. Thank you for your endless love and care, all the supports and strength you have given me. I will never be able to thank you enough for always be by my side in every step of my life. To my fiancé Moo, thanks for all your love and support, and for being with me through the ups and downs of my PhD journey.

Author's Declaration

I declare that this thesis is my own composition and has not been submitted elsewhere for any other degree, diploma or professional qualification. The work presented in this thesis has been carried out by me except where otherwise acknowledged.

Patamat Patanapirunhakit

Definitions/Abbreviations

ΔF	Active wall force
ΔP	Active effective pressure
ΔT	Active wall tension
A1AT	α-1-antitrypsin
ABCA1	ATP-binding cassette transporter A1
ABCG1	ATP-binding cassette transporter G1
ADP	Adenosine diphosphate
AGE	Advance glycation end product
AGP2	α-1-acid glycoprotein 2
AIM-HIGH	Atherothrombosis Intervention in Metabolic Syndrome with Low HDL/High Triglycerides: Impact on Global Health Outcomes
APC	Antigen-presenting cell
Apo	Apolipoprotein
aPTT	Activated partial thromboplastin time
AUC	Area under the curve
BCR	B cell receptor
BMI	Body mass index
CAMP	Cathelicidin antimicrobial peptide
cDNA	Complementary deoxyribonucleic acid
CERS	Ceramide synthases
CERT	Ceramide transfer protein
CETP	Cholesteryl ester transfer protein
cGMP	Cyclic guanosine monophosphate
CHO	Chinese hamster ovary
CML	Carboxymethyl-lysine
COX-2	Cyclooxygenase 2
C_T	Threshold cycle
CV	Coefficient of variation
D	Lumen diameter
DPBS	Dulbecco's phosphate buffered saline
ED50	Half maximal effective dose
EDTA	Ethylenediaminetetraacetic acid
EEV	Endothelium-derived EV
EL	Endothelial lipase
eNOS	Endothelial-derived nitric oxide synthase
EPS	Early Pregnancy Study
ETP	Endogenous Thrombin Potential
EV	Extracellular vesicle
EVT	Extravillous trophoblast
F	Wall force
FCR	Fraction catabolic rate
FET	Frozen embryo transfer
FL	Fructosyl-lysine
FMD	Flow-mediated dilatation
GI	Gastrointestinal
HAEC	Human aortic endothelial cell
HASMC	Human smooth muscle cell
HCAEC	Human coronary artery endothelial cell

hCG	Human chorionic gonadotropin
HDL	High density lipoprotein
HL	Hepatic lipase
HMEC	Human microvascular endothelial cells
HPS2-THRIVE	Heart Protection Study 2–Treatment of HDL to Reduce the Incidence of Vascular Events
HUVEC	Human umbilical vein endothelial cells
IC	Internal circumference
ICAM-1	Intercellular adhesion molecule 1
IDL	Intermediate density lipoprotein
Ig	Immunoglobulin antibodies
IL	interleukin
IUGR	Intrauterine growth restriction
KPSS	High potassium physiological salt solution
LCAT	Lecithin/cholesterol acyltransferase
LDL	Low density lipoprotein
LFQ	Label-free quantification
LH	Luteinising hormone
LOOH	Lipid hydroperoxides
LpDF	Lipoprotein-depleted fraction
LpDP	Lipoprotein-depleted plasma
LPL	Lipoprotein lipase
LPS	Lipopolysaccharide
LPS	Lipotoxicity in Pregnancy Study
LTA	Lipoteichoic acid
MAC	Membrane attack complex
MCP-1	Monocyte chemotactic protein 1
Met110	Methionine residues at position 110 of apolipoprotein A-I
Met136	Methionine residues at position 136 of apolipoprotein A-I
Met172	Methionine residues at position 172 of apolipoprotein A-I
MG-H1	Methylglyoxal-derived hydroimidazolone 1
MHC I	Major histocompatibility complex class I
MHC II	Major histocompatibility complex class II
mRNA	Messenger ribonucleic acid
nLC-MS/MS	Nano liquid chromatography coupled to tandem mass spectrometry
NO	Nitric oxide
NOS	Nitric oxide synthase
OPLS-DA	Orthogonal Projections to Latent Structures Discriminant Analysis
oxLDL	Oxidised low density lipoprotein
P	Effective pressure
PAI-1	Plasminogen activator inhibitor
PGI-2	prostaglandin I 2
PIGF	Placental growth factor
PLTP	Phospholipid transfer protein
PON1	Paraoxonase-1
PON3	Paraoxonase-3
PPAE	Porcine pulmonary artery endothelial cell
PPP	Platelet-poor plasma
PSS	Physiological salt solution
QC	Quality control

qRT-PCR	Quantitative reverse transcription polymerase chain reaction
Rap-1b	Ras-related protein
RCT	Reverse cholesterol transport
ROS	Reactive oxygen species
S1P	Sphingosine-1-phosphate
S1PR	Sphingosine-1-phosphate receptor
SAA1	Serum amyloid A 1
SAT	Subcuteneous adipose tissue
SD	Standard deviation
SEC	Size exclusion chromatography
sFlt-1	soluble fms-like tyrosine kinase-1
SGPL	Sphingosine-1-phosphate lyase
SGPP	Sphingosine-1-phosphate phosphatase
SPHK	Sphingosine kinase
SPT	Serine palmitoyl transferase
SR-B1	Scavenger receptor B1
T	Wall tension
TCR	T cell receptor
TEER	Transendothelial electrical resistance
TF	Tissue factor
TLR	Toll-like receptor
TNF	Tumor necrosis factor
TRL	Triglyceride-rich lipoproteins
ttPeak	Time to peak
VAT	Visceral adipose tissue
VCAM-1	Vascular adhesion molecule 1
VEGF	Vascular endothelial growth factor
VEGFR-1	Vascular endothelial growth factor receptor 1
VEGFR-2	Vascular endothelial growth factor receptor 2
VI	Velocity index
VLDL	Very low density lipoprotein
VSMC	Vascular smooth muscle cell
vWF	von Willebrand factor

Chapter 1 Introduction

High density lipoprotein (HDL) is well-recognized for its protective role against atherosclerosis, including reverse cholesterol transport (RCT), anti-inflammatory effect, anti-oxidative capability and vascular tone regulation. Increasing plasma HDL cholesterol concentrations, however, does not reduce the risk of atherosclerotic vascular events (Schwartz et al. 2012; Landray et al. 2014; Boden et al. 2011). Therefore, attention has shifted towards HDL composition, both protein and lipid, and function in the maintenance of vascular function.

In healthy pregnancy, maternal metabolism adapts to provide an optimal environment to maintain pregnancy and provide nutrients for the developing fetus. These changes include insulin resistance, inflammation and oxidative stress, all of which could cause vascular damage. However, vascular function is enhanced in healthy pregnancy. The mechanism for this phenomenon remains to be elucidated. Elevated plasma HDL concentration in pregnancy combined with HDL's, perhaps enhanced, vasculo-protective functions could protect maternal vascular endothelium (Sulaiman et al. 2016). In contrast, HDL concentration is lower in complications of pregnancy with vascular dysfunction such as preeclampsia (Belo et al. 2002; Sattar, Bendomir, et al. 1997). These findings might suggest that HDL has a protective impact on vascular function in healthy pregnancy and that HDL protection is reduced in preeclampsia.

This chapter provides an overview of preeclampsia as a complication of pregnancy. Endothelial function, lipid and lipoprotein in the non-pregnant population are reviewed, focusing on HDL's contribution to the protection of endothelial function. Lastly, maternal adaptations in healthy pregnancy and preeclampsia are reviewed. How HDL could be involved in the normal physiology of pregnancy and in the pathophysiology of pre-eclampsia is explored.

1.1 Preeclampsia

Preeclampsia is a vascular complication of pregnancy that affects 2-8% of all pregnancies and attributes to 12% of maternal deaths according to the World Health Organization (Högberg 2005; 'WHO recommendations for prevention and treatment of pre-eclampsia and eclampsia' 2011). Preeclampsia is defined as

the new onset of hypertension with proteinuria or end-organ dysfunction such as liver impairment, renal insufficiency or pulmonary edema which usually occurs after 20 weeks of gestation. Primarily, clinical manifestations of preeclampsia result from a generalised maternal endothelial dysfunction. For instance, impaired regulation of vascular tone causes hypertension, increased vascular permeability results in oedema and proteinuria, and glomerular damage leads to renal insufficiency.

Maternal complications of preeclampsia include hemolysis, elevated liver enzymes, low platelet count (HELLP) syndrome, eclampsia, heart failure, renal failure, hepatic rupture and disseminated intravascular coagulation [reviewed in (Pankiewicz et al. 2019)]. Consequences of preeclampsia to the fetus include intrauterine growth restriction (IUGR) and preterm delivery. Epidemiologic studies showed that up to 25% of all fetus with IUGR and small for gestational age infants and 15-20% of preterm infants are associated with preeclampsia (Jeyabalan 2013). There is growing evidence that preeclampsia affects both mothers and offspring in the long term. A meta-analysis of 22 epidemiological studies revealed a link between preeclampsia and cardiovascular disease with a 4-fold increased risk of heart failure and a 2-fold increased risk of coronary heart disease, stroke, and cardiovascular death (Wu et al. 2017). A 20-year-follow-up study reported increased incidence of hypertension in offspring born to pregnancies complicated by pre-eclampsia, compared to normotensive pregnancies (Davis et al. 2015).

Many risk factors for preeclampsia have been identified. A systematic review of over 100 controlled cohort studies revealed that the risk of preeclampsia was increased in women with chronic hypertension, pre-existing diabetes, raised body mass index (BMI) before pregnancy or at booking, antiphospholipid syndrome, autoimmune disease and renal disease (Duckitt and Harrington 2005). Additional risk factors include maternal age ≥ 40, a previous diagnosis of preeclampsia, multiple pregnancy and nulliparity (Duckitt and Harrington 2005).

Despite being the leading cause of maternal and perinatal mortality, management of preeclampsia is limited to symptomatic/supportive treatment. Preeclampsia can only be cured by delivery and increased risks of future cardiovascular disease remain for women with preeclampsia and their offspring.

Thus, it is important to understand the mechanisms underlying the pathophysiology of preeclampsia. Preeclampsia is probably a collection of a number of disease phenotypes. Several classifications of preeclampsia have been proposed to subclassify preeclampsia based on gestation at disease onset, underlying cause of disease and disease severity to facilitate a better understanding of preeclampsia pathophysiology. Based on the gestation at onset of symptoms, preeclampsia can be divided into two phenotypes: early-onset and late-onset preeclampsia. Early-onset preeclampsia is preeclampsia that develops before 34 weeks of gestation while late-onset preeclampsia develops at or after 34 weeks of gestation (Tranquilli et al. 2013; Raymond and Peterson 2011). Preeclampsia can also be categorized by its severity into preeclampsia with and without severe features. Preeclampsia with severe features includes systolic blood pressure of 160 mmHg or more, or diastolic blood pressure of 110 mmHg or more, thrombocytopenia, impaired liver function, renal insufficiency, pulmonary edema, new onset headache and visual disturbances (American College of Obstetricians and Gynecologists 2013).

1.1.1 Pathophysiology of preeclampsia

Preeclampsia is considered a multi-factorial disorder. Early-onset preeclampsia tends to be associated with placental impairment, IUGR, multi-organ dysfunction and detrimental maternal and neonatal outcomes, while late-onset preeclampsia is likely to result from maternal underlying diseases that predispose to vascular insufficiency and leans toward a normal placenta size and function and normal fetal growth (Tsatsaris et al. 2003; Raymond and Peterson 2011).

Preeclampsia, especially early-onset preeclampsia, is thought to be mediated by abnormal development of the placental vasculature resulting in placental hypoperfusion/ischemia and the release of antiangiogenic factors that disturb maternal endothelial function (Maynard et al. 2003). Disruption to placenta development in preeclampsia ranges from decidualization to spiral artery remodelling. Decidualization is a process of endometrial stromal cell differentiation into decidual stromal cells in preparation for pregnancy. An *in vitro* study showed that endometrial stromal cells isolated from non-pregnant women with a previous history of severe preeclampsia failed to decidualize, demonstrated by lack of morphological change and expression of appropriate

stage-specific markers (Garrido-Gomez et al. 2017). In healthy pregnancy, decidualized cells produce secretory products that promote trophoblast invasion and spiral artery remodelling in placental development [reviewed in (Gellersen and Brosens 2014)]. Thus, decidualization defects in preeclampsia can contribute to downregulated trophoblast invasion and aberrant placentation. In a cell culture experiment, conditioned medium from severe preeclampsia decidual cells was added to cultured cytotrophoblasts and invasion was measured by counting the number of cytotrophoblasts that migrated across a filter. The results showed that conditioned medium from severe preeclampsia decidual cells failed to promote cytotrophoblast invasion, whereas cytotrophoblast invasion was observed in the presence of conditioned medium from healthy control pregnancy decidual cells (Garrido-Gomez et al. 2017). During normal placental development, trophoblasts, which consist of cytotrophoblasts and syncytiotrophoblasts, invade spiral arteries in the endometrium. Spiral arteries then undergo physiological remodelling to have a wider diameter and improve placental perfusion. In preeclampsia, however, spiral arteries remain narrow, leading to placental hypoperfusion or ischemia [reviewed in (Ngene and Moodley 2018)].

A poorly perfused or ischemic placenta causes an imbalance of pro- and antiangiogenic factors which contributes to the pathogenesis of preeclampsia. The key angiogenic factors in preeclampsia are placental growth factor (PlGF) and soluble fms-like tyrosine kinase-1 (sFlt-1). In healthy pregnancy, vascular endothelial growth factor (VEGF) stimulates eNOS activity and promotes vasodilation predominantly through VEGF receptor 2 (VEGFR-2). This was demonstrated by greater eNOS activation by VEGF in uterine artery endothelial cells isolated from pregnant sheep versus those from non-pregnant sheep, a response that was blocked by an VEGFR-2 inhibitor (Grummer et al. 2008). PlGF is a member of the VEGF family and is produced mainly by the placenta (Shore et al. 1997). PlGF competitively binds to the VEGF-1 or Flt-1, but not VEGF-2, and thus promotes VEGF-VEGFR-2 interaction which has a stronger vasodilatory signal [reviewed in (Chau, Hennessy, and Makris 2017)]. In healthy pregnancy, serum PIGF concentration increased from the first to the third trimester, peaking at 32 weeks of gestation and decreasing thereafter (Ng et al. 2019; Lobmaier et al. 2014). sFlt-1 is a soluble form of VEGFR-1 and is mainly

expressed in placenta (Thomas et al. 2009). sFlt-1 serves as an antagonist of VEGF and PlGF. Binding of sFlt-1 to VEGF or PlGF limits the access of these ligands to their signalling receptors [reviewed in (Roberts and Rajakumar 2009)]. Placenta is the main source of circulating sFlt-1. Placental sFlt-1 expression increased throughout gestation of healthy pregnancy, especially in the third trimester (Sela et al. 2008). Also, serum sFlt-1 concentration increased in the third trimester of healthy pregnancy (Ng et al. 2019; Lobmaier et al. 2014).

In preeclampsia, there was a lower serum PlGF and higher sFlt-1 concentrations in pregnant women who later developed preeclampsia than healthy pregnant women (Levine et al. 2004). Reduced PIGF concentration in preeclampsia started as early as 13 weeks of gestation, and elevation of sFlt-1 level began as early as 5 weeks before the onset of preeclampsia (Levine et al. 2004). The change in PIGF and sFlt-1 levels in preeclampsia is thought to be from placental ischemia. When cultured cytotrophoblast obtained from the first trimester placenta were exposed to different oxygen condition, sFlt-1 concentration in the cultures increased, while PIGF concentration decreased, with a decrease of oxygen concentration (Nagamatsu et al. 2004). There was also upregulated sFlt-1 expression in placenta of preeclampsia relative to healthy pregnancy (Sela et al. 2008; Thomas et al. 2009). Low circulating PlGF levels and excess levels of sFlt-1, as found in preeclampsia, could impair vascular tone regulation, leading to widespread endothelial dysfunction and the clinical presentation of preeclampsia.

There is limited research studying vascular function prior to the onset of preeclampsia. The endothelial dysfunction of preeclampsia could either be the consequence of placental ischemia and angiogenic factor imbalance or could be the underlying vascular pathology of pregnant women or both. The pathological lesion in the spiral artery of preeclampsia, spiral atherosis, is compatible with the atherosclerotic process in the non-pregnant population in which the early lesion is an accumulation of lipid-laden macrophages in the vascular bed [reviewed in (Sattar and Greer 1999)]. Moreover, there is excess fat accumulation in several tissues of preeclampsia including glomerular cells (glomerular endotheliosis) and the liver [reviewed in (Sattar and Greer 1999)]. Ectopic lipid accumulation in organs involved in the pathogenesis of

preeclampsia suggests a potential role of lipid disturbance in the endothelial dysfunction of preeclampsia which will be discussed later. Also, lipid-lowering medication such as statins have been studied for their contribution in the management of preeclampsia. Not only is there a potential benefit of statin's cholesterol-lowering effect by inhibiting hydroxymethylglutaryl-coenzyme A (HMG-CoA) reductase in cholesterol synthesis, but statins also have other properties which could enhance endothelial function. Statins can promote nitric oxide (NO) bioavailability by various mechanisms including increasing endothelial-derived nitric oxide synthase (eNOS) phosphorylation, restoring eNOS activity by decreasing caveolin-1 in caveolae and reducing reactive oxygen species (ROS) production and oxidative stress [reviewed in (Lecarpentier et al. 2012)]. It was shown that pravastatin reduced sFlt-1 secretion from primary endothelial cells, purified cytotrophoblast cells, and placental explants obtained from women with preterm preeclampsia (Brownfoot et al. 2015). However, research concerning the effect of statins on preeclampsia clinical outcomes is controversial. Women with preeclampsia who received daily pravastatin had reduced serum sFlt-1 level and stabilized blood pressure and proteinuria (Brownfoot et al. 2015). In contrast, other studies showed no difference in plasma sFlt-1, PIGF, the sFlt-1:PlGF ratio and blood pressure between women with preeclampsia treated with pravastatin and the placebo groups (Ahmed et al. 2020; Costantine et al. 2016)."

1.2 Endothelial function

1.2.1 Physiology of the endothelium

The vascular endothelium is the inner layer lining the lumen of blood vessels. It functions as a physical barrier between the blood and the vascular wall, regulation of vascular tone and modulation of vascular inflammation. Endothelial cells produce and secrete a variety of vasoconstrictors and vasodilators. The most important vasodilatory substance derived from endothelial cells is NO (Ignarro et al. 1987). NO is a gaseous molecule synthesized from an L-arginine by the enzyme nitric oxide synthase (NOS). Endothelial-derived NOS (eNOS) is the main isoform of NOS and predominates in the regulation of vascular tone. eNOS activity can be stimulated by shear stress and vasodilators such as acetylcholine and bradykinin, thereby inducing NO synthesis (Fisslthaler et al. 2000; Kuchan

and Frangos 1994; Furchgott and Zawadzki 1980; Ignarro et al. 1987; Fleming, Hecker, and Busse 1994). NO then activates the enzyme guanylate cyclase in vascular smooth muscle cells (VSMC) to form cyclic guanosine monophosphate (cGMP) which subsequently reduces cytosolic calcium levels within VSMC and leads to vasodilation (Rapoport and Murad 1983). Endothelium-derived NO can also prevent leukocyte adhesion to endothelial cells, contributing to inflammatory inhibition (Kubes, Suzuki, and Granger 1991). Under physiological conditions, endothelial cells regulate vascular tone by balancing the production and secretion of vasoconstrictors and vasodilators to maintain blood flow and blood pressure.

With respect to the balance between coagulation and fibrinolysis, the endothelium plays an anti-thrombotic role to maintain coagulation in a quiescent state. Coagulation is a process of blood clotting in response to vascular injury to prevent blood loss and limit injury to the vessels. Coagulation includes primary platelet aggregation which is initially reversible and secondary hemostasis which generates fibrinogen to augment the platelet plug. Primary hemostasis involves platelet adhesion, activation and aggregation. Upon vessel injury, von Willebrand factor (vWF) in the subendothelial space is exposed and interacts with glycoprotein Ib/IX/V receptors in platelets. This interaction initiates platelet adhesion to the endothelium. After that, platelets are activated by adenosine diphosphate (ADP), thrombin, or thromboxane A2 to promote glycoprotein IIb/IIIa interaction among platelets, leading to platelet aggregation. Endothelium-derived NO can be released into the blood, activating cGMP in platelets, and thus reducing platelet activation and adherence to endothelial cells (Hogan, Lewis, and Henderson 1988; Sneddon and Vane 1988).

Secondary hemostasis involves fibrin clot formation through three pathways: extrinsic, intrinsic and common pathways. The extrinsic pathway starts when tissue factor (TF) is exposed to the circulation. TF is a transmembrane protein expressed on extravascular cells such as VSMC and adventitial cells. Interaction of TF and clotting factor VIIa activates factor X in the common pathway. The intrinsic pathway involves activation of factor XII and downstream proteins: factor XI, IX, VIII and X, respectively. Activation of factor X by extrinsic and intrinsic pathways initiates the common pathway. Activated factor X, together

with factor V, promotes prothrombin conversion into thrombin via a prothrombinase complex. The prothrombinase complex is a combination of a protease factor Xa and a protein cofactor factor Va and anionic phospholipid membranes and the presence of calcium ions are required for the prothrombinase complex to cleave prothrombin to thrombin (Walker and Krishnaswamy 1994). Thrombin then converts fibrinogen to fibrin which lead to formation of fibrin clot. Endothelial cells express thrombomodulin which is an inhibitor of the coagulation cascade (Maruyama, Bell, and Majerus 1985). Thrombomodulin binds to thrombin. The thrombin-thrombomodulin complex then activates protein C which subsequently inactivates coagulation factor Va and inhibits the downstream coagulation cascade (Esmon and Owen 1981; Owen and Esmon 1981; Esmon, Owen, and Esmon 1982).

1.2.2 Pathophysiology of endothelial dysfunction

The term “endothelial dysfunction” is generally defined as changes in the endothelium that impair its function. Endothelial dysfunction is associated with atherogenic phenotypes including increased vasoconstriction, inflammation and thrombosis. An imbalance of vasoconstrictors and vasodilators, particularly a reduction of NO bioavailability, is the main mediator of endothelial dysfunction. Decreased NO bioavailability can lead to impaired VSMC response to vasodilators and thus, vasoconstriction. Other functions of NO may also be affected, for example its ability to inhibit platelet aggregation and leukocyte trafficking, leading to enhanced coagulation and an inflammatory state.

A reduction of NO bioavailability by enhanced NO degradation can be the result of enhanced oxidative stress (Rubanyi and Vanhoutte 1986b, 1986a). Oxidative stress is defined as “an imbalance between oxidants and antioxidants in favor of the oxidants, potentially leading to damage” (Sies 1997). Oxidants include free radical or single electron oxidants and two electron oxidants such as ROS. ROS is a term describing highly reactive chemicals formed from O_2, for example lipid hydroperoxides (LOOH) generated from lipid peroxidation and hydrogen peroxide (H_2O_2) derived from the action of oxidases such as glucose oxidase on O_2. Under physiological conditions, oxidants are normally produced from aerobic metabolism. However, a greater production of oxidants can occur under pathophysiological conditions (Sies 1997). Many pathological conditions

associated with endothelial dysfunction, such as hypertension, insulin resistance and atherosclerosis, are associated with increased oxidative stress (reviewed in (Cai and Harrison 2000)). Oxidative stress is one of the main mechanisms in the pathogenesis of endothelial dysfunction.

Another mechanism of endothelial dysfunction is inflammation. Endothelial cells can release a broad spectrum of pro- and anti-inflammatory cytokines, chemokines and growth factors, for example interleukin-1 (IL-1), IL-5, IL-6, IL-10 and monocyte chemotactic protein 1 (MCP-1) [reviewed in (Mai et al. 2013)]. During inflammation, endothelial cells are activated and release additional pro-inflammatory cytokines which contribute to inflammatory pathways. Treatments with bacterial lipopolysaccharide (LPS) or tumor necrosis factor α (TNFα) to induce inflammation in cultured human umbilical vein endothelial cells (HUVEC) and human coronary artery endothelial cells (HCAEC) revealed increased production of IL-6, a pro-inflammatory cytokine (von Asmuth et al. 1991; Krishnaswamy et al. 1998). Moreover, activated endothelial cells express adhesion molecules including intercellular adhesion molecule 1 (ICAM-1) and vascular adhesion molecule 1 (VCAM-1) (Zeuke et al. 2002). Upregulation of adhesion molecules expression facilitates leukocyte adhesion to endothelial cells and leukocyte transmigration across the endothelium to the underlying tissue or the site of inflammation.

Inflammation can stimulate coagulation and thrombosis. C-reactive protein, an inflammatory stimulator, was associated with reduced expression of thrombomodulin by endothelial cells, resulting in pro-coagulant effects (Nan et al. 2005). Additionally, inflammation-associated cytokines including TNF-α and CD40 ligand were found to stimulate expression of TF by endothelial cells (Del Turco et al. 2014; Bavendiek et al. 2002). Under physiological conditions, endothelial cells do not express active TF. After vascular injury or stimulation by inflammation, coagulation factor VIIa binds to TF expressed on the endothelial cell surface, initiates the coagulation cascade and contributes to intravascular thrombosis. Moreover, activated endothelial cells release vWF which promotes platelet aggregation and prevents rapid degradation of coagulation factor VIII (Bernardo et al. 2004). Studies in mice showed that endothelial cell-derived vWF

is a major contributor to atherosclerosis by promoting vascular thrombo-inflammation (Doddapattar et al. 2018; Dhanesha et al. 2016).

1.3 Lipid and lipoprotein

Lipids are water-insoluble compounds which are formed mainly from carbon, hydrogen and oxygen. Lipid serves as energy storage, is essential for cellular and mitochondrial membranes, and is a constituent of steroid hormones, bile salts, fat-soluble vitamins and lipoproteins. Lipids can be categorized into derived, simple and complex lipids. Derived lipids are the basic components of simple and complex lipids, including fatty acid and cholesterol. Simple lipids are lipids that produce up to two products by hydrolysis, mainly fatty acid and alcohol components. Examples of simple lipids are monoacylglycerol, diacylglycerol and triglyceride. Lastly, complex lipids are lipids that produce three or more products by hydrolysis, for example, sphingolipids which are esters of fatty acid, alcohol sphingosine, and phosphate or sugars (glucose or galactose).

1.3.1 Sphingolipid metabolism

Ceramide can be considered as the central hub metabolite in sphingolipid metabolism. It is an important precursor for other sphingolipids and all sphingolipids are catabolized back into ceramide before degradation. Ceramide can either be synthesised through the *de novo* pathway, via sphingomyelin hydrolysis or via the salvage pathway (Figure 1-1).

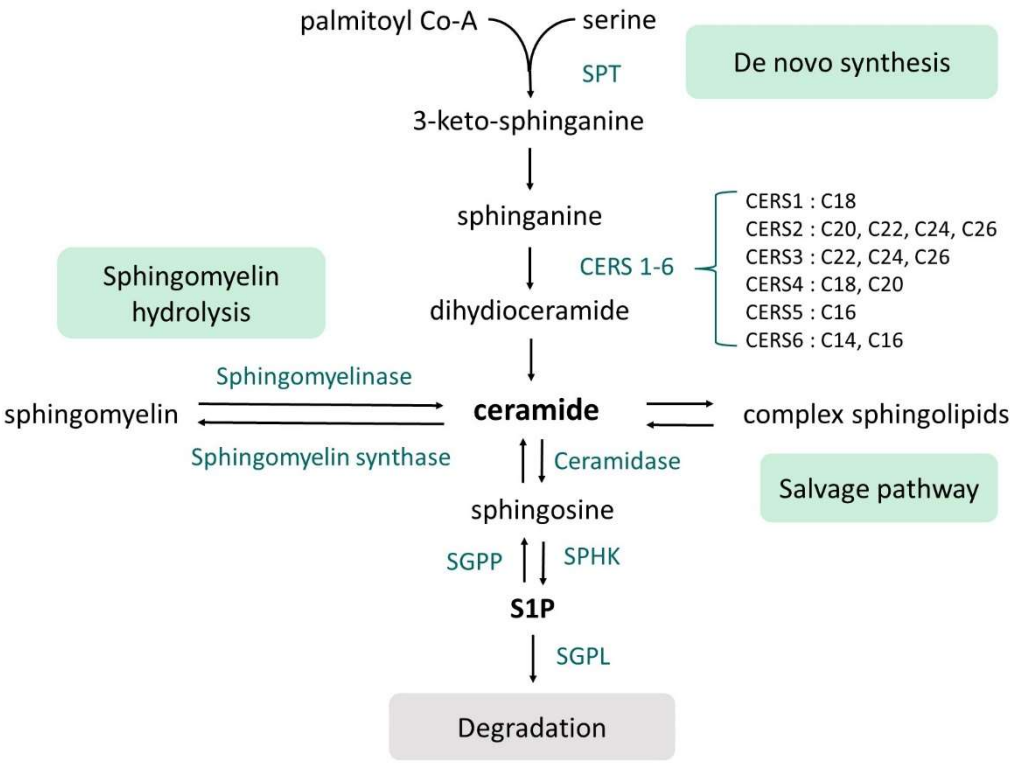

Figure 1-1 . Sphingolipid metabolism SPT, serine palmitoyl transferase; CERS, ceramide synthases; SPHK, sphingosine kinase; SGPP, S1P phosphatase; SGPL, S1P lyase

De novo synthesis takes place in the endoplasmic reticulum, where the enzyme serine palmitoyl transferase (SPT) catalyzes the condensation of palmitoyl Co-A and serine to generate 3-keto-sphinganine. This reaction is the rate-limiting step of *de novo* synthesis. The 3-keto-sphinganine produced by this reaction is then rapidly transformed into sphinganine. The enzyme ceramide synthases (CERS) 1-6 convert sphinganine into dihydroceramides of different acyl-chain lengths depend on the specificities of each CERS. In the final step, dihydroceramide is converted to ceramide with a variety of fatty acids acyl-chain lengths. Despite its low solubility, ceramide can move to the Golgi by either ceramide transfer protein (CERT) or vesicle transport. In the Golgi, ceramide is converted to other complex sphingolipids such as sphingomyelin and glucosylceramide. Other pathways for ceramide synthesis are sphingomyelin hydrolysis and the salvage pathway. Sphingomyelin hydrolysis is the process of sphingomyelin conversion to ceramide by the enzyme sphingomyelinase in plasma membranes or lysosomes and the salvage pathway is the process that allows complex sphingolipids conversion back into ceramide.

The sole breakdown pathway for all sphingolipids is through ceramide catabolism in the endoplasmic reticulum. All sphingolipids are degraded into ceramide. The enzymes ceramidase and sphingosine kinase (SPHK) then convert ceramide to sphingosine and sphingosine-1-phosohate (S1P), respectively. S1P can be reconverted to sphingosine by a reversible process catalysed by the enzyme S1P phosphatase (SGPP). In addition, S1P lyase (SGPL) degrades S1P into hexadecenal and phosphoethanolamine in an irreversible manner [reviewed in (Gault, Obeid, and Hannun 2010; Chaurasia and Summers 2015)].

In plasma, most of the S1P and ceramide are carried in lipoproteins, 60% for S1P and 98% for ceramide, and the remainder is carried by albumin, blood cells, and platelets (Okajima 2002; Boon et al. 2013; Hammad et al. 2010).

1.3.2 Lipoproteins

Lipoproteins consist of lipid and protein components. Triglyceride and cholesteryl ester are the hydrophobic lipids at the core of lipoproteins, surrounded by proteins and other amphipathic lipids such as cholesterol and phospholipid. The main function of lipoproteins is to transport hydrophobic lipids, in the highly aqueous environment including the blood and other extracellular fluids. Lipoproteins can be classified into five major types based on their density: chylomicrons (density<0.95 g/mL), VLDL (density 0.95-1.006 g/mL), IDL (density 1.006-1.019 g/mL), LDL (density 1.019-1.063 g/mL), and HDL (density 1.063-1.21 g/mL). HDL can be divided by its density into two major subfractions: HDL2 and HDL3. HDL2 has the lower density (1.063-1.125 g/mL), larger size and is relatively lipid-rich, while HDL3 is denser (1.125-1.21 g/mL), smaller and richer in protein. LDL consists of 7 subclasses (LDL1-7) based on electrophoretic mobility (Kalogirou et al. 2007). LDL1 and LDL2 are considered large buoyant LDL, and LDL3-7 are small dense LDL. Small dense LDL is more prevalent in patients with coronary artery disease than healthy controls (Campos et al. 1992; Coresh et al. 1993). It is possibly due to the increased susceptibility of small dense LDL to oxidation, and oxidised LDL (oxLDL) is atherogenic (Yoshino, Hirano, and Kazumi 2002).

Chylomicron, the lowest density lipoprotein, is the largest lipoprotein in size and the highest in triglyceride content. Lipoprotein size decreases and contains less

triglyceride progressing from VLDL, IDL, LDL to HDL. Therefore, chylomicron, VLDL and IDL are considered as triglyceride-rich lipoprotein (TRL) while LDL and HDL are cholesterol-rich lipoprotein. The apolipoprotein content of lipoproteins also differs. The main protein in VLDL, IDL and LDL is apolipoprotein B (apoB) while HDL contains apolipoprotein A-I (apoA-I) as the major protein. The general characteristics of lipoproteins are shown in Table 1.1.

Table 1.1 The general characteristics of lipoproteins

Lipoprotein	Diameter (nm)	Density (g/mL)	% Protein	% Triglyceride	% Cholesterol and Cholesteryl Ester
Chylomicrons	100–500	1–2	0.95	85–90	4–8
VLDL	30–80	0.95–1.006	5–10	50–65	15–25
IDL	25–35	1.006 –1.019	10–20	20–30	40–45
LDL	18–25	1.019–1.063	20–25	7–15	45–50
HDL	5–12	1.063–1.210	40–55	3–10	15–20

The normal function of VLDL, IDL and LDL is to transport fatty acids and cholesterol to peripheral tissues for energy production and storage. VLDL is synthesized in the liver by the assembly of endogenously produced lipids including triglyceride and cholesteryl ester. The major protein coating the lipid core of VLDL is apolipoprotein B-100 (apoB-100). From the time VLDL is secreted into the bloodstream, VLDL acquires apolipoprotein C-II (apoC-II) and apolipoprotein E (apoE) from HDL and undergoes triglyceride hydrolysis by lipoprotein lipase (LPL) and its co-factor, apoC-II [reviewed in (Bayly 2014)]. Additionally, the triglycerides in VLDL can be transferred to HDL by cholesteryl ester transfer protein (CETP) in exchange for cholesteryl ester from HDL to VLDL

(Morton and Zilversmit 1983). Progressive removal of triglyceride from VLDL leads to the formation of cholesteryl ester and apoE-rich remnant particles called VLDL remnants or IDL. About half of IDL are taken up and degraded by the liver, whereas the other half of IDL proceeds through triglyceride hydrolysis by LPL and becomes LDL. LDL mainly consists of cholesteryl ester in the core with apoB-100 as the major protein on the surface. The amount of cholesterol that LDL carries in the form of cholesteryl ester accounts of around 70% of total cholesterol in plasma [as reviewed in (Bayly 2014)]. LDL transports cholesterol to peripheral tissues where apoB-100 on the surface of LDL is recognized and binds to LDL receptors on the membrane of target cells, leading to LDL endocytosis. The LDL particle is then degraded intracellularly and releases cholesterol to be utilized within the cell such as steroid hormone synthesis in steroid hormone-producing tissue and bile acid production in the liver [reviewed in (Goldstein, Anderson, and Brown 1982)].

1.3.3 TRL and LDL contribution to endothelial dysfunction

TRL and LDL are known to impair endothelial function via various mechanisms including disruption of endothelial integrity and vascular tone regulation, promotion of an inflammatory environment and a pro-thrombotic state. TRL lipolysis products and altered TRL concentration and composition under pathological conditions can impair endothelial function. When flow-mediated dilatation (FMD) of the brachial artery, a method of determining arterial diameter changes in response to reactive hyperemia using ultrasound, was determined in healthy individuals, there were inverse correlations of FMD with plasma triglyceride and apoB concentrations. This finding supports a role of TRL in vasomotor dysfunction. Products generated from TRL lipolysis including remnant lipoproteins, free fatty acids, monoglycerides, diglycerides and phospholipids also decreased endothelial barrier function. A transendothelial electrical resistance study in human aortic endothelial cells (HAEC) incubated with TRL lipolysis products, derived from TRLs treated with LPL, exhibited a time-dependent decrease in transendothelial resistance i.e. an increase in endothelial permeability (Eiselein et al. 2007). Immunofluorescent studies also revealed morphological changes in endothelial junction proteins demonstrated by discontinuity and irregularity in the distribution of zona occludens-1, VE-cadherin and occludin, and disruption of the F-actin network (Eiselein et al.

2007). In addition, TRL lipolysis products induced apoptosis in HAEC (Eiselein et al. 2007). Increased endothelial permeability could contribute to lipid diffusion into the sub-endothelial space via intercellular pathways. Lipid peroxidation and lipoprotein degradation in the sub-endothelial space releases aldehydes and oxidized phospholipids which oxidise LDL lipid components and apoB, thereby forming oxLDL [reviewed in (Hartley, Haskard, and Khamis 2019).

OxLDL is associated with endothelial dysfunction. OxLDL reduces NO production and thus impairs vasodilation. Studies in porcine pulmonary artery endothelial cells (PPAE) revealed that oxLDL promoted eNOS translocation from caveolae, a lipid domain on the plasma membrane, to intracellular membranes (Blair et al. 1999). This process inactivates eNOS and reduces NO production. Adding oxLDL to PPAE cell culture resulted in a reduction in acetylcholine-mediated eNOS activation (Blair et al. 1999). In addition, oxLDL may promote inflammatory processes. HUVECs incubated with oxLDL resulted in increased endothelial expression of ICAM-1 and VCAM-1 in a dose-dependent manner (Cominacini et al. 1997). OxLDL can also activate endothelial inflammation, mostly through phospholipid oxidation products such 1-palmitoyl-2-arachidonyl-sn-glycero-3-phosphorylcholine (reviewed in (Berliner and Gharavi 2008)). Lastly, the interaction of oxLDL with isolated platelets activated platelet aggregation *in vitro* (Meraji et al. 1992). One of the mechanisms could be an oxLDL-mediated reduction of NO bioavailability which not only impairs vasodilatory function, but also promotes platelet activation.

1.4 High density lipoprotein

1.4.1 HDL metabolism

1.4.1.1 HDL biogenesis

HDL synthesis is initiated when apoA-I is secreted, mainly from the liver and the intestine, into the blood circulation (Zannis et al. 1985). Circulating apoA-I interacts with ATP-binding cassette transporter A1 (ABCA1) which is expressed in macrophages, adipocytes and various human tissues with the highest expression in placenta, liver and lungs (Kielar et al. 2001; Langmann et al. 1999). ABCA1 preferentially interacts with lipid-free apoA-I, but not with mature HDL particles, and markedly enhances cellular cholesterol and phospholipid efflux to

lipid-free apoA-I (Wang et al. 2000). Progressive lipidation of apoA-I converts apoA-I to nascent discoid HDL particles, enriched in unesterified cholesterol. Afterwards, lecithin/cholesterol acyltransferase (LCAT) interacts with discoidal HDL. LCAT activates the transesterification between phospholipids and unesterified cholesterol by transferring the 2-acyl group of lecithin or phosphatidylethanolamine to cholesterol to form cholesteryl ester (Fielding, Shore, and Fielding 1972). Eventually, cholesterol esterification in HDL by LCAT converts nascent discoid HDL to mature spherical HDL (Chroni et al. 2005). HDL biogenesis is illustrated in Figure 1-2.

The most recognizable HDL function is RCT, a process by which HDL removes cholesterol from peripheral tissues to the liver for excretion. The mechanisms for cholesterol efflux from the plasma membrane to HDL include passive diffusion and active pathways mediated by ABCA1 and ATP-binding cassette transporter G1 (ABCG1). ABCA1 preferentially enhances cell interaction with lipid-free apoA-I and, thus, promotes cholesterol efflux to apoA-I thereby forming nascent HDL. In contrast, ABCG1 induces cellular cholesterol efflux to more mature HDL. ABCG1 expression on human embryonic kidney 293 (HEK293) cells promoted cellular sterol efflux to HDL without any effect on sterol efflux to apoA-I (Wang et al. 2008). After cholesterol is transported to HDL, LCAT converts cholesterol to cholesteryl ester which is later removed from HDL via scavenger receptor B1 (SR-B1)-mediated selective uptake of HDL cholesteryl ester into the liver in the absence of HDL endocytosis and degradation.

1.4.1.2 HDL remodelling

HDL undergoes remodelling by proteins in the blood circulation, resulting in alteration of HDL properties such as HDL size. The conversion between HDL2 and HDL3 can be activated by various HDL remodelling pathways as detailed below and are shown in Figure 1-2.

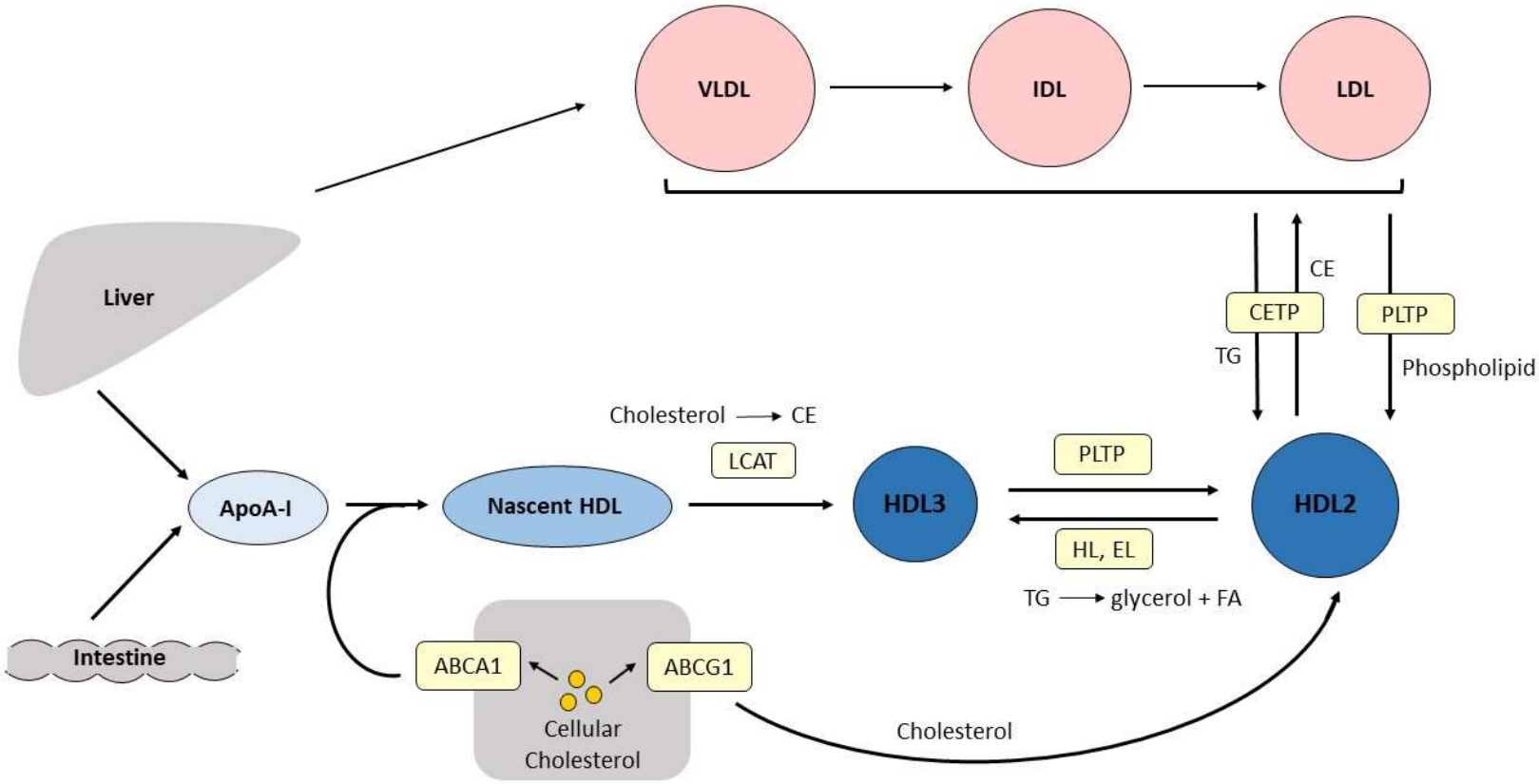

Figure 1-2 HDL synthesis and remodeling ApoA-I is secreted from liver and intestine. Cellular cholesterol is then transferred to plasma apoA-I by ABCA1, form nascent discoid HDL and eventually mature HDL3 by LCAT. Mature HDL3 can be remodeled by ABCG1, HL, EL, PLTP and CETP. CE; cholesteryl ester, TG; triglyceride, FA; fatty acid

Hepatic lipase (HL) and endothelial lipase (EL)

Hepatic lipase (HL) and endothelial lipase (EL) are plasma lipolytic enzymes derived from the liver and endothelial cells, respectively. HL hydrolyses triglycerides and phospholipids of circulating lipoproteins, and thus promotes conversion of HDL2 to HDL3 (Figure 1-2). Polymorphisms in the HL gene associated with lower HL activity showed an association with higher HDL2 concentration (Couture et al. 2000; Zambon et al. 1998). EL hydrolyses triglycerides and phospholipids of lipoproteins, but with a greater affinity for phospholipid than triglyceride hydrolysis (Jaye et al. 1999). HDL isolated from EL-overexpressing mice showed a decreased percentage of phospholipid and cholesterol content, unchanged triglyceride content and an increased percentage of protein (Maugeais et al. 2003; Ishida et al. 2003). Gel-filtration chromatography and nondenaturing gradient gel electrophoresis revealed a marked reduction in HDL size of EL-overexpressing mice (Maugeais et al. 2003). These findings suggest that both HL and EL are involved in interconverting HDL2 to HDL3 and nascent HDL.

Phospholipid transfer protein (PTLP)

Phospholipid transfer protein (PTLP) is a transfer protein for phospholipid, cholesterol and other lipids among lipoproteins and between lipoproteins and cells (Rao et al. 1997; Nishida and Nishida 1997). Several *in vitro* studies found that PLTP promoted cholesterol and phosphatidylcholine efflux from macrophages and vesicles to HDL, compared to conditions in the absence of PLTP (Vikstedt et al. 2007; Tall, Forester, and Bongiovanni 1983). PLTP also transfers VLDL/IDL/LDL surface phospholipid to HDL (Figure 1-2) (Cheung, Wolfbauer, and Albers 1996; Jiang et al. 1999). An approximately 60% reduced HDL phospholipid and cholesterol in PLTP-knockout mice suggests a significant contribution of PLTP in transferring these lipids to HDL (Jiang et al. 1999). Interestingly, PTLP promotes fusion of HDL3 particles and generates HDL2 and nascent HDL. HDL and PLTP co-incubation showed increased nascent HDL formation and a higher proportion of large HDL particles or HDL2, while HDL3 subfractions decreased (Vikstedt et al. 2007; Tall, Forester, and Bongiovanni 1983). Observing the remodelling of enlarged reconstituted HDL particles incubated with PLTP by electron microscopy revealed a fusion of HDL3 particles

rather than increased lipid influx into HDL3 to form HDL2 (Lusa et al. 1996). These results illustrate that the PLTP mediates the fusion of HDL3 and promotes the formation of HDL2 and nascent HDL (Figure 1-2).

CETP

CETP is responsible for transferring HDL cholesteryl esters to VLDL/IDL/LDL in exchange for triglyceride to HDL (Figure 1-2) (Morton and Zilversmit 1983). This HDL remodelling by CETP results in triglyceride-rich HDL which can be further converted from HDL2 to HDL3 by HL. An increased HDL2 to HDL3 ratio was found in patients with CETP deficiency (Inazu et al. 1990). Coronary heart disease patients receiving anacetrapib, a CETP inhibitor, had higher plasma HDL cholesterol concentration than patients receiving placebo treatment (Brinton et al. 2015). Thus, smaller HDL particles resulting from HL action on triglyceride-rich HDL may facilitate HDL clearance, leading to lower plasma HDL levels. Moreover, accelerated HDL remodelling by PLTP activity was found in triglyceride-enriched HDL versus triglyceride-depleted HDL (Settasatian et al. 2001). This is likely due to the destabilization of apoA-I as a spectroscopic study revealed a less stable apoA-I in triglyceride-enriched HDL than that in triglyceride-depleted HDL (Settasatian et al. 2001). These processes may underlie the inverse relationship observed between high plasma triglycerides and low plasma HDL as observed in metabolic syndrome. CETP activity also affects the ABCG1-dependent pathway of cholesterol efflux to HDL. HDL isolated from patients with homozygous genetic deficiency of CETP or from subjects receiving CETP inhibitors exhibited an enhanced ability of HDL to promote ABCG1-dependent cholesterol efflux from macrophages (Matsuura et al. 2006; Yvan-Charvet et al. 2007; Yvan-Charvet et al. 2010). This could be due to the increased HDL concentration and LCAT-mediated production of cholesteryl ester found in CETP-deficient patients and subjects treated with CETP inhibitors (Yvan-Charvet et al. 2010; Matsuura et al. 2006).

1.4.1.3 HDL catabolism

HDL can be degraded by gradual removal of HDL components. Several of the plasma enzymes involved in HDL remodeling are involved in HDL catabolism. HL and EL promote plasma clearance of HDL. Western blot of lipoproteins from HL-

overexpressing rabbits, resolved by electrophoresis in a 1% agarose gel and visualized using fat red 7B staining, revealed a marked reduction of the HDL fraction (Fan et al. 1994). HDL clearance was studied in transgenic mice by injection of ^{125}I-HDL into mice and assaying the plasma for ^{125}I-HDL radioactivity. The HDL apolipoprotein fraction catabolic rate (FCR), calculated from plasma decay curve of radiolabelled HDL, significantly increased in both HL- and EL-overexpressing mice than the control mice (Braschi et al. 1998; Maugeais et al. 2003).

HDL catabolism can also be promoted by CETP. Patients with genetic CETP deficiency have a marked increase in HDL cholesterol and apoA-I (Inazu et al. 1990; Maruyama et al. 2003). Reduced CETP activity can be found in around 65% of hyperalphalipoproteinemic patients and these patients exhibited a markedly lower cholesterol turnover, studied using radiolabelled cholesterol turnover studies (Maruyama et al. 2003; Nestel and Miller 1980). Thus, decreased CETP activity may affect cholesterol turnover by decreasing CETP-mediated removal of cholesteryl ester from HDL. In fact, this may explain the failure of HDL raising medications such as CETP inhibitors to reduce CVD risk. In contrast to HL, EL and CETP, PLTP (which promotes lipid incorporation into HDL) helps maintain HDL levels. A study in PLTP-knockout mice revealed a significant reduction of HDL lipid and protein levels including reduced apoA-I (Jiang et al. 1999).

Enhancement of HDL clearance by HL, EL and CETP could be due to their lipolytic activity. HDL preincubated with HL or EL increased cholesterol delivery from HDL to cultured rat hepatoma cells and SR-B1-expressing, LDL receptor-deficient cells, respectively (Bamberger, Glick, and Rothblat 1983; Nijstad et al. 2009). HDL cholesteryl ester FCR in EL-overexpressing mice was higher than wild-type mice (Nijstad et al. 2009). Regarding apoA-I destabilization, transgenic mice and rabbits with enhanced HL activity not only had reduced lipid content in HDL, but also reduced HDL apolipoproteins including apoA-I (Braschi et al. 1998; Fan et al. 1994). Moreover, enhancement of small HDL (HDL3) production by HL, EL and CETP might promote HDL catabolism. An estimate of HDL size by HDL cholesterol/(apoA-I+apoA-II), which represents the core-to-surface ratio of HDL, was inversely related with apoA-I FCR, studied in humans using radioiodinated apoA-I (Brinton, Eisenberg, and Breslow 1994). ApoA-I FCR was found to be

inversely correlated with HDL cholesterol levels (Brinton, Eisenberg, and Breslow 1994). Renal uptake of apoA-I was studied in isolated rabbit kidney perfused with modified and unmodified HDL. Triglyceride-enriched HDL incubated with LPL and HL had a smaller size than unmodified HDL (Horowitz et al. 1993). Perfusion of this small, modified HDL revealed a greater apoA-I accumulation in kidney cortex than when the kidney was perfused with unmodified HDL (Horowitz et al. 1993). Lipid-free or minimally lipidated apoA-I is mainly degraded by the kidney (Woollett and Spady 1997). Since HDL is too large to be filtered via glomerular filtration, only apoA-I is filtered, reabsorbed through proximal tubules in kidney cortex and degraded intracellularly (Kozyraki et al. 1999). These data suggest that the mechanism whereby the triglyceride enrichment of HDL by CETP facilitates hydrolysis of HDL triglycerides in the HDL core by LPL, HL or EL, leading to smaller particle size, leading to destabilization of apoA-I binding on HDL surface, free apoA-I uptake by the kidney for degradation and therefore increased HDL FCR.

Sites of HDL catabolism were assessed using a ^{125}I-tyramine-cellobiose–labelled HDL assay. The uptake of labelled HDL by the liver and the kidney were significantly enhanced in transgenic mice with EL overexpression (Maugeais et al. 2003). In the absence of SR-B1, EL-overexpressing mice lost their selective hepatic uptake of HDL cholesteryl ester over HDL protein (Nijstad et al. 2009). This result suggests that selective hepatic uptake by EL can be attributed to SR-B1 expression. SR-B1 is a membrane protein which is primarily expressed in the liver and steroidogenic tissues such as ovary and adrenal gland (Acton et al. 1996). The main function of SR-B1 is as an HDL receptor. HDL exhibited high affinity binding to cells expressing SR-B1 *in vitro* (Xu et al. 1997). After HDL interacts with SR-B1, SR-B1 exerts its ability to selectively uptake cholesteryl ester, free cholesterol, triglycerides, and phospholipids, but not protein, from HDL into SR-B1-expressing cells (Acton et al. 1996; Greene, Skeggs, and Morton 2001; Thuahnai et al. 2001; Nijstad et al. 2009). Studies in SR-B1 knockout mice demonstrated an approximately 55% lower secretion rate of cholesterol into bile and cholesterol content of bile, but not biliary phospholipids or bile salts, relative to wild type mice (Mardones et al. 2001). Increased plasma cholesterol concentration and larger HDL size were also found in SR-B1-deficient mice versus wild-type mice (Rigotti et al. 1997). These findings suggest that SR-B1 is a large

contributor to the removal of HDL cholesteryl ester for biliary excretion and can influence HDL size. In addition, the unchanged hepatic cholesteryl ester levels, bile acid pool size and faecal excretion of bile found in SR-B1 knockout mice illustrates that SR-B1 selectively takes up plasma and HDL cholesteryl ester in a way that does not influence hepatic cholesteryl ester content and the overall biliary metabolism (Mardones et al. 2001).

1.4.2 Clinical trials that increased HDL concentration and their lack of effect on cardiovascular outcomes

It is established that HDL has many properties that might protect the vascular endothelium including RCT, vasodilatory, anti-inflammatory, anti-oxidative and anti-thrombotic activities. Raising HDL concentrations might be expected to reduce the risk of atherosclerosis-related disease. Initially, in 1977, the Framingham Heart Study observed a strong inverse relationship between HDL cholesterol levels and subsequent incidence of coronary heart disease in a four-year follow up study of both men and women, aged 49 to 82 years (Gordon et al. 1977). Low HDL cholesterol concentration was found to associate with progressive atherosclerosis as measured by coronary arteriography and greater risk of ischemic stroke and carotid atherosclerosis [as reviewed in (Maron 2000)]. However, clinical trials have failed to show that HDL cholesterol-increasing medication decreases atherosclerotic risks, even though the medication did increase HDL cholesterol concentration.

Treatment with niacin can increase plasma HDL cholesterol concentrations by promoting apoA-I production and reducing apoA-I catabolism in the liver. The Atherothrombosis Intervention in Metabolic Syndrome with Low HDL/High Triglycerides: Impact on Global Health Outcomes (AIM-HIGH) study revealed that adding niacin to statin therapy in patients with established atherosclerosis increased plasma HDL cholesterol concentration compared to statin therapy alone. However, there was no significant difference in the number of deaths from coronary heart disease and stroke between the statin and statin plus niacin groups in the AIM-HIGH study (Boden et al. 2011). The Heart Protection Study 2–Treatment of HDL to Reduce the Incidence of Vascular Events (HPS2-THRIVE) study compared the combination of niacin and laropiprant, a PD2 antagonist which decreases niacin-induced flushing and improves adherence to niacin

therapy, versus placebo in a large randomized-controlled trial of patients with cardiovascular disease. Again, there was no significant different in the incidence of major coronary events between niacin-laropiprant and placebo groups, despite higher HDL cholesterol concentration in niacin-laropiprant group by 6 mg/dL than placebo group (Landray et al. 2014). Dalcetrapib, a CETP inhibitor, was also used to assess the clinical benefit of raising HDL cholesterol concentrations in the dal-OUTCOMES study. In this study of coronary heart disease patients with recent acute coronary syndrome, dalcetrapib showed no benefit in reducing cardiovascular mortality, despite elevating plasma HDL cholesterol concentration (Schwartz et al. 2012).

Mendelian randomisation analyses have revealed an inconsistent association between genes that elevate plasma HDL concentrations and the effect of these genes on reducing the risk of myocardial infarction. HDL cholesterol exhibited an association with reduced risk of myocardial infarction in an observational epidemiological study (Voight et al. 2012). However, this study also showed that genetic carriers of the LIPG 396Ser allele in the EL gene, which results in higher plasma HDL cholesterol levels than non-carriers, did not have any lower risk of myocardial infarction (Voight et al. 2012). Therefore, increased HDL plasma concentrations *per se* might not diminish the risk of atherosclerotic vascular disease. Rather, research should also focus on HDL composition and functionality in diminishing the risk of vascular disease.

1.4.3 Protein components of HDL

HDL consists of approximately 50% protein and 50% lipid. The protein components of HDL can be divided into four groups: apolipoproteins, enzymes, lipid transfer proteins and minor proteins (<5% of total HDL proteins) including immune-associated proteins, acute phase reactants and protease inhibitors. There was endogenous circadian rhythm of HDL level with the peak in the afternoon and early evening (3-5 pm) under 8 hours:16 hours sleep:wake schedule (Grant et al. 2021). The mean coefficient of variation (CV) for diurnal variation were 3.5% for HDL cholesterol and 6.5% for apoA (Wasenius et al. 1990). The mean CV for monthly variation were 4.1% for HDL cholesterol and 9.4% for apoA (Wasenius et al. 1990). A day-to-day variation of other protein compositions of HDL has not been widely studied apart from apoA.

1.4.3.1 Apolipoproteins

ApoA-I is the major protein in HDL accounting for 70% of the total protein in mature HDL particles, followed by apoA-II. Other apolipoproteins include apoA-IV, apoC-I, apoC-II, apoC-III, apoE, apoM and apoL-I. ApoA-I is produced in hepatocytes and enterocytes as a prepro-protein. The 18 amino acid prepeptide is cleaved to create pro-apoA-I before secretion and a 6 amino acid propeptide is cleaved during pro-apoA-I maturation to apoA-I in the circulation. Secretion of apoA-I initiates HDL biogenesis via apoA-I activation of LCAT. ApoA-I is involved in many of the anti-atherosclerotic properties of HDL such as RCT and antioxidant. Therefore, apoA-I is considered as the main structural and functional protein of HDL.

ApoA-II is the second major protein in HDL accounting for 15-20% of the total HDL protein. Approximately 50% of HDL particles may consist of apoA-II [reviewed in(Kontush et al. 2015)]. Unlike HDL particles containing apoA-I, but not apoA-II (LpAI) which are anti-atherogenic, HDL particles containing both apoA-I and apoA-II (LpAI-AII) might be anti- or pro-atherogenic. HAEC and smooth muscle cells coculture incubated with HDL from apoA-II transgenic mice resulted in increased LDL oxidation, while HDL from apoA-I transgenic and non-transgenic mice did not (Castellani et al. 1997). ApoA-I/apoA-II transgenic mice fed an atherogenic diet developed a 15-fold larger atherosclerotic lesion on aorta than apoA-I transgenic mice (Schultz et al. 1993). Whereas another study showed a smaller atherosclerotic lesion in apoA-II transgenic mice than non-transgenic mice (Tailleux et al. 2000).

ApoM is a 26 kDa glycoprotein primarily produced by the liver. In the circulation, apoM is mainly bound to HDL and is involved in HDL metabolism and function, particularly through its property as a S1P carrier. Cholesterol efflux from RAW macrophages incubated with apoM-deficient HDL was 50% lower than apoM-expressing HDL, as measured by cholesterol secreted into cell medium. (Wolfrum, Poy, and Stoffel 2005). This finding suggests apoM role in promoting cellular cholesterol efflux to HDL. ApoM is required in HDL as a carrier of S1P, a sphingolipid contributing to many of the endothelium-protective functions of HDL. When separating human HDL into HDL with and without apoM by affinity chromatography, S1P was found exclusively in fractions of human HDL with apoM

and did not appear in HDL without apoM (Christoffersen et al. 2011). ApoM also promotes S1P efflux from erythrocytes. Erythrocytes incubated with HDL showed greater S1P efflux from erythrocytes in the presence of apoM than apoM-deficient HDL (Christensen et al. 2017).

1.4.3.2 Enzymes and lipid transfer proteins

HDL contains enzymes and lipid transfer proteins as described in Section 1.4.1.2. An additional key enzyme is paraoxonase-1 (PON1) which can hydrolyse paraoxone, other organophosphate substrates and aromatic carboxylic acid esters. PON1 is mainly synthesized by the liver and is predominantly associated with HDL in the circulation (Mackness et al. 2010). PON1's main biological function is as an antioxidant enzyme that plays a vital role in the antioxidant function of HDL. Purified PON1 and HDL-associated PON1 protected LDL from oxidation, probably by hydrolysing lipid peroxides to a harmless form (Mackness et al. 1993). There was reduced lipid peroxide content in coronary and carotid atherosclerotic lesion homogenates incubated with serum PON1 (Aviram et al. 2000). Decreased cholesteryl linoleate hydroperoxide (CL-OOH) and cholesteryl linoleate hydroxide (CL-OH) and increased linoleic acid hydroperoxide (L-OOH) and linoleic acid hydroxide (L-OH) content in the lesions suggested there was an esterase-like activity of PON1 since esterase hydrolyses the ester bond between cholesterol and linoleic acid hydroperoxide/hydroxide (Aviram et al. 2000). PON1 and purified L-OOH co-incubation showed decreased L-OOH with elevated L-OH concentrations, suggesting that a peroxidase activity of PON1 reduces L-OOH to L-OH (Aviram et al. 2000). Many human studies revealed a negative correlation of PON1 activity with oxidative stress or risk of cardiovascular disease (Mackness et al. 2003; van Himbergen et al. 2008; Tang et al. 2012). Therefore, PON1 activity is one of the key players in determining HDL's antioxidant capacity.

1.4.3.3 Minor proteins

Minor proteins represent <5% of the total protein of HDL. Examples of minor proteins are proteins involved in the immune response such as complement components, proteins involved in hemostasis, acute-phase response proteins and protease inhibitors. Minor proteins in HDL may not have an established role in

HDL functionality but have been gaining more attention over the past decades owing to the advances in proteomic technologies which provide extensive identification of over 250 proteins in HDL according to the HDL Proteome Watch list established by the Davidson and Shah research group (Davidson S.). An increasing number of proteins involved in complement system, acute-phase response proteins and protease inhibitors have been found in HDL and highlight the possibility of HDL's role in immune system as well as other atheroprotective function of HDL (Hoofnagle and Heinecke 2009).

Complement C1 to C9 are proteins of the complement system which is an enzyme amplification cascade leading to lysis of pathogens' cells. There are three pathways of activating the complement system: classical, lectin and alternative. All three pathways are induced by microbial which lead to activation of the complement components cascade resulting in the generation of membrane attack complex (MAC) (Figure 1-3). MAC is a complex of the complement C5b, C6, C7, C8 and C9 that can generate pores in cell membranes, leading to lysis of target cells and prevent host infection by pathogens [reviewed in (Ehrnthaller et al. 2011)]. The complement components found associated with HDL are C3, C4 and C9 [reviewed in (Kontush et al. 2015)].

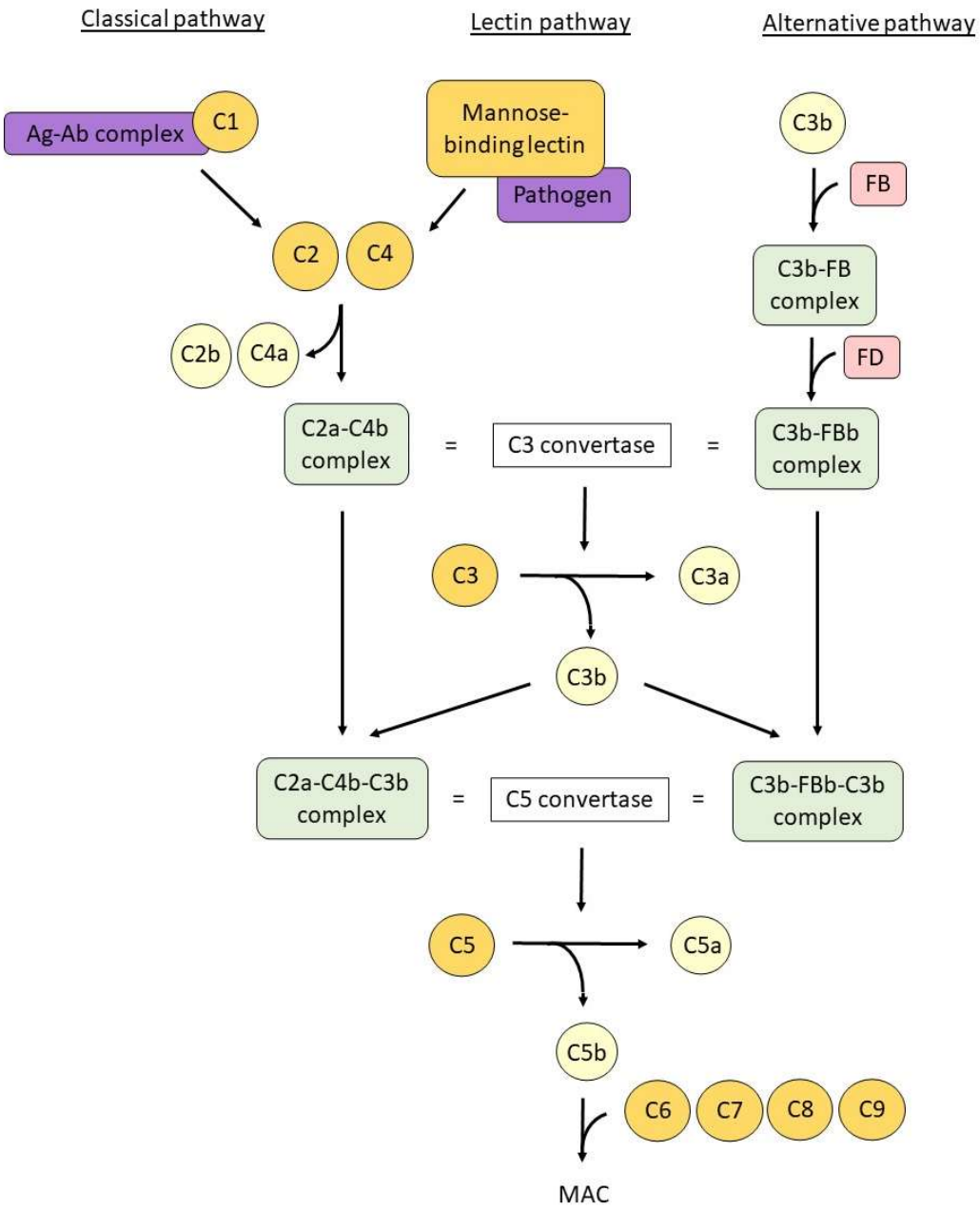

Figure 1-3: The complement system There are three pathways initiating the complement system. The classical pathway begins with recognition of antigen-antibody complexes by C1 which then cleaves C2 and C4 to create the C2a-C4b complex which is a C3 convertase. Mannose-binding lectin initiates the lectin pathway by binding the pathogen membrane and also generating the C2a-C4b complex. The alternative pathway involves C3b binding to FB to form the C3b-FB complex which is then cleaved by FD to form the C3b-FBb complex which is a C3 convertase. C3 convertase cleaves C3 to C3a and C3b after which C3b bind to the C2a-C4b and C3b-FBb complexes to create C5 convertases. The C5 convertase cleaves C5 to C5a and C5b. Finally, a combination of C5b, C6, C7, C8 and C9 form MAC which can generate pores in cell membranes, leading to lysis of target cells and prevent host infection by pathogens. Ag; antigen, Ab; antibody, FB; factor B, FD; factor D, MAC; membrane attack complex

Acute-phase-response proteins are proteins released from the liver and other peripheral tissues in response to different stimuli such as inflammation, infection and tissue injury. There are two categories of acute phase proteins: positive and negative acute response proteins. Positive acute-phase-response proteins are released at an increased rate into the circulation during the acute phase response while negative acute-phase-response proteins are decreased. Positive acute-phase-response proteins can also be divided into type I and type II proteins based on the mechanisms underlying their release. Type I proteins are stimulated by IL-1-like cytokines, for example IL-1, TNF-α and tumor necrosis factor ß (TNF-ß), whereas type II proteins are induced by IL-6. Acute phase proteins can control the inflammatory response, inhibit undesired pathogens and reduce cell cytotoxicity during tissue injury [reviewed in (Arnhold 2020)]. For instance, serum amyloid A 1 (SAA1) is a positive acute-phase-response protein which reflects overall inflammatory status. Under inflammatory conditions, SAA1 is increasingly associated with HDL, leading to enhanced cholesterol efflux from injury sites and lipid recycling for tissue healing (Banka et al. 1995).

1.4.4 HDL proteome

Proteomics is a large-scale approach to understand the characteristic of protein including expression and modification of proteins. The method of choice for proteomics is mass spectrometry which is able to provide high-content quantitative data for biological samples [reviewed in (Cravatt, Simon, and Yates Iii 2007)]. The HDL proteome was initially investigated by Karlsson et al. in 2015 using two-dimensional gel electrophoresis and mass spectrometry in which 13 proteins were identified in HDL of healthy participants (Karlsson et al. 2005). Since then, proteomic studies of human HDL using mass spectrometry have been tracked and recorded by the Davidson and Shah group on the website “HDL Proteome Watch” (Davidson S.). Currently, there are 45 articles and over 900 proteins identified in HDL. Only 25 proteins were reported in >75% of articles of which 12 were apolipoproteins. ApoA-I, apoA-IV and apoL-I are three proteins that appeared in all studies. These findings reflect a large variability in the HDL proteome. To identify HDL-associated proteins and avoid nonspecific co-isolation, the Davidson and Shah group propose a criterion that only proteins identified by at least three independent laboratories should be classified as HDL-associated proteins. According to this criterion, HDL currently contains 251

associated proteins. A review by Shao and Heinecke pointed out the importance of focussing on function and clinical importance when identifying HDL-associated proteins (Shao and Heinecke 2018).

1.4.5 Lipid components of HDL

The lipid composition of HDL comprises mainly phospholipids (40%), followed by neutral lipids such as cholesteryl ester (35%) and free cholesterol (10%), and sphingolipids (6%), respectively. Cholesteryl ester is at the core of HDL while phospholipids, free cholesterol and sphingolipids makes up the lipid monolayer surface of HDL.

1.4.5.1 S1P

Among the lipid components of HDL, the sphingolipid S1P has a well-recognized anti-atherogenic function (Figure 1-4). HDL-S1P helps maintain endothelial tight junctions and thus, can protect against inflammation-induced vascular leakage. Incubation of HUVEC with S1P resulted in a dose-dependent increase of transendothelial electrical resistance (TEER), an index of endothelial cell barrier function, estimated by measuring electrical resistance across cultured cell monolayers in real time (Argraves et al. 2008). Adding pertussis toxin, an inhibitor of S1P receptors, to HUVEC culture media at the same time as HDL abolished the TEER response of HUVEC monolayers to HDL treatment, suggesting that S1P receptors are required for HDL-mediated improvement of endothelial cell barrier function (Argraves et al. 2008). S1P has also been shown to promote vasorelaxation. When adding S1P to the myograph bath of a mouse aortic segment precontracted with phenylephrine, S1P induced a dose-dependent vasodilatory response (Nofer et al. 2004). Moreover, intra-arterial administration of S1P reduced mean arterial pressure in Wistar rats (Nofer et al. 2004). Addition of S1P to HUVEC culture resulted in dose-dependent increases of Akt and eNOS phosphorylation (Nofer et al. 2004). In addition, HDL-S1P exerts its vasodilatory properties through enhancing cyclooxygenase 2 (COX-2) and prostaglandin I 2 (PGI-2) production. Incubation of cultured VSMC with S1P at concentrations compatible with those in physiological levels in HDL resulted in increased COX-2 expression in a time- and dose-dependent manner, which could promote PGI-2

production, a vasodilator (González-Díez et al. 2008).

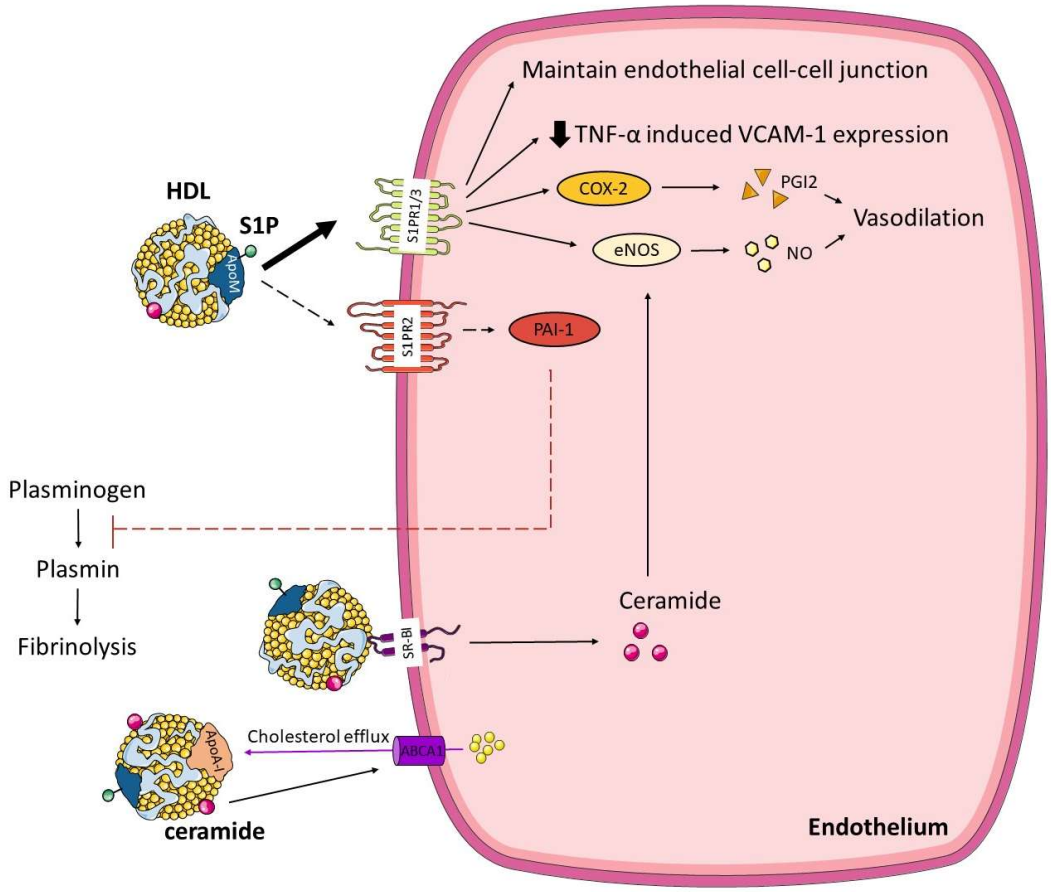

Figure 1-4 HDL sphingolipid effects on vascular function HDL-S1P and HDL-ceramide exert their role in vascular protection through various pathways. In HDL particles, ApoM enhances S1P's interaction with S1PR1 and S1PR3 which predominantly protect endothelial function. S1P-S1PR1 and S1P-S1PR3 signalling help maintain endothelial cell-cell junctions, inhibit TNF-α induced VCAM-1 expression and enhance vasodilation via eNOS and COX-2 stimulation. On the other hand, apoM in HDL weakens S1P-S1PR2 interaction, resulting in reduced PAI-1 expression, and a reduced prothrombotic state. Binding of HDL to SR-B1 leads to increased intracellular total ceramide levels which are involved in the vasodilatory effects of HDL by stimulating eNOS. Ceramide also increases ABCA1 expression which improves cholesterol efflux to HDL. This figure was modified from (Patanapirunhakit et al. 2021). S1P; sphingosine-1-phosphate, S1PR1-3; S1P receptors 1-3, TNF-α; tumor necrosis factor α, VCAM-1; vascular adhesion molecule-1, eNOS; endothelial nitric oxide synthase, NO; nitric oxide, COX-2; cyclooxygenase-2, PGI2; prostaglandin I2, PAI-1; plasminogen activator inhibitor-1, SR-B1; scavenger receptor class B type I, ABCA1; ATP Binding Cassette transporter A1, apoM; apolipoprotein M, apoA-I; apolipoprotein A-I

There are 5 types of S1P receptors, S1P receptors (S1PR) 1-5. Each S1PR shows different effects when interact with circulating S1P. Binding of S1P to S1PR1 and S1PR3 provides protection against endothelial dysfunction. Preincubating HUVEC with VPC23019, an S1PR1 and S1PR3 inhibitor, inhibited HDL-induced COX-2 expression and PGI-2 release, while preincubation of HUVEC with JTE, an S1PR2 inhibitor, did not affect COX-2 expression and PGI-2 release (Xiong, Liu, and Yi 2014). Myograph studies of aortic segments from S1PR3-knockout mice revealed no vasodilatory response of isolated aorta with S1P treatment and approximately 60% less vasodilatory response of isolated aorta with HDL treatment, compared to wild-type mice aorta (Nofer et al. 2004). These findings suggest that an HDL S1P-S1PR3 interaction partially contributes to the vasodilatory effects of HDL. HUVEC transfected with siRNA specifically against S1PR1 down-regulated S1PR1 expression and suppressed HDL-induced inhibition of the TNF-α induced VCAM-1 expression (Kimura et al. 2006). Whereas S1P-S1PR2 interaction increased plasminogen activator inhibitor 1 (PAI-1) expression, an inhibitor of plasminogen activators, thereby reducing plasminogen activation and fibrinolysis, macrophage recruitment and inflammation which are pro-atherogenic events (Skoura et al. 2011; Takahashi et al. 2017).

As S1P effects on endothelial function depend on which S1P receptor S1P interacts with, apoM may promote the anti-atherogenic effects of HDL-S1P by selectively modulating the S1P-S1PR interaction. S1P bound to apoM on HDL exerts different responses than S1P bound to albumin. Incubation of HUVEC with HDL from wild type mice (apoM-containing HDL) inhibited TNF-α induced VCAM-1 expression, whereas HDL from apoM-deficient mice and albumin-bound S1P did not suppress TNF-α action (Galvani et al. 2015). Since inhibition of TNF-α induced endothelial VCAM-1 expression is attributed to S1PR1 signalling, S1P bound to apoM might promote the S1P-S1PR1 interaction. In contrast, a study in 3T3L1 adipocyte culture showed that S1P bound to apoM-rich vehicles increased PAI-1 expression to a lesser extent than control vehicles (Takahashi et al. 2017). S1P bound to apoM-depleted vehicles increased PAI-1 expression in 3T3L1 adipocytes to a greater extent than control vehicles, while S1P bound to albumin-depleted vehicles induced PAI-1 expression to a lesser extent that control vehicles (Takahashi et al. 2017). These findings suggest that apoM might weaken S1P's ability to induce PAI-1 expression which is ascribed to the S1P-

S1PR2 interaction. Thus, apoM could enhance the anti-atherogenic effects of HDL-S1P by promoting the S1P-S1PR1 interaction while weakening the S1P-S1PR2 interaction.

1.4.5.2 Ceramide

The major ceramide species associated with HDL are C24:0 and C24:1 ceramide (Argraves et al. 2011). HDL ceramide seems to have anti-atherogenic effects as there was significantly lower C24:1 ceramide concentration in HDL of individuals with ischemic heart disease, relative to those without ischemic heart disease (Argraves et al. 2011). Ceramide can contribute to HDL's vasculo-protective role via various pathways (Figure 1-4). It promotes RCT of HDL by promoting both ABCA1 expression and the interaction between apoA-I and ABCA1. ABCA1-expressing cells including Chinese hamster ovary (CHO) cells and human aortic smooth muscle cells treated with ceramide revealed a dose-dependent increase of cholesterol efflux from cells to lipid-free apoA-I (Witting, Maiorano, and Davidson 2003; Ghering and Davidson 2006). CHO cells treated with ceramide showed increased ABCA1 protein expression in both whole cell protein and surface protein extracts, and increased apoA-I binding at the cell surface demonstrated using fluorescence-labelled apoA-I (Witting, Maiorano, and Davidson 2003). Ceramide is also involved in HDL-induced eNOS activation through SR-B1. Treating CHO cells expressing SR-B1 with HDL resulted in increased intracellular ceramide levels and eNOS activity (Li et al. 2002).

It is noteworthy that ceramide function can be heterogeneous depending on fatty acid chain length and contrasting effects of long-chain (C16 and C18) and very-long-chain (C24) ceramides are proposed. A diet-induced model of non-alcoholic fatty liver disease and atherosclerosis, LDLR(-/-) mice, exhibited increased ceramide C16:0 and C18:0 but decreased ceramide C24:0 in the liver (Kasumov et al. 2015). Also, there was elevated ceramide C16:0 but reduced ceramide C24:0 concentrations found in HDL of type 1 diabetes patients (Denimal et al. 2015). Increased long-chain ceramide and decreased very-long-chain ceramide may be associated with cardiovascular pathology as plasma ceramide C16:0 to C24:0 ratio was strongly correlated with cardiovascular incidence (Laaksonen et al. 2016).

1.4.6 HDL function: protection of the vascular endothelium

1.4.6.1 Reverse cholesterol transport

Elimination of excess cholesterol from macrophages via RCT is a key vaso-protective function of HDL. Cholesterol-loaded macrophages in arterial wall are the hallmark of atherosclerotic lesions in which they promote local inflammation, growth of atherosclerotic plaques, formation of necrotic lipid core and rupture-prone plaques [reviewed in (Lee-Rueckert et al. 2022)]. Measuring the thickness of the intima and media of carotid artery can be used to determine the extent of plaques and is proposed to be a surrogate marker for atherosclerosis [reviewed in (Bartels, Franco, and Rundek 2012)]. There was an inverse association between the cholesterol efflux capacity of HDL and carotid intima-media thickness and coronary artery disease, independent of HDL cholesterol concentration (Khera et al. 2011; Saleheen et al. 2015). In a 10-year-follow-up study, there was also an inverse relationship between cholesterol efflux capacity and atherosclerotic cardiovascular disease as a primary outcome (Rohatgi et al. 2014). Therefore, HDL's ability to remove cholesterol from peripheral tissues is a clinically relevant measure of the vasculo-protective function of HDL.

1.4.6.2 Vascular tone regulation

HDL has been shown to have a vasodilatory effect. Adding HDL to a myograph bath of rat thoracic aorta pre-contracted with phenylephrine resulted in around 50% vasorelaxation (Nofer et al. 2004). HDL can exert its vasodilatory effects through interaction with SR-B1 and S1P receptors. There was increased eNOS activity in SR-B1-expressing CHO cells incubated with HDL, while HDL had no effect on eNOS activity in SR-B1-deficient cells (Yuhanna et al. 2001). Binding of HDL to SR-B1 on the endothelium initiates various intracellular signals including intracellular calcium mobilization, increased intracellular ceramide levels and Akt-mediated eNOS phosphorylation/dephosphorylation, all resulting in eNOS activation [reviewed in (Kontush 2014)]. Moreover, apoA-I is required for eNOS stimulation via the HDL–SR-B1 interaction. Lipid-free apoA-I in the absence of HDL did not affect eNOS activity, however, adding apoA-I antibodies to isolated endothelial plasma membrane in the presence of HDL attenuated eNOS

activation (Yuhanna et al. 2001). Another pathway of HDL induced vasodilation involved S1P signalling as described in section 1.4.5.1.

1.4.6.3 Antioxidant properties

HDL can protect LDL and other lipoproteins from oxidative damage, thus preventing the generation of oxLDL and avoiding oxLDL-induced endothelial dysfunction. Intravenous injection of HDL reduced lipid peroxidation in hypercholesterolemic rabbits (Klimov et al. 1993). The first step of the antioxidant mechanism mediated by HDL is the removal of oxidants from lipoproteins and cells. HDL removes LOOH from LDL, either spontaneously or mediated by CETP or lipid-free apoA-I (Christison, Rye, and Stocker 1995). HDL reduced hydroperoxide levels and increased cell viability of Cu^{2+}-oxidized human astrocyte culture (Ferretti et al. 2003). Similarly, incubation of Cu^{2+}-oxidized erythrocytes with HDL resulted in LOOH accumulation in HDL (Klimov et al. 2001).

Following its transfer to HDL, LOOH can be hydrolysed to an harmless form by PON1 or redox-inactivated by apoA-I using the methionine residues at position 110, 136 and 172 of apoA-I (Met110, Met136, Met172, respectively)(Pankhurst et al. 2003). This position number of an amino acid in apoA-I is designated from the prepro-protein of apoA-I, thus this position number includes pre- and propeptide of apoA-I. Isolated apoA-I incubated with cholesteryl linoleate hydroperoxides (CEOOH) decreased CEOOH concentration with concomitant increases in redox-inactive cholesteryl linoleate hydroxides (CEOH) and apoA-I methionine oxidation content (Garner et al. 1998). Incubation of HDL3 with oxLDL markedly transformed apoA-I Met136 and Met172 into oxidized forms, and decreased phosphatidylcholine hydroperoxide (PCOOH) levels and increased redox-inactive phosphatidylcholine hydroxides (PCOH) in the HDL3 and oxLDL mixture (Zerrad-Saadi et al. 2009). In addition, pre-oxidation of Met136 and Met172 diminished the capacity of HDL to reduce PCOOH (Zerrad-Saadi et al. 2009). Thus, methionine residues in apoA-I have a key role in the antioxidant ability of HDL. Oxidants can also be removed from HDL by hepatic selective uptake. Perfusion of rat liver with HDL containing CEOOH resulted in faster removal of CEOOH from HDL than CEOH, and enhanced reduction of HDL CEOOH content (Christison et al. 1996). The removal of CEOOH by the liver showed specificity for HDL-

associated CEOOH over LDL-associated CEOOH (Christison et al. 1996). To conclude, the oxidation status of apoA-I methionine residues and PON1 activity are the key factors mediating HDL's antioxidant capacity.

1.4.6.4 Anti-thrombotic properties

HDL affects primary hemostasis by impairing platelet production and aggregation through interaction with apoE and SR-B1 receptors, leading to decreased thrombosis. HDL was found to impair megakaryocyte proliferation and platelet production in mice (Murphy et al. 2013). HDL also inhibits platelet aggregation via the apoE and SR-B1 receptors on the platelet surface. Platelet aggregation was determined by the threshold concentration, or the minimum concentration of ADP, adrenaline or collagen required to induce aggregation of isolated platelets *in vitro*. The apoE-rich HDL subclass, from the fractionation of whole HDL and HDL2 by heparin-Sepharose affinity chromatography, exhibited a potent inhibitory effect on platelet aggregation compared to the apoE-poor fraction (Desai et al. 1989). Radiolabelled apoE-rich HDL could be observed to be bound to cell surface receptors, likely the apoE receptor on the platelet surface (Desai et al. 1989). Moreover, flow cytometric analysis revealed that rhodamine isothiocyanate-labelled HDL3 bound specifically to platelets and that the HDL-platelet interaction was inhibited by competition with ligands of SR-B1 (Brodde et al. 2011). Pre-incubation of platelets from wild type mice with HDL3 inhibited thrombin-induced platelet aggregation and calcium elevation, whereas HDL3 failed to inhibit aggregation of platelets obtained from SR-B1 knockout mice (Brodde et al. 2011).

In regard of secondary hemostasis (Figure 1-5), HDL was found inversely related with plasma PAI-1 concentrations and with levels of prothrombin fragment (F1+2), a protein fragment released during the prothrombin conversion to thrombin that is a marker of thrombin generation (MacCallum et al. 2000; Asselbergs et al. 2007). HDL can activate protein C which is factor Va and VIIIa inhibitors (Griffin et al. 1999). Also, incorporation of apoA-I into anionic vesicles prevented the particle binding to clotting factor Va, thus inhibiting prothrombinase complex formation (Oslakovic et al. 2009). Thus apoA-I appears to inhibit the prothrombinase complex formation, and this could be one of the mechanisms for the anti-thrombotic effects of HDL.

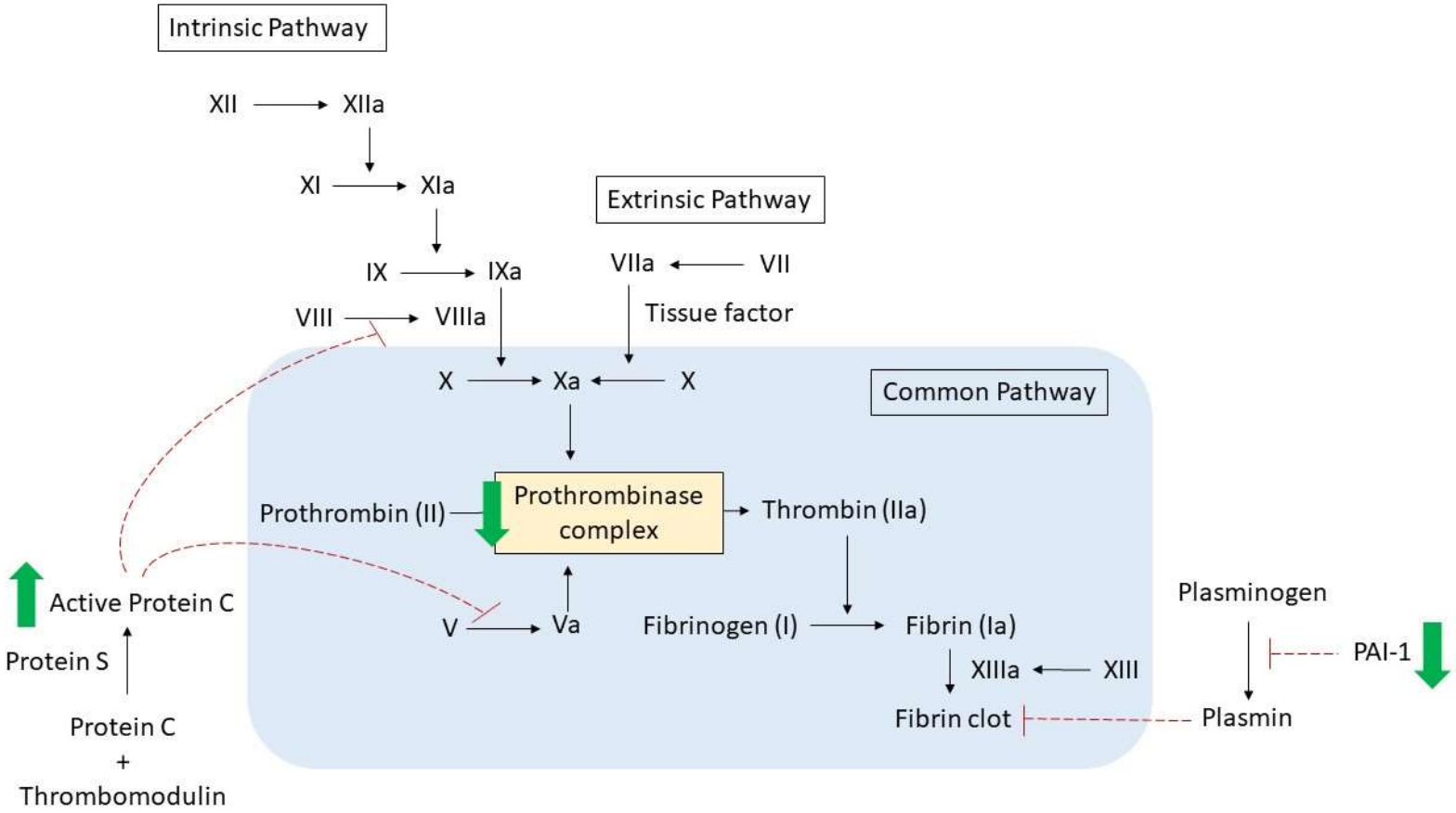

Figure 1-5 Coagulation cascades and the anti-thrombotic properties of HDL Secondary hemostasis consists of intrinsic, extrinsic and common pathways. Activation of factor XII activates downstream proteins in the intrinsic pathway: factor XI, IX, VIII and X. Factor X is also activated by tissue factor and factor VIIa in the extrinsic pathway. Factor Xa together with factor Va form a prothrombinase complex which convert prothrombin to thrombin, leading to fibrin clot formation. Green arrows demonstrate anti-thrombotic actions of HDL. HDL activates protein C which further inhibits factor VIIIa and Va. HDL also inhibits formation of prothrombinase complex and reduces PAI-1 expression.

1.4.6.5 Anti-inflammatory and immunomodulatory properties

Inflammatory mechanisms include the secretion of chemotactic factors or antibodies to recruit leukocytes to injury sites, upregulation of adhesion molecules on endothelial cells that promotes leukocyte adhesion and extravasation, increased blood flow and vasodilation [reviewed in (Nair et al. 2021)]. Under an inflammatory state, phagocytic leukocytes including neutrophils, eosinophils, monocytes, macrophages and dendritic cells are recruited into acute inflammation sites to engulf and ingest organisms intracellularly. While neutrophils, monocytes (macrophage precursors) and macrophages phagocytose smaller pathogens, eosinophils are specialized in destroying bigger organisms such as parasites. HDL protects the endothelium against chronic inflammation in atherosclerosis through various mechanisms.

An inhibitory effect of HDL was found on monocyte migration. A co-culture of a monolayer HAEC on top of a human smooth muscle cell (HASMC) matrix on a membrane was incubated with LDL and HDL. This resulted in an approximately 90% lower LDL-induced monocyte transmigration compared to the coculture with no added HDL (Navab et al. 1991). The inhibitory activity of HDL was attributed to the HDL2 rather than HDL3. Adding HDL2 to HAEC and HASMC cultures with LDL exhibited a similar inhibition of monocyte migration to that seen with whole HDL, while HDL3 showed no inhibitory effect on LDL-induced monocyte migration (Navab et al. 1991). HDL can inhibit the expression of endothelial adhesion molecules. HDL inhibits TNFα-stimulated VCAM-1 expression in endothelial cells by activating eNOS via apoA-I-SR-B1 interaction and S1P-S1PR interaction (Kimura et al. 2006; Ashby et al. 1998). A study in cultured HUVEC displayed the superiority of HDL3 in comparison to HDL2 in inhibiting VCAM-1 expression (Ashby et al. 1998). By downregulating VCAM-1 expression, leukocyte adhesion to the endothelium and transmigration across the endothelium are reduced, leading to an inhibition of the inflammatory process.

HDL also acts as an antimicrobial agent due to the actions of several proteins on HDL. Apolipoprotein L-I (apoL-I) directly interferes with parasites by depolarizing the lysosomal membrane of *Trypanosoma brucei*, resulting in lysosome swelling and lysis (Pérez-Morga et al. 2005). HDL can neutralize the proinflammatory effects of bacterial membrane components such as LPS and lipoteichoic acid

(LTA). HDL's ability to inhibit both LPS- and LTA-induced TNF-α secretion was observed in an *in vitro* study of the murine macrophage cell line, RAW 264.7 (Grunfeld et al. 1999). An *in vivo* study also showed that New Zealand white rabbits treated with HDL before they were infused with LPS maintained a lower plasma TNF-α concentration and mean arterial pressure compared to those not treated with HDL (Cué et al. 1994). HDL is required in plasma to convert LPS to a form that loses its ability to induce a pyogenic response and rapid neutropenia (Ulevitch, Johnston, and Weinstein 1979).

Moreover, HDL can inhibit antigen-presenting cell (APC) activation at the level of both innate and adaptive receptors of immune system. Innate immunity is the first line of defense mechanism to limit invasion and spread of infections and adaptive immunity is required once the infection is established inside the body to recognize and responses to the specific foreign substances. Cellular components of innate immunity, macrophages and dendritic cells, can be categorized as APC which, after they digest the pathogen intracellularly, present fragments of pathogen on the surface for recognition by T lymphocytes in the adaptive immune response. Thus, they provide a link between innate and adaptive immunity [reviewed in (Delves 2020; Actor 2019).

The function of the adaptive immune system is based on two cell types: B and T lymphocytes. B lymphocytes act as APCs in which the B cell receptor (BCR) on the surface of B lymphocytes binds and endocytoses antigens. The antigens are then processed and presented by major histocompatibility complex class II (MHC II) to helper T cells. In addition to their antigen-presenting role, B lymphocytes produce immunoglobulin antibodies (Ig) in response to interaction with antigens. In humans, the Ig antibody classes are IgG, IgA, IgM, IgD, and IgE. They can activate several immune responses including the classical pathway of complement activation, antigen binding to cytotoxic T cells and the cellular component of innate immunity [reviewed in (Delves 2020; Actor 2019). T lymphocytes including cytotoxic, helper and regulatory T cells participate in the cellular component of adaptive immunity. The T cell receptor (TCR) on cytotoxic T cells interacts with major histocompatibility complex class I (MHC I) on target cells, leading to breakdown of intracellular pathogens or apoptosis of the infected cells. For helper T cells, they bind to MHC II on APCs (macrophages,

dendritic cells and B lymphocytes) and become activated. Activated helper T cells can be subdivided into Th1 and Th2 cells depending on the type of antigen helper T cells recognized and they produce different sets of cytokines either pro- or anti-inflammatory cytokines. Lastly, regulatory T cells suppress an excessive immune response by various mechanisms such as inhibiting T cell proliferation and cytokine production to maintain homeostasis.

A study in human microvascular endothelial cells (HMEC) showed that apoA-I treatment inhibited toll-like receptor (TLR) trafficking into lipid rafts and subsequently prevented NF-κB activation of pro-inflammatory signals (Cheng et al. 2012). Overexpression of apoA-I in mice reduced endothelial expression of TLRs and NF-κB dependent signaling, assessed by gene expression of IL-6, MCP-1 and TNF-α in mouse thoracic aorta (Cheng et al. 2012). Treatment with HDL and apoA-I inhibited the ability of APCs, including C57BL/6 mouse B cells, bone marrow-derived dendritic cells and peritoneal macrophages, to stimulate T-cell activation (Wang et al. 2012). Thus, HDL exerts its anti-inflammatory properties through effects on both innate and adaptive immunity.

1.4.7 HDL and extracellular vesicle (EV)

1.4.7.1 HDL isolation protocols

Density ultracentrifugation is considered as the gold standard method to isolate HDL in research (Hafiane and Genest 2015). This technique is used to separate lipoprotein fractions from plasma, in which lipoproteins are classified based on particle density. Gradient density ultracentrifugation is a technique of creating a density gradient by overlaying layers of different densities and separating lipoproteins with a single ultracentrifugation until the lipoprotein bands reach their isopycnic equilibrium (Chapman et al. 1981). In contrast, sequential density ultracentrifugation comprises of sequences of ultracentrifugation, each at increasing density, that separates HDL from plasma and other lipoproteins (Henderson, Vaisar, and Hoofnagle 2016). Disadvantages of this technique can be the sheer force HDL experiences during ultracentrifugation which may affect the integrity of the HDL particle. Stripping of apoA-I and other HDL associated proteins occurred as centrifugal force increased (Kunitake and Kane 1982; Munroe, Phillips, and Schumaker 2015). Another limitation is a co-isolation of

other plasma particles with overlapping density ranges, for example, circulating extracellular vesicles (EV) which have the density of 1.08-1.21 g/mL which is in the range of 1.063-1.21 g/mL density of HDL.

Another method for HDL isolation is immunoaffinity chromatography (immunosorption) with an apoA-I-specific antibody. The principle of HDL isolation by immunosorption is capturing apoA-I-containing particles with antibodies specific to apoA-I immobilized on Sepharose beads (Cheung and Albers 1984; McVicar et al. 1984). ApoA-I-containing particles isolated by immunosorption are enriched in protein but lower in cholesterol and phospholipid content relative to HDL particles isolated by density ultracentrifugation (McVicar et al. 1984). Noteworthy, apoA-I is the main protein but is not specific to HDL particles as apoA-I can also appear in other lipoproteins including VLDL and LDL (Lepedda et al. 2013; Diffenderfer and Schaefer 2014). Thus, approach to HDL isolation by immunoaffinity chromatography will co-isolate VLDL and LDL as apoA-I-containing particles. Lastly, HDL can also be isolated based on particle size by size exclusion chromatography (SEC) (Collins and Olivier 2010; Collins et al. 2010). However, any plasma proteins which have overlapping ranges of particle size with HDL can be co-isolated with HDL whether they are associated with the HDL particle or not.

1.4.7.2 Co-isolation of HDL and EV

An EV is a spherical vesicle with an outer lipid bilayer containing nucleic acids and proteins originating from the source cell. Normal cells release two major types of EVs including exosomes and microvesicles. The most abundant and smaller type of EV are exosomes which range from 40-120 nm and are formed by fusion of multivesicular bodies and the plasma membrane. In contrast, microvesicles (100 nm -1 μm) bud directly from plasma membranes and consist of cytoplasmic cargo. Under specific conditions, cells can release different types of EVs, for example, dying cells release apoptotic bodies (50 nm-2 μm) and malignant cells release oncosomes (1-10 μm).

There are a variety of techniques to separate EV based on its biophysical and biochemical properties including density and size. Similar to lipoprotein

isolation, EV can be isolated based on its density using density gradient or sequential centrifugation. The major limitation of this technique is co-isolation of HDL which has a comparable density and LDL which showed possible physical interactions with EV (Sódar et al. 2016). SEC separates particles by size and allows EV which are larger than HDL to elute earlier from a size-exclusion chromatography column. EV isolation by SEC with Sepharose CL-2B, which has a pore size of 75 nm, removes around 95% of HDL and protein with EV recovery of 43% (Böing et al. 2014). All particles in the EV fraction are larger than 75 nm, leaving the possibility that smaller EV (<75 nm), which comprise approximately 50% of all EV, co-elute with HDL in later fractions after SEC (Böing et al. 2014). To separate EV based on both size and density, differential centrifugation is applied by sequentially centrifuging at increasing speed to pellet cells, cell debris and EV. Disadvantages of this method is not only co-isolation of non-EV component such as protein aggregates, but also increased possibility of EV clumping and EV damaging from the ultracentrifugation step [reviewed in (Coumans et al. 2017)].

Therefore, HDL and EV are commonly co-isolated due to their overlapping densities in the range of 1.063-1.21 g/mL. Transmission electron microscopy of plasma fractions isolated by density ultracentrifugation at density range of 1.063-1.21 g/mL showed HDL particles with diameter around 10 nm and the presence of apoA-I was confirmed in this fraction (Yuana et al. 2014). Larger vesicular structures with a diameter of around 100 nm were also found in this density range fraction and were most likely to be EVs with a typical cup-shaped morphology and the ability to bind to lactadherin and anti-CD61, markers of EV particles (Yuana et al. 2014). Similarly, EV isolated from plasma using sucrose-density gradient ultracentrifugation will include HDL which has a comparable density (Théry et al. 2006). In regard of particle number, EV accounts for only 1% of total particles in the HDL fraction isolated by density ultracentrifugation (Yuana et al. 2014). However, taking into account EV diameter which is approximately 10-fold larger than HDL particle, the total volume of EV would be much more than the total volume of HDL and could be a significant contamination in term of interfering each other’s function and experimental outcome.

1.4.7.3 Possible contribution of EV to HDL functionality

EV can be released from almost all living cells and are known for their role in intercellular communication by the delivery of biological messages from one cell to target cells. In the cardiovascular system, EV can mediate vascular function in both anti- and pro-atherogenic ways. Similar to HDL, EV have shown to have vasculo-protective effects and exhibit anti-inflammation, anti-oxidation and vascular tone regulation properties. Endothelium-derived EV (EEV) can suppress monocyte activation by transferring miRNA-10a to monocytes leading to suppression of NF-κB signalling and reduced proinflammatory gene expression, including TNF-α and IL-1β, in monocytes (Njock et al. 2015). This was demonstrated in both an *in vitro* study of THP-1 monocytic cells and in an *in vivo* study of a mouse peritonitis model. EEV also inhibited TNF-α induced endothelial ICAM-1 expression via miRNA-222 transfer into endothelial cells, demonstrated in human coronary artery endothelial cell culture and apoE-deficient mice (Jansen et al. 2015). In addition, EEV protected endothelial cells against oxidative stress. Palmitate-induced oxidative stress in HUVEC was inhibited by EEV from TNF-α stimulated HUVEC via promoting NO production, increasing superoxide dismutase and suppressing ROS production (Mahmoud et al. 2017).

However, EV also exhibit pathogenic effects that impair endothelial function. EEV promotes monocyte transmembrane migration and monocyte adhesion to endothelial cells demonstrated in an *in vitro* transwell migration assay and in a cell adhesion assay of THP-1 monocytes to HUVEC monolayers, respectively (Hosseinkhani et al. 2018). EV released from inflamed cells could drive endothelial cells toward a pro-inflammatory state. EEV derived from TNF-α stimulated HUVEC up-regulated expression of ICAM-1 and a variety of pro-inflammatory cytokines and chemokines including IL-6, IL-8 and MCP-1 in HUVEC culture (Hosseinkhani et al. 2018). Adding EV derived from LPS-stimulated monocytes into HUVEC culture resulted in increased mRNA and protein expression of ICAM-1, IL-6 and MCP-1 (Tang et al. 2016).

A role of EV in mediating vascular function is complex, but there are a considerable number of common properties of EV and HDL in protecting endothelial function, particularly anti-inflammatory and anti-oxidative properties. There are also overlapping mechanisms underlying these properties

such as enhanced NO production. Thus, co-isolation of HDL and EV could confound the outcome of either HDL or EV functional studies, leading to misinterpretation of some biological effect being attributed to HDL or EV.

1.2 Maternal adaptation to pregnancy: healthy pregnancy and preeclampsia

Pregnancy is divided into three trimesters: the first trimester (0-13 weeks), the second trimester (14-26 weeks) and the third trimester (27 weeks to delivery). The first trimester is associated with implantation and establishment of the maternal-fetal circulation. After fertilization, zygote cells undergo cleavage and form a blastocyst which implants into maternal decidua at around 1-week post-fertilization. During this period, the trophoblast cell layer encircles the blastocyst and differentiates into syncytiotrophoblasts, an outer multinucleated syncytium, and cytotrophoblasts, an inner layer of mononuclear cells. After implantation, trophoblasts differentiate into two domains: villous and extravillous trophoblasts. Villous trophoblasts contribute to chorionic villi that is in contact with the fetal circulation. Extravillous trophoblasts (EVT) invade the maternal decidua and myometrium to form a placental bed at the maternoplacental interface and surrounding spiral arteries. A subset of EVT called endovascular trophoblasts penetrate the maternal spiral artery lumens and modify the vessel media by replacing smooth muscle and connective tissue with fibrinoid material. This process transforms muscular, narrow-lumen spiral arteries into wide diameter, low-resistance uteroplacental vessels. During the first trimester, these vessels are plugged by EVT to block oxygenated blood from entering the placental circulation thus creating a low oxygen tension in the intervillous space. Low oxygen is required for normal fetal development in this early period as the fetus lacks protective mechanisms against ROS damage. At around 12-16 weeks of gestation, when embryogenesis is completed, the EVT plug starts to dissolve, allowing maternal blood flow through spiral arteries into the intervillous space of the placenta and exchanges oxygen and nutrients with fetal circulation in the chorionic villi [reviewed in (Cunningham et al. 2018; Schoots et al. 2018)].

Pregnancy is associated with increased reproductive hormone levels including estrogen and progesterone. A longitudinal study of hormone concentration

during pregnancy revealed a progressive increase of maternal plasma estrogen and progesterone concentration from the first trimester to the third trimester before sharply dropping at postpartum (Alvarez et al. 1996). Estrogen and progesterone are primarily produced by the ovary of reproductive-age women and additionally produced by the placenta during pregnancy. Estrogen and progesterone are involved in the adaptation to, and the maintenance of pregnancy including metabolic adaptation and enhanced vascular function. During pregnancy, maternal biological systems adapt to provide adequate nutrients for fetus and maintain maternal homeostasis, corresponding to different stages of fetal and placental development. The main maternal adaptations to healthy pregnancy and preeclampsia are reviewed below, including those to lipid and lipoprotein metabolism, sphingolipid metabolism, glucose metabolism, coagulation system, immune system, oxidative status and vascular adaptation.

1.2.1 Glucose metabolism

During pregnancy, basal endogenous glucose production which mainly comes from the liver increases as gestational age advances. Longitudinal studies of basal endogenous glucose production measured by prime constant infusion of stable isotope labelled glucose in normal pregnant women before conception, at the second and third trimesters showed increased basal endogenous production with advancing gestation (Catalano et al. 1992; Sivan et al. 1997). By the third trimester of pregnancy, despite an increase in basal endogenous glucose production, there is a significant increase of fasting insulin concentration and a reduction of insulin suppression of endogenous glucose production measured by insulin infusion during a hyperinsulinemic-euglycemic clamp (Catalano et al. 1992; Sivan et al. 1997). These finding suggest a decreased hepatic insulin sensitivity during pregnancy. Decreased insulin sensitivity in pregnancy occurs from the beginning of the second trimester. Insulin sensitivity, defined as a decreased glucose infusion rate to maintain plasma glucose constant at 90 mg/dL plus any endogenous glucose production during a hyperinsulinemic-euglycemic clamp, decreased progressively from pre-gravid to 12-14 weeks of gestation and further decreased at 34-36 weeks of gestation (Catalano et al. 1993; Catalano et al. 1991). An overall decrease in insulin sensitivity during

pregnancy attributed 40% at 12-14 weeks of gestation and 60% at 34-36 weeks of gestation (Catalano et al. 1993; Catalano et al. 1991).

A study in pregnant women at mid-gestation showed that the frequency of glucose, insulin, and insulin resistance, calculated using the surrogate indices of homeostasis model assessment (HOMA-IR), of ≥75th percentile significantly increased with increasing BMI (Hauth et al. 2011). Thus, obese pregnant women were more likely to have higher fasting glucose, insulin and insulin resistance than normal weight pregnancy. Preeclampsia is associated with hyperinsulinemia and insulin resistance. There were higher frequency of fasting maternal glucose, insulin and HOMA-IR of ≥75th percentile in pregnant women who subsequently developed preeclampsia compared with women who remained normotensive (Hauth et al. 2011). In the third trimester, plasma insulin concentrations in fasting state and after oral glucose ingestion were significantly higher in preeclampsia compared to healthy pregnancy, despite similar plasma glucose concentrations between preeclampsia and healthy pregnancy (Martinez Abundis et al. 1996).

1.2.2 Lipid and lipoprotein metabolism

Maternal metabolism during the first to mid second trimester is an anabolic phase during which maternal fat accumulation increases (Pipe et al. 1979; Clapp et al. 1988). Fat mass and percent body fat estimated by hydrodensitometer and subcutaneous fat thickness measured from 7 sites: triceps, biceps, subscapular, subcostal, suprailiac, mid and lower thigh increased in early pregnancy (12-14 weeks of gestation) relative to before conception (Catalano et al. 1998). Later by mid-pregnancy, there is a switch to maternal catabolic state to increase availability of nutrients to the fetus. The rate of fat oxidation estimated by indirect calorimetry during a hyperinsulinemic-euglycemic clamp demonstrated a net lipogenesis before conception and in early pregnancy (12-14 weeks of gestation) while evidence of net lipolysis was shown during the third trimester (Catalano et al. 1998). Central subcutaneous fat thickness measured by ultrasonography at the abdomen during each trimester of pregnancy showed a significant reduction at the third trimester compared to the first and the second trimesters (Kinoshita and Itoh 2006). This change in fat accumulation during pregnancy can be driven by insulin sensitivity of adipose tissue, as demonstrated

by enhanced insulin effects on lipogenesis and anti-lipolysis in early pregnancy, and by insulin resistance in late pregnancy in a study of adipocytes isolated from pregnant rat (Ramos et al. 2003). In this study, insulin sensitivity of adipose tissue lipolysis and lipogenesis were determined in pregnant rat adipocytes by measuring glycerol (product of lipolysis) in cell medium and lipid extracted from cells, respectively, in the presence of insulin.

A longitudinal study of lipid profile during pregnancy showed a progressive increase of plasma triglyceride and cholesterol concentration during the second trimester which peaked in the third trimester (Alvarez et al. 1996). Both triglyceride and cholesterol increase with gestation in all lipoprotein fractions including VLDL, LDL and HDL. There was a greater increase in triglyceride and cholesterol concentration in LDL which increased after the second trimester and HDL which increased as early as the first trimester (Alvarez et al. 1996; Sulaiman et al. 2016). HDL cholesterol starts to rise from 10 weeks of gestation and reaches its peak concentration (42% increase) at 20 weeks of gestation, followed by a slow fall to a plateau (7% above early pregnant level) after which HDL remains stable until delivery (Sulaiman et al. 2016). Also, apoA-I concentration increases in the second trimester and remains stable at the third trimester (Alvarez et al. 1996). Significant decreases of HDL triglyceride and cholesterol during the second trimester are consistent with CETP activity which peaks at the second trimester and could promote HDL degradation during the second trimester of pregnancy (Iglesias et al. 1994). The increase in HDL level is mainly explained by elevated HDL2 concentration with a slight fall in HDL3 (Fahraeus, Larsson-Cohn, and Wallentin 1985; Alvarez et al. 1996). This can be a consequence of reduced HL activity after the first trimester and a further decrease during the second and third trimesters, resulting in a reduction in the conversion of HDL2 to HDL3 during pregnancy (Alvarez et al. 1996).

Pregnancy hormones such as human placental lactogen (hPL) and estrogen could be responsible for the key changes in maternal lipid metabolism. hPL is a hormone secreted by placenta that increases throughout pregnancy (Newbern and Freemark 2011). hPL has been shown to promote insulin resistance, pancreatic beta cell replication and insulin production *in vivo* [reviewed in (Newbern and Freemark 2011; S. Handwerger and M. Freemark 2000)]. An *in*

vitro study showed that incubation of adipose tissue with hPL resulted in increased adipose tissue lipolysis (Williams and Coltart 1978). With regard of estrogen, healthy women receiving estrogen supplementation showed higher VLDL triglyceride, VLDL apoB, HDL cholesterol and HDL apoA-I concentrations than non-estrogen users (Walsh et al. 1991). The mechanism underlying estrogen effects in increasing VLDL triglyceride is augmented triglyceride production rate as demonstrated by reduced VLDL triglyceride concentration and its turnover rate after estrogen was discontinued (Glueck, Fallat, and Scheel 1975). Also, radiodinated VLDL and HDL kinetic studies showed enhanced VLDL apoB and HDL apoA-I synthesis during estrogen administration (Schaefer et al. 1983). There was also reduced HL activity in normolipidemic women during estrogen administration compared to the baseline activity before estrogen administration (Schaefer et al. 1983).

Studies in preeclampsia showed hypercholesterolemia at the same extent as in healthy pregnancy but a significant increase in plasma triglyceride concentration in preeclampsia compared to healthy pregnancy (Potter and Nestel 1979; Sattar, Bendomir, et al. 1997). Elevated plasma triglyceride concentration in preeclampsia can reach double the concentration found in healthy pregnancy during the third trimester (Sattar, Bendomir, et al. 1997; Hubel et al. 1996). Importantly, higher plasma triglyceride concentration in preeclampsia can occur as early as 16-18 weeks of gestation which is prior to the clinical onset of preeclampsia (Lorentzen et al. 1994). Hypertriglyceridemia is reflected in a markedly elevated VLDL concentration in preeclampsia (Sattar, Bendomir, et al. 1997). While IDL and total LDL concentrations in preeclampsia are similar to those in healthy pregnancy (Sattar, Bendomir, et al. 1997). The concentration of small dense LDL is 3-fold higher in preeclampsia (Sattar, Bendomir, et al. 1997). On the other hand, HDL cholesterol concentration is significantly lower in preeclampsia relative to healthy pregnancy (Sattar, Bendomir, et al. 1997).

Healthy pregnant women with higher HDL cholesterol concentration throughout gestation tend to have infants with lower birth weight, especially in late pregnancy as HDL cholesterol concentrations at 24 and 36 weeks of gestation were inversely related with neonatal birth weight (Wang et al. 2020). This may be due to gestational hyperlipidemia that might affect lipid transport from

maternal HDL to the fetus via the placenta. Gestational hyperlipidemia enhances the RCT function of HDL to counter increased cholesterol availability and prevent excessive lipid peroxidation. There was increased cholesterol efflux from primary human trophoblasts to apoA-I obtained from pregnant women with supraphysiological hypercholesterolemia (total cholesterol≥280 mg/dL) relative to those with physiological hypercholesterolemia (total cholesterol<280 mg/dL) (Fuenzalida et al. 2020). It was shown that an exposure to high fat diet in mice during gestation resulted in fetal growth restriction and reduced placental weight (Sasson et al. 2015). In preeclampsia, HDL concentration during the second and third trimesters was associated with reduced neonatal birth weight (Boghossian et al. 2017). Epidemiological studies showed that preeclampsia is associated with small for gestational age infants (Jeyabalan 2013). This could be explained by the pathology of the placenta in preeclampsia resulting in limited nutrient transport to fetus.

1.2.3 Sphingolipid metabolism

1.4.7.3 S1P

S1P is important in the implantation and placentation process (Figure 1-6). During *in vitro* decidualization, gene expression of SPHK1 and SGPP1 were up-regulated in proliferative human endometrial stromal cells, while SGPL1 expression was not, suggesting high turnover of S1P during decidualization (Brünnert et al. 2014). SPHK1 expression and activity in decidua also increases with gestation, suggesting the importance of S1P in normal decidualization of pregnancy (Yamamoto et al. 2010). In placental development, S1P appears to inhibit cytotrophoblast differentiation, but its effect on trophoblast invasion is heterogenous depending on types of S1P receptor on EVT that S1P interacts with (Singh et al. 2012; Johnstone et al. 2005). S1P-S1PR1 interaction results in enhanced EVT migration, while S1P-S1PR2 interaction leads to inhibition of EVT migration (Westwood et al. 2017; Yang, Li, and Pan 2014). Incubation of isolated dNK cells with sphingosine analogue showed reduced S1PR5 receptor expression on dNK cells, impairment of dNK-mediated EVT migration estimated by immunohistochemistry of human placental explants with treated-dNK cells, and impaired endothelial angiogenesis demonstrated by HUVEC branching after incubated with culture media of treated-dNK cells (Zhang, Dunk, and Lye 2013).

Thus, modulation of S1P metabolism could be involved in EVT migration and spiral artery remodelling during pregnancy. At term, there were more S1PR1 (anti-atherosclerotic receptor) expression than S1PR2 (pro-atherosclerotic receptor) expression on arteries from healthy pregnant women including omental arteries, myometrial arteries and chorionic plate arteries (Hudson et al. 2007; Hemmings et al. 2006). These findings suggest a role for S1P in protecting vessels in the maternal and placental circulation from endothelial dysfunction.

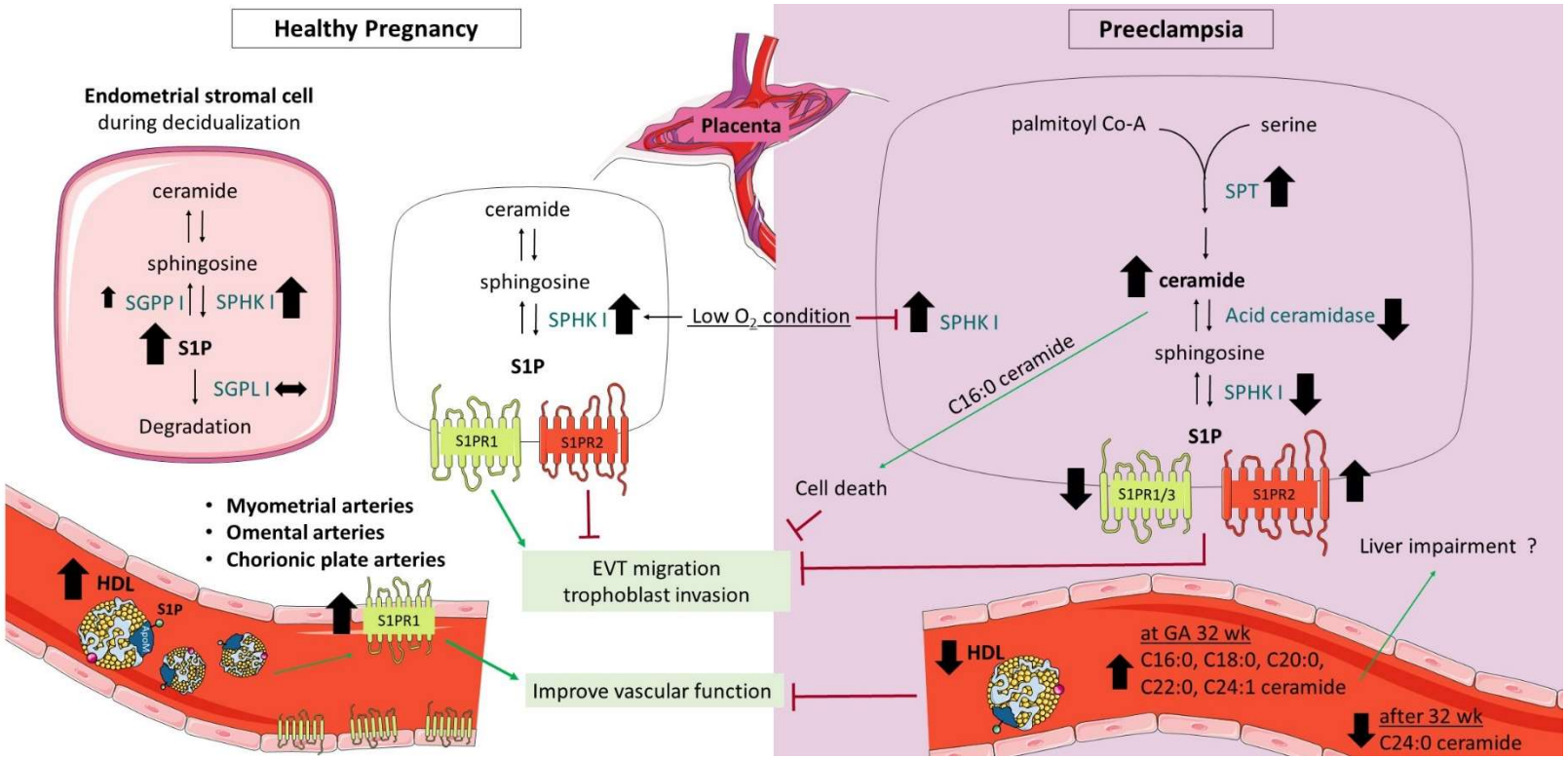

Figure 1-6 Sphingolipid roles in healthy pregnancy and preeclampsia After decidualization, there is up-regulated SPHK I and SGPP I expression and stable SGPL I expression, suggesting high turnover of S1P and a role for S1P in normal decidualization. Higher S1PR1 than S1PR2 expression in omental arteries, myometrial arteries and chorionic plate arteries, together with increased plasma HDL concentrations could lead to improved maternal vascular function. EVT migration and trophoblast invasion are enhanced by S1P-S1PR1 interaction in healthy pregnancy but inhibited by S1P-S1PR2 signalling. Under low oxygen conditions, impaired sensitivity to hypoxia in placenta and an inability to up-regulate SPHKI expression were found in preeclampsia. Decreased S1PR1 and S1PR3, and increased S1PR2 expression in placenta suggest impaired EVT migration and trophoblast invasion. SPT activation and decreased acid ceramidase expression result in ceramide accumulation, cell death and impaired trophoblast invasion in preeclampsia. Compared to healthy pregnancy, lower HDL concentrations, increased plasma C16:0, C18:0, C20:0, C22:0 and C24:1 ceramide at 32 weeks of gestation, and decreased C24:0 ceramide concentration at 32-36 weeks of gestation in preeclampsia could lead to endothelium and liver impairment. This figure was modified from (Patanapirunhakit et al. 2021). S1P; sphingosine-1-phosphate, S1PR1-3; S1P receptors 1-3, SPHK I; sphingosine kinase I, SGPP I; S1P phosphatase I, SGPL I; S1P lyase I, EVT; extravillous trophoblast, SPT; Serine-palmitoyltransferase

In preeclampsia, there is impaired sensitivity to hypoxia of placenta and an inability to up-regulate SPHK1 expression (Figure 1-6). Exposure of explant human placental chorionic villi from preeclampsia to a low oxygen environment resulted in reduced gene and protein expression of SPHK1, while the explants from normotensive patients showed higher SPHK1 mRNA and protein expression when exposed to low oxygen content (Dobierzewska et al. 2016). There were down-regulated mRNA expression of S1PR1 and S1PR3 and up-regulated mRNA expression of S1PR2 in chorionic villi of preeclampsia (Dobierzewska et al. 2016). A shift of S1P-S1PR interaction towards anti-angiogenic activity could be involved in the aberrant angiogenesis observed during placentation in preeclampsia. Comparison of plasma S1P concentrations in patients with preeclampsia relative to those in healthy pregnancy are inconsistent. A study focused on patients with mild preeclampsia revealed higher plasma S1P concentrations relative to healthy pregnancy, whereas a lower concentration of serum S1P was found in another study focused on early-onset preeclampsia (Charkiewicz et al. 2017; Melland-Smith et al. 2015). This inconsistency can be explained by differences in S1P concentrations between serum and plasma or the categories of preeclampsia (mild/severe preeclampsia or early/late-onset preeclampsia) (Hammad et al. 2010).

1.4.7.3 Ceramide

In healthy pregnant women, the major ceramide species in the circulation are C24:0 and C24:1 (Hammad et al. 2010; Dobierzewska et al. 2017). Plasma concentrations of specific ceramide species including C24:0, C18:0 and C16:0 continuously increase from the first to the third trimester, whereas C24:1 ceramide does not change throughout pregnancy (Dobierzewska et al. 2017). There is limited research concerning ceramide metabolism in pregnant humans, but studies in livestock could provide clues on the role of ceramide in pregnancy since bovine pregnancy has similar metabolic adaptations to pregnant humans (increased insulin resistance and lipolysis). Comparison of plasma ceramide levels between lean and overweight pregnant cattle showed that most plasma ceramide species are further increased in overweight pregnant cattle, relative to those with a lean phenotype, during pre- and postpartum (Rico et al. 2015; Rico et al. 2017). In overweight pregnant cows, increased plasma fatty acid is associated with increased hepatic lipid accumulation, indicating enhanced fatty

acid supply for lipid accumulation in the liver, which is consistent with increased total ceramide and C24:0 ceramide accumulation in the liver of overweight cows during the late gestational period (Rico et al. 2015; Rico et al. 2017). These findings suggest that increased circulating fatty acids in overweight individuals may enhance ceramide synthesis in the liver, resulting in higher ceramide in plasma, hepatic lipid accumulation and insulin resistance.

Aberrant ceramide metabolism is observed in preeclampsia (Figure 1-6). There was higher ceramide accumulation in placenta from early-onset preeclampsia, especially C16:0 and C24:0 ceramide in trophoblast layers and syncytial knots demonstrated by imaging and immunofluorescent staining of placenta. This study showed increased *de novo* synthesis via SPT activation and decreased breakdown of ceramides to sphingosine in lysosomes through reduced *ASAH1* (acid ceramidase gene) expression and activity, resulting in increased ceramide accumulation (Melland-Smith et al. 2015). Also, *ASAH1* expression can be inhibited by oxidative stress, leading to C16:0 and C18:0 ceramide accumulation (Melland-Smith et al. 2015). Accumulation of C16:0 ceramide in trophoblast cells was shown to promote apoptosis, autophagy and necroptosis which then interfered with the normal process of trophoblast cell fusion and trophoblast invasion (Melland-Smith et al. 2015; Bailey et al. 2017). Therefore, increased ceramide accumulation due to enhanced *de novo* synthesis and oxidative stress-induced reduction of lysosomal breakdown could lead to placental dysfunction and cell death in preeclampsia. There were increased plasma C16:0, C18:0, C18:1, C20:0, C22:0 and C24:1 ceramide concentrations in preeclampsia at around 32 weeks of gestation, whereas C24:0 ceramide concentration deceased at 32-36 weeks of gestation in preeclampsia, compared to healthy pregnancy (Melland-Smith et al. 2015; Charkiewicz et al. 2017; Dobierzewska et al. 2017).

1.2.4 Coagulation system

Platelet count during the last month of pregnancy was significantly lower than in non-pregnant women (Boehlen et al. 2000). However, platelet volume and platelet volume distribution width increased in the third trimester, indicating increased platelet consumption which could contribute to the reduced platelet count in late pregnancy (Fay, Hughes, and Farron 1983). There is a physiological hypercoagulable state in which most of the coagulation factors increase and

anticoagulants decrease during pregnancy. In the intrinsic pathway, levels of clotting factor VIII significantly increased in the second and third trimester (Drury-Stewart et al. 2014), whereas the data on clotting factors XI and IX levels is equivocal since they have been reported as increased, decreased and unchanged [reviewed in (Thornton and Douglas 2010)]. In addition, the activity of clotting factor VII in the extrinsic pathway and its downstream effects on clotting factors X and II in the common pathway were higher in the third trimester of pregnancy than in non-pregnant women (And and Prydz 1984). Concentration of fibrinogen, a substate for fibrin clot formation, increased with gestation during pregnancy with higher fibrin monomer concentration in the third trimester (Manten et al. 2004; Shamshirsaz et al. 2021a). Moreover, anti-coagulants including antithrombin and protein S decreased during pregnancy. Antithrombin, which inactivates clotting factor Xa and thrombin, decreased throughout gestation (Shamshirsaz et al. 2021a). The concentration and activity of protein S which promotes protein C activation and inactivates factor Va and VIIa was also decreased as gestational age advanced (Kristoffersen et al. 2017). Lastly, coagulation tests including activated partial thromboplastin time (APTT) and prothrombin time (PT) and thrombin time (TT) remain within normal ranges in healthy pregnancy (Shamshirsaz et al. 2021b; Xu et al. 2021). Whereas a study in severe preeclampsia found prolonged APTT which represents impaired intrinsic coagulation pathway (Han et al. 2014). Moreover, there were significantly higher fibrinogen level and TT in preeclampsia, suggesting profound changes of the common coagulation pathway (Han et al. 2014).

1.2.5 Immune system

As the fetus develops throughout gestation, maternal immunological response continuously adapts and is described in three immunological stages corresponding to stages of fetal development. The first stage is a pro-inflammatory state associated with implantation and placentation. The characteristic of endometrium when it becomes receptive for implantation is similar to the inflammatory response. Immune cells including natural killer cells and macrophages accumulated in human decidua, at the implantation site (King, Loke, and Chaouat 1997; Mor, Straszewski-Chavez, and Abrahams 2006). A meta-analysis of transcriptome studies in receptive-phase endometrium also showed a greater proportion of genes expressed that are involved in the immune system

including those involved in the inflammatory response and complement system (Altmäe et al. 2017). Moreover, Th1-type cytokines such as IL-1, IL-6, IL-8 and TNF-α, which mainly promote cellular immunity including macrophage and cytotoxic T cell activation, were dominant during the first trimester of pregnancy (Yoshinaga 2008; Mor et al. 2011). It is thought that the inflammatory response is activated during the first trimester due to breakthrough of the epithelial lining and endometrium of the uterus for implantation and placentation, and that inflammation is required to remove cell debris and provide proper epithelium/endometrium modification for these processes. Inflammation, including an activated complement system, is essential for normal implantation and placental development. Culture of mouse embryos with complement C3 derivatives supplemented in cell medium resulted in larger blastocysts, suggesting embryotrophic activity of C3 (Lee et al. 2004). An important role for C3 in normal placentation was demonstrated in C3-deficient mice which have fewer conceptus with markedly smaller fetuses and placenta in early pregnancy (Chow et al. 2009).

The second trimester is associated with fetal growth and development and inflammation is not as required as it is during the first trimester. The Th1/Th2 balance shifts toward a Th2 response including IL-4, IL-5, IL-10, and IL-13 which promotes the humeral immunity by promoting antibody production from B lymphocytes [reviewed in (Mor et al. 2011)]. Finally, at term when parturition commences, a pro-inflammatory response again dominates during this last immunological phase. Parturition is associated with leukocyte infiltration in maternal myometrium and increased expression of pro-inflammatory cytokines such as IL-1, IL-6 and TNF-α in placental tissue and amnion (Keelan et al. 2003). There is also a role for complement C5a in myometrial contraction demonstrated by an increased frequency of contraction in human myometrium strips incubated with C5a in a myograph study (Gonzalez, Pedroni, and Girardi 2014). In the circulation, SAA concentration during the third trimester of pregnancy was not significantly different from non-pregnant women (Kristensen et al. 2009). However, serial SAA concentration measurements during parturition showed markedly increased SAA concentration immediately after delivery which further increased at 24 hours after delivery, suggesting an inflammatory state associated with parturition (de Villiers et al. 1990).

In preeclampsia, peripheral neutrophils and monocytes are excessively activated as demonstrated by upregulated expression of activating molecules such as ICAM-1 and selectin on neutrophils and monocytes in preeclampsia compared to healthy pregnancy [reviewed in]. Expression of HLA-DR, a cell-surface marker of activation, on helper T cells and cytotoxic T cells was also higher in preeclampsia than in healthy pregnancy (Saito et al. 1999). Th1-type immunity is dominant in preeclampsia. There were more Th-1 type cytokines (IL-2, interferon-γ, and TNF-α) secreted from cultured peripheral blood mononuclear cells from preeclampsia (Saito et al. 1999). Whereas concentration of IL-4, a Th2-type cytokine, were similar in cultures of cells from healthy pregnancy and preeclampsia (Saito et al. 1999).

1.2.6 Oxidative status

Oxidative status is enhanced during healthy pregnancy. Plasma concentration of the ROS superoxide, which is a strong oxidant was increased after the first trimester and remained stable throughout gestation (Mannaerts et al. 2018). Systemic oxidative stress, estimated by plasma redox balance, also strongly increased throughout gestation from the first to the third trimester (Stefanović et al. 2012). The main source of systemic oxidative stress is the placenta which produces ROS throughout pregnancy. At the end of the first trimester, there is a transition from a low to high oxygen tension in the intervillous space when the EVT plug dissolved, allowing a gradual increase of maternal blood flow into the placenta and increased oxygen tension (Jauniaux et al. 2000). Increased oxygen tension can promote ROS generation through increased generation of superoxide radicals. During this period, expression of oxidative stress markers including heat shock protein 70 and nitrotyrosine, estimated by immunohistochemical staining of first trimester human placental tissue, increased suggesting enhanced oxidative stress as the maternal circulation is established (Jauniaux et al. 2000). Moreover, exposure of organ cultures of first trimester human placental villi to elevated oxygen concentration resulted in syncytiotrophoblast deterioration demonstrated by vacuolization of the cells and loss of structural-integrity of mitochondria (Watson et al. 1998). Syncytiotrophoblasts are sensitive to ROS, since they lack sufficient antioxidant enzymes, such as mitochondrial superoxide dismutase, and they are also the first cells of the placental villi that are exposed to oxygen-rich maternal blood (Watson et al. 1998). These characteristics of

syncytiotrophoblast augment ROS production as the fetal-maternal circulation is established. Further in the second and third trimester, decreased antioxidant activity could involve an oxidant/antioxidant imbalance and enhanced oxidative stress. A longitudinal study of plasma PON1 activity estimated by diazoxon hydrolysis rates showed a significant decrease during late pregnancy (32 and 38 weeks of gestation) compared to the first and second trimester (Stefanović et al. 2012).

Oxidative stress is further enhanced in preeclampsia. There was increased concentration of malondialdehyde (MDA), a pro-oxidant, in plasma and placenta of preeclampsia compared to healthy pregnancy (Rani et al. 2010; Aydın et al. 2004). It is proposed that partial invasion of spiral arteries in preeclampsia could lead to intermittent placental perfusion and fluctuation of oxygen tension [reviewed in (Hung and Burton 2006)]. Sharp increase of oxygen tension rather than gradual increase like in healthy pregnancy could then enhance ROS production. Another proposed mechanism is that antioxidant defence in preeclampsia is disturbed, resulting in enhanced oxidative stress. Decreased plasma total antioxidant (TA) content was evident in preeclampsia, together with increased plasma MDA to TA ratio (Bharadwaj et al. 2018). Plasma and placental antioxidants, such as superoxide dismutase and glutathione/glutathione peroxide, decreased in preeclampsia (Rani et al. 2010; Aydın et al. 2004; Kumar and Das 2000). Moreover, preeclampsia showed lower PON1 activity than healthy pregnancy in all trimesters and started as early as 10-14 weeks of gestation (Genc et al. 2011; Al-Kuraishy, Al-Gareeb, and Al-Maiahy 2018).

1.2.7 Vascular adaptation

Vascular function appears to be enhanced in healthy pregnancy. There was decreased peripheral vascular resistance, calculated from the ratio of mean arterial pressure and cardiac output, during the first and second trimesters and an increase during the third trimester (Atkins et al. 1981; Mahendru et al. 2014). In parallel with peripheral vascular resistance, aortic augmentation index (calculated from aortic pressure waveform and reflects systemic arterial stiffness) decreased during the first and second trimester, with the majority of reduction in the first trimester, and rebounds in the third trimester (Mahendru

et al. 2014; Chapman et al. 1998). Arterial reservoir-like properties calculated from aortic pressure waveforms also increased during the first trimester and maintain the level throughout gestation (Poppas et al. 1997). These findings reflect increased vascular compliance as part of the physiology of pregnancy. Decreased peripheral vascular resistance, and increased vascular compliance occurred in early pregnancy beginning as early as 6 weeks of gestation (Chapman et al. 1998; Mahendru et al. 2014). There were higher FMD in each trimester of pregnancy compared to non-pregnant controls (Dørup, Skajaa, and Sørensen 1999). As a result of maternal vascular adaptation, blood pressure, measured either by a sphygmomanometer or an automated blood pressure measuring device, decreased from the first trimester, reached a nadir in the second trimester and rose to the pre-pregnant level in the third trimester and postpartum period (Atkins et al. 1981; Mahendru et al. 2014).

Healthy pregnancy are found to develop refractoriness of vascular reactivity toward vasoconstrictors, for example norepinephrine and angiotensin II [reviewed in (Gant et al. 1980)]. Thus, refractoriness of pregnant vessels to vasoconstrictors can contribute to vasodilation during pregnancy. Other factors contributing to maternal vascular adaptation is increased NO availability. Investigation of serum nitrate and nitrite concentrations as a marker of NO production showed the increase in first trimester of pregnancy compared to non-pregnant women (Choi, Im, and Pai 2002). Increased nitrate and nitrite concentrations remained throughout gestation to the third trimester and returned to non-pregnant concentration at 9-12 weeks postpartum (Choi, Im, and Pai 2002). Estrogen is known to promote NO production by upregulating eNOS expression via estrogen receptor ER-α and ER-ß signalling [reviewed in (Chambliss and Shaul 2002)]. Progesterone has also been shown to promote NO production through enhancing eNOS expression (Simoncini et al. 2007).

Endothelial dysfunction occurs in preeclampsia, especially impaired vasodilatory response. Incubation of myometrial resistance arteries from healthy pregnant women with plasma from patients with preeclampsia resulted in reduced endothelium-dependent vasodilatory capacity to bradykinin (Hayman et al. 2000). The vascular dysfunction seems to be targeted to the endothelium as there was no significance difference in endothelium-independent vasodilatory

response to sodium nitroprusside between myometrial arteries incubated with plasma from healthy pregnancy and preeclampsia (Hayman et al. 2000). Reduced NO availability was shown in preeclampsia as there were reduced nitrate and nitrite concentrations in serum of preeclampsia compared to gestational-age-matched healthy pregnancy (Choi, Im, and Pai 2002).

1.3 HDL's role in vascular protection in pregnancy

The maternal physiological adaptation to healthy pregnancy includes enhanced insulin resistance and hyperlipidemia, which provides for adequate glucose and lipid for fetal growth, and a proinflammatory state associated with implantation, placentation and parturition. There is also a hypercoagulable state, a preparation for parturition, and increased oxidative stress during pregnancy. In a non-pregnant population, these conditions would be expected to lead to vascular damage and endothelial dysfunction. However, there is improved vascular function in healthy pregnancy whereby healthy pregnant women have decreased peripheral vascular resistance, increased vascular compliance and vasodilation. HDL plays a key role in preventing vascular dysfunction in the non-pregnant population and its concentration increases during pregnancy which could exert protective effects in healthy pregnancy [reviewed in (Sulaiman et al. 2016)]. There was a strong correlation between decreased systemic arterial stiffness, estimated by aortic augmentation index, and increased HDL cholesterol concentration during the first trimester, suggesting a contribution from HDL in enhancing vascular function in pregnancy (Mahendru et al. 2014). In addition to HDL quantity, the quality of HDL could be involved in a protective role in pregnancy but there is very little information on HDL structure and function in pregnancy. Further investigation into pregnant HDL composition and function is needed.

There is only one published proteomic study of HDL composition from pregnant women (Sreckovic et al. 2013). This cross-sectional study revealed 35 HDL-associated proteins in pregnant women at term. Half of these proteins were associated with lipid and lipoprotein metabolism including apoA-I, apoC-II, apoC-III and apoM. Other proteins included acute-phase-response proteins such as SAA1 and PON1, and proteins involved in the immune system and coagulation processes. These data suggest a role for HDL in regulation of lipid and

lipoprotein metabolism, inflammation, the immune system and the coagulation system in pregnancy. Pilot data from our laboratory comparing the HDL proteome of non-pregnant women and healthy pregnant women in the third trimester showed that the concentrations of 23 proteins in HDL were significantly different (W. Sulaiman, unpublished). Eleven proteins were in higher concentration in healthy pregnant HDL while 12 proteins were lower. The proteins that differed were involved in many biological pathways such as lipid metabolism, coagulation and inflammation and the change in HDL composition may be linked to the efficacy of HDL function in pregnancy. HDL function has not been extensively investigated in pregnancy. There was increased cholesterol efflux to exogenous apoA-I from primary human trophoblast obtained from pregnant women with supraphysiological hypercholesterolemia (total cholesterol ≥280 mg/dL) relative to those with physiological hypercholesterolemia (total cholesterol <280 mg/dL), despite similar ABCA1 expression (Fuenzalida et al. 2020). The finding suggests increased ABCA1 activity due to increased cholesterol availability in pregnancy. Similar result was found in cholesterol efflux to apoA-I from endothelial cells obtained from human term placenta which was higher than from HUVEC (Stefulj et al. 2009)

Reduced plasma concentrations of HDL are typical in preeclampsia a condition where endothelial dysfunction is evident. Incubation of myometrial arteries obtained from healthy pregnant women with plasma from preeclampsia caused reduced endothelium-dependent vasodilation, compared to plasma from healthy pregnancy (Hayman et al. 1999). Interestingly, there was a significant association between endothelium-dependent response of the arteries and circulating apoA-I concentration (Hayman et al. 1999). Whether only lower concentrations of HDL or also dysfunctional HDL occur in preeclampsia requires to be elucidated. Validation of dysfunctional HDL involvement in the pathogenesis of preeclampsia could support HDL modulation as a novel treatment for preeclampsia. Recombinant HDL (rHDL) with improved vasoprotective function could be developed to restore the specific function of HDL that was impaired in preeclampsia. For example, wild type apoA-I-containing rHDL has been shown to have increased efficacy of RCT and anti-inflammatory functions [reviewed in (Vucic and Rosenson 2011)]. Patients with peripheral artery disease who received a single intravenous infusion of human

apoA-I-phosphatidylcholine complex, rHDL CSL-111, showed reduced plaque lipid content and VCAM-1 expression (Shaw et al. 2008). rHDL could be given to high-risk pregnant women to prevent the development of preeclampsia or given in preeclampsia to counter endothelial dysfunction and its clinical manifestation.

1.4 Hypothesis

I hypothesize that HDL with of greater vascular protective function is synthesised in pregnant women in order to protect maternal vascular function against the unfavourable metabolic environment associated with the maternal metabolic adaptation to pregnancy. This newly formed HDL has a different lipid and protein composition to that of non-pregnant HDL which is associated with improved HDL function. In metabolic complications of pregnancy such as preeclampsia, dysfunctional HDL is formed, secondary to changes in composition, and in pre-eclampsia HDL fails to adequately protect the maternal endothelial function.

1.5 Objectives

- To compare HDL protein composition and function at different gestational ages throughout pregnancy

- To compare HDL protein composition and function between healthy pregnancies and those complicated by early and late-onset pre-eclampsia

- To establish an assay to assess vasodilatory and anti-thrombotic functions of HDL

- To examine sphingolipid metabolism in pregnancy including sphingolipid composition in HDL, and sphingolipid synthesis enzyme gene expression in adipose tissue and placenta of healthy pregnancy and preeclampsia

- To establish an HDL isolation protocol that removes potential EV contamination

Chapter 2 General Methodology

2.1 Participant recruitment

2.1.1 Recruitment of healthy pregnant women

Healthy pregnant women samples were from the archival collection of the Early Pregnancy Study (EPS) and the Lipotoxicity in Pregnancy Study (LIPS) in the Freeman laboratory, University of Glasgow. The detail of these studies is provided below.

2.1.1.1 Early Pregnancy Study (EPS)

This cohort was collected originally for the study entitled 'Pre-conception maternal erythrocyte saturated to unsaturated fatty acid ratio predicts pregnancy after natural cycle frozen embryo transfer' (Onyiaodike et al. 2018). This study was conducted at the Assisted Conception Unit at Glasgow Royal Infirmary between October 2007 and June 2010 and received ethical approval from the Glasgow Royal Infirmary Research Ethics Committee (07/S0704/49). Written informed consent was obtained from all participants. Women who were undergoing frozen embryo transfer (FET) and had a regular menstrual cycle without exogenous hormone use were recruited (Table 2.1). Blood samples were obtained daily to detect the luteinising hormone (LH) surge and FET was performed on day 3 after the LH surge. Positive pregnancy test was confirmed by urinary human chorionic gonadotropin (hCG) at day 18 post-LH surge and ultrasound at day 45 post-LH surge. Blood samples from 10 women were used in this experiment, each with 4 time points: pre-partum, day 18 post-LH surge, day 29 post-LH surge and day 45 post-LH surge. Pre-partum samples were blood obtained at 3 days before the LH surge (6 days prior to FET). To convert the time of LH surge to gestational age, the LH surge was considered to be day 14 after the last menstrual period, assuming a 28-day menstrual cycle, and therefore was classed as equivalent to 2 weeks of gestation. Therefore, day 18, 29 and 45 post-LH surge were equivalent to 4.6, 6.1 and 8.4 weeks of gestation, respectively.

Table 2.1: Inclusion and exclusion criteria of women in the Early Pregnancy Study (EPS)

Inclusion criteria	Exclusion criteria
1. Women with a regular menstrual cycle	1. Administration of exogenous hormones for fertility treatment
2. Undergoing FET in a natural cycle	
3. Positive pregnancy test for both urinary hCG at day 18 post-LH surge and ultrasound at day 45 post-LH surge	

2.1.1.2 Lipotoxicity in Pregnancy Study (LIPS)

LIPS covered from 16 weeks of gestation to 13 weeks after delivery. Participants were recruited from National Health Service Greater Glasgow and Clyde maternity units between March 2010 and November 2011 as part of the PhD thesis entitled 'Anatomical fat distribution and accumulation and lipotoxicity in lean and obese pregnancy' by Dr Eleanor Jarvie at University of Glasgow. The study received ethical approval from the West of Scotland Research Ethics Committee (09/S0701/105) and written informed consent was taken from all participants. Healthy Caucasian women between the ages of 16-40 years with no history of assisted conception, no significant past medical history and no known metabolic disease (e.g. diabetes mellitus, thyroid disease, polycystic ovarian syndrome, or cardiovascular disease) were recruited at their first antenatal appointment (Table 2.2). Women who had multiple pregnancies, gestational diabetes, or developed obstetric antenatal complications throughout the study were retrospectively excluded.

Table 2.2: Inclusion and exclusion criteria of women from 2nd trimester to post-pregnancy

Inclusion criteria	Exclusion criteria
1. Caucasian women between the ages of 16-40 years	1. Significant past medical or obstetric history 2. Previous pregnancies through assisted conception 3. Known metabolic disease e.g., diabetes, thyroid disease, polycystic ovarian syndrome, and cardiovascular disease 4. Multiple pregnancy 5. Gestational diabetes or an obstetric antenatal complication developed during the study

2.1.2 Recruitment of women with preeclampsia and women with gestational-age-matched healthy pregnancy

Preeclampsia and healthy pregnant women samples were from an archival collection provided by Dr Hiten Mistry, University of Nottingham. This cohort of samples were collected as part of a biobank of samples under ethics entitled: 'Studies into nurturing and development of pregnancies – understanding the genetics of pregnancy and setting up a biobank' (REC 15/EM/0523). A couple of studies that have been published using these samples were (Seamon et al. 2020; Scaife et al. 2021). Preeclampsia and healthy pregnancy were recruited according to the following criteria. Pre-eclampsia was defined as gestational

hypertension (systolic blood pressure >140 mmHg and diastolic blood pressure >90 mmHg, determined on 2 occasions >4 hours apart and arising after 20 weeks of gestation in a previously normotensive woman) and de novo proteinuria (protein: creatinine ratio >30; urine protein concentration >3 g/L in 2 random clean-catch midstream specimens collected >4 hours apart) with no evidence of urinary tract infection (Brown et al. 2001). Even though women with preeclampsia were recruited under the criteria described earlier, they still fit the updated criteria in which proteinuria is not mandatory but an alternative symptom for a diagnosis of preeclampsia (Brown et al. 2018). Preeclampsia patients were categorized into early- (diagnosis ≤34 weeks of gestation) and late- (diagnosis >34 weeks of gestation) onset preeclampsia (Tranquilli et al. 2013). Healthy normotensive pregnant women were matched for gestational age with preeclampsia, had no complications and no evidence of any urinary tract infections. All participants were informed and signed consent following HRA-REC ethics committee approval of the study gained by the University of Nottingham (REF: 15/EM/0523). Medical and obstetric histories and venous blood samples were obtained before delivery (Mistry et al. 2008).

2.2 Blood collection

Blood (20-40 mL) was taken via venepuncture from study participants by a medically trained person. Blood samples were collected in tubes that contained ethylenediaminetetraacetic acid (EDTA), an anticoagulant. EDTA blood tubes were then centrifuged at 3000 revolutions per minute (rpm)/1500g, 4ºC for 15 minutes. Supernatant was collected as plasma and stored in aliquots at -80ºC until use. This blood preparation method was used with samples from healthy pregnant women for Chapter 3, 6 and 7, preeclampsia for Chapter 4 and non-pregnant and healthy pregnant women for the wire myography study in Chapter 5. Blood sample preparation for the thrombin generation study in Chapter 5 was prepared differently with collection in sodium citrate tubes and platelet removal process and was described in section 5.3.1.1 in Chapter 5.

2.3 HDL isolation

2.3.1 Preparation of density solutions for HDL isolation

Density solutions of 1.182 g/mL, 1.063 g/mL, 1.478 g/mL and 1.21 g/mL were prepared as follows:

- Stock density solution (density=1.006 g/mL)

  11.4 g sodium chloride (VWR international), 0.1 g EDTA (VWR International) and 1 M sodium hydroxide (1 mL, VWR International) was added into 1 L distilled water.

- Density solution (density=1.182 g/mL)

  29.98 g sodium bromide (VWR international) was added to 100mL stock density solution (density=1.006 g/mL).

- Density solution (density=1.063 g/mL)

  Stock density solution (density=1.006 g/mL) was mixed with density solution (density=1.182 g/mL) at a ratio of 2:1.

- Density solution (density=1.478 g/mL)

  78.32 g sodium bromide was mixed with 100mL stock density solution (density=1.006 g/mL).

- Density solution (density=1.21 g/mL)

  Density solution (density = 1.063 g/mL) was mixed with density solution (density=1.478 g/mL) at a ratio of 2:1.

Density of all solutions was checked using a density meter (PAAR DMA 35 Density meter, Paar Scientific Ltd) before use.

2.3.2 Sequential ultracentrifugation

HDL was isolated from plasma by using two-step sequential ultracentrifugation. This method separates lipoprotein fractions from plasma based on their density and is the gold standard technique for isolation of lipoproteins.

Plasma (500 µL) was mixed with 1.182 g/mL density solution (250 µL) in thick-wall polycarbonate ultracentrifuge tubes (Beckman Coulter, 11 x 34mm, catalogue no: 342303) and was overlaid with 1.063g/mL density solution (250 µL). This was then centrifuged at 100,000 rpm (435,680 g for maximum radius and 274,400 g for minimum radius), 23ºC for 2.5 hours (TL100 Beckman Coulter, Life Sciences) in a fixed angled rotor (TLA 120.2, Beckman Coulter, Life Sciences). VLDL and LDL fractions (density<1.063 g/mL) were gently removed from the top in a volume of 500 µL using a glass pipette. The infranatant (500 µL) was then mixed with 1.478g/mL density solution (250 µL), overlaid with density solution 1.21g/mL (250 µL) and centrifuged at 100,000 rpm (435,680 g for maximum radius and 274,400 g for minimum radius), 23ºC for 5 hours. The top 500 µL (HDL fraction, density 1.063-1.21 g/mL) was collected from the top of the tube using a glass pipette leaving 500-uL infranatant (lipoprotein-depleted plasma, density >1.21g/mL).

2.3.3 Desalting

The HDL fraction was desalted using a PD MiniTrap G-25 column (GE Healthcare BioSciences) following the manufacturer's instructions for the spin protocol. The column was prepared by removing the upper and lower caps, storage solution and the upper filter from the column. Dulbecco's phosphate buffered saline (2 mL) (DPBS 1X, Thermo Fisher Scientific, 14190144) was passed through each column twice, followed by DPBS (3 mL) and centrifugation (Jouan, CR 412) at 2400 rpm/1187 g, room temperature for 2 minutes. The HDL fraction (500 µL) was then pipetted onto the column and centrifuged at 3000 rpm/1855 g, room temperature for 5 minutes. Desalted HDL fraction was then collected from the eluate and stored in aliquots at -80ºC until further analysis.

2.4 Plasma and lipoprotein composition analyses

2.4.1 Total protein concentration

Total protein concentration of HDL samples was determined by using a Bradford assay (Bradford 1976). Study participant number identification was labelled on each HDL sample and could be read by the researcher. Briefly, protein standards (1 mg/mL, 0.75 mg/mL, 0.5 mg/mL, 0.25 mg/mL and 0.1 mg/mL) were prepared from 1 mg/mL bovine serum albumin (BSA) standard stock (Sigma-Aldrich, P0914) and distilled water. Each protein standard (5µL), diluted HDL samples (1: 4) (5µL) and negative control (distilled water, 5µL) was added to separate wells on a 96-well plate in duplicate, followed by Bradford reagent (250 µL) (Sigma Aldrich, B6916) in each well. The plate was then mixed and incubated at room temperature for 15 minutes. Absorbance was measured at 620 nm by a plate reader (Multiskan EX Thermofisher). Protein concentration of HDL samples was calculated from absorbance values of samples compared to the standard curve. Protein quantification of HDL in Chapter 3 had an intra-assay CV of 9.02%. The inter-assay CV of the protein standard ranged from 5.96 – 14.96%.

2.4.2 HDL proteomic analysis

HDL proteomic analysis took place at the Occupational and Environmental Medicine Center, Department of Clinical and Experimental Medicine, Linköping University. I was able to perform HDL proteomic analysis in healthy pregnancy at different gestation throughout pregnancy (Chapter 3) with the assistances of Dr Helen Karlsson and Dr Stefan Ljunggren. The HDL proteomic studies in preeclampsia (Chapter4) and EV (Chapter 7) were carried out by Dr Stefan Ljunggren. Study participant number identification was labelled on each HDL sample and could be read by the researcher. Proteomic analysis of HDL samples from the same study (gestational series in Chapter 3, preeclampsia in Chapter 4 or HDL/EV in Chapter 7) were performed in the same batch and analysed together within the study, separately from other studies.

2.4.2.1 Preparation of solutions used for HDL proteomics analysis

- 25 mM ammonium bicarbonate (Sigma)

Ammonium bicarbonate (0.19765 g) was made up to 100 mL with distilled water.

- 8 M urea (Sigma) in 25mM ammonium bicarbonate

  Urea (4.8048 g) was made up to 10mL with 25mM ammonium bicarbonate solution.

- 0.25 mM dithiothreitol (Sigma)

  Dithiothreitol (0.0386 g) was made up to 1 mL with 25 mM ammonium bicarbonate solution.

- 0.75 M iodoacetamide (Sigma)

  Iodoacetamide (0.1387 g) was made up to 1mL with 25 mM ammonium bicarbonate solution

- 0.1% formic acid

  10% formic acid (100 uL) was made up to 10mL with distilled water.

2.4.2.2 Isolation of HDL protein

Each desalted HDL fraction was used in a volume containing 10 µg of total protein determined by a Bradford assay. Samples were vacuum-dried using a vacuum centrifugation system (SpeedVac, ThermoFisher Scientific) at 35ºC for 10 minutes. Protein pellets were then dissolved in 8 M urea in 25 mM ammonium bicarbonate (30 µL) for 10 minutes to denature proteins, followed by adding 0.25 mM dithiothreitol in 25 mM ammonium bicarbonate (2 µL) and left for 15 minutes to prevent disulfide bonds from forming between cysteine residues of proteins. To alkylate the proteins, 0.75 M iodoacetamide in 25 mM ammonium bicarbonate (2 µL) was added and left for 15 minutes at room temperature. The protein mixture was then diluted (1:10) in 25 mM ammonium bicarbonate (2.25 mL) and trypsinised [1:25 (weight/weight; trypsin:protein)] with the trypsin stock solution (200 µg/mL stock solution (Promega)). After that, the mixture was incubated overnight at 37ºC. The next day the protein solution was dried for 4

hours using a vacuum centrifugation system. The pellet was then dissolved in 0.1% formic acid (160 µL) to give a final protein concentration of 0.0625 µg/µL.

2.4.2.3 Nano liquid chromatography coupled to tandem mass spectrometry (nLC-MS/MS)

Peptides isolated from HDL (4 uL of 0.0625 µg/µL) were loaded onto a nano liquid chromatograph (EASY-nLC, Thermo Scientific, Waltham, MA, USA) with a C18 column (100 mm × 0.75 µm, Agilent Technologies, Santa Clara, CA, USA). The mobile phase comprised 2% to 40% acetonitrile supplemented with 0.1% formic acid for 82 minutes with an increase to 90% acetonitrile for a further 8 min. Eluted peptides were then transferred by an electrospray ionization interface to a tandem mass spectrometer (LTQ Velos Orbitrap Pro, Thermo Scientific) where the sequences of the peptides were determined by the collision-induced dissociation method with data-dependent acquisition. MaxQuant software version 1.6.3.4 (Max Planck Institute of Biochemistry, Martinsried, Germany) was used to analyse the data and identify peptides through comparison with the human Uniprot/Swissprot database. The identification criteria for proteins to use in further analysis were proteins which had at least 2 identified peptides and were found in more than 50% of all the samples analysed.

2.4.2.4 ApoA-I glycation

Glycation at amino acid positions 36, 47, 83, 118, 120, 130, 131, 157, 206, 219, 230, 232, 250, 262 and 263 (including pre- and pro-peptide) on apoA-I was searched as the modification variable in the mass spectrometry data. The intensity of glycated peptides and the ratio between glycated and non-glycated peptides were obtained from MaxQuant software and were corrected with each sample's apoA-I concentration before statistical analysis.

2.4.2.5 ApoA-I methionine oxidation

Methionine oxidation at amino acid positions 110, 136 and 172 (including pre- and pro-peptide) on apoA-I was searched as the modification variable in the mass spectrometry data. The intensity of modified peptides and the ratio between modified and unmodified peptides were obtained from MaxQuant

software and were corrected with each sample's apolipoprotein A-I concentration before statistical analysis.

2.4.2.6 Orthogonal Projections to Latent Structures Discriminant Analysis (OPLS-DA)

Orthogonal Projections to Latent Structures Discriminant Analysis (OPLS-DA) is a regression and prediction method used in multivariate data analysis. The OPLS-DA model consists of simultaneous projection of dependent variables (Y) and predictor variables (X) on hyper planes. The OPLS-DA algorithm processes the data to find the linear relationship between a matrix of Y and X that provides good approximation of the original data tables and maximizes the covariance between the observation positions on the hyper planes. To handle variation in X that is unrelated to Y, OPLS-DA divides the systematic variability in X into two parts: the systematic part that is linearly correlated (predictive) to Y and one that is uncorrelated (orthogonal) to Y. This partitioning of X data helps improve interpretability and prediction. Cross validation was used to determine the number of significant model dimensions by removing observations from the model one at a time and comparing the Y predicted by this model with the actual values. OPLS-DA was performed in proteomic data using Soft Independent Modelling of Class Analogy (SIMCA) to provide insights into separations between groups of samples. The analysis was carried out by Dr Stefan Ljunggren.

2.4.3 Total cholesterol, apoA-I and apoB concentration

Total cholesterol, apoA-I and apoB concentrations of plasma and lipoprotein fractions were measured by the Roche cobas c311 analyser at the Vascular Biochemistry Unit, University of Glasgow. Measurement of apoA-I and cholesterol concentration of HDL samples in the preeclampsia study (Chapter 4) was provided by Dr Monique Mulder at Erasmus University Medical Center, Rotterdam, the Netherlands.

2.4.4 SAA1 concentration

SAA1 in HDL samples was determined by a Human Serum Amyloid A1 DuoSet ELISA (R&D Systems, catalogue number: DY3019-05). This was performed according to the manufacturer's protocol as previous described in (Ljunggren et

al. 2017). I was able to measure SAA1 concentration in healthy pregnancy at different gestation throughout pregnancy (Chapter 3) with the assistance of Dr Helen Karlsson and Dr Stefan Ljunggren. SAA1 analyses in preeclampsia (Chapter4) and EV (Chapter 7) were carried out by Dr Stefan Ljunggren. Study participant number identification was labelled on each HDL sample and could be read by the researcher.

Briefly, a 96-well plate was coated with a capture antibody overnight. After that, the plate was washed and blocked for 1 hour using 5% Tween-20 in phosphate-buffered saline. Human SAA1 standard (part number 844410) was reconstituted, and serial diluted with 5% Tween-20 in phosphate-buffered saline to become 200, 100, 50, 25, 12.5, 6.25, 3.13 and 1.56 ng/mL. HDL in 0.8 M urea diluted 1:5 in 5% Tween-20 in phosphate-buffered saline (100 µL), standards (100 µL) or negative control (5% Tween-20 in phosphate-buffered saline, 100 µL) were added to the plate in duplicate and incubated for 2 hours at room temperature. The plate was washed, and a detection antibody was added to the plate and incubated for 2 hours, whereafter the plate was washed, streptavidin-HRP was added and incubated for 20 minutes in the dark. After a final wash, a substrate solution was added and incubated for 20 minutes in the dark. At the end of the incubation, stop solution was added and absorbance was measured at 450 nm with correction at 570 nm using a Spectramax 190 plate reader (Molecular devices, Sunnyvale, CA, USA). SAA1 concentration of HDL samples was calculated from absorbance values of samples compared to the standard curve and expressed as ng/mL. SAA1 concentration of HDL in Chapter 3 showed an intra-assay CV of 5.13%. The inter-assay CV of human SAA1 standards ranged from 1.18 – 8.11%.

2.4.5 PON1 arylesterase activity measurement

PON1 arylesterase activity was measured as the conversion of phenyl acetate to phenol using an enzymatic assay as previously described in (Ljunggren et al. 2014). Phenol, the product of this reaction, was measured by spectrophotometry. I was able to measure PON1 activity in healthy pregnancy at different gestation throughout pregnancy (Chapter 3) with the assistance of Dr Helen Karlsson and Dr Stefan Ljunggren. PON1 activity measurements in preeclampsia samples (Chapter4) and EV (Chapter 7) were carried out by Dr

Stefan Ljunggren. Study participant number identification was labelled on each HDL sample and could be read by the researcher.

Salt buffer was prepared by mixing 20 mM Trizma (Sigma) and 1.0 mM calcium chloride (Sigma) with distilled water and made up to 1 L. Hydrochloric acid was added to the solution to adjust pH to 8. The HDL sample was diluted with this salt buffer (1:80). Diluted HDL samples (20 µL) were added to each well of a 96-well plate (Sigma-Aldrich) in triplicate. Salt buffer (20 µL) was also added to the 96-well plate as a negative control. After that, 3.26 mM phenyl acetate solution (200 µL) was added to each well of HDL samples or negative control. The phenyl acetate solution was prepared by diluting phenyl acetate (44.4 µL) in salt buffer (100 mL). Lastly, a high performance spectrophotometry SpectraMax 190 plate reader (Molecular Devices, Sunnyvale, CA, USA) was used to measure the absorbance of phenol over time at 270 nm with 250 nm as background. The initial period when the reaction was linear was used for calculation of activity, expressed as U/mL. The activity was then adjusted with the total protein concentration in HDL obtained from Bradford assay and expressed as U/mg HDL protein.

A pilot study was performed to compare PON1 activity of HDL isolated from blood collected with different anticoagulants. HDL was isolated from blood collected with EDTA (n=4), lithium heparin (n=4) and no coagulant (serum, n=4). The result showed similar PON1 activity among three groups (mean PON1 activity 12.46, 12.48 and 11.22 U/mg HDL for EDTA, lithium heparin and serum respectively, p=0.99). Therefore, PON1 activity assay in this thesis was performed in HDL isolated from EDTA blood due to their availability. The intra assay CV in this pilot was 12.08%.

3 HDL protein compositional changes throughout gestation in healthy pregnancy

3.1 Introduction

During pregnancy, maternal metabolism goes through significant adaptation in order to provide energy and nutrition for the fetus. Increased maternal lipogenesis and fat accumulation occurs in early gestation and in later gestation increased insulin resistance and lipolysis lead to high plasma glucose and lipid levels (Huda, Sattar, and Freeman 2009). Inflammation, coagulation and oxidative stress are also elevated in late pregnancy (Sulaiman et al. 2016). Despite this unfavourable environment for the vascular endothelium, vascular function in pregnant women appears to be enhanced. Healthy pregnant women have lower systemic vascular resistance due to vasodilation compared to non-pregnant women, leading to a gradual decrease in blood pressure (Sulaiman et al. 2016). The concentration of HDL, which is well-known for its anti-atherogenic properties in non-pregnant populations, also changes during gestation. In healthy pregnancy, plasma HDL concentration starts to rise at 10-15 weeks of gestation and peaks (42% increase) at 20 weeks of gestation (Sulaiman et al. 2016). HDL cholesterol concentration is significantly lower in preeclampsia relative to healthy pregnancy (Sattar, Bendomir, et al. 1997). Based on the increase in healthy pregnancy and the lower levels in preeclampsia, one might speculate that HDL could be a protective factor for vascular function in healthy pregnancy and fails in preeclampsia resulting in endothelial dysfunction.

The main source of circulating HDL in pregnancy could be the liver where HDL production could be enhanced by increased estrogen during pregnancy. A radio-iodinated HDL kinetic study showed enhanced HDL apoA-I synthesis during estrogen administration (Schaefer et al. 1983). Healthy women receiving estrogen supplementation showed higher HDL cholesterol and HDL apoA-I concentrations than non-estrogen users (Walsh et al. 1991). There was also reduced HL activity in normolipidemic women during estrogen administration compared to the baseline activity before estrogen administration (Schaefer et al. 1983). HDL concentration was shown to be different between males and females. There was lower HDL2 and HDL3 levels in men than women (Anagnostis et al. 2015). Also, a higher prevalence of low-HDL cholesterol was found in

males compared to females (Ge et al. 2015). It is noteworthy that the time when HDL begins to increase is around the time when the feto-placental circulation is fully established. Significant amounts of apoA-I secretion from the maternal side of placenta have been demonstrated using human perfused placenta and primary trophoblast cell culture (Melhem et al. 2019). Thus, fully formed placenta may contribute to HDL concentration and/or HDL with enhanced function in terms of vascular protection. HDL composition in pregnancy may differ from that in non-pregnant women and may be related to the efficacy of HDL function. HDL produced in pregnancy could play a key role in preventing vascular dysfunction.

The composition of HDL, both protein and lipid, in the non-pregnant population has been shown to be central to the vasculo-protective properties of HDL. For example, apoA-I is the major structural and functional protein in HDL. ApoA-I and PON1 content of HDL has a significant role in HDL's anti-oxidative effects (Soran, Schofield, and Durrington 2015; Karlsson, Kontush, and James 2015). ApoA-I and S1P in HDL are involved in the enhancement of vascular function (Yuhanna et al. 2001; Nofer et al. 2004). Moreover, a study in metabolic syndrome demonstrated an altered HDL lipidome and lower cholesterol efflux capacity in metabolic syndrome patients compared with a healthy population. Interestingly, weight loss and exercise interventions modified these patients' HDL lipidome toward that of healthy individuals and improved its cholesterol efflux function (Khan et al. 2018). This information emphasizes the crucial role of HDL composition on its efficacy.

A cross-sectional study of the proteome of HDL from pregnant women revealed 35 HDL-associated proteins in pregnant women at term (Sreckovic et al. 2013). Half of these proteins are associated with lipid and lipoprotein metabolism including apoA-I, apoC-II, apoC-III and apoM. Other proteins included acute-phase-response proteins such as SAA1 and PON1, and proteins involved in immune system and coagulation process. The finding suggests a role for HDL in lipid and lipoprotein metabolism, inflammation, immune system and coagulation system in pregnancy. Pilot data from our laboratory comparing the HDL proteome of non-pregnant women and healthy pregnant women in the third trimester showed that the concentrations of 23 proteins in HDL were significantly different (Sulaiman, unpublished). Eleven proteins were in higher

concentration in healthy pregnant HDL while 12 proteins were lower. The proteins that differed are involved in many biological pathways such as lipid metabolism, coagulation and inflammation and the change in HDL composition may be linked to the efficacy of HDL function in pregnancy.

In this chapter, using a proteomic approach, the protein composition of HDL was determined in a longitudinal study of healthy pregnancy from pre-conception to after delivery to identify the temporal changes in HDL composition during pregnancy. It is extremely difficult to collect samples across an entire pregnancy from before conception to after delivery. This difficulty was overcome in this analysis by matching two independent cohorts of women, pre-pregnancy to 8.4 weeks of gestation (early pregnancy group) and 16 weeks of gestation to 13 weeks post-partum (late pregnancy group), for BMI, age and parity. BMI of participants at 8.4 weeks of gestation from the early pregnancy group were matched one-to-one with booking BMI of participants in the late pregnancy group within difference of ±2 kg/m^2 followed by matching age and parity with the least difference possible. The two cohorts were combined to represent an entire pregnancy timeline from pre-pregnancy to post-natal. However, each cohort was analysed independently as a separate longitudinal study to avoid overinterpreting the data, apart from in the multivariate data modelling where first trimester samples were combined. The pre-pregnancy timepoint was used as the non-pregnant referent for the early pregnancy group and the post-partum timepoint was used as the non-pregnant referent for the late pregnancy. The results from pre-pregnancy and post-partum timepoint were also compared to determine the comparability between the two cohorts.

Quantitation of apoA-I amino acid glycation and methionine oxidation was also assessed from the proteomic data to verify the existence and extent of apoA-I modifications during healthy pregnancy. Such modifications can compromise HDL vasculo-protective properties such as cholesterol efflux and anti-oxidative activity (Hoang et al. 2007; Shen et al. 2015; Shao et al. 2010). Other components measured in HDL from this gestational series were a direct assessment of apoA-I, cholesterol and SAA1 content. PON1 activity was also determined throughout gestation as a reflection of HDL's antioxidant function during healthy pregnancy.

3.1.1 Hypothesis

HDL protein composition begins to change at around 10-13 weeks of gestation when the maternal-fetal circulation is fully established and returns to pre-pregnancy composition in the post-natal period.

3.1.2 Objectives

- To determine protein composition, apoA-I concentration, glycation and methionine oxidation, cholesterol concentration and SAA1 concentration in HDL pre-pregnancy, at 4.6, 6.1, 8.4, 16, 25, 35 weeks of gestation and at 13 weeks after delivery

- To determine PON-1 activity of HDL pre-pregnancy, at 4.6, 6.1, 8.4, 16, 25, 35 weeks of gestation and at 13 weeks after delivery

3.2 Methodology

3.2.1 Recruitment of healthy pregnant women

Healthy pregnant women samples were from two archival collections of longitudinal cohorts throughout pregnancy recruited according to section 2.1.1, chapter 2. Sample size of n=10 was chosen for this study based on several previous studies on the HDL proteome. A significant longitudinal difference in HDL proteome was evident after LPS challenge in n=10 (Levels et al. 2011). Also, a significant difference in HDL proteome between pregnant and non-pregnant women was observed in n=10 per group (Sulaiman W., unpublished).

In this study, ten participants were identified from each cohort that matched for BMI, age and parity. The first cohort (EPS) included 4 timepoints from pre-pregnancy, 4.6, 6.1 and 8.4 weeks of gestation. The second cohort (LIPS) covered 4 time points as follows: 16 (range 14-19), 25 (range 23-28), 35 (range 34-38) weeks of gestation and 13 weeks (range 10-14 weeks) postpartum. Age, parity and BMI at 8.4 weeks of gestation of participants in the EPS study were matched with age, parity and BMI at 16 weeks of gestation of participants in the LIPS study.

3.2.2 HDL sample preparation

Blood was processed according to section 2.2, chapter 2, followed by HDL preparation from plasma according to section 2.3, chapter 2. Desalted HDL fractions were then stored in -80ºC until use.

3.2.3 Proteomic analysis of HDL

HDL samples from 8 different timepoints throughout pregnancy were used for proteomic analysis. Isolation of HDL protein, nLC-MS/MS analysis, apoA-I glycation and methionine oxidation identification and quantitation and OPLS-DA multivariate data modelling were carried out as described in section 2.4.2, chapter 2.

In the OPLS-DA of this gestational series of HDL samples, protein composition, BMI and age were assigned as co-variables. Samples were grouped into five classes: pre-pregnancy, 1st trimester (4.6, 6.1 and 8.4 weeks of gestation), 2nd trimester (16 and 25 weeks of gestation), 3rd trimester (35 weeks of gestation) and postpartum in this analysis.

3.2.4 Measurement of HDL total cholesterol, apoA-I and SAA1 concentration

HDL total cholesterol, apoA-I and SAA1 concentrations were measured (according to section 2.4.5 and 2.4.3, chapter 2) in all samples.

3.2.5 PON1 activity assessment

PON1 activity was assessed in each HDL sample following the protocol in section 2.4.6, chapter 2.

3.2.6 Statistical analysis

Data from the EPS cohort (pre-pregnancy, 4.6, 6.1 and 8.4 weeks of gestation) and the LIPS cohort (16, 25, 35 weeks of gestation and post-pregnancy) were analysed separately. For the EPS study, there were uneven numbers of samples at each timepoint. Repeated measures ANOVA can cope with these missing numbers and can be performed in parametric data as usual. However, the

Friedman test cannot analyse groups with uneven numbers of samples. Thus, non-parametric data analysed by Friedman test was only from 9 women, each with 3 timepoints: before pregnancy (n=9), 4.6 weeks (n=9) and 8.4 weeks (n=9). Data from the two cohorts (EPS and LIPS) were displayed together in the same time plot with a broken line between the cohorts to indicate independent analyses. To determine the comparability between the two cohorts, pre-pregnancy EPS data and post-partum LIPS data were compared, by unpaired t-test for parametric data or Mann-Whitney test for non-parametric data.

Protein quantity output from the proteomic analysis was expressed as label-free quantification (LFQ) intensity from the MaxQuant software (version 1.6.3.4) and was considered as non-parametric data for statistical analysis because it represents a relative value. Friedman tests followed by *post hoc* Wilcoxon signed rank tests were carried out to compare the difference of LFQ intensity median for each protein quantity between each timepoint. ApoA-I glycation and methionine oxidation data were corrected for HDL apoA-I concentration before analysis by Friedman test followed by *post hoc* Wilcoxon signed rank test for both LFQ intensity and the ratio between modified and unmodified peptides.

Total cholesterol, apoA-I, SAA1 concentration and PON1 activity data was checked for normal distribution using a Ryan-Joiner test. Log- or square root transformation was applied to achieve normal distribution if necessary. Repeated measures ANOVA with *post hoc* Tukey test was then performed for parametric data and Friedman test followed by *post hoc* Wilcoxon signed rank test were performed for non-parametric data. Minitab version 19 was used for statistical analysis.

3.3 Results

3.3.1 General characteristics of the healthy pregnant women

From the EPS, 10 women were selected with a mean age of 35.6 (SD±5.6) years and body mass index (BMI) of 24.4 kg/m^2 (SD±3.6). All were nulliparous and non-smokers. Five 6.1 weeks of gestation samples and one 8.4 weeks of gestation samples were unavailable. Therefore, the total number of samples were pre-pregnancy (n=10), 4.6 weeks (n=10), 6.1 weeks (n=5) and 8.4 weeks (n=9). Ten

women were selected from the LIPS cohort by matching BMI, age and parity with individuals selected from the early pregnancy study. Their mean age was 32.3 (SD±2.7) years and mean BMI was 24.2 kg/m^2 (SD±4.0). All participants were nulliparous and non-smokers. There were no missing samples from the LIPS cohort. General characteristics of the healthy pregnant women were shown in Table 3.1.

Table 3.1: Demographics of selected participants from EPS and LIPS studies

	EPS study (n=10)	LIPS study (n=10)	p
Age	35.6 (5.6)	32.3 (2.7)	0.12
BMI	24.4 (3.6)	24.2 (4.0)	0.91
Parity	100% Primiparous	100% Primiparous	-
Smoking status	100% non-smoker	100% non-smoker	-

Note: Data expressed as mean (SD).

3.3.2 HDL total cholesterol and apoA-I concentration

Total cholesterol and apoA-I concentrations were measured in all HDL samples. Total cholesterol and apoA-I concentrations in HDL showed no significant difference between pre-pregnancy and post-partum. HDL cholesterol concentrations were 1.8±0.5 and 1.5±0.1 mmol/L at pre-pregnancy and post-partum, respectively (p=0.087). While HDL apoA-I concentrations were 1.0±0.2 g/L at pre-pregnancy and 0.9±0.2 g/L after delivery (p=0.27). HDL apoA-I concentration significantly decreased at 13 weeks after delivery (0.9±0.2 g/L) compared to concentration at 16, 25 and 35 weeks of gestation (1.2±0.2, 1.2±0.2 and 1.3±0.3 g/L respectively) (Figure 3-1). HDL apoA-I concentration at 16, 25 and 35 weeks of gestation were 31.5, 28.8 and 39.7% higher than the concentration at postpartum (Figure 3-1). Cholesterol concentration in HDL did not differ throughout pregnancy (Figure 3-2). HDL cholesterol concentration at 16, 25 and 35 weeks of gestation were 6.8, 9.7 and 25.1% higher than the concentration at postpartum (Figure 3-2). The ratio of HDL cholesterol to apoA-I

concentration significantly increased at 13-week postpartum (1.7±0.4 mmol/g), relative to those at 16, 25 and 35 weeks of gestation (1.3±0.2, 1.4±0.3 and 1.5±0.3 mmol/g, respectively) (Figure 3-3). The ratio of HDL cholesterol to apoA-I concentration at 16, 25 and 35 weeks of gestation were 25.4, 20.0 and 16.7% lower than the ratio at postpartum (Figure 3-3).

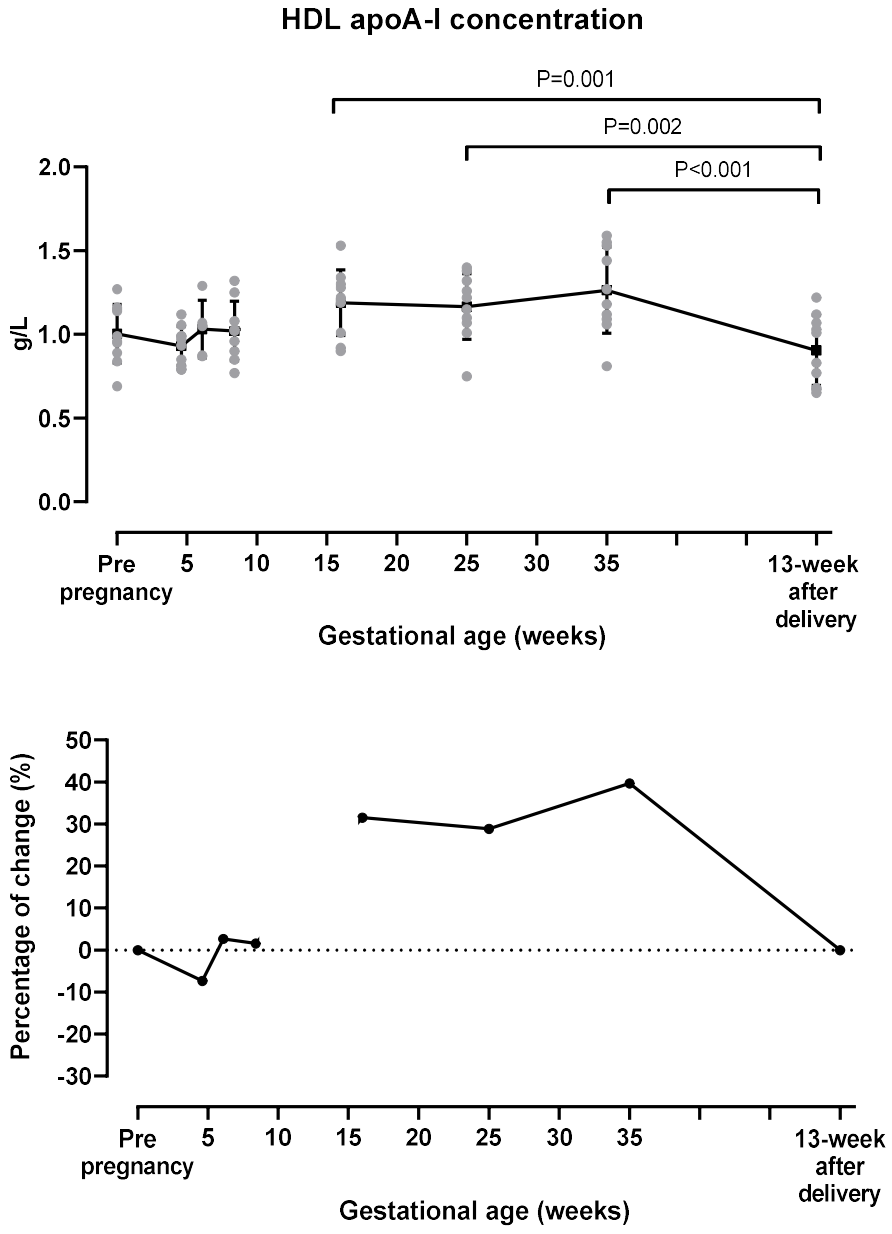

Figure 3-1 Apolipoprotein A-I concentration in HDL throughout pregnancy: Data is shown as mean±SD of the concentration (above) and percentage of change (below). Percentage of change was calculated from the change of mean value at 4.6, 6.1 and 8.4 weeks of gestation relative to mean value at pre-pregnancy and mean value at 16, 25 and 35 weeks of gestation relative to mean value at postpartum. Repeated measures ANOVA with *post hoc* Tukey test was carried out in each cohort separately and there is a discontinuous line between the two groups of participants. $p<0.05$ was taken as statistically significant.

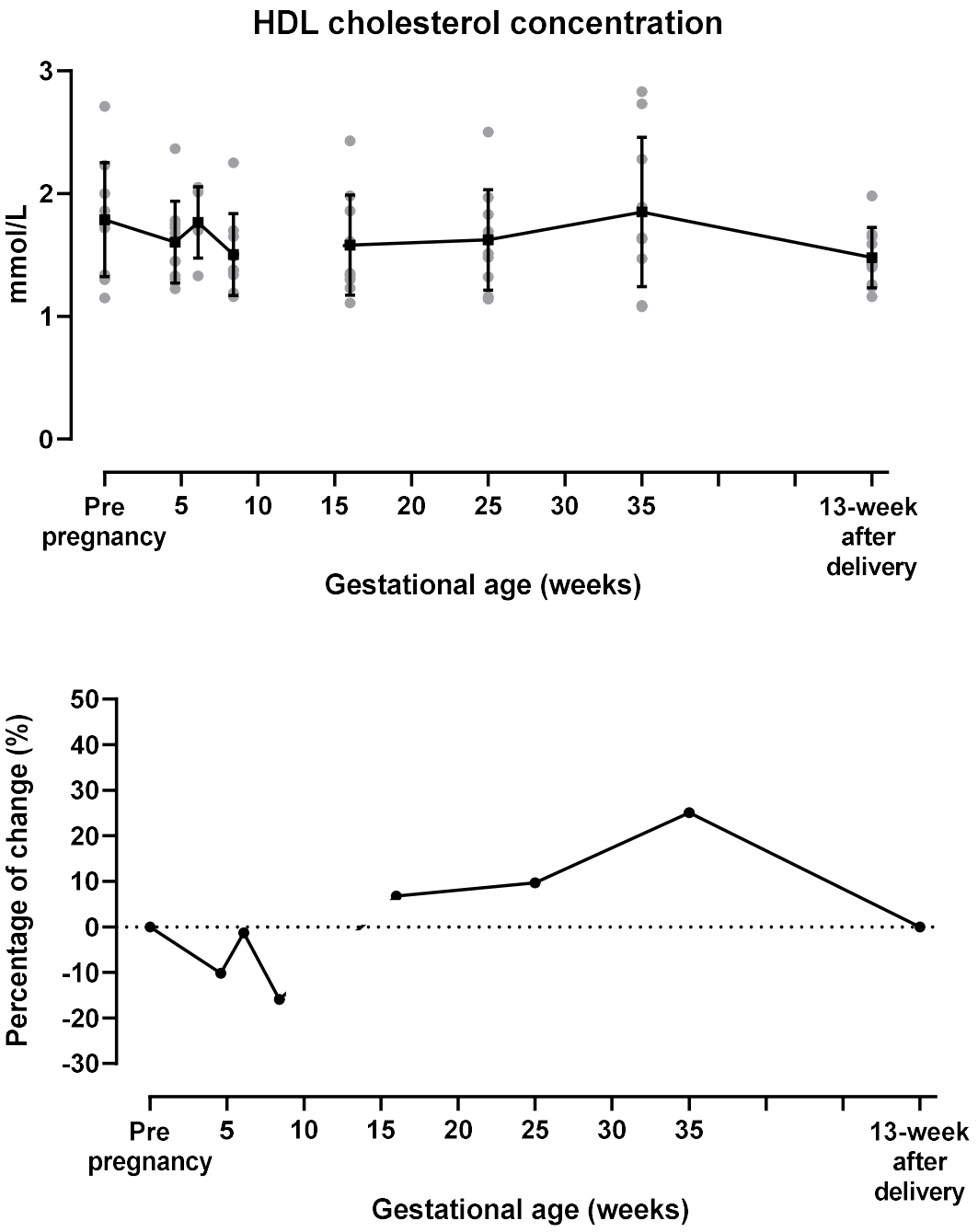

Figure 3-2 Cholesterol concentration in HDL throughout pregnancy Data is shown as mean±SD of the concentration and percentage of change. Percentage of change was calculated from the change of mean value at 4.6, 6.1 and 8.4 weeks of gestation relative to mean value at pre-pregnancy and mean value at 16, 25 and 35 weeks of gestation relative to mean value at postpartum. Repeated measures ANOVA with *post hoc* Tukey test was carried out in log transformed data of each cohort separately and there is a discontinuous line between the two groups of participants. $p<0.05$ was taken as statistically significant.

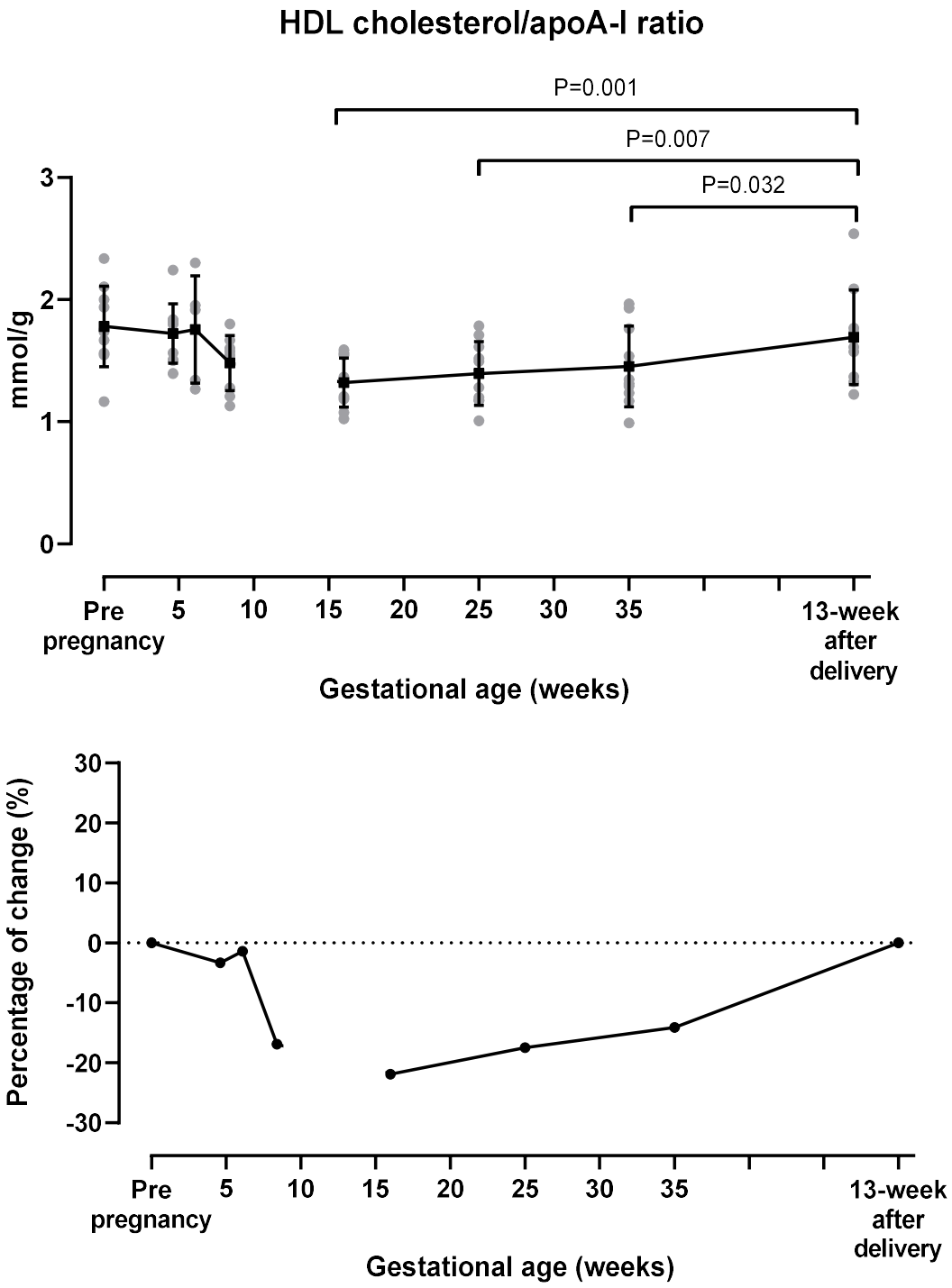

Figure 3-3 The ratio of cholesterol to apoA-I concentration in HDL throughout pregnancy: Data is shown as mean±SD of the concentration and percentage of change. Percentage of change was calculated from the change of mean value at 4.6, 6.1 and 8.4 weeks of gestation relative to mean value at pre-pregnancy and mean value at 16, 25 and 35 weeks of gestation relative to mean value at postpartum. Repeated measures ANOVA with *post hoc* Tukey test was carried out in each cohort separately (non-transformed data of EPS study and log transformation of LIPS data) and there is a discontinuous line between the two groups of participants. $p<0.05$ was taken as statistically significant.

3.3.3 Protein composition of HDL throughout gestation in healthy pregnancy

From nLC-MS/MS analysis, there was a total of 120 proteins detected in at least one HDL sample. HDL-associated proteins were then identified by including only proteins found in more than 50% of all HDL samples; 63 proteins were identified (Table 3.2). Among these 63 proteins, there were apolipoproteins, lipid transfer proteins and enzymes known to be associated with HDL metabolism such as CETP and PLTP, acute-phase proteins, complement proteins and coagulation proteins.

Table 3.2: List of proteins identified in >50% of all HDL samples throughout pregnancy

α-1-acid glycoprotein 1
α -1-acid glycoprotein 2
α -1-antichymotrypsin
α -1-antitrypsin
α -1B-glycoprotein
α -1-microglobulin/bikunin precursor
α -2-antiplasmin
α -2-Heremans-Schmid-glycoprotein
Angiotensinogen
Antithrombin-III
Apolipoprotein A-I
Apolipoprotein A-II
Apolipoprotein A-IV
Apolipoprotein B-100
Apolipoprotein C-I
Apolipoprotein C-II
Apolipoprotein C-III
Apolipoprotein C-IV
Apolipoprotein D
Apolipoprotein E
Apolipoprotein F
Apolipoprotein L-I
Apolipoprotein M
Apolipoprotein(a)
ß-2-glycoprotein 1
ß-2-microglobulin
Cathelicidin antimicrobial peptide
Cholesteryl ester transfer protein
Clusterin
Complement C3
Complement C4-A
Complement C4-B
Fibrinogen α chain
Fibrinogen ß chain

Haptoglobin
Haptoglobin-related protein
Hemopexin
Heparin cofactor 2
Ig γ-1 chain C region
Ig κ chain C region
Ig λ-6 chain C region
Kininogen-1
Leucine-rich α-2-glycoprotein
Methylated in normal thymocytes protein
Phosphatidylcholine-sterol acyltransferase
Phospholipid transfer protein
Pigment epithelium-derived factor
Platelet basic protein
Platelet factor 4
Prenylcysteine oxidase 1
Retinol-binding protein 4
Serotransferrin
Serum albumin
Serum amyloid A-1
Serum amyloid A-4
Serum paraoxonase/arylesterase 1
Serum paraoxonase/lactonase 3
Sorting nexin-29
Thymosin beta 4
Transthyretin
Vitamin D-binding protein
Vitronectin
Zinc-α-2-glycoprotein

3.3.4 Differences in HDL protein composition throughout gestation in healthy pregnancy

Of the 63 proteins identified in more than 50% of all HDL samples from healthy pregnancy, 16 proteins were found to have significant differences in LFQ intensity throughout gestation including apoA-IV, apoC-II, apoC-III, apoC-IV, apoF, apoL-I, α-1-acid glycoprotein 2 (AGP2), α-1-antitrypsin (A1AT), angiotensinogen, cathelicidin antimicrobial peptide (CAMP), fibrinogen α chain, fibrinogen ß chain, prenylcysteine oxidase 1, SAA1, paraoxonase-3 (PON3) and vitronectin (Table 3.3). LFQ intensity is a quantitative measure in mass spectrometry which quantifies the relative amount of peptides and proteins without using stable-isotope labels. These 16 proteins showed no significant difference between pre-pregnancy EPS and post-partum LIPS samples, except

apoA-IV which was significantly higher in pre-pregnancy HDL than in post-partum HDL (p=0.045).

There were 6 proteins; apoL-I, A1AT, angiotensinogen, fibrinogen α chain, fibrinogen β chain and SAA1 that significantly increased during the first trimester (4.6, 6.1 or 8.4 weeks of gestation) (Figure 3-9, 3-11, 3-12, 3-14, 3-15, 3-17), while apoA-IV and apoC-III decreased (Figure 3-4, 3-6). During 16, 25 or 35 weeks of gestation, LFQ intensity of apoL-I, angiotensinogen, CAMP, prenylcysteine oxidase 1 and vitronectin were significantly higher than their LFQ intensity after delivery (Figure 3-9, 3-12, 3-13, 3-16, 3-19). ApoF and PON3 were also elevated at 16 weeks of gestation compared to 25 and 35 weeks of gestation (Figure 3-8, 3-18) but only apoF had a lower LFQ intensity at 35 weeks of gestation compared to postpartum (Figure 3-8). Lastly, apoC-II, apoC-IV and AGP2 revealed lower LFQ intensity at 16 or 25 weeks of gestation than at 35 weeks of gestation or 13 weeks post-partum (Figure 3-5, 3-7, 3-10). The ratio of HDL apoC-II/apoC-III was also analysed and showed significantly decreased LFQ at 8.4 weeks of gestation and increased LFQ at 35 weeks of gestation and 13-week postpartum (Figure 3-20).

Table 3.3 List of protein contents in HDL that changed during pregnancy: protein name and their function

Protein	Function
ApoA-IV	• Negative acute phase reactant • Enhances RCT and anti-inflammation
ApoC-II	LPL activator
ApoC-III	• Inhibits LPL activity • Inhibits TRL uptake by liver and other tissues • Impairs protective properties of HDL, such as endothelial anti-apoptosis and RCT
ApoC-IV	Promotes hypertriglyceridemia
ApoF	Inhibits CETP activity
ApoL-I	Promotes lysosomal lysis of *Trypanosoma brucei*
AGP2	• Positive acute phase reactant • Pro- and anti-inflammatory effects
A1AT	• Serine protease inhibitor

	• Protects RCT function of HDL from protease-induced deterioration
Angiotensinogen	• Substrate of angiotensin in renin-angiotensin-aldosterone system • Increases blood pressure • Decreases blood volume
CAMP	Antimicrobial activity
Fibrinogen α chain	• Converted to fibrin and forms fibrin clots • Positive acute phase reactant
Fibrinogen ß chain	• Converted to fibrin and forms fibrin clots • Positive acute phase reactant
PON3	Protects LDL oxidation
Prenylcysteine oxidase 1	Pro-oxidant enzyme
SAA1	Impairs anti-inflammatory effect of HDL
Vitronectin	Inhibits the extracellular complement system

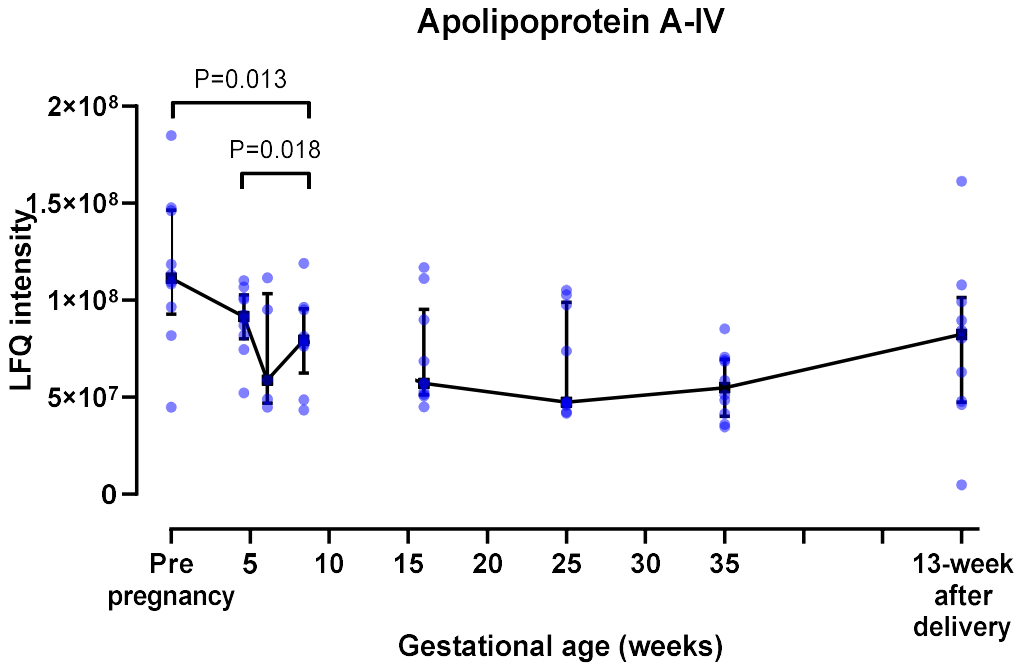

Figure 3-4 LFQ intensity of apoA-IV throughout gestation: Data is expressed as median±interquartile range. Friedman test followed by *post hoc* Wilcoxon signed rank test were carried out in each cohort separately and there is a discontinuous line between the two groups of participants. $p<0.05$ was taken as statistically significant.

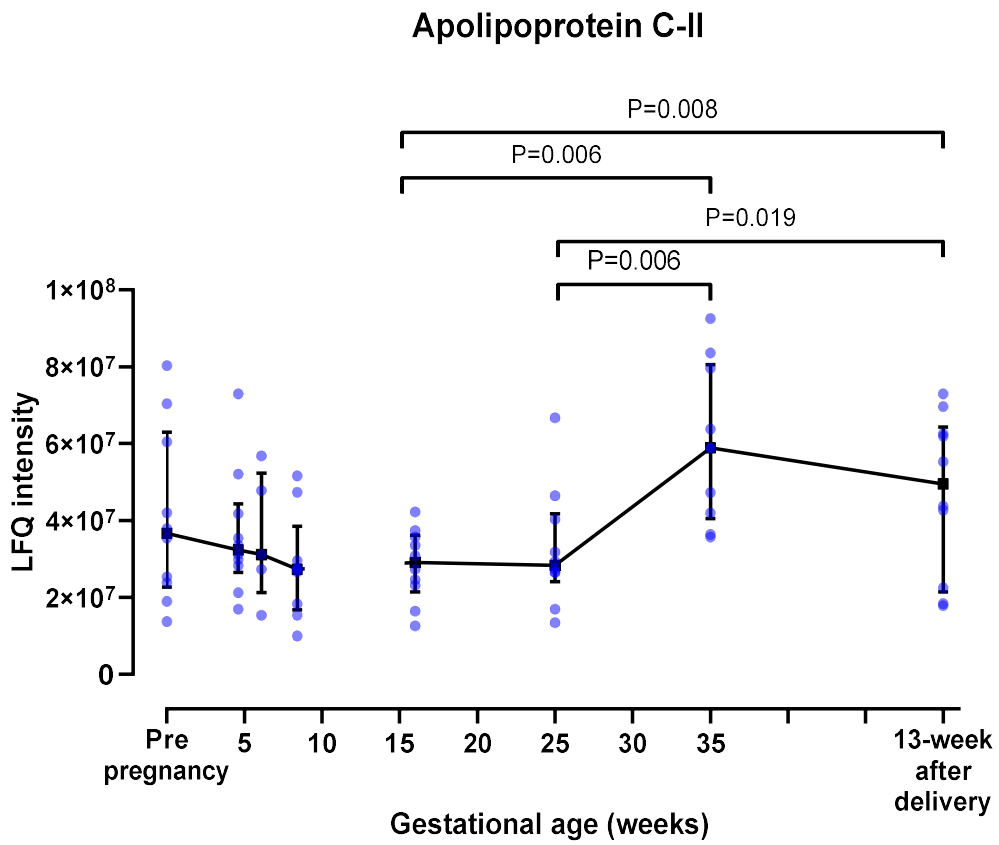

Figure 3-5 LFQ intensity of apoC-II throughout gestation: Data is expressed as median±interquartile range. Friedman test followed by *post hoc* Wilcoxon signed rank test were carried out in each cohort separately and there is a discontinuous line between the two groups of participants. p<0.05 was taken as statistically significant.

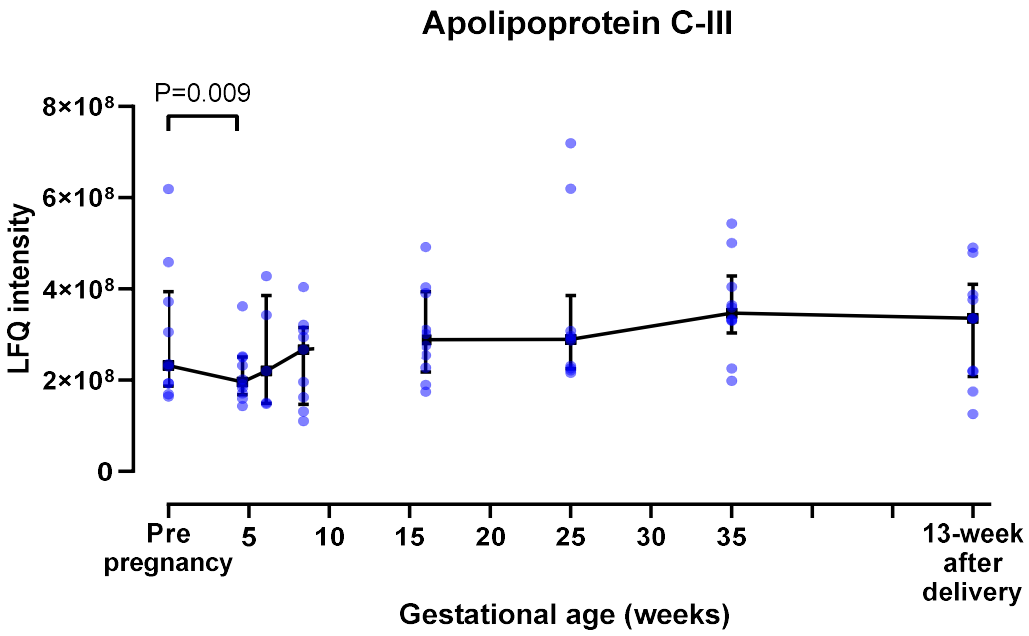

Figure 3-6 LFQ intensity of apoC-III throughout gestation: Data is expressed as median±interquartile range. Friedman test followed by *post hoc* Wilcoxon signed rank test were carried out in each cohort separately and there is a discontinuous line between the two groups of participants. p<0.05 was taken as statistically significant.

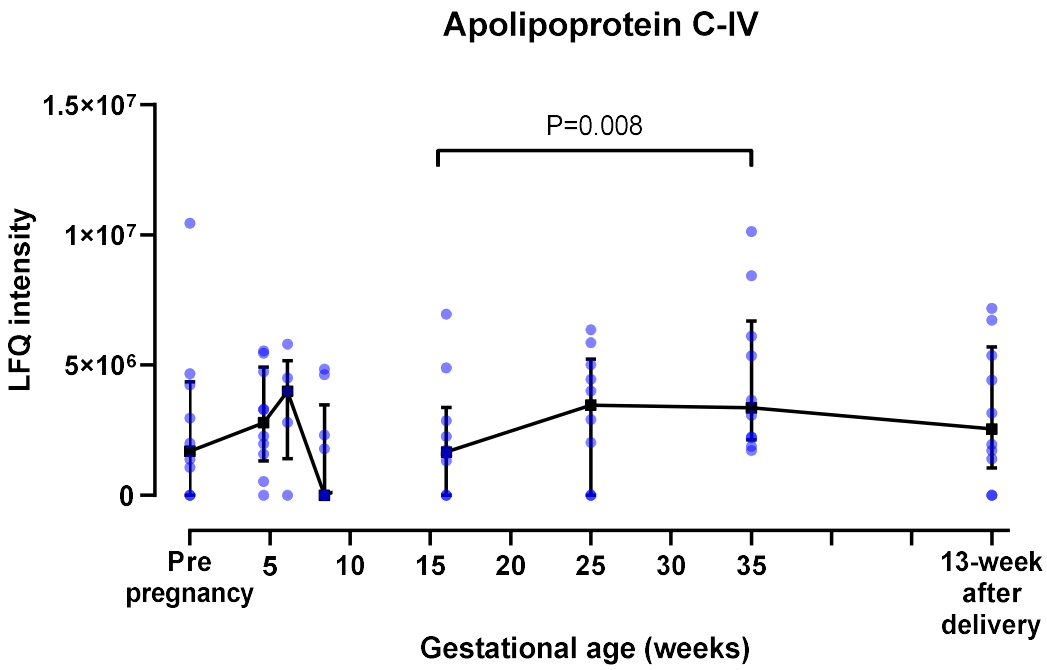

Figure 3-7 LFQ intensity of apoC-IV throughout gestation: Data is expressed as median±interquartile range. Friedman test followed by *post hoc* Wilcoxon signed rank test were carried out in each cohort separately and there is a discontinuous line between the two groups of participants. p<0.05 was taken as statistically significant.

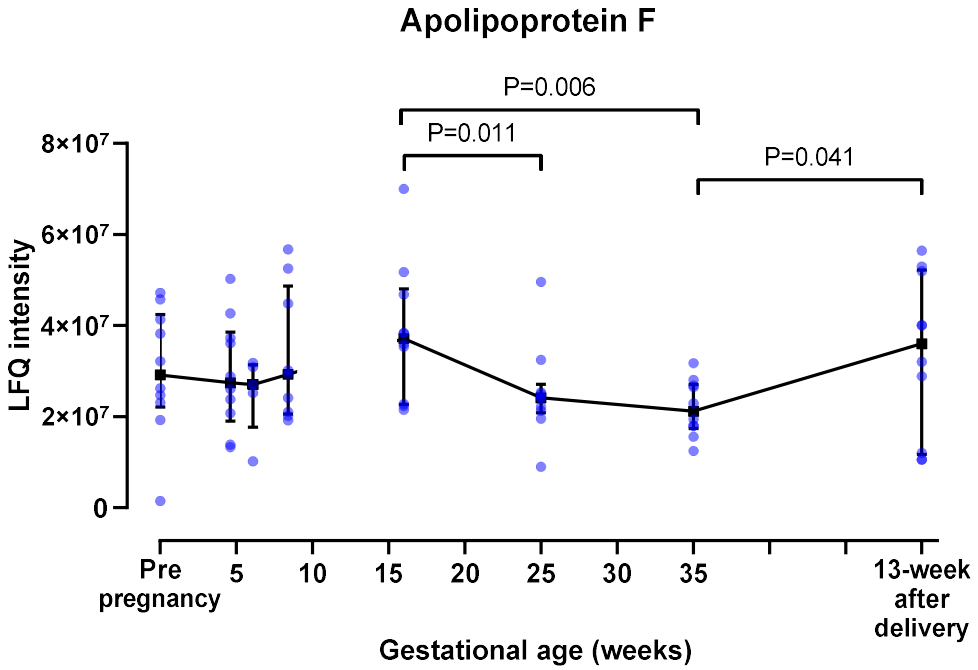

Figure 3-8 LFQ intensity of apoF throughout gestation: Data is expressed as median±interquartile range. Friedman test followed by *post hoc* Wilcoxon signed rank test were carried out in each cohort separately and there is a discontinuous line between the two groups of participants. p<0.05 was taken as statistically significant.

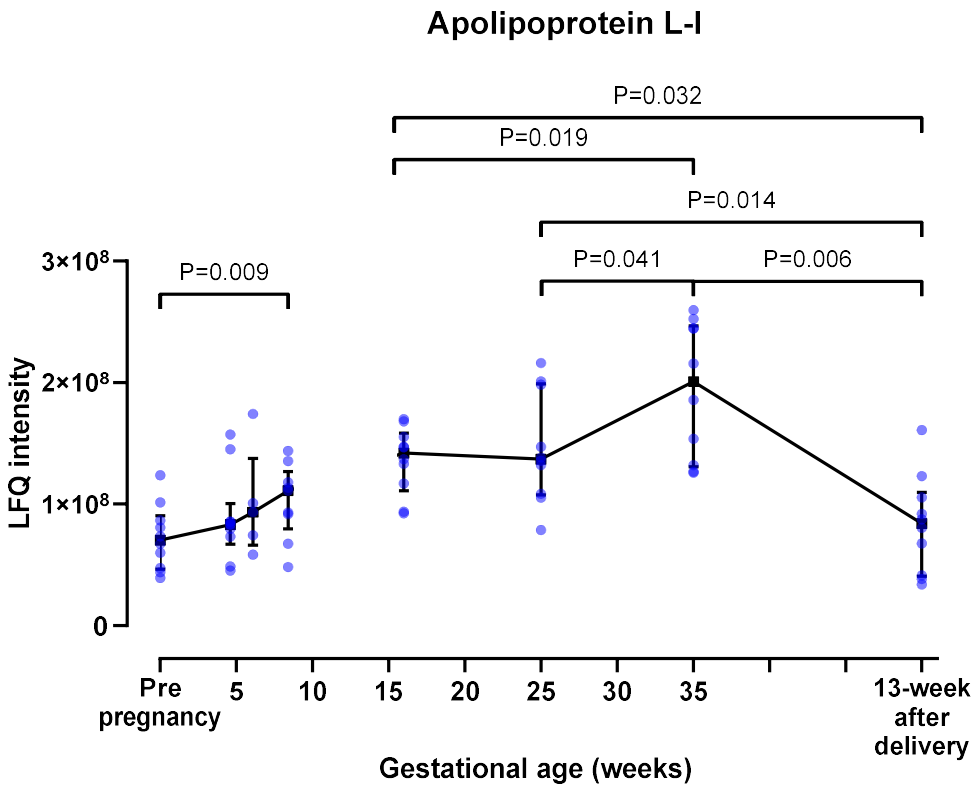

Figure 3-9 LFQ intensity of apoL-I throughout gestation: Data is expressed as median±interquartile range. Friedman test followed by *post hoc* Wilcoxon signed rank test were carried out in each cohort separately and there is a discontinuous line between the two groups of participants. p<0.05 was taken as statistically significant.

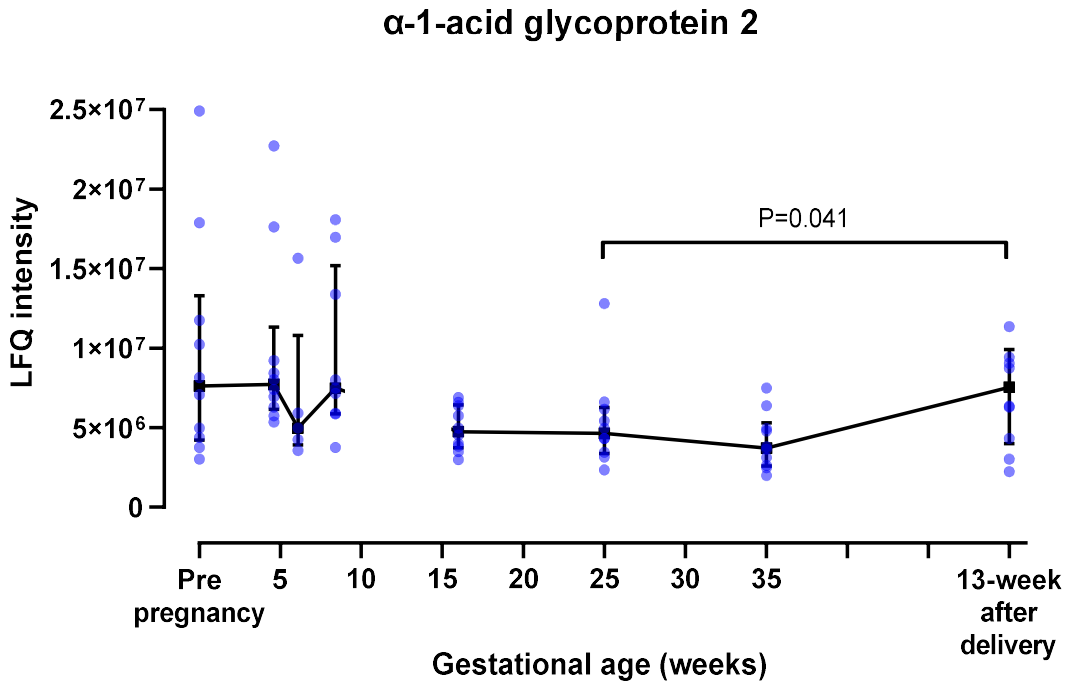

Figure 3-10 LFQ intensity of AGP2 throughout gestation: Data is expressed as median±interquartile range. Friedman test followed by *post hoc* Wilcoxon signed rank test were carried out in each cohort separately and there is a discontinuous line between the two groups of participants. p<0.05 was taken as statistically significant.

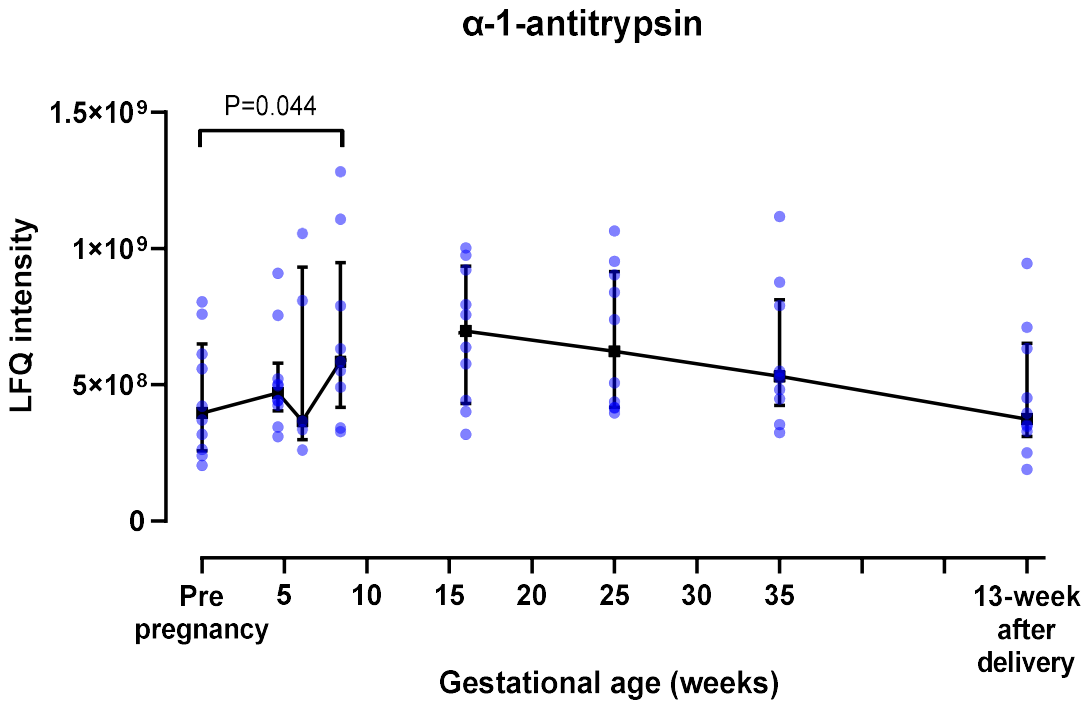

Figure 3-11 LFQ intensity of A1AT throughout gestation: Data is expressed as median±interquartile range. Friedman test followed by *post hoc* Wilcoxon signed rank test were carried out in each cohort separately and there is a discontinuous line between the two groups of participants. p<0.05 was taken as statistically significant.

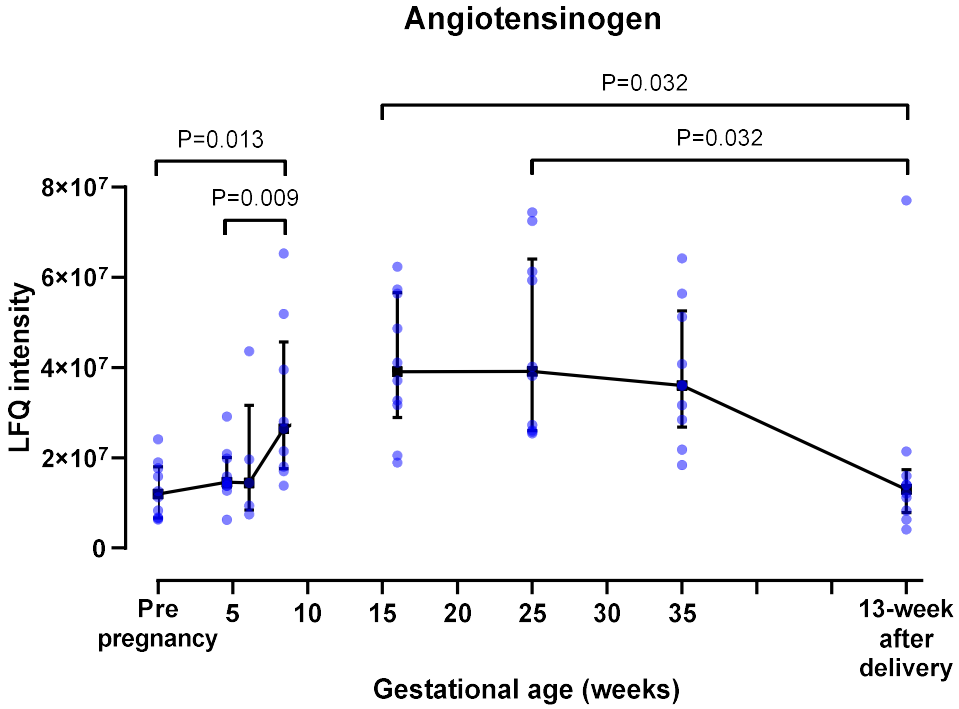

Figure 3-12 LFQ intensity of angiotensinogen throughout gestation: Data is expressed as median±interquartile range. Friedman test followed by *post hoc* Wilcoxon signed rank test were carried out in each cohort separately and there is a discontinuous line between the two groups of participants. p<0.05 was taken as statistically significant.

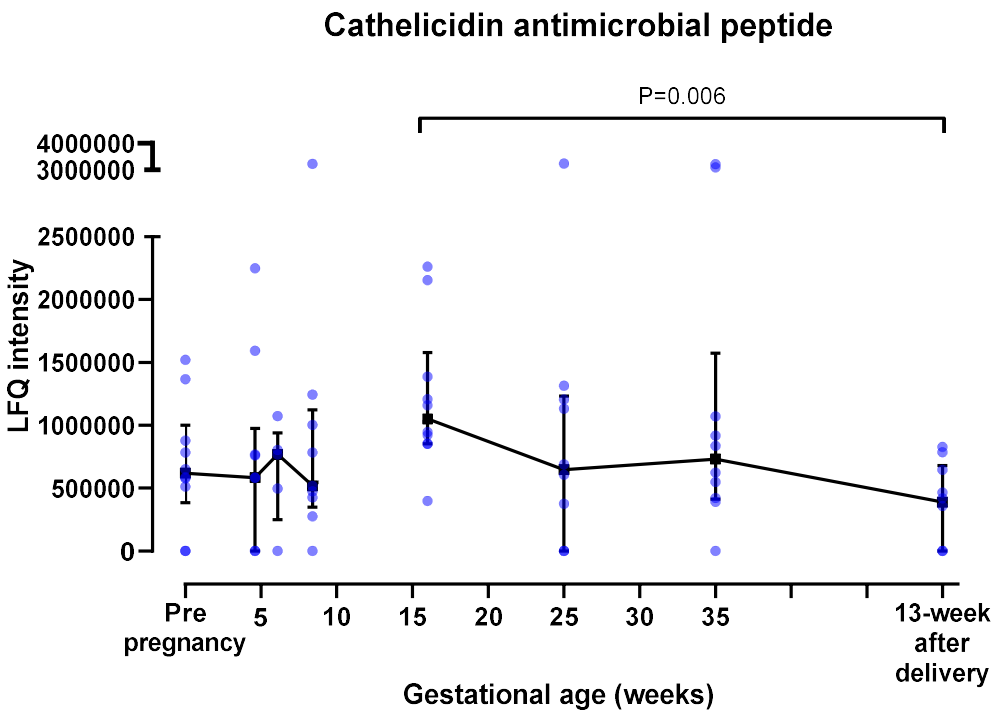

Figure 3-13 LFQ intensity of CAMP throughout gestation: Data is expressed as median±interquartile range. Friedman test followed by *post hoc* Wilcoxon signed rank test were carried out in each cohort separately and there is a discontinuous line between the two groups of participants. p<0.05 was taken as statistically significant.

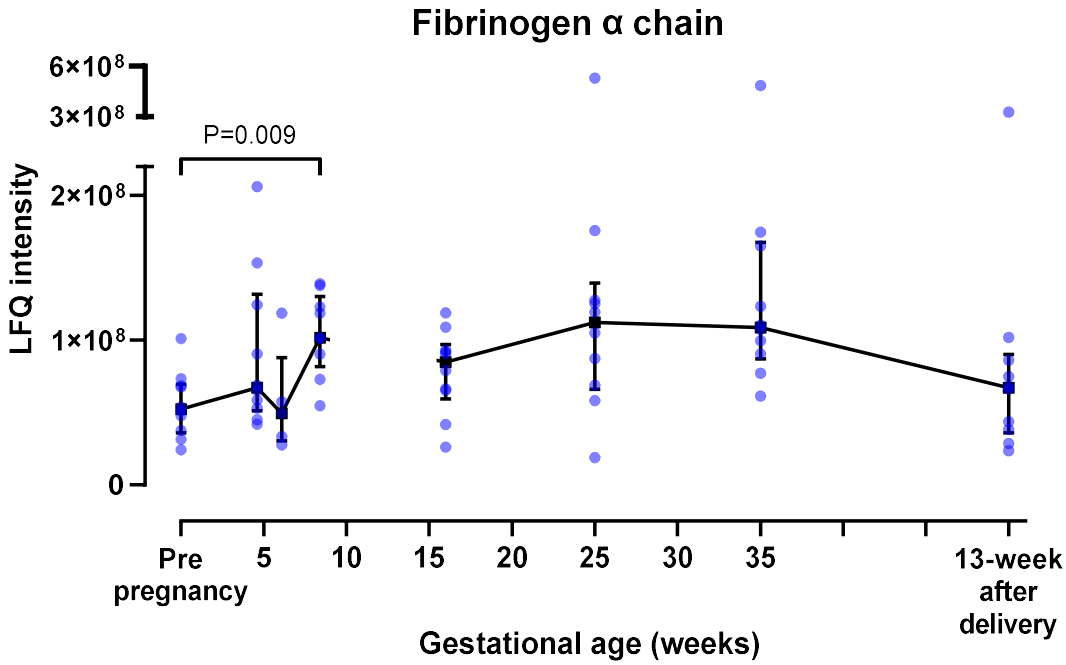

Figure 3-14 LFQ intensity of fibrinogen α chain throughout gestation: Data is expressed as median±interquartile range. Friedman test followed by *post hoc* Wilcoxon signed rank test were carried out in each cohort separately and there is a discontinuous line between the two groups of participants. p<0.05 was taken as statistically significant.

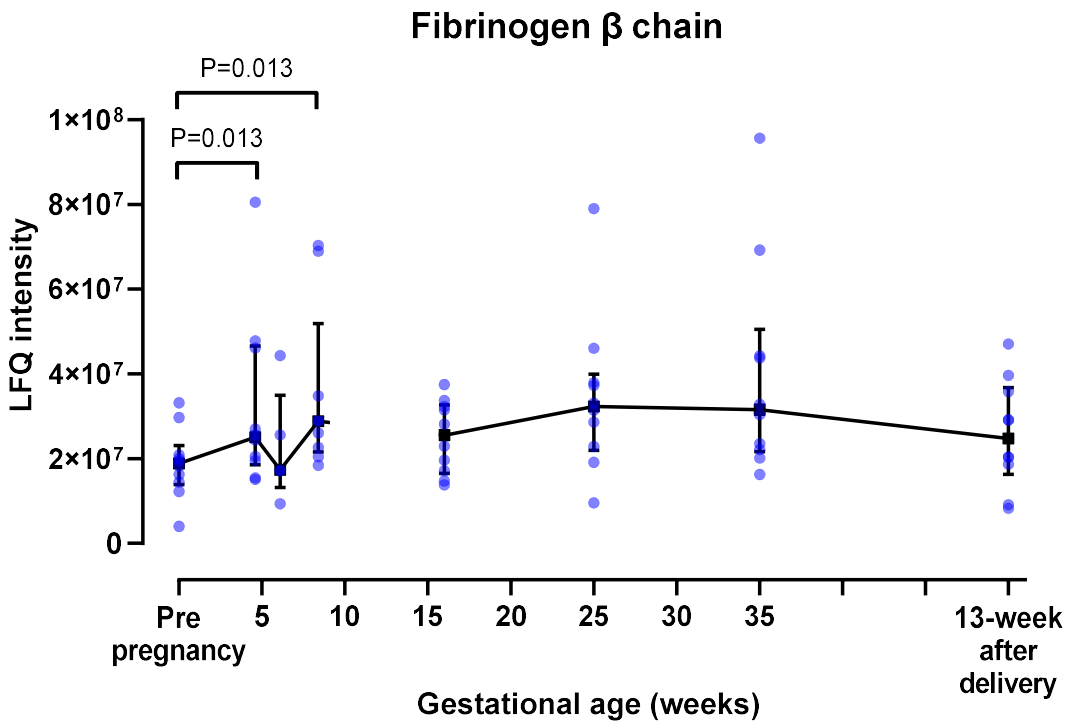

Figure 3-15 LFQ intensity of fibrinogen β chain throughout gestation: Data is expressed as median±interquartile range. Friedman test followed by *post hoc* Wilcoxon signed rank test were carried out in each cohort separately and there is a discontinuous line between the two groups of participants. p<0.05 was taken as statistically significant.

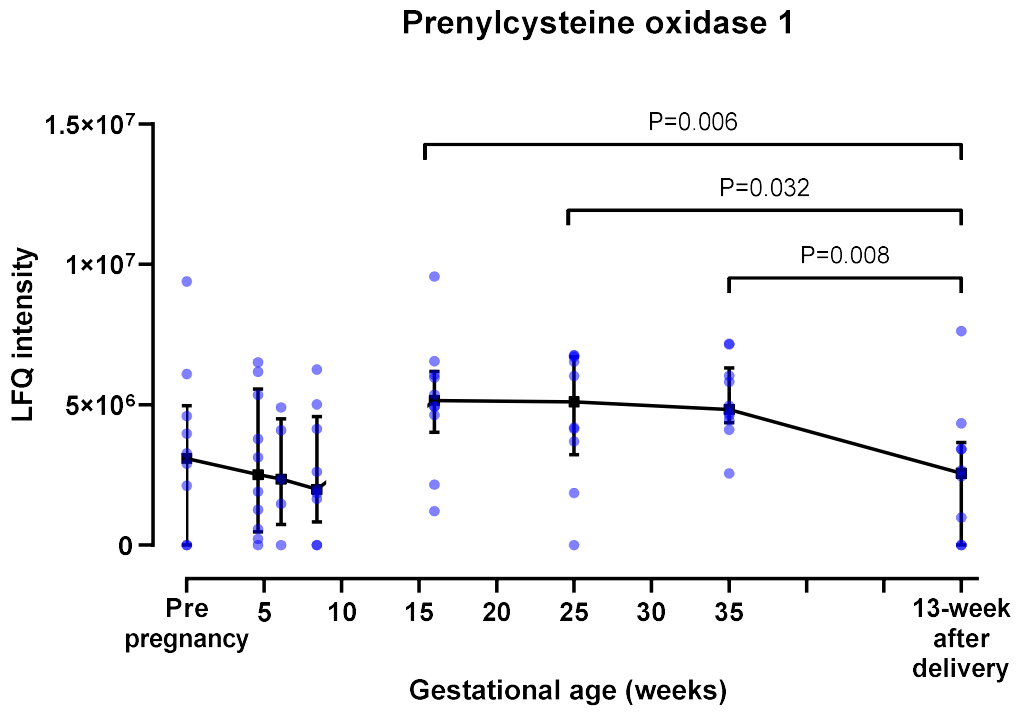

Figure 3-16 LFQ intensity of prenylcysteine oxidase 1 throughout gestation: Data is expressed as median±interquartile range. Friedman test followed by *post hoc* Wilcoxon signed rank test were carried out in each cohort separately and there is a discontinuous line between the two groups of participants. p<0.05 was taken as statistically significant.

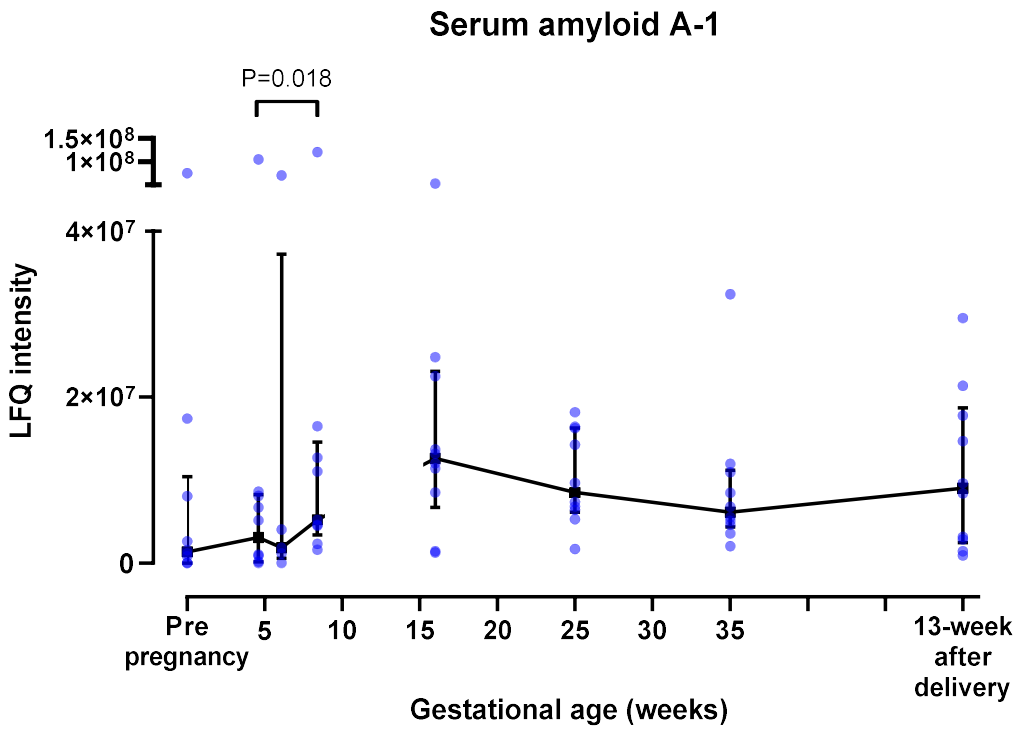

Figure 3-17 LFQ intensity of SAA1 throughout gestation: Data is expressed as median±interquartile range. Friedman test followed by *post hoc* Wilcoxon signed rank test were carried out in each cohort separately and there is a discontinuous line between the two groups of participants. p<0.05 was taken as statistically significant.

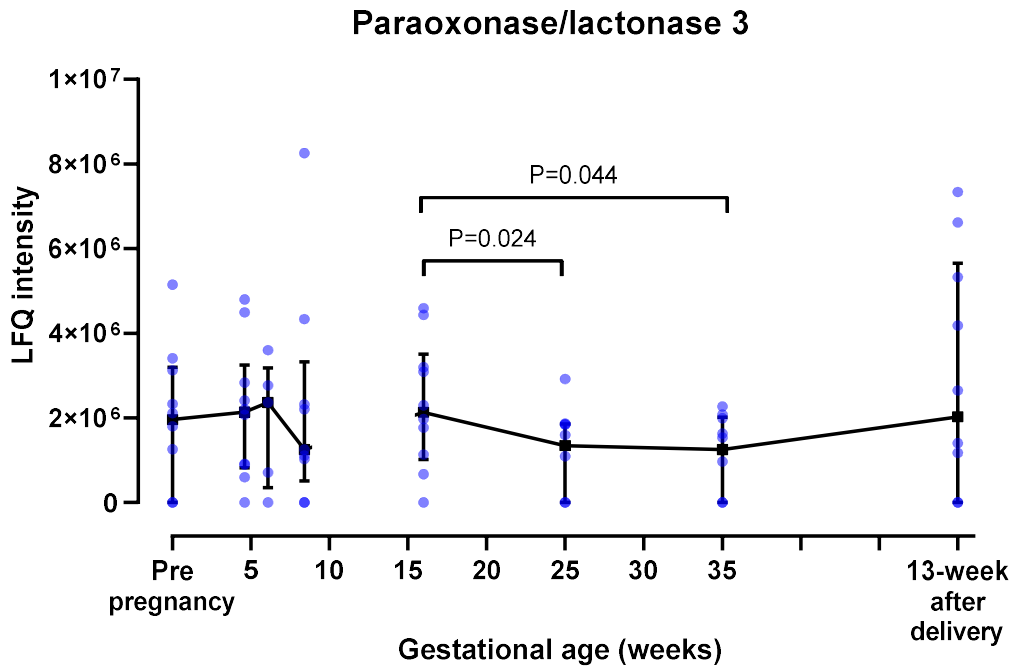

Figure -3-18 LFQ intensity of PON3 throughout gestation: Data is expressed as median±interquartile range. Friedman test followed by *post hoc* Wilcoxon signed rank test were carried out in each cohort separately and there is a discontinuous line between the two groups of participants. p<0.05 was taken as statistically significant.

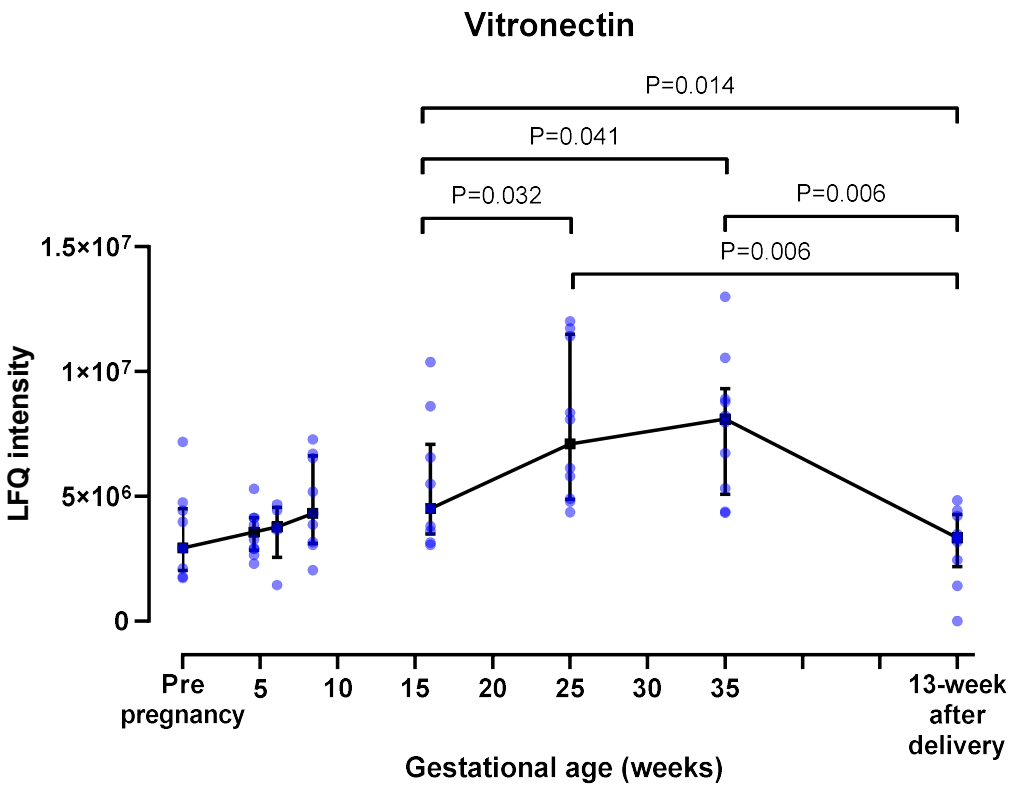

Figure 3-19 LFQ intensity of vitronectin throughout gestation: Data is expressed as median±interquartile range. Friedman test followed by *post hoc* Wilcoxon signed rank test were carried out in each cohort separately and there is a discontinuous line between the two groups of participants. $p<0.05$ was taken as statistically significant.

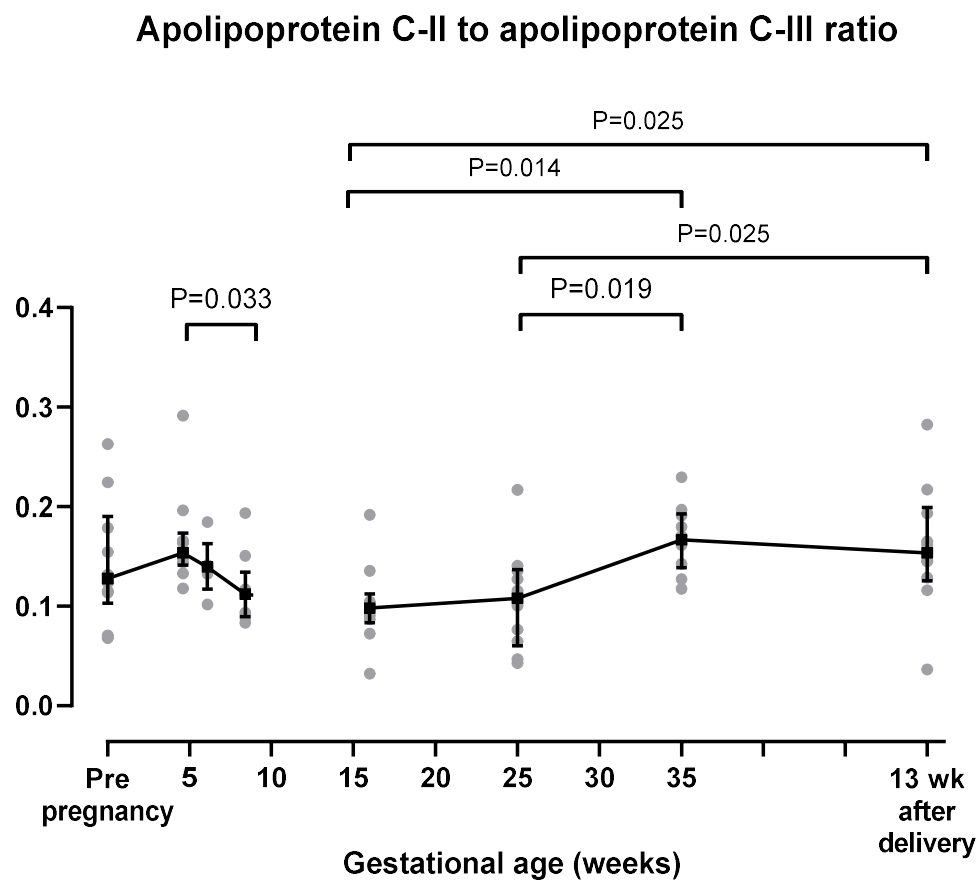

Figure 3-20 Ratio of apoC-II to apoC-III throughout gestation: Data is expressed as median±interquartile range. Friedman test followed by *post hoc* Wilcoxon signed rank test were carried out in each cohort separately and there is a discontinuous line between the two groups of participants. $p<0.05$ was taken as statistically significant.

3.3.5 Orthogonal Projections to Latent Structures Discriminant Analysis (OPLS-DA)

Variations in HDL proteome, BMI and age between the 5 sampling timepoints - pre-pregnancy, the first trimester (4.6, 6.1 and 8.4 weeks of gestation), the second trimester (16 and 25 weeks of gestation), the third trimester (35 weeks of gestation) and postpartum - were evaluated by OPLS-DA.

A score plot was created to visualize the differences in the proteomes of each sample with the x-axis representing between-timepoint variation and the y-axis representing within-timepoint variation (Figure 3-21). This score plot revealed a gradient of separation of sample according to the timepoint in pregnancy. Pre-pregnant samples were displayed at the right end of the x-axis. As one moves along the x-axis to the left then HDL of increasing gestational age appears,

firstly, HDL from the first trimester (4.6, 6.1 and 8.4 weeks of gestation), then the second trimester (16 and 25 weeks of gestation) and finally the third trimester (35 weeks of gestation). Samples from after delivery (13-week postpartum) appeared back at the far right the x-axis close to the pre-pregnancy samples.

A loading plot was also created to illustrate the inter-relationship between different types of HDL proteins (Figure 3-22). Proteins located closer to each other represent their greater correlation. Together with the score plot, the location of protein in the loading plot may be used to indicate how proteins change in each group of samples in the score plot. Proteins located to the left end of x-axis of the loading plot (for example, apoL-I, vitronectin and angiotensinogen) were higher in the samples that located to the left end of x-axis of the score plot (the second and third trimester) and lower in the samples to the right.

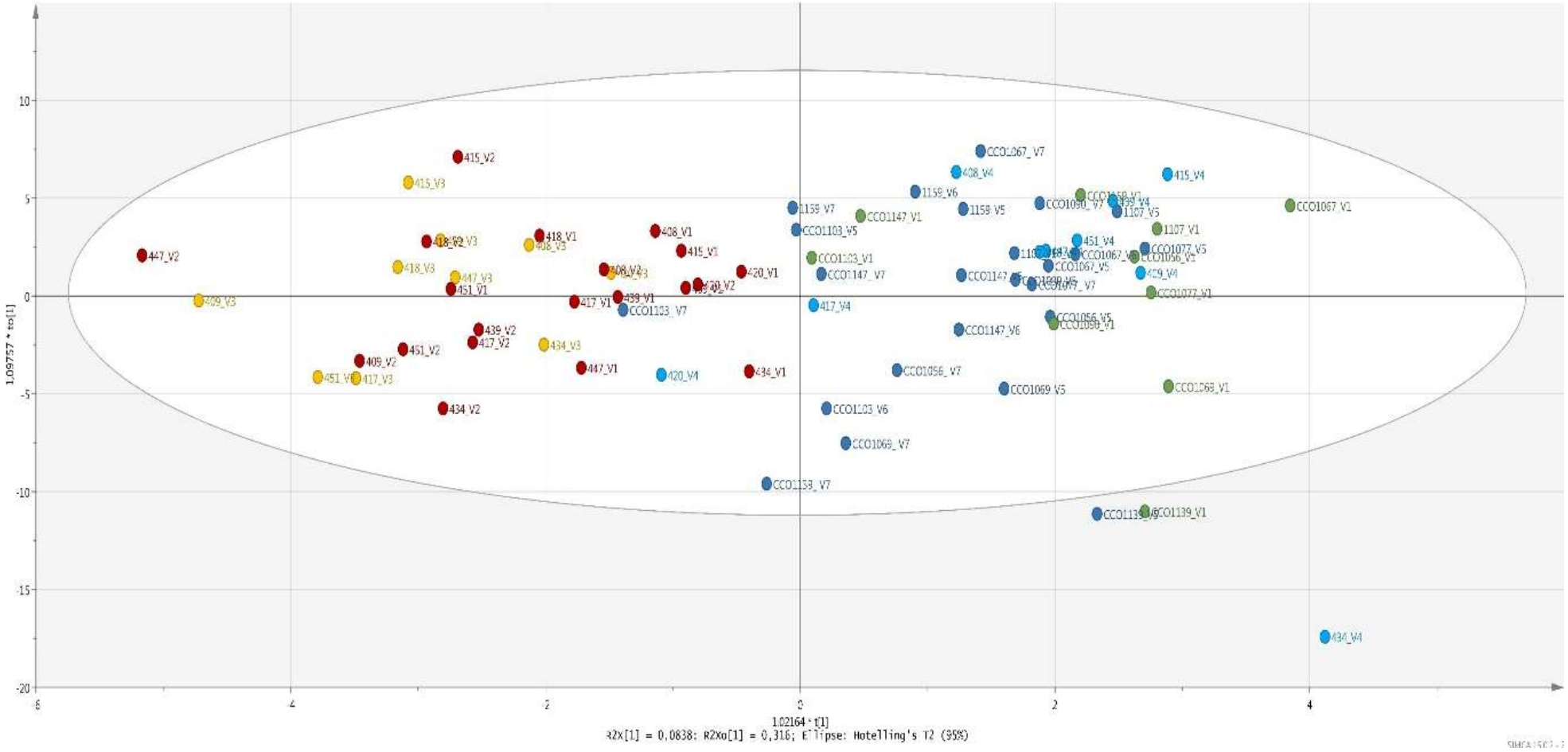

Figure 3-21 Score plot of Orthogonal Projections to Latent Structures Discriminant Analysis (OPLS-DA). Five timepoints were analysed: pre-pregnancy (green), the first trimester (dark blue), the second trimester (red), the third trimester (yellow) and post-pregnancy (light blue). HDL proteins, BMI and age were assigned as variables. The x-axis represents between-group variation, and the y-axis represents within-group variation. The ellipse represents the confidence region for a two-dimensional score plot with the significance level of 0.05. Observations situated outside the ellipse may be considered outliers. The plot shows a gradient of separation of sample according to gestational age of pregnancy.

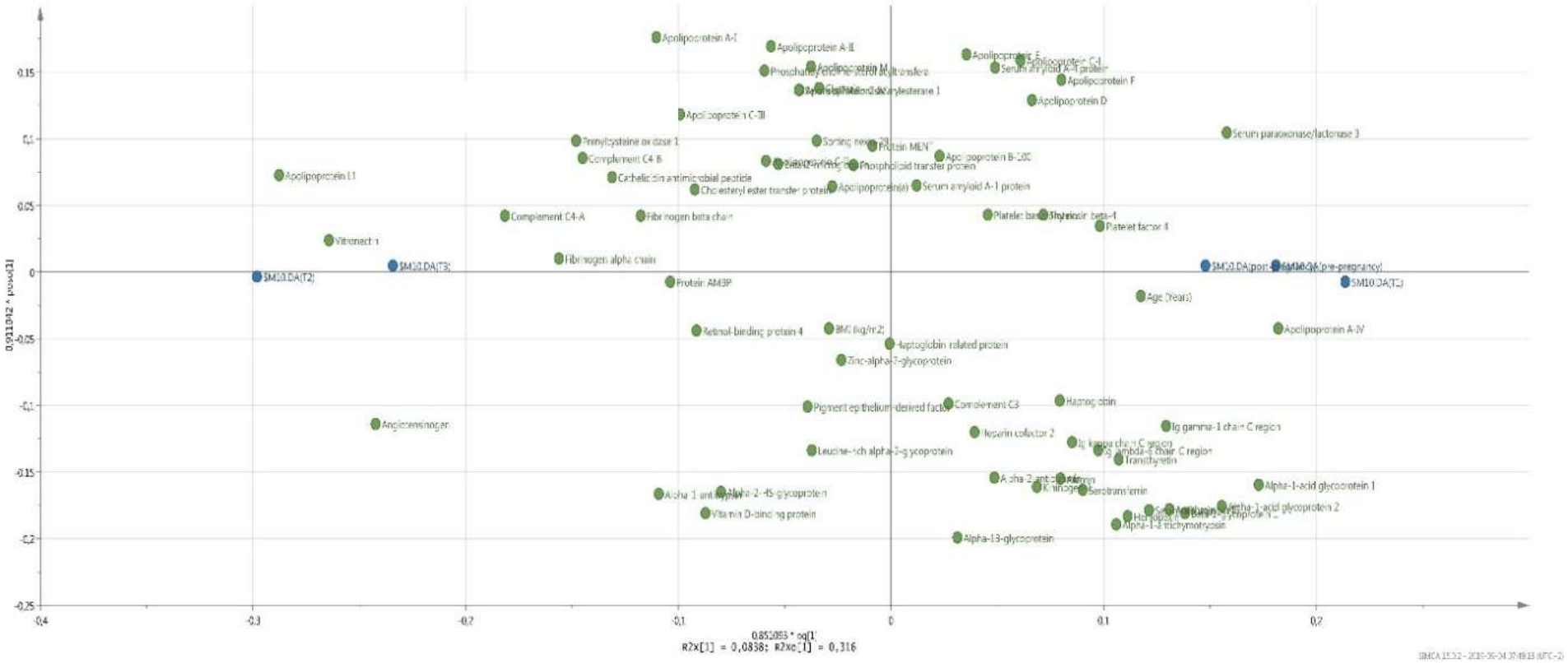

Figure 3-22 Loading plot of Orthogonal Projections to Latent Structures Discriminant Analysis (OPLS-DA) This plot shows the inter-relationship between different types of HDL proteins. Proteins located closer to each other represent their greater correlation. The blue points are the point from which all the green points are distanced.

3.3.6 ApoA-I glycation in HDL throughout gestation in healthy pregnancy

Both LFQ intensity of apoA-I peptide containing glycated amino acid and ratio of glycated to non-glycated amino acid at position 36, 47, 83, 118, 120, 130, 131, 157, 206, 219, 230, 232, 250, 262 and 263 (including pre- and pro-peptide) on apoA-I did not significantly differ between pre-pregnancy and post-partum HDL. There was no significant difference in the LFQ intensity of glycated peptide at all the 15 amino acid positions on apoA-I studied throughout pregnancy. The ratio of glycated to non-glycated amino acid at position 36, 83, 118, 130, 131, 157, 206, 219, 230, 232, 250, 262 and 263 on apoA-I also showed no difference throughout gestation of healthy pregnancy. Only amino acid positions 47 and 120 of apoA-I (Figure 3-23) showed a significant change in glycation during pregnancy. The ratio of glycated to non-glycated amino acid at position 47 and 120 of apo A-I, corrected for apoA-I concentration, was significantly lower at 8.4 weeks of pregnancy than at 4.6 weeks (Figure 3-24). Moreover, the ratio of glycated to non-glycated amino acid at position 120 of apoA-I significantly increased at 4.6 weeks of gestation compared to pre-pregnancy (Figure 3-24).

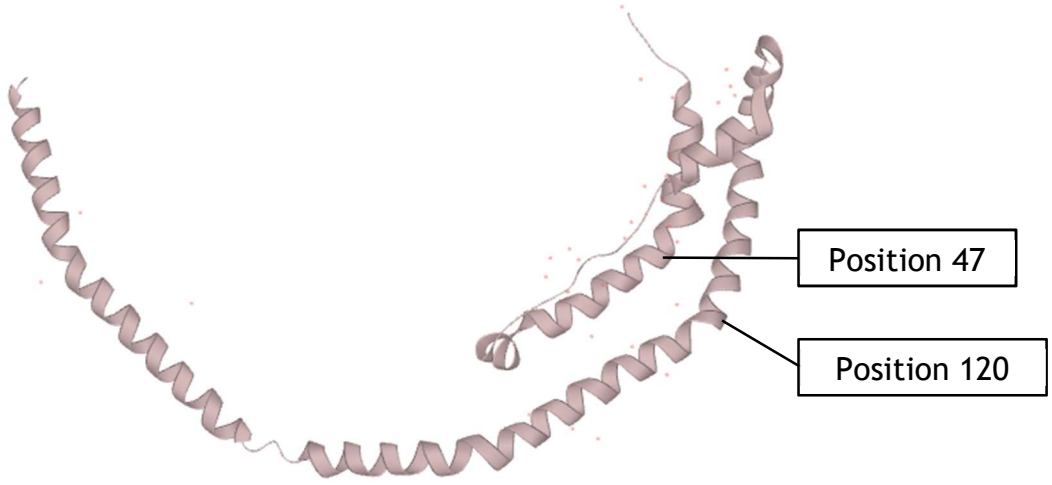

Figure 3-23 The structure of apoA-I with amino acid at position 47 and position 120 indicated The figure was modified from UniProt (Consortium 2020).

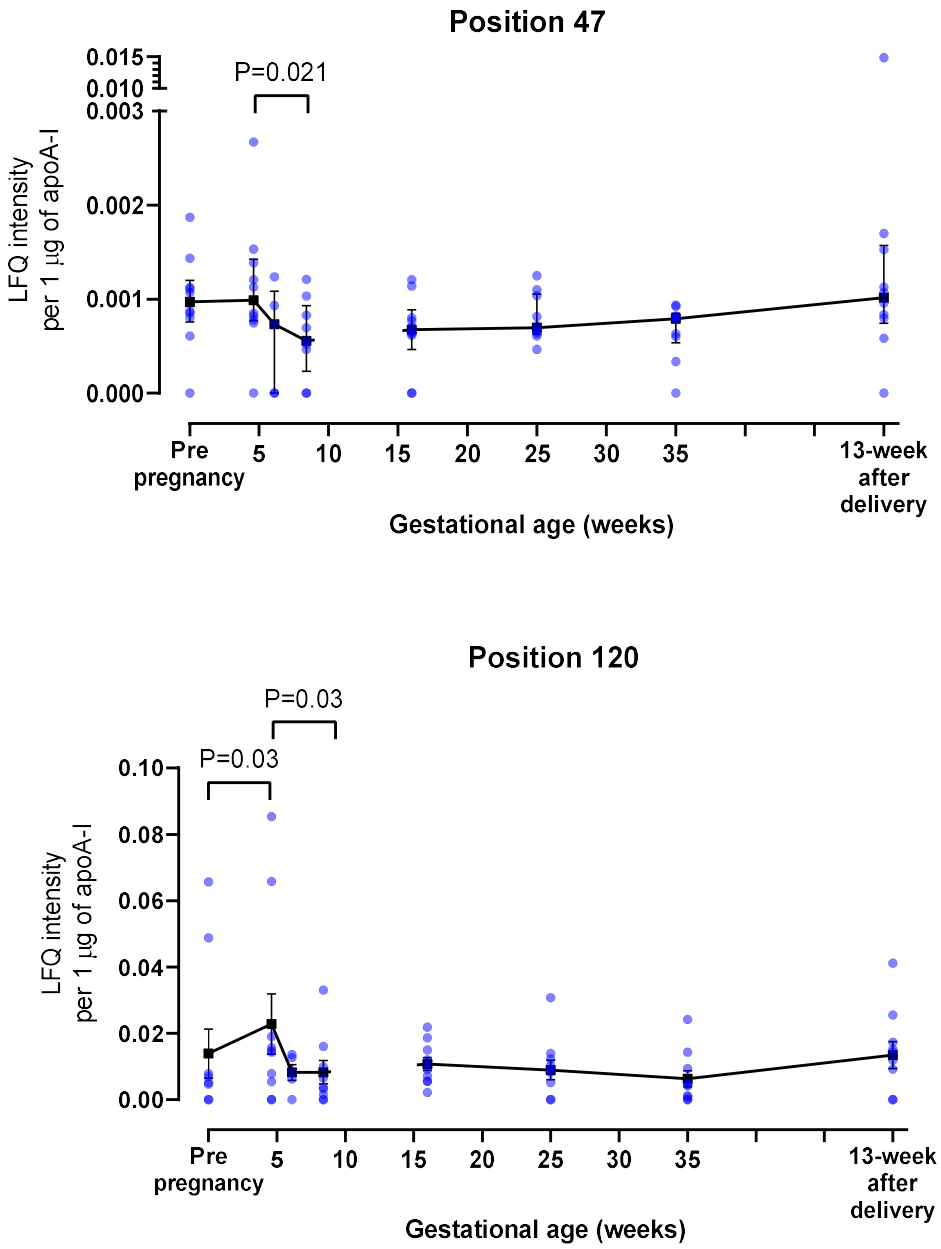

Figure 3-24 Ratio of glycated to non-glycated amino acid at position 47 and 120 on apoA-I throughout pregnancy (corrected for apoA-I concentration). Data is expressed as median±interquartile range. Friedman test followed by *post hoc* Wilcoxon signed rank test were carried out in each cohort separately and there is a discontinuous line between the two groups of participants. $p<0.05$ was taken as statistically significant.

3.3.7 ApoA-I methionine oxidation in HDL throughout gestation in healthy pregnancy

Oxidised methionine residues were identified in HDL samples throughout gestation at position 110, 136 and 172 (including pre- and pro-peptide) on the apoA-I protein (Figure 3-25). There was no significant difference between pre-pregnant and post-partum HDL in term of intensity of oxidised methionine and ratio of oxidised to non-oxidised methionine at all 3 positions. The intensity of oxidised methionine at these 3 positions on apoA-I did not significantly differ (Figure 3-26). The ratio of oxidised to non-oxidised methionine at position 110 and 172 on apoA-I also revealed no difference, while only the ratio at position 136 showed a significant increase at 13 weeks after delivery compared to 35 weeks of gestation (Figure 3-27).

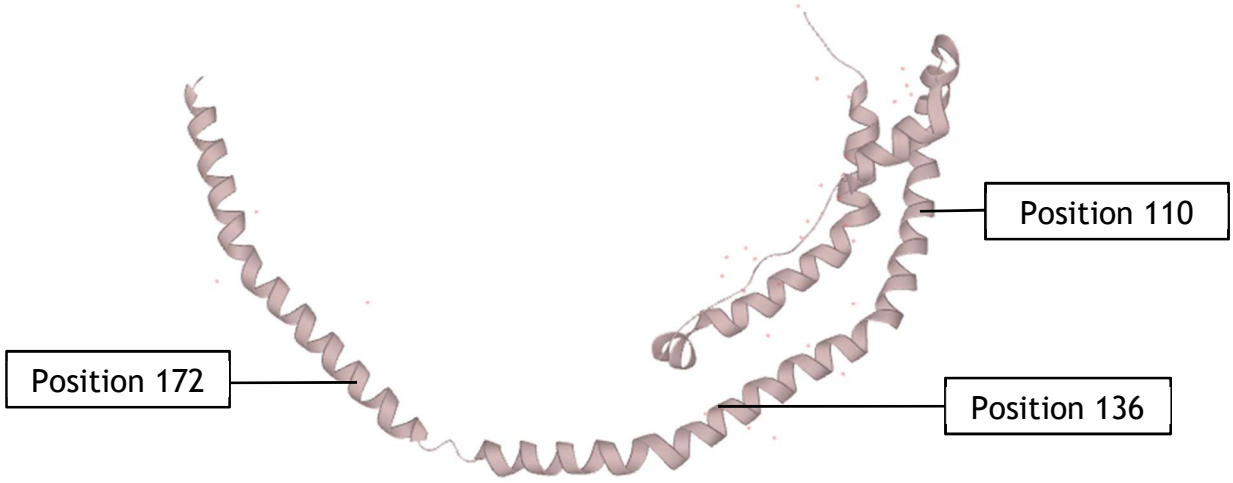

Figure 3-25 The structure of apoA-I with amino acid at position 110, 136 and 172 indicated The figure was modified from UniProt (Consortium 2020).

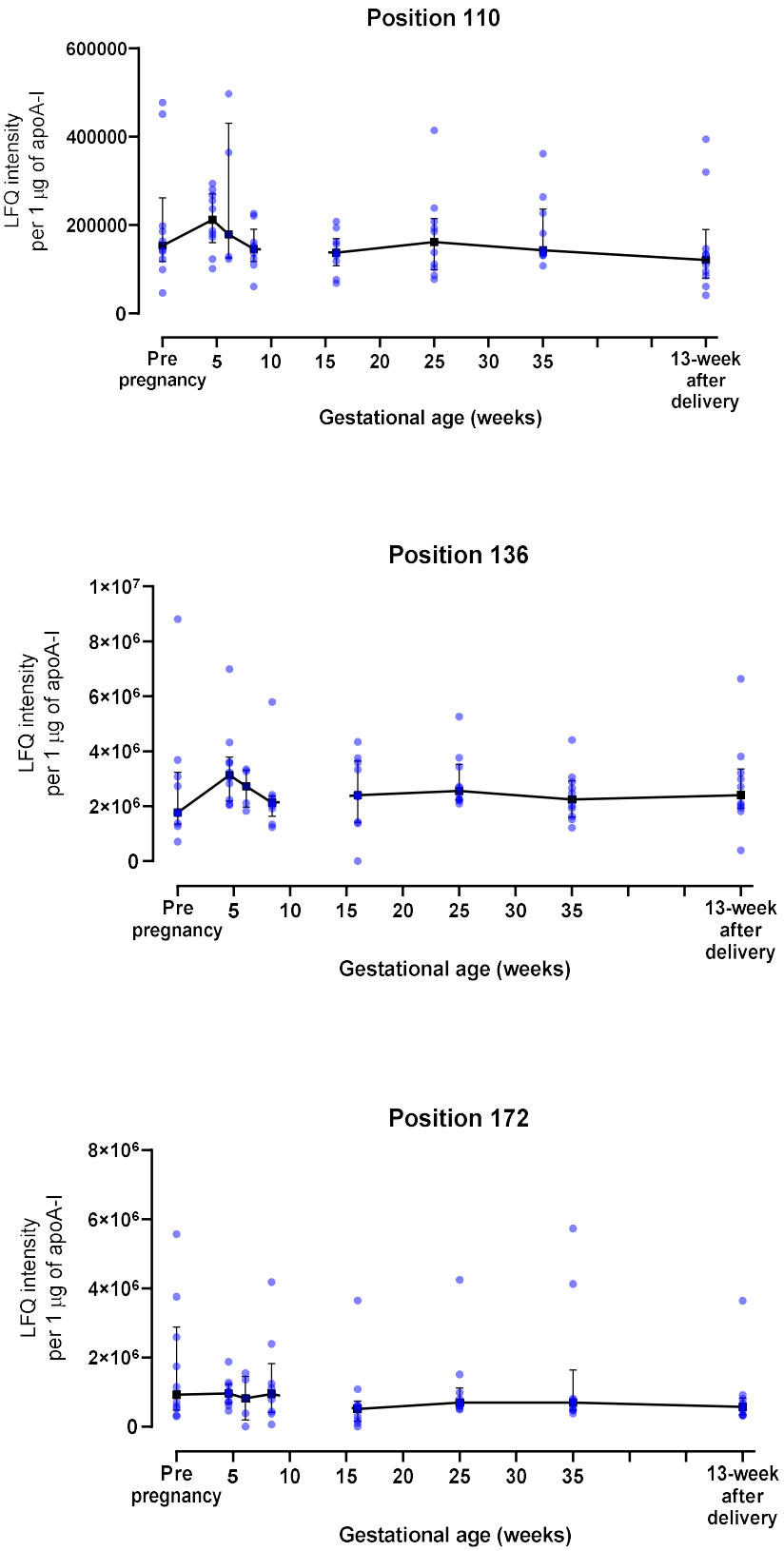

Figure 3-26 LFQ intensity of oxidised methionine residue at position 110, 136 and 172 of apoA-I throughout pregnancy (corrected for apoA-I concentration) Data is expressed as median±interquartile range. Friedman test followed by *post hoc* Wilcoxon signed rank test were carried out in each cohort separately and there is a discontinuous line between the two groups of participants. $p<0.05$ was taken as statistically significant.

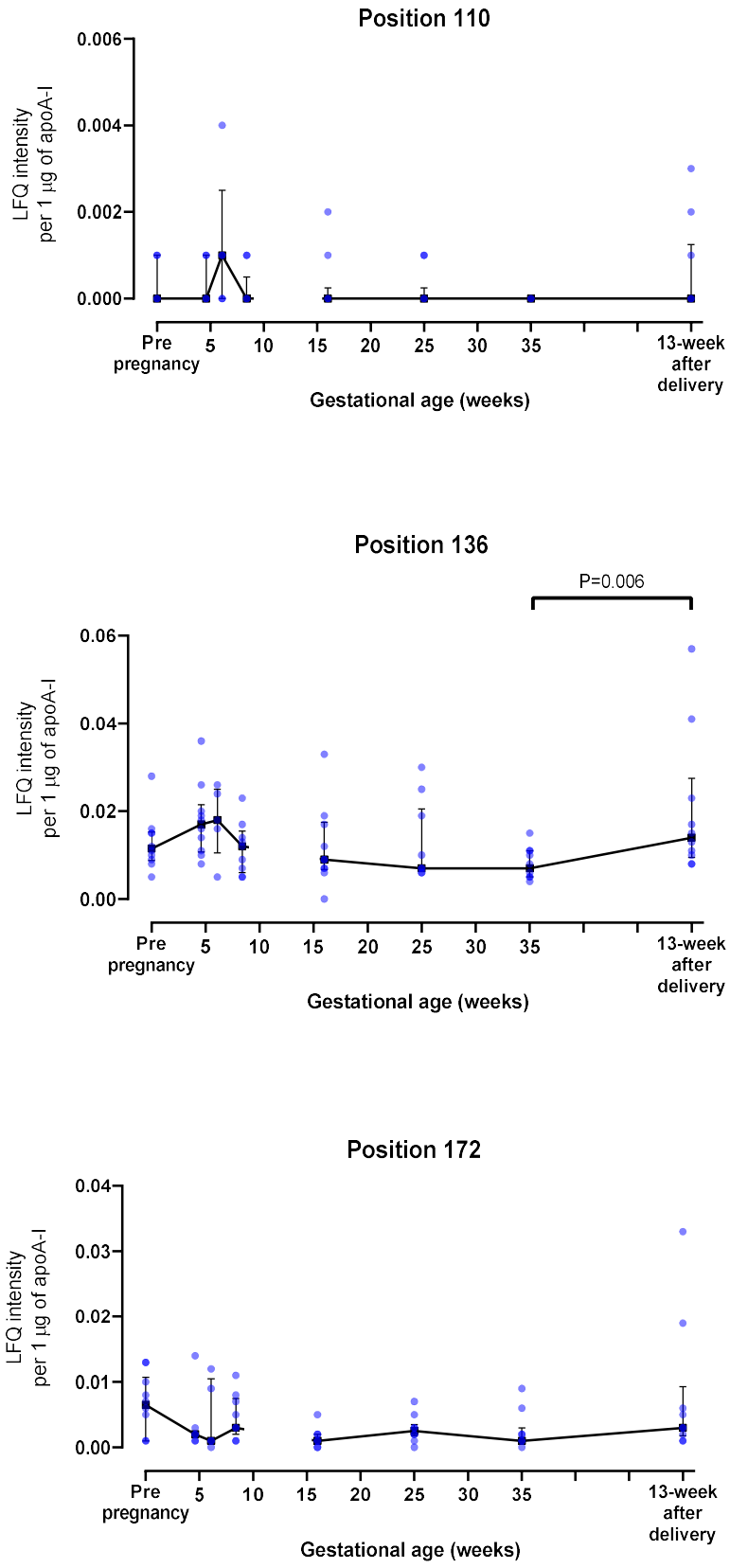

Figure 3-27 Ratio of oxidised to non-oxidised methionine residues at position 110, 136 and 172 of apoA-I throughout pregnancy (corrected for apoA-I concentration). Data is expressed in median±interquartile range. Friedman test followed by *post hoc* Wilcoxon signed rank test were carried out in each cohort separately and there is a discontinuous line between the two groups of participants. $p<0.05$ was taken as statistically significant.

3.3.8 SAA1 concentration in HDL throughout gestation in healthy pregnancy

There was no statistically significant difference of SAA1 concentration in HDL samples among pre-pregnancy, 4.6, 6.1, 8.4 weeks of gestation and 16, 25, 35 weeks of gestation and postpartum (Figure 3-28). Also, SAA1 concentration in HDL at pre-pregnancy and postpartum were not significantly different.

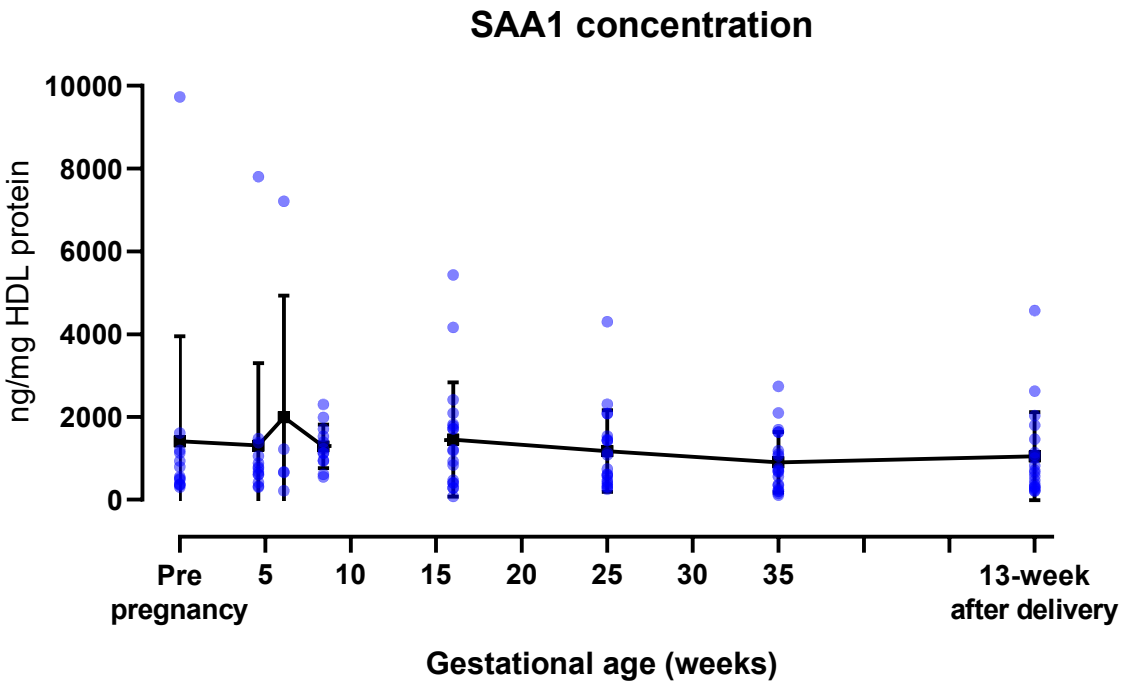

Figure 3-28 SAA1 concentration in HDL throughout gestation Data is expressed as mean±SD. Friedman test followed by *post hoc* Wilcoxon signed rank test were carried out in EPS study and repeated measures ANOVA with *post hoc* Tukey test were carried out in log-transformed data of LIPS study. There is a discontinuous line between the two groups of participants. $p<0.05$ was taken as statistically significant.

3.3.9 PON1 activity of HDL samples throughout pregnancy

The PON1 activity of HDL samples showed no significant difference between pre-pregnancy, 4.6, 6.1, 8.4 weeks of gestation and 16, 25, 35 weeks of gestation and postpartum (Figure 3-29). There was also no significant difference between PON1 activity of HDL samples at pre-pregnancy and postpartum. The ratio of SAA1 concentration to PON1 activity at postpartum was higher than at 35 weeks of gestation (Figure 3-30).

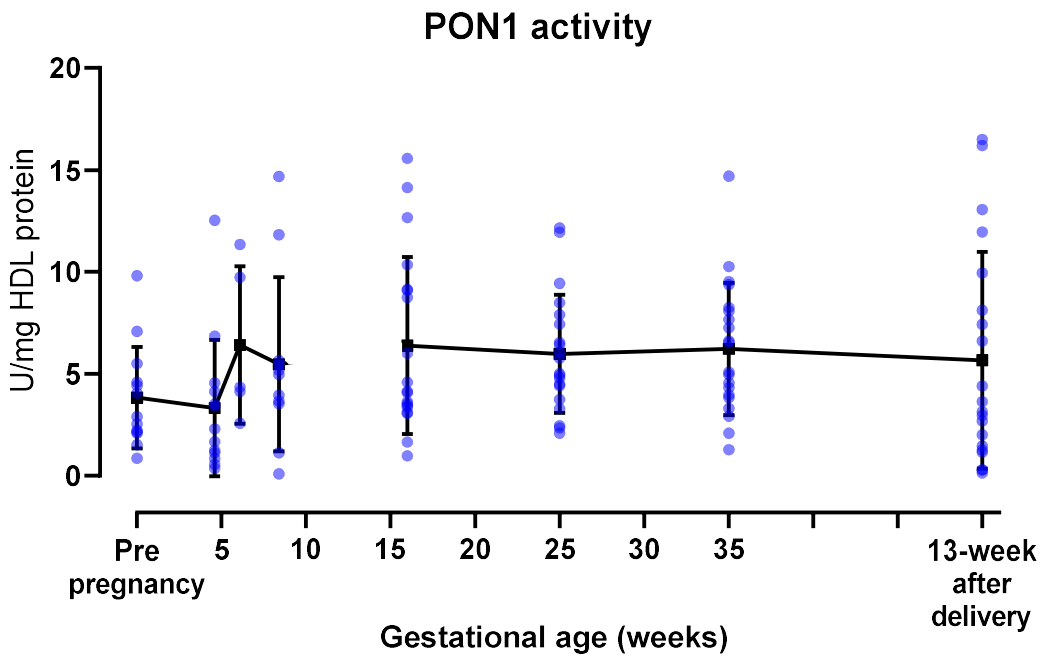

Figure 3-29 PON1 activity of HDL throughout gestation Data is expressed as mean±SD. Repeated measures ANOVA with *post hoc* Tukey test were carried out in square-root-transformed data of each cohort separately and there is a discontinuous line between the two groups of participants. $p<0.05$ was taken as statistically significant.

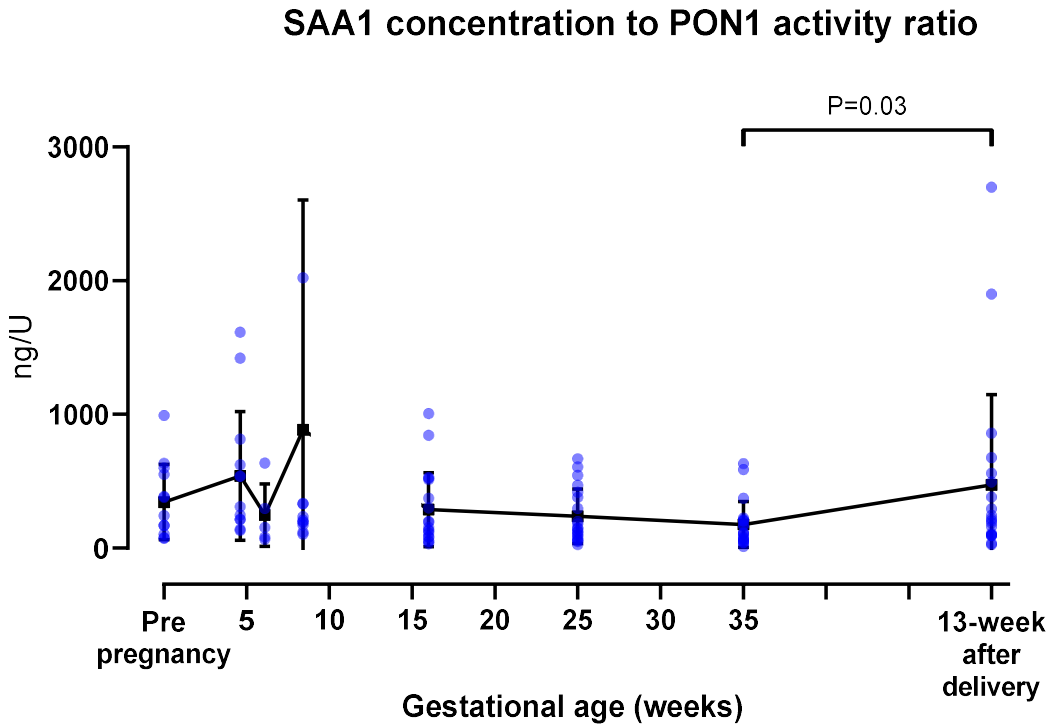

Figure 3-30 The ratio of SAA1 concentration to PON1 activity in HDL throughout gestation Data is expressed as mean±SD. Friedman test was carried out in EPS study and repeated measures ANOVA with *post hoc* Tukey test were carried out in log-transformed data of LIPS study. There is a discontinuous line between the two groups of participants. $p<0.05$ was taken as statistically significant.

3.4 Discussion

This chapter showed increased apoA-I in HDL of pregnant women in the second and third trimester. It may be inferred from the increased apoA-I concentration that overall HDL function including RCT, anti-inflammatory, antioxidant and vasodilation increased during pregnancy (Pankhurst et al. 2003; Zerrad-Saadi et al. 2009; Yuhanna et al. 2001; Garner et al. 1998). HDL apoA-I increased by around 30-40% while HDL cholesterol increased by only 20% during pregnancy. This is also reflected in reduced HDL cholesterol/apoA-I ratio in the second and third trimester of pregnancy. The HDL cholesterol/apoA-I ratio can be used as a surrogate for HDL size, being directly related to HDL particle size. The lower ratio as pregnancy progressed may imply the production of smaller HDL particles (Mazer et al. 2013). HDL particle size showed a positive correlation with major cardiovascular event in a population study (van der Steeg et al. 2008). Similarly, small HDL particle was inversely related to serum concentration of N-terminal pro-brain natriuretic peptide, a marker of heart failure, and high-sensitive cardiac troponin T, a marker of myocardial dysfunction (Duparc et al. 2020). Therefore, elevated HDL apoA-I concentration and reduced HDL cholesterol/apoA-I ratio may reflect smaller particle size and improved HDL functionality during pregnancy. However, inferring smaller HDL particle size from a decreased HDL cholesterol/apoA-I ratio is problematic as the apoA-I content of different HDL particles varies. Using this inference, the data presented here are inconsistent with the increased proportion of large HDL in late pregnancy demonstrated by various studies. HDL2b which is a larger HDL subfraction measured by gradient gel electrophoresis increased during the second and third trimester of pregnancy compared to the first trimester (Alvarez et al. 1996). Using nuclear magnetic resonance (NMR) spectroscopy to determine HDL size also showed increased diameter of overall HDL particles and increased concentration of large HDL in pregnancy compared to HDL from non-pregnant women (Melchior et al. 2021). HDL cholesterol/apoA-I ratio represents the core cholesterol volume relative to apoA-I and if the apo-A1 content of HDL is increased during pregnancy the ratio would suggest a smaller particle size. It could be that HDL particles in the second and third trimester of pregnancy have a different apoA-I content but does not necessarily cause a shift of HDL subfraction size from HDL2 or HDL3. It would be important to directly measure

HDL particle size in our samples to increase our understanding of the gestational changes in HDL size.

There was a significantly higher HDL apoA-I concentration during pregnancy, but not HDL cholesterol. HDL cholesterol historically has been used as a marker for HDL functionality with respect to RCT, one of the key protective properties of HDL. Many studies of HDL cholesterol in populations showed a negative relationship with cardiovascular risk (Gordon et al. 1977; Miller and Miller 1975). However, raising HDL cholesterol repeatedly failed to provide beneficial impact on cardiovascular outcome (Boden et al. 2011; Landray et al. 2014; Schwartz et al. 2012). Moreover, the protective properties of HDL include not only RCT, but also anti-inflammation, anti-oxidation, vasodilation, etc. Thus, HDL cholesterol alone may not reflect overall function of HDL in vascular protection and therefore my observation of no change throughout pregnancy does not mean that HDL function does not change. In most pregnant populations the increase in HDL cholesterol is of the order of 20-50% (Sulaiman et al. 2016; Fahraeus, Larsson-Cohn, and Wallentin 1985; Sattar, Greer, et al. 1997). It is likely that with the small sample size used in the present study, powered for the proteomics analysis, may have been underpowered to detect a difference in HDL cholesterol. The sample size for HDL cholesterol in pregnancy was calculated from an *a priori* power calculation based on a study by Alvarez et al. regarding HDL cholesterol concentration at the first and second trimester of healthy pregnancy. The standardised pooled SD of HDL cholesterol concentration of those two timepoints was 15. This suggested that n=12-15 women per group are required to achieve 80%-90% power at α=0.05 for a paired comparison of HDL cholesterol concentration in pregnancy.

There was a moderate change in HDL protein composition throughout pregnancy as HDL proteomic analysis showed that of the 63 HDL-associated proteins identified across gestation to the postpartum period, 16 proteins significantly differed in concentration throughout pregnancy. Multivariate modelling of all 63 identified HDL-associated proteins in pregnancy, adjusted for BMI and age, illustrated a gradual transition of HDL protein composition from pre-pregnancy, continuing throughout the first and second trimester, reaching the biggest transition in the third trimester of pregnancy. It was also clear that the protein

composition of HDL at 13 weeks after delivery reverted to the pre-partum HDL composition. This analysis provides evidence for a gestational change in HDL protein composition as part of the normal adaptation to pregnancy which reverts to a non-pregnant HDL composition after delivery and may reflect changes in overall HDL function as an element of the maternal adaptation to pregnancy.

HDL protein composition changes during pregnancy included changes in concentrations of apoC-II, apoC-III, apoC-IV and apoF which are all involved in plasma lipid metabolism. ApoC-III is known to interrupt triglyceride breakdown by inhibiting LPL, so diminished HDL apoC-III at 4.6 weeks of gestation could enhance LPL activity in triglyceride hydrolysis, resulting in reduced triglyceride concentration [reviewed in (Ooi et al. 2008; Kontush et al. 2015)]. Even though plasma triglyceride level at 4.6 weeks of gestation did not significantly differ from that at pre-pregnancy, lower apoC-III could contribute to enhancing plasma triglyceride breakdown to promote triglyceride accumulation in maternal peripheral tissue which is consistent with lipid accumulation in the first trimester of pregnancy (Catalano et al. 1998; Zamai et al. 2020). ApoC-III can inhibit TRL uptake by the liver and other tissues such as adipose tissue. Decreased apoC-III could then lead to TRL uptake in adipose tissue which is consistent with lipid accumulation stage in early pregnancy to provide energy for fetal growth later in pregnancy. HDL apoC-III is also associated with coronary artery disease risk whereby HDL with apoC-III was positively associated and HDL without apoC-III was negatively associated with coronary heart disease risk. While increased apoC-III content in HDL was revealed to impair the protective properties of HDL, including apoptosis of endothelial cells and RCT (Jensen et al. 2012; Riwanto et al. 2013; Luo et al. 2017). Thus, decreased apoC-III content in HDL may indicate improved HDL function in early pregnancy.

In the first trimester, HDL apoC-II content did not change. However, HDL apoC-II/apoC-III ratio decreased at 8.4 weeks of gestation. ApoC-II is an important LPL activator that displaces the lid region of the LPL protein and promotes triglyceride binding to the active site, leading to increased triglyceride breakdown (Hill et al. 1998; LaRosa et al. 1970). This ratio represents the balance of activation and inhibition of LPL activity by the apolipoprotein Cs. Reduction of this ratio may reflects a predominance of LPL inhibition over

activation maintaining plasma triglyceride levels at 8.4 weeks of gestation. Later on in pregnancy, the amount of HDL apoC-II, apoC-IV and the apoC-II/apoC-III ratio increased at 35 weeks of gestation which is consistent with increased plasma triglyceride concentration in late pregnancy (Potter and Nestel 1979). ApoC-IV can promote hypertriglyceridemia, probably by inhibiting VLDL uptake by the liver and promoting plasma VLDL accumulation (Allan and Taylor 1996). My proteomic findings suggest that apoC-IV and apoC-II both contribute to maternal hypertriglyceridemia in the third trimester and promote placental lipid transport to the fetus. The estimated fetal growth velocity reached a peak at 35 weeks of gestation (Grantz et al. 2018). After delivery, plasma triglyceride concentration continuously declined (Potter and Nestel 1979). ApoC-II and apoC-II/apoC-III ratio, but not apoC-IV, remained elevated at 13 weeks postpartum compared to 16 and 25 weeks of gestation. This suggests a role for apoC-II in reducing triglyceride concentration after delivery. ApoC-II may promote triglyceride breakdown to provide lipids for breast-feeding. The proteomics data presented here suggest a role for HDL in modulating maternal triglyceride metabolism through pregnancy and the post-natal period.

ApoF can inhibit CETP activity in transferring cholesteryl ester from HDL to TRL in exchange for triglyceride in the reverse direction, thus apoF inhibits enrichment of triglyceride in HDL, leading to an increased HDL retention time in plasma (Wang, Driscoll, and Morton 1999; Morton, Liu, and Izem 2019). Decreased HDL apoF content from 16 to 25 weeks of gestation is consistent with the observed second trimester peak in CETP activity and the increasing percent triglyceride content in HDL at 16 weeks of gestation that peaked at 35 weeks of gestation (Iglesias et al. 1994; Zamai et al. 2020). Triglyceride-rich HDL in the third trimester could facilitate HDL degradation, resulting in a decline in plasma HDL concentration which was found in pregnant women after the peak of plasma HDL concentration at 20 weeks of gestation (Sulaiman et al. 2016). Increased HDL apoF content at 13 weeks postpartum could lead to the decline in CETP activity and the decreased HDL triglyceride content postpartum (Iglesias et al. 1994; Potter and Nestel 1979). After delivery, the loss of estrogen-induced HDL synthesis would be expected to cause a reduction in plasma HDL concentration, however, HDL concentration postpartum remain unchanged from the third trimester and just starts to decline after 10 weeks postpartum (Sulaiman et al.

2016). This suggests that apoF may regulate CETP activity and triglyceride enrichment of HDL in order to regulate plasma HDL concentration in the third trimester and in the postpartum period.

Proteins with immunomodulatory activity also changed in HDL throughout pregnancy. It is noteworthy that the majority of immune system proteins that were altered in HDL during pregnancy were part of innate immunity rather than active in the adaptive immune system. Pregnant women are susceptible to infections including parasite infection. Increased HDL apoL-1 content during the first and third trimesters may support the maternal immune system against parasite infection during pregnancy. ApoL-I is a key protein related to the anti-parasitic activity of HDL (Pérez-Morga et al. 2005). It can form anion channels in the lysosomal membrane of *Trypanosoma brucei* and promote chloride influx resulting in lysosome swelling and lysis (Pérez-Morga et al. 2005). Also, CAMP which is known for its broad antimicrobial activity and for reducing bacterial product-induced inflammation increased in HDL during the second trimester, also potentially enhancing the maternal immune response against bacterial infection (Dürr, Sudheendra, and Ramamoorthy 2006).

The concomitant increase in four positive acute-phase-response proteins, SAA1, A1AT and fibrinogen α and ß chain and a decrease in apoA-IV, a negative acute phase reactant, detected in HDL by proteomics at 8.4 weeks of gestation are consistent with a dominant Th1 (pro-inflammatory) immune system in the first trimester to facilitate tissue remodelling in response to implantation and placentation. In the process of inflammation, pro-inflammatory cytokines not only induce inflammation, but also induce acute-phase reactant secretion to control and terminate inflammation. High concentrations of SAA has previously been found to remodel HDL to a greater size, higher density and relatively lower apoA-I content (Coetzee et al. 1986). SAA was found to impair the anti-inflammatory effect of HDL *in vitro*. HDL supplemented with SAA inhibited endothelial NO production and induced endothelial ROS production, leading to increased VCAM-1 expression on the endothelial cell surface (Zewinger et al. 2015). Non-pregnant individuals with elevated SAA also showed a positive relationship between higher HDL cholesterol concentration and increased cardiovascular mortality, in contrast to patients with low SAA that showed the

opposite association (Zewinger et al. 2015). These findings imply that increased HDL SAA content is pro-inflammatory. HDL proteomic analysis is a semi-quantitative measurement and the quantitative study of SAA1 in HDL by ELISA showed no significant change of SAA1 concentration throughout gestation. It can be interpreted that SAA1 protein level relative to all HDL proteins increased, but not the actual SAA1 concentration. Considering that HDL SAA1 concentration did not change throughout gestation, it may not have a role in enhancing Th1 dominance in the first trimester.

Other acute phase proteins are fibrinogen α and ß chains which can be converted to fibrin and form fibrin clots as part of the coagulation cascade. Elevated fibrinogen in HDL at 8.4 weeks of gestation parallels with hypercoagulable state that begins early in pregnancy. Thrombin generation, coagulation factor VIII, and plasma fibrinogen increased at 8.4 weeks of gestation (Bagot et al. 2017; Bagot et al. 2019). This result might support a role of HDL fibrinogen in promoting coagulation to contain tissue damage and promote tissue remodelling during placentation. With respect to inflammation, fibrinogen can modulate inflammation in both an enhancing and a suppressing way. Many fibrinogen derivatives can act as chemotactic agents for leukocytes and the fibrin network provides specific contact sites to promote macrophage migration, whereas high concentrations of fibrinogen can cause tight fibrin clot structure that reduces macrophage migration (Pillay et al. 2013; Hoppe 2014). Moreover, the specific form of fibrinogen might affect the action of fibrinogen toward inflammation. Immobilized fibrinogen is more likely to promote inflammation while soluble fibrinogen leans toward anti-inflammation (Pillay et al. 2013). However, no evidence exists regarding the role of HDL fibrinogen content in inflammation.

Another acute-phase response protein increased in HDL at 8.4 weeks of gestation was A1AT which is a serine protease inhibitor. A1AT has shown an anti-elastase activity and could have a role in protecting RCT function of HDL. Serine proteases such as neutrophil elastase are released in response to inflammatory stimuli and have been shown to affect HDL function. Incubation of macrophages isolated from neutrophil elastase-deficient mice with exogenous neutrophil elastase resulted in reduced ABCA1 protein expression in macrophages and reduced cholesterol efflux from macrophages to apoA-I (Wen et al. 2018). A1AT

binding to HDL was shown to be protected from oxidative deterioration of anti-elastase activity *in vitro* (Gordon et al. 2015). This suggests a role for A1AT in protecting HDL function from Th1 inflammatory state in early pregnancy. In addition, apoA-IV, a negative acute-phase reactant or protein that declines in an acute-phase response, has been shown to enhance RCT, anti-inflammation and inhibit platelet function (Peng and Li 2018). Even though HDL has anti-inflammatory effects in the non-pregnant population, the decrease in apoA-IV together with the increases of fibrinogen α and ß chains in HDL at 8.4 weeks of gestation illustrate HDL proteome changes that promote inflammation and coagulation in pregnancy and may negatively impact RCT. This latter function may be preserved in pregnancy by the increased A1AT content in HDL.

By the end of the third trimester, maternal Th1 immune system is dominant again to promote uterine contraction and delivery. Fewer proteins involved in the immune system changed in HDL during the third trimester compared to the first trimester. Apart from apoL-I mentioned earlier, AGP2, an acute-phase response protein, increased in HDL from 25 weeks of gestation to the postpartum period. This protein has both pro- and anti-inflammatory effects, for example, it can promote neutrophil aggregation at low concentration but inhibit their aggregation at high concentration [reviewed in (Hochepied et al. 2003)]. The net function of AGP2 is hard to predict and it is rather considered as a part of a wider system that modulates immune response [reviewed in (Hochepied et al. 2003)]. However, increased AGP2 in HDL in the third trimester may suggest that its pro-inflammatory effects may enhance uterine contraction and parturition.

Vitronectin which is known to inhibit the end step of all three pathways in the extracellular complement system (Figure 1-3) was found to progressively increase in HDL from 16 weeks to 25 and 35 weeks of gestation (Vikstedt et al. 2007). The complement system is part of innate immunity and is as important as inflammation in maintaining healthy pregnancy from conception to labour. Complement C3 has an embryotrophic activity and is required for normal placentation (Lee et al. 2004; Chow et al. 2009). There is also a role for complement C5a in myometrial contraction demonstrated by increased frequency of contraction of human myometrium strips incubated with C5a in myograph study (Gonzalez, Pedroni, and Girardi 2014). However, excessive

complement activation can cause pregnancy complications, such as preterm delivery. There was increased C5a levels in myometrium of a mouse model of preterm labor induced by vaginal administration of LPS, relative to age-matched control or term myometrium (Gonzalez, Pedroni, and Girardi 2014). Vitronectin inhibits complement activation by stopping the insertion of C5b, C6, C7, C8 and C9 into MAC, and also inhibits the main complement protein during parturition C5a which promotes uterine contraction and therefore may protect against preterm labor (Gonzalez, Pedroni, and Girardi 2014). To conclude, HDL proteome changes signal a significant role for HDL in mediating the pregnant immune system and inflammation in the first trimester and maintaining pregnancy in the third trimester.

HDL proteins involved in oxidation did not show any significant changes during pregnancy except for PON3 which decreased during the second and third trimester. This study showed that HDL PON1 arylesterase activity did not change throughout gestation which is consistent with another study that measured PON1 activity in plasma by paraoxon hydrolysis rates during pregnancy (Stefanović et al. 2012). However, a longitudinal study of plasma PON1 activity estimated by diazoxon hydrolysis rates did show a significant decrease during late pregnancy (32 and 38 weeks of gestation) compared to the first and second trimester (Stefanović et al. 2012). This could be due to different PON1 enzyme activities towards different substrates measured in the studies as described in section 1.4.3.2, chapter 1. SAA1 concentration to PON1 activity ratio increased at postpartum relative to at 35 weeks of gestation. This ratio has been proposed to be a marker of dysfunctional HDL [reviewed in (Kotani, Yamada, and Gugliucci 2013)]. SAA1 is pro-inflammatory and was shown to reduce anti-inflammatory function of HDL (Zewinger et al. 2015). A condition of increased SAA1 content and decreased PON1 activity in HDL could render HDL function toward reduced efficacy of anti-inflammatory and antioxidant effects. Increased SAA1 concentration to PON1 activity ratio at postpartum may reflect a functional-deficient HDL after delivery, compared to functional HDL in the third trimester.

In contrast to PON1, PON3 displays limited arylesterase activity and has no paraoxonase activity (Draganov et al. 2000). PON3 is an antioxidant enzyme that can protect LDL against oxidative damage. In the presence of purified rabbit

PON3, copper-induced LDL oxidation was delayed in a dose-dependent manner (Draganov et al. 2000). Decreased PON3 in HDL during the second and third trimester is consistent with decreased antioxidant activity and enhanced oxidative stress in late pregnancy (Stefanović et al. 2012). After delivery, prenylcysteine oxidase 1 decreased in HDL at 13 weeks after delivery. This result might suggest increased HDL antioxidant function resulting from reduced content of the pro-oxidant enzyme (prenylcysteine oxidase 1). However, the ratio of oxidised to non-oxidised Met136 of apoA-I increased at 13 weeks after delivery. Oxidation of Met136 was found to reduce the anti-oxidative properties of HDL but to enhance RCT *in vitro* (Cukier et al. 2017). Increased oxidised Met136 at postpartum might be the consequence of increased oxidative stress during pregnancy. The consequent reduction in anti-oxidative activity of HDL could be compensated by decreased prenylcysteine oxidase 1 activity postpartum. Furthermore, improved HDL-mediated RCT may be of paramount importance to remove excess cholesterol from macrophages and peripheral cells after delivery.

Lastly, angiotensinogen was the only protein involved in renin-angiotensin-aldosterone system that was found in pregnant HDL. HDL angiotensinogen was elevated at 8.4 weeks of pregnancy which is consistent with the increase in plasma angiotensinogen concentration at this gestation (Baker, Broughton Pipkin, and Symonds 1990). The renin-angiotensin-aldosterone system is activated as early as 6-8 weeks of gestation leading to increased plasma volume thereby helping to maintain blood pressure in early pregnancy [reviewed in (Sanghavi and Rutherford 2014)]. However, there is no evidence of angiotensinogen influencing HDL function so increased HDL angiotensinogen content may only reflect increased angiotensinogen concentration in plasma.

Moreover, this study found decreased glycation at position 47 and 120 of apoA-I at 8.4 weeks of gestation. HDL glycation is primarily induced by hyperglycemia, so, decreased glycated apoA-I found at 8.4 weeks of gestation is consistent with the transient increase in insulin sensitivity and reduced fasting plasma glucose level in the first trimester (Mills et al. 1998). Glycation of lysine residues at position 47 and 120 of apoA-I was found to associate with impaired reverse cholesterol efflux and anti-inflammatory effect of HDL (Liu et al. 2018; Domingo-Espin et al. 2018). The observed decreased glycated apoA-I at these

residues might imply improved RCT and anti-inflammatory function of HDL in the first trimester.

The strength of this study is that it is a longitudinal study from pre-conception to postpartum, allowing the study of HDL changes throughout gestation. Even though this study includes two independent longitudinal cohorts of pre-pregnancy to 8.4 weeks of gestation and 16 weeks of gestation to postpartum, participants from these two studies were matched with BMI, age, parity and smoking status. Also, comparisons of pre-pregnancy and postpartum results of HDL proteome (except for apoA-IV), apoA-I modification (methionine oxidation and glycation), apoA-I, cholesterol and SAA1 concentration, and PON1 activity showed no significant difference between pre-pregnancy and postpartum data. This suggests the comparability of these two groups of participants.

The limitation of this study is that the lab researcher was not blinded to the participant IDs which may cause the bias toward different groups of samples. However, all the measurements in this study was by objective assay, All samples were assayed in batches or during the same time period which reduced the bias. There is also a concern regarding the long-term stability of HDL in human plasma. HDL samples in this study were isolated from plasma in archival collections stored at -70ºC for up to 13 years which had never been thawed before. Previous studies demonstrated that HDL concentration isolated from serum stored at -70ºC for 10 and 13 years remained unchanged compared to those at baseline (Muzakova, Beekhof, and Jansen 2020; Yu et al. 2017). Another limitation is semi-quantitative measurement of proteomic approach in which it does not show an exact amount of protein, but a relative level of protein to all proteins in the samples in term of LFQ intensity. Identification and quantification of minor proteins can be interfered by the presence of higher abundance proteins, so some minor protein may not be detected by proteomic approach [reviewed in (Chandramouli and Qian 2009)]. With this in mind, HDL protein of interest could be quantified for a more precise outcome in the future experiment.

As proteomic analysis is a high throughput approach which detects a large number of proteins and as the data is presented as a relative value, the data contains a lot of zero values. Some minor proteins may be present in a few

samples but go undetected in others. For example, in this study, there was a total of 120 proteins detected in at least one HDL sample while only 63 proteins were identified in more than half of all HDL samples. To cope with data that contains a lot of zeros, it is difficult to obtain a normal distribution of data by taking logarithm or square root transformations. Therefore, all the proteomic data was treated as a non-parametric. In this study, treating proteomic data as a non-parametric data led to another limitation in which there were uneven numbers of samples at each timepoint in the EPS study and the Friedman test, the appropriate repeated measures non-parametric statistic test, cannot analyse groups with uneven numbers of samples. Thus, non-parametric data analysed by Friedman test was only from 9 women, each with 3 timepoints: before pregnancy (n=9), 4.6 weeks (n=9) and 8.4 weeks (n=9), instead of 4 timepoints: pre-pregnancy (n=10), 4.6 weeks (n=10), 6.1 weeks (n=5) and 8.4 weeks (n=9). An alternative statistical analysis could be carried by a mixed effects model which can cope with uneven numbers of samples so all 4 timepoints of samples can be included and the EPS and LIPS can be modelled together in the same analysis. The downfall of using ANOVA which is a parametric test to a non-normal distributed data is that there may be increased probability of a type I error (a false positive) (Wilcox and Keselman 2003). Comparison of the results from mixed effects model with *post hoc* Tukey test and Friedman test with *post hoc* Wilcoxon signed rank test showed similar results for significant changes in α-1-glycoprotein 2, angiotensinogen, apoA-IV, apoC-II, apoL-I, prenylcysteine oxidase 1 and vitronectin throughout gestation. While A1AT, apoC-III, apoC-IV, CETP, fibrinogen α and ß chain, SAA1 and PON3 lost their statistical significance in mixed effects model analysis. There were three additional proteins that showed their significant changes after mixed effects model, but not Friedman test. α-1-microglobulin was more abundance in HDL at 35 weeks compared to 6.1 weeks of gestation. ß-2-microglobulin was less abundant in HDL at 6.1 weeks of gestation compared to 4.6 weeks of gestation. The LFQ intensity of complement C4-A decreased at postpartum compared to 25 weeks of gestation.

Multiple pair-wise comparisons in this study can be a limitation as the probability of obtaining a type I error increases when performing multiple hypothesis tests on a set of data. Thus, there can be increased rate of statistically significant result by chance in this study. Bonferroni correction can be used to adjust p

values for a set of statistic tests to reduce the error rate. To test n hypotheses at once¸ significance level for each hypothesis should be 1÷n times of that for one comparison. In this study, p=0.05 was used originally for each hypothesis. Based on Bonferroni correction, p value for each hypothesis of proteomic data (63 proteins) comparison among three timepoints during early pregnancy (before pregnancy, 4.6 and 8.4 weeks of gestation) should be reduced to 0.05÷189 = 0.00026. The significance level for proteomic data among four timepoints in late pregnancy should be 0.05÷378 = 0.00013. Based on these readjusted p values, there was no significant difference in HDL proteome throughout gestation. The weakness of Bonferroni correction is that the interpretation of a result depends on the number of tests performed (Perneger 1998). Bonferroni correction can be very conservative especially when many tests or outcomes are being conducted (VanderWeele and Mathur 2019). Also, Bonferroni correction is less relevant when the outcome measured may not be independent of each other i.e. sets of proteins in HDL might change together, one protein might change if another protein changes. Another way to deal with multiple comparison may be looking at levels of significance ranking. Those with lowest p are results with greatest certainty.

In summary, this chapter demonstrated a significant transition of HDL protein composition throughout pregnancy. A possible contribution of HDL in maternal adaptation, especially lipid metabolism, has been shown. The changes of HDL protein content and modification during pregnancy also suggest improved RCT and anti-inflammatory function of HDL. It would be important to determine cholesterol efflux capacity and anti-inflammatory effect of HDL throughout gestation to confirm the relevance of HDL protein changes and to improve our understanding of HDL function in pregnancy. Lastly, this study suggests that HDL particle size could be smaller after the first trimester when the maternal-fetal circulation is established and may suggest the contribution of fully formed placenta to HDL vascular-protective function. It is necessary to measure HDL particle size throughout gestation to understand the certain HDL physiology during pregnancy.

4 Protein composition of HDL from pregnant women with preeclampsia

4.1 Introduction

Preeclampsia is a vascular complication of pregnancy defined as new onset hypertension with proteinuria or end-organ dysfunction. According to the World Health Organization, preeclampsia affects 2-8% of all pregnancies and contributes to 12% of maternal deaths. The pathophysiology of preeclampsia is heterogenous and can present as early-onset preeclampsia which is associated with poor placentation and fetal growth restriction, or late-onset preeclampsia which tends to be associated with maternal underlying diseases that predispose to vascular insufficiency (Tsatsaris et al. 2003; Raymond and Peterson 2011). Preeclampsia, particularly early-onset preeclampsia, is thought to result from abnormal development of the placenta including all steps from decidualization to spiral artery remodelling ultimately leading to placental ischemia (Maynard et al. 2003). On the other hand, the cause of late-onset preeclampsia is more likely to be an uteroplacental malperfusion at term, coupled with maternal predisposition to vascular inflammation, rather than disrupted placenta development [reviewed in (Staff 2019)]. Both pathways of abnormal placentation and placental malperfusion at term lead to oxidative stress of the syncytiotrophoblast and the release of antiangiogenic factors that disturb maternal endothelial function resulting in the clinical manifestation of preeclampsia.

There is aberrant lipid metabolism and an atherogenic pattern of lipoproteins with decreased HDL concentration in preeclampsia which potentially contributes to the endothelial dysfunction of preeclampsia. High plasma HDL concentration and function are associated with decreased cardiovascular risk and enhanced endothelial function in the non-pregnant as described in section 1.4, Chapter 1. HDL may also play a role in the healthy maternal adaptation to pregnancy (section 1.5 and 1.6, Chapter 1). Thus, the lower HDL concentrations observed in preeclampsia might suggest reduced vascular protection. In Chapter 3, I showed that there was also a change in HDL composition during pregnancy with several protein changes potentially associated with increased HDL function. HDL is well-recognized in the non-pregnant for its vascular protective function including

vasodilatory, anti-inflammatory, anti-thrombotic and anti-oxidative activities and these protective properties are often lost in pathological situations such as coronary heart diseases, metabolic syndrome and type 2 diabetes mellitus (Gordon et al. 1977; Khan et al. 2018; Wilson et al. 2007). In addition to a reduction in HDL concentration it is possible that HDL function is also adversely affected in preeclampsia. A combination of reduced concentration and decreased function would mean that HDL might fail to protect the maternal endothelium against the adverse lipid and inflammatory environment that comprises the maternal adaptation to pregnancy. In the absence of HDL's protection, endothelial dysfunction might be more likely to develop contributing to the clinical manifestation of preeclampsia.

This chapter aimed to compare the protein composition of HDL in the third trimester of preeclampsia and healthy pregnancy using the same proteomic approach as in Chapter 3. The third trimester of preeclampsia was selected due to clinical presentation of preeclampsia which mostly presents in the third trimester. Early- and late-onset preeclampsia tend to associate with different pathophysiology. HDL composition and function may also differ in early- and late-onset preeclampsia. Thus, HDL protein was compared between early-onset preeclampsia and its gestational-age-matched healthy pregnancy, and between late-onset preeclampsia and its gestational-age-matched healthy pregnancy. Glycation and methionine oxidation of apoA-I amino acids, which can compromise HDL functions such as RCT and anti-oxidation activity, were quantitated (Hoang et al. 2007; Shen et al. 2015; Shao et al. 2010). Preeclampsia and diabetes may share a common pathophysiology and HDL protein could be glycated. Pre-existing diabetes and gestational diabetes increase risk of preeclampsia [reviewed in (Weissgerber and Mudd 2015)]. Fructosyl-lysine (FL), the major early-stage protein glycation product, methylglyoxal-derived hydroimidazolone 1 (MG-H1) and carboxymethyl-lysine (CML), the major advance glycation end product (AGE) were determined for assessing glycation of HDL protein. Finally, HDL concentrations were assessed by apoA-I and cholesterol concentrations, and SAA1 concentration was measured as an acute inflammatory marker. PON1 activity was determined as a reflection of an antioxidant properties of HDL.

4.1.1 Hypotheses

- There is a change in protein composition of HDL from early-onset preeclampsia toward HDL dysfunction in protecting against oxidative stress and inflammation, compared to HDL from gestational-age-matched healthy pregnancy

- There is a change in protein composition of HDL from late-onset preeclampsia toward HDL dysfunction in removing excess cholesterol, compared to HDL from gestational-age-matched healthy pregnancy

4.1.2 Objectives

- To compare HDL protein composition, apoA-I concentration and modification, cholesterol and SAA1 concentration in HDL from early-onset preeclampsia with its gestational-age-matched healthy pregnant HDL

- To compare HDL protein composition, apoA-I concentration and modification, cholesterol and SAA1 concentration in HDL from late-onset preeclampsia with its gestational-age-matched healthy pregnant HDL

- As a validation exercise to identify difference in HDL protein composition, apoA-I concentration and modification, cholesterol and SAA1 concentration in third trimester HDL that result from preeclampsia *per se* independent of gestation of onset, the early- and late-onset preeclampsia groups were combined and compared to their combines with healthy pregnant HDL.

4.2 Methodology

4.2.1 Recruitment of healthy pregnant women and women with preeclampsia

Early-onset preeclampsia and its gestational-age-matched healthy pregnancy, and late-onset preeclampsia and its gestational-age-matched healthy pregnancy were recruited according to section 2.1.2, chapter 2. It should be noted that the gestation-matched control cohort of early-onset preeclampsia may not be

strictly healthy as it included pregnant women with preterm delivery (before 37 weeks of gestation).

4.2.2 Plasma preparation

Venous blood samples were obtained before delivery collected in chilled tubes containing EDTA as described by (Mistry et al. 2008). Plasma was stored at −80ºC until use.

4.2.3 HDL sample preparation

HDL was prepared from plasma according to the protocol in section 2.3, chapter 2. Desalted HDL fractions were then stored at -80ºC.

4.2.4 Proteomic analysis of HDL samples

HDL samples from early-onset preeclampsia, late-onset preeclampsia and their matching control groups were used for proteomics analysis. Isolation of HDL protein, nLC-MS/MS, methionine oxidation and OPLS-DA were carried out as described in section 2.4.2, chapter 2.

In this OPLS-DA, protein composition, BMI and age were assigned as variables. There were 3 sets of data models undertaken with 2 classes designated for each analysis.

1) Preeclampsia (early and late onset combined) and matched healthy pregnancy controls combined

2) Early-onset preeclampsia and their matched healthy pregnancy controls

3) Late-onset preeclampsia and their matched healthy pregnancy controls

Lastly, FL, MG-H1 and CML were searched as the modification variable in the mass spectrometry data. The intensity of glycated peptides and the ratio between glycated and non-glycated peptides were obtained from MaxQuant software.

4.2.5 Measurement of total cholesterol, apoA-I and SAA1 concentration in HDL

Total cholesterol, apoA-I and SAA1 concentrations were measured (according to section 2.4.3 and 2.4.5, chapter 2) in all HDL samples prepared from preeclampsia and healthy pregnancy.

4.2.6 General characteristics of women with early-onset preeclampsia and their gestation-matched healthy pregnant controls

Demographic data of early-onset preeclampsia women (n=11) and their gestational-age-matched healthy pregnancy controls (n=10) are shown in Table 4.1. Mean ages were 31.3 and 33.0 years for healthy pregnancy and early-onset preeclampsia, respectively. Early-onset preeclampsia women had a higher mean BMI of 31.9 kg/m^2 compared to the mean BMI of healthy pregnancy controls (24.6 kg/m^2) with p=0.026. Systolic and diastolic blood pressures at diagnosis of early-onset preeclampsia women were also higher than those of healthy pregnancy controls. Gestational age at delivery and baby birthweight were similar between the two groups.

Table 4.1 General characteristics of early-onset preeclampsia women and their matched healthy pregnancy controls

	Healthy Pregnancy (n=10)	Early-onset Preeclampsia (n=11)	p value
Age (years)	31.3(5.0)	33.0(5.2)	0.48
BMI (kg/m^2)	24.6(3.6)	31.9(8.3)	0.026
Caucasian	8(80%)	10(91%)	0.214
Non-smoker	7(70%)	9(82%)	0.635
Primiparous	1(10%)	8(73%)	0.008
Systolic blood pressure at diagnosis (mmHg)	115(20)	149(5)	<0.001
Diastolic blood pressure at diagnosis (mmHg)	71(9)	95(3)	<0.001

Gestational age at delivery (weeks)	33.6(2.1)	34.0(2.2)	0.67
Baby birthweight (g)	2087(565)	2111(663)	0.94
Male baby	4(40%)	9(82%)	0.080
Caesarean section	6(60%)	9(82%)	0.36

Note: Data was expressed as mean (SD)

4.2.7 PON1 arylesterase activity assessment

PON1 arylesterase activity of HDL samples from preeclampsia and healthy pregnant women was determined according to the protocol in section 2.4.6, chapter 2.

4.2.8 Statistical analysis

There were 3 analyses undertaken with 2 groups in each analysis.

1) Early-onset preeclampsia and its gestational-age-matched healthy pregnancy

2) Late-onset preeclampsia and its gestational-age-matched healthy pregnancy

3) Preeclampsia (early and late onset combined) and matched healthy pregnancy controls combined

Protein quantity output from proteomic analysis was expressed as LFQ intensity from the software and was considered as non-parametric data for statistical analysis because of its relative value. Mann-Whitney test were carried out to compare the difference of LFQ intensity median between 2 groups of samples in each protein. The glycation and methionine oxidation of apoA-I to apoA-I concentration ratio were also analysed using Mann-Whitney test for both intensity and the ratio between modified and unmodified peptides. Total cholesterol, apoA-I and SAA1 concentration data was checked for normal distribution using Ryan-Joiner test. Log- or square root transformation were applied to achieve normal distribution if necessary. Unpaired t-test was then

performed for parametric data and Mann-Whitney test was performed for non-parametric data. Minitab version 19 was used for statistical analysis.

4.3 Results

4.3.1 General characteristics of women with late-onset preeclampsia and their matched healthy pregnant controls

Mean age, BMI, gestational age and baby birthweight were similar between late-onset preeclampsia and healthy pregnancy (Table 4.2). Systolic and diastolic blood pressure at diagnosis of late-onset preeclampsia were significantly higher than those of healthy pregnancy with p <0.001 (Table 4.2).

Table 4.2 General characteristics of late-onset preeclampsia and its matched healthy pregnancy

	Healthy Pregnancy (n=10)	Late-onset Preeclampsia (n=9)	p value
Age (years)	30.1(5.7)	27.6(5.0)	0.34
BMI (kg/m^2)	27.7(6.2)	29.7(3.6)	0.43
Caucasian	10 (100%)	9 (100%)	1.00
Non-smoker	8 (80%)	9 (100%)	0.47
Primiparous	4 (40%)	4 (44%)	1.00
Systolic blood pressure at diagnosis (mmHg)	119(9)	146(4)	<0.001
Diastolic blood pressure at diagnosis (mmHg)	68(7)	94(3)	<0.001
Gestational age at delivery (weeks)	38.9(0.6)	38.5(1.6)	0.56
Baby birthweight (g)	3350(420)	3138(667)	0.45
Male baby	6 (60%)	3 (33%)	0.37
Caesarean section	5 (50%)	4 (44%)	1.00

Note: Data was expressed as mean (SD).

4.3.2 General characteristics of healthy pregnant women and women with preeclampsia

Mean maternal age, gestational age and baby birthweight of the combined preeclampsia and combined healthy pregnancy groups were similar with maternal ages of 30.6 and 30.7 years old, gestational ages of 36.1 and 36.2 weeks, and baby birthweight of 2573 and 2718 g for preeclampsia and healthy pregnancy, respectively (Table 4.3). The mean BMI of the preeclampsia group was 30.9 kg/m^2 which was significantly higher than the mean BMI of the healthy pregnancy group (26.2 kg/m^2) with p=0.013 (Table 4.3). Systolic and diastolic blood pressure at diagnosis of preeclampsia were both significantly higher than those of healthy pregnancy (p value <0.001). Mean blood pressures were 148/95 and 117/70 mmHg for preeclampsia and healthy pregnancy, respectively (Table 4.1). Other demographic data for combined preeclampsia and healthy pregnancy groups including ethnicity, smoking status, parity, baby gender and mode of delivery are shown in Table 4.3.

Table 4.3 General characteristics of healthy pregnancy and preeclampsia

	Healthy Pregnancy (n=20)	Preeclampsia (n=20)	p value
Age (years)	30.7(5.4)	30.6(5.8)	0.93
BMI (kg/m^2)	26.2(5.3)	30.9(6.7)	0.013
Caucasian	18 (90%)	19 (95%)	0.49
Non-smoker	15 (75%)	18 (90%)	0.41
Primiparous	5 (25%)	12 (60%)	0.054
Systolic blood pressure at diagnosis (mmHg)	117(16)	148(5)	<0.001
Diastolic blood pressure at diagnosis (mmHg)	70(8)	95(3)	<0.001
Gestational age at delivery (weeks)	36.2(3.1)	36.1(3.0)	0.85
Baby birthweight (g)	2718(804)	2573(839)	0.59
Male baby	10 (50%)	12 (60%)	0.75

Caesarean section	11 (55%)	13 (65%)	0.75

Note: Data was expressed as mean (SD).

4.3.3 Total cholesterol and apoA-I concentration in HDL samples

There was no significant difference in apoA-I and cholesterol concentration in HDL between, early-onset preeclampsia and matched controls, late-onset preeclampsia and matched controls, and combined preeclampsia and healthy pregnancy (Figure 4-1 and 4-2). There was no significance difference in the ratio of cholesterol to apoA-I concentration between early- or late-onset preeclampsia and their matched controls, while this ratio was significantly lower in HDL from combined preeclampsia than in HDL from combined healthy pregnancy (Figure 4-3).

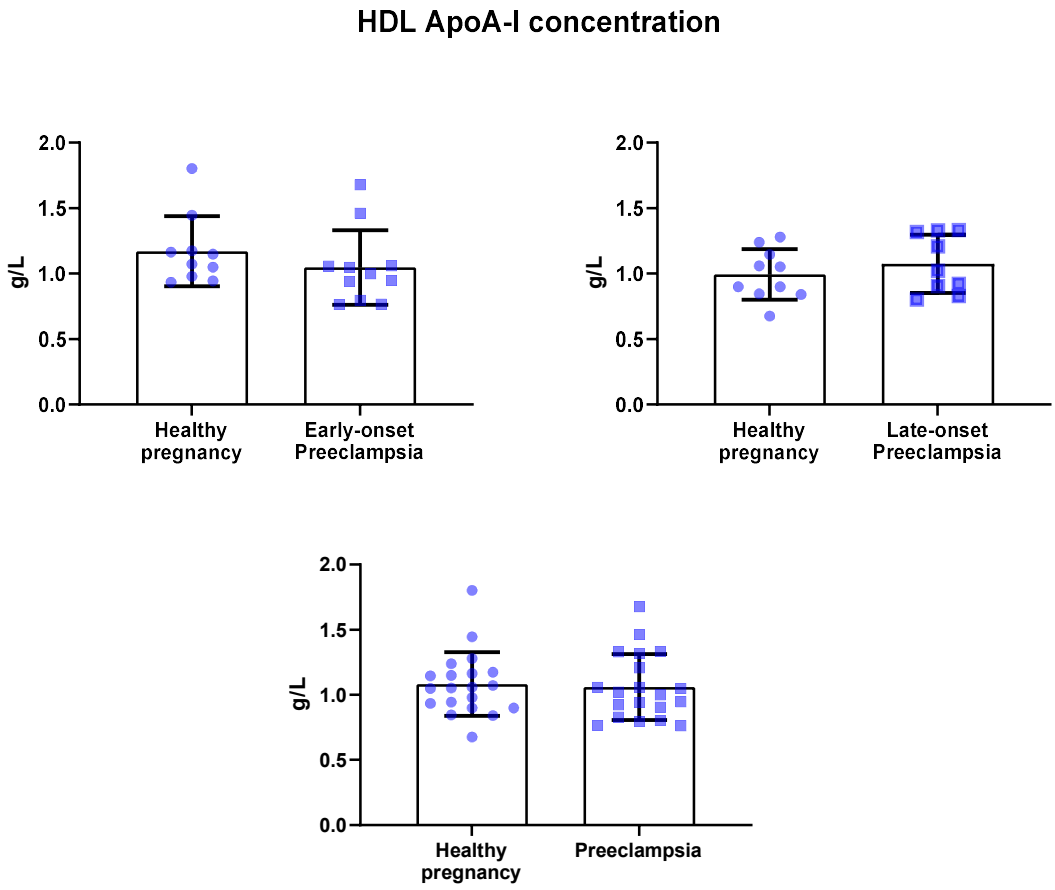

Figure 4-1 ApoA-I concentration in HDL of healthy pregnancy and preeclampsia: Data is expressed as mean±SD. Unpaired t-test was carried out in log transformed apoA-I concentration between preeclampsia and healthy pregnancy (below), and early-onset preeclampsia and its control (left above). Comparison of apoA-I concentration between late-onset preeclampsia and its control (right above) was carried out on raw data by unpaired t-test. $p<0.05$ was taken as statistically significant.

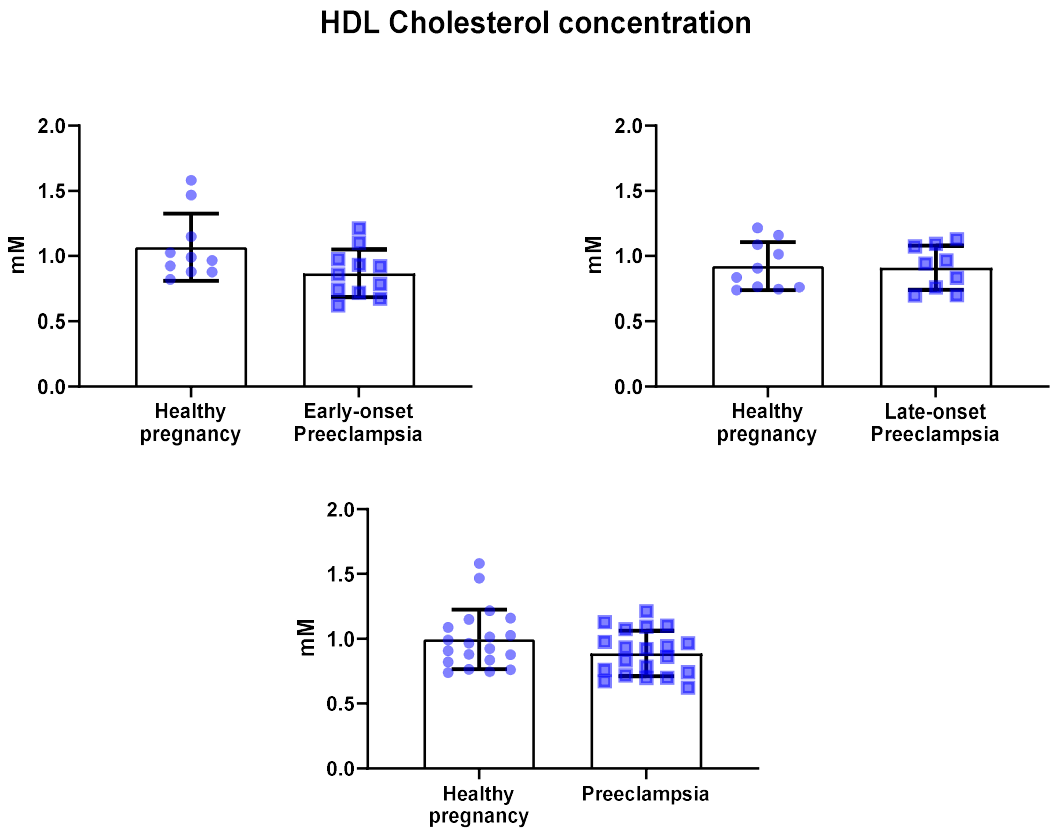

Figure 4-2 Cholesterol concentration in HDL of healthy pregnancy and preeclampsia: Data is expressed as mean±SD. Comparison of cholesterol concentration between early-onset preeclampsia and its control (left above), and between late-onset preeclampsia and its control (right above) were carried out on raw data by unpaired t-test. Unpaired t-test was carried out on log transformed cholesterol concentration between preeclampsia and healthy pregnancy (below). $p<0.05$ was taken as statistically significant.

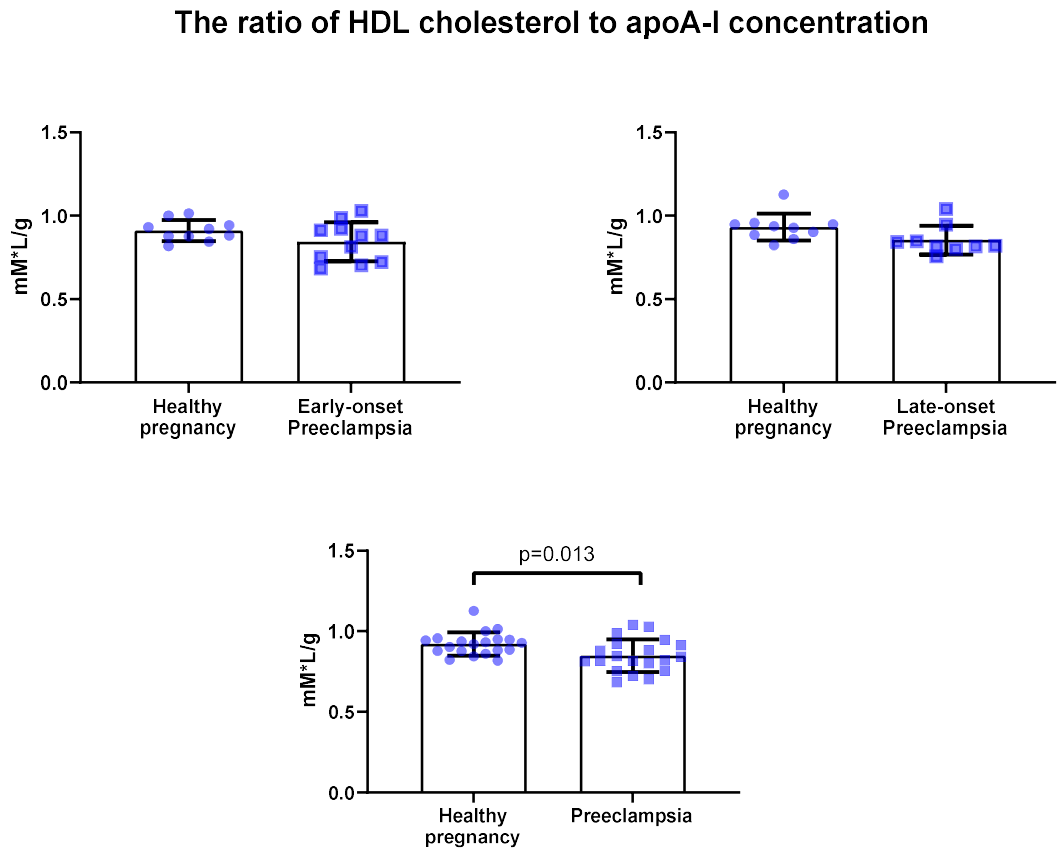

Figure 4-3 The ratio of cholesterol to apoA-I concentration in HDL of healthy pregnancy and preeclampsia: Data is expressed as mean±SD. Unpaired t-test was carried out to compare this ratio between early-onset preeclampsia and its control (left above), late-onset preeclampsia and its control (right above), and preeclampsia and healthy pregnancy (below). $p<0.05$ was taken as statistically significant.

4.3.4 HDL protein composition in early-onset preeclampsia compared to healthy pregnancy

There were 6 proteins with a significantly different LFQ intensity between early-onset preeclampsia HDL and gestation matched healthy pregnancy HDL including apoA-IV, L-selectin, peroxtredoxin-2, zinc-α-2-glycoprotein, ß-2-microglobulin and Ras-related protein (Rap-1b). The LFQ intensities of apoA-IV and L-selectin were lower specifically in early-onset preeclampsia HDL than in their matched control HDL, while there was no significant difference between combined preeclampsia and combined healthy pregnancy group (Figure 4-4 and 4-5). The LFQ intensities of peroxiredoxin-2 and zinc-α-2-glycoprotein were lower in early-onset preeclampsia HDL than in their matched control HDL and were lower in combined preeclampsia than in combined healthy pregnancy group (Figure 4-6 and 4-7). ß-2-microglobulin and Rap-1b were higher in early-onset preeclampsia

HDL than in their matched control HDL and were higher in combined preeclampsia than in combined healthy pregnancy group (Figure 4-8 and 4-9).

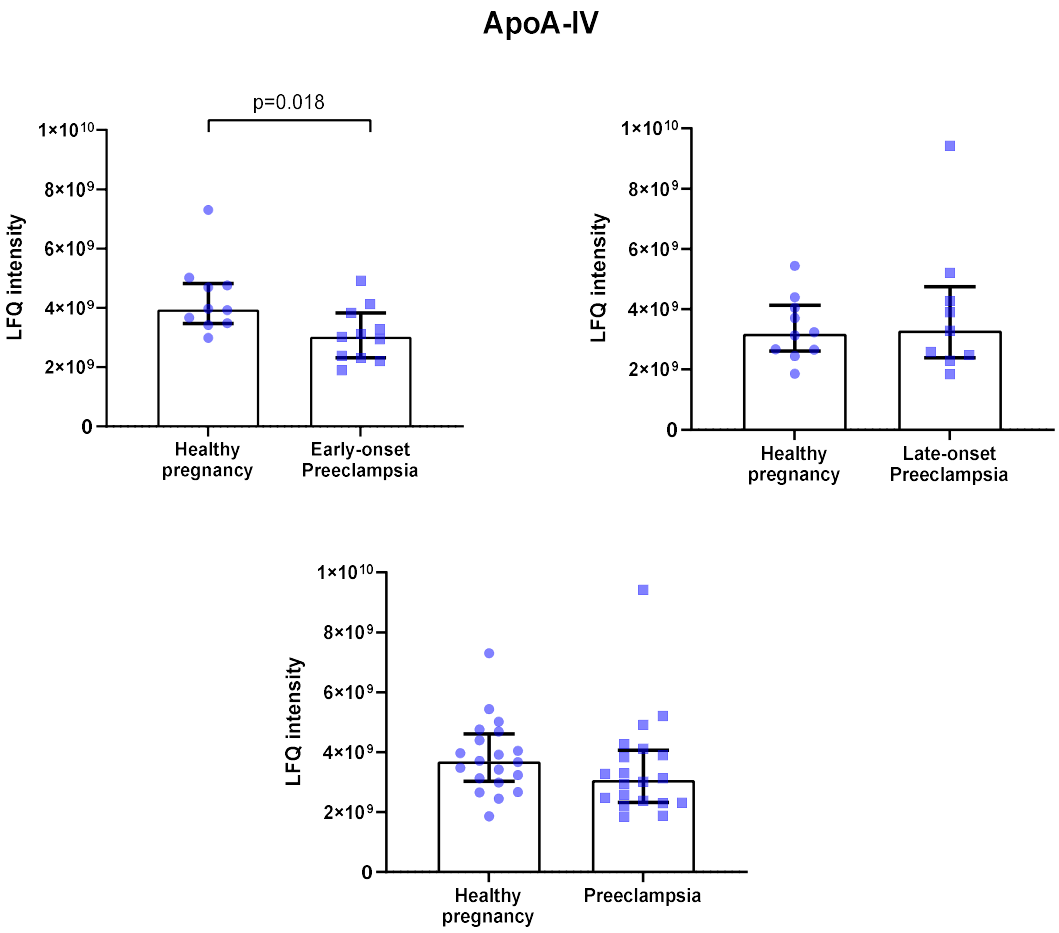

Figure 4-4 LFQ intensity of apoA-IV of healthy pregnancy and preeclampsia: Data was expressed as median±interquartile range. Mann-Whitney tests were carried out to compare the data between early-onset preeclampsia HDL and gestation matched controls (left above), late-onset preeclampsia HDL and gestation matched controls (right above), and preeclampsia HDL and gestation matched healthy pregnancy HDL (below). $p<0.05$ was taken as statistically significant.

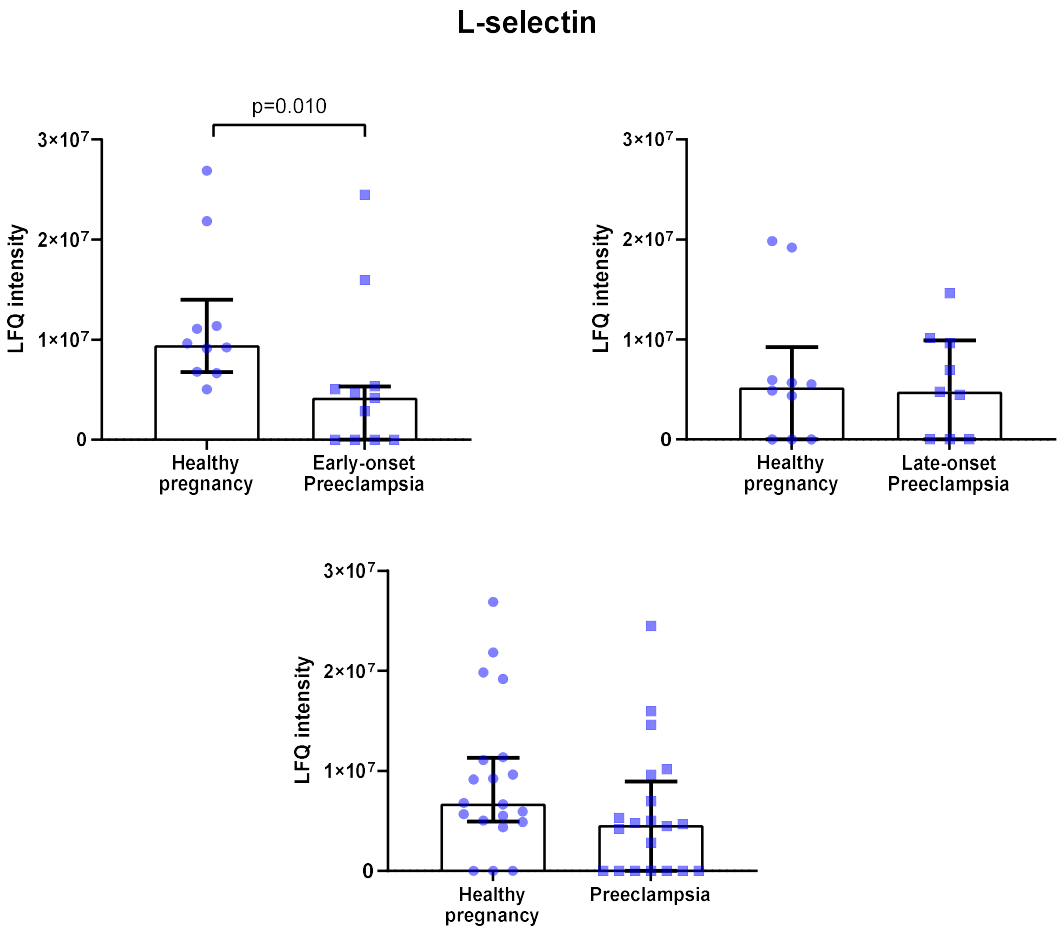

Figure 4-5 LFQ intensity of L-selectin of healthy pregnancy and preeclampsia: Data was expressed as median±interquartile range. Mann-Whitney tests were carried out to compare the data between early-onset preeclampsia HDL and gestation matched controls (left above), late-onset preeclampsia HDL and gestation matched controls (right above), and preeclampsia HDL and gestation matched healthy pregnancy HDL (below). $p<0.05$ was taken as statistically significant.

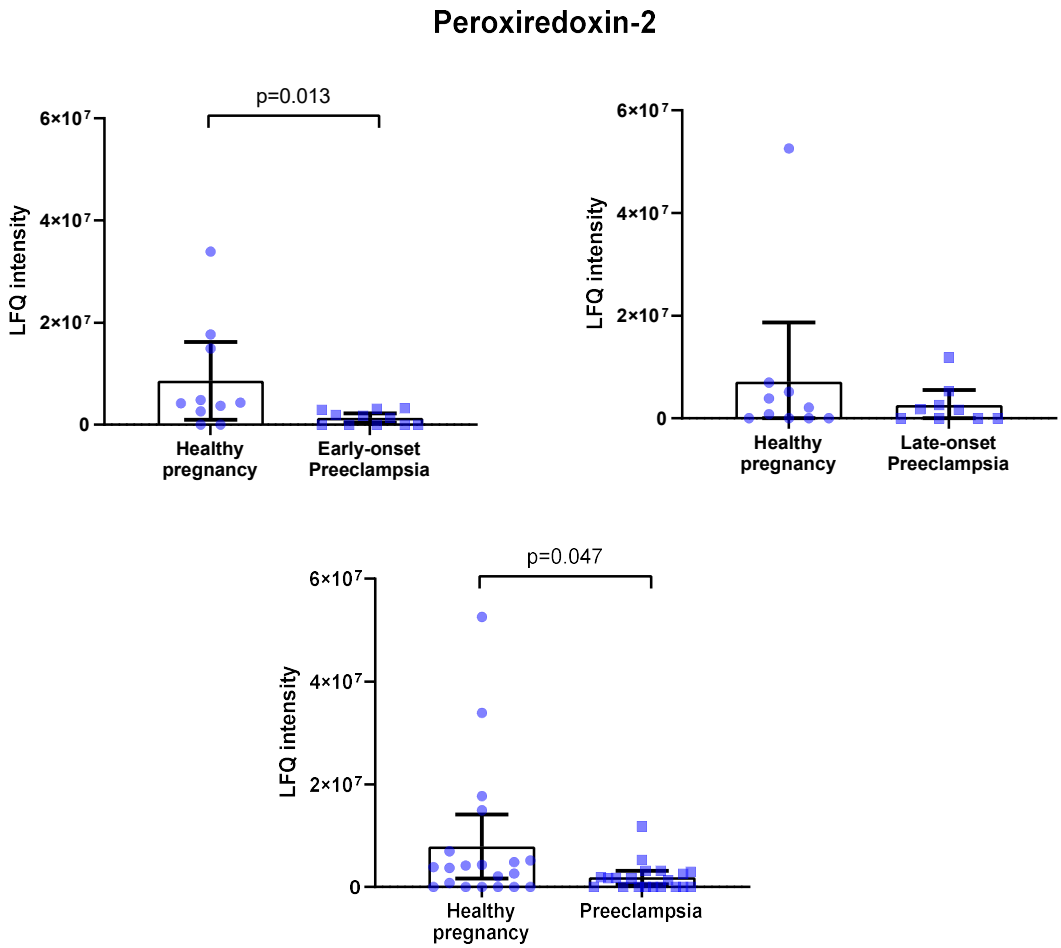

Figure 4-6 LFQ intensity of peroxiredoxin-2 of healthy pregnancy and preeclampsia: Data was expressed as median±interquartile range. Mann-Whitney tests were carried out to compare the data between early-onset preeclampsia HDL and gestation matched controls (left above), late-onset preeclampsia HDL and gestation matched controls (right above), and preeclampsia HDL and gestation matched healthy pregnancy HDL (below). $p<0.05$ was taken as statistically significant.

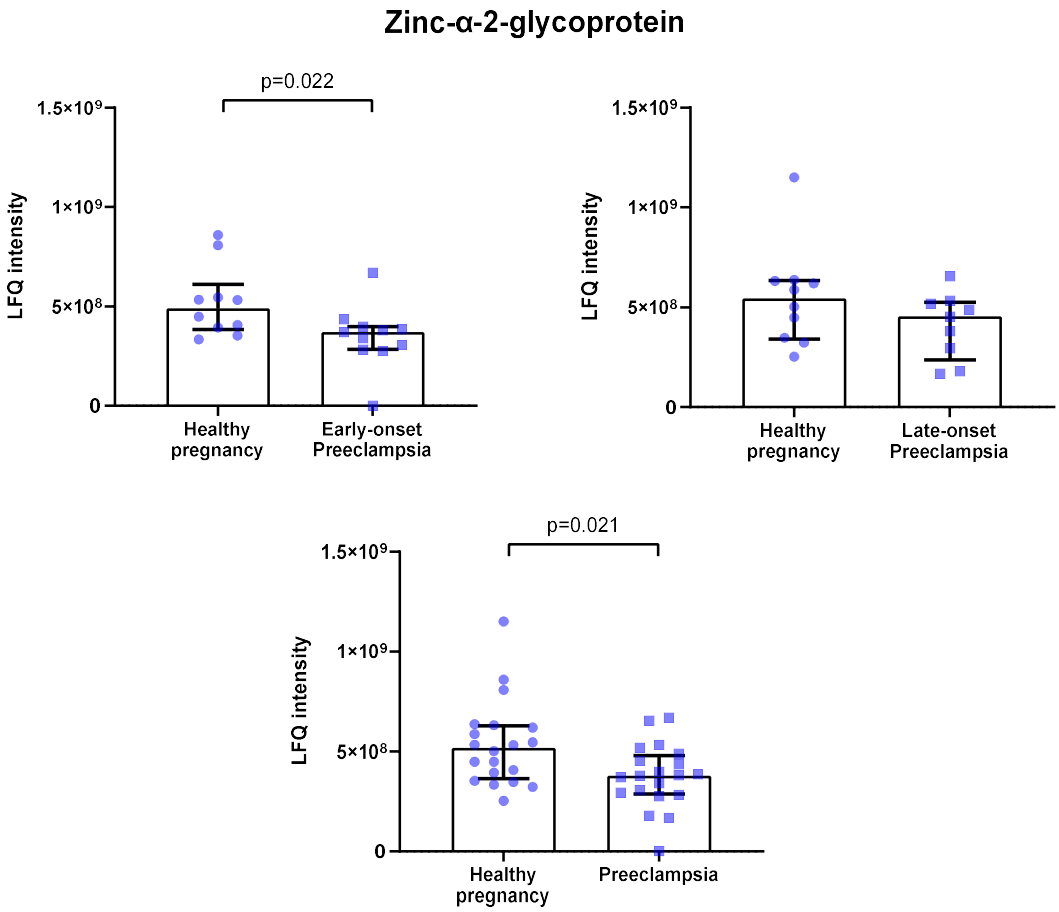

Figure 4-7 LFQ intensity of zinc-α-2-glycoprotein of healthy pregnancy and preeclampsia: Data was expressed as median±interquartile range. Mann-Whitney tests were carried out to compare the data between early-onset preeclampsia HDL and gestation matched controls (left above), late-onset preeclampsia HDL and gestation matched controls (right above), and preeclampsia HDL and gestation matched healthy pregnancy HDL (below). $p<0.05$ was taken as statistically significant.

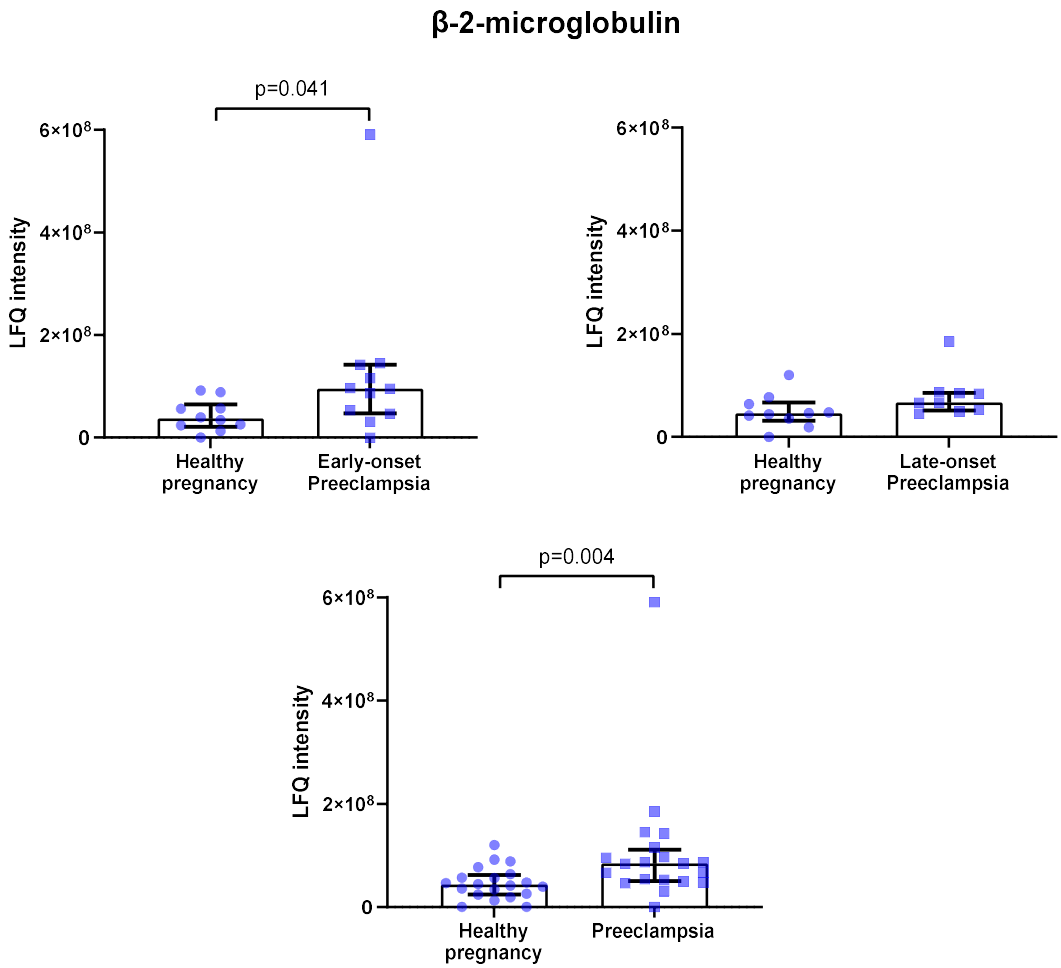

Figure 4-8 LFQ intensity of β-2-microglobulin of healthy pregnancy and preeclampsia: Data was expressed as median±interquartile range. Mann-Whitney tests were carried out to compare the data between early-onset preeclampsia HDL and gestation matched controls (left above), late-onset preeclampsia HDL and gestation matched controls (right above), and preeclampsia HDL and gestation matched healthy pregnancy HDL (below). $p<0.05$ was taken as statistically significant.

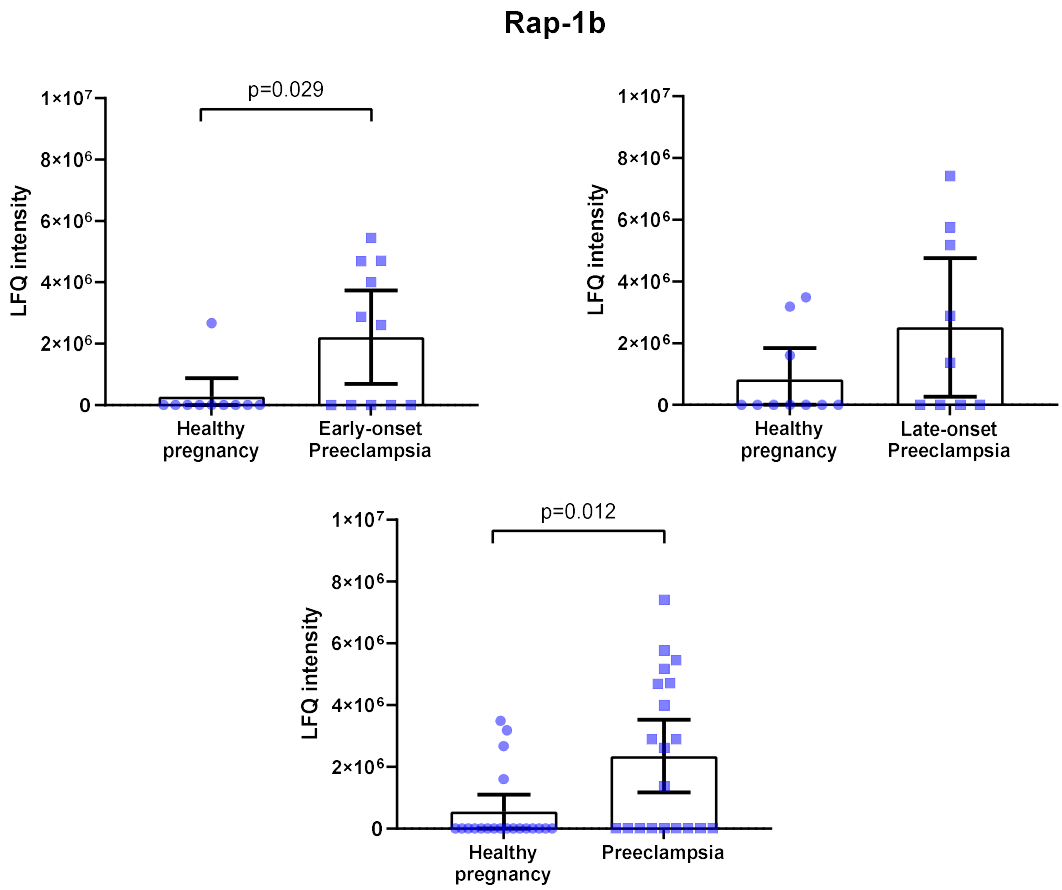

Figure 4-9 LFQ intensity of Rap-1b of healthy pregnancy and preeclampsia: Data was expressed as median±interquartile range. Mann-Whitney tests were carried out to compare the data between early-onset preeclampsia HDL and gestation matched controls (left above), late-onset preeclampsia HDL and gestation matched controls (right above), and preeclampsia HDL and gestation matched healthy pregnancy HDL (below). $p<0.05$ was taken as statistically significant.

4.3.5 HDL protein composition in late-onset preeclampsia and gestation matched healthy pregnancy

There were 14 proteins exhibited significant different LFQ intensity between late-onset preeclampsia and healthy pregnancy. The LFQ intensities of BPI fold-containing family B member 1 and protease C1 inhibitor were significant lower in late-onset preeclampsia HDL than in their matched control HDL, but there was no difference between combined preeclampsia and combined healthy pregnancy group (Figure 4-10 and 4-11). The LFQ intensity of myosin-9 was higher specifically in late-onset preeclampsia HDL than in their matched control HDL, while there was no significant difference between combined preeclampsia and combined healthy pregnancy group (Figure 4-12). Antithrombin, ß-2-glycoprotein 1, complement C9 and prothrombin had lower LFQ intensities in late-onset

preeclampsia HDL than in their matched control HDL and had lower LFQ intensities in combined preeclampsia than in combined healthy pregnancy group (Figure 4-13 to 4-16). ApoC-III, complement factor D, collagen α-1 chain, keratinocyte differentiation-associated protein, LCAT, PLTP and ribonuclease pancreatic had higher LFQ intensities in late-onset preeclampsia HDL compared to healthy pregnant HDL and had higher LFQ intensities in combined preeclampsia than in combined healthy pregnancy group (Figure 4-17 to 4-23).

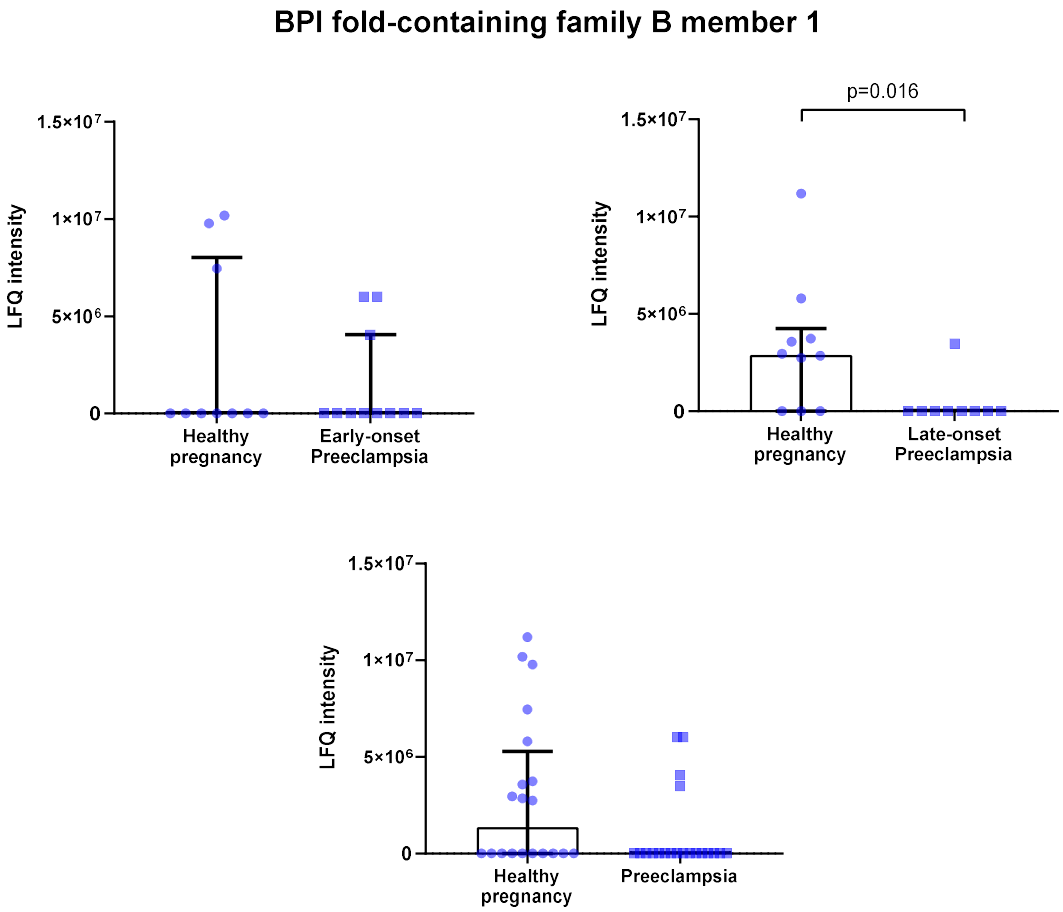

Figure 4-10 LFQ intensity of BPI-fold containing family B member 1 of healthy pregnancy and preeclampsia: Data was expressed as median±interquartile range. Mann-Whitney tests were carried out to compare the data between early-onset preeclampsia HDL and gestation matched controls (left above), late-onset preeclampsia HDL and gestation matched controls (right above), and preeclampsia HDL and gestation matched healthy pregnancy HDL (below). $p<0.05$ was taken as statistically significant.

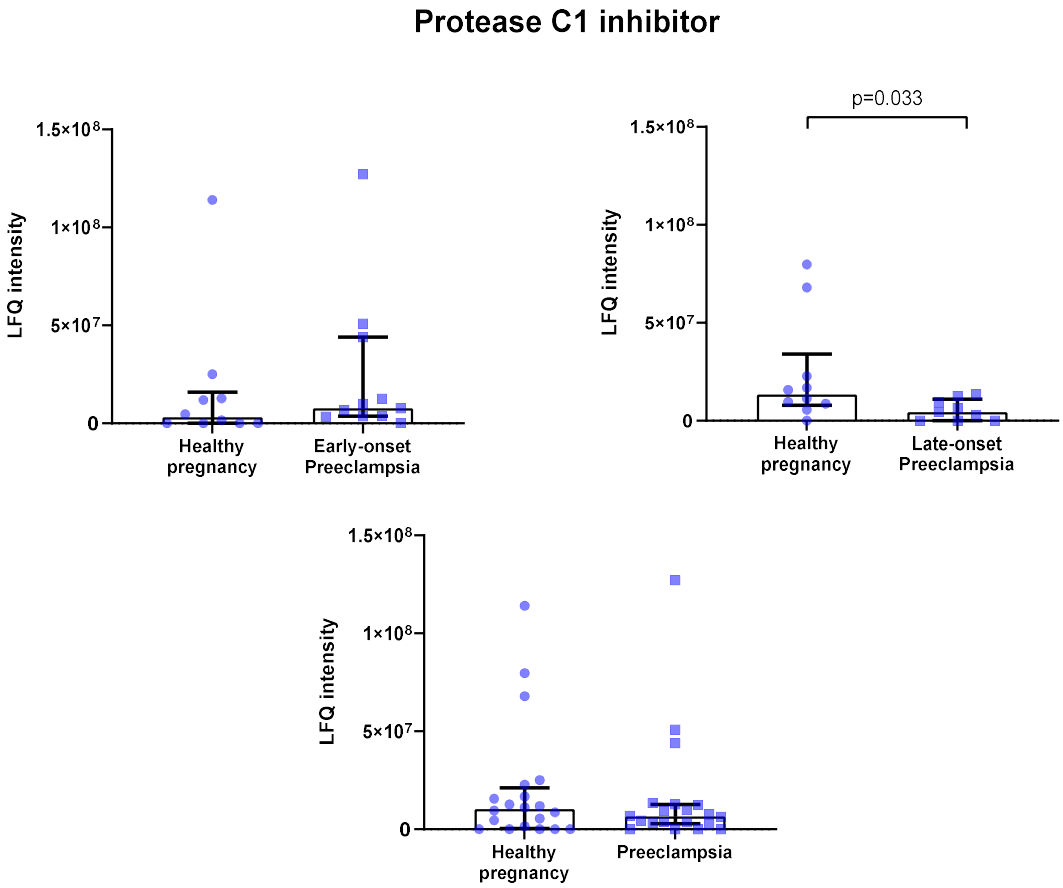

Figure 4-11 LFQ intensity of protease C1 inhibitor of healthy pregnancy and preeclampsia: Data was expressed as median±interquartile range. Mann-Whitney tests were carried out to compare the data between early-onset preeclampsia HDL and gestation matched controls (left above), late-onset preeclampsia HDL and gestation matched controls (right above), and preeclampsia HDL and gestation matched healthy pregnancy HDL (below). $p<0.05$ was taken as statistically significant.

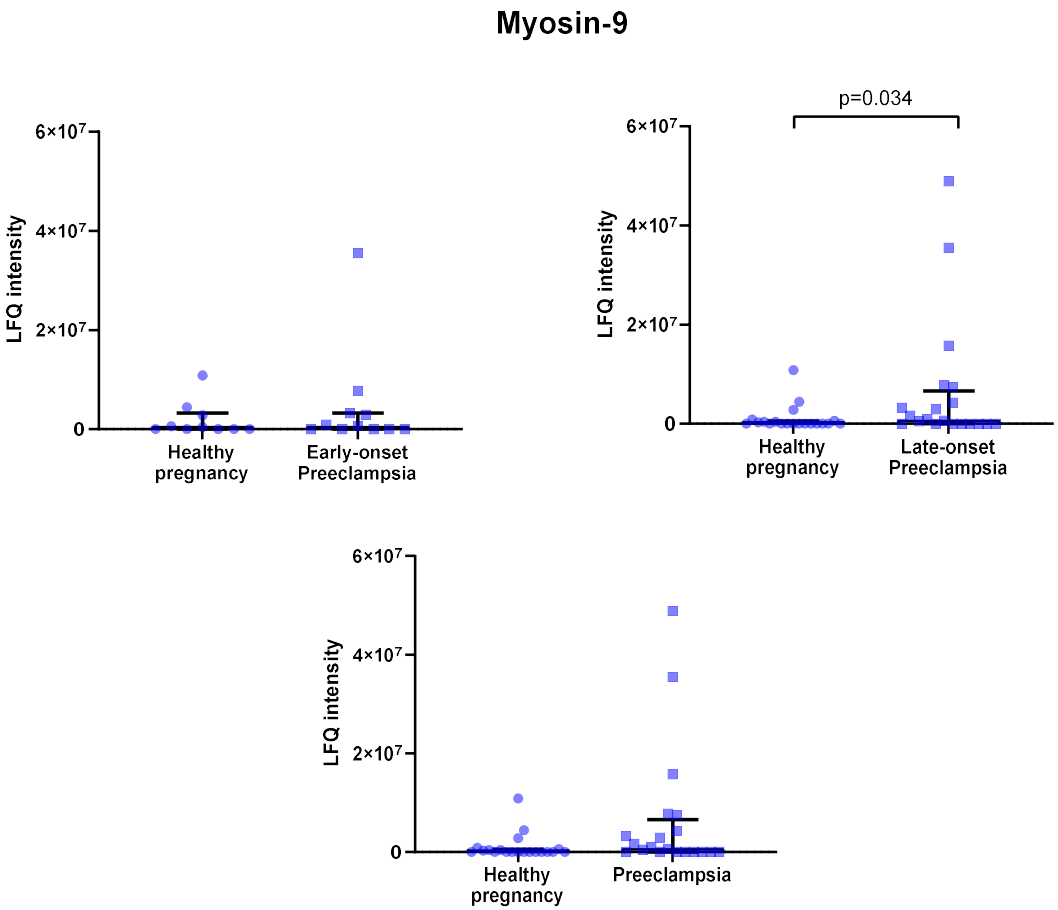

Figure 4-12 LFQ intensity of myosin-9 of healthy pregnancy and preeclampsia: Data was expressed as median±interquartile range. Mann-Whitney tests were carried out to compare the data between early-onset preeclampsia HDL and gestation matched controls (left above), late-onset preeclampsia HDL and gestation matched controls (right above), and preeclampsia HDL and gestation matched healthy pregnancy HDL (below). $p<0.05$ was taken as statistically significant.

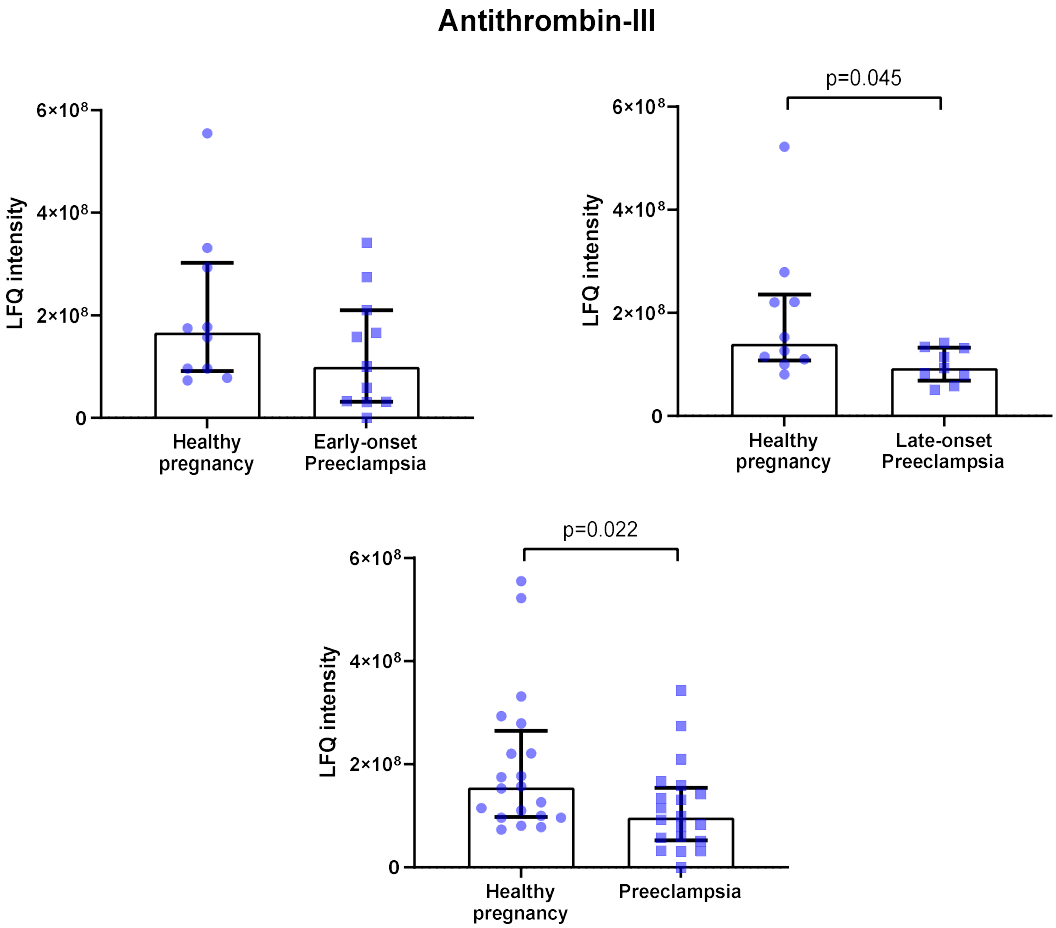

Figure 4-13 LFQ intensity of antithrombin-III of healthy pregnancy and preeclampsia: Data was expressed as median±interquartile range. Mann-Whitney tests were carried out to compare the data between early-onset preeclampsia HDL and gestation matched controls (left above), late-onset preeclampsia HDL and gestation matched controls (right above), and preeclampsia HDL and gestation matched healthy pregnancy HDL (below). $p<0.05$ was taken as statistically significant.

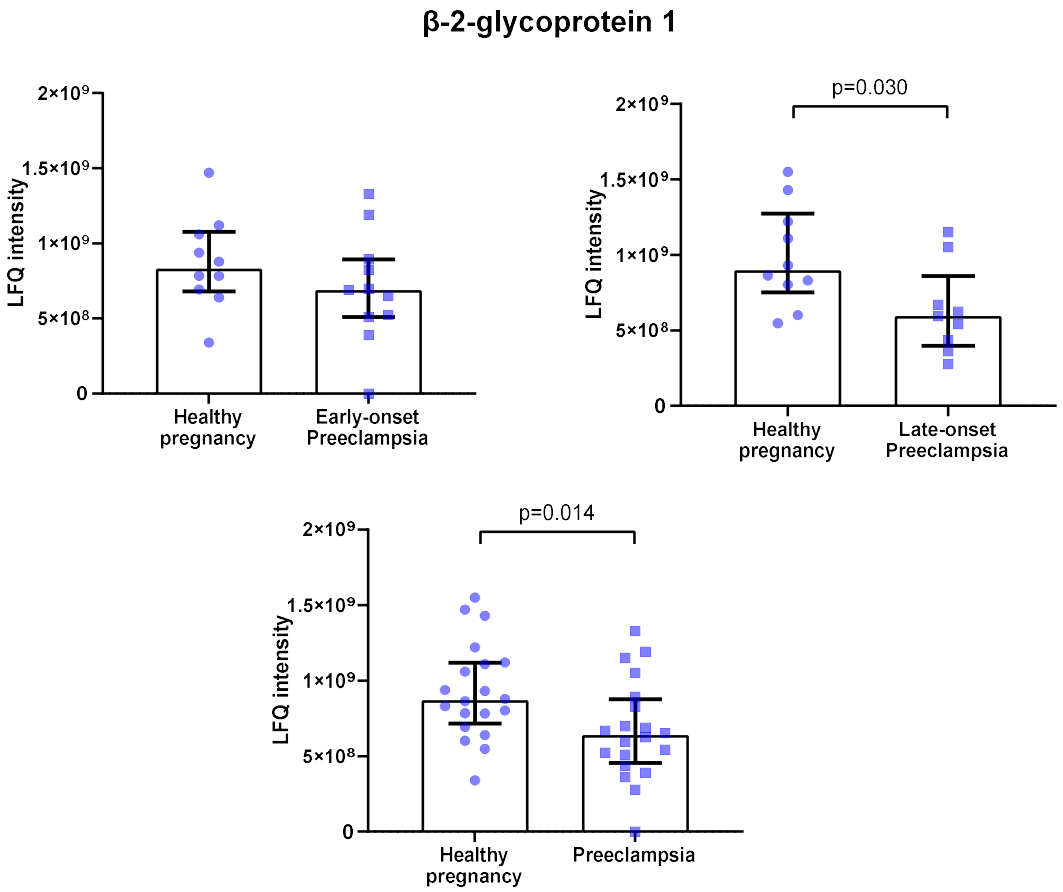

Figure 4-14 LFQ intensity of β-2-glycoprotein 1 of healthy pregnancy and preeclampsia: Data was expressed as median±interquartile range. Mann-Whitney tests were carried out to compare the data between early-onset preeclampsia HDL and gestation matched controls (left above), late-onset preeclampsia HDL and gestation matched controls (right above), and preeclampsia HDL and gestation matched healthy pregnancy HDL (below). $p<0.05$ was taken as statistically significant.

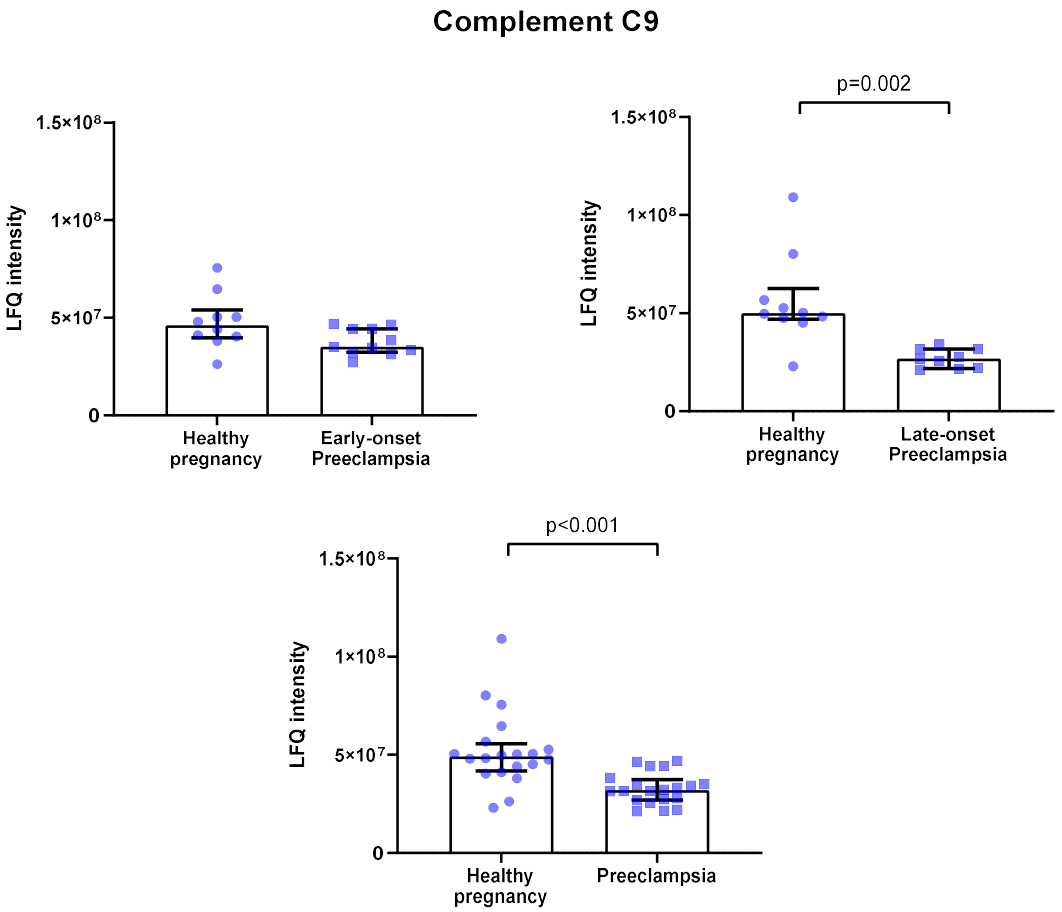

Figure 4-15 LFQ intensity of complement component C9 of healthy pregnancy and preeclampsia: Data was expressed as median±interquartile range. Mann-Whitney tests were carried out to compare the data between early-onset preeclampsia HDL and gestation matched controls (left above), late-onset preeclampsia HDL and gestation matched controls (right above), and preeclampsia HDL and gestation matched healthy pregnancy HDL (below). $p<0.05$ was taken as statistically significant.

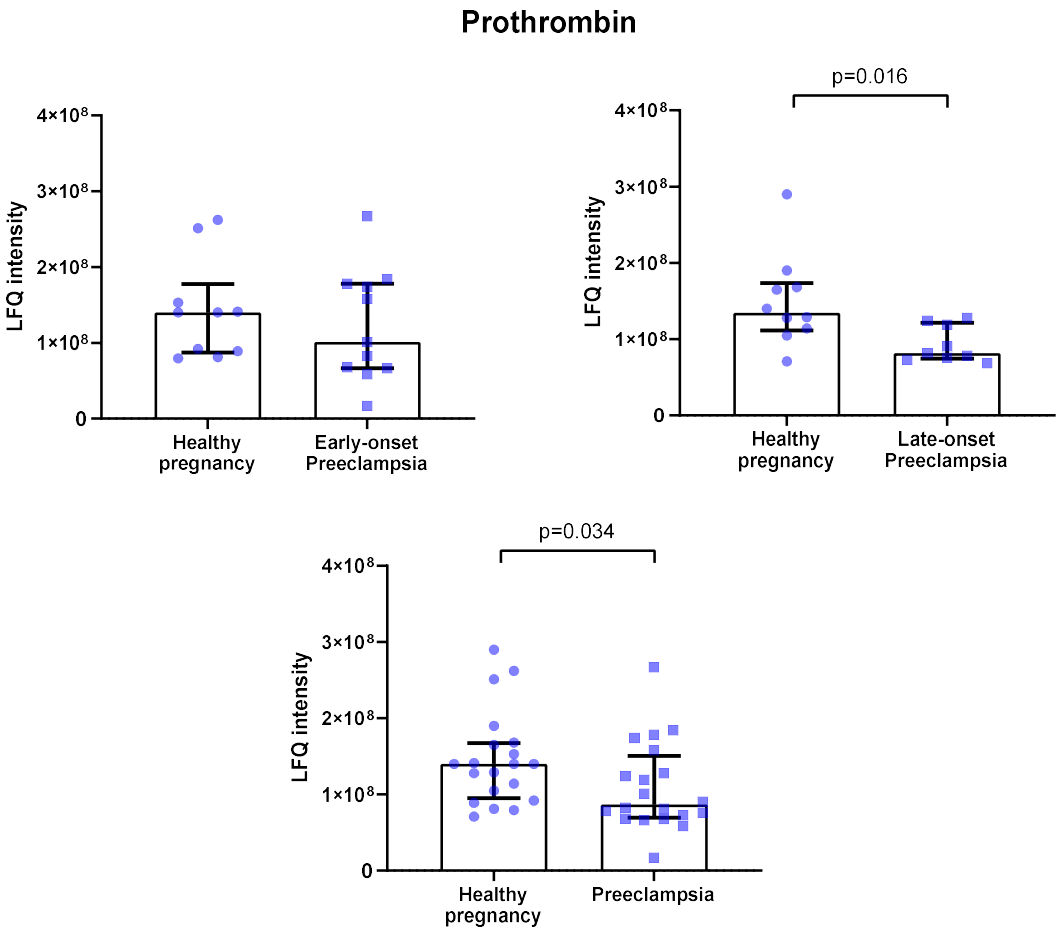

Figure 4-16 LFQ intensity of prothrombin of healthy pregnancy and preeclampsia: Data was expressed as median±interquartile range. Mann-Whitney tests were carried out to compare the data between early-onset preeclampsia HDL and gestation matched controls (left above), late-onset preeclampsia HDL and gestation matched controls (right above), and preeclampsia HDL and gestation matched healthy pregnancy HDL (below). $p<0.05$ was taken as statistically significant.

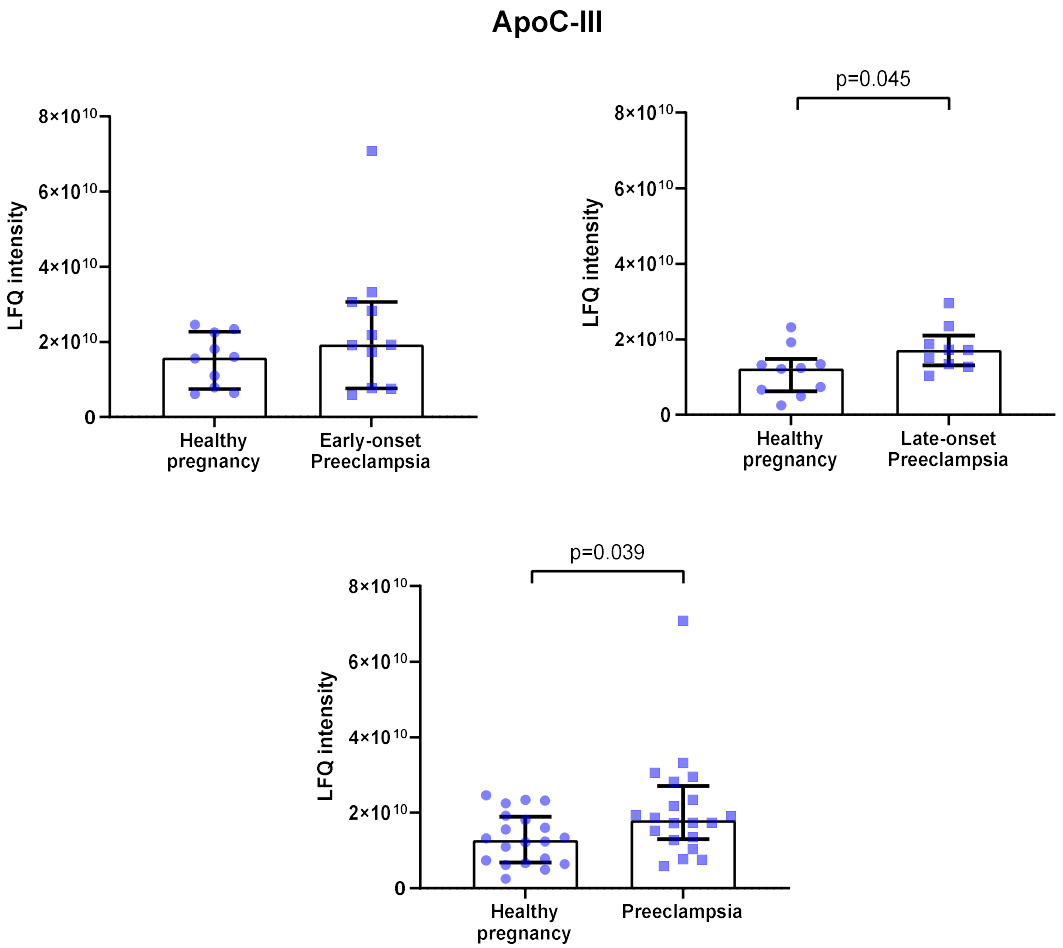

Figure 4-17 LFQ intensity of apoC-III of healthy pregnancy and preeclampsia: Data was expressed as median±interquartile range. Mann-Whitney tests were carried out to compare the data between early-onset preeclampsia HDL and gestation matched controls (left above), late-onset preeclampsia HDL and gestation matched controls (right above), and preeclampsia HDL and gestation matched healthy pregnancy HDL (below). $p<0.05$ was taken as statistically significant.

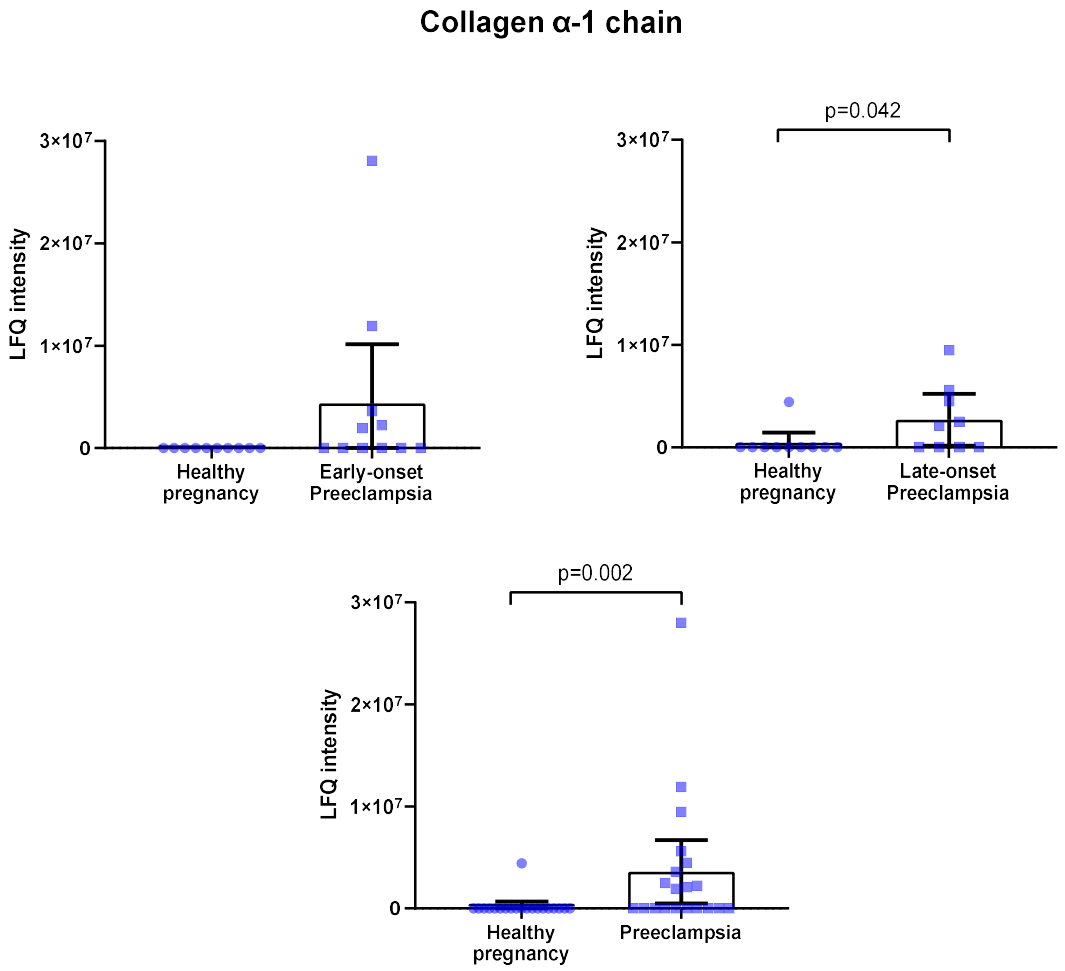

Figure 4-18 LFQ intensity of collagen α-1 chain of healthy pregnancy and preeclampsia: Data was expressed as median±interquartile range. Mann-Whitney tests were carried out to compare the data between early-onset preeclampsia HDL and gestation matched controls (left above), late-onset preeclampsia HDL and gestation matched controls (right above), and preeclampsia HDL and gestation matched healthy pregnancy HDL (below). $p<0.05$ was taken as statistically significant.

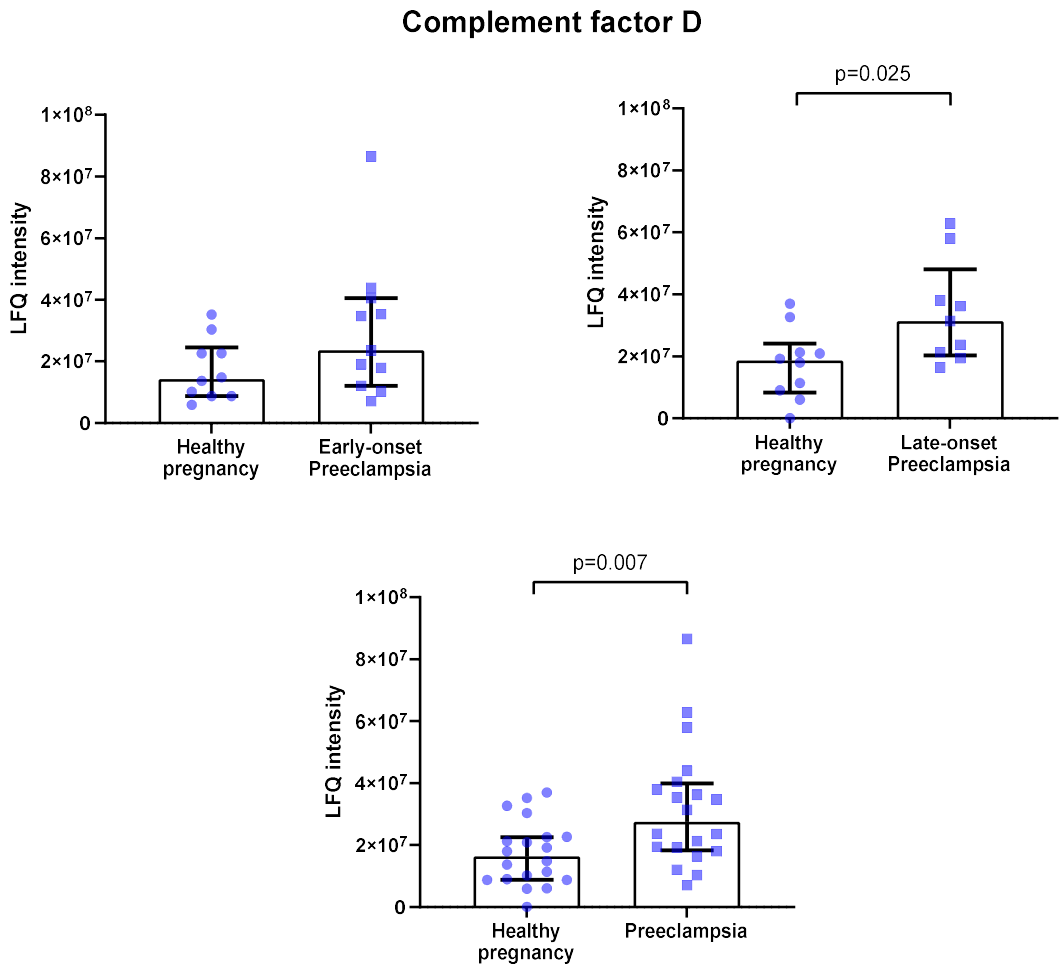

Figure 4-19 LFQ intensity of complement factor D of healthy pregnancy and preeclampsia: Data was expressed as median±interquartile range. Mann-Whitney tests were carried out to compare the data between early-onset preeclampsia HDL and gestation matched controls (left above), late-onset preeclampsia HDL and gestation matched controls (right above), and preeclampsia HDL and gestation matched healthy pregnancy HDL (below). $p<0.05$ was taken as statistically significant.

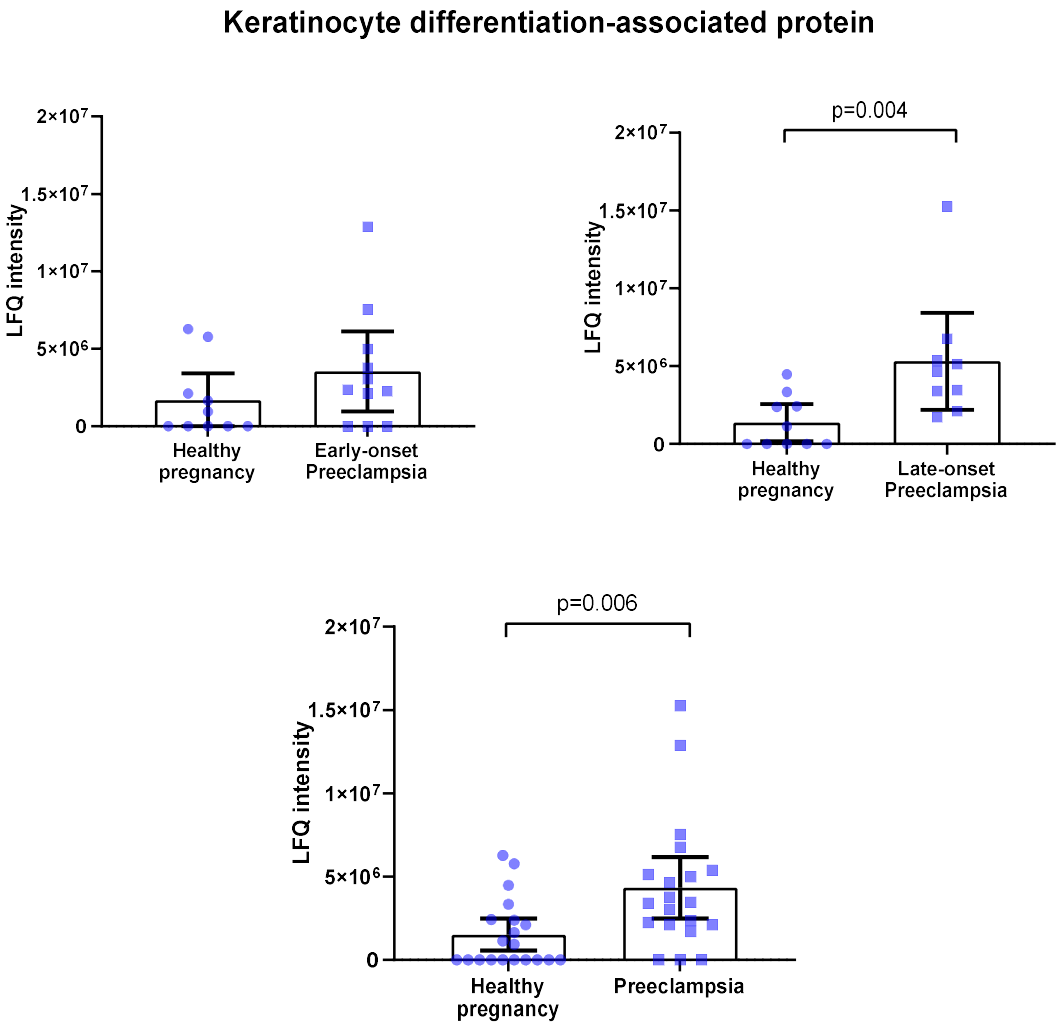

Figure 4-20 LFQ intensity of keratinocyte differentiation-associated protein of healthy pregnancy and preeclampsia: Data was expressed as median±interquartile range. Mann-Whitney tests were carried out to compare the data between early-onset preeclampsia HDL and gestation matched controls (left above), late-onset preeclampsia HDL and gestation matched controls (right above), and preeclampsia HDL and gestation matched healthy pregnancy HDL (below). $p<0.05$ was taken as statistically significant.

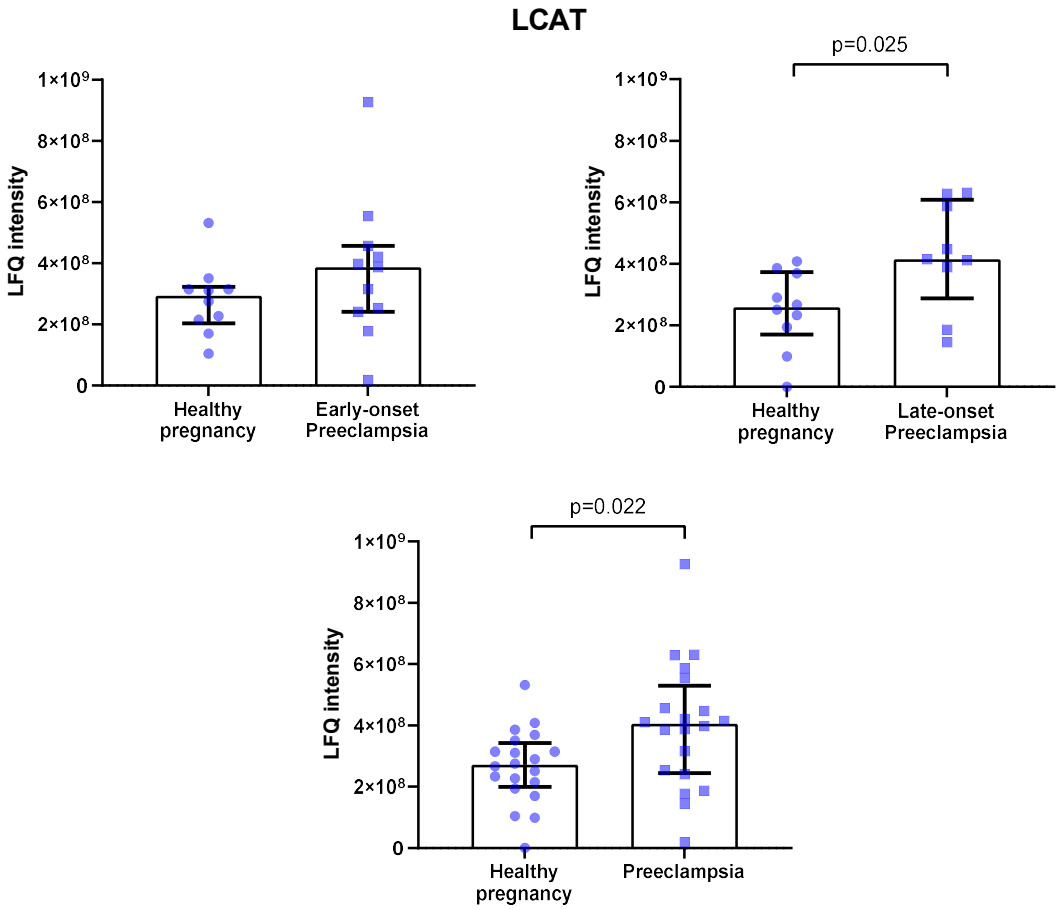

Figure 4-21 LFQ intensity of LCAT of healthy pregnancy and preeclampsia: Data was expressed as median±interquartile range. Mann-Whitney tests were carried out to compare the data between early-onset preeclampsia HDL and gestation matched controls (left above), late-onset preeclampsia HDL and gestation matched controls (right above), and preeclampsia HDL and gestation matched healthy pregnancy HDL (below). $p<0.05$ was taken as statistically significant.

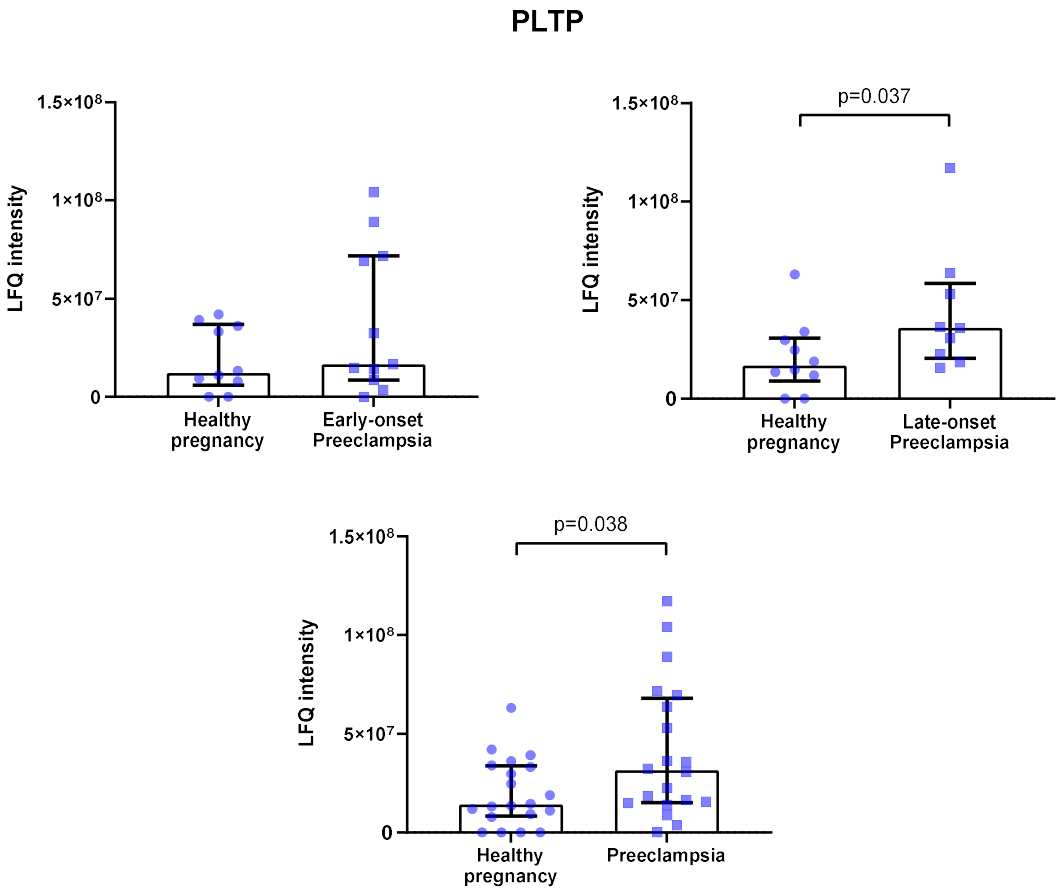

Figure 4-22 LFQ intensity of PLTP of healthy pregnancy and preeclampsia: Data was expressed as median±interquartile range. Mann-Whitney tests were carried out to compare the data between early-onset preeclampsia HDL and gestation matched controls (left above), late-onset preeclampsia HDL and gestation matched controls (right above), and preeclampsia HDL and gestation matched healthy pregnancy HDL (below). $p<0.05$ was taken as statistically significant.

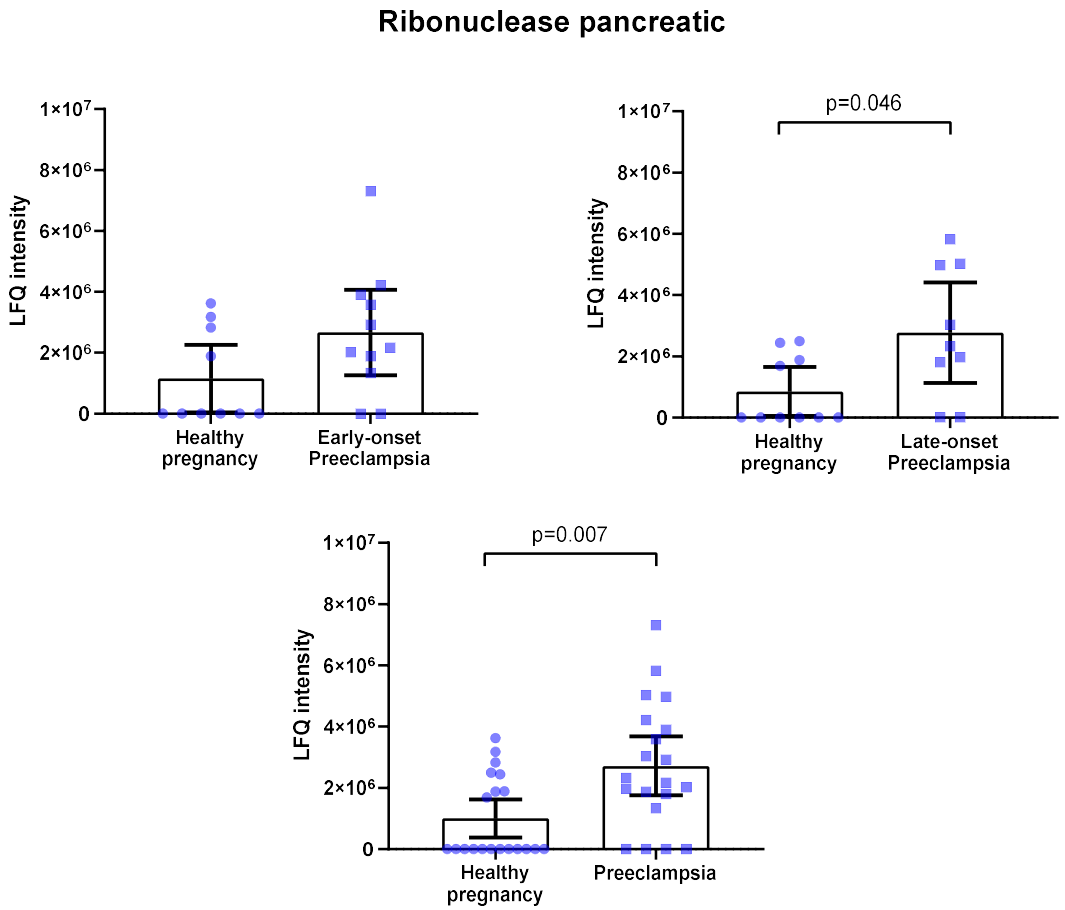

Figure 4-23 LFQ intensity of ribonuclease pancreatic protein of healthy pregnancy and preeclampsia: Data was expressed as median±interquartile range. Mann-Whitney tests were carried out to compare the data between early-onset preeclampsia HDL and gestation matched controls (left above), late-onset preeclampsia HDL and gestation matched controls (right above), and preeclampsia HDL and gestation matched healthy pregnancy HDL (below). $p<0.05$ was taken as statistically significant.

4.3.6 HDL protein composition in combined preeclampsia and combined healthy pregnant women

In preeclampsia (early and late onset combined) and matched healthy pregnancy combined, proteomic analysis identified a total of 285 proteins detected in at least one HDL sample. There were 151 HDL-associated proteins identified as proteins found in more than 50% of all HDL samples as shown in Table 4.4. Among these 151 proteins, there were 15 apolipoproteins, proteins involved in immune system such as immunoglobulin and complement, acute-phase response proteins and proteins involved in coagulation.

There were 20 proteins that showed statistical differences in LFQ intensities between HDL from combined preeclampsia and combined healthy pregnancy with $p<0.05$ (Table 4.4). As shown in section 4.3.5 and 4.3.6 of this chapter, the LFQ intensities of peroxiredoxin-2 and zinc-α-2-glycoprotein were lower in early-onset preeclampsia HDL than in their matched control HDL and were lower in combined preeclampsia than in combined healthy pregnancy group (Figure 4-6 and 4-7). β-2-microglobulin and Rap-1b were higher in early-onset preeclampsia HDL than in their matched control HDL and were higher in combined preeclampsia than in combined healthy pregnancy group (Figure 4-8 and 4-9). Antithrombin, β-2-glycoprotein 1, complement C9 and prothrombin had lower LFQ intensities in late-onset preeclampsia HDL than in their matched control HDL and had lower LFQ intensities in combined preeclampsia than in combined healthy pregnancy group (Figure 4-13 to 4-16). ApoC-III, complement factor D, collagen α-1 chain, keratinocyte differentiation-associated protein, LCAT, PLTP and ribonuclease pancreatic had higher LFQ intensities in late-onset preeclampsia HDL compared to healthy pregnant HDL and had higher LFQ intensities in combined preeclampsia than in combined healthy pregnancy group (Figure 4-17 to 4-23). There were 5 proteins including hemopexin, prosaposin, vitamin D-binding protein, calmodulin-3 and complement C4a that showed significant differences in LFQ intensities between the combined preeclampsia group and controls but not in either the early-onset or late-onset preeclampsia groups relative to their gestation matched healthy pregnancy controls. Hemopexin, prosaposin and vitamin D-binding protein showed lower LFQ intensities in combined preeclampsia HDL than in combined healthy pregnancy HDL (Figure 4-24 to 4-26). On the other hand, calmodulin-3 and complement C4a showed significant higher LFQ intensities in the combined preeclampsia than combined healthy pregnancy (Figure 4-27 and 4-28).

Table 4.4: List of 151 proteins identified in >50% of all HDL samples from the combined preeclampsia group and healthy pregnant control women

Protein	P value
Complement component C9	< 0.001
Collagen α-1 chain	0.002
β-2-microglobulin	0.004
Keratinocyte differentiation-associated protein	0.006
Complement factor D	0.007
Ribonuclease pancreatic	0.007
LCAT	0.012
Rap-1b	0.012
β-2-glycoprotein 1	0.014
Zinc-α-2-glycoprotein	0.021
Antithrombin-III	0.022
Calmodulin-3	0.022
Prothrombin	0.034
PLTP	0.038
Apolipoprotein C-III	0.039
Vitamin D-binding protein	0.041
Prosaposin	0.043
Hemopexin	0.047
Peroxiredoxin-2	0.047
Complement C4-A	0.048
L-selectin	0.053
Cofilin-1	0.054
Transgelin-2	0.056
Profilin-1	0.057
BPI fold-containing family B member 1	0.059
Myosin-9	0.062
Kininogen-1	0.068
α-1-acid glycoprotein 1	0.081
Apolipoprotein A-V	0.081
Cystatin-C	0.082
Ig γ-3 chain C region	0.088
Coagulation factor XII	0.092
Hemicentin-1	0.093
SAA4	0.102
PON1	0.102
Talin-1	0.109
α-1-acid glycoprotein 2	0.114
Apolipoprotein B-100	0.114
Apolipoprotein A-IV	0.12
Complement C4-B	0.12
Protein MENT	0.12
Apolipoprotein C-II	0.133
Apolipoprotein M	0.133
Serum albumin	0.14
C4b-binding protein α chain	0.148
Plasma serine protease inhibitor	0.148

α-2-HS-glycoprotein	0.156
Gelsolin	0.156
Insulin-like growth factor-binding protein complex acid labile subunit	0.168
Tropomyosin α-4 chain	0.171
Apolipoprotein E	0.172
Haptoglobin-related protein	0.172
Carboxypeptidase B2	0.181
Myosin light polypeptide 6	0.182
Phosphatidylinositol-glycan-specific phospholipase D	0.183
Insulin-like growth factor-binding protein 3	0.19
Carbonic anhydrase 1	0.196
Plasminogen	0.204
α-1B-glycoprotein	0.208
Apolipoprotein A-II	0.208
Platelet-activating factor acetylhydrolase	0.208
Keratin, type I cytoskeletal 9	0.21
TATA box-binding protein-associated factor RNA polymerase I subunit A	0.21
α-1-antichymotrypsin	0.234
Complement C3	0.25
Ig λ-1 chain C regions	0.259
Complement factor B	0.26
Fibrinogen α chain	0.273
Fibrinogen γ chain	0.273
Apolipoprotein A-I	0.298
Ig γ-1 chain C region	0.298
Flavin reductase (NADPH)	0.307
Filamin-A	0.314
Platelet factor 4	0.323
Serotransferrin	0.323
Fibroblast growth factor-binding protein 2	0.337
Heparin cofactor 2	0.344
CETP	0.351
Proprotein convertase subtilisin/kexin type 9	0.39
Hemoglobin α	0.394
Platelet basic protein	0.425
Corticosteroid-binding globulin	0.457
Inhibin ß C chain	0.457
Lipopolysaccharide-binding protein	0.457
Vitronectin	0.457
Insulin-like growth factor-binding protein 4	0.464
Hemoglobin ß	0.473
Hyaluronan-binding protein 2	0.473
Plasma protease C1 inhibitor	0.488
Apolipoprotein L1	0.49
Coagulation factor XIII A chain	0.506
Ig kappa chain C region	0.507
Retinol-binding protein 4	0.525
Inter-α-trypsin inhibitor heavy chain H2	0.533

α-2-antiplasmin	0.534
Lysozyme C	0.56
Apolipoprotein C-IV	0.561
CD44 antigen	0.578
Actin, cytoplasmic 2	0.579
N-acetylmuramoyl-L-alanine amidase	0.579
CD5 antigen-like	0.583
Ig mu chain C region	0.588
Keratin, type II cytoskeletal 1	0.597
Ig gamma-2 chain C region	0.611
Integrin α-IIb	0.625
Angiogenin	0.634
Tetranectin	0.646
Thymosin ß-4	0.664
Apolipoprotein C-I	0.675
Clusterin	0.675
Protein S100-A9	0.678
Inter-α-trypsin inhibitor heavy chain H4	0.695
Protein AMBP	0.695
HLA class I histocompatibility antigen, B-7 α chain	0.699
Lumican	0.731
Retinoic acid receptor responder protein 2	0.735
Thyroxine-binding globulin	0.755
Apolipoprotein F	0.756
Ig α-1 chain C region	0.787
Sex hormone-binding globulin	0.797
Haptoglobin	0.812
Apolipoprotein(a)	0.818
Fibrinogen ß chain	0.818
Leucine-rich α-2-glycoprotein	0.818
Neutrophil defensin 3	0.82
Insulin-like growth factor II	0.829
Insulin-like growth factor I	0.838
Chorionic somatomammotropin hormone 2	0.857
Pregnancy-specific ß-1-glycoprotein 1	0.877
Pregnancy-specific ß-1-glycoprotein 2	0.877
Leucyl-cystinyl aminopeptidase	0.879
Immunoglobulin λ constant 3	0.882
Apolipoprotein D	0.903
SAA1	0.903
Kinesin heavy chain isoform 5C	0.918
Prenylcysteine oxidase 1	0.92
Pigment epithelium-derived factor	0.925
Afamin	0.946
Angiotensinogen	0.946
Fibronectin	0.946
ß-Ala-His dipeptidase	0.966
SAA2	0.968
PON3	0.968
α-1-antitrypsin	0.989

Cathelicidin antimicrobial peptide	0.989
HLA class I histocompatibility antigen, A-3 α chain	0.989
Monocyte differentiation antigen CD14	0.989
Protein Z-dependent protease inhibitor	0.989
Kallistatin	1
Proline-rich acidic protein 1	1
Transthyretin	1

P value was calculated from Mann-Whitney test comparing the difference of LFQ intensity median between combined preeclampsia group and healthy pregnancy in each protein.

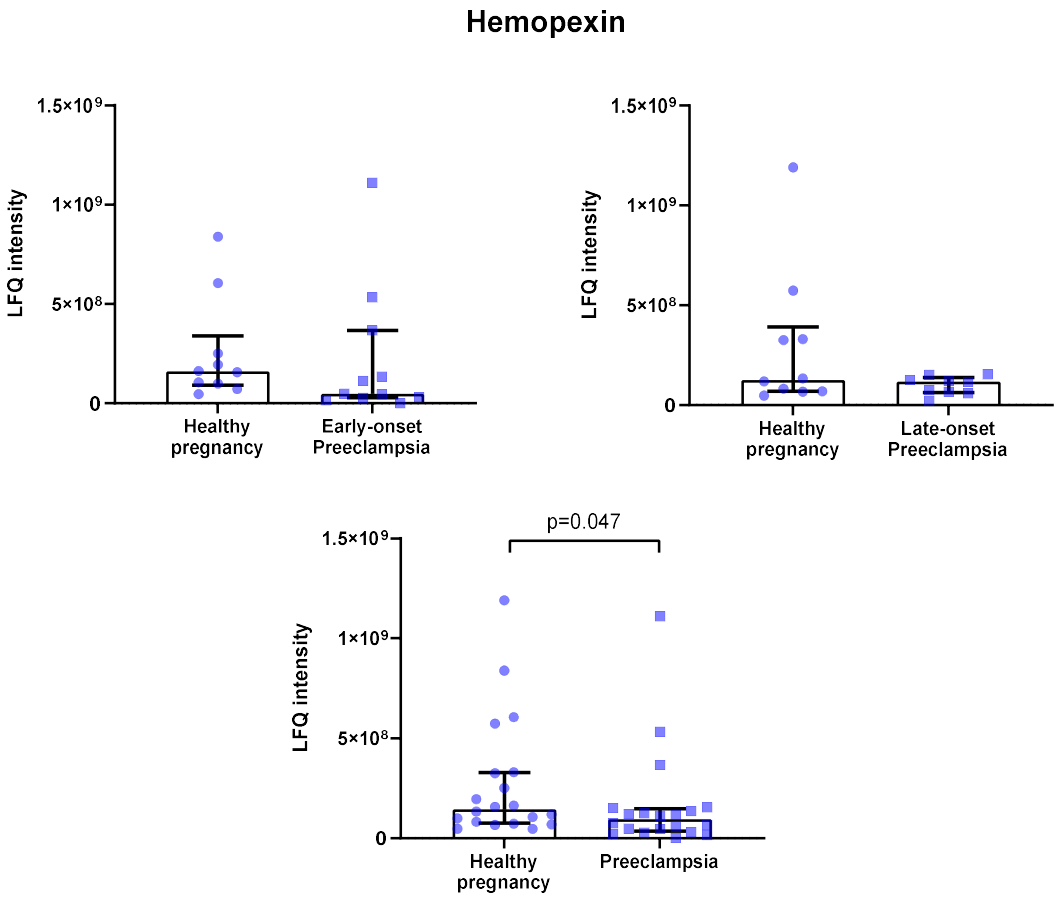

Figure 4-24 LFQ intensity of hemopexin of healthy pregnancy and preeclampsia: Data was expressed as median±interquartile range. Mann-Whitney tests were carried out to compare the data between early-onset preeclampsia HDL and gestation matched controls (left above), late-onset preeclampsia HDL and gestation matched controls (right above), and preeclampsia HDL and gestation matched healthy pregnancy HDL (below). $p<0.05$ was taken as statistically significant.

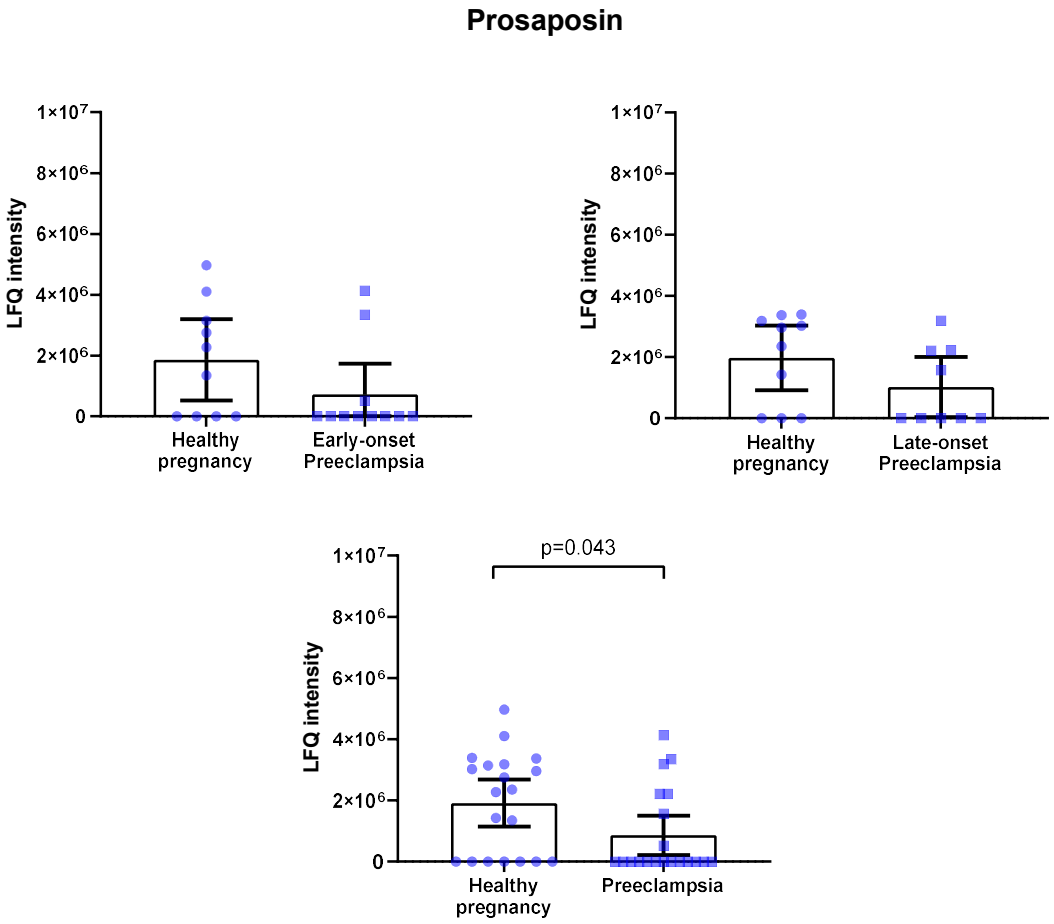

Figure 4-25 LFQ intensity of prosaposin of healthy pregnancy and preeclampsia: Data was expressed as median±interquartile range. Mann-Whitney tests were carried out to compare the data between early-onset preeclampsia HDL and gestation matched controls (left above), late-onset preeclampsia HDL and gestation matched controls (right above), and preeclampsia HDL and gestation matched healthy pregnancy HDL (below). $p<0.05$ was taken as statistically significant.

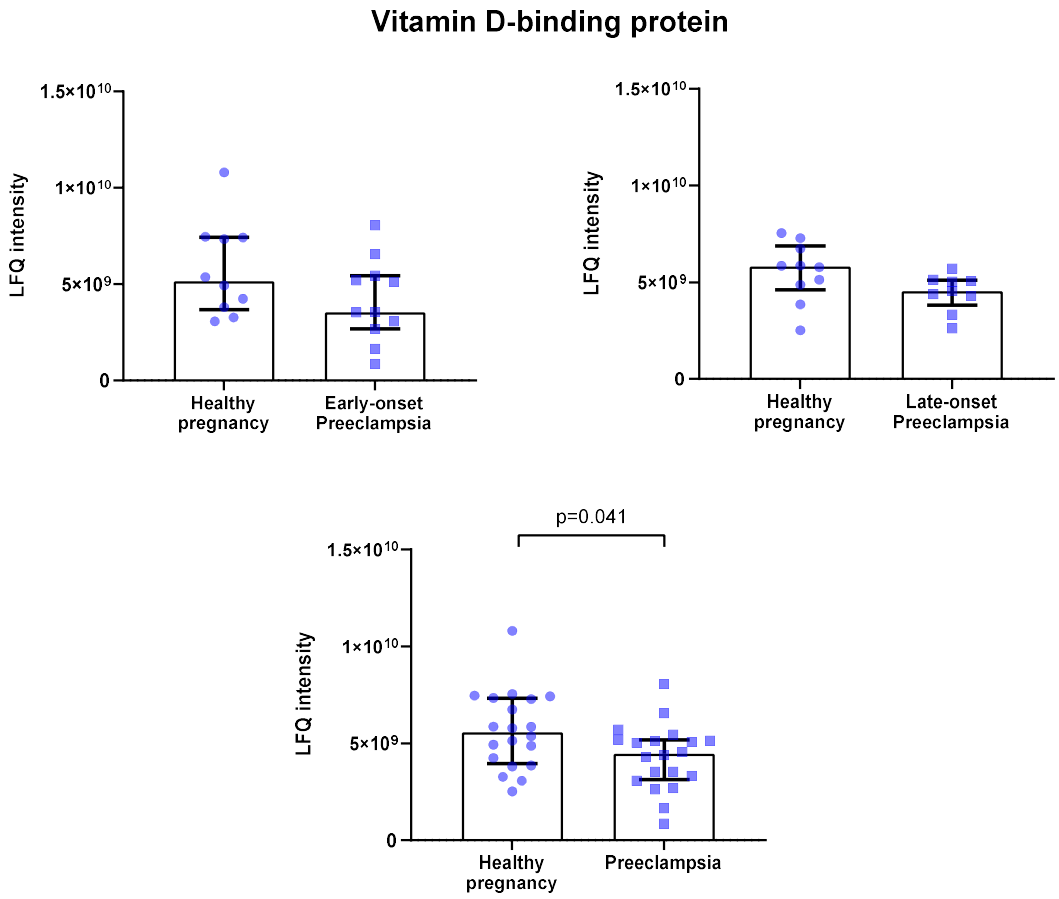

Figure 4-26 LFQ intensity of vitamin D-binding protein of healthy pregnancy and preeclampsia: Data was expressed as median±interquartile range. Mann-Whitney tests were carried out to compare the data between early-onset preeclampsia HDL and gestation matched controls (left above), late-onset preeclampsia HDL and gestation matched controls (right above), and preeclampsia HDL and gestation matched healthy pregnancy HDL (below). $p<0.05$ was taken as statistically significant.

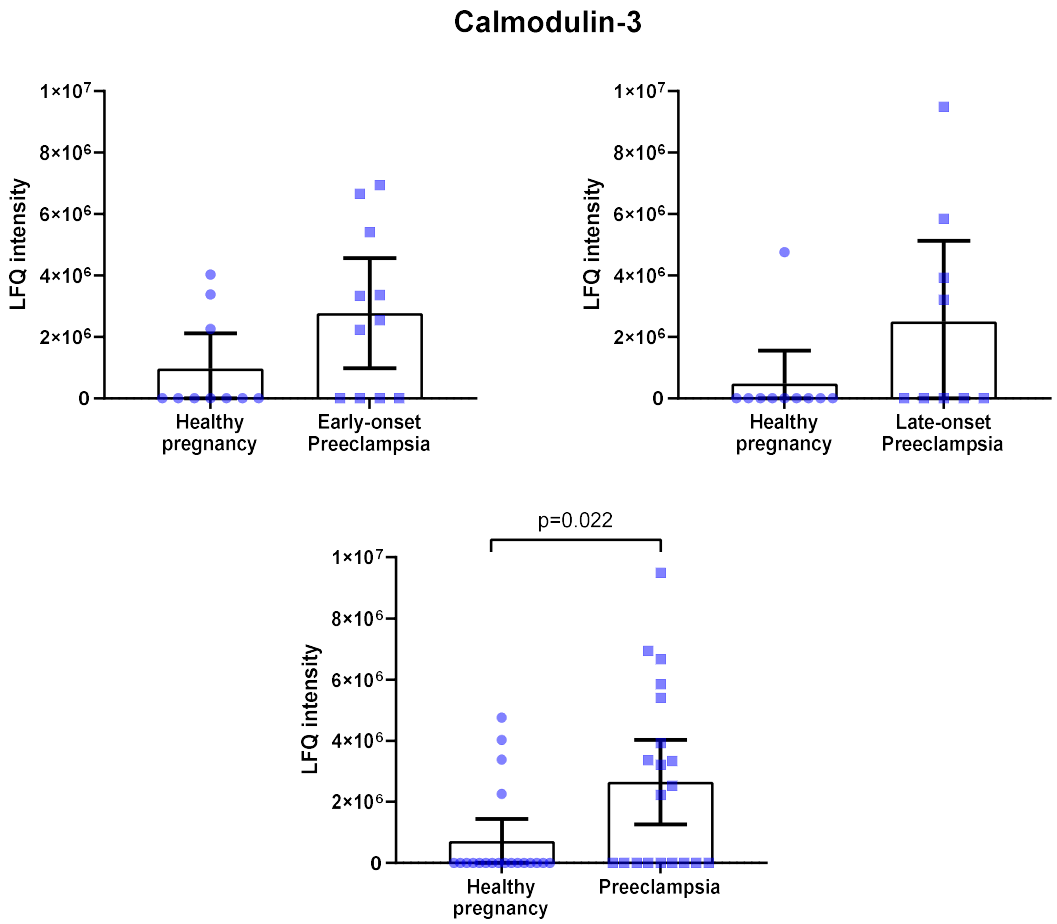

Figure 4-27 LFQ intensity of calmodulin-3 of healthy pregnancy and preeclampsia: Data was expressed as median±interquartile range. Mann-Whitney tests were carried out to compare the data between early-onset preeclampsia HDL and gestation matched controls (left above), late-onset preeclampsia HDL and gestation matched controls (right above), and preeclampsia HDL and gestation matched healthy pregnancy HDL (below). $p<0.05$ was taken as statistically significant.

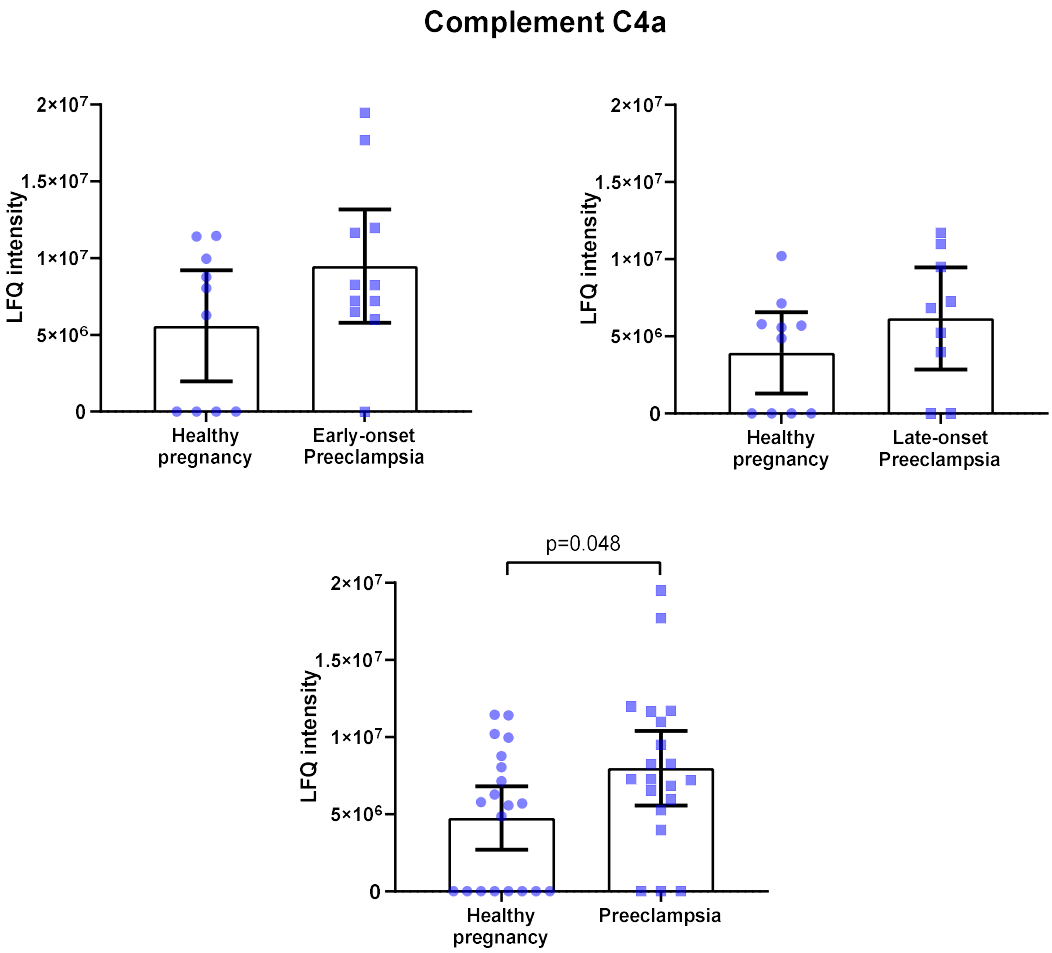

Figure 4-28 LFQ intensity of complement C4a of healthy pregnancy and preeclampsia: Data was expressed as median±interquartile range. Mann-Whitney tests were carried out to compare the data between early-onset preeclampsia HDL and gestation matched controls (left above), late-onset preeclampsia HDL and gestation matched controls (right above), and preeclampsia HDL and gestation matched healthy pregnancy HDL (below). $p<0.05$ was taken as statistically significant.

4.3.7 Orthogonal Projections to Latent Structures Discriminant Analysis (OPLS-DA)

There were 3 discriminant analyses undertaken 1) preeclampsia (early and late onset combined) and healthy pregnancy, 2) early-onset preeclampsia and matched healthy pregnancy controls and 3) late-onset preeclampsia and matched healthy pregnancy controls. OPLS-DA was expressed as a score plot and a loading plot for each data. A score plot was created to visualize the differences in the proteomes of each sample with the x-axis representing between-group variation and the y-axis representing within-group variation. A loading plot was created to show the inter-relationship between different types of HDL proteins. Proteins located closer to each other represent their greater correlation. Together with the score plot, the location of protein in the loading plot may be used to indicate how proteins change in each group of samples in the score plot. Proteins located to the left end of x-axis of the loading plot were higher in the samples that located to the left end of x-axis of the score plot and lower in the samples to the right.

OPLS-DA of early-onset preeclampsia HDL and matched healthy pregnancy control HDL showed no significant separation. However, OPLS-DA with variable importance for the projection (VIP), which includes only variables (proteins) important for separation, revealed a significant separation between early-onset preeclampsia HDL and matched healthy pregnancy HDL with p=0.041 (Figure 4-29). It was shown that kallistatin (SERPINA4), apoC-II (APOC2) and clusterin (CLU) were higher in early-onset preeclampsia HDL, while protein S100A9, apoA-IV and complement C9 were lower in early-onset preeclampsia HDL (Figure 4-29). OPLS-DA of late-onset preeclampsia HDL versus matched healthy pregnancy control HDL showed no separation (p=0.7) (Figure 4-30). OPLS-DA with combined preeclampsia HDL versus combined healthy pregnancy HDL exhibited a significant separation between the two groups (p=0.005) (Figure 4-31). Integrin α-IIb (ITGA2B) was higher in preeclampsia HDL, while complement C9 was lower in preeclampsia HDL (Figure 4-31). It should be noted that the y-axes of Figures 4-29, 4-30 and 4-31 are not on the same scale.

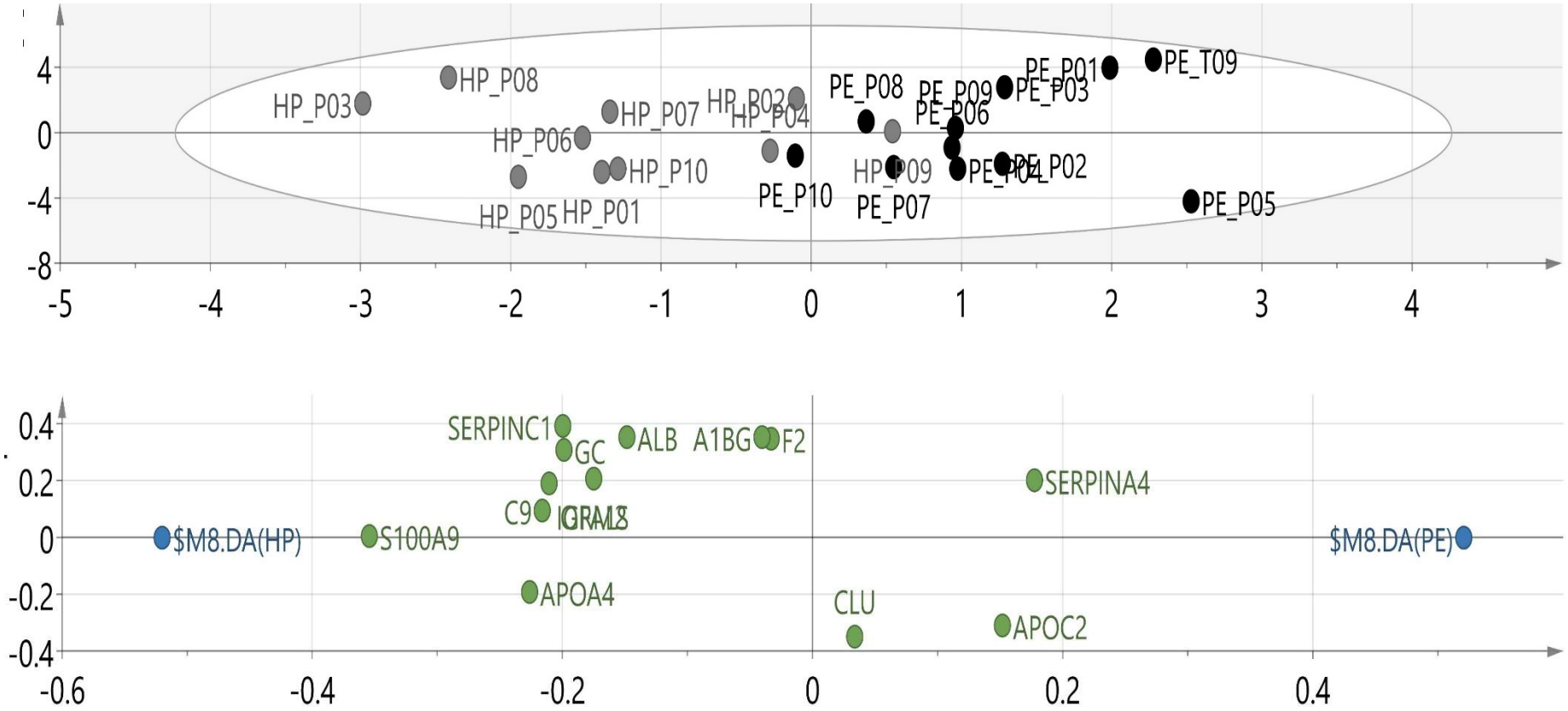

Figure 4-29 Score plot and loading plot of OPLS-DA (VIP) with two categories of samples (early-onset preeclampsia and matched healthy pregnancy controls): HDL proteins, BMI and age were assigned as variables. The score plot (upper) showed a significant separation of samples between early-onset preeclampsia HDL and matched healthy pregnancy control HDL (p value=0.041). The x-axis represents between-group variation, and the y-axis represents within-group variation. Proteins located to the right end of x-axis of the loading plot (lower) such as kallistatin (SERPINA4), apoC-II (APOC2) and clusterin (CLU) were higher in the samples that located to the right end of x-axis of the score plot (early-onset preeclampsia HDL) and lower in the samples to the left (healthy pregnancy HDL). The blue points are the point from which all the green points are distanced.

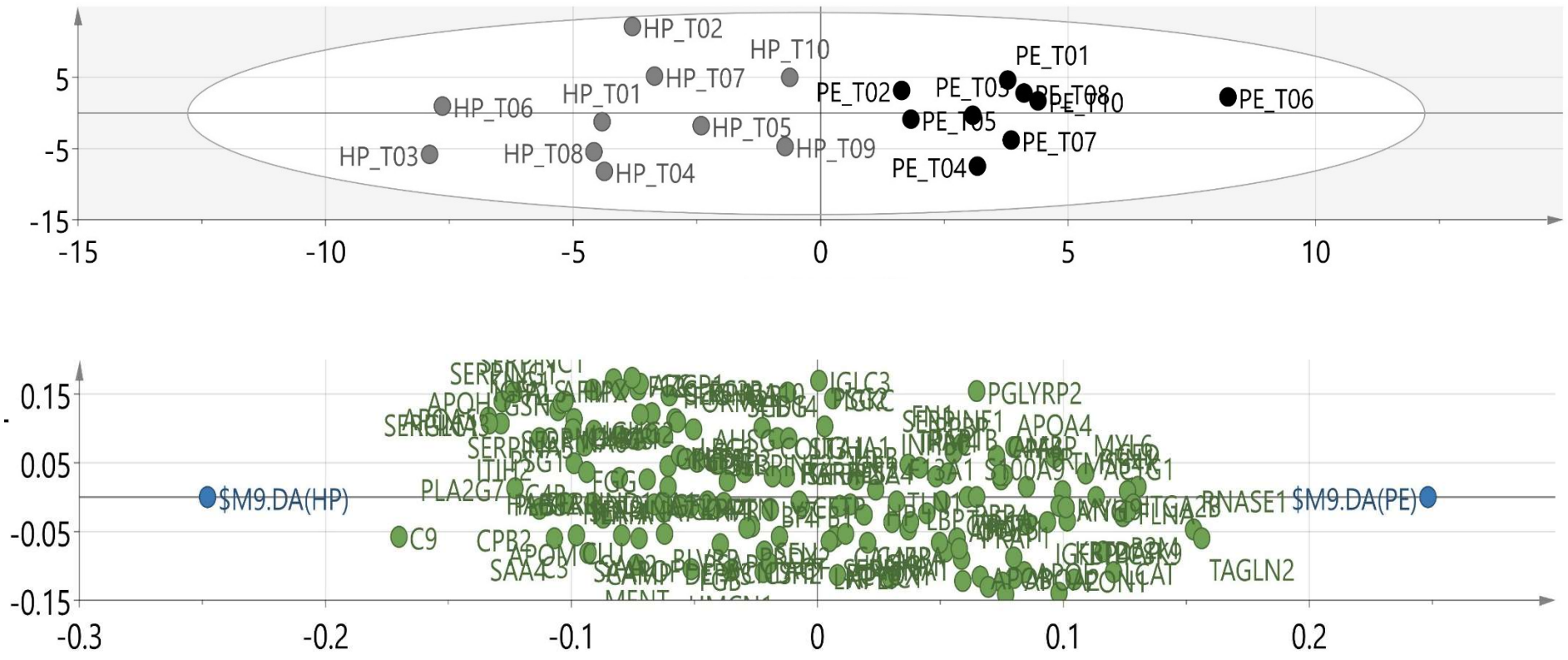

Figure 4-30 Score plot and loading plot of OPLS-DA with two categories of samples (late-onset preeclampsia HDL and matched healthy pregnancy control HDL): HDL proteins, BMI and age were assigned as variables. The score plot (upper) showed an insignificant separation of samples between late-onset preeclampsia HDL and matched healthy pregnancy control HDL (p value=0.71). The x-axis represents between-group variation, and the y-axis represents within-group variation. Proteins located to the left end of x-axis of the loading plot (lower) were higher in the samples that located to the left end of x-axis of the score plot and lower in the samples to the right. The blue points are the point from which all the green points are distanced.

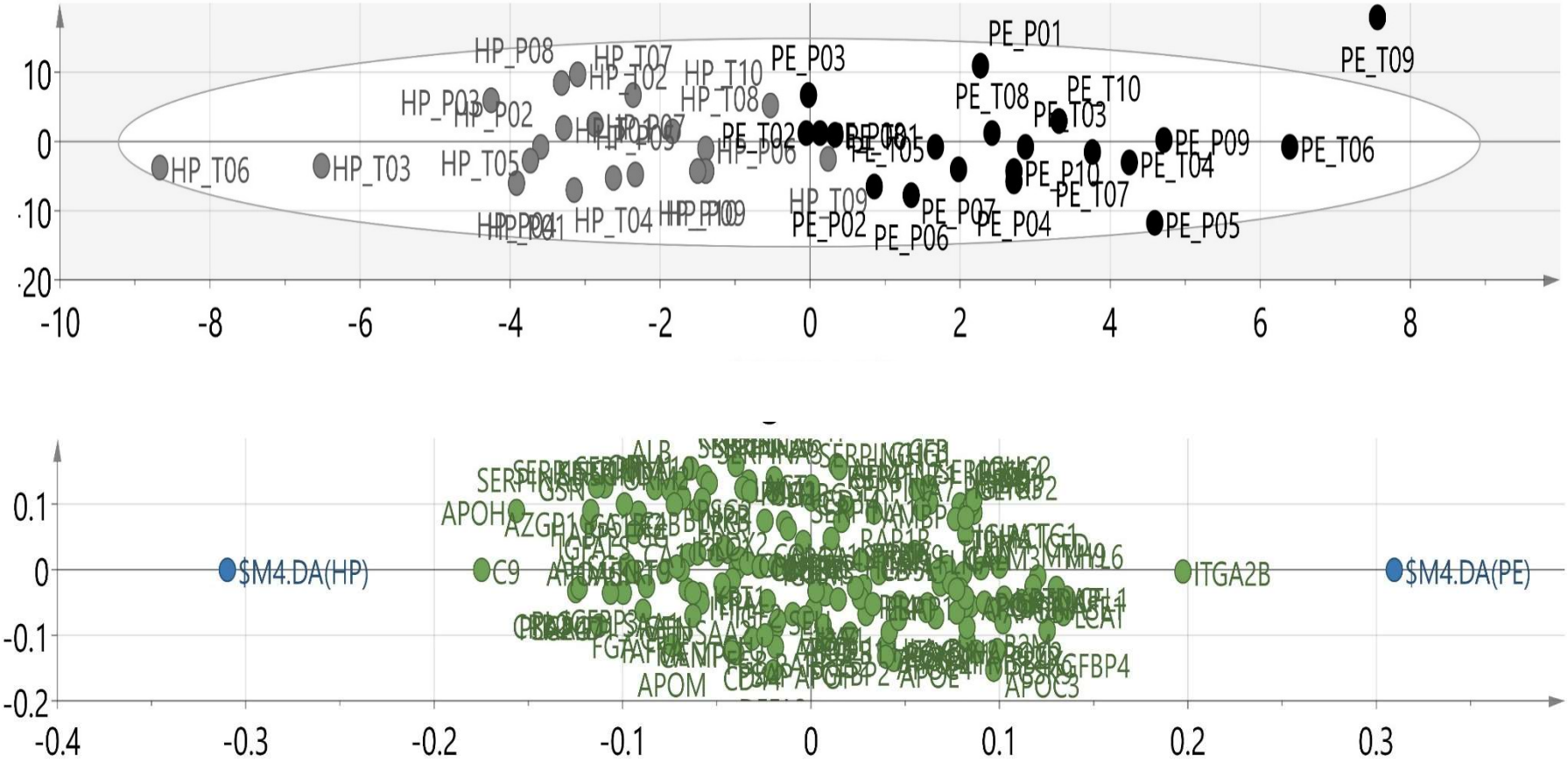

Figure 4-31 Score plot and loading plot of OPLS-DA with two categories of samples, preeclampsia and healthy pregnancy: HDL proteins, BMI and age were assigned as variables. The score plot (upper) showed a significant separation of samples between preeclampsia and healthy pregnancy (p value=0.005). The x-axis represents between-group variation, and the y-axis represents within-group variation. Proteins located to the right end of x-axis of the loading plot (lower) such as integrin α-IIb (ITGA2B) were higher in the samples that located to the right end of x-axis of the score plot (preeclampsia HDL) and lower in the samples to the left (healthy pregnancy HDL). The blue points are the point from which all the green points are distanced.

4.3.8 Glycation modification on HDL proteins of preeclampsia and healthy pregnancy

There was FL detected on apoA-I, apoA-II, apoD, apoE, apoJ, fibrinogen α chain, kinesin heavy chain isoform 5C, plasma serine protease inhibitor, tropomyosin α-4 chain and talin-1 of preeclampsia and healthy pregnant HDL (Table 4.5). CML was detected on 26 proteins and MG-H1 was detected on 11 proteins in preeclampsia and healthy pregnant HDL (Table 4.5). FL intensity and ratio on position 232 of apoA-I was found to be significantly lower in early-onset preeclampsia HDL compared to matched healthy pregnancy control HDL (Figure 4-32 and 4-33). There was no significant difference in CML and MG-H1 intensity and ratio between early- or late-onset preeclampsia HDL and their controls. All glycation modifications did not significantly differ between combined preeclampsia and combined healthy pregnant HDL.

Table 4.5: List of modified proteins in preeclampsia and healthy pregnant HDL and the amino acid position within proteins where FL, CML or MG-H1 modifications were found

Protein name	Amino acid position within proteins
FL	
α-1-antitrypsin	298
Apolipoprotein A-I	36, 47,120,131, 142, 157, 164, 206, 230, 232, 219, 250
Apolipoprotein A-II	46, 51, 53, 62, 69, 77
Apolipoprotein D	75
Apolipoprotein E	161
Apolipoprotein J	62, 68
Fibrinogen α chain	467, 480, 581
Kinesin heavy chain isoform 5C	348, 350
Plasma serine protease inhibitor	295
Tropomyosin α-4 chain	215
Talin-1	535
CML	
α-1-acid glycoprotein 1	12
α-1-acid glycoprotein 2	12
α-1-antitrypsin	24
Angiotensinogen	13
Antithrombin-III	5, 15
Apolipoprotein A-I	2, 5, 10, 11, 12, 14, 18, 27
Apolipoprotein A-II	1, 2, 8, 20, 25
Apolipoprotein B-100	1, 11, 13

Apolipoprotein C-II	5
Apolipoprotein C-III	3, 11
Apolipoprotein D	1, 6, 13
Apolipoprotein J	3
Β-2-glycoprotein 1	2
Cholesteryl ester transfer protein	11
Complement factor B	7
Complement C3	1
Fibrinogen alpha chain	4, 6, 11, 17, 18
Gelsolin	20
Hyaluronan-binding protein 2	1
Ig alpha-1 chain C region	1
Kinesin heavy chain isoform 5C	3, 5
Phospholipid transfer protein	6
Serotransferrin	5
Serum paraoxonase/arylesterase 1	9, 14, 24, 30
Vitamin D-binding protein	1, 4, 8
Vitronectin	9, 10

Protein name	Amino acid position within proteins
MG-H1	
α-1-antitrypsin	22
Apolipoprotein E	6
Apolipoprotein J	10
Complement factor B	8
Fibrinogen α chain	2, 3
Hyaluronan-binding protein 2	10
N-acetylmuramoyl-L-alanine amidase	20
Talin-1	6
Tropomyosin α-4 chain	6, 7

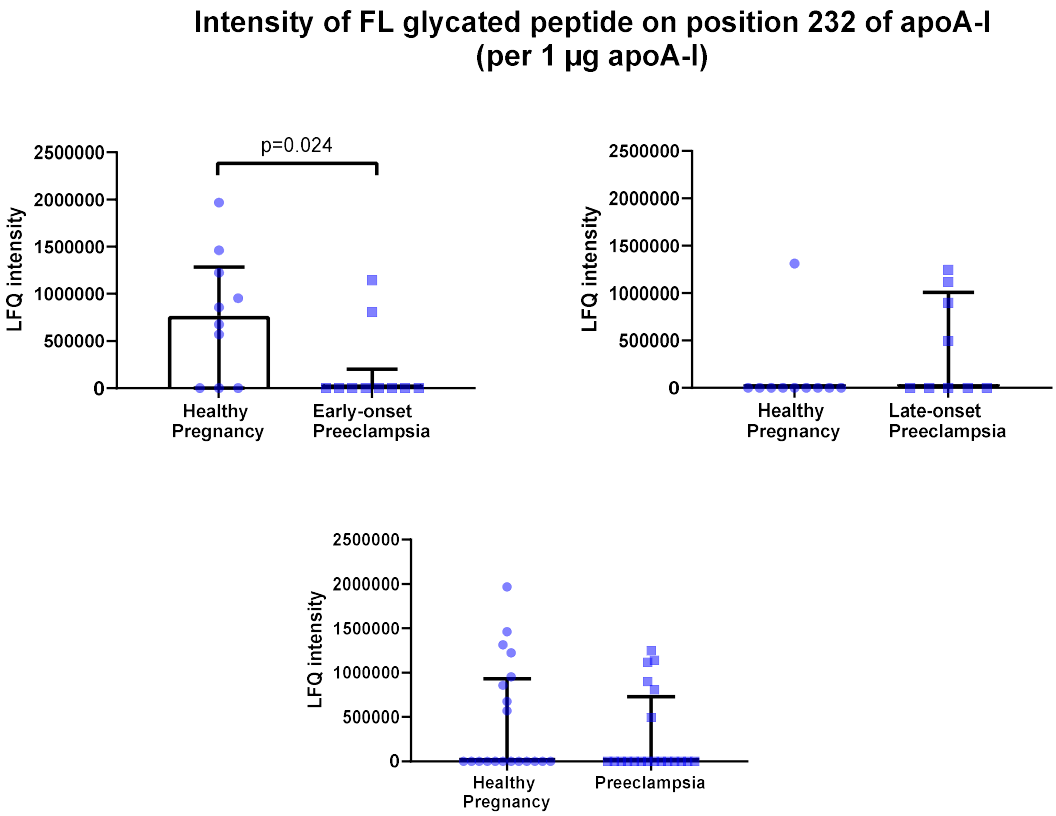

Figure 4-32 Intensity of FL glycation at position 232 on apoA-I Data was expressed as median±interquartile range. Mann-Whitney tests were carried out to compare the data between early-onset preeclampsia HDL and gestation matched controls (left above), late-onset preeclampsia HDL and gestation matched controls (right above), and preeclampsia HDL and gestation matched healthy pregnancy HDL (below). $p<0.05$ was taken as statistically significant.

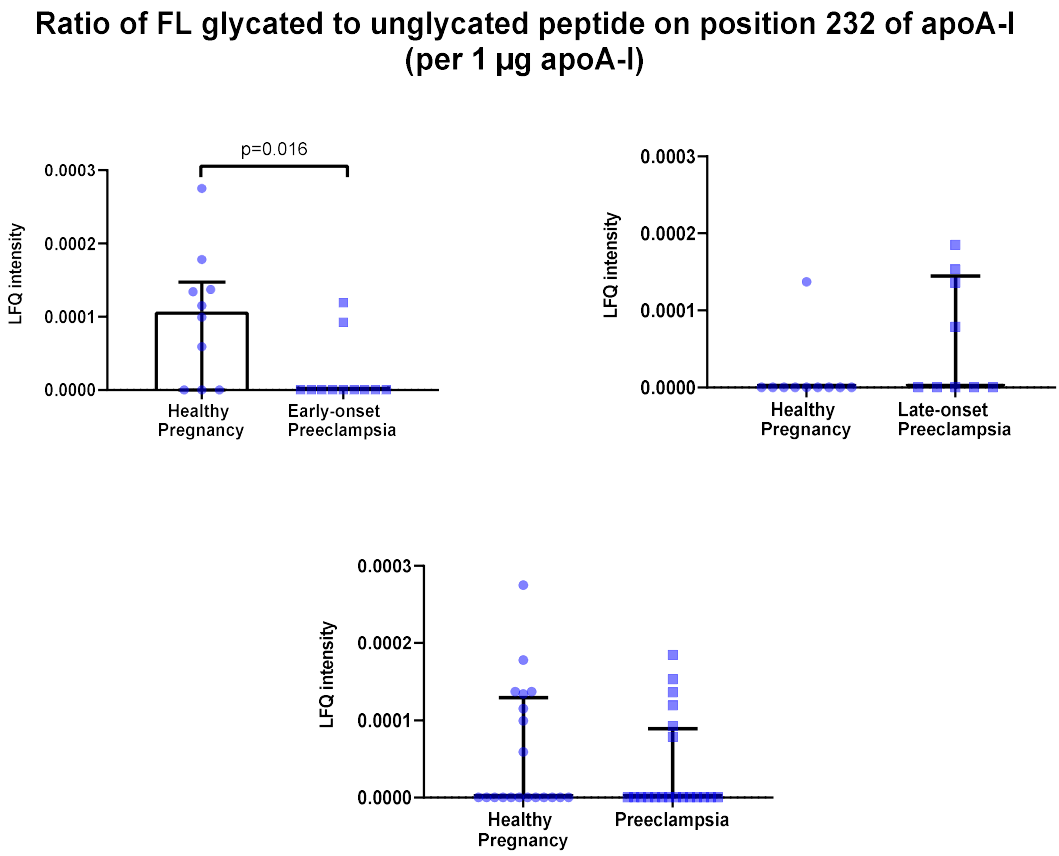

Figure 4-33 Ratio of FL glycated to non-glycated amino acid at position 232 on apoA-I Data was expressed as median±interquartile range. Mann-Whitney tests were carried out to compare the data between early-onset preeclampsia HDL and gestation matched controls (left above), late-onset preeclampsia HDL and gestation matched controls (right above), and preeclampsia HDL and gestation matched healthy pregnancy HDL (below). $p<0.05$ was taken as statistically significant.

4.3.9 ApoA-I methionine oxidation in HDL from preeclampsia and healthy pregnancy

Oxidised methionine residues were identified at position 110, 136 and 172 on the ApoA-I protein of preeclampsia and healthy pregnant HDL. There was no significance difference of oxidised methionine LFQ intensity in all three positions of apoA-I between early- or late-onset preeclampsia and their matched control. The LFQ intensity of oxidised methionine at position 110 of apoA-I was higher in combined preeclampsia than in healthy pregnancy (Figure 4-34). The ratio of oxidised to non-oxidised methionine at position 172 of apoA-I was significantly higher in early-onset preeclampsia, compared to that in matched healthy pregnancy (Figure 4-35). This ratio was also significantly higher in combined preeclampsia than that in healthy pregnancy control (Figure 4-35).

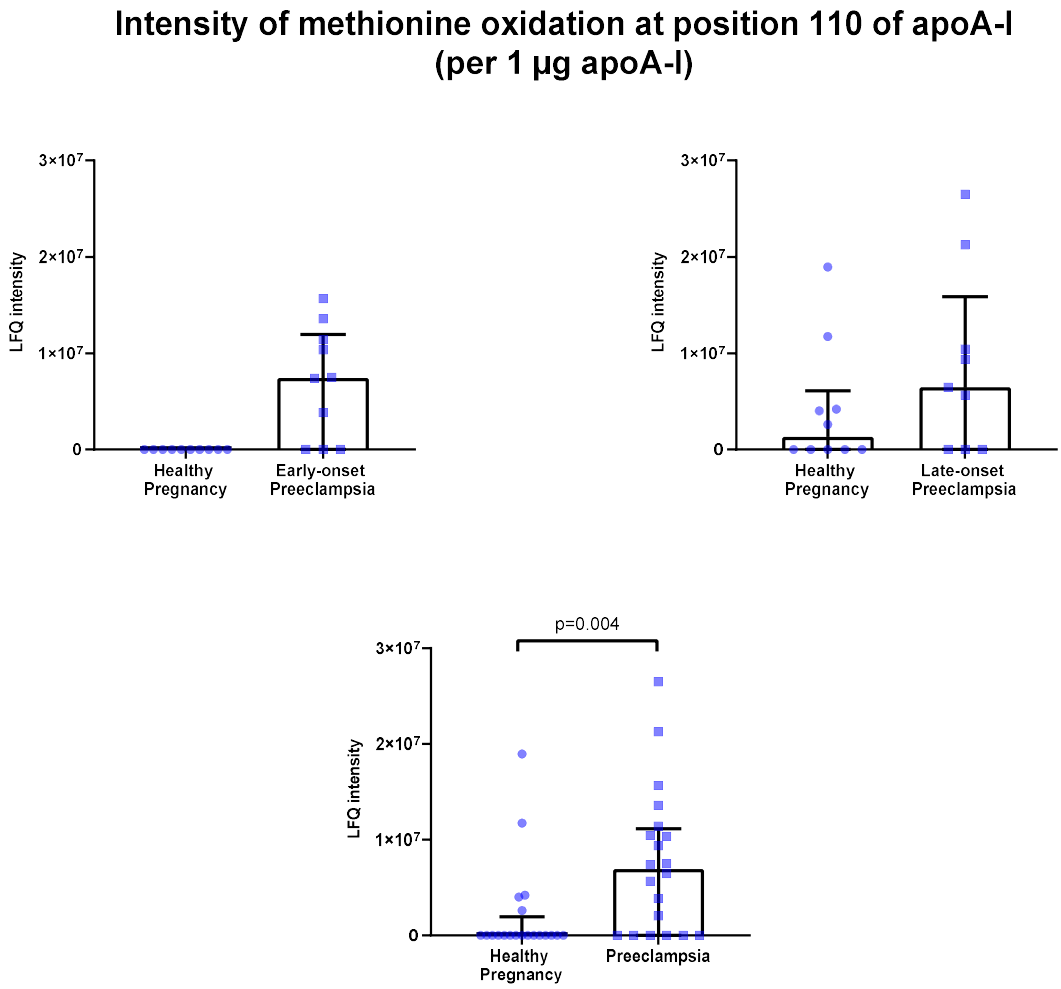

Figure 4-34 Intensity of oxidised methionine at position 110 on apoA-I Data was expressed as median±interquartile range. Mann-Whitney tests were carried out to compare the data between early-onset preeclampsia HDL and gestation matched controls (left above), late-onset preeclampsia HDL and gestation matched controls (right above), and preeclampsia HDL and gestation matched healthy pregnancy HDL (below). $p<0.05$ was taken as statistically significant.

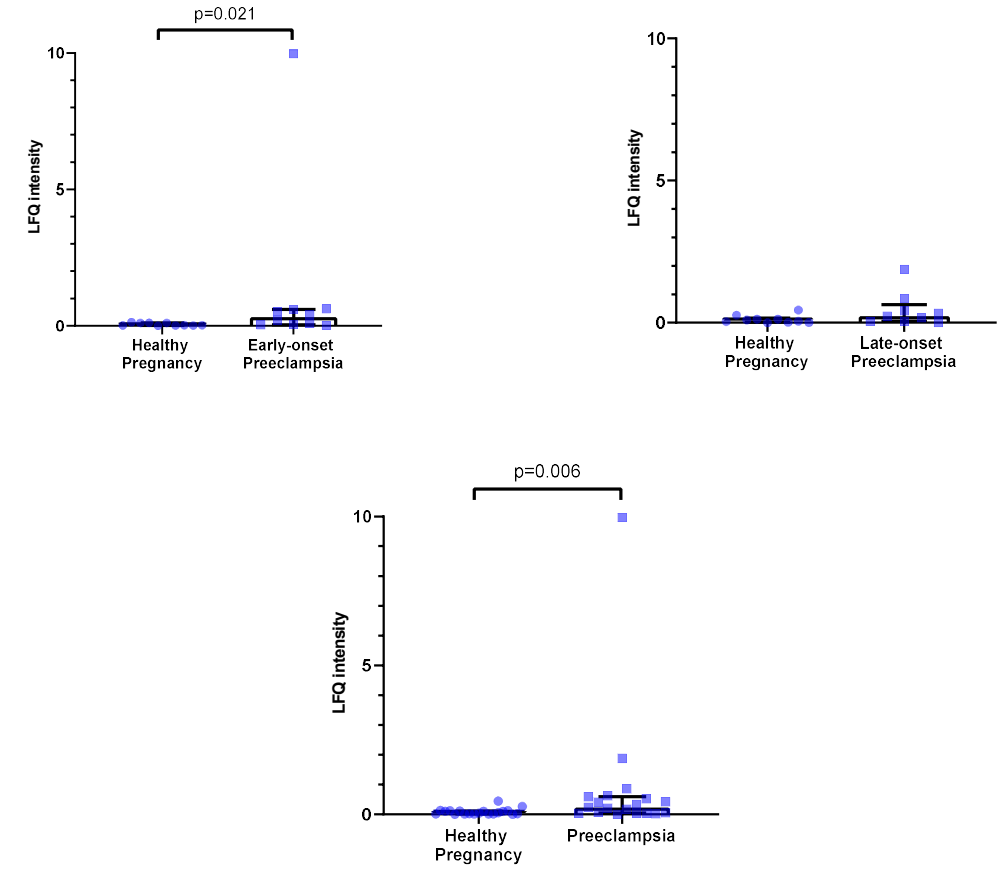

Figure 4-35 Ratio of oxidised to non-oxidised methionine at position 172 on apoA-I Data was expressed as median±interquartile range. Mann-Whitney tests were carried out to compare the data between early-onset preeclampsia HDL and gestation matched controls (left above), late-onset preeclampsia HDL and gestation matched controls (right above), and preeclampsia HDL and gestation matched healthy pregnancy HDL (below). $p<0.05$ was taken as statistically significant.

4.3.10 SAA1 concentration in HDL of preeclampsia and healthy pregnancy

There was no significant difference in SAA1 concentration between early- or late-onset preeclampsia HDL and their controls as well as between combined preeclampsia and combined healthy pregnancy (Figure 4-36).

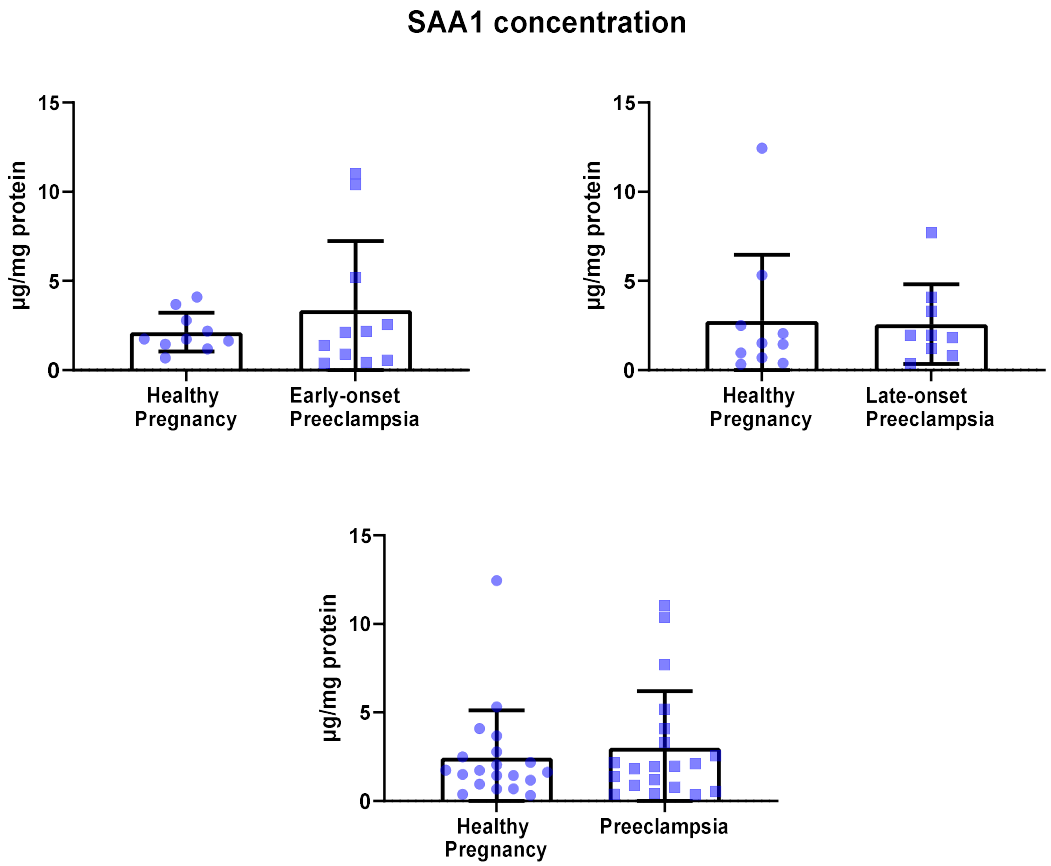

Figure 4-36 SAA1 concentration in HDL of healthy pregnancy and preeclampsia: Data was expressed as mean±SD. Unpaired t-tests were carried out on log transformed SAA1 concentration between early-onset preeclampsia HDL and gestation matched controls (left above), late-onset preeclampsia HDL and gestation matched controls (right above), and preeclampsia HDL and gestation matched healthy pregnancy HDL (below). $p<0.05$ was taken as statistically significant.

4.3.11 PON1 activity in HDL from preeclampsia and healthy pregnancy

There was no significant difference in PON1 activity between early- or late-onset preeclampsia HDL and their controls as well as between combined preeclampsia and combined healthy pregnancy (Figure 4-37). The ratio of SAA1 concentration to PON1 activity did not differ between early- or late-onset preeclampsia HDL and their controls as well as between combined preeclampsia and combined healthy pregnancy (Figure 4-38).

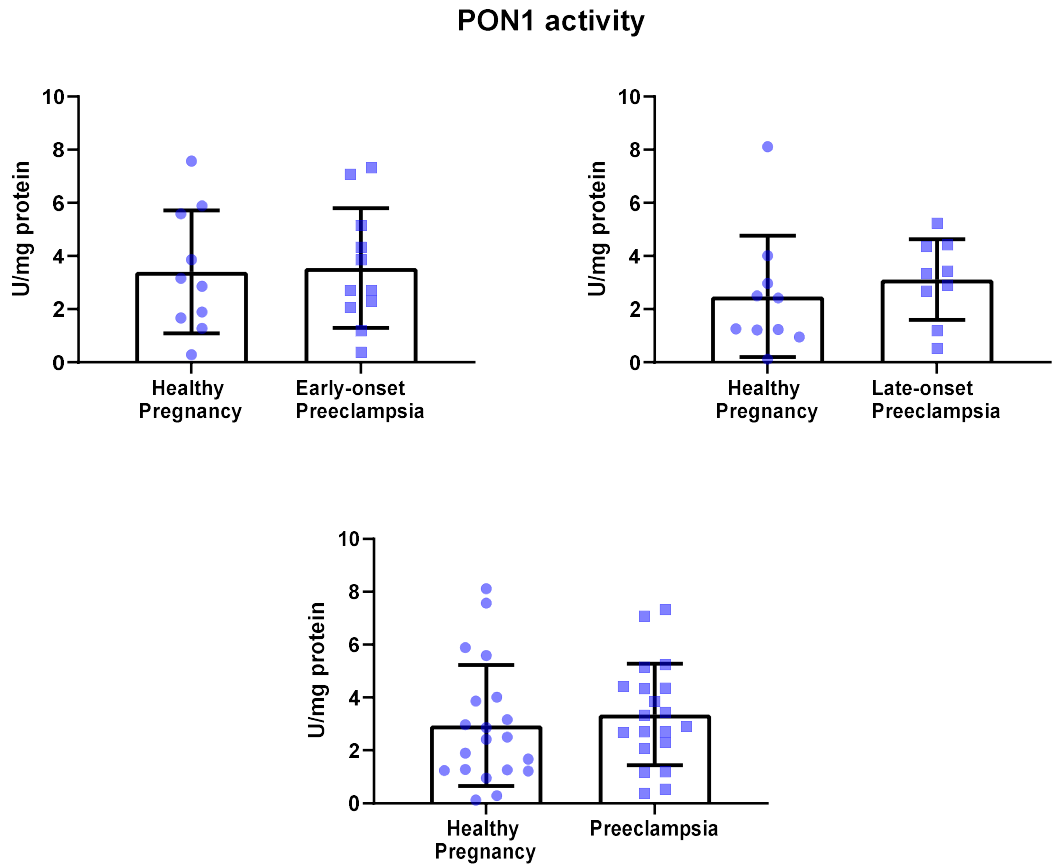

Figure 4-37 PON1 activity of HDL in healthy pregnancy and preeclampsia: Data was expressed as mean±SD. Unpaired t-tests were carried out to compare PON1 activity between early-onset preeclampsia HDL and gestation matched controls (left above), late-onset preeclampsia HDL and gestation matched controls (right above), and preeclampsia HDL and gestation matched healthy pregnancy HDL (below). $p<0.05$ was taken as statistically significant.

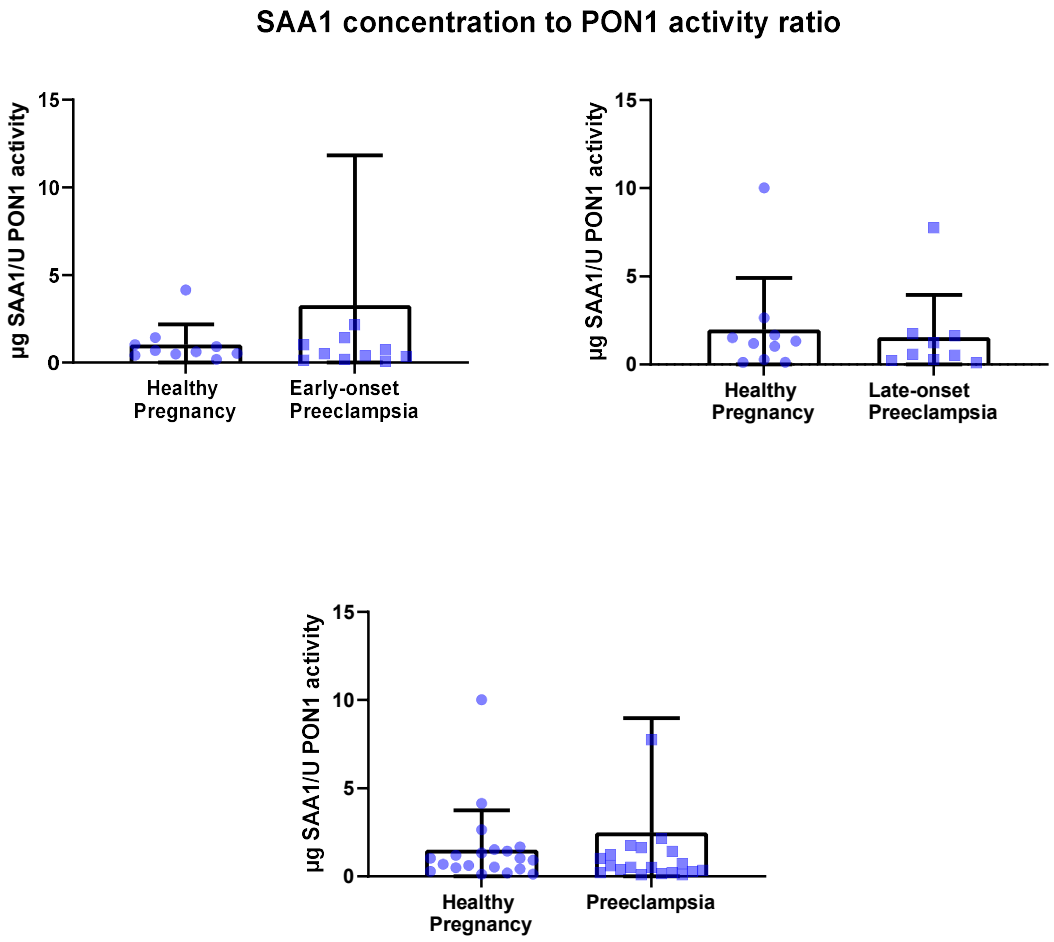

Figure 4-38 PON1 activity of HDL in healthy pregnancy and preeclampsia: Data was expressed as mean±SD. Unpaired t-tests were carried out on log transformed SAA1 to PON1 ratio between early-onset preeclampsia HDL and gestation matched controls (left above), late-onset preeclampsia HDL and gestation matched controls (right above), and preeclampsia HDL and gestation matched healthy pregnancy HDL (below). $p<0.05$ was taken as statistically significant.

4.4 Discussion

This chapter reveals a similar HDL apoA-I and cholesterol concentration between early- or late-onset preeclampsia and their matched controls, and between combined preeclampsia and healthy pregnancy. This is inconsistent with other HDL studies that showed lower HDL cholesterol concentration in preeclampsia relative to healthy pregnancy (Sattar, Bendomir, et al. 1997; Al-Kuraishy, Al-Gareeb, and Al-Maiahy 2018). While there is a study showed similar HDL concentration between preeclampsia and healthy pregnancy (Rodie et al. 2004). The lack of detection of reduced HDL concentration in preeclampsia of this study could be due to heterogeneity of pathophysiology of early- and late-onset preeclampsia and a different proportion of these two types of preeclampsia in each study. Another reason can be that a sample size of n=10 per group of this

study, powered for the proteomics analysis, may have been underpowered to detect a difference in HDL cholesterol. Effect size for HDL cholesterol in preeclampsia was calculated from a priori power calculation based on a study by (Al-Kuraishy, Al-Gareeb, and Al-Maiahy 2018) comparing HDL cholesterol concentration of preeclampsia and healthy pregnancy. Pooled SD of HDL cholesterol concentration in those two groups was 9.16. It was calculated that n=20 women per group are required to achieve 90% power at α=0.05 to detect the expected difference in HDL cholesterol concentration between preeclampsia and healthy pregnancy.

There were 151 HDL-associated proteins identified in preeclampsia and healthy pregnancy while 63 HDL-associated proteins were identified throughout gestation of healthy pregnancy (Chapter 3). This suggests more complex mixture of HDL protein changes in preeclampsia than in a healthy pregnancy process. However, there was a small difference of HDL protein composition between preeclampsia and healthy pregnancy with only 20 out of 151 proteins showing a significant difference. Considering that 16 out of 63 HDL-associated proteins were significantly altered throughout gestation, it seems that there was a greater magnitude of fewer HDL protein changes affected by gestation *per se*. Whereas HDL protein changes were subtler in a more complex change in preeclampsia.

There were six proteins that showed differences between early-onset preeclampsia HDL and matched control HDL. Even though early-onset preeclampsia and combined preeclampsia had higher BMI than their controls and might affect HDL composition, OPLS-DA which corrected for BMI showed significant separation of early-onset preeclampsia HDL proteins from their matched healthy pregnancy controls and combined preeclampsia HDL proteins from healthy pregnant HDL. On the other hand, OPLS-DA of late-onset preeclampsia HDL proteins and its controls were not significantly separated perhaps due multiple overlapping aetiologies. The insignificant separation of late-onset preeclampsia and healthy pregnant HDL proteins may be due to the multifactorial pathophysiology of late-onset preeclampsia i.e., maternal age, BMI and cardiovascular risks, unlike in early-onset preeclampsia where the pathophysiology may be less heterogenous resulting from placental dysfunction.

Proteins that significant differed between late-onset preeclampsia HDL and matched healthy pregnancy HDL were different from proteins that significant differed between early-onset preeclampsia HDL and matched healthy pregnancy HDL. These findings emphasize the difference in pathophysiology of early- and late-onset preeclampsia that may result in or be the consequence of different HDL protein composition. HDL protein composition appears to be affected by both preeclampsia pathology.

ApoA-IV and L-selectin were lower specifically in early-onset preeclampsia HDL than in matched control HDL without difference between combined preeclampsia HDL and combined healthy pregnancy HDL. It is likely that apoA-IV and L-selectin were affected by pathology of early-onset preeclampsia and not preeclampsia in general. Whereas peroxiredoxin-2, zinc-α-2-glycoprotein, ß-2-microglobulin and Rap-1b showed differences between early-onset preeclampsia HDL and matched control HDL, and between combined preeclampsia and combined healthy pregnancy group. These protein changes can be either the effect of pathology of early-onset preeclampsia or preeclampsia. Lower levels of the anti-inflammatory protein, apoA-IV, and the antioxidant enzyme, peroxiredoxin-2, in early-onset preeclampsia HDL compared to controls is consistent with an excessive inflammatory and oxidative state in preeclampsia (Hochepied et al. 2003; Duka et al. 2013). This suggests HDL dysfunction in modulating inflammatory and oxidative state, resulting in excessive inflammation ad oxidative stress in early-onset preeclampsia. Reduction of L-selectin in early-onset preeclampsia HDL might seem incompatible with the previous suggestion since it is an adhesion molecule on leukocytes facilitating leukocyte migration and inflammation. However, this finding is consistent with previous data showing that lower surface L-selectin was found on neutrophils in preeclampsia (Sacks et al. 1998). In addition, one study showed increased L-selectin expression in placenta of an early-onset preeclampsia group and that placental L-selectin correlated with angiotensin type 2 receptor expression in preeclampsia (Mistry et al. 2020). These findings may suggest a role for L-selectin in the pathophysiology of early-onset preeclampsia through its placental expression rather than in HDL. It was shown in this chapter that SAA1 concentration, PON1 activity and the ratio of SAA1 concentration to PON1 activity between preeclampsia and healthy pregnancy HDL did not differ. This is

inconsistent with other studies that showed higher SAA concentration and lower PON1 activity in preeclampsia serum than in healthy pregnancy serum (Genc et al. 2011; Al-Kuraishy, Al-Gareeb, and Al-Maiahy 2018; Engin-Ustün et al. 2007). This can be due to a sample size of n=10 in this chapter which was powered for the proteomics analysis may have been underpowered to detect a difference in HDL SAA concentration and PON1 activity. The only data available online for SAA concentration in preeclampsia and healthy pregnancy was a median and maximum to minimum range so effect size for SAA in preeclampsia was calculated based on the difference in medians and estimated SD assuming that the data was normally distributed (Engin-Ustün et al. 2007). It was calculated that n=13 women per group are required to achieve 90% power at α=0.05 to compare HDL SAA concentration between preeclampsia and healthy pregnancy. For PON1 activity in preeclampsia, n=17 women per group were required to achieve 90% power at α=0.05 (Genc et al. 2011). Another difficulty in comparing PON1 activity result from different laboratory settings is that different substrates may be used and the phenyl acetate used to assay PON1 activity in this thesis has a higher rate of hydrolysis than paraoxon that was used in (Genc et al. 2011). When stored at -80ºC, PON1 activity towards phenyl acetate is more stable than that toward paraoxon [reviewed in (Ceron, Tecles, and Tvarijonaviciute 2014)]. It is therefore difficult to compare data from different laboratory settings and to interpret absolute PON1 activity.

Zinc-α-2-glycoprotein is well-known as an adipokine that promotes lipid catabolism in adipose tissue but its role in plasma and HDL is still unresolved (Hassan et al. 2008). Even though the structure of zinc-α-2-glycoprotein is remarkably similar to that of the MHC-I molecule, no evidence for a role of zinc-α-2-glycoprotein in the immune response has been found (Hassan et al. 2008). Lower zinc-α-2-glycoprotein in early-onset preeclampsia HDL is in contrast to previous data showing higher serum zinc-α-2-glycoprotein concentration in the third trimester of early-onset preeclampsia (Stepan et al. 2012). Zinc-α-2-glycoprotein in HDL and serum both originate from the liver, thus, this finding might suggest that there may be an alteration in the distribution of zinc-α-2-glycoprotein among plasma compartments in early-onset preeclampsia or preeclampsia in general. More information on the properties of zinc-α-2-glycoprotein in plasma and HDL is required to elucidate the significance of our

finding. ß-2-microglobulin is a subunit of MHC-I molecule which is important in presenting endogenous antigen to cytotoxic T cells inducing the adaptive immune response (Bernier 1980). Rap-1b is a key regulator of integrin, the marker of immune stimulation, and has a key role in early B cell development and T-dependent humoral immunity (Stefanini and Bergmeier 2019; Haiyan Chu 2008). Both proteins are involved in the adaptive immune system and were higher in early-onset preeclampsia and preeclampsia, suggesting activated adaptive immunity in early-onset preeclampsia or preeclampsia *per se*.

Regarding late-onset preeclampsia, BPI fold-containing family B member 1, protease C1 inhibitor and myosin-9 showed differences specifically between late-onset preeclampsia HDL and matched control HDL. These changes were potentially resulted from pathology of late-onset preeclampsia. While there were eleven proteins including proteins involved the immune system (complement factor D and C9), lipoprotein metabolism (apoC-III, PLTP and LCAT), the gastrointestinal system (keratinocyte differentiation-associated protein and ribonuclease pancreatic), the coagulation system (ß-2-glycoprotein 1, antithrombin and prothrombin) and collagen α-1 chain that showed differences between late-onset preeclampsia and matched control and between combined preeclampsia and combined healthy pregnancy group. These changes can be either the effect of pathology of late-onset preeclampsia or preeclampsia. BPI fold-containing family B member 1, protease C1 inhibitor, myosin-9, complement factor D and C9 are all involved in complement activation or the innate immune response (Shao et al. 2015; Nam et al. 2014; Tsai et al. 2014). These findings suggest a difference in immune pathophysiology between early- and late-onset preeclampsia with more activated adaptive immunity in early-onset preeclampsia and more activated innate immunity in late-onset preeclampsia.

Collagen α-1 chain is a fibril-forming collagen found in most connective tissue which is encoded by *COL1A1* gene. Several studies via weighted gene co-expression network analysis which create a scale-free network from gene expression data found that *COL1A1* polymorphisms were the most relevant gene to dyslipidemia in an obese population (Miao et al. 2019; Kathiresan et al. 2007). The mechanism underlying this association is still unclear. The higher collagen α-

1 chain in late-onset preeclampsia HDL may suggest its involvement in dyslipidemia in late-onset preeclampsia. Next, apoC-III is known to inhibit LPL, an enzyme that converts VLDL to IDL and LDL, and reduce TRLs uptake into the liver [reviewed in (Ooi et al. 2008; Kontush et al. 2015)]. Thus, increased apoC-III may result in increased VLDL which is found in preeclampsia. HDL apoC-III is also shown to be associated with coronary artery disease risk in which HDL containing apoC-III was positively associated and HDL without apoC-III was negatively associated with coronary heart disease risk. Increased apoC-III content in HDL was revealed to impair the protective properties of HDL, for example, endothelial anti-apoptosis and RCT(Jensen et al. 2012; Riwanto et al. 2013; Luo et al. 2017). Thus, increased apoC-III in HDL may contribute to the pathophysiology of late-onset preeclampsia by impairing the vasculo-protection properties of HDL leading to endothelial dysfunction. Higher LCAT, a cholesterol esterifying enzyme, was also found which, in contrast, can improve RCT function of HDL. Whether the RCT ability of HDL is affected in late-onset preeclampsia is not yet determined.

Elevation of both LCAT and PLTP in HDL observed in late-onset preeclampsia may lead to altered lipid composition and a shift in HDL subfraction distribution to HDL2. LCAT promotes formation of mature HDL from nascent HDL via small, dense HDL3 to eventually larger HDL2, and PLTP, a transfer protein that mainly moves phospholipid between lipoproteins, was also shown to promote fusion of HDL3 particles and generate HDL2 (Vikstedt et al. 2007; Tall, Forester, and Bongiovanni 1983; Lusa et al. 1996). This is consistent with increased HDL diameter found in preeclampsia, relative to healthy pregnancy (Einbinder et al. 2018). However, we found that the HDL cholesterol/apoA-I ratio, which was found directly related with HDL particle size and can be used as a surrogate for HDL size, was lower in preeclampsia compared to healthy pregnancy, implying smaller HDL size in preeclampsia (Mazer et al. 2013). This inconsistency could be due to the heterogenous pathophysiology of preeclampsia. This chapter only suggests larger HDL particles (inferred from increased LCAT and PLTP in HDL) in late-onset preeclampsia, but not early-onset preeclampsia. Whereas the HDL cholesterol/apoA-I ratio did not differ between early- or late-onset preeclampsia and their controls. Increased HDL particle size has been shown to be related with major cardiovascular event (van der Steeg et al. 2008). Small HDL particle

was also inversely related to serum concentration of N-terminal pro-brain natriuretic peptide, a marker of heart failure, and high-sensitive cardiac troponin T, a marker of myocardial dysfunction (Duparc et al. 2020). Thus, it would be useful to directly measure HDL particle size in our samples to increase our understanding of pathophysiology of early- and late-onset preeclampsia in HDL size.

Next, the gastrointestinal (GI) tract associated proteins, keratinocyte differentiation-associated protein and ribonuclease pancreatic, were found to be higher in late-onset preeclampsia HDL than in healthy pregnancy HDL. This may suggest increased intestinal permeability that allows more proteins to enter from the gut lumen into the circulation. Intestinal permeability was shown to be positively related to unfavourable glucose and lipid metabolism, metabolic endotoxemia (LPS) and low-grade inflammation in overweight pregnant women (Mokkala et al. 2017). Positive correlations between intestinal permeability and plasma triglyceride and total cholesterol concentrations were found in both non-pregnant and pregnant populations. In contrast, HDL showed a positive correlation only in pregnancy and was negatively correlated with intestinal permeability in non-pregnancy (Mokkala et al. 2017; Robertson et al. 2018; Moreno-Navarrete et al. 2012). This suggests that the adaptation of pregnant HDL to protect against metabolic risk in healthy pregnancy may fail to happen in late-onset preeclampsia.

Preeclampsia is associated with hypercoagulable state with increased APTT and TT (Han et al. 2014). Early-onset severe preeclampsia is the high-risk group for super hyper-coagulation while late-onset preeclampsia and moderate preeclampsia mostly show similar coagulation values compared to healthy pregnancy (Heilmann, Rath, and Pollow 2007). However, our findings in late-onset preeclampsia show some degree of coagulation abnormalities. Ꞵ-2-glycoprotein 1 has shown both anti- and pro-coagulative effects including binding to thrombin to downregulate its activity as the anticoagulant effect, and inhibiting thrombomodulin and protein C activation which is a procoagulant effect [reviewed in (McDonnell et al. 2020)]. Antithrombin can inactivate thrombin and other coagulation factors while prothrombin is a substrate for thrombin generation and subsequently, clot formation. Effects of Ꞵ-2-

glycoprotein 1, antithrombin and prothrombin on coagulation cascade are correlated with HDL function (Figure 4-38). Our findings concerning low expression of ß-2-glycoprotein 1 and prothrombin in HDL may suggest improved antithrombotic effect of HDL while low expression of antithrombin and ß-2-glycoprotein 1 may support dysfunction of HDL in protecting against prothrombotic state.

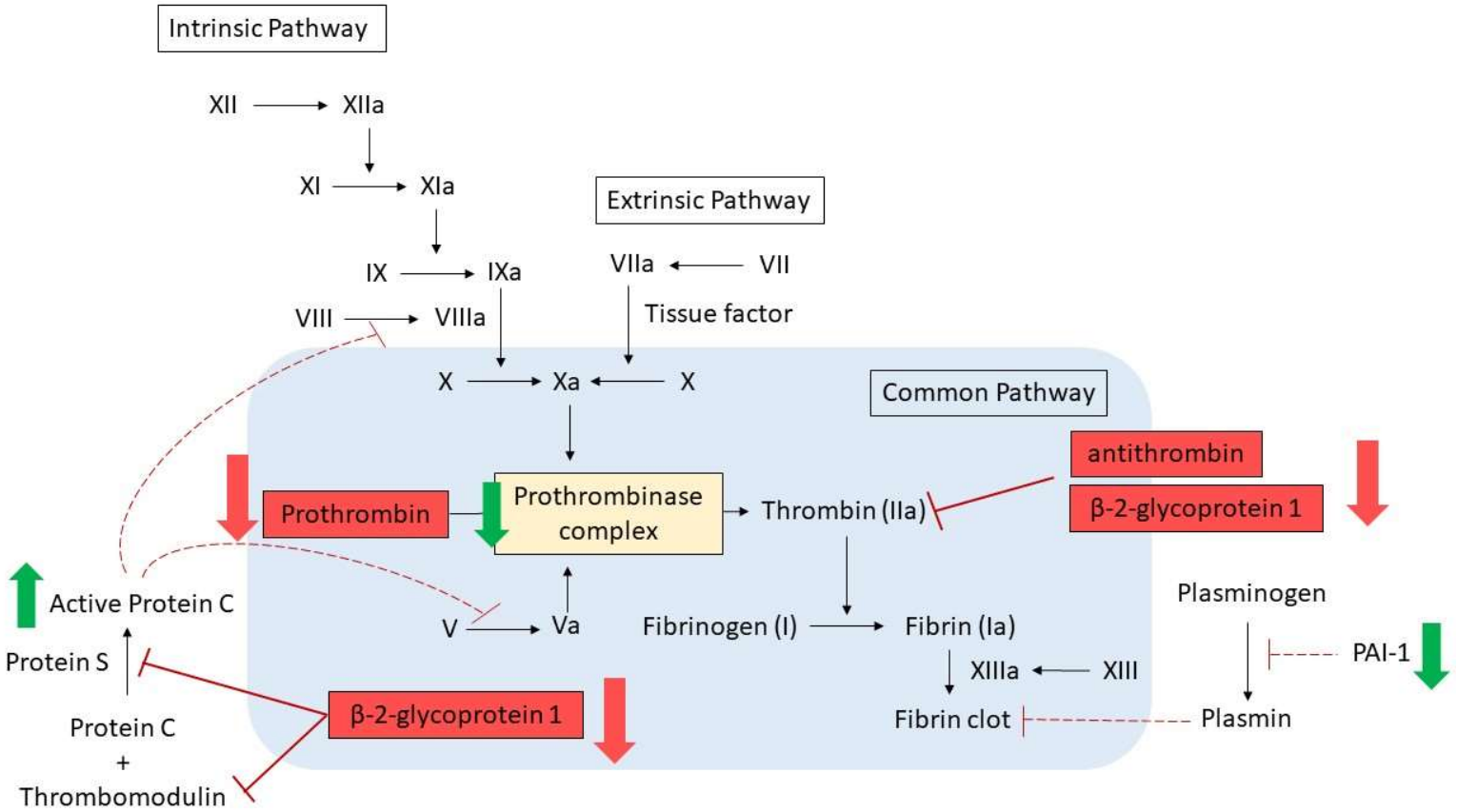

Figure 4-39 Role of β-2-glycoprotein 1, antithrombin and prothrombin in the coagulation cascade and anti-thrombotic properties of HDL Green arrows demonstrate anti-thrombotic actions of HDL. HDL activates protein C which further inhibits factor VIIIa and Va. HDL also inhibits formation of prothrombinase complex and reduces PAI-1 expression. Red arrows represent changes of LFQ intensity of proteins (in red box) in preeclampsia HDL. β-2-glycoprotein 1 can inhibit protein C activation, binding to thrombin to downregulate its activity and inhibiting thrombomodulin. Antithrombin can inactivate thrombin while prothrombin is a substrate for thrombin generation.

Lastly, calmodulin-3, prosaposin, hemopexin, vitamin D-binding protein and complement C4a showed differences between combined preeclampsia and combined healthy pregnancy group without differences between either the early-onset or late-onset preeclampsia groups and their gestation matched healthy pregnancy controls. Calmodulin-3 and complement C4a were higher in preeclampsia HDL while hemopexin, prosaposin and vitamin D-binding protein were lower in preeclampsia compared to those of healthy pregnancy. It is suggested that these protein changes were the result of pathology of preeclampsia rather than early- or late-onset preeclampsia alone. Calmodulin involves in calcium signal transduction and regulating cells in various biological pathways (reviewed in (Cheung 1980)). Studies *in vitro* observed an interaction between calmodulin and ABCA1 which was increased by calcium and zinc (Iwamoto et al. 2010; Lu et al. 2021). This binding of calmodulin protected degradation of ABCA1. Calmodulin-knockdown cells showed accelerated ABCA1 degradation, thus reduced cellular cholesterol efflux to HDL and HDL biogenesis (Iwamoto et al. 2010). Higher calmodulin in preeclampsia HDL may result in enhanced RCT function of HDL and HDL biogenesis. Plasma concentration of HDL was lower in preeclampsia compared to healthy pregnancy, suggesting that calmodulin may not affect HDL production in preeclampsia, but it may be a compensatory mechanism to increased RCT. Lower prosaposin in preeclampsia HDL might be associated with reduced HDL biogenesis in preeclampsia. Prosaposin is a precursor of saposin which activates degradation of sphingolipids and is required in membrane localization of ABCA1 (Sandhoff and Kolter 2003; Basford et al. 2011). Inhibition of the prosaposin conversion to saposin resulted in sphingolipid accumulation in lysosomes and reduced availability of ceramide to promote ABCA1 membrane translocation, thus decreased membrane ABCA1 and reduced cholesterol efflux to HDL and decreased HDL production (Haidar et al. 2006; Witting, Maiorano, and Davidson 2003). Reduction of prosaposin in preeclampsia HDL is consistent with and could be one of mechanisms in reducing HDL concentration in preeclampsia.

Lower hemopexin in preeclampsia HDL may indicate impaired anti-oxidative and anti-inflammatory function of HDL in preeclampsia. Hemopexin is a transport protein that has the highest binding affinity for heme (Altruda et al. 1985). Cellular uptake of heme promotes heme degradation and, thus, prevent heme-

mediated ROS production and oxidative stress (Smith and Morgan 1981; Puppo and Halliwell 1988). Treatment of mouse hepatoma cells and human promyelocytic cells with heme-hemopexin complex also induced mRNA expression of metallothionine which reduced oxidative stress likely by inhibiting lipid peroxidation (Alam and Smith 1992; Thornalley and Vasák 1985; Hidalgo et al. 1988). In terms of HDL, apoE-knockout mice lacking hemopexin showed higher heme, ROS and proinflammatory HDL in plasma, resulting in higher atherosclerotic lesions than apoE-knockout mice with hemopexin (Mehta et al. 2016). Macrophages of this mouse model lacking hemopexin also revealed reduced cholesterol efflux capacity (Mehta et al. 2016).

Another protein reduced in preeclampsia HDL was vitamin D-binding protein. Vitamin D-binding protein is the main carrier of vitamin D and its metabolites (Daiger, Schanfield, and Cavalli-Sforza 1975). It is also an actin scavenger preventing filament formation which may cause vascular obstruction (Speeckaert et al. 2006). Our observation of reduced vitamin D-binding protein in preeclampsia HDL is consistent with decreased plasma concentration and placental expression of this protein as reported in other preeclampsia studies. The normal gestational increase in plasma vitamin D-binding protein was lost in preeclampsia patients (Bikle et al. 1984; Tannetta, Redman, and Sargent 2014). An immunostaining study showed reduced expression of vitamin D-binding protein in syncytiotrophoblasts of placenta from preeclampsia pregnancies compared to those in healthy placenta (Ma et al. 2012). Induction of oxidative stress also resulted in downregulated expression of vitamin D-binding protein in cultured trophoblasts from healthy placenta (Ma et al. 2012). Reduced vitamin D-binding protein in plasma, HDL and placenta of preeclampsia suggests a role for reduced availability of vitamin D or vitamin D-binding protein activity in the pathogenesis of preeclampsia. The exact role of vitamin D in preeclampsia is still unclear, but lower plasma vitamin D levels were detected in pregnant women who subsequently developed preeclampsia and were related to an increased risk of preeclampsia (Bodnar et al. 2007). Vitamin D-binding protein also helps to cleave excessive actin released from damaged cells during pregnancy thereby preventing actin’s thrombotic effects (Tannetta, Redman, and Sargent 2014). Loss of this function could contribute to a procoagulant state in preeclampsia.

Early-stage protein glycation of apoA-I lysine at position 232 but not AGE was found to be lower in apoA-I in early-onset preeclampsia. This finding illustrates decreased early-stage glycation but still similar advanced glycation of apoA-I in early-onset preeclampsia and healthy pregnancy. Advanced glycated apoA-I has been shown to impair anti-atherogenic properties of HDL such as RCT, anti-oxidation and anti-inflammation. Treatment of reconstituted HDL with glycated lysine in apoA-I reduced its capacity to promote cholesterol efflux from cultured macrophages (Domingo-Espín et al. 2018). Glycation of apoA-I lysine (including lysine at position 232) has been shown to reduce glucose uptake in cultured mouse myotubes without any impact on plasma glucose clearance in an insulin-resistant mouse model or insulin secretion from cultured INS-1E beta cells (Domingo-Espín et al. 2018). However, we found no difference of advanced glycation of apoA-I in early- or late-onset preeclampsia compared to their gestation matched controls. This may imply that glycation modification of apoA-I is unlikely to involved in preeclampsia pathophysiology.

Oxidation of Met172 was higher in early-onset preeclampsia HDL than its matched control HDL and higher in combined preeclampsia HDL than combined healthy pregnancy HDL. A study of the amphipathic helical domain of apoA-I suggested the importance of residues 66-120 in LCAT activation [reviewed in (Segrest et al. 1992)]. Oxidation of Met172 has been reported to diminish RCT of HDL by impairing the ABCA1 pathway and LCAT activation (Shao et al. 2014; Shao et al. 2008). It may also induce inflammation by producing pro-inflammatory molecules (Witkowski et al. 2019). Thus, increased Met172 oxidation may imply dysfunctional RCT of HDL and enhancing inflammatory environment in early-onset preeclampsia and/or preeclampsia *per se*. A significantly higher level of methionine oxidation at positions 110 of apoA-I were also found in combined preeclampsia compared to healthy pregnancy. Cellular studies revealed enhanced cholesterol removal from human monocyte-derived macrophages when incubated with apoA-I containing Met110 oxidation compared to apoA-I without methionine oxidation (Panzenböck et al. 2000). This is in contrast with the possibility that RCT of HDL is impaired in preeclampsia. It would be important to directly determine RCT efficacy of HDL in early- and late-onset preeclampsia.

This study is the first HDL proteomic study in preeclampsia. The strength of this study is the focus of HDL data in early- or late-onset preeclampsia relative to their matched healthy pregnancy rather than preeclampsia *per se* to avoid the heterogenous of pathophysiology between early- and late-onset preeclampsia. Comparison of early- or late-onset preeclampsia with their gestational-age-matched healthy pregnancy also help reduce the confounding effect of gestation on HDL protein composition. There was also a validation analysis to identify difference in HDL data resulted from preeclampsia *per se* independent of gestation of onset, the early- and late-onset preeclampsia. The limitation of this study is that it is a cross-sectional study of preeclampsia and healthy pregnancy. Even though these two groups of participants were matched with gestational age, there was a significant difference of BMI between preeclampsia or early-onset preeclampsia with their controls. Different BMI could reflect differences in maternal lipid metabolism and may be HDL composition and function. A longitudinal study of pregnant women who later develop preeclampsia would be useful to observe the changes during preeclampsia development without this limitation. Multivariate analysis of HDL proteins was performed in this study with correction. Another limitation to be considered in this study is multiple comparison which could increase a false positive. It is important to look at levels of significance ranking for those with lower p as results with greater certainty and to give more credence to those difference with lower p.

In summary, this study showed small changes in HDL protein composition in early- and late-onset preeclampsia. A difference of HDL pathophysiology of early- and late-onset preeclampsia was shown as HDL proteins that showed differences between early-onset preeclampsia and their matched controls, and late-onset preeclampsia and their matched controls were completely different. This study of HDL proteome suggests that there could be impaired RCT and anti-inflammatory effect of HDL in early-onset preeclampsia. There may be impaired antioxidant effects of HDL in early-onset preeclampsia or in preeclampsia in general. HDL protein changes in late-onset preeclampsia suggests a possible contribution of HDL in hypertriglyceridemia and increased intestinal permeability. RCT and anti-thrombotic effect of HDL might be impaired in late-onset preeclampsia. Larger HDL particle size was also suggested in late-onset preeclampsia. It would be useful to directly examine HDL size in late-onset

preeclampsia for a better understanding in pathophysiology of HDL in preeclampsia. HDL function including RCT, anti-inflammatory and antioxidant function should be investigated in early-onset preeclampsia and RCT and anti-thrombotic function should be investigated in late-onset preeclampsia.

5 HDL functional assay development

5.1 Introduction

It is well-known that HDL has many properties that might protect the vascular endothelium including RCT, vasodilatory, anti-inflammatory, anti-oxidative and anti-thrombotic activities. It was evident that low HDL cholesterol concentration positively associated with progressive atherosclerosis as demonstrated by coronary arteriography and greater risk of ischemic stroke and carotid atherosclerosis [as reviewed in (Maron 2000)]. A strong inverse relationship between HDL cholesterol levels and subsequent incidence of coronary heart disease was also observed in the Framingham Heart Study, a four-year follow up study of both men and women, aged 49 to 82 years (Gordon et al. 1977). In healthy pregnancy, HDL cholesterol and apoA-I concentration increased (Alvarez et al. 1996; Sulaiman et al. 2016). While HDL cholesterol concentration is significantly lower in preeclampsia relative to healthy pregnancy (Sattar, Bendomir, et al. 1997). This thesis has shown a significant change of HDL protein composition throughout gestation of healthy pregnancy and between preeclampsia and healthy pregnancy in Chapter 3 and 4. The changes of HDL proteins during pregnancy suggest improved vascular protective function of HDL, for example, increased A1AT in the first trimester that could protect RCT function of HDL from protease-induced deterioration and reduced apoA-I glycation in the first trimester that could reduce impairment of RCT and anti-inflammatory function from glycation. While differences of HDL proteins between preeclampsia and healthy pregnancy might link to dysfunctional HDL in preeclampsia including anti-inflammatory activity in early-onset preeclampsia and anti-thrombotic effect of HDL in late-onset preeclampsia. In order to link HDL composition to HDL function, I aim to develop assays that could directly measure HDL function, especially the vasodilatory and anti-thrombotic properties of HDL.

Vascular endothelium has a key role in regulating vascular tone, anti-thrombotic effects and anti-inflammatory effects under physiological conditions. Assessment of endothelial function mainly aims to investigate vascular reactivity following a stimulus. The gold standard of endothelial function assessments are methods that measure vascular reactivity intravascularly under *in vivo* conditions such as

intravascular ultrasound or coronary angiography following an administration of endothelial vasoactive substances. Due to their invasiveness, these applications are limited to patients that require the procedure as clinical interventions. Less invasive methods such as flow-mediated dilation of the brachial artery are more frequently used in research settings. Flow-mediated dilation of the brachial artery is a method of determining arterial diameter changes using ultrasound following an occlusion of brachial artery by a blood pressure cuff to increase blood flow and endothelial shear stress, leading to NO stimulation. Flow-mediated dilation is used to indirectly determine HDL function by associating HDL concentration with vascular reactivity measured by flow-mediated dilation. HDL administration would be required to directly determine HDL effect on vascular reactivity, and it is not widely available particularly in human.

Other options for investigations into vascular reactivity *in vitro* include wire myography and pressure myography. Both methods are designed to examine vascular reactivity of isolated arteries in response to stimuli *in vitro* but under different conditions. In wire myography, arteries are prepared as ring segments, mounted onto wires and maintained under isometric conditions throughout the experiment. This method allows the examination of isometric responses of small resistance arteries by keeping the internal circumference of the artery segments constant and measuring the circumferential wall tension. In pressure myography, artery segments are cannulated and connected to a perfusion circuit that controls pressure and flow and keeps vessels under isobaric conditions. In addition to testing responses to pharmacological agents, pressure myography allows adjustable pressure and flow as stimuli for vascular responses which provides more physiological than wire myography. However, wire myography is more suitable for studies focusing on the mechanical properties of vessels. It is also relatively easy to set up and is able to run multiple artery segments at the same time to improve experimental output. Finally, plasma biomarkers such as adhesion molecules, proinflammatory markers and prothrombotic agents can be measured as an indirect assessment of endothelial function.

HDL is known to protect vessels from endothelial dysfunction through various mechanisms including vasodilatory effects and reducing coagulation and inflammation. HDL contributes to vascular tone regulation mainly by activating

NO production and thus promoting NO-mediated vasodilation (Jeffrey T. Kuvin and Richard H. Karas 2002; Yuhanna et al. 2001). In pregnancy, HDL concentration rose from 10 to 20 weeks of gestation and remains stable until delivery (Sulaiman et al. 2016). Reduced peripheral vascular resistance which reflects vasodilation also started early in the first trimester and continued during the second trimester (Atkins et al. 1981). These coincident events raise the possibility of HDL's contribution to vasodilation in pregnancy. Previous data collected by Sulaiman W. in our lab (unpublished) measured vascular reactivity of non-pregnant rat uterine arteries, pregnant rat uterine arteries, and human pregnant subcutaneous adipose tissue (SAT) arteries following HDL incubation. Wire myography was adopted to assess endothelial function and the concentration of 2% pooled HDL was used in this study based on the evidence of reduced endothelium-dependent relaxation of myometrial arteries after incubation with 2% of pooled plasma from women with preeclampsia (Hayman et al. 2000). These previous data revealed that pregnant HDL significantly reduced contractility and improved vasodilation of non-pregnant rat uterine arteries compared to non-pregnant HDL. The study in pregnant rat uterine arteries also showed that pregnant HDL markedly decreased vasoconstriction compared to non-pregnant HDL effect, while changes in vasodilation were not detected probably due to gestationally associated remodelling providing a background maximum relaxation of the arteries.

The previous studies in SAT arteries of pregnant women showed no statistical difference in contractile and relaxation response between pregnant and non-pregnant HDL due to small sample size, but the pattern of reduced vasoconstriction was identical to that seen in pregnant rat uterine arteries. Since human SAT arteries did show a trend towards reduced contractility in response to pregnant HDL compared to non-pregnant HDL it is important to examine HDL's vascular effects further. Wire myography was chosen for this experiment to allow 1) a direct comparison of pregnant and non-pregnant HDL impact on vascular reactivity of arteries from the same participant, 2) an ability to study small resistance arteries which are highly muscular and are important in blood flow regulation by contracting or dilating the vessels, and 3) a focus on mechanical properties of artery. The wire myography protocol used in this thesis was adapted from Professors Mulvany and Halpern's protocol (Mulvany and

Halpern 1977) including the mounting procedure, normalization of internal circumference and the functional assessment based on mesenteric arteries of rats. This protocol is well established in the lab for determining rat mesenteric artery function and function of uterine arteries from non-pregnant and pregnant rats. There was difficulty in collecting wire myography data from human SAT arteries due to a lower abundance of vessels in human SAT and difficulty in dissecting vessels from SAT as certain branch arteries cannot be found easily in human SAT compared to the easy dissection of rat mesenteric or uterine arteries. These difficulties with dissection led to inconsistency of vessel size and increased risk of damage to the vascular endothelium during vessel dissection so vessels did not reliably respond throughout the experiment. I sought to circumvent the problems with SAT artery dissection by using another type of human artery i.e., those from visceral adipose tissue (VAT). VAT is more vascularised than SAT and so the arteries are easier to identify and handle. In summary, I aimed to examine pregnant HDL's effect on vascular reactivity of VAT arteries of pregnant women using wire myography.

In addition to vasodilatory effects, HDL helps maintain endothelial function by promoting an anti-thrombotic state via impairing both platelet function and the coagulation cascade. Studies in mice showed that HDL can inhibit megakaryocyte proliferation, platelet production and aggregation via the apoE and SR-B1 receptors on the platelet surface (Murphy et al. 2013; Brodde et al. 2011). An *in vitro* study showed that HDL reduced coagulation factor Va activity through activation of protein C and protein S (Griffin et al. 1999). This mechanism of HDL stimulating protein C was argued by the loss of the ability of HDL to inactivate factor Va after additional purification of HDL by SEC (Oslakovic, Norstrøm, and Dahlbäck 2010). After ultracentrifugation and SEC, the HDL fraction showed no effect on factor Va activity whereas the activity that enhanced factor Va inactivation eluted in the void fraction containing anionic phospholipid (Oslakovic, Norstrøm, and Dahlbäck 2010). It is possible that the factor Va inactivation ability of HDL prepared by ultracentrifugation was not due to HDL itself but the contaminating anionic phospholipids. However, HDL effects in regulating the coagulation cascade has still been shown by other mechanism. It was shown that in a mixture of serum and liposomes containing natural phospholipids that labelled phospholipids transferred from liposomes to apoB

and apoA-I-containing particles and that apoA-I-containing particles neutralized procoagulant property of anionic phospholipids (Oslakovic et al. 2009). Anionic phospholipid incorporated into rHDL with purified apoA-I was unable to bind factor Va and did not stimulate factor X and prothrombin activation, in contrast to the control liposomes (Oslakovic et al. 2009). Thus, HDL seems to exert its anti-thrombotic properties through impairing conversion of prothrombin to thrombin. The formation of the prothrombinase complex in previous studies of HDL function was assessed by the prothrombinase assay which measured thrombin generated from a mixture of HDL and the factors required for prothrombinase complex formation and thrombin generation (clotting factor V and Xa, calcium and prothrombin).

In plasma, a thrombin generation assay is normally used to assess the clotting potential of plasma (Bennett et al. 2014) and is a kinetic assay of coagulation. The principle of this method is to trigger coagulation in plasma by adding tissue factor, calcium and phospholipids to generate thrombin. Thrombin generated over time is then measured by adding a fluorogenic substrate to cleave thrombin to generate a fluorescent product which can be measured by a microplate fluorometer. The principles of prothrombinase assay and the thrombin generation assay are similar, but the thrombin generation assay has an advantage over the prothrombinase assay in that plasma is used instead of clotting factors V and Xa, calcium and prothrombin mixture, thus is closer to human physiological conditions. Therefore, I aimed to adapt an existing commercial thrombin generation assay protocol used for plasma into an assay able to determine the anti-clotting potential of HDL. All the coagulation factors and proteins necessary in generating thrombin are in plasma but in the case of assessing HDL, these factors would be fractionated into the lipoprotein-depleted plasma (LpDP) fraction after the lipoprotein isolation process. Thus thrombin generation in the presence of high and low density lipoprotein fractions (HDL and VLDL/LDL), lipoprotein-depleted plasma (LpDP) and with lipoprotein fractions combined with LpDP or plasma were compared.

In this chapter, the development of two assays for determining HDL function has been described. The HDL functional assays include assessment of the

vasodilatory effects of HDL on vascular reactivity by small-vessel wire myography and the anti-coagulation effect of HDL by a thrombin generation assay.

5.1.1 Aims of study

- To develop an assay for determining the effect of HDL on vascular tone regulation in isolated human small arteries

- To develop an assay for determining the anti-coagulation effects of HDL on thrombin generation

5.2 Establishment of a pregnant VAT artery wire myography protocol to assess the effects of HDL on vascular tone

5.2.1 Methodology

5.2.1.1 Preparation of physiological salt solution (PSS)

Physiological salt solution (PSS) contained 119.0 mM NaCl, 4.7 mM KCl, 1.2 mM $MgSO_4$, 24.9 mM $NaHCO_3$, 1.2 mM KH_2PO_4, 11.1 mM Glucose and 2.5 mM $CaCl_2$. The method used to prepare PSS was as follows:

- Stock solution A (1 L): 139.1 g sodium chloride (Sigma-Aldrich), 7 g potassium chloride (Sigma-Aldrich) and 2.885 g magnesium sulphate (Sigma-Aldrich) was added to 1 L deionised water.

- Stock solution B (1 L): 42 g sodium bicarbonate (Sigma-Aldrich) and 3.2 g monopotassium phosphate (Sigma-Aldrich) was added to 1 L deionised water.

- Physiological salt solution (2 L): Stock solution A (100 mL), stock solution B (100 mL), 4 g glucose (Fisher Scientific), 1 M calcium chloride (5 mL, Fisher Scientific) and deionised water (up to 1.5 L) was mixed. The solution was bubbled with 95% O_2/5% CO_2 before deionised water was added to a final volume of 2 L and pH was checked to be in range of 7.3 to 7.5.

5.2.1.2 Preparation of high potassium physiological salt solution (KPSS)

High potassium physiological salt solution (KPSS) contained 0.58 mM $MgSO_4$, 123.7 mM KCl, 24.9 mM $NaHCO_3$, 1.2 mM KH_2PO_4, 2.5 mM $CaCl_2$ and 11.1 mM glucose. The method used to prepare KPSS is as follows:

- Stock solution A for KPSS (500 mL): 92.23 g potassium chloride (Sigma-Aldrich) and 1.44 g magnesium sulphate (Sigma-Aldrich) was added to 500 mL deionised water.

- High potassium physiological salt solution (500 mL): Stock solution A for KPSS (25 mL), stock solution B (25 mL), 1 g glucose (Fisher Scientific), 1 M calcium chloride (1.25 mL, Fisher Scientific) and deionised water (up to 300 mL) was mixed. The solution was bubbled with 95% O_2/5% CO_2 before deionised water was added to a final volume of 500 mL and pH was checked to be in range of 7.3 to 7.5.

5.2.1.3 Drug preparation

Stock solutions of vasoconstrictors (noradrenaline, U46619, vasopressin, serotonin and angiotensin II) and vasodilators (acetylcholine, bradykinin, carbachol and sodium nitroprusside) were prepared by adding distilled water to noradrenaline (Sigma-Aldrich), U46619, vasopressin, serotonin, angiotensin II acetylcholine (Sigma-Aldrich), bradykinin, carbachol and sodium nitroprusside to a concentration of $1x10^{-2}$M and stored at -20ºC. Before the experiment, the solutions were diluted with distilled water to the required concentration and kept on ice.

5.2.1.4 Recruitment of non-pregnant women

Non-pregnant women were recruited from students and staff at the Institute of Cardiovascular and Medical Sciences, College of Medical, Veterinary and Life Sciences, University of Glasgow by members of the Freeman laboratory and me. This group was recruited for blood collection to act as a control group for healthy pregnant women. The inclusion and exclusion criteria are listed in Table 5.1. Ethical approval was obtained from University of Glasgow, MVLS College Ethics Committee (Project No: 200160064). Women who met the criteria were

fully informed regarding the study and written consent was obtained before blood collection.

Table 5.1 Inclusion and exclusion criteria for non-pregnant women

Inclusion criteria	Exclusion criteria
1. Non-pregnant women	1. Metabolic disease (such as diabetes and hypertension)
2. Age 16 to 45	2. Undergoing treatment for metabolic disease (e.g. statins)
	3. Any known transmissible disease
	4. Rheumatoid arthritis or any other autoimmune disease
	5. *Taking any form of estrogen medication (e.g. combined contraceptive pill/patch, hormone replacement therapy, tamoxifen) or on high dose norethistrone (e.g. 5 mg) *This criteria is only for participants in thrombin generation assay

5.2.1.5 Recruitment of healthy pregnant women

Healthy pregnant women were recruited from the maternity unit, Queen Elizabeth University Hospital by members of the Freeman laboratory and me. The inclusion and exclusion criteria are listed in Table 5.2. Ethical approval was granted by the West of Scotland Research Ethics Committee (Ethics Ref: 11/AL/0017; R&D Ref: GN11OB034). Pregnant women at term who met the criteria were identified from the Caesarean section (C-section) operating theatre

list, informed about the study and written consent was taken prior to blood collection and VAT biopsy by the obstetric surgeon during the C-section.

Table 5.2 Inclusion and exclusion criteria of healthy pregnant women

Inclusion criteria	Exclusion criteria
1. Pregnant women at third trimester undergoing elective Caesarean section (non-labouring)	1. Metabolic disease (such as diabetes and hypertension)
2. Age 18 to 45	2. Undergoing treatment for metabolic disease (e.g. statins)
3. Range of body mass indices (BMI)	3. Any known transmissible disease
	4. Rheumatoid arthritis or any other autoimmune disease

5.2.1.6 Preparation of blood and HDL samples

Blood collection and preparation were performed according to section 2.2, chapter 2 using EDTA tubes for both non-pregnant and healthy pregnant blood samples. HDL was isolated from plasma using two-step sequential ultracentrifugation according to section 2.3, chapter 2. Pregnant HDL from n=10 pregnant women were pooled and labelled as pooled pregnant HDL. Non-pregnant HDL from n=10 non-pregnant women were also pooled and labelled as pooled non-pregnant HDL. Pooled pregnant and non-pregnant HDL were stored at -80 ºC until use.

5.2.1.7 VAT vessel dissection

VAT was collected from healthy pregnant women undergoing elective Caesarean section. During surgery, VAT of an approximate size of 3 to 6 cm^3 was dissected

from the greater omentum by the obstetric surgeon. VAT was then placed in PSS and transferred on ice to the laboratory for artery dissection.

5.2.1.8 VAT arteries dissection, incubation and mounting

Within 2 hours after biopsy, VAT was placed in a petri dish filled with cold PSS. VAT was fixed to the petri dish by the fixing pins. Resistance-sized arteries of 200 to 550 μm were dissected from VAT under a dissecting microscope, perivascular adipose tissue was removed, and arteries were then cut into 2mm segments.

To prepare the incubation media, pooled HDL (20 μL) was added to PSS (980 μL) to make 2% pooled HDL for incubation. Artery segments were divided into 3 groups to be incubated in 2% pooled non-pregnant HDL, 2% pooled pregnant HDL or PSS for 16-20 hours at 4ºC.

After incubation, artery segments were carefully threaded onto two 40μm wires. Both wires were fixed onto each jaw of a wire myograph bath units in a 4-multichannel wire myograph system 620M (Danish Myo Technology (DMT), Denmark) which contained cold PSS (5 mL per bath unit) oxygenated with 95% oxygen and 5% carbon dioxide. Firstly, each end of one wire was screwed onto the jaw and both jaws were pulled close together, before the other wire was screwed to the other jaw. The length of the artery was measured under a dissecting microscope using the micrometer eye piece at 2.5 times magnification. The wires were checked that they were aligned and positioned close without touching each other leaving a zero force on the artery segments. Finally, the bath units were heated to 37 ºC for 30 minutes.

5.2.1.9 Normalization of the artery segments

All artery segments were normalized to the optimal tension that provides the maximum response to vasoconstrictors and vasodilators. Artery segments were stretched in steps of 50 μm diameter until the effective pressure was 100 mmHg or 13.3 kPa which is assumed to be the transmural pressure that provides the internal circumference of a fully relaxed artery (Mulvany and Halpern 1977). Laplace's formula is applied to calculate the effective pressure (P) from the internal circumference (IC), given by the equation:

$$P = \frac{2\pi \text{ x wall tension}}{IC} \quad \text{(kPa)}.$$

An exponential curve was created by the DMT normalization software to fit the internal circumference-pressure data. The optimal internal circumference was calculated from the internal circumference on the curve where effective pressure is 100 mmHg multiplied by 0.9 which was found to give the maximum active force and sensitivity to vasoactive agents (Aalkjaer and Mulvany 1981). Artery segments were all set to their optimal internal circumference and left to rest for 1 hour.

5.2.1.10 "Wake-up" protocol

Before the experiment, a wake-up protocol was carried out to reactivate vascular responses and to check vascular viability by checking the response to different types of stimulators including an endothelium-dependent vasodilator. KPSS (123mM) was used to induce contractility via depolarization of vascular smooth muscle cells. Firstly, KPSS (5 mL) was added to each bath unit. The contractile response was observed until it reached a maximal contraction. Arteries were then washed three times with PSS. After the vascular response reached baseline, vascular contraction was activated again with KPSS. Any artery segments that did not respond to either the first or second KPSS were excluded. Next, noradrenaline ($1x10^{-5}$ M, 5mL) was added to each bath unit to activate an α adrenoreceptor-mediated contraction. The contractile response was observed until it reached maximal contraction. Endothelial function was then checked by exposing the vessels to acetylcholine ($3x10^{-6}$ M) which induces NO release from intact endothelial cells and causes vasodilation. Arteries were washed with PSS three times before leaving to rest for 20 minutes.

5.2.1.11 Assessment of vascular tone response

Increasing doses of noradrenaline ($1x10^{-9}$, $3x10^{-9}$, $1x10^{-8}$, $3x10^{-8}$, $1x10^{-7}$, $3x10^{-7}$, $1x10^{-6}$, $3x10^{-6}$, $1x10^{-5}$ M) were added to each wire myograph bath unit with 3 minutes interval in between each dose. After the vessel had reached maximal contraction, increasing doses of acetylcholine ($1x10^{-8}$, $3x10^{-8}$, $1x10^{-7}$, $3x10^{-7}$, $1x10^{-6}$, $3x10^{-6}$, $1x10^{-5}$ M) were added with two-minute intervals in between each

dose. The vessels were then washed with PSS and exposed to KPSS to confirm artery viability.

5.2.1.12 Wire myograph data analysis

The force produced by the artery segments during the experiment was recorded and active wall force (ΔF) was calculated by subtracting baseline force from recorded force using the data analysis software (Labchart version 8, AdInstruments). The outcome measurements from wire myography data that were used for statistical analysis were active wall tension, active effective pressure, half maximal effective dose (ED50) and area under the curve (AUC). The calculations were as follows:

- Wall tension (T) is the force response per unit vessel length, given by

$$T = \frac{F}{2 \text{ x segme} \quad \text{length}} \qquad \text{(mN/mm).}$$

- Active wall tension (ΔT) is the change in wall tension, which is an isometric activation during wire myograph experiment, given by

$$\text{active wall tension} = T_{\text{active}} - T_{\text{baseline}}$$

or $$active\ wall\ tension = \frac{\Delta F}{2 \text{ x segment length}}$$

(mN/mm).

- Lumen diameter (D) is calculated based on measured internal circumference (IC), given by

$$D = \frac{IC}{\pi} \qquad \text{(mm).}$$

- Effective pressure (P) is the transmural pressure required to maintain the lumen diameter taking the length and diameter of vessel into account. P is calculated from Laplace formula, given by the equation

$$P = \frac{2\pi \times T}{IC}$$

or $$P = \frac{2 \times T}{D}$$ (mN/mm^2 or kPa).

- Active effective pressure (ΔP) is the change in effective pressure, which is an isometric activation during wire myograph experiment, given by

$$\text{active effective pressure} = P_{\text{active}} - P_{\text{baseline}}$$

or $$active\ effective\ pressure = \frac{2 \times \text{active wall tension}}{D}$$

(mN/mm^2 or kPa).

- Half maximal effective dose (ED50) is the dose or amount of treatment that produces half of the maximal response. Firstly, the linear trend that best fits the treatment dose-response curve is generated using the least squares method. The linear equation is as follow:

$$y = mx + b,$$

where "x" is the independent variable. The two concentrations on either side of the half of maximal response was input in the calculation for ED50.

"y" is the dependent variable. The two responses on either side of the half of maximal response was input in the calculation for ED50.

"m" is the slope of the line.

"b" is a constant which is equal to the value of y when x=0.

After the predicted linear equation was generated, ED50 was calculated from "y" in the linear equation, given x=half of the maximal response.

- Area under the curve (AUC) is calculated using Graphpad software for the concentration response curve of vasoconstrictors or vasodilators.

5.2.1.13 Inclusion and exclusion of wire myography traces in data analysis

From n=9 healthy pregnant women recruited as VAT donors, 59 artery segments were dissected (3-8 artery segments per VAT donor) and used in wire myography to compare pregnant and non-pregnant HDL effects on vascular responses. A total of 24 artery segments from n=9 pregnant VAT donors were incubated with pregnant HDL. An additional 24 artery segments from n=9 pregnant VAT donors were incubated with non-pregnant HDL. The remaining 11 artery segments from n=6 pregnant VAT donors were incubated with PSS as a control. There were 4 artery segments that did not respond to KPSS and were excluded from the experiment, including 2 artery segments (from n=1 VAT donor) in the pregnant HDL group, 1 artery segment in non-pregnant HDL group and 1 artery segment in PSS. For the 55 artery segments remaining, wire myograph parameters were calculated and noradrenaline response curves were plotted for each individual artery segment. The mean±SD of active wall tension and active effective pressure at maximum concentration of noradrenaline were 2.0±1.5 mN/mm and 9.2±7.1 kPa, respectively. The outliers were identified according to specific criteria and excluded from statistical analysis based on active wall tension and active effective pressure and looking at the individual noradrenaline response curves of all artery segments together. The criteria were as follow:

- Noradrenaline response curves showing an atypical pattern
- active wall tension at maximum concentration of noradrenaline <0.4 mN/mm
- active effective pressure at maximum concentration of noradrenaline <2.1 kPa

From the criteria above, 11 artery segments were excluded for having an active effective pressure at maximum concentration of noradrenaline <2.1 kPa. There were 9 out of 11 artery segments that also showed active wall tension at maximum concentration of noradrenaline <0.4 mN/mm.

5.2.1.14 Statistical analysis

Sample size was determined by an *a priori* power calculation based on the effect size observed in non-pregnant rat uterine arteries and human SAT arteries by Sulaiman W. described in chapter 1. A SD=0.57 was chosen based on the SD of human SAT artery response in PSS provided by Sulaiman W. Using the highest sample size observed for the vasodilatory response of non-pregnant rat uterine arteries to carbachol, it was calculated that n=13-16 women per group were required to provide 80%-90% power at α=0.05. Therefore, at least n=16 women per group is required to elucidate a physiological effect in human arteries.

5.2.2 Results

5.2.2.1 General characteristics of participants who donated HDL samples

Demographic data from healthy pregnant (n=10) and non-pregnant women (n=10) from whom HDL was isolated are shown in Table 5.2. Healthy pregnant women (n=10) had a mean (SD) age of 32.7 (3.7) years and a mean (SD) BMI of 30.8 (3.7) kg/m^2. Their gestational ages ranged from 38 to 41 weeks of gestation. Non-pregnant women (n=10) had a mean (SD) age of 26.7 (5.5) years and a mean (SD) BMI of 23.6 (3.5) kg/m^2. All pregnant and non-pregnant women had no active underlying medical disease and were non-smokers. However, the mean age and mean BMI of the pregnant women were significantly higher than those of the non-pregnant women (p=0.012 and <0.001, respectively).

Table 5.2 General characteristic of pregnant and non-pregnant women contributed to HDL samples

	Pregnant women (n=10)	Non-pregnant women (n=10)	p
Age (years)	32.7 (3.7)	26.7 (5.5)	0.012
BMI (kg/m^2)	30.8 (3.7)	23.6 (3.5)	<0.001
Gestational age (weeks)	39.4 (0.8)	-	-
Smoking status	100% non-smoker	100% non-smoker	-

* Data were expressed as mean (SD).

5.2.2.2 General characteristics of pregnant VAT donors

A total of n=9 pregnant women were recruited as VAT donors for the comparison of pregnant and non-pregnant HDL effects on VAT vascular responses. All women were at 39 weeks of gestation and had no other medical condition requiring their exclusion. Their mean (SD) age and BMI were 34 (2.9) years old and 32.3 (6.9) kg/m^2, respectively. All were non-smokers except one person that was a smoker prior to pregnancy. Demographic data of n=9 pregnant VAT donors were shown in Table 5.3.

Table 5.3 General characteristic of pregnant VAT donors

Sample ID	Age (years)	BMI (kg/m^2)	Gestational age (weeks+days)	Smoking status (pre-pregnancy)
PP02	35	29.0	39	Yes
PP03	32	36.4	39	No
PP04	38	28.7	39	No
PP05	30	47.2	39+2	No
PP06	35	25.0	39	No
PP07	38	32.4	39	No
PP09	33	31.1	39	No
PP12	32	28.7	39+1	No
PP13	m.d.	m.d.	m.d.	m.d.
Total (mean±SD)	34.1±2.9	32.3±6.9	39.0±0.1	

* m.d. represents missing data.

5.2.2.3 Characteristic of VAT arteries from pregnant women

The final wire myography data included in the statistical analysis consisted of 44 artery segments from n=8 VAT donors. There were 16 artery segments from n=7 VAT donors in the pregnant HDL group, 19 artery segments from n=8 VAT donors in the non-pregnant HDL group and 9 artery segments from n=5 VAT donors in the PSS or control group (1-3 artery segments per VAT donor).

Segment length, optimal internal circumference and diameter of pregnant VAT artery segments are shown in Table 5.4. There were no statistically significant differences in segment length, optimal internal circumference and diameter among the three treatment groups of pregnant HDL, non-pregnant HDL and PSS ($p>0.05$).

Table 5.4 Specific characteristics of VAT artery segments from pregnant women used in the three treatment groups

Treatment group	Segment length (mm)	Optimal internal circumference (μm)	Optimal internal diameter (μm)
Pregnant HDL	1.9 (0.1)	1386 (91)	441 (29)
Non-pregnant HDL	1.8 (0.2)	1361 (125)	433 (40)
PSS	1.9 (0.1)	1246 (150)	396 (48)

***** Data were expressed as mean (SD).

5.2.2.4 Effect of HDL from pregnant and non-pregnant women on artery response to KPSS

Maximal responses (active wall tension and active effective pressure) to KPSS of arteries exposed to pregnant HDL, non-pregnant HDL and PSS were compared and are shown in Figure 5-1. There was no significant difference in maximal active wall tension and active effective pressure in response to KPSS among the 3 treatments (active wall tension [mean±SD]: pregnant HDL 0.41±0.26, non-pregnant HDL 0.39±0.21 mN/mm, PSS 0.35±0.21 mN/mm, p=0.21 mN/mm, active effective pressure [mean±SD]: pregnant HDL 1.85±1.05 kPa, non-pregnant HDL 1.83±1.03 kPa, PSS 1.75±0.95 kPa, p=0.48).

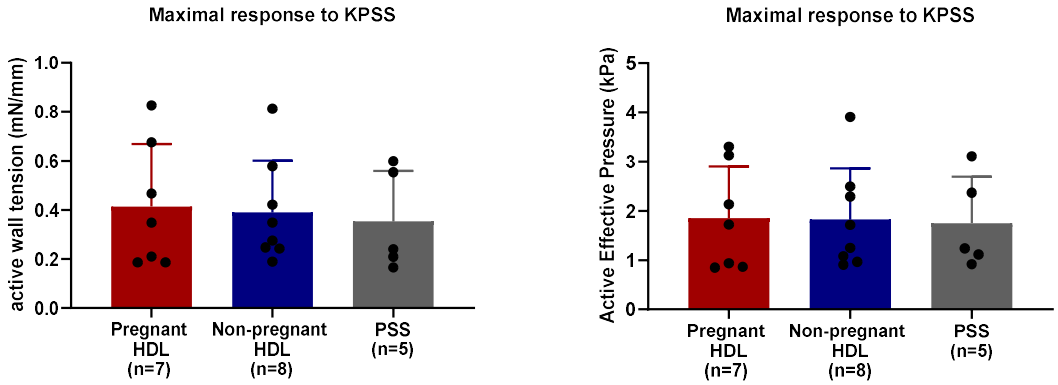

Figure 5-1 Active wall tension and active effective pressure of maximal response to KPSS of VAT arteries incubated with pregnant HDL, non-pregnant HDL and PSS. Data were expressed as mean±SD.

5.2.2.5 Comparison of the effects of non-pregnant and pregnant HDL on vasoconstriction responses of VAT arteries from pregnant women using wire myography

The contractile response curves of VAT arteries incubated in pregnant HDL, non-pregnant HDL or PSS are shown in Figure 5-2. Both active wall tension and active effective pressure responses to increasing dose of noradrenaline revealed no significant difference between exposures at all concentrations of noradrenaline ($p>0.05$). Similar results were observed for the noradrenaline ED50 (both active wall tension and active effective pressure) as shown in Figure 5-3 (active wall tension [mean±SD]: pregnant HDL $2.15x10^{-7}$±$1.07x10^{-7}$ mN/mm, non-pregnant HDL $2.48x10^{-7}$±$1.92x10^{-7}$ mN/mm, PSS $2.29x10^{-7}$±$1.27x10^{-7}$ mN/mm, p=0.91, active effective pressure [mean±SD]: pregnant HDL $2.14x10^{-7}$±$1.10x10^{-7}$ kPa, non-pregnant HDL $2.50x10^{-7}$±$1.90x10^{-7}$ kPa, PSS $2.53x10^{-7}$±$1.82x10^{-7}$ kPa, p=0.89) and for AUC of the noradrenaline response curve (both active wall tension and active effective pressure) as shown in Figure 5-4 (active wall tension [mean±SD]: pregnant HDL 9.75±6.63, non-pregnant HDL 9.61±5.74, PSS 8.57±3.35, p=0.621, active effective pressure [mean±SD]: pregnant HDL 44.30±29.00, non-pregnant HDL 44.46±25.03, PSS 43.88±17.37, p=0.859).

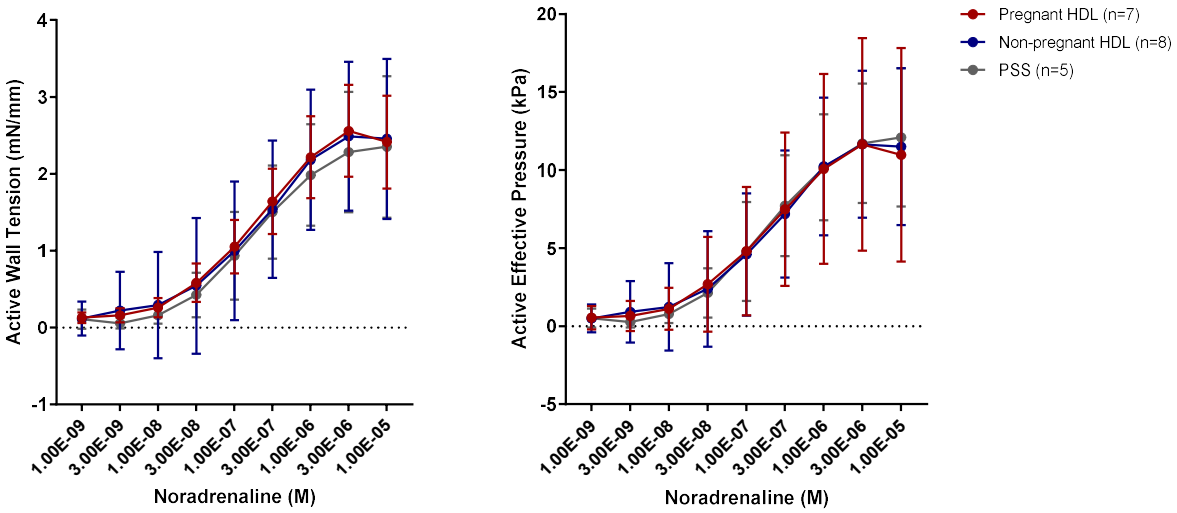

Figure 5-2 Contractile response curves (active wall tension and active effective pressure) of VAT arteries incubated in pregnant HDL, non-pregnant HDL or control group. Data were expressed as mean with SD.

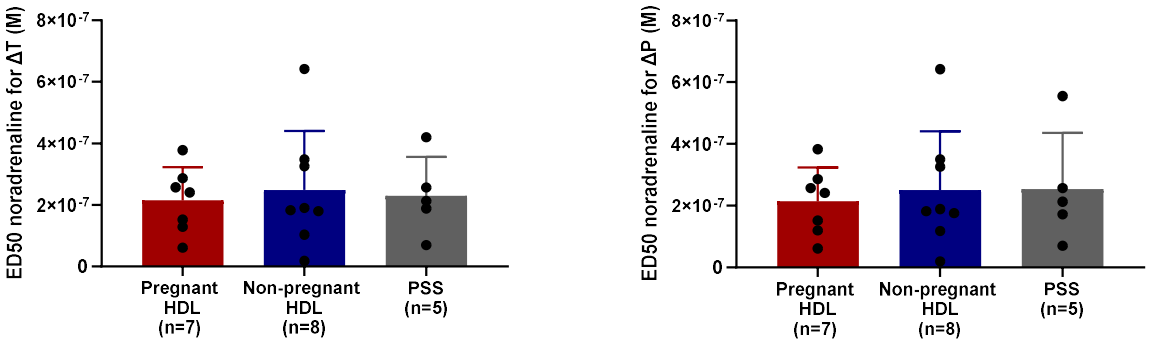

Figure 5-3 ED50 of noradrenaline (active wall tension and active effective pressure) of VAT arteries incubated in pregnant HDL, non-pregnant HDL or control group. Data were expressed as mean with SD.

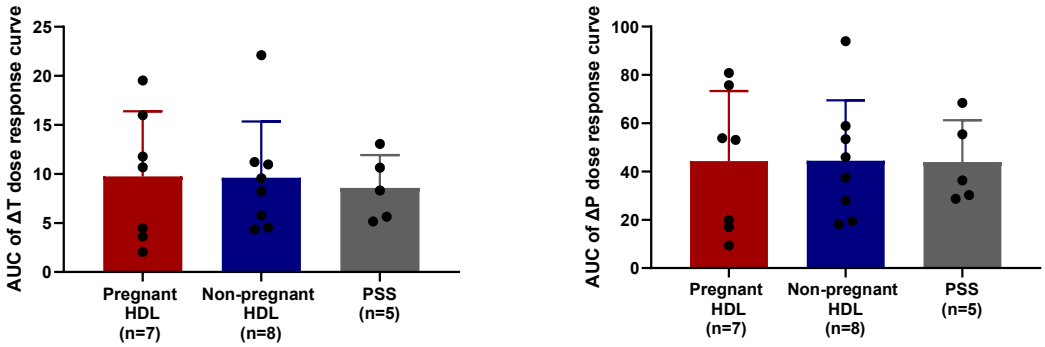

Figure 5-4 AUC of active wall tension and active effective pressure contractile response curve to noradrenaline of pregnant VAT arteries incubated in pregnant HDL, non-pregnant HDL or control group. Data were expressed as mean and SD.

5.2.2.6 Comparison of the effects of non-pregnant and pregnant HDL on vasorelaxation of VAT arteries using wire myography

Relaxation response data from this experiment could not be analyzed because most of the vessels that were contracted to the maximum dose of noradrenaline were not stable enough to test the relaxation response. After the maximum dose of noradrenaline, most of the vessels continuously relaxed before acetylcholine was added (Figure 5-5). There is no clear relaxation response due to acetylcholine administration at any of the doses used. Thus, there is a need to develop an improved protocol for assessment of vascular reactivity in human VAT arteries using wire myography.

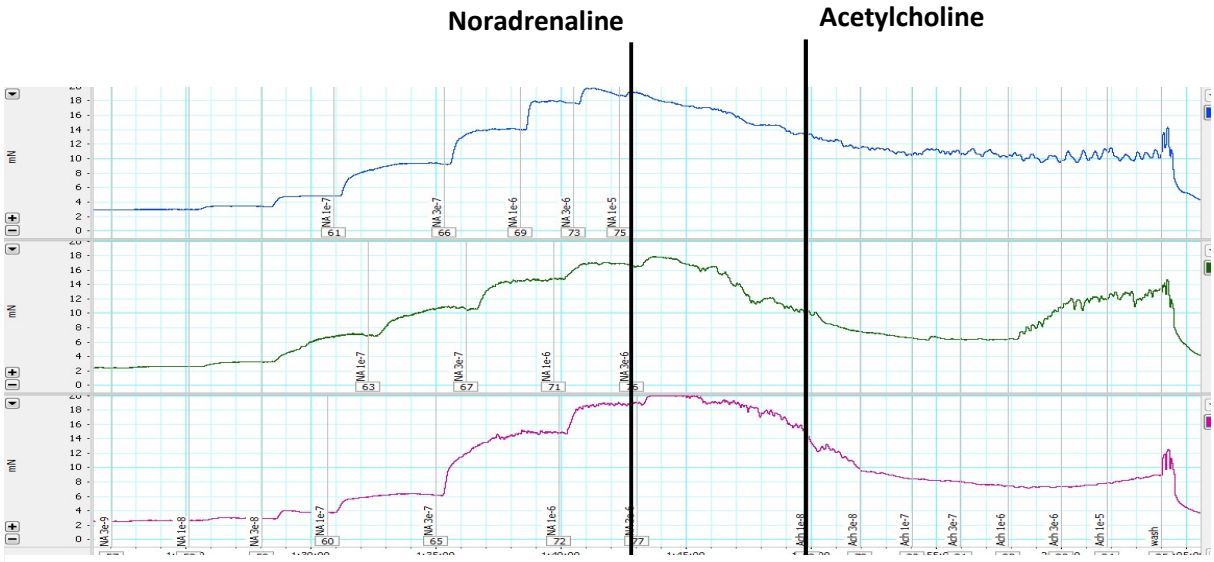

Figure 5-5 Representative wire myography traces of pregnant VAT arteries during the assessment of vascular response to increasing doses of noradrenaline, followed by increasing doses of acetylcholine.

5.2.2.7 Development of wire myography protocol

Development of wire myography protocol was with the help of Elisabeth Beattie, Laura Haddow and John McAbney. To improve the wire myography protocol, different vasoconstrictors and vasodilators were used with VAT arteries incubated with PSS overnight. Initially, the experiment was carried out using VAT arteries from 3 donors with two biological replicates per donor. Noradrenaline at different concentrations; $3x10^{-6}$ and $1x10^{-5}$ M was used as a pre-constrictor before adding a vasodilator. No concentration of adrenaline gave a stable enough contraction to test the relaxation response or show a clear relaxation response to acetylcholine (Figure 5-6). U46619, a synthetic thromboxane A2 agonist, was the next vasoconstrictor to be tested for pre-constriction. U46619, both at $3x10^{-8}$ and $1x10^{-7}$ M, showed more stable contraction than noradrenaline and was chosen as the pre-constrictor for assessment of relaxation response. Increasing doses of different vasodilators: acetylcholine, bradykinin and carbachol ($1x10^{-10}$- $3x10^{-5}$ M) were then tested with U46619 ($3x10^{-8}$ and $1x10^{-7}$ M) as a pre-constrictor. There was no clear relaxation response to these vasodilators (Figure 5-7). Whereas a single dose of sodium nitroprusside ($3x10^{-5}$ M) following U46619 ($3x10^{-8}$ M) gave a clear relaxation response (Figure 5-8). In contrast to other vasodilators (acetylcholine, bradykinin and carbachol) which are endothelium-dependent vasodilators, sodium nitroprusside is an endothelium-independent vasodilator. This result suggests a lack of endothelium function in pregnant visceral adipose tissue arteries prepared according to this protocol, however previous literatures have shown endothelium-dependent relaxation in pregnant visceral adipose arteries (Ashworth et al. 1996; Pascoal et al. 1998; Brewster et al. 2010; Mishra et al. 2011; Boisramé-Helms et al. 2015). The possible factors contributing to the issues observed in our protocol could be the preparation protocol, the skill in dissection and mounting, the duration of incubation or the types of vasoconstrictors and vasodilators used.

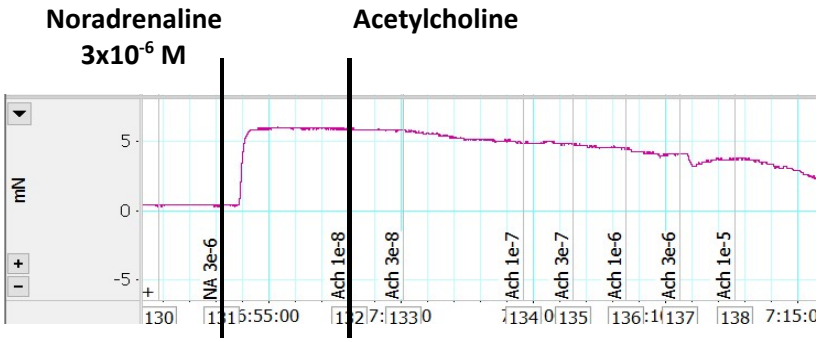

Figure 5-6 Representative wire myograph trace of vascular response to noradrenaline at $3x10^{-6}$ M as a pre-constrictor, following by increasing dose of acetylcholine ($1x10^{-8}$- $3x10^{-5}$ M). There was no clear relaxation response to acetylcholine in studies of VAT arteries from three donors.

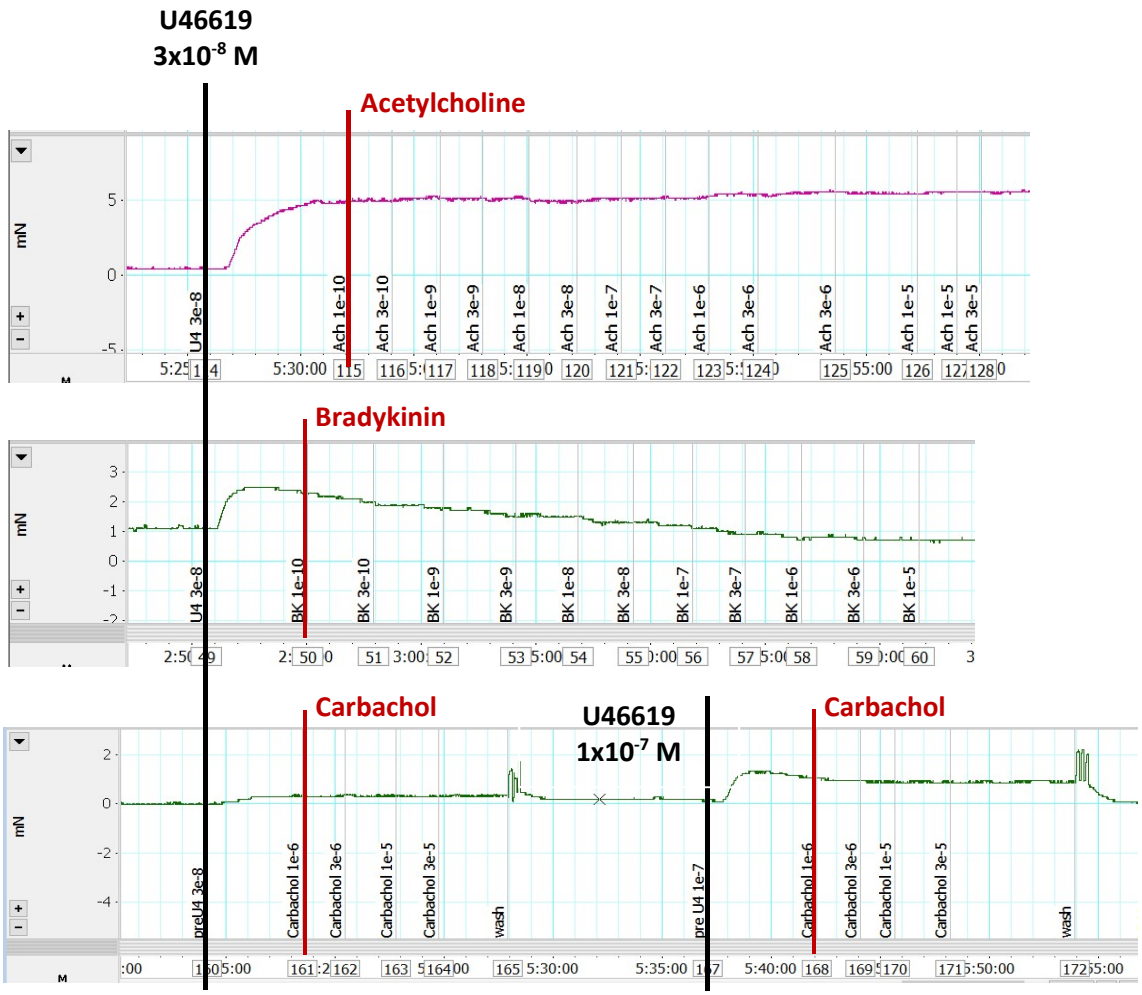

Figure 5-7 Representative wire myograph traces of vascular response to U46619 ($3x10^{-8}$ and $1x10^{-7}$ M) as a pre-constrictor, following by increasing dose of different vasodilators: acetylcholine, bradykinin and carbachol ($1x10^{-10}$- $3x10^{-5}$ M). There was no clear relaxation response to any vasodilators which are all endothelium-dependent vasodilators.

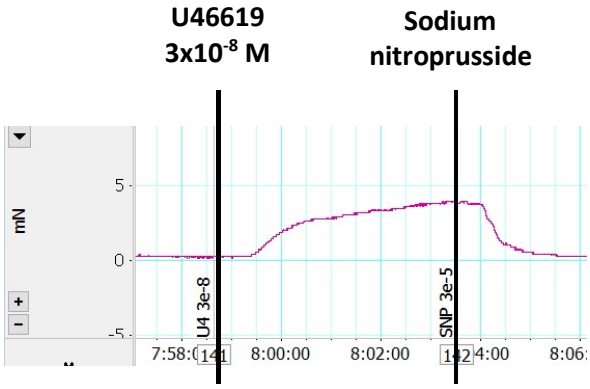

Figure 5-8 Representative wire myograph trace of vascular response to U46619 ($3x10^{-8}$ M) as a pre-constrictor, following by a single dose of sodium nitroprusside ($3x10^{-5}$ M). There was a clear relaxation response to sodium nitroprusside, an endothelium-independent vasodilator.

To exclude poor dissection skills as a factor, vessels were prepared according to this protocol in the same tissue and at the same time as an experienced wire myography user, Elisabeth Beattie. Our results show the same response with unstable contractile response to noradrenaline, stable contraction from U46619, no relaxation following increasing dose of acetylcholine ($1x10^{-10}$-$3x10^{-5}$ M) and a clear relaxation response to sodium nitroprusside ($3x10^{-5}$ M). Thus, poor quality dissection could be excluded, and further improvement of the protocol was focused on different types of vasoconstrictors and vasodilators and duration of incubation.

The next stage of protocol development involved vessels being dissected and mounted on wire myography immediately after biopsy instead of overnight incubation. Increasing doses of 5 vasoconstrictors: noradrenaline ($1x10^{-10}$-$3x10^{-5}$ M), vasopressin ($1x10^{-10}$-$3x10^{-5}$ M), serotonin ($1x10^{-10}$-$3x10^{-5}$ M), U46619 ($1x10^{-10}$-$3x10^{-6}$ M) and angiotensin II ($1x10^{-10}$-$3x10^{-7}$ M), were tested in the same tissue. In these pilot studies, n=2 VAT donors with 8 biological replicates per donor were completed. Noradrenaline and angiotensin II give unstable contraction that spontaneously relaxed without vasodilators. Vasopressin showed stable contraction but, after washing with PSS several times, vessels remained contracted or unpredictably relaxed and contracted. U46619 and serotonin seemed to be promising vasoactive agents that give stable contraction, but more replicates would need to be tested to confirm this result.

5.2.3 Discussion

This study found similar effects of pregnant and non-pregnant HDL on VAT artery contraction which is inconsistent with the previously observed effect of pregnant HDL found in rat uterine arteries using the same wire myography protocol (Sulaiman W., unpublished). Sulaiman found that pregnant HDL reduced active wall tension and active effective pressure noradrenaline response curves, and maximal active wall tension and active effective pressure in response to noradrenaline in non-pregnant rat uterine arteries compared to those incubated with non-pregnant HDL. Her study in pregnant rat uterine arteries also showed a reduced maximal active wall tension response to noradrenaline in arteries exposed to pregnant HDL compared to those exposed to non-pregnant HDL. There may be a difference between rat uterine and human VAT artery reactivity in response to HDL. The higher BMI of pregnant HDL donors may impair the vasodilatory effect of HDL and mask any differences in impact on vascular tone regulation between pregnant and non-pregnant HDL. Research in obesity-related conditions such as diabetes has demonstrated loss of the vasodilatory effect of HDL in these population (Sorrentino et al. 2010; Perségol et al. 2006). The impact of HDL on vasorelaxation was also inversely related to triglyceride content in HDL, which increases in obesity (Perségol et al. 2006). Also, our study lacked power. The sample size of this study was only six per group which did not reach a sample size of 16 per group that is required to provide 80% power to identify a difference between an effect of HDL from pregnant and non-pregnant women in VAT arteries according to an *a priori* power calculation based on the effect size observed in non-pregnant rat uterine arteries and human SAT arteries by Sulaiman W. Therefore, the lack of a significant difference in contractile response to noradrenaline cannot confirm whether pregnant HDL affects pregnant VAT arteries or not. There were barriers to increasing sample size: time limitations, a long study protocol from recruitment to artery dissection and wire myography which needed to be continuous and most importantly, an inability to determine the vasodilatory response of the wire myography protocol. Thus, the decision was made to develop a protocol to be able to measure both vasoconstriction and vasodilation properties before continuing the experiment.

Regarding protocol development, the wire myograph protocol from Sulaiman W. was adopted in this study since it was shown to be an effective protocol for the

study of HDL effect on rat uterine arteries and identified similar trends in human SAT artery response to HDL. However, difficulties in the dissection and handling of suitable arteries from SAT biopsies meant the decision was made to isolate arteries from VAT tissue for this study. Pregnant VAT was chosen due to the greater content of appropriate vasculature when compared to SAT, to their anatomy as maternal systemic arteries and to their accessibility. However, the same wire myograph protocol seemed to act differently on SAT and VAT arteries. Pregnant VAT arteries showed unstable vasoconstriction with noradrenaline and lacked clear vasorelaxation in response to acetylcholine. I assessed several factors that could interfere with vascular tone regulation, however poor skill in vessel dissection could be excluded considering the similar results obtained by an experienced wire myograph user. Future experiments should include histological study to confirm the presence of endothelial cells. Moreover, the optimal duration of HDL incubation before mounting on wire myograph should be examined. Previous research has shown that human VAT arteries dissected within 2 hours after biopsy can be stored at 4 ºC for up to 48 hours without any significant deleterious effect on vascular tone regulation (Ashworth et al. 1996). In addition, human uterine arteries incubated with plasma for 1 and 16 hours also exhibit similar contractile responses (Hayman et al. 2000). However, differences in the tissue collection protocol and wire myograph set up may differentially plan to optimise the wire myograph protocol for pregnant VAT arteries from tissue collection, vascular dissection, HDL incubation, and types of vasoconstrictors and vasodilators is required.

5.3 Development of a thrombin generation assay in HDL

5.3.1 Methodology

5.3.1.1 Samples preparation

Non-pregnant women were recruited as described in section 5.2.1.4 and Table 5.1 of this chapter. Non-pregnant blood was collected in sodium citrate tubes and was then centrifuged at room temperature, 3,000 rpm (1,500g) for 10 minutes. Supernatant was collected and centrifuged again at room temperature 3,000 rpm (1,500g) for 10 minutes to remove platelets. Platelet-poor plasma (PPP) was stored in aliquots at -80ºC until use.

HDL was isolated from PPP using sodium bromide density-gradient ultracentrifugation according to section 2.3, chapter 2. The VLDL/LDL fraction and lipoprotein-depleted plasma (LpDP) were also collected. Samples were then desalted by gel filtration using PD MiniTrap G-25 column (GE Healthcare BioSciences) according to section 2.4. All samples were collected in aliquots and stored at -80 ºC.

5.3.1.2 Thrombin generation assay

Thrombin generation was assessed by the Calibrated Automated Thrombogram (CAT) method using the Fluoroskan Ascent microplate fluorometer (Thermo Scientific) at the Department of Haematology, Glasgow Royal Infirmary with help from Dr Vivienne Gibson. The fluorometer was primed with distilled water (5 mL) twice and all reagents and samples were prepared as follow before the experiment.

- Warm distilled water and Fluo substrate buffer (Thrombinoscope, TS50.20) were prepared in water bath at 37ºC.

- Distilled water (1 mL) was added to PPP Low reagent (1pM TF, Thrombinoscope TS31.0), Calibrator (Thrombinoscope, TS20.0) and NIBSC ref standard (TGT reference plasma 06/232, The National Institute for Biological Standards and Control) and left for 10 minutes before use.

- A working solution of thrombomodulin (0.4nM) was prepared by adding PPP Low reagent (97 µL) to thrombomodulin (1 µM stock from CARIM Lots ST09-009 Batch 00510 7/7/10, 3 µL) to make a stock solution of thrombomodulin (30nM). The stock solution (36 µL) was then mixed with PPP Low reagent (414 µL) to make a working solution of thrombomodulin (0.4nM).

- Fluo substrate was prepared by adding Fluo substrate (40 µL) (Thrombinoscope, TS50.10) to preheated Fluo substrate buffer (1.6 mL)

- All samples were stored frozen and thawed in a water bath for 10 minutes prior to use.

PPP Low reagent, PPP Low reagent with thrombomodulin or Calibrator (20 µL) was added to a 96-well plate in duplicate. PPP Low reagent contained defined concentrations of tissue factor and phospholipid and was used to stimulate thrombin generation. Thus, wells with PPP Low reagent provided measurement of thrombin generation in a standardized environment. Wells with PPP Low reagent and thrombomodulin represented the effect of thrombomodulin inhibition on thrombin generation in those samples. Wells with calibrator provided a calibrated amount of thrombin activity which was used to calculate thrombin generation in each sample to correct for donor-to-donor variation such as differences in colour of the plasma.

After that, NIBSC reference plasma or patient sample (80 µL) was added into each well containing PPP Low reagent, PPP Low reagent with thrombomodulin or Calibrator. The plate was then loaded into the fluorometer and incubated for 10 minutes. After incubation, the dispenser was washed with pre-warmed distilled water followed by Fluo substrate (20 µL) which was then dispensed into each well. The amount of thrombin generated over time was measured through fluorescence production at an excitation wavelength of 390 nm and an emission wavelength of 460 nm. Thrombinoscope® software was used to convert the fluorescent signal into nM/L thrombin activity with adjustment for the inner filter effect and α-2-macroglobulin thrombin complex that was used in the calibrator.

5.3.1.3 Data analysis

The outcome measurements from the thrombin generation assay that were used for statistical analysis were as follows:

- Lag time (min), a measure of time to start of thrombin formation.

- Endogenous Thrombin Potential (ETP, nM/min), the area under the curve of thrombin concentration-time curve. ETP represents the total amount of enzymatic activity by thrombin during the time it was active.

- Peak (nM), the maximum thrombin concentration produced

- Time to peak (ttPeak, min), the time to the peak thrombin concentration.
- Velocity Index (VI, nM/min), the slope between lag time and time to peak
- Start Tail (min), the time when thrombin generation has come to an end

Thrombin activity in NIBSC plasma was checked that it was within the standard range (Table 5.5) as a quality control for each plate.

Table 5.5 NISBC reference plasma acceptance range

	Acceptance range	
	PPP low reagent	**PPP low reagent + thrombomodulin**
Lag time (min)	4.9-6.5	4.8-6.3
ETP (nM*min)	985-1474	525-1055
Peak (nM)	86-182	66-154
ttPeak (min)	10-13	9-11
VI (nM/min)	10-38	13-37
Start Tail (min)	28-34	26-30

5.3.1.4 Development of thrombin generation assay protocol for HDL

The first experiment was to assess the effect of the lipoprotein isolation process on the thrombin generation assay. To assess the effect of ultracentrifugation, thrombin generation was determined in every fraction along the lipoprotein isolation process (PPP, VLDL/LDL, HDL and LpDP) and recombination of all fractions (VLDL/LDL, HDL and LpDP) to make the recombined PPP. In addition,

thrombin generation was assessed in each fraction with and without desalting to assess the effect of the desalting process.

The recombined PPP was created by combining the same volume (1 mL) of VLDL/LDL fraction, HDL fraction and LpDP (total volume=3 mL). This mixture was then concentrated using Amicon ultra-15 centrifugal filter units (3,000 MWCO, Sigma-Aldrich) to reduce volume to 1 mL. Centrifugal filter columns were washed by adding Dulbecco's phosphate buffered saline (15 mL, DPBS) (Thermo Fisher Scientific, 14190144) and centrifuged at 4,400 rpm/3990 g, 4 ºC for 10 minutes. The washing step was repeated using 0.1 M NaOH (15 mL) and DPBS (15 mL) with the same centrifugation. Recombined VLDL/LDL, HDL and LpDP sample (3 mL, 1:1:1 volume ratio) was added to prepared centrifugal filter columns and centrifuged at 4,400 rpm/3,990 g, 4 ºC until the volume of retained solution decreased to 1 mL (one third of recombined samples' volume). The retentate was collected as concentrated recombined PPP. The list of all tested samples is shown in Table 5.6.

Table 5.6 Lists of samples tested in experiment 1 to assess the effect of lipoprotein isolation process on thrombin generation assay

PPP
VLDL/LDL fraction
• with desalting
• without desalting
HDL fraction
• with desalting
• without desalting
LpDP
• with desalting
• without desalting
Recombined PPP (VLDL/LDL + HDL + LpDP)
• without concentration and desalting
• without concentration, but with desalting
• with concentration and desalting

The second experiment was to assess the effect of sodium bromide (NaBr) added during the lipoprotein isolation process on thrombin generation. NaBr is a denaturing salt that can denature proteins and disturb many biological pathways (van Logten et al. 1974; Loeber, Franken, and van Leeuwen 1983). NaBr at the concentration of 0.32 M (the calculated concentration of NaBr left in HDL after ultracentrifugation, assuming 90% of NaBr was removed by gel filtration) was added to PPP and was assessed by thrombin generation assay. Multiple desalting by gel filtration (1 to 5 times) to reduce NaBr concentration were also tested. The list of all tested samples is shown in Table 5.7.

Table 5.7 Lists of samples tested in experiment 2 to assess the effect of NaBr on thrombin generation assay

0.32 M NaBr in PPP
Recombined PPP from desalted VLDL/LDL + HDL + LpDP without concentration
• 2 times desalting
• 3 times desalting
• 4 times desalting
• 5 times desalting
Recombined PPP from desalted VLDL/LDL + HDL + LpDP with concentration
• 2 times desalting
• 3 times desalting
• 4 times desalting
• 5 times desalting

Finally, the third experiment was to assess the effect of desalting method of HDL sample on thrombin generation assay. HDL was desalted by 3 protocols: gel filtration, dialysis and desalting column. Desalting by gel filtration was done using PD MiniTrap G-25 column (GE Healthcare BioSciences) according to section 2.4, chapter 2. Another desalting protocol was dialysis using GeBAflex-tube (3,500 MWCO, Gene Bio-Application Ltd.). Distilled water (3 mL) was added to a GeBAflex-tube and incubated for 5 minutes before emptying it. HDL sample (1 mL) was then loaded into the GeBAflex-tube and placed in a beaker containing DPBS (5 L) with stirring for 36 hours. DPBS (5 L) was changed every 12 hours, 3 times in total, before the sample was collected and stored at -80 ºC. The last

method was desalting HDL by using Amicon ultra-15 centrifugal filter units (3,000 MWCO, Sigma-Aldrich) to reduce the concentration of contaminating salt and reconstituting the concentrate to the original volume. A centrifugal filter column was washed by adding DPBS (15 mL) and centrifuged at 4,400 rpm/3990 g, 4 ºC for 10 minutes. The washing step was repeated using 0.1 M NaOH (15 mL) and DPBS (15 mL) with the same centrifugation. HDL was then loaded into the column and centrifuged at 4,400 rpm/3,990 g, 4 ºC until the volume of retained solution decreased to around 1 mL. DPBS (15 mL) was added to the retentate and centrifuged at 4,400 rpm/3,990 g, 4 ºC until the volume of retained solution decreased to around 1 mL. This step was repeated 6 times. The retentate was collected and reconstituted with DPBS to the original volume. HDL samples were mixed with PPP (1:1 volume ratio) before tested for thrombin generation. The list of all tested samples is shown in Table 5.8.

Table 5.8 Lists of samples tested in experiment 3 to assess the effect of NaBr in HDL sample on thrombin generation assay

Gel filtrated HDL in PPP (1:1 volume ratio) • 1 time desalting • 2 times desalting • 3 times desalting • 4 times desalting • 5 times desalting
Dialysed HDL in PPP (1:1 volume ratio)
Centrifuged HDL in PPP (1:1 volume ratio)

5.3.2 Results

5.3.2.1 Experiment 1: to assess the effect of lipoprotein isolation process on thrombin generation assay

In the first experiment to assess the effect of the lipoprotein isolation process on the thrombin generation assay, samples from each step of HDL isolation including PPP, VLDL/LDL, HDL, LpDP, recombined PPP (VLDL/LDL, HDL and LpDP) with and without concentration were analysed in thrombin generation assay. The results are shown in Table 5.9 and Table 5.10. NIBSC reference

plasma showed thrombin generation activity within the acceptable range. PPP was the only sample that exhibited identifiable thrombin generation activity. In contrast, VLDL/LDL, HDL, LpDP, recombined PPP and concentrated-recombined PPP with and without desalting did not demonstrate any detectable thrombin generation. Only post-processed samples lost their activity to generate thrombin, thus there could be factors, such as residual NaBr, interfering with thrombin generation added during lipoprotein isolation. NaBr may interfere with clotting as binding of many of the enzymes which have cofactors will be affected by high salt. Therefore, I further assessed the effect of NaBr added during the lipoprotein isolation process on thrombin generation in the second experiment.

Table 5.9 Thrombin generation parameters of Experiment 1 in PPP Low reagent

Sample	ETP (nM•min)	Peak (nM)	Lag time (min)	ttPeak (min)	VI (nM/min)	Start Tail (min)
NIBSC reference plasma	1424.6	138.2	6.3	12.4	22.4	32.9
PPP	718.8	46.2	6.3	15.1	5.2	41.9
VLDL	0	0	0	0	0	0
Desalted VLDL	0	0	0	0	0	0
HDL	0	0	0	0	0	0
Desalted HDL	0	0	0	0	0	0
LpDP	0	0	0	0	0	0
Desalted LpDP	0	0	0	0	0	0
Recombined PPP (VLDL+HDL+LpDP)	0	0	0	0	0	0
Desalted recombined PPP	0	0	0	0	0	0
Desalted and concentrated recombined PPP	0	0	0	0	0	0

Table 5.10 Thrombin generation parameters of Experiment 1 in PPP Low reagent with thrombomodulin

Sample	ETP (nM•min)	Peak (nM)	Lag time (min)	ttPeak (min)	VI (nM/min)	Start Tail (min)
NIBSC reference plasma	729.2	100.0	5.8	10.4	21.4	27.0
PPP	199.7	26.0	5.3	10.6	4.9	26.2
VLDL	0	0	0	0	0	0
Desalted VLDL	0	0	0	0	0	0
HDL	0	0	0	0	0	0
Desalted HDL	0	0	0	0	0	0
LpDP	0	0	0	0	0	0
Desalted LpDP	0	0	0	0	0	0
Recombined PPP (VLDL+HDL+LpDP)	0	0	0	0	0	0
Desalted recombined PPP	0	0	0	0	0	0
Desalted and concentrated recombined PPP	0	0	0	0	0	0

5.3.2.2 Experiment 2: to assess the effect of NaBr on thrombin generation assay

The effect of NaBr on thrombin generation was assessed in experiment 2. The results are shown in Table 5.11 and Table 5.12. NIBSC reference plasma showed thrombin generation activity within the acceptance range. Thrombin generation was not detected in PPP with NaBr and all recombined PPP samples with and without concentration which were desalted by gel filtration 2 to 5 times. This suggests that NaBr abolished the thrombin generation activity of PPP in the assay and reducing the concentration of NaBr in recombination of VLDL/LDL, HDL and LpDP by gel filtration up to 5 times could not recover thrombin generation activity. Next experiment, HDL fraction was added directly to PPP to examine the effect of NaBr on thrombin generation activity of HDL. The effect of different desalting methods of HDL (gel filtration, dialysis and desalting column) on thrombin generation were also assessed.

Table 5.11 Thrombin generation parameters of Experiment 2 in PPP Low reagent

Sample	ETP (nM•min)	Peak (nM)	Lag time (min)	ttPeak (min)	VI (nM/min)	Start Tail (min)
NIBSC reference plasma	1296.3	122.28	6.17	12.67	18.82	33.33
PPP + NaBr	0	0	0	0	0	0
Recombined PPP desalt x2	0	0	0	0	0	0
Recombined PPP desalt x3	0	0	0	0	0	0
Recombined PPP desalt x4	0	0	0	0	0	0
Recombined PPP desalt x5	0	0	0	0	0	0
Concentrated-recombined PPP desalt x2	0	0	0	0	0	0

Concentrated-recombined PPP desalt x3	0	0	0	0	0	0
Concentrated-recombined PPP desalt x4	0	0	0	0	0	0
Concentrated-recombined PPP desalt x5	0	0	0	0	0	0

Table 5.12 Thrombin generation parameters of Experiment 2 in PPP Low reagent with thrombomodulin

Sample	ETP (nM•min)	Peak (nM)	Lag time (min)	ttPeak (min)	VI (nM/min)	Start Tail (min)
NIBSC reference plasma	748	101.18	5.50	10	22.51	26.67
PPP + NaBr	0	0	0	0	0	0
Recombined PPP desalt x2	0	0	0	0	0	0
Recombined PPP desalt x3	0	0	0	0	0	0
Recombined PPP desalt x4	0	0	0	0	0	0
Recombined PPP desalt x5	0	0	0	0	0	0
Concentrated-recombined PPP desalt x2	0	0	0	0	0	0

Concentrated-recombined PPP desalt x3	0	0	0	0	0	0
Concentrated-recombined PPP desalt x4	0	0	0	0	0	0
Concentrated-recombined PPP desalt x5	0	0	0	0	0	0

5.3.2.3 Experiment 3: to assess the effect of NaBr in HDL sample on thrombin generation assay

The results of experiment 3 are shown in Tables 5.13 and 5.14. Adding the HDL fraction directly to PPP seems to show some thrombin generation activity. Comparison between 1- to 5-time desalting by gel filtration of HDL samples with PPP (1:1 volume ratio) exhibited more thrombin generation as desalting times increased. PPP with dialysed HDL showed no thrombin generation, while PPP with HDL desalted by centrifugal column revealed a small amount of thrombin generation activity (Table 5.13 and 5.14).

Table 5.13 Thrombin generation parameters of Experiment 3 in PPP Low reagent

Sample	ETP (nM•min)	Peak (nM)	Lag time (min)	ttPeak (min)	VI (nM/min)	Start Tail (min)
NIBSC reference plasma	1517.69	145.05	6.67	12.67	24.18	32.83
PPP + gel filtrated x1 HDL	814.4	48.8	6.7	14.5	6.3	49.3
PPP + gel filtrated x2 HDL	1064.4	56.1	6.7	15.3	6.5	52.3
PPP + gel filtrated x3 HDL	1072.9	60.8	6.3	14.7	7.3	46.7
PPP + gel filtrated x4 HDL	1191.4	84.2	5.7	12.7	12.1	44.2
PPP + gel filtrated x5 HDL	1119.7	65.7	5.5	14.0	7.7	47.0
PPP + Dialysed HDL	0	0	0	0	0	0
PPP + Centrifuged HDL	0	1.46	9.67	43	0.04	0

Table 5.14 Thrombin generation parameters of Experiment 3 in PPP Low reagent with thrombomodulin

Sample	ETP (nM•min)	Peak (nM)	Lag time (min)	ttPeak (min)	VI (nM/min)	Start Tail (min)
NIBSC reference plasma	772.04	103.97	6	10.67	22.28	28.17
PPP + gel filtrated x1 HDL	572.7	43.5	6.3	13.0	6.5	41.0
PPP + gel filtrated x2 HDL	529.6	45.9	6.0	12.3	7.3	39.7
PPP + gel filtrated x3 HDL	424.4	35.4	5.3	11.3	5.9	38.7
PPP + gel filtrated x4 HDL	559.1	53.8	5.0	10.3	10.1	36.3
PPP + gel filtrated x5 HDL	492.8	56.3	4.7	9.7	11.3	30.3
PPP + Dialysed HDL	0	0	0	0	0	0
PPP + Centrifuged HDL	0	0	0	0	0	0

5.3.3 Discussion

From the first experiment that assessed the effect of lipoprotein isolation process on thrombin generation. PPP was the only sample that exhibited identifiable thrombin generation activity. It is reasonable that PPP but not lipoprotein fractions (VLDL/LDL and HDL) showed detectable thrombin generation activity since there are proteins and clotting factors required for thrombin production in PPP but not in lipoprotein fractions. After isolating VLDL, LDL and HDL from plasma, other proteins including clotting factors should be in LpDP fraction. Therefore, LpDP should be able to generate thrombin. Recombination of VLDL/LDL, HDL and LpDP should also provide an identifiable thrombin generation activity. However, LpDP and recombination of the lipoprotein and LpDP fractions did not show any detectable thrombin generation

activity. Since only post-processed samples lost their activity to generate thrombin, there could be factors, such as residual NaBr, interfering with thrombin generation added during lipoprotein isolation. NaBr is likely to interfere with clotting as binding of many of the enzymes which have cofactors will be affected by high salt. NaBr is the most common chemical used to create specific densities required in lipoprotein isolation process. The disadvantage of using this salt is that it creates a high ionic strength of the solution which may affect HDL stability. NaBr can denature proteins and may affect biological pathways (Bello, Haas, and Bello 1966). Studies of NaBr effects in rats showed a dose-dependent disturbance in various systems, for example motor incoordination, growth retardation, increased percentage of neutrophil and endocrine system (van Logten et al. 1974). There were also histologic and functional changed in thyroid, testes and adrenal of rats intoxicated with high-dose NaBr (van Logten et al. 1974; Loeber, Franken, and van Leeuwen 1983). My data showed that thrombin generation was not detected in PPP with NaBr at the concentration of 0.32 M which is the calculated concentration of NaBr remaining in HDL samples after desalting by gel filtration, assuming that 90% of NaBr was removed. This finding suggests that NaBr abolished the thrombin generation activity of PPP in the assay.

Reducing the concentration of NaBr in recombination of VLDL/LDL, HDL and LpDP by gel filtration up to 5 times still could not recover thrombin generation activity. The calculated concentrations of NaBr in these samples were $2.5x10^{-2}$ M, $2.5x10^{-3}$ M, $2.5x10^{-4}$ M, $2.5x10^{-5}$ M for recombined PPP desalted 2 to 5 times, respectively. Concentrating recombined PPP to decrease volume to the original could also remove some NaBr. The manufacturer's instructions for Amicon ultra-15 centrifugal filter units (3,000 MWCO, Sigma-Aldrich) indicated that centrifuging a solution of vitamin B-12 which has molecular weight of 1,350 Da at 4,000 g for 1 hour removed >75% of vitamin B-12. NaBr has a markedly smaller molecular weight (102.89 Da) than vitamin B-12 and MWCO of Amicon ultra-15 centrifugal filter units. Thus, there could be NaBr loss during the concentration step but it is difficult to calculate how much precisely. Concentrated recombined PPP desalted up to 5 times still did not exhibit any detectable thrombin generation.

Interestingly, adding the HDL fraction directly to PPP seems to show some thrombin generation activity. This finding suggests that HDL may carry some key component of thrombin generation which may not be found in LpDP. Comparison between 1- to 5-time desalting by gel filtration of HDL samples with PPP (1:1 volume ratio) exhibited more thrombin generation as desalting times increased. The calculated NaBr concentration of these samples were 0.16 M, $1.6x10^{-2}$ M, $1.6x10^{-3}$ M, $1.6x10^{-4}$ M, $1.6x10^{-5}$ M for PPP with HDL desalted 1 to 5 times, respectively. These data seem to provide the evidence of a dose-dependent deleterious effect of NaBr to thrombin generation activity *in vitro*.

Nevertheless, PPP with dialysed HDL which had a lower NaBr concentration than that in HDL desalted by 5-time gel filtration did not show any detectable activity of thrombin production. The calculated NaBr concentration was 0.13 ρM for the dialysed HDL fraction with PPP. PPP with HDL desalted by centrifugal column, on the other hand, had a higher NaBr concentration than that in HDL desalted by 5-time gel filtration but did show a small activity of thrombin generation. The calculated NaBr concentration of PPP with HDL desalted by centrifugal columns was 0.39 M, assuming that at least 75% of NaBr was removed according to manufacturer's manual of Amicon ultra-15 centrifugal filter units (3,000 MWCO, Sigma-Aldrich). These finding suggest that there could be other factors apart from NaBr that interfere with thrombin generation activity. The sheer force of ultracentrifugation can damage surface-bound protein of HDL (Collier et al. 2018). A study found shredding of HDL-associated proteins and lower HDL density as rotor speed increases (Munroe, Phillips, and Schumaker 2015). Therefore, it may affect HDL proteins involved in coagulation cascade. Also, extremely long processing time (up to 96 hours for HDL isolation and dialysis) may affect protein activities. Some key components of the coagulation cascade may become detached from HDL during this long period of dialysis.

In summary, our data suggest that thrombin generation activity in plasma can be impaired by NaBr used in the lipoprotein isolation process. PPP with 5-time gel filtrated HDL exhibited the highest thrombin generation activity among all samples. The limitation of this assay is the difficulty in determining whether there is a degree of deteriorated thrombin generation activity of HDL desalted by 5-time gel filtration, leading to the difficulty in standardize thrombin

generation activity measured in HDL isolated with the protocol using NaBr. In the future, iodixanol may be used as an alternative to build a step density for HDL isolation protocol since it produces iso-osmotic solution at all densities, is non-toxic to cells and non-inhibitory to enzymes (Ford, Graham, and Rickwood 1994; Harman, Griffin, and Davies 2013).

5.4 Overview discussion

This chapter showed development of two assays for determining HDL function including assessment of the vasodilatory effects of HDL on vascular reactivity by small-vessel wire myography and the anti-coagulation effect of HDL by a thrombin generation assay. The strength of small-vessel wire myography is that it is an *ex vivo* approach that allows an assessment of HDL impact on vascular reactivity of human arteries. It also allows a direct comparison of pregnant and non-pregnant HDL impact on vascular reactivity of arteries from the same participant. However, this study still lacks power, and BMI of pregnant and non-pregnant HDL donors were not matched which might affect the vasodilatory effect of HDL. Importantly, pregnant VAT arteries showed unstable vasoconstriction with noradrenaline and lacked clear vasorelaxation in response to acetylcholine, thus it is unable to determining vasodilatory effect of HDL in pregnant VAT arteries with this protocol of wire myography. Optimization of the wire myograph protocol for pregnant VAT arteries from tissue collection, vascular dissection, HDL incubation, and types of vasoconstrictors and vasodilators is required to establish this protocol. The strength of thrombin generation assay is that it allows a direct measurement of thrombin generation function of HDL, especially that thrombin generation is a centre of the anti-thrombotic effect of HDL. However, this assay of determining thrombin generation function of HDL has a limitation that NaBr interfered with thrombin generation activity, leading to the difficulty in standardize thrombin generation activity measured in HDL isolated with the protocol using NaBr. It would be important to find an alternative protocol to isolate HDL to be used in this assay. Iodixanol may be useful as an alternative to build a step density for HDL isolation protocol since it produces iso-osmotic solution at all densities, is non-toxic to cells and non-inhibitory to enzymes (Ford, Graham, and Rickwood 1994; Harman, Griffin, and Davies 2013). Also, assays that are able to determine other functions

of HDL such as anti-inflammatory function should be developed to assess HDL function in healthy pregnancy and preeclampsia.

6. Sphingolipid metabolism in pregnancy

6.1 Introduction

A sphingolipid is defined as a sphingoid base connected to a fatty acid via an amide bond. This class of lipids includes S1P and ceramides. Sphingolipids are lipid components of HDL that have an established role in the function of HDL. In particular, S1P promotes HDL-induced inhibition of the TNF-α induced VCAM-1 expression through S1P-S1PR1 signalling (Kimura et al. 2006). S1P has also been shown to induce vasorelaxation through several mechanisms including eNOS activation and enhancement of COX-2 and PGI-2 production (Nofer et al. 2004; González-Díez et al. 2008). Myograph studies of aortic segments from S1PR3-knockout mice showed approximately 60% less vasodilatory response of isolated aorta to HDL treatment, compared to HDL effects on wild-type mice aorta (Nofer et al. 2004). In HDL particles, S1P is carried by apoM. When separating human HDL into HDL with and without apoM by affinity chromatography, S1P was found exclusively in fractions of human HDL with apoM and did not appear in HDL without apoM (Christoffersen et al. 2011). In addition to being a carrier for S1P, apoM can also modulate S1P metabolism by promoting S1P efflux from erythrocytes and promoting anti-atherogenic properties of HDL-S1P (Christensen et al. 2017). ApoM is required for S1P-meadiated inhibition of the TNF-α induced VCAM-1 expression. Incubation of HUVEC with HDL from wild type mice (apoM-containing HDL) inhibited TNF-α induced VCAM-1 expression, whereas HDL from apoM-deficient mice and albumin-bound S1P did not suppress TNF-α action (Galvani et al. 2015).

The ceramide content of HDL also appears to have anti-atherogenic effects. A study in individuals with ischemic heart disease revealed a significantly lower C24:1 ceramide concentration in HDL, compared to individuals without ischemic heart disease (Argraves et al. 2011). Ceramide promotes ABCA1 expression and the interaction of apoA-I and ABCA1 which induces cellular cholesterol efflux to HDL (Witting, Maiorano, and Davidson 2003; Ghering and Davidson 2006). Ceramide is also involved in HDL-mediated eNOS activation. Treating CHO cells expressing SR-B1 with HDL resulted in increased intracellular levels of ceramide and eNOS activity (Li et al. 2002). Interestingly, ceramide function can be heterogeneous depending on its fatty acid chain length and there is a potential

reciprocal relationship between long-chain (C16 and C18) and very-long-chain (C24) ceramides. There were increased ceramide C16:0 and C18:0, but decreased ceramide C24:0 observed in the liver of LDLR(-/-) mice, a diet-induced model of non-alcoholic fatty liver disease and atherosclerosis (Kasumov et al. 2015). The ratio of plasma ceramide C16:0 and C24:0 was also markedly associated with cardiovascular incidence (Laaksonen et al. 2016). These findings suggest that elevated long-chain ceramide and reduced very-long-chain ceramide may be associated with cardiovascular pathology.

Even though HDL concentration increases during pregnancy and could have a role in maintaining maternal vascular function, the role of HDL-S1P and HDL-ceramide has not been established in the physiology of pregnancy (Sulaiman et al. 2016). However, there are some data that might suggest potential roles for S1P and ceramide in enhancing vascular function in pregnancy. S1P is important in implantation and placentation. During decidualization, there is up-regulated *SPHK1* and *SGPP1* expression and stable *SGPL1* expression, suggesting high turnover of S1P (Brünnert et al. 2014). *SPHK1* expression and activity in decidua also increases with gestation, suggesting the importance of S1P in the normal decidualization of pregnancy (Yamamoto et al. 2010). During placental development, EVT migration and spiral artery remodelling can be modulated by S1P. S1P promotes EVT migration through S1P-S1PR1 interaction while S1P-S1PR2 interaction results in inhibition of EVT migration (Westwood et al. 2017; Yang, Li, and Pan 2014). Incubation of isolated dNK cells with a sphingosine analogue revealed down-regulated *S1PR5* expression in dNK cells, impairment of dNK-mediated EVT migration estimated by immunohistochemistry in co-culture of human placental explants and treated-dNK cells, and impaired endothelial angiogenesis demonstrated by HUVEC branching after incubation with culture media of treated-dNK cells (Zhang, Dunk, and Lye 2013). At term, there was higher *S1PR1* (anti-atherogenic receptor) expression than *S1PR2* (pro-atherogenic receptor) expression in omental, myometrial and chorionic plate arteries of healthy pregnancy (Hudson et al. 2007; Hemmings et al. 2006). As S1P effects on endothelial function depend on the type of S1P receptor S1P interact with, these findings suggest a role for S1P in protecting vessels in the maternal and placental circulation from endothelial dysfunction.

In preeclampsia, there is impaired placental sensitivity to hypoxia and an inability to up-regulate placental *SPHK1* expression (Dobierzewska et al. 2016). There was also down-regulated *S1PR1* and *S1PR3* expression and up-regulated *S1PR2* expression in chorionic villi of preeclampsia which could be involved in the impaired EVT migration and trophoblast invasion observed in preeclampsia (Dobierzewska et al. 2016). With respect to ceramide, there was increased *de novo* synthesis via SPT activation and decreased breakdown of ceramides to sphingosine in placental lysosomes resulting from reduced *ASAH1* (acid ceramidase gene) expression and activity, leading to increased ceramide accumulation in placenta of early-onset preeclampsia (Melland-Smith et al. 2015). Ceramide C16 was shown to promote trophoblastic cell apoptosis, autophagy and necrosis (Melland-Smith et al. 2015; Bailey et al. 2017). Thus, accumulation of ceramide C16 in trophoblast cells could interfere with the normal process of trophoblast cell fusion and trophoblast invasion. There were elevated plasma ceramide C16:0, C18:0, C18:1, C20:0, C22:0 and C24:1 concentrations in preeclampsia at 32 weeks of gestation, while ceramide C24:0 concentration deceased at 32-36 weeks of gestation in preeclampsia, compared to healthy pregnancy (Melland-Smith et al. 2015; Charkiewicz et al. 2017; Dobierzewska et al. 2017). As increased ratio of long-chain to very-long-chain ceramide was associated with liver cirrhosis and cardiovascular disease, increased C16:0 and C18:0 ceramide and decreased C24:0 ceramide in the third trimester may relate to liver and vascular complications of preeclampsia (Laaksonen et al. 2016; Grammatikos et al. 2015).

In this chapter, S1P and ceramide concentrations in HDL were assessed at different gestations of pregnancy to examine a possible association of these HDL-sphingolipids with maternal vascular function. ApoM concentration was also examined in HDL throughout pregnancy. Gene expression of sphingolipid synthesis enzymes was assessed in SAT from healthy pregnant and non-pregnant women as a surrogate for sphingolipid expression in the liver, the potential source of HDL sphingolipids. The source of S1P residing in HDL could be hepatocytes since HDL synthesis mainly occurs in the liver and aberrant lipid handling in the liver can lead to decreased S1P in HDL (Kurano et al. 2020). Ceramide can be incorporated into newly synthesized VLDL and LDL in the liver, thus ceramide content in HDL could possibly be acquired from VLDL and LDL in

the circulation via lipid transfer proteins (Memon et al. 1998; Memon et al. 1999; Merrill et al. 1995). Measurement of sphingolipid synthesis enzyme gene expression in the liver of pregnant women would be ideal to understand the source of S1P and ceramide in HDL of healthy pregnancy. However, liver biopsy is a high-risk procedure and would not be appropriated to perform in healthy pregnant women. It was shown in one study that gene expression of long chain polyunsaturated fatty acid (LC-PUFA) synthesis enzyme in SAT reflected that in the liver (Mackay et al. 2012). The study demonstrated lower LC-PUFA concentration in erythrocyte from preeclampsia compared to healthy pregnancy. LC-PUFA concentration in SAT between preeclampsia and healthy pregnancy were similar which did not suggest SAT as a major source of lower erythrocyte LC-PUFA concentration in preeclampsia. However, there was lower LC-PUFA synthesis enzyme gene expression in SAT of preeclampsia. Thus, SAT may not be a main site for LC-PUFA synthesis, but the gene expression in SAT may reflect other potential sites of synthesis such as the liver. In this thesis, SAT was chosen because of its potential in reflecting sphingolipid synthesis gene expression in the liver and its accessibility in pregnant women undergoing caesarean section. The five chosen genes (*SPTLC1*, *SMPD1*, *SMPD3*, *SMPD4* and *ENPP7*) are genes encoding enzymes involved in sphingolipid generation via either the *de novo* pathway or sphingomyelin hydrolysis (Figure 6-1). The *SPTLC1* gene expresses the SPT enzyme which is the rate-limiting step of *de novo* ceramide synthesis, and it was chosen to represent the *de novo* pathway. There are 4 subunits of sphingomyelinase: *SMPD1*, *SMPD3*, *SMPD4* and *ENPP7* which generate ceramide by hydrolysing sphingomyelin. These 4 genes were chosen to represent the sphingomyelin hydrolysis pathway.

Finally, gene expression of sphingolipid synthesis enzymes was assessed in placentae from healthy, IUGR and preeclampsia pregnancies to determine whether placental sphingolipid metabolism in healthy pregnancy and preeclampsia, as well as IUGR, which is a fetal complication associated with placental vascular dysfunction, placental insufficiency and preeclampsia (Jeyabalan 2013). The five genes (*SPTLC1, SMPD1, SMPD3, SMPD4* and *ENPP7*) were chosen as they are key enzymes in sphingolipid generation by the *de novo* pathway and in sphingomyelin hydrolysis. An additional five genes (*SGMS1, SGMS2, CERS1, CERS4, CERS6*) were selected based on the sphingolipid profile of

this same set of placentae published in (Brown et al. 2016). The sphingolipid profile of placentae from healthy pregnancy, IUGR and preeclampsia was estimated by mass spectrometry and showed eight species of ceramide ranging from C16:0, C18:0, C20:0, C22:0, C23:0, C24:0, C24:1 and C24:2 with ceramide C16:0 and C24:0 as the major ceramide species in placentae. There were no differences in these ceramide species between placentae from healthy pregnancy, IUGR and preeclampsia, while there were 20% higher sphingomyelin (SM) 14:0 content in placentae of preeclampsia and 2-fold higher SM 18:0 content in placentae of IUGR and preeclampsia, relative to healthy pregnancy (Brown et al. 2016). Therefore, *SGMS1* and *SGMS2* which encode sphingomyelin synthase enzymes that convert ceramide to sphingomyelin were chosen to assess sphingomyelin synthesis (Figure 6-1). *CERS1, CERS4* and *CERS6* which encode specific ceramide synthases that promote the generation of ceramide C18 (*CERS1* and *CERS4*) and ceramide C14 (*CERS6*) were also chosen to represent specific ceramide species synthesis which may influence the synthesis of specific sphingomyelin species observed at a higher amount in placentae of preeclampsia and IUGR (Figure 6-1).

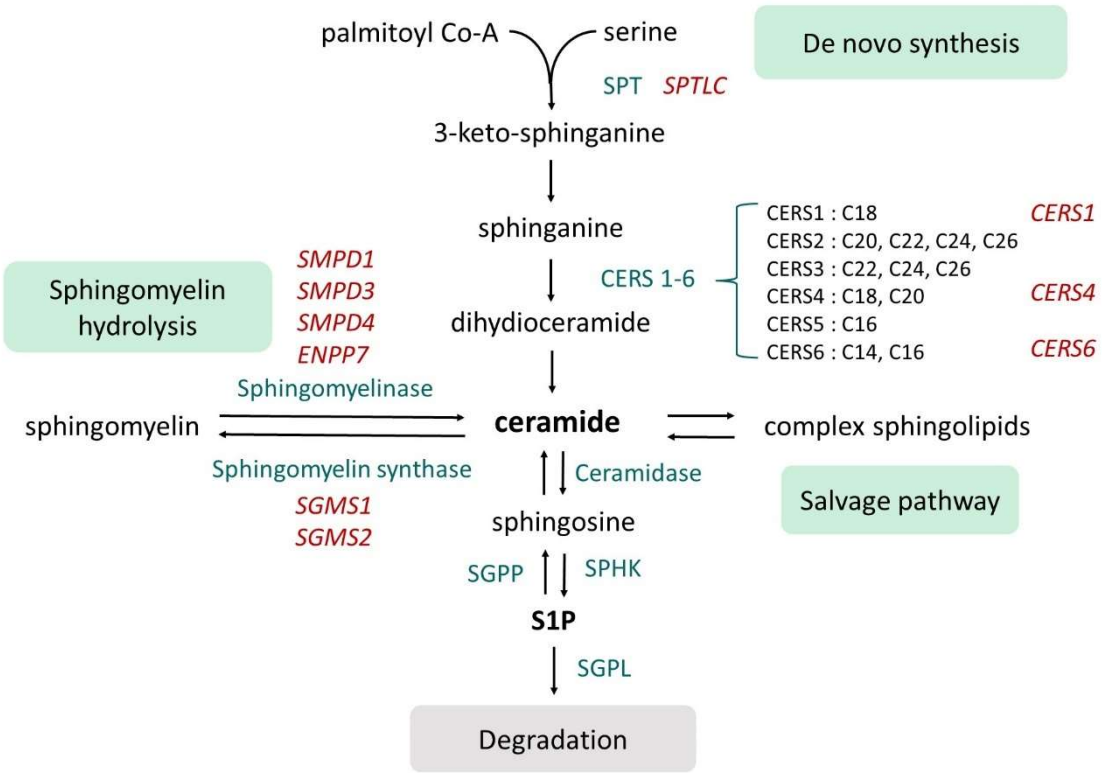

Figure 6-1 Sphingolipid metabolism Red, italic words indicate genes expressing the corresponding enzymes in green. SPT, serine palmitoyl transferase; CERS, ceramide synthases; SPHK, sphingosine kinase; SGPP, S1P phosphatase; SGPL, S1P lyase

6.1.1 Hypotheses

- There are increased concentration of S1P and ceramide content, ratio of very-long-chain ceramide to long-chain ceramide and apoM concentration in HDL as gestational age advances.

- There is up-regulated sphingolipid synthesis enzyme expression in SAT of healthy pregnancy, compared to non-pregnant women.

- There is up-regulated sphingolipid synthesis enzyme expression in placentae of preeclampsia and IUGR, compared to healthy pregnancy.

6.1.2 Objectives

- To determine S1P, ceramide and apoM concentration in HDL of healthy pregnant women at different gestational ages throughout gestation

- To compare gene expression of sphingolipid synthesis enzymes in SAT of healthy pregnant and non-pregnant women

- To compare gene expression of sphingolipid synthesis enzymes in placentae of healthy pregnancy, IUGR and preeclampsia

6.2 Methodology

6.2.1 Recruitment of healthy pregnant women as HDL donors

Healthy pregnant women samples were from an archival collection of two cohorts undergoing longitudinal studies throughout pregnancy recruited according to section 2.1.1, chapter 2. Ten participants were recruited from each cohort (EPS and LIPS) and matched for BMI, age and parity as indicated in section 3.3.1, chapter 3. The first cohort (EPS) included 4 timepoints from before pregnancy, 4.6, 6.1 and 8.4 weeks of gestation. The second cohort (LIPS) covered from 16 weeks of gestation to 13 weeks after delivery.

Blood was processed according to section 2.2, chapter 2, followed by HDL preparation from plasma according to section 2.3, chapter 2. Desalted HDL fractions were then stored in -80ºC until use.

6.2.2 Recruitment of non-pregnant and healthy pregnant women as SAT donors

SAT samples of non-pregnant and healthy pregnant women were from an archival collection of the Freeman group.

6.2.2.1 Non-pregnant women

Non-pregnant women undergoing gynaecological procedures for benign conditions (at Glasgow Royal Infirmary) and those undergoing cholecystectomy, hernia removal or renal transplant (donor) (at Western Infirmary, Glasgow) were recruited (n=10). Ethical approval was granted by the West of Scotland Research Ethics Committee (Ethics Ref: 11/AL/0017; R&D Ref: GN11OB034). All participants were aged between 18-45 years old and did not present with any systemic disease unrelated to their condition. SAT biopsies were obtained during the procedures and were obtained from under the skin at an abdominal incision site appropriate to the surgery being undertaken.

6.2.2.2 Healthy pregnant women

Healthy pregnant women (n=10) were recruited from the maternity unit, Queen Elizabeth University Hospital, Glasgow, United Kingdom. The inclusion and exclusion criteria are listed in Table 6-2. Ethical approval was granted by the West of Scotland Research Ethics Committee (Ethics Ref: 11/AL/0017; R&D Ref: GN11OB034). Pregnant women at term who met the criteria were identified from the C-section operating theatre list, informed about the study and written consent was taken prior to SAT biopsy by the obstetric surgeon during the C-section. SAT was flash frozen in liquid nitrogen and stored at -80ºC until use.

Table 6-2: Inclusion and exclusion criteria for healthy pregnant women

Inclusion criteria	Exclusion criteria
1. Pregnant women at third trimester undergoing elective C-section (non-labouring)	1. Metabolic disease (such as diabetes and hypertension)
2. Age 18 to 45	2. Undergoing treatment for metabolic disease (e.g. statins)
3. Range of BMI	3. Any known transmissible disease
	4. Rheumatoid arthritis or any other autoimmune disease
	5. Any adverse pregnancy outcome

6.2.3 Recruitment of healthy pregnant women, pregnant women with IUGR and with preeclampsia as placenta donors

Placenta samples were from an archival collection of healthy pregnant women (n=68), pregnant women with IUGR (n=10) and with preeclampsia at the third trimester (n=23). The study was performed at the Princess Royal Maternity Hospital, Glasgow and ethic approval was given by the Glasgow Royal Infirmary Local Research Ethics Committee (Ethics approval and R&D reference number 01OB006 and 01OB007, Ethics approval 06/S0704/14 and R&D approval reference number RN05BI013). All participants provided written informed consent. Preeclampsia was defined according to the ISSHP criteria mentioned in section 2.1.2, chapter 2. IUGR was defined as an estimated fetal weight<5th percentile for gestation with associated oligohydramnios (amniotic fluid index<5) and/or abnormal umbilical artery blood flow on doppler ultrasound. Women with metabolic disease or suspected fetal anomalies likely to contribute to reduced

fetal growth were excluded. At delivery, full thickness biopsy (approximately five grams) of placenta was collected from four separate pre-determined areas on each placenta (distinct from the umbilical cord insertion) and then samples were randomised. All samples were flash frozen in liquid nitrogen and stored at -70ºC.

6.2.4 Measurement of sphingolipid concentrations in HDL samples at different gestation throughout healthy pregnancy

Measurement of sphingolipid concentration in HDL samples was provided by Dr Monique Mulder, Gardi Voortman and Kristien Dorst, Erasmus University Medical Center, Rotterdam, the Netherlands, using Liquid Chromatography-Tandem Mass Spectrometry according to (den Hoedt et al. 2021). Briefly, an LC-30A autosampler (Shimadzu, Kyoto, Japan) injected HDL lipid extracts into a Shimadzu HPLC system (Shimadzu) equipped with a Kinetex C8 column (50 mm × 2.1 mm, 2.6 µm, 00B-4497-AN, Phenomenex, Maarssen, Netherlands) at 30ºC. The mobile phase comprised 95% mobile phase A [MQ/methanol (50/50, v/v) containing 1.5 mM ammonium formate and 0.1% formic acid] and 5% mobile phase B (methanol containing 1 mM ammonium formate and 0.1% formic acid) for 2 mins, following by a linear gradient from 95% mobile phase A and 5% mobile phase B to 7% mobile phase A and 93% mobile phase B in 5.5 min and was held for 4.5 min. After that, the column was flushed with 99% mobile phase B for 2 min followed by a 2 min re-equilibration. The effluent was transferred to a Sciex Qtrap 5500 quadruple mass spectrometer (AB Sciex Inc., Thornhill, ON, Canada) and analysed in positive ion mode following electrospray ionization using multiple reaction monitoring. S1P and seven ceramide species for which standards were commercially available (ceramide C14:0, C16:0, C18:0, C20:0, C22:0, C24:0, C24:1, Avanti polar lipids) were quantified using nine-point calibration curves which were constructed by plotting analyte to internal standard peak area ratios versus the corresponding analyte concentration. Correlation coefficients (R2) were >0.99. Analyses of spectral data were performed using MultiQuant software (AB Sciex Inc.).

6.2.5 Measurement of apoM concentrations in HDL samples at different gestation throughout healthy pregnancy

Measurement of apoM concentration in HDL samples at different gestation throughout healthy pregnancy was provided by Dr Christina Christoffersen using a sandwich ELISA according to the protocol in (Axler, Ahnström, and Dahlbäck 2007). Briefly, A 96-well plate (Costar 3590, Corning) was coated with monoclonal M58 (100 µL) at a concentration of 10 µg/mL in carbonate buffer, pH 9.6. The plate was quenched with 2% bovine serum albumin (200 µL, Sigma-Aldrich) in Tris-buffered saline overnight at 4ºC. HDL samples, together with a plasma standard curve, were diluted in Tris-buffered saline with 1% Triton X-100 (Sigma-Aldrich) and 1% bovine serum albumin, and 100 µL was added to each well. After an overnight incubation at room temperature, the plate was washed by Tris-buffered saline with 0.1% Triton X-100. Biotinylated M42 secondary antibody (100 µL) diluted to a final concentration of 0.5 µg/mL in Tris-buffered saline with 0.1% Triton X-100 and 1% bovine serum albumin, was then added to the plate and incubated at room temperature for 2 hours, followed by washing. Streptavidin-avidin complex with horseradish peroxidase (Dako) was prepared according to the manufacturer's instructions, diluted in Tris-buffered saline with 0.1% Triton X-100 and 1% bovine serum albumin, and 100 µL was added. After washing, peroxide and o-phenylenediamine dihydrochloride (Dako) was prepared according to the manufacturer's instructions, and 100 µL was added. The reaction was terminated after 9 minutes, and absorbance at 490 nm was read by plate reader (EL808; BioTek Instruments) with Deltasoft 3 software. ApoM concentration was calculated by applying least-squares principles to a five-parameter sigmoidal model of the standard curve. Calculated apoM concentration was expressed as µmol/l or µM.

6.2.6 Measurement of gene expression of enzymes involved in sphingolipid metabolism in SAT of healthy pregnant and non-pregnant women

Quantitative reverse transcription polymerase chain reaction (qRT-PCR) was used to quantitate the messenger ribonucleic acid (mRNA) expression after pre-amplification of complementary deoxyribonucleic acid (cDNA) of sphingolipid synthesis enzyme genes in SAT of healthy pregnant and non-pregnant women.

6.2.6.1 RNA isolation from SAT

The RNeasy Lipid Tissue Mini Kit (QIAGEN) was used to isolate RNA from SAT, as per the manufacturer's instructions. Tissue (100-200 mg) was homogenised in QIAzol lysis reagent (1mL) using a hand-held tissue homogeniser (Omni UH Motor Battery Pack & Charger, Camlab). The homogenate was transferred to a 1.5-mL centrifuge tube and incubated at room temperature for 5 minutes. Chloroform (200 µL) was added to the homogenate and shaken vigorously for 15 seconds followed by incubation at room temperature for a further 3 minutes. The sample was subsequently centrifuged at 12,000 g (13,000 rpm) for 15 minutes at 4ºC. The upper aqueous phase (400-500 µL) was transferred to a clean 1.5-mL centrifuge tube, to which 75% ethanol (500 µL) was added and the sample was vortexed. The sample was then transferred into RNeasy spin columns and centrifuged for 15 seconds at 8,000 g (10,000 rpm). The flow-through was discarded and this step was repeated until the entire sample was processed. The sample was subsequently washed with RW1 buffer (700 µL) and spun at 8,000 g (10,000rpm) for 15 seconds followed by disposal of the flow through. RPE buffer (500 µL) was then used to wash the column at 8,000 g (10,000 rpm) for 15 seconds, followed by the second round of RPE buffer wash (500 µL) for 2 minutes. The column was placed in new 2-mL tube and centrifuged at 8,000 g (10,000 rpm) for 1 minutes to fully dry the membrane. Finally, the filter portion of the spin column was transferred to a 1.5-mL tube where nuclease free water (30 µL) was added before a centrifugation at 8,000g (10,000 rpm) for 1 minute. The flow through was transferred to a fresh Eppendorf tube for storage at -80ºC.

6.2.6.2 RNA quantification

A Nanodrop spectrophotometer with Nanodrop 1000 software version 3.7.1 was used to quantify RNA (Thermo Fisher Scientific). RNA sample was thawed on ice and centrifuged at 8,000g (10,000 rpm) at 4ºC for 5 minutes. Ethanol was decanted from the tube and the pellet left to dry at room temperature for 10 minutes before adding nuclease-free water (20 µL). The sample was vortexed and incubated at 65ºC for 5 minutes then vortexed and incubated again for a further 5 minutes before use. RNase-free water (1.5 µL) and RNA (1.5 µL) were loaded on to Nanodrop spectrophotometer separately to allow measuring the concentrations in ng/µL and the ratio of absorbance at 260 nm and 280 nm and

concentration. The 260/280 ratio of approximately 2 is generally accepted as "pure" for RNA. The RNA was stored at -80ºC until required.

6.2.6.3 DNase treatment of RNA

Contaminating genomic DNA was removed from the extracted RNA samples using a DNA-free kit (Ambion, cat. no.AM1906). Each of the RNA sample (21.5 µL) was added to a microcentrifuge tube followed by 10X Dnase 1 buffer (2.5 µL) and rDnase 1 (1 µL). The sample was incubated at 37ºC for 30 minutes in an OMN-E thermal cycler. DNase Inactivation Reagent (3 µL) was added to each sample and incubated for 2 minutes at room temperature. After that, the sample was centrifuged at 13,000 rpm for 1 minute to pellet the DNase Inactivation Reagent. The supernatant was collected as DNase-treated RNA.

6.2.6.4 Reverse transcription

A High capacity cDNA Reverse Transcription Kit (Applied Biosystems, cat. no. 4368813) was used to reverse transcribe DNase-treated RNA to complementary DNA (cDNA). The 2X RT Mastermix was prepared by mixing 10X RT Buffer (2 µL), 25X dNTPs (0.8 µL), 10X random primers (2 µL), Multiscribe reverse transcriptase (1 µL), Superasin 1U/ul (1 µL) and nuclease-free water (3.2 µL) for each reaction. The no-RT Mastermix was also prepared for a no-RT control using the same volumes of reagents but without Multiscribe reverse transcriptase. The 2X RT Mastermix (10 µL) was added to Dnase-treated RNA (10 µL). The sample was then incubated at 25ºC for 10 minutes followed by 37ºC for 120 minutes and 85ºC for 5 seconds using the ThermoFisher Hybaid PCR Express Thermal Cycler. The samples were stored at -20ºC.

6.2.6.5 Pre-amplification of cDNA

Since a small quantity of RNA and cDNA can be obtained from SAT, cDNA was pre-amplified to increase the concentration of a specific gene and reduce the required sample's volume for PCR reaction. Pre-amplification was performed using the TaqMan PreAmp Master Mix Kit (Applied Biosystems, cat. no. 4384266) with the same primer set that was used in PCR reaction for genes including *STPLC1, SMPD1, SMPD3, SMPD4, ENPP7* and *PPIA* (Taqman® gene expression assays, Thermo Fisher Scientific) (Table 6.1). All Taqman® gene expression

assays were pooled and mixed with Tris-EDTA (TE) PH 8 buffer (Ambion, cat. no. AM9849) at 1:1 volume ratio. Pooled Taqman assay mix (12.5 µL), TaqMan PreAmp Master Mix (25 µL), nuclease-free water (7.5 µL) and cDNA (5 µL) were added to each well of a 96-well plate. The plate was sealed and briefly centrifuged in Jouan CR412 centrifuge followed by 10 pre-amplification cycles in a thermocycler (StepOnePlus Real-Time PCR System, Applied Biosystems) which was programmed to incubate the sample at 95 ºC for 10 minutes then 10 cycles of 95 ºC for 15 seconds followed by 60 ºC for 4 minutes. Each sample was then diluted with TE buffer in a 1:4 ratio.

Table 6.1 Taqman® gene expression assays

Gene	Taqman® gene expression assay	Assay ID
SPTLC1	Serine palmitoyl transferase (subunit 1)	Hs00272311_m1
SMPD1	Acid sphingomyelinase	Hs03679346_g1
SMPD3	Neutral sphingomyelinase	Hs00920354_m1
SMPD4	Neutral sphingomyelinase	Hs04187047_g1
ENPP7	Alkaline sphingomyelinase	Hs00698717_m1
PPIA	Peptidyl-protyl Isomerase A	4333763T
CDKN1B	cyclin dependent kinase inhibitor 1B	Hs00153277_m1
SGMS1	sphingomyelin synthase 1	Hs00983630_m1
SGMS2	sphingomyelin synthase 2	Hs00380453_m1
CERS1	ceramide synthase 1	Hs04195319_s1
CERS4	ceramide synthase 4	Hs00226114_m1

CERS6	ceramide synthase 6	Hs00826756_m1
TOP1	DNA topoisomerase 1	Hs00243257_m1

The uniformity of pre-amplification was checked using ΔΔCT method following the protocol published by Thermo Fisher. Gene expressions of each target gene (*STPLC1, SMPD1, SMPD3, SMPD4 and ENPP7*) were determined in pre-amplified and non-pre-amplified cDNA in duplicate with *CDKN1B* as a reference gene. calculated threshold cycle (C_T) values for each target gene and *CDKN1B* were obtained for different dilutions of pre-amplified and non-pre-amplified cDNA. $\Delta\Delta C_T$ values for each target gene were calculated as followed:

ΔC_T = averaged C_T of target gene – averaged C_T of *CDKN1B*

$\Delta\Delta C_T$ = ΔC_T of pre-amplified cDNA - ΔC_T of non-pre-amplified cDNA

The $\Delta\Delta C_T$ values of pre-amplified cDNA at different dilution for *STPLC1, SMPD1, SMPD3, SMPD4* and *ENPP7* were within ±1.5 (Figure 6-2). A $\Delta\Delta C_T$ value close to zero indicates preamplification uniformity and a $\Delta\Delta C_T$ value within ±1.5 is acceptable since 90% of TaqMan® Gene Expression Assays produce $\Delta\Delta C_T$ within ±1.5.

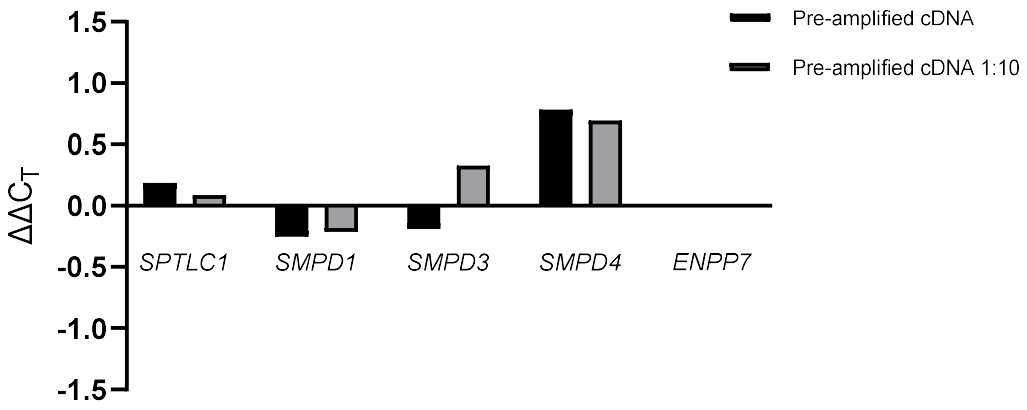

Figure 6-2 The $\Delta\Delta C_T$ values of pre-amplified cDNA at different dilution for *STPLC1, SMPD1, SMPD3, SMPD4* and *ENPP7*

6.2.6.6 Quantitative real-time PCR reaction

A PCR reaction mixture was prepared for each gene (*STPLC1, SMPD1, SMPD3, SMPD4, ENPP7* and *PPIA*) by mixing TaqMan Universal PCR Mastermix (12.5 µL), Taqman® gene expression assay probe corresponding to each gene as shown in Table 6.1 (1.25 µL) and nuclease-free water (5 µL) per reaction. PCR mixture (18.7 µL) was added to each well of a 96-well plate followed by pre-amplified cDNA (6.25 µL) in duplicate for each sample. Negative control and no-RT control were carried out for all samples by using nuclease-free water (negative control) and samples with no-RT Mastermix (no-RT control) instead of cDNA. The plate was then sealed and briefly centrifuged. The plate was then loaded onto a StepOnePlus Real-Time PCR System (Applied Biosystems) which completed a standard RT-PCR cycle by incubating the plate at 50ºC for 2 minutes, 95ºC for 10 minutes and 40 cycles of 95ºC for 15 seconds and the final incubation at 60ºC for 1 minute.

An amplification plot and calculated threshold cycle (C_T) values were obtained from the StepOnePlus Real-Time PCR System using StepOnePlus™ Software version 2.3. C_T values of each gene were normalised to an endogenous reference gene, *PPIA* which previous shown to be a stable control gene for adipose tissue (Neville et al. 2011), by subtracting averaged C_T of *PPIA* from averaged C_T of target gene as followed:

$$\Delta C_T = \text{averaged } C_T \text{ of target gene} - \text{averaged } C_T \text{ of } PPIA$$

The ΔC_T value was then converted to linear form by $2^{-\Delta CT}$ calculation and presented as percentage to represent the fold difference of target gene expression relative to the endogenous reference gene. The percentage of relative expression of target genes to controls has an inter-assay coefficient of variation (CV) <13% in adipose tissue for a wide variety of target genes when carried out using a commercial primer process from Applied Biosystems (unpublished data from our lab).

6.2.7 Measurement of gene expression of enzymes involved in sphingolipid metabolism in placentae from healthy pregnancy, IUGR and preeclampsia

The qRT-PCR was used to quantitate the mRNA expression of sphingolipid synthesis enzyme genes in placentae of healthy pregnant, IUGR and preeclampsia. Measurement of *STPLC1, SMPD1, SMPD3, SMPD4* and *ENPP7* expression was performed by Swati Patil.

6.2.7.1 RNA isolation from placenta

Placental tissue (100 mg) was homogenised in TRIzol lysis reagent (Thermo Fisher Scientific, 1 mL) using a hand-held tissue homogeniser. The homogenate was transferred to a 1.5-mL centrifuge tube and incubated at room temperature for 5 minutes. Chloroform (200 µL) was added to the homogenate and shaken vigorously for 15 seconds followed by incubation at room temperature for a further 3 minutes. The sample was subsequently centrifuged at 12,000g (13,000 rpm) for 15 minutes at 4ºC. The upper aqueous phase (400-500 µL) was transferred to a clean 1.5-mL centrifuge tube. Isopropanol (500 µL) was added to each sample and incubated at room temperature for 10 minutes. The sample was then centrifuged at 12,000g (13,000 rpm) for 10 minutes at 4ºC. Isopropanol was decanted from the centrifuge tube to leave the pellet at the bottom and was replaced with 75% ethanol (1 mL), vortexed and stored at -80 ºC.

6.2.7.2 RNA quantification, DNase treatment of RNA and reverse transcription reaction

RNA sample was thawed on ice and centrifuged at 8,000g (10,000 rpm) at 4ºC for 5 minutes. Ethanol was decanted from the tube and the pellet left to dry at room temperature for 10 minutes before adding nuclease-free water (30 µL). The sample was vortexed and incubated at 65ºC for 5 minutes then vortexed and incubated again for a further 5 minutes before use. A Nanodrop spectrophotometer with Nanodrop 1000 software version 3.7.1 was used to quantify RNA (Thermo Fisher Scientific) according to the protocol in section 6.2.6.2 in this chapter. Contaminating genomic DNA was then removed from the extracted RNA samples using a DNA-free kit (Ambion, cat. no.AM1906), followed by reverse transcription of DNase-treated RNA to cDNA using a High capacity

cDNA Reverse Transcription Kit (Applied Biosystems, cat. no. 4368813) according to the protocol in section 6.2.6.3 and 6.2.6.4 in this chapter.

6.2.7.3 Quantitative real time PCR reaction

A PCR reaction mixture was prepared for each gene (*STPLC1, SMPD1, SMPD3, SMPD4, ENPP7, SGMS1, SGMS2, CERS1, CERS4, CERS6* and *TOP1*) by mixing TaqMan Universal PCR Mastermix (12.5 µL), Taqman® gene expression assay probe corresponding to each gene as shown in Table 6.1 (1.25 µL) and nuclease-free water (10.25 µL) per reaction. PCR mixture (24 µL) was added to each well of a 96-well plate followed by cDNA (1 µL) in duplicate for each sample. Negative control and no-RT control were carried out for all samples by using nuclease-free water (negative control) and samples with no-RT Mastermix (no-RT control) instead of cDNA. The plate was then sealed and briefly centrifuged. The plate was then loaded onto a StepOnePlus Real-Time PCR System (Applied Biosystems) which completed a standard RT-PCR cycle by incubating the plate at 50ºC for 2 minutes, 95ºC for 10 minutes and 40 cycles of 95ºC for 15 seconds and the final incubation at 60ºC for 1 minute.

An amplification plot and C_T values were obtained from the StepOnePlus Real-Time PCR System using StepOnePlus™ Software version 2.3. C_T values of each gene were normalised to an endogenous reference gene, *TOP1* which previous shown to be a stable control gene for placenta (Kaitu'u-Lino et al. 2014) as followed

ΔC_T = averaged C_T of target gene – averaged C_T of *TOP1*.

The ΔC_T value was then converted to linear form by $2^{-\Delta CT}$ calculation and presented as percentage to represent the fold difference of target gene expression relative to the endogenous reference gene.

Since this placental gene expression experiment involved a large sample size and the intra-assay variation has not yet been examined in this setting of assay, CV and $2^{-\Delta\Delta CT}$ were calculated from *SPTLC1, SMPD1, SMPD3, SMPD4* and *TOP1* data as indicators of the intra-assay or inter-plate variation. The $2^{-\Delta\Delta CT}$ method was used to examining the impact of intra-assay variation to gene expression comparison

outcome by comparing the result of gene expression calculated by $2^{-\Delta\Delta CT}$ with the result from $2^{-\Delta CT}$. The $2^{-\Delta\Delta CT}$ value represents the fold change of target gene expression normalised to an endogenous reference gene and relative to the inter-plate control (QC) sample, while $2^{-\Delta CT}$ represents the fold change of target gene expression relative to the endogenous reference gene only. If the result from $2^{-\Delta\Delta CT}$ and $2^{-\Delta CT}$ calculation were compatible, the impact of inter-plate variation is insignificant. A placenta biopsy from one specific pregnant woman was used as a QC sample and *SPTLC1, SMPD1, SMPD3, SMPD4* and *TOP1* expression were measured in placenta of QC repeatedly across all plated of qRT-PCR reaction. The $\Delta\Delta C_T$ of each target gene was calculated by subtracting the ΔC_T of QC in each plate from the ΔC_T of placenta from other participants in the same plate of qRT-PCR reaction as followed

$\Delta\Delta C_T = \Delta C_T$ of each sample – ΔC_T of QC.

The $\Delta\Delta C_T$ value was then converted to linear form by $2^{-\Delta\Delta CT}$ calculation. This $2^{-\Delta\Delta CT}$ value for each gene represents the fold change of target gene expression normalised to an endogenous reference gene and relative to the QC sample in the same plate. The intra-assay CV of placental expression of target genes relative to controls for *SPTLC1, SMPD1, SMPD3, SMPD4* and *TOP1* was evaluated by calculating CV of ΔC_T of the QC sample across all plates of qRT-PCR as followed

%CV of ΔC_T = (SD of $\Delta C_T \div$ mean of ΔC_T) x 100.

6.2.8 Statistical analysis

All data was check for normal distribution using Ryan-Joiner test. Log- or square root transformation were applied to achieve normal distribution if necessary. Data from the EPS cohort (pre-pregnancy, 4.6, 6.1 and 8.4 weeks of gestation) and the LIPS cohort (16, 25, 35 weeks of gestation and post-pregnancy) were analysed separately. To determine the comparability between the two cohorts, pre-pregnancy EPS data and post-partum LIPS data were compared as indicated in section 3.2.6, chapter 3. HDL sphingolipid concentrations were also presented as ratios of sphingolipid to apoA-I or cholesterol concentration in HDL. Since apoA-I is a major protein in HDL and can be considered as a marker for HDL

particle, HDL sphingolipid to apoA-I concentration ratio represents sphingolipid content per HDL particle. HDL cholesterol is another HDL marker which is widely used as a biomarker for assessing cardiovascular disease focusing on RCT function of HDL. The HDL sphingolipid to HDL cholesterol ratio could give an insight into how lipid distribution changes in HDL (perhaps related to HDL size) and how S1P relates with functional (RCT) unit of HDL. HDL sphingolipid concentrations (uncorrected, corrected with apoA-I and corrected with cholesterol) within each cohort, as well as apoM concentration which were all normally distributed were analysed by repeated measures ANOVA followed by *post hoc* Tukey's test.

Relative expression ($2^{-\Delta CT}$) of each gene in SAT was analysed by unpaired t-test for parametric data and Mann-Whitney test for non-parametric data. For $2^{-\Delta CT}$ and $2^{-\Delta\Delta CT}$ value of each gene in placenta, one-way ANOVA was used for parametric data and Kruskal-Wallis test was used for non-parametric data to compare the percentage of relative gene expression in placenta among preeclampsia, IUGR and healthy pregnancy. Minitab version 19 was used for statistical analysis.

6.3 Results

6.3.1 General characteristics of HDL donors

HDL donors were the same group of participants as the study in chapter 3. General characteristics of HDL donors were shown in section 3.3.1, chapter 3 and Table 3.3. Participants from EPS and LIPS were matched for BMI, age and parity. All participants were nulliparous and non-smokers.

6.3.2 S1P and apoM concentration in HDL samples at different gestation in healthy pregnancy

HDL S1P concentration decreased at 8.4 weeks of gestation compared to those before pregnancy, rose at 35 weeks of gestation compared to those at 15 and 25 weeks of gestation and then dropped again after delivery. Similarly, S1P corrected for apoA-I concentration decreased at 8.4 weeks of gestation, increased at 35 weeks of gestation but then increased again after delivery. However, after correction for cholesterol concentration, S1P concentration in

HDL were not different across gestation (Figure 6-3). There was no significant difference in S1P concentration (uncorrected, corrected for apoA-I and corrected for cholesterol) between HDL from pre-pregnancy and postpartum (Table 6.2). ApoM concentration in HDL of pregnant women at 6.1 weeks of gestation was significantly lower than those in HDL at pre-pregnancy (Figure 6-4). ApoM concentration of HDL at postpartum (1.2±0.3 μM) was significantly higher than that before pregnancy (0.9±0.3 μM) with $p=0.032$. There was no significant difference of S1P to apoM concentration ratio throughout gestation ($p>0.05$) (Figure 6-5).

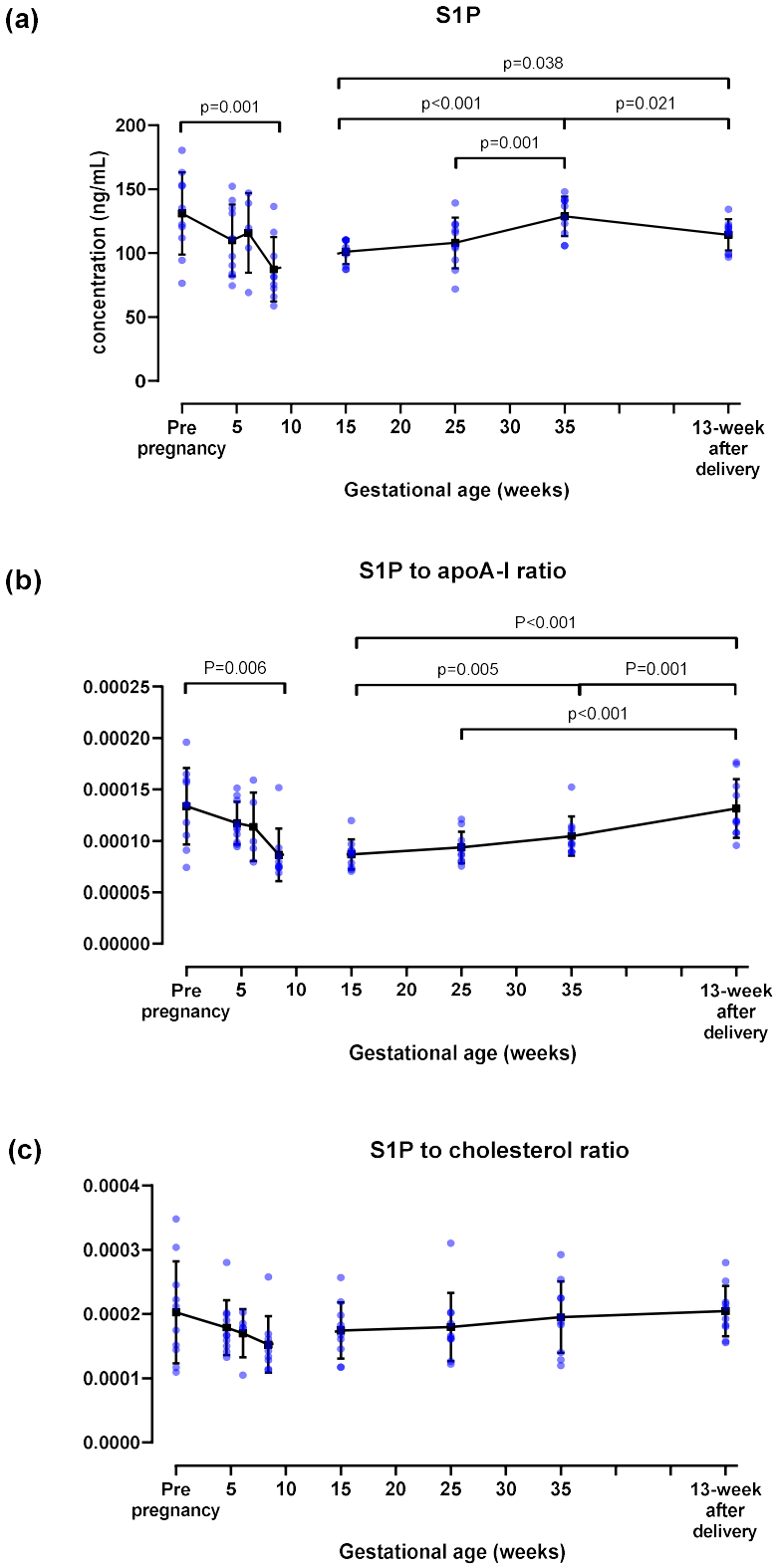

Figure 6-3 S1P concentration [uncorrected (a), corrected for apoA-I concentration (b) and corrected for cholesterol concentration (c)] in HDL at different gestations throughout pregnancy Data was expressed as mean±SD. Repeated measures ANOVA followed by Tukey's test was carried out for S1P concentration (both EPS and LIPS), S1P concentration corrected for apoA-I (EPS) and S1P concentration corrected for cholesterol (LIPS). S1P concentration corrected for apoA-I (LIPS) and S1P concentration corrected for cholesterol (EPS) were log-transformed before analysis by repeated measures ANOVA followed by Tukey's test. $p<0.05$ was taken as statistically significant.

Table 6.2 Comparison of S1P concentration (uncorrected, corrected for apoA-I and corrected for cholesterol) between HDL from pre-pregnancy and postpartum

	Pre-pregnancy	Postpartum	p
S1P concentration (ng/mL)	131.0±30.6	114.4±11.6	0.16
S1P to apoA-I ratio	0.00013±0.00004	0.00013±0.00003	0.90
S1P to cholesterol ratio	0.00020±0.00008	0.00021±0.00004	0.95

Data was expressed in mean±SD. Unpaired t-test was carried out to compare S1P concentration between pre-pregnancy and postpartum. $p<0.05$ was taken as statistically significant.

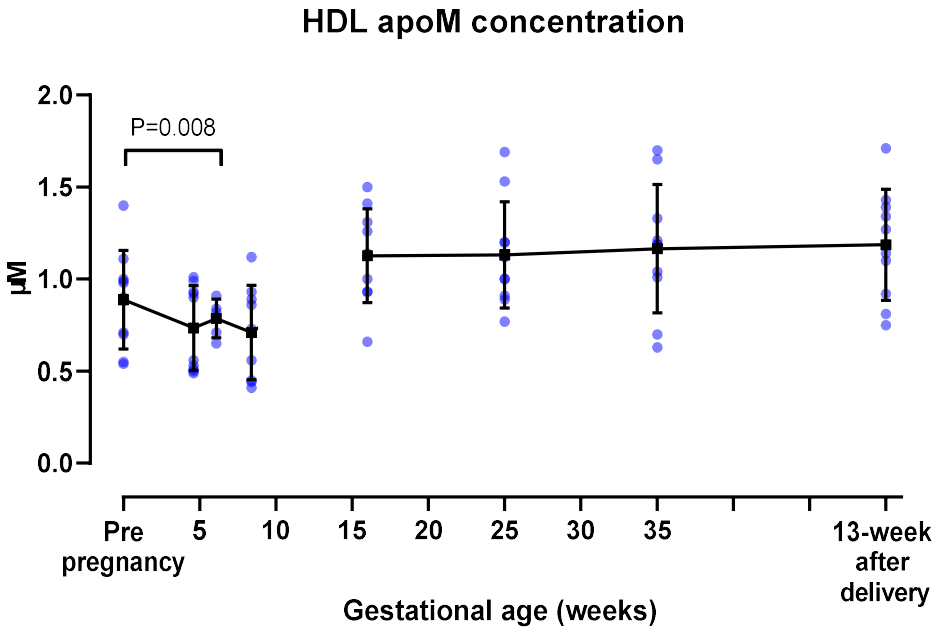

Figure 6-4 ApoM concentration in HDL throughout pregnancy: Data is shown as mean±SD. Repeated measures ANOVA followed by *post hoc* Turkey's test were carried out in each cohort separately and is shown with no line between these two groups of participants. $p<0.05$ was taken as statistically significant.

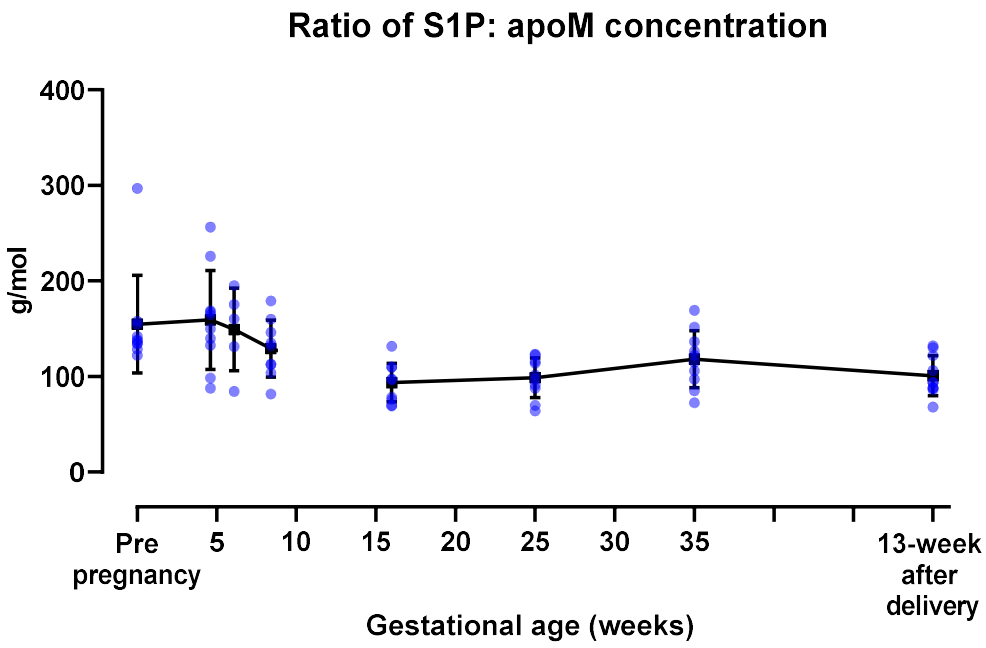

Figure 6-5 Ratio of S1P to apoM concentration in HDL at different gestations throughout pregnancy Data was expressed as mean±SD. Repeated measures ANOVA was carried out for the ratio (LIPS). The ratio (EPS) was log-transformed before analysis by repeated measures ANOVA. $p<0.05$ was taken as statistically significant.

6.3.3 Ceramide concentration in HDL samples at different gestations in healthy pregnancy

Ceramide C14:0 concentration in HDL did not change from pre-pregnancy to 8.4 weeks of gestation and from 16 to 35 weeks of gestation. It then decreased after delivery compared to the concentration at 16, 25 and 35 weeks of gestation (Figure 6-6). After correction for apoA-I concentration, ceramide C14:0 concentration in HDL did not significantly differ throughout the gestation from pre- to post-partum (Figure 6-6). However, correction with cholesterol concentration revealed an elevation of ceramide C14:0 concentration at 8.4 weeks of gestation compared to the concentration at 4.6 weeks of gestation and a decrease at 13-week after delivery compared to concentrations at 16 and 25 weeks of gestation (Figure 6-6). On the other hand, HDL ceramide C16:0 concentration either uncorrected, corrected for apoA-I or cholesterol concentration showed no significant alteration across gestation (Figure 6-7).

HDL ceramide C18:0 concentration remained stable in the first trimester and then rose at 25 and 35 weeks of gestation compared to those at 15 weeks of gestation. Thereafter, it dropped at 13-week postpartum compared to those at

25 and 35 weeks of gestation (Figure 6-8). Correction for apoA-I concentration revealed only an increase of HDL ceramide C18:0 concentration at 25 and 35 weeks of gestation, while correction for cholesterol concentration showed an increase at 35 weeks of gestation and a decrease after delivery (Figure 6-8).

Similar to shorter-chain ceramides, ceramide C20:0 concentration in HDL showed no significant difference in the first trimester. It increased at 35 weeks of gestation compared to 16 weeks of gestation and decreased after delivery compared to those at 35 weeks of gestation. Correction for apoA-I or cholesterol concentration revealed the same pattern of elevated ceramide C20:0 concentration in HDL at 35 weeks of gestation. However, only HDL ceramide C20:0 concentration corrected with apoA-I concentration increased after delivery compared to those at 16 weeks of gestation (Figure 6-9).

HDL ceramide C22:0 concentration (uncorrected, correct for apoA-I and corrected for cholesterol) rose at 35 weeks of gestation compared to 16 weeks of gestation. Corrected ceramide C22:0 concentration for apoA-I and cholesterol also increased at postpartum compared to those at 16 and 25 weeks of gestation (Figure 6-10).

Ceramide C24:0 concentration in HDL (uncorrected, correct for apoA-I and corrected for cholesterol) demonstrated elevations at 13-week after delivery compared to those at 16 weeks of gestation (Figure 6-11). HDL ceramide C24:1 concentration, both uncorrected and after correction for apoA-I, rose at 35 weeks of gestation and at postpartum, while HDL ceramide C24:1 corrected for cholesterol concentration only showed an increase after delivery (Figure 6-12).

The ratio of ceramide C24:0 to ceramide C16:0 increased at 35 weeks of gestation and 13-week postpartum compared to the ratio at 15 weeks of gestation (Figure 6-13). To determine the comparability between the two cohorts: EPS and LIPS, pre-pregnancy EPS data and post-partum LIPS data were also compared. There were no significant differences in HDL ceramide C14:0, C16:0, C18:0, C20:0, C22:0, C24:0 and C24:1 concentrations, either as absolute concentration or corrected for apoA-I and for cholesterol concentration, between pre- and post-pregnant timepoints, except for uncorrected ceramide C14:0 and C16:0 concentration. Ceramide C14:0 and C16:0 concentrations in HDL

prior to pregnancy (8.9±2.1 and 29.1±8.8 ng/mL, respectively) were significantly higher than those after delivery (6.2±1.3 and 20.6±6.4 ng/mL, respectively) with p=0.004 and 0.026, respectively.

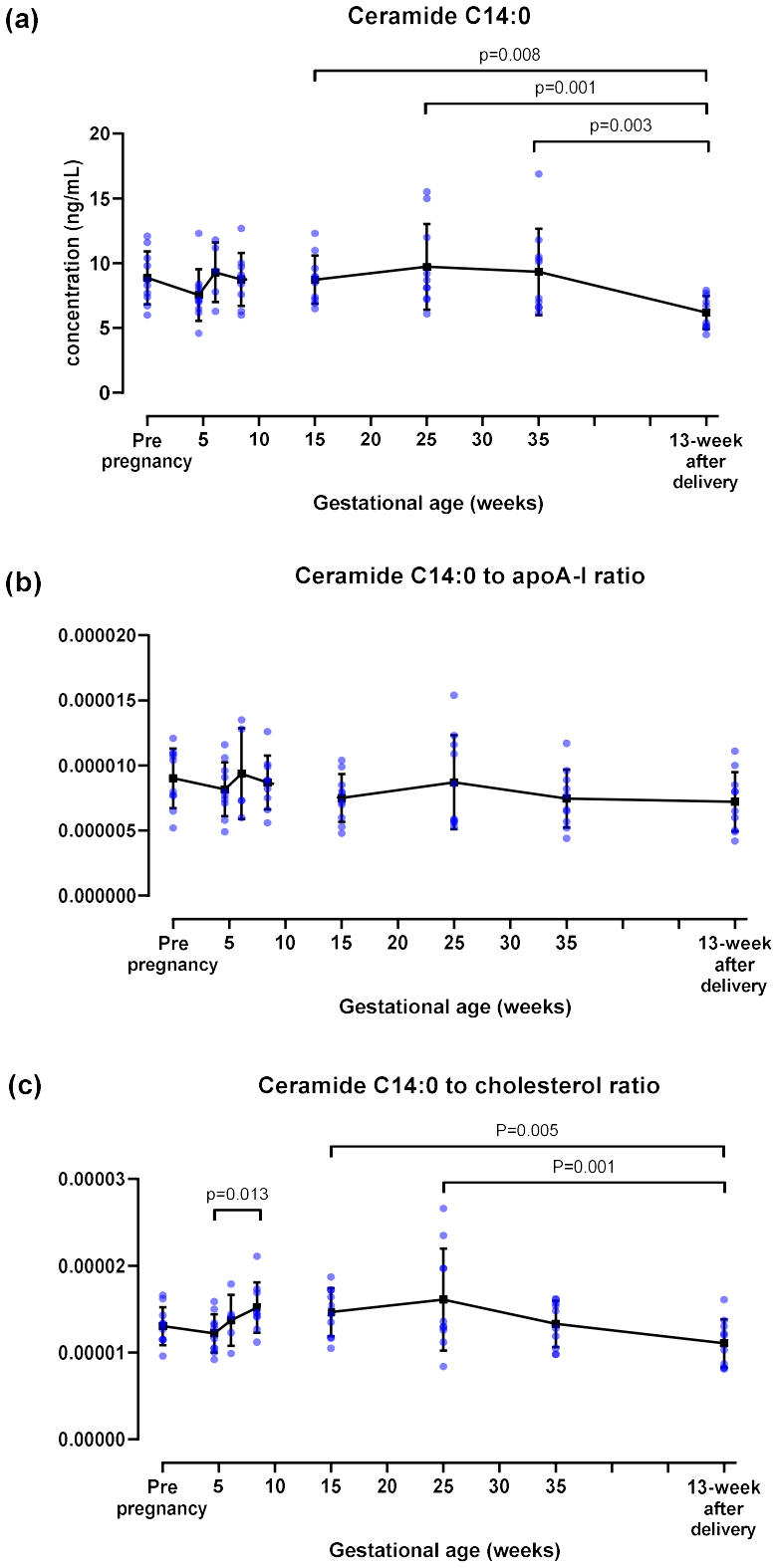

Figure 6-6 Ceramide C14:0 concentration [uncorrected (a), corrected for apoA-I concentration (b) and corrected for cholesterol concentration (c)] in HDL at different gestation throughout pregnancy Data was expressed as mean±SD. Repeated measures ANOVA followed by Tukey's test was carried out for EPS data of ceramide C14:0 concentration (uncorrected, corrected for apoA-I concentration and corrected for cholesterol concentration). LIPS data of ceramide C14:0 concentration (uncorrected, corrected for apoA-I concentration and corrected for cholesterol concentration) were log-transformed before analysis by repeated measures ANOVA followed by Tukey's test. $p<0.05$ was taken as statistically significant.

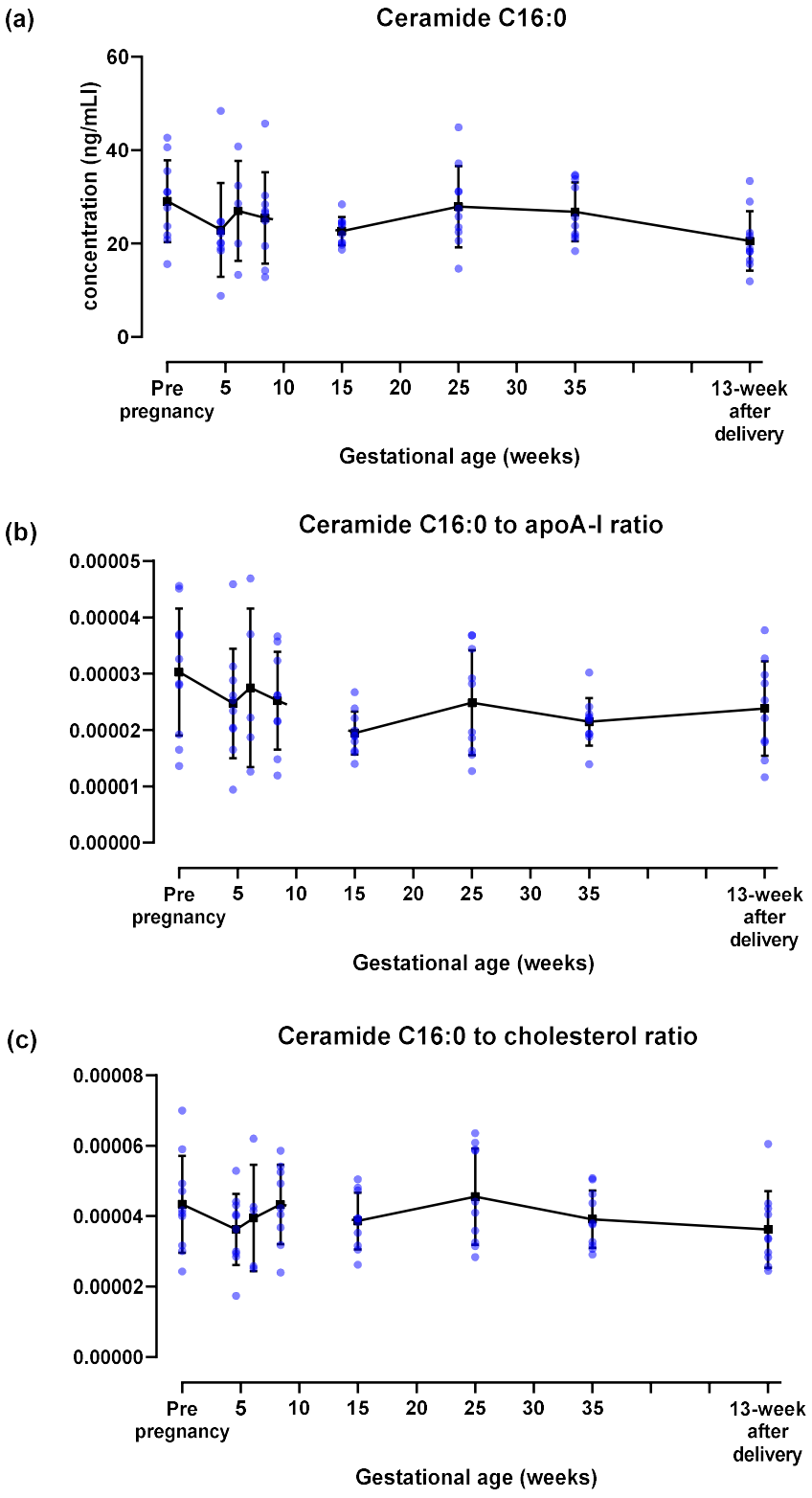

Figure 6-7 Ceramide C16:0 concentration [uncorrected (a), corrected for apoA-I concentration (b) and corrected for cholesterol concentration (c)] in HDL at different gestation throughout pregnancy Data was expressed as mean±SD. Repeated measures ANOVA followed by Tukey's test was carried out for ceramide C16:0 concentration (both EPS and LIPS), ceramide C16:0 concentration corrected for apoA-I (both EPS and LIPS) and ceramide C16 concentration corrected for cholesterol (EPS). Ceramide C16:0 concentration corrected for cholesterol (LIPS) was log-transformed before analysed by repeated measures ANOVA followed by Tukey's test. $p<0.05$ was taken as statistically significant.

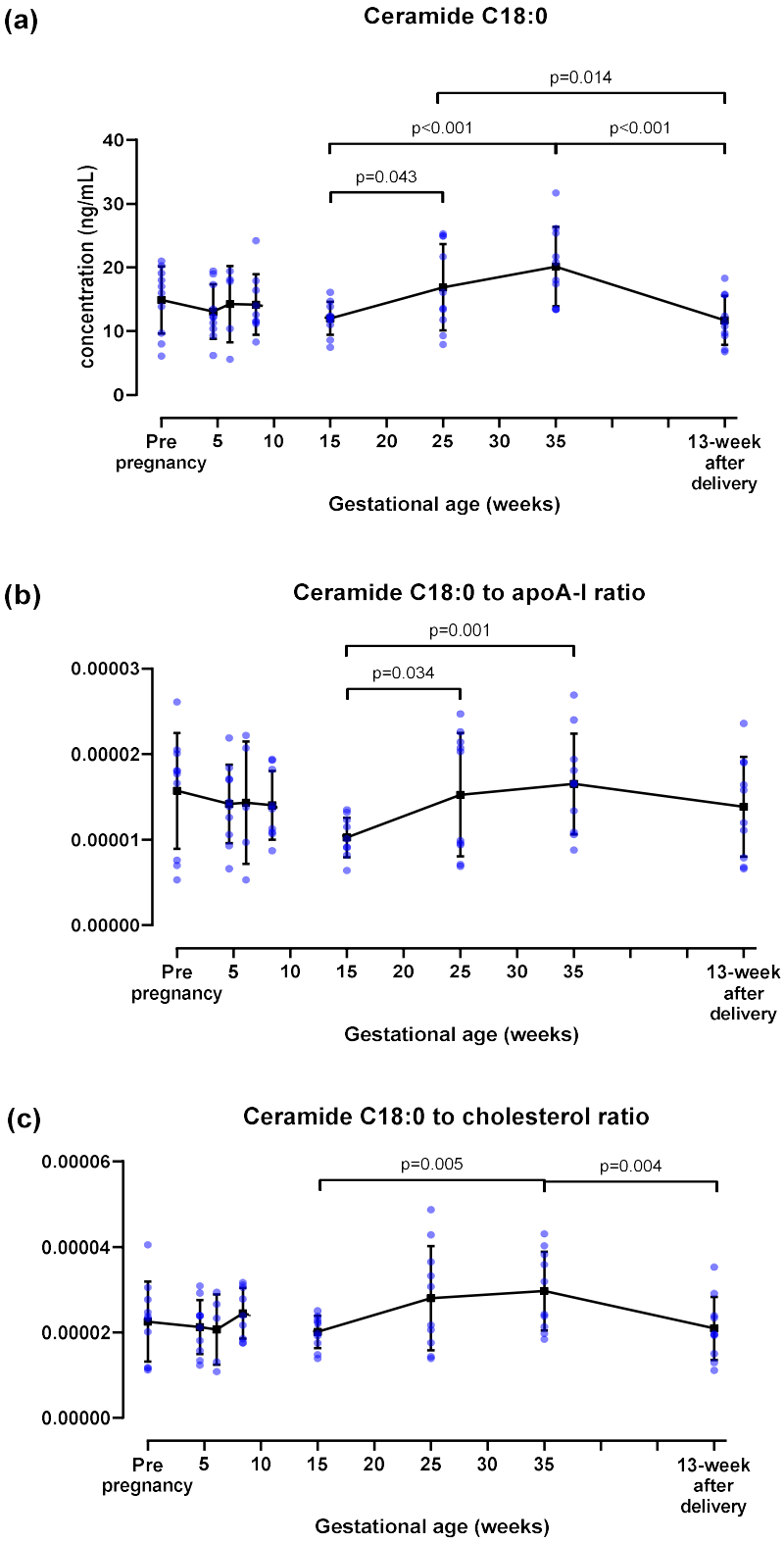

Figure 6-8 Ceramide C18:0 concentration [uncorrected (a), corrected for apoA-I concentration (b) and corrected for cholesterol concentration (c)] in HDL at different gestation throughout pregnancy Data was expressed as mean±SD. Repeated measures ANOVA followed by Tukey's test was carried out for EPS data of ceramide C18:0 concentration (uncorrected, corrected for apoA-I concentration and corrected for cholesterol concentration). LIPS data for ceramide C18:0 concentration (uncorrected, corrected for apoA-I concentration and corrected for cholesterol concentration) were log-transformed before analysis by repeated measures ANOVA followed by Tukey's test. $p<0.05$ was taken as statistically significant.

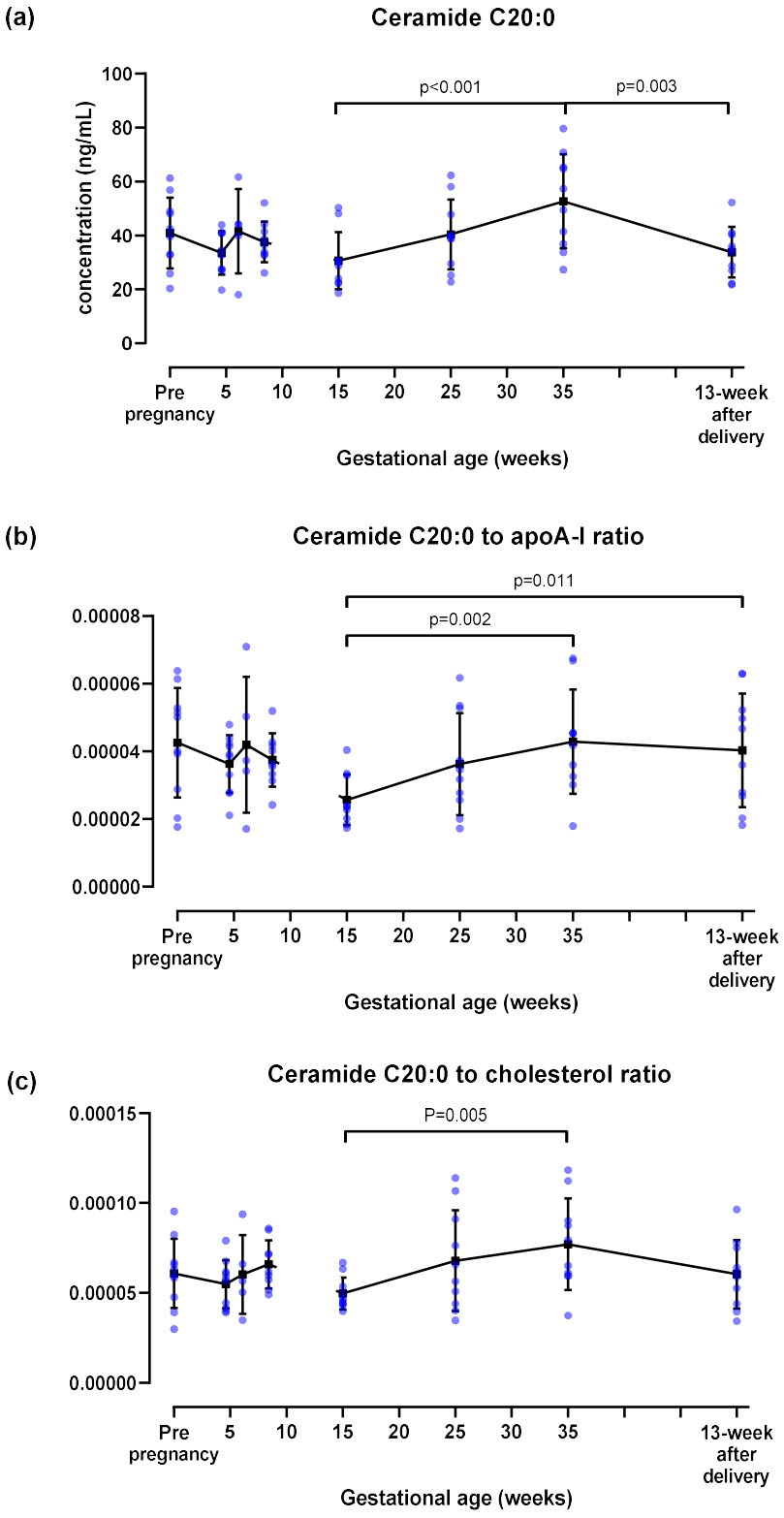

Figure 6-9 Ceramide C20:0 concentration [uncorrected (a), corrected for apoA-I concentration (b) and corrected for cholesterol concentration (c)] in HDL at different gestation throughout pregnancy Data was expressed as mean±SD. Repeated measures ANOVA followed by Tukey's test was carried out in EPS data of ceramide C20:0 concentration (uncorrected, corrected for apoA-I concentration and corrected for cholesterol concentration). LIPS data for ceramide C20:0 concentration (uncorrected, corrected for apoA-I concentration and corrected for cholesterol concentration) were log-transformed before analysis by repeated measures ANOVA followed by Tukey's test. $p<0.05$ was taken as statistically significant.

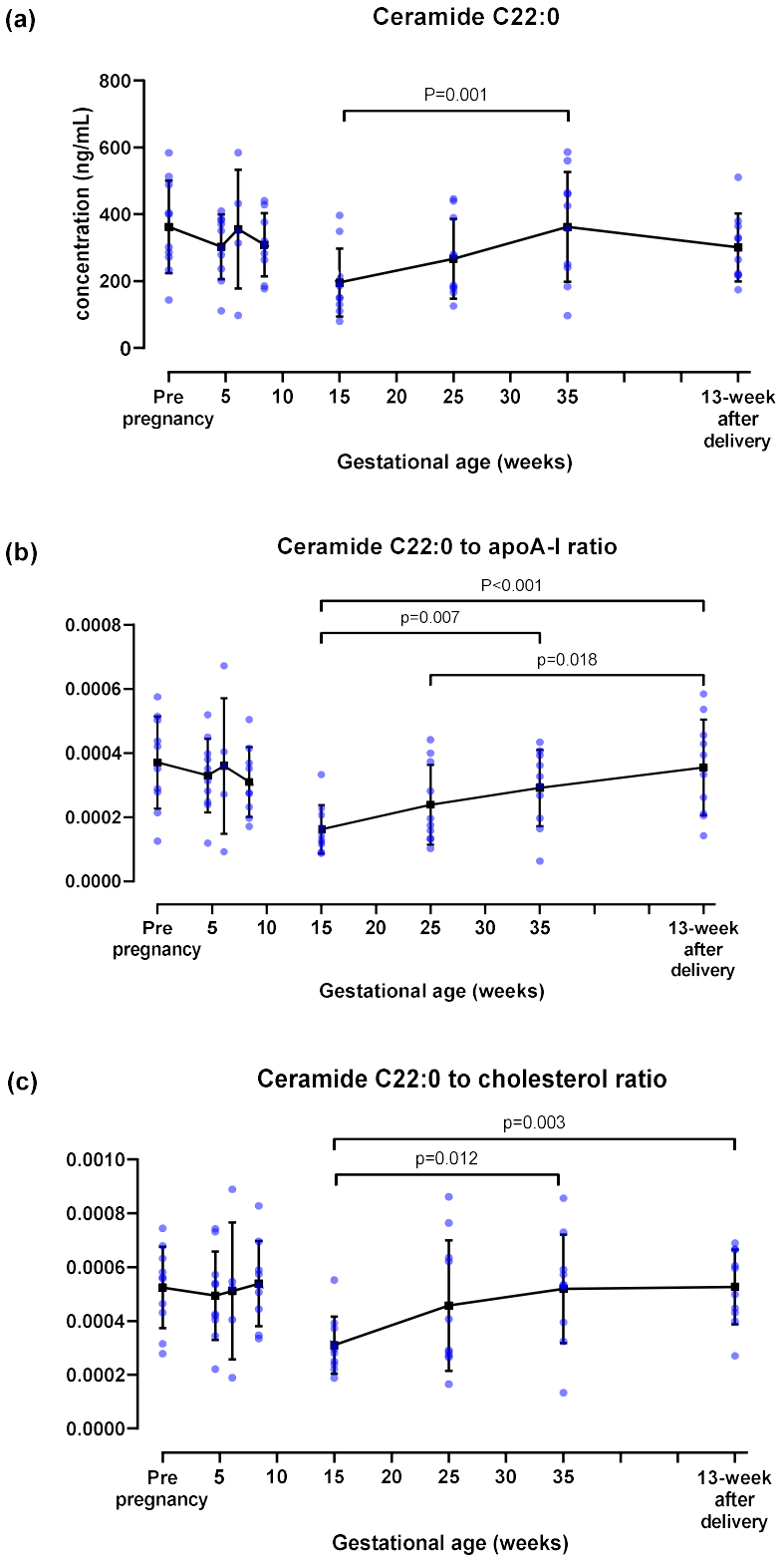

Figure 6-10 Ceramide C22:0 concentration [uncorrected (a), corrected for apoA-I concentration (b) and corrected for cholesterol concentration (c)] in HDL at different gestation throughout pregnancy Data was expressed as mean±SD. Repeated measures ANOVA followed by Tukey's test was carried out for ceramide C22:0 concentration (both EPS and LIPS), ceramide C22:0 concentration corrected for apoA-I (both EPS and LIPS) and ceramide C22:0 concentration corrected for cholesterol (EPS). Ceramide C22:0 concentration corrected for cholesterol (LIPS) was log-transformed before analysis by repeated measures ANOVA followed by Tukey's test. $p<0.05$ was taken as statistically significant.

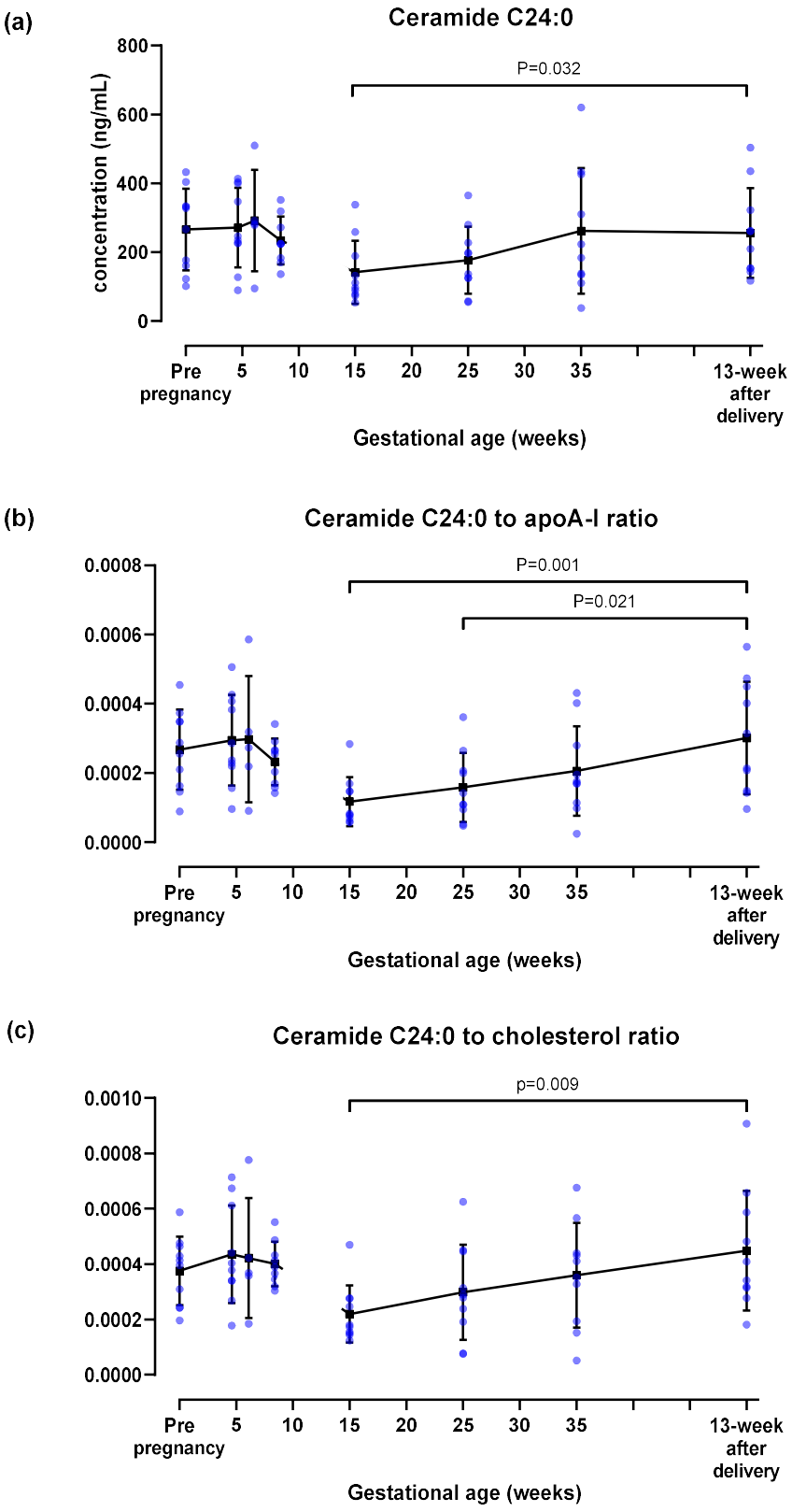

Figure 6-11 Ceramide C24:0 concentration [uncorrected (a), corrected for apoA-I concentration (b) and corrected for cholesterol concentration (c)] in HDL at different gestation throughout pregnancy Data was expressed as mean±SD. Repeated measures ANOVA followed by Tukey's test was carried out in EPS data of ceramide C24:0 concentration (uncorrected, corrected for apoA-I concentration and corrected for cholesterol concentration). LIPS data of ceramide C24:0 concentration (uncorrected, corrected for apoA-I concentration and corrected for cholesterol concentration) were log-transformed before analysis by repeated measures ANOVA followed by Tukey's test. $p<0.05$ was taken as statistically significant.

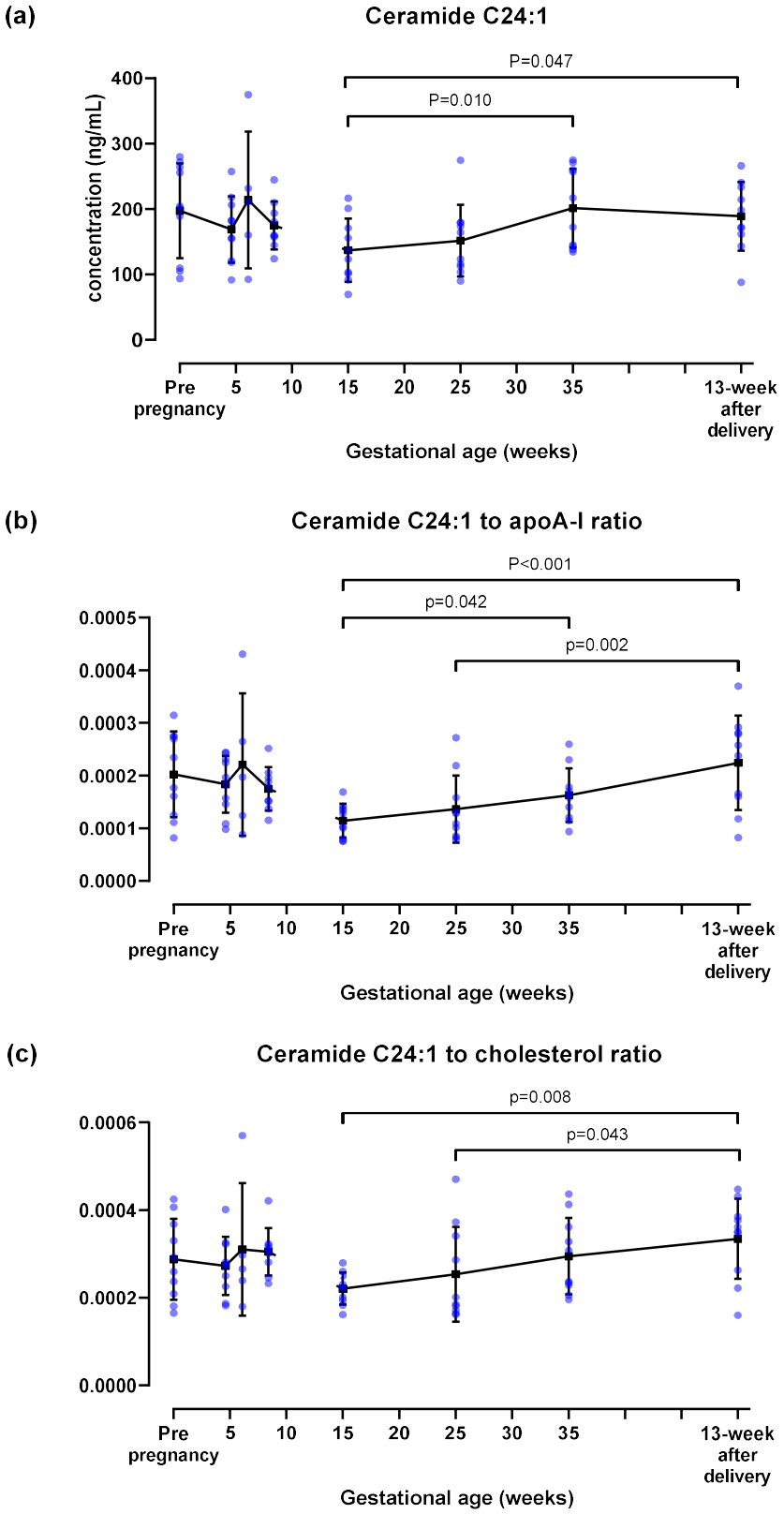

Figure 6-12 Ceramide C24:1 concentration [uncorrected (a), corrected for apoA-I concentration (b) and corrected for cholesterol concentration (c)] in HDL at different gestation throughout pregnancy Data was expressed in mean±SD. Repeated measured ANOVA was carried out in ceramide C24:1 concentration (both EPS and LIPS) and ceramide C24:1 concentration corrected for apoA-I (EPS). Ceramide C24:1 concentration corrected for apoA-I (LIPS) and ceramide C16 concentration corrected for cholesterol (both EPS and LIPS) were log-transformed before analysed by repeated measured ANOVA. $p<0.05$ was taken as statistically significant.

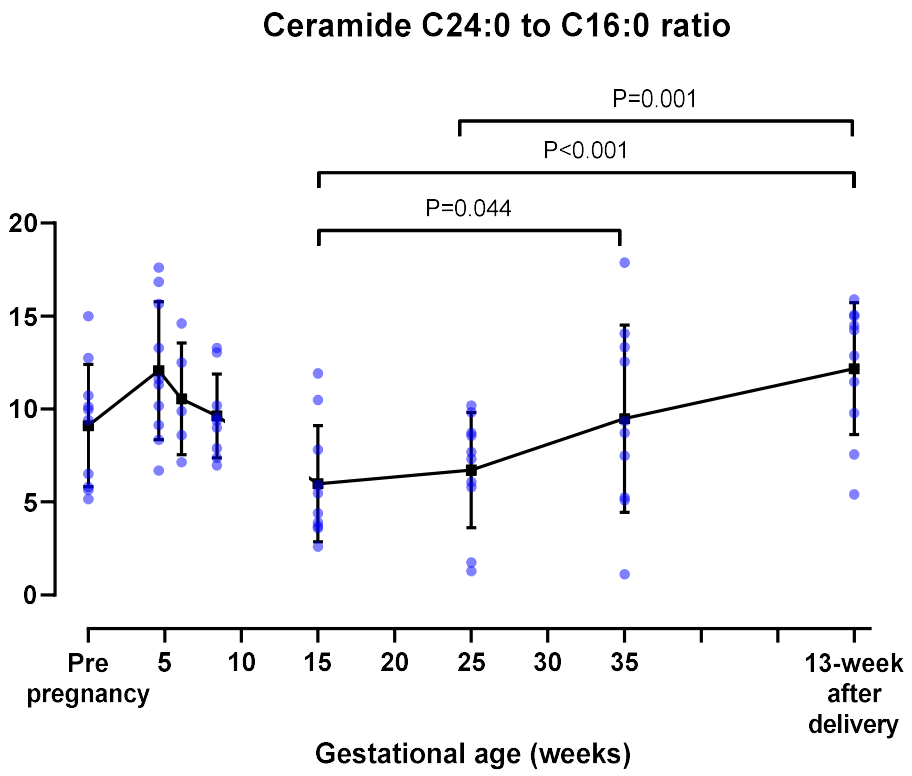

Figure 6-13 Ratio of ceramide C24:0 to ceramide C16:0 concentration in HDL at different gestation throughout pregnancy Data was expressed as mean±SD. Repeated measures ANOVA followed by Tukey's test was carried out to compare the ratio at different timepoints. $p<0.05$ was taken as statistically significant.

6.3.4 General characteristics of SAT donors

There was no significant difference of age, smoking status, systolic and diastolic blood pressure between healthy pregnancy and non-pregnant women (Table 6.3). Mean BMI of healthy pregnant women was significantly higher than those of non-pregnant women (Table 6.3).

Table 6.3 Demographics of SAT donors

	Healthy pregnancy (n=10)	Non-pregnancy (n=10)	p
Age	32.0 (3.0)	35.7 (7.7)	0.19
BMI	30.7 (3.8)	26.6 (4.3)	0.044
Non-smoker	10 (100%)	7 (70%)	0.090
Systolic blood pressure (mmHg)	118.3 (8.8)	122.7 (12.6)	0.43
Diastolic blood pressure (mmHg)	72.8 (6.5)	76.6 (9.0)	0.35
Gestational age at delivery (days)	277.1 (5.3)	-	-
Mode of delivery: caesarean section	10 (100%)	-	-
Male fetus	4 (44.4%)	-	-

Note: Data was expressed as mean (SD). Significant level $p<0.05$.

6.3.5 Sphingolipid synthesis enzyme gene expression in SAT of healthy pregnant and non-pregnant women

The expression of ceramide synthesis enzyme genes: S*TPLC1*, *SMPD1* and *SMPD4* in SAT was significantly lower in pregnancy, compared to non-pregnant women. While *SMPD3* and *ENPP7* expression in SAT showed no significant difference between these two groups (Figure 6-14).

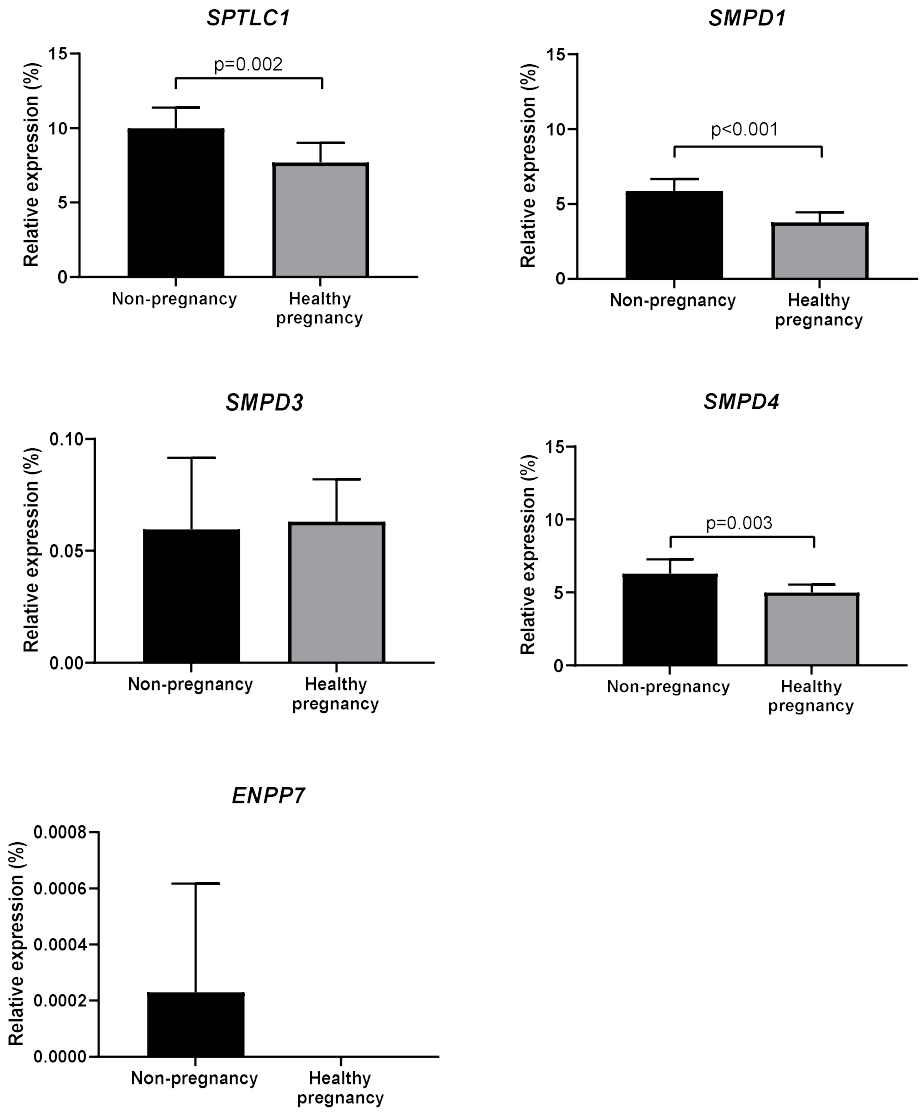

Figure 6-14 Relative expression of *STPLC1, SMPD1, SMPD3*, *SMPD4* and *ENPP7* expression ($2^{-\Delta CT}$) between SAT from pregnant (n=10) and non-pregnant women (n=10) Data was expressed as mean±SD. Unpaired t test was carried out on relative expression of *SPTLC1, SMPD1*, *SMPD3* and *SMPD4.* Mann-Whitney test was carried out in *ENPP7* data. p<0.05 was taken as statistically significant.

6.3.6 General characteristics of placenta donors

Placenta were obtained from healthy pregnancy (n=68), IUGR (n=10) and preeclampsia (n=23) subjects. The mean age, BMI, percentage of primiparous, smoking status, mode of delivery and fetal sex were not significantly different among the groups (Table 6.4). Systolic and diastolic blood pressure were higher in the preeclampsia group, compared to the healthy pregnancy and IUGR groups. Gestational age at delivery and birth weight centile were lower in preeclampsia and IUGR, compared to healthy pregnancy.

Table 6.4 Demographics of placenta donors

	Healthy pregnancy (n=68)	IUGR (n=10)	Preeclampsia (n=23)	p
Age	30.4 (5.1)	29.7 (4.9)	29.5 (5.8)	0.83
BMI	28.9 (6.4)	24.7 (5.5)	30.1 (7.4)	0.068
Primiparous	27 (40%)	4 (40%)	14 (61%)	0.20
Non-smoker	54 (79%)	5 (50%)	19 (83%)	0.10
Systolic blood pressure (mmHg)	121 (15)[a]	113 (4)[a]	144 (25)[b]	<0.001
Diastolic blood pressure (mmHg)	71 (10)[a]	72 (3)[a,b]	91 (16)[b]	<0.001
Gestational age at delivery (days)	275 (9)[a]	253 (21)[b]	253 (21)[b]	<0.001
Mode of delivery: Caesarean section	54 (79.4%)	9 (90%)	17 (73.9%)	0.55
Birth weight centile	55 (31)[a]	1 (2)[b]	22 (26)[b]	<0.001
Male fetus	32 (49%)	3 (33%)	13 (57%)	0.50

Note: Data was expressed as mean (SD). Different superscript letters indicate differences between individual groups. Significant level $p<0.05$.

6.3.7 Sphingolipid synthesis enzymes gene expression in placenta of healthy pregnancy, IUGR and preeclampsia

STPLC, *SMPD1, SMPD3, SMPD4, ENPP7, SGMS1, SGMS2, CERS1* and *CERS4* placental gene expression did not demonstrate any significant difference between preeclampsia, IUGR and healthy pregnancy (Figure 6-15). Only *CERS6* placental expression was significantly reduced in IUGR, compared to healthy pregnant women. However, there was no difference in CERS6 placental expression between preeclampsia and healthy pregnancy or IUGR. (Figure 6-15).

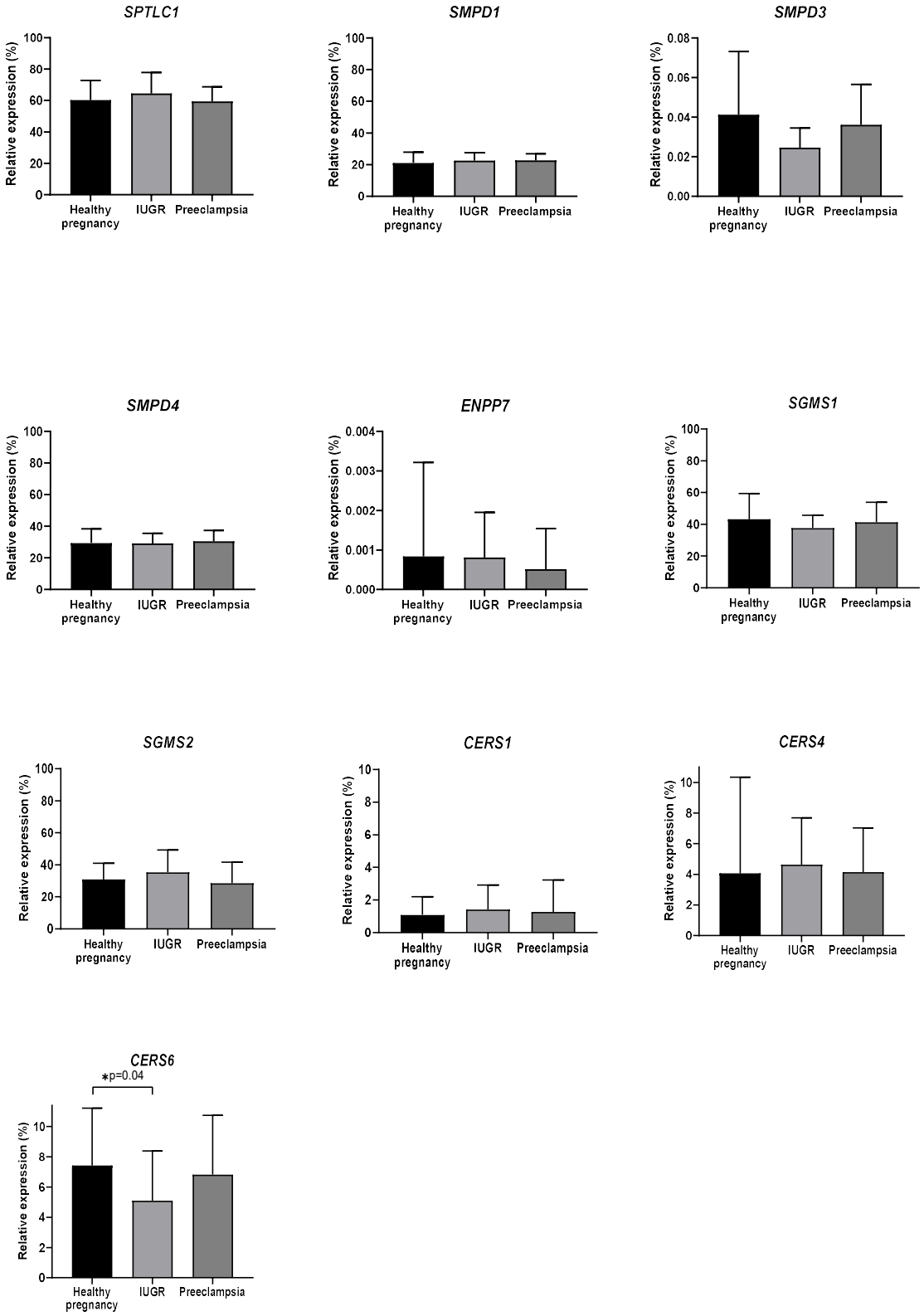

Figure 6-15 Relative expression ($2^{-\Delta Ct}$) of *STPLC1, SMPD1, SMPD3*, *SMPD4, ENPP7, SGMS1, SGMS2, CERS1, CERS4* and *CERS6* among placentae from healthy pregnancy (n=68), IUGR (n=10) and preeclampsia (n=23) Data was expressed as mean±SD. One-way ANOVA was carried out in log-transformed data of *SPTLC1* and non-transformed data of *SMPD1*. Kruskal-Wallis test followed by Dunn's test was carried out in *SMPD3*, *SMPD4, ENPP7, SGMS1, SGMS2, CERS1, CERS4 and CERS6* data. $p<0.05$ was taken as statistically significant.

The $2^{-\Delta\Delta CT}$ values of placentae from healthy pregnancy, IUGR and preeclampsia were compared and revealed no significant difference of *SPTLC1, SMPD1, SMPD3* and *SMPD4* expression among placentae from healthy pregnancy, IUGR and preeclampsia (Figure 6-16). This result of placental STPLC, SMPD1, SMPD3 and SMPD4 expression from $2^{-\Delta\Delta CT}$, which represents the fold change of target gene expression normalised to an endogenous reference gene and relative to the QC sample, was similar to the result from $2^{-\Delta CT}$, which represents the fold change of target gene expression relative to the endogenous reference gene only, with no significant difference among healthy pregnancy, IUGR and preeclampsia. This finding suggests no impact of the inter-plate variation to gene expression comparison outcome.

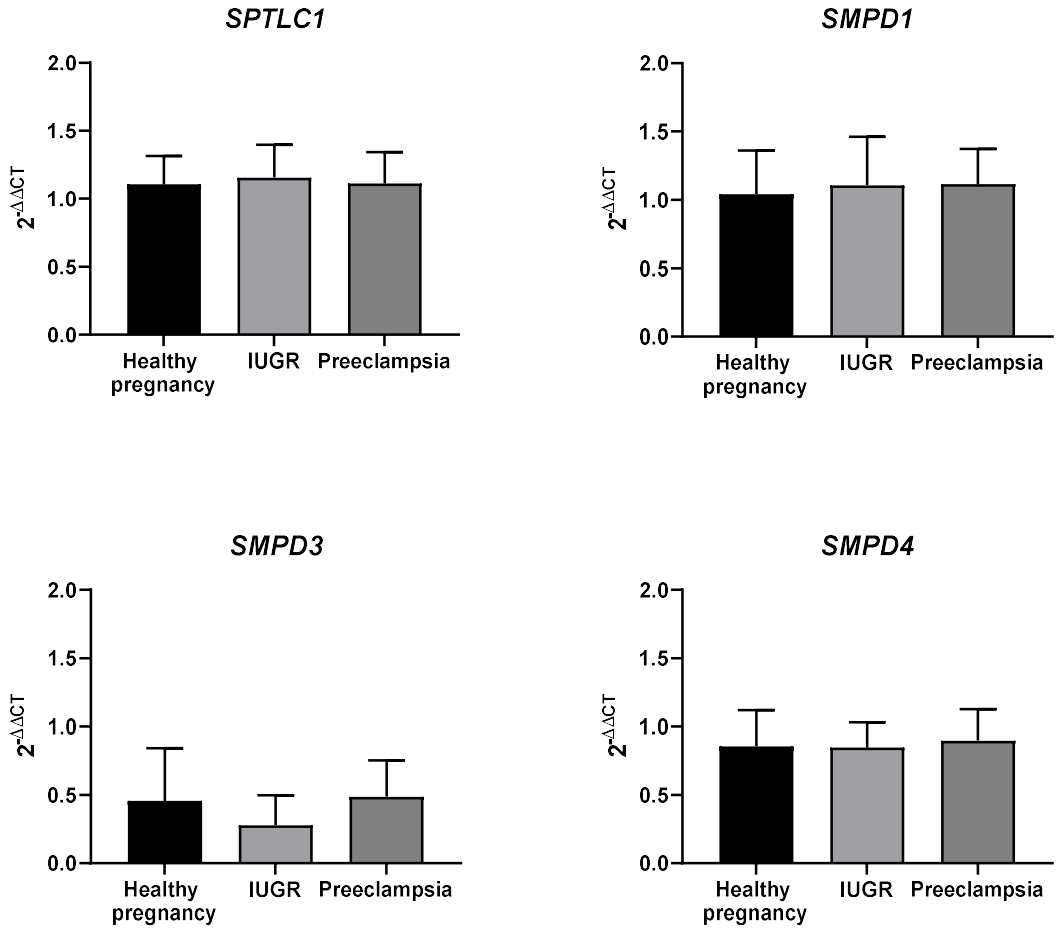

Figure 6-16 The fold change of *STPLC1, SMPD1, SMPD3* and *SMPD4* expression relative to the QC sample ($2^{-\Delta\Delta Ct}$) among placentae from healthy pregnancy (n=68), IUGR (n=10) and preeclampsia (n=23) Data was expressed as mean±SD. One-way ANOVA was carried out in log-transformed data of *SPTLC1* and non-transformed data of *SMPD1*. Kruskal-Wallis test was carried out in *SMPD3* and *SMPD4* data. $p<0.05$ was taken as statistically significant.

The intra-assay CV of ΔC_T of the QC sample across 15 plates of qRT-PCR for *SPTLC1, SMPD1, SMPD3, SMPD4* and *TOP1* were 0.61%, 0.74%, 6.65%, 0.35% and 0.34%, respectively (Table 6.5). The CV was all less than 10% which shows an acceptable variation between plates of qRT-PCR experiment.

Table 6.5 Descriptive statistics of ΔC_T of the QC sample across 15 plates of qRT-PCR

	STPLC1	*SMPD1*	*SMPD3*	*SMPD4*	*TOP1*
Mean	25.80	27.23	34.56	26.46	24.93
%CV	0.61	0.74	6.65	0.35	0.34
SD	0.16	0.20	2.30	0.09	0.09

6.4 Discussion

In this chapter, sphingolipid composition in HDL was measured throughout pregnancy. There was a decrease in HDL-S1P concentration in the first trimester and an increase in the third trimester to a level higher than that postpartum by 35 weeks of gestation. S1P has been shown to promote anti-inflammatory function of HDL in which it promotes HDL-induced inhibition of the TNF-α induced VCAM-1 expression (Kimura et al. 2006). S1P can also induce vasodilatory properties of HDL by eNOS activation and enhancing COX-2 and PGI-2 production (Nofer et al. 2004; González-Díez et al. 2008). Thus, anti-inflammatory and vasodilatory function of HDL-S1P may decrease during the first trimester but increase in the third trimester. Decreased S1P concentration in the first trimester may be due to the observed decrease in HDL apoM concentration which is a carrier of S1P on HDL, as well as an apoM property in promoting S1P efflux from erythrocytes (Christensen et al. 2017). Also, apoM is required for S1P-mediated inhibition of the TNF-α induced VCAM-1 expression (Galvani et al. 2015). Therefore, the anti-inflammatory function of HDL-S1P could decrease during the first trimester as we found reduced S1P and apoM concentration in HDL during the first trimester. This suggests that HDL S1P may not be important in early pregnancy and that there is no additional importance during early pregnancy to that seen in the non-pregnant state. Low HDL S1P in early gestation could be because S1P has been transported to the placenta and endometrium where S1P is involved in decidualization, EVT migration and spiral

artery remodelling as discussed in section 1.5.3, Chapter 1. It may be more important to have S1P at the site of decidualization and placentation than to be in circulating HDL to improve vascular function in early pregnancy. On the other hand, as S1P concentration increases in HDL during the third trimester, HDL-S1P may help maintain maternal vascular function by its anti-inflammatory and vasodilatory functions in the third trimester.

HDL S1P to apoA-I concentration showed a similar pattern to the uncorrected data suggesting that the change of S1P concentration in HDL was not only due to changes in HDL levels but also to S1P concentration per HDL particle (assuming apoA-I is a marker of HDL particle number). Interestingly, HDL-S1P concentration per unit cholesterol in this HDL sample remained stable throughout gestation. Increased HDL S1P in the third trimester may be counteracted by increased HDL cholesterol due to enhanced RCT to counter increased cholesterol availability (Fuenzalida et al. 2020; Stefulj et al. 2009). The magnitude of increased S1P in pregnancy was large enough to prevent a deficiency of S1P per unit HDL cholesterol. Another consideration in the interpretation of HDL S1P data is the lipid distribution in HDL subfractions, in addition to the lipid concentration in total HDL, which may affect HDL functionality. It was shown that patients with type 1 diabetes mellitus (T1DM) had similar plasma S1P and higher HDL cholesterol levels, but lower S1P/HDL-cholesterol ratio compared to controls (Frej et al. 2017). S1P was shown to shift toward low density (larger) HDL particles in T1DM patients and that lower density HDL particles were unable to inhibit TNF-α induced VCAM-1 expression in contrast to a significant inhibition by denser HDL particles with the same amount of S1P (Frej et al. 2017). Thus, it would be important to directly measure S1P content in HDL subfractions, HDL size distribution and HDL function in this sample to validate the relevance of changes in HDL S1P concentration in pregnancy.

With respect to ceramide, there were small changes in HDL ceramides between the first and second trimester but the major changes in HDL ceramide concentration happened during the third trimester and postpartum period. Only HDL ceramide C14:0 to cholesterol ratio increased during the first trimester and ceramide C18:0 (uncorrected and corrected for apoA-I) increased during the second trimester. Most of the HDL ceramide species (ceramide C18:0, C20:0,

C22:0, C24:1) increased at 35 weeks of gestation. This is consistent with the published observations where plasma ceramide concentrations (C16:0, C18:0 and C24:0) were continuously elevated throughout pregnancy (Dobierzewska et al. 2017). The role of ceramide in HDL has not been well established but ceramides may be involved in HDL function. Ceramide can promote RCT of HDL by promoting ABCA1 expression and interaction of apoA-I and ABCA1 which induces cellular cholesterol efflux. (Witting, Maiorano, and Davidson 2003; Ghering and Davidson 2006). Ceramides are also involved in HDL-induced eNOS activation. Treating CHO cells expressing SR-B1 with HDL resulted in increased intracellular ceramide concentration and eNOS activity (Li et al. 2002). Thus, increased HDL-ceramide concentration during pregnancy, particularly during the third trimester, may result in improved HDL functions such as RCT and vasodilatory effects. After delivery, different ceramide species changed in different directions. Ceramide C14:0, C18:0 and C20:0 decreased, while ceramide C22:0, C24:0 and C24:1 increased at 13 weeks after delivery. This finding represents a reciprocal relationship between long-chain ceramides (C16 and C18) and very-long-chain ceramides (C24). A study showed that the ratio of plasma ceramide C16:0 and C24:0 was markedly associated with cardiovascular incidence (Laaksonen et al. 2016). The presented data revealed a significantly higher ratio of HDL ceramide 24:0 to C16:0 during the third trimester and postpartum, thus may suggest a less association with cardiovascular pathology during the third trimester of pregnancy and postpartum. A study showed that ceramide C24:1 concentration in HDL of individuals with ischemic heart disease was significantly lower than in those without ischemic heart disease (Argraves et al. 2011).

In this chapter, sphingolipid synthesis gene expression in SAT of healthy pregnant women was also measured as a surrogate for sphingolipid expression in the liver, the potential source of HDL sphingolipids. Reduced expression of ceramide synthesis enzymes in both the *de novo* pathway (*SPTLC1*) and the sphingomyelin hydrolysis pathway (*SMPD1* and *SMPD4*) were found in SAT of pregnant women, suggesting lower level of ceramide accumulation in SAT of pregnant women. This finding is in contrast to plasma ceramide concentrations (C16:0, C18:0, C24:0) which continuously increase from the first trimester to third trimester (Dobierzewska et al. 2017) and our data that showed the increase of ceramide content (C14:0, C18:0, C20:0, C22:0, C24:0, C24:1) in HDL from the first

trimester to third trimester. Comparison of *SMPD3* and *ENPP7* expression in SAT from pregnant and non-pregnant women may be difficult due to their limited expression in SAT, especially *ENPP7* that had very low expression in SAT from non-pregnant and then was undetermined in SAT from pregnant women. The reduced expression of genes involved in generating ceramide might be expected to be associated with reduced ceramide generation in adipose tissue, however, expression of genes involved in ceramide catabolism such as ceramidase that convert ceramide to sphingosine and ceramide synthase that convert sphingosine back to ceramide have not been investigated. Also, synthesis enzyme activity and sphingolipid level in SAT have not been measured in this study. The turnover rate of sphingolipid synthesis, synthesis enzyme level and activity, and sphingolipid accumulation in adipose tissue cannot be predicted from our result. There was down-regulated sphingolipid synthesis gene expression in SAT of pregnant women, but the turnover rate, synthesis enzyme level and activity as well as sphingolipid level may decrease, stay the same or increase. SAT is not necessarily a good surrogate for the liver. It is still undetermined whether the liver or potential erythrocyte/plasma lipids is the main source of the sphingolipid content in HDL of pregnant women or not. It should also be noted that participants from the pregnancy group showed higher BMI than those from non-pregnant women. There is no evidence on the association between BMI and these sphingolipid gene expressions in SAT, but BMI was found to be associated with SAT depth in pregnancy. Early pregnancy BMI was positively correlated with SAT depth measured by ultrasonography during the second trimester (Lindberger et al. 2021). It may be possible for the BMI balance to affect lipid synthesis gene expression, however *SPTLC1*, *SMPD1* and *SMPD4* expression was still significantly reduced in healthy pregnancy with BMI as a covariate in the analysis. Thus, reduction of *SPTLC1*, *SMPD1* and *SMPD4* expression was independent of BMI.

Lastly, sphingolipid synthesis gene expression in placentae from healthy, IUGR and preeclampsia pregnancies was measured to determine whether placental sphingolipid metabolism might be altered in preeclampsia and IUGR. Placental expression of sphingolipid synthesis enzymes for both *de novo* synthesis and sphingomyelin hydrolysis, excepted for *CERS6*, did not differ among healthy pregnancy, IUGR and preeclampsia. These data are consistent with a comparison of sphingolipid content where no significant difference in placental levels were

found between healthy pregnancy, IUGR and preeclampsia (Brown et al. 2016). However, it is in contrast to a report of higher placental ceramide accumulation (C16:0, C18:0, C20:0, C24:0) in early-onset preeclampsia (Melland-Smith et al. 2015). The lack of detection of a difference in the present study may be due to a heterogeneity of preeclampsia pathophysiology, especially between early-onset preeclampsia which leans toward placental dysfunction and late-onset preeclampsia which is mostly associated with normal placenta.

Only *CERS6* expression was significantly reduced in placenta from IUGR pregnancy compared to that of healthy pregnancy. CERS6 is an enzyme that specifically catalyses the generation of ceramide C14 and C16. The reduction of placental *CERS6* expression in IUGR may result in reduced ceramide C16 production in IUGR placenta. *CERS6* knockout mice challenged with a high-fat diet showed reduced ceramide C16:0 in white and brown adipose tissue, and liver and were protected from diet-induced obesity by increasing rate of energy expenditure (Turpin et al. 2014). These mice were also protected from macrophage infiltration and activation of proinflammatory gene expression in white adipose tissue and had improved glucose tolerance and insulin sensitivity (Turpin et al. 2014). Whereas overexpressing CERS6 in primary hepatocytes isolated from C57BL6/J mice resulted in increased ceramide C16 in liver, inhibited Akt/PKB activation, promoted triglyceride accumulation and impaired mitochondrial oxidation of fatty acids by inhibiting complex II of the electron transport chain (Raichur et al. 2014). These suggested cytotoxic effects of CER6 and ceramide C16 in various tissues such as adipose tissue inflammation and lipid accumulation and mitochondrial dysfunction in the liver. In placenta, treatment of primary cytotrophoblast cells and chorionic villous explants with ceramide C16 promoted cell apoptosis and necrosis (Melland-Smith et al. 2015; Bailey et al. 2017). Thus, our result of reduced placental *CERS6* expression may indicate reduced placental ceramide C16 levels and placental cell death. This is consistent with reduced maternal lipolysis and long-chain fatty acid flux in IUGR which could lead to inadequate lipid supply from the mother (Diderholm et al. 2006; Mackay et al. 2012). However, a lipidomic study of placenta from the same set of participants showed no significant differences in placental ceramide C14 and C16, and sphingomyelin SM14 and SM16 concentrations between IUGR and healthy pregnancy (Brown et al. 2016). Thus, aberrant sphingolipid

metabolism in placenta may not play a role in the mechanism of placental impairment in IUGR.

The strength of this study was that it was the longitudinal study of maternal HDL throughout pregnancy. Even though this study includes two longitudinal cohorts of pre-pregnancy to 8.4 weeks of gestation and 16 weeks of gestation to postpartum, participants from these two studies were matched with BMI, age, parity and smoking status. There was also no significant difference between pre-pregnancy and postpartum data of S1P and most of ceramide species in HDL, as well as HDL proteome, apoA-I modification (methionine oxidation and glycation), apoA-I, cholesterol and SAA1 concentration, and PON1 activity as shown in chapter 3. This suggests the comparability of these two groups of participants. The limitation of this study includes using SAT as a surrogate of the liver since liver biopsy is too invasive, especially in pregnant women. Another limitation is a lack of preeclampsia subgroup analysis between early- and late-onset preeclampsia which could avoid the confounding factor of the heterogenous pathophysiology of preeclampsia in term of placental pathology.

In summary, S1P and ceramide content in HDL increased throughout gestation of healthy pregnancy, particularly in the third trimester. The ratio of very-long-chain ceramides (C24:0) and long-chain ceramides (C16:0) also increased in the third trimester and postpartum. Potentially, this may indicate improved vascular protective function of HDL during pregnancy, especially in the third trimester and postpartum. Alteration of gene expression of sphingolipid synthetic enzymes in SAT favours reduced ceramide production in adipose tissue of pregnant women compared to non-pregnancy. However, ceramide turnover as well as sphingolipid content in SAT of pregnant women have not yet been investigated. SAT is a poor surrogate of the liver therefore it is still undetermined whether the liver is the main source of sphingolipid content in HDL of pregnant women or not. Lastly, placental gene expression of sphingolipid synthesis enzymes was not different between placenta of preeclampsia and healthy pregnancy. However, there was a study in early-onset preeclampsia that showed higher placental ceramide accumulation (C16:0, C18:0, C20:0, C24:0) (Melland-Smith et al. 2015). It is possible that the indifference in our result is due to the heterogenous pathophysiology of preeclampsia, especially between early-onset preeclampsia

which leans toward placental dysfunction and late-onset preeclampsia which is mostly associated with normal placenta. In the future, HDL function, especially vasodilatory, anti-inflammatory and RCT properties, should be investigated throughout gestation to validate the relevant of sphingolipid content of HDL in healthy pregnancy. Sphingolipid content in SAT of pregnant women should be investigated to confirm the result of sphingolipid synthesis gene expression in SAT and for a better understanding of sphingolipid metabolism in pregnancy. Finally, it would be useful to compare placental sphingolipid synthesis gene expression between early- and late-onset preeclampsia to avoid the confounding factor of the heterogenous pathophysiology of preeclampsia in term of placental pathology.

7 Development of an HDL and EV separation protocol

7.1 Introduction

HDL can be isolated by several techniques including immunoaffinity chromatography (immunosorption), size exclusion chromatography (SEC) and the gold standard, density ultracentrifugation (Collins and Olivier 2010; Collins et al. 2010). The immunosorption technique was applied to isolate HDL by capturing apoA-I-containing particle with antibodies specific to apoA-I immobilized on Sepharose beads (Cheung and Albers 1984; McVicar et al. 1984). ApoA-I is the major protein of HDL however, it is not specific to HDL particles. ApoA-I can appear in either VLDL, LDL or HDL as well as free form in plasma, so apoA-I-containing particles isolated by immunoaffinity chromatography will include not only HDL but also VLDL and LDL (Lepedda et al. 2013; Diffenderfer and Schaefer 2014). SEC can also be applied to isolate HDL from plasma based on particle size (Collins and Olivier 2010; Collins et al. 2010). However, any plasma proteins which have overlapping ranges of particle size with HDL can be co-isolated with HDL whether they are associated with the HDL particle or not.

The gold standard HDL isolation method is density ultracentrifugation (Hafiane and Genest 2015). The principle of density ultracentrifugation is to separate lipoprotein fractions from plasma based on particle density and can be categorized into gradient and sequential density ultracentrifugation. Gradient density ultracentrifugation is a technique of creating a density gradient by overlaying layers of different densities and separating lipoprotein with a single ultracentrifugation until the lipoprotein bands reach their isopycnic equilibrium (Chapman et al. 1981) and sequential density ultracentrifugation comprises of a sequence of ultracentrifugation steps to separate HDL from plasma and other lipoproteins (Henderson, Vaisar, and Hoofnagle 2016). Even though density ultracentrifugation is the gold standard technique for isolating HDL from plasma, HDL isolated by this technique may lose attached proteins due to high salt solution and centrifugal force. It can also be contaminated with other plasma particles with overlapping density range, for example, circulating EV which has the density of 1.08-1.21 g/mL which is in the range of 1.063-1.21 g/mL density of HDL (Figure 7-1). A study of plasma fractions isolated using density

ultracentrifugation at density range of 1.063-1.21 g/mL revealed that not only HDL particles with a diameter of around 10 nm, identified by transmission electron microscopy and the presence of apoA-I, were confirmed in this fraction, larger vesicular structures with a diameter of around 100 nm were also found (Yuana et al. 2014). These vesicles were most likely EV as they had the typical cup-shaped morphology of EV and an ability to bind to lactadherin and anti-CD61, both biological markers of EV particles (Yuana et al. 2014).

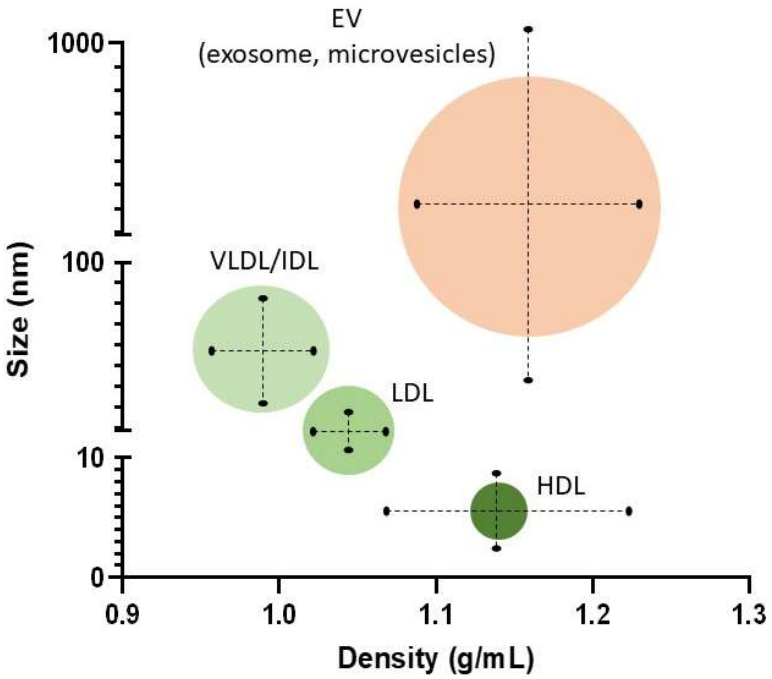

Figure 7-1 Particle size and density of HDL, LDL, VLDL/IDL and EV

EVs are spherical vesicles which have an outer lipid bilayer and contain nucleic acids and proteins originating from the source cell. EV released from normal cells can be categorized into exosomes (40-120 nm) and microvesicles (100 nm -1 µm). Exosomes are the most abundant EV and are formed by fusion of multivesicular bodies with the plasma membrane while microvesicles bud directly from plasma membrane and contain cytoplasmic cargo. Under specific conditions, cells can release different types of EVs such as apoptotic bodies (50 nm-2 µm) which are released from dying cells. Similar to HDL isolation methods, EV can be isolated based on their density using density centrifugation. However, EV isolated by this technique were found to be contaminated with HDL, which has an overlapping range of density, and LDL which showed possible interaction

with EV (Sódar et al. 2016). Another method to isolate EV is SEC which separates particles based on particle size. This method allows EV which are larger than HDL (Figure 7-1) to elute sooner from a size-based chromatography column, since larger particles cannot enter the gel and travel through a shorter distance in the column while smaller particles travel through the gel and elute later from the column. EV isolation by SEC with Sepharose CL-2B which has a pore size of 75 nm has been shown to remove around 95% of HDL and protein with 43% EV recovery (Böing et al. 2014). However, this study showed that all particles in the EV fraction were larger than 75 nm, thus smaller EV (<75 nm) which account for approximately 50% of all EV may have co-eluted with HDL in the later fractions of SEC (Böing et al. 2014). Lastly, EV can be isolated based on both density and size using differential centrifugation. The principle of this technique is to sequentially centrifuge at increasing speed to pellet cells, cell debris and then EV. Limitations of this method include co-isolation of non-EV components such as protein aggregates and increased possibility of EV clumping and EV damage from the ultracentrifugation step [reviewed in (Coumans et al. 2017)].

Not only are HDL and EV commonly co-isolated, but there is also a considerable number of common properties between HDL and EV regarding endothelial function protection. EV has shown several properties similar to HDL including anti-inflammatory, antioxidant and vasodilatory effects. EV derived from endothelial cells (EEV) were shown to inhibit TNF-α induced endothelial ICAM-1 expression by transferring miRNA-222 into endothelial cells, demonstrated in human coronary artery endothelial cell culture and apoE-deficient mice (Jansen et al. 2015). EEV can transfer miRNA-10a to monocytes and suppress NF-κB signalling and reduce proinflammatory gene expression, including TNF-α and IL-1ß, in monocytes (Njock et al. 2015). Moreover, EV derived from TNF-α stimulated HUVEC were shown to promote NO production, increase superoxide dismutase and suppress ROS production, thus protecting HUVEC from palmitate-induced oxidative stress (Mahmoud et al. 2017). There are also EV properties that are opposite to the functions of HDL. A study of EEV in an *in vitro* transwell migration assay and a cell adhesion assay of THP-1 monocytes to a HUVEC monolayer revealed that EEV can promote monocyte transmembrane migration and monocyte adhesion to endothelial cells (Hosseinkhani et al. 2018). Incubation of HUVEC with EEV resulted in increased endothelial MCP-1

expression (Hosseinkhani et al. 2018). Additionally, EV released from inflamed cells such as EV from TNF-α stimulated HUVEC and LPS-stimulated monocytes have been shown to up-regulate ICAM-1 expression and various pro-inflammatory cytokines and chemokines such as IL-6, IL-8 and MCP-1 in HUVEC culture (Hosseinkhani et al. 2018; Tang et al. 2016).

It is noteworthy that there are overlapping properties between HDL and EV in regard to protecting vascular function especially anti-inflammatory and anti-oxidative properties. There are also some common mechanisms underlying these properties such as enhanced NO production. Co-isolation of HDL and EV could interfere with outcomes of either HDL or EV functional studies, leading to misinterpretation of some biological effects being attributed to HDL or EV. Even though EV accounts for only 1% of total particles in the HDL fraction isolated by density ultracentrifugation, the diameter of EV is approximately 10-fold larger than HDL particle (Yuana et al. 2014). The total volume of EV could be much more than the total volume of HDL and could be a significant contamination in term of confounding each other's function and outcome of their functional studies. Therefore, isolation protocols of HDL and EV with reduced HDL or EV cross-contamination are required to establish specific properties to each entity.

In this chapter, a protocol to isolate HDL and EV separately from plasma was developed to remove potential EV contamination from HDL samples. A combination of SEC and density ultracentrifugation was applied for this protocol as illustrated in Figure 7-2. Firstly, plasma particles were separated by size using SEC similar to the EV isolation protocol in (Böing et al. 2014). Particle size and concentration, total protein concentration and apoA-I concentration were assayed in each fraction eluted from SEC to determine EV-rich and HDL-rich fractions. EV-rich fractions were pooled and collected as EV samples while HDL-rich fractions were pooled and further underwent a density ultracentrifugation to remove potential contamination of VLDL, IDL and LDL. HDL isolated from this protocol was labelled as EV-free HDL. HDL was also isolated from plasma of the same set of participants using density ultracentrifugation only and was labelled as HDL. Protein composition of EV, EV-free HDL and HDL obtained by nLC-MS/MS were compared to determine the difference in proteins that appear in EV and

EV-free HDL in comparison to proteins in HDL isolated by the gold standard with a potential EV contamination.

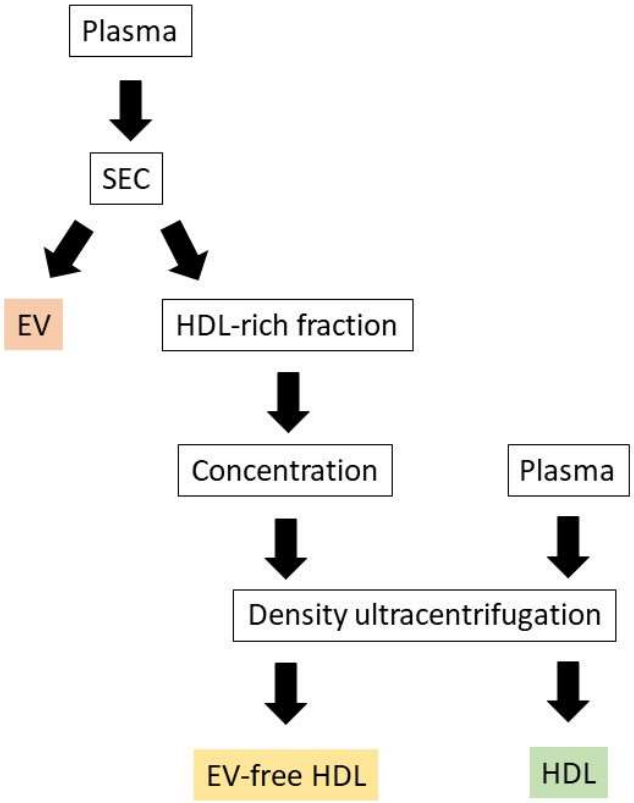

Figure 7-2 Flow chart of the isolation protocol of HDL, EV and EV-free HDL

7.1.1 Hypotheses

- There is co-isolation of EV particles when isolating HDL from plasma by sequential ultracentrifugation.

7.1.2 Objectives

- To establish a protocol to separately isolate EV and HDL from plasma.

7.2 Methodology

7.2.1 HDL and EV isolation protocol development

Plasma was obtained from an archival collection of pregnant women at 16 weeks of gestation according to section 2.1.1.2, chapter 2. Plasma samples (n=6) were

used in the first pilot study. the isolation protocol of HDL and EV from plasma included the combination of SEC and density ultracentrifugation as illustrated in Figure 7-2. Firstly, plasma particles were separated by size using SEC as described in section 7.2.1.1 of this chapter. Particle size and concentration, total protein concentration and apoA-I concentration were measured in each fraction eluted from the SEC column to determine EV-rich and HDL-rich fractions (section 7.2.1.2 of this chapter and section 2.4.1 and 2.4.3, chapter 2). EV-rich fractions were pooled and labelled as EV samples while HDL-rich fractions were pooled and concentrated to reduce the volume as described in section 7.2.1.3 of this chapter. The HDL-rich fraction then underwent a density ultracentrifugation to remove potential contamination of VLDL, IDL and LDL (section 7.2.1.4 of this chapter). HDL isolated from this protocol was labelled as EV-free HDL.

7.2.1.1 Size-exclusion chromatography (SEC)

The first step was to separate EV from lipoprotein particles by SEC similar to the protocol in (Böing et al. 2014). Size-exclusion chromatography was prepared by adding Sepharose CL-2B (14mL, Sigma-Aldrich CL2B300) into 10-mL polypropylene columns (Thermo Fisher Scientific, 29924) with a porous filter disc at the bottom and a bottom lid in place. This was left at room temperature for 30 minutes and then at 4 ºC for at least 48 hours to allow packing. After that, the prepared column was left at room temperature for 30 minutes before use. Another porous filter disc was placed on top of the Sepharose at the 10-ml mark on the column. The liquid inside the column was drained and washed with Dulbecco's phosphate buffered saline (10 mL, DPBS) (Thermo Fisher Scientific, 14190144). Columns were then ready to use.

Plasma (500 µL) was centrifuged at 2,000 g (5,200 rpm) for 30 minutes to pellet apoptotic bodies. The supernatant was transferred to another microcentrifuge tube and was then centrifuged again at 12,000 g (13,000 rpm) for 45 minutes to pellet microvesicles. After that, the supernatant was transferred to the prepared Sepharose column. The eluate was immediately collected in 25 fractions of 500 µL. Particle size and concentration (by nanoparticle tracking analysis described below in section 7.2.1.2), apoA-I (by a chemical analyser according to section 2.4.3, chapter 2) and total protein (by Bradford assay according to section 2.4.1, chapter 2) concentrations were measured in each fraction.

Each column was used 2-3 times. After each use, columns were washed with DPBS (10 mL), 0.5 M NaOH until the pH reached 14 and then DPBS until the pH decreased to 7. Columns were then ready to use for the next sample.

7.2.1.2 EV particle size and concentration measurement

EV particle size and concentration in each fraction from SEC was measured using nanoparticle tracking analysis on a NanoSight NS500 using NanoSight NTA v3 software. Each fraction was diluted with DPBS to 1:100 dilution and was added to the sample chamber where a laser beam passed through the sample. The camera was then set to capture two 30-second videos at camera settings: screen gain 1, camera setting 14 and process settings: screen gain 10, threshold 5. Particle size and concentration were then analysed from the video files using NanoSight NTA v3 software.

7.2.1.3 Fraction concentration

Amicon ultra-15 centrifugal filter units (100,000 molecular weight cut-off, Ultracel-100K, Sigma-Aldrich, UFC910096) were used to concentrate pooled fractions 14-23 from the SEC. Centrifugal filter columns were washed by adding DPBS (15 mL) followed by centrifugation at 4,000 g (4,400 rpm), 4 ºC for 10 minutes. The washing step was repeated using 0.1 M NaOH (15 mL) and PBS (15 mL) followed by centrifugation as before. Fractions 14-23 from the SEC were pooled and added to the centrifugal filter column. This was centrifuged at 4,000 g (4,400 rpm), 4 ºC until the volume of retained solution decreased to 500 µL (Figure 7-3). Retentate was collected for further HDL isolation.

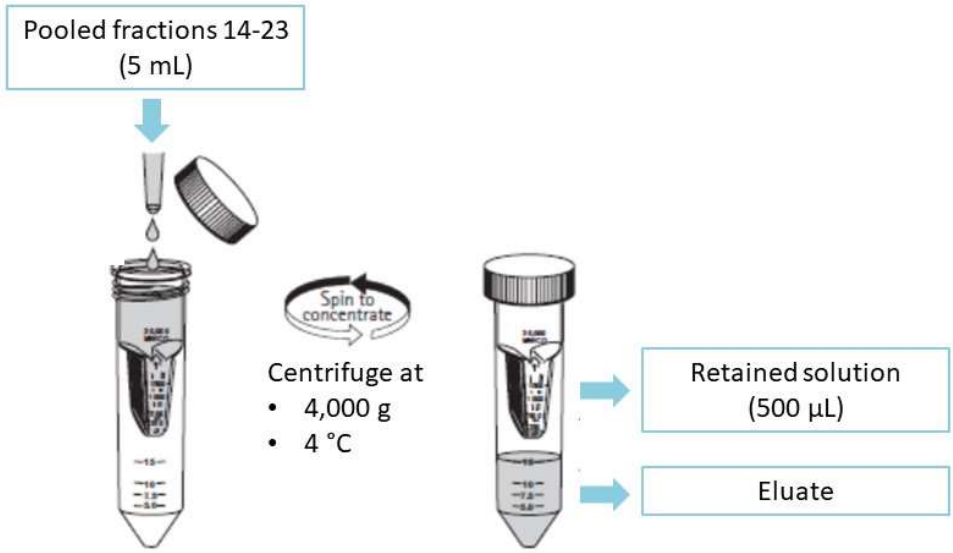

Figure 7-3 Pooled fractions 14-23 concentration protocol

To test whether there was any HDL or other lipoproteins eluted through the filter into the eluate, eluate from the first centrifugation was transferred from below the filter to above the filter in the same centrifugal filter column. This was centrifuged at 4,000 g (4,400 rpm), 4 ºC until the volume of retained solution decreased to 500 µL. Retained solution and eluate from both runs were assayed for apoA-I and apoB concentration (by a chemical analyser according to section 2.4.3, chapter 2).

7.2.1.4 Density ultracentrifugation

Concentrated fractions 14-23 then underwent a sequential density ultracentrifugation to isolate HDL. A single step and two-step density ultracentrifugation were performed. ApoA-I and apoB concentration were measured in HDL samples to determined which protocol of density ultracentrifugation provided higher HDL recovery and less VLDL/LDL contamination.

The single step density ultracentrifugation isolated all lipoproteins (VLDL, LDL and HDL) together at the final density of 1.006-1.21 g/mL. Concentrated fractions 14-23 (500 µL) were mixed with 1.478 g/mL density solution (385 µL) and overlaid with 1.21 g/mL density solution (115 µL). This was centrifuged at 100,000 rpm (435,680 g for maximum radius and 274,400 g for minimum radius), 23ºC for 5 hours. Supernatant (250 µL or 500 µL) was collected as total

lipoprotein fraction and infranatant was collected as lipoprotein-depleted fraction (LpDF).

The two-step density ultracentrifugation was used to remove VLDL/LDL from the solution before isolating HDL similar to HDL isolation protocol in section 2.3.2, chapter 2. Concentrated fractions 14-23 (500 µL) was mixed with 1.182 g/mL density solution (250 µL) and layered with 1.063 g/mL density solution (250 µL). This was centrifuged at 100,000 rpm (435,680 g for maximum radius and 274,400 g for minimum radius), 23ºC for 2.5 hours. The supernatant (500 µL) was collected as the VLDL and LDL fraction (density<1.063 g/mL). The infranatant was then mixed with 1.478 g/mL density solution (250 µL) and overlaid with 1.21 g/mL density solution (250 µL). This was centrifuged at 100,000 rpm (435,680 g for maximum radius and 274,400 g for minimum radius), 23ºC for 5 hours. The supernatant (500 µL) was collected as HDL (density 1.063-1.21 g/mL).

All lipoprotein fractions were desalted according to section 2.3.3, chapter 2 using PD MiniTrap G-25 columns (spin protocol). ApoA-I and apoB concentrations were measured in HDL samples according to section 2.4.3, chapter 2.

7.2.2 Comparison of EV, EV-free HDL and HDL protein composition

Plasma was obtained from an archival collection of pregnant women at 16 weeks of gestation according to section 2.1.1.2, chapter 2. Plasma samples (n=10) were used in this study. EV and EV-free HDL were isolated from these plasma samples according to the protocol in section 7.2.1 of this chapter. HDL was also isolated from plasma of the same set of participants using density ultracentrifugation only as previously described in section 2.3, chapter 2. The isolation protocol of EV, EV-free HDL and HDL is summarized in Figure 7-4.

Proteomic analysis, SAA1 concentration and PON1 activity were determined in EV, EV-free HDL and HDL fractions according to sections 2.4.2, 2.4.4 and 2.4.5, chapter 2.

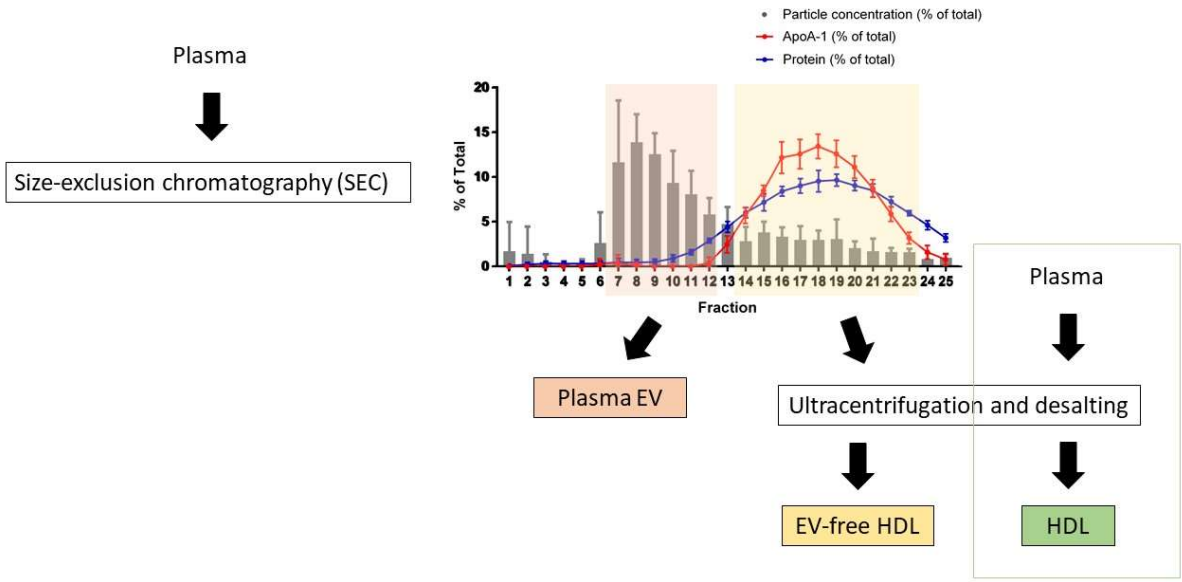

Figure 7-4 Isolation protocol of EV, EV-free HDL and HDL from plasma

7.2.3 Statistical analysis

Protein quantities from the proteomic analysis was expressed as LFQ intensity from the MaxQuant software (version 1.6.3.4) and was considered as non-parametric data for statistical analysis because it represents a relative value. Friedman tests followed by *post hoc* Wilcoxon signed rank tests were carried out to compare LFQ intensity of each protein among EV, EV-free HDL and HDL.

SAA1 concentration and PON1 activity data were checked for normal distribution using Ryan-Joiner test. Log or square root transformation were applied to achieve normal distribution if necessary. Repeated measures ANOVA followed by *post hoc* Tukey's test was performed for parametric data and Friedman test followed by *post hoc* Wilcoxon signed rank test was performed for non-parametric data to test for differences among HDL, EV-free HDL and EV.

7.3 Results

7.3.1 HDL and EV isolation protocol development

7.3.1.1 Size-exclusion chromatography (SEC)

Plasma was added into SEC column to isolate plasma particles by size. The eluate was collected in 25 fractions of 500 µL. Particle size and concentration, apoA-I and protein concentration were measured in each fraction. Both mean and mode of particle size of fractions 1 to 3 were 185.62 and 178.43 nm, 153.78 and 141.87 nm, and 186.60 and 170.22 nm, respectively (Figure 7-5). Particle size continuously decreased from fractions 3 to 10 and remained at a plateau until fraction 25.

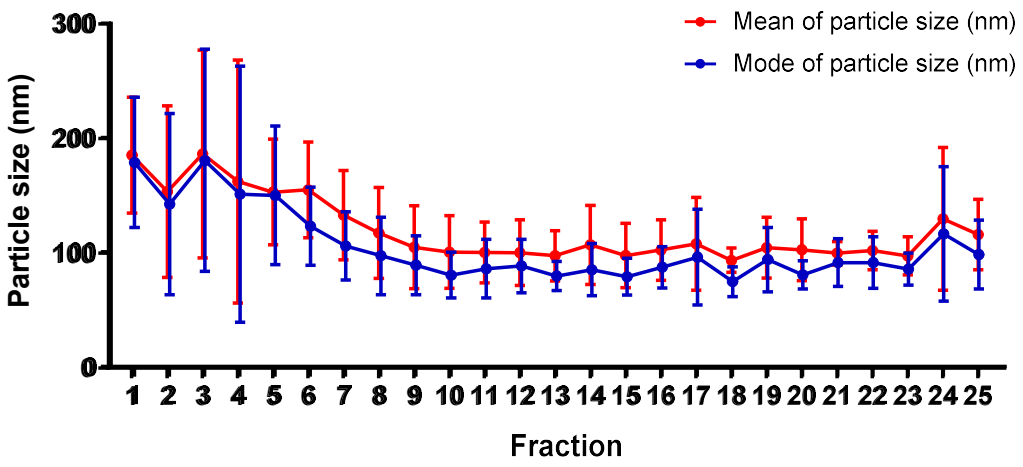

Figure 7-5 Mean and mode of particle size in each fraction after SEC. Data is expressed as mean±SD. n=6.

The distributions of particle number, protein and apoA-I concentration in each fraction are shown in Figure 7-6. Fractions 1-6 contain 6.8% of total particles in all fractions. Most of the particles, 65.8% of total particle concentration, were present in fractions 7-12, whereas fractions 13-25 contain 27.4% of total particles. Regarding total protein concentration, the first half of the 25 fractions (fractions 1-12) contain only 7.9% of total protein, while 92.1% of the total protein was in fractions 13-25.

Similarly, 94.0% of the total apoA-I concentration across all 25 fractions was found in fractions 14-23. ApoA-I concentration in fractions 14-23 accounted of

57.3% of total amount of apoA-I in plasma before SEC. ApoA-I rarely presented in fractions other than fractions 14-23 (Figure 7-6 and 7-7). Of the total amount of apoB in plasma before SEC, 2.8% of apoB was present in fractions 7-12, 34.6% in fractions 14-23 and 0% in other fractions (Figure 7-7).

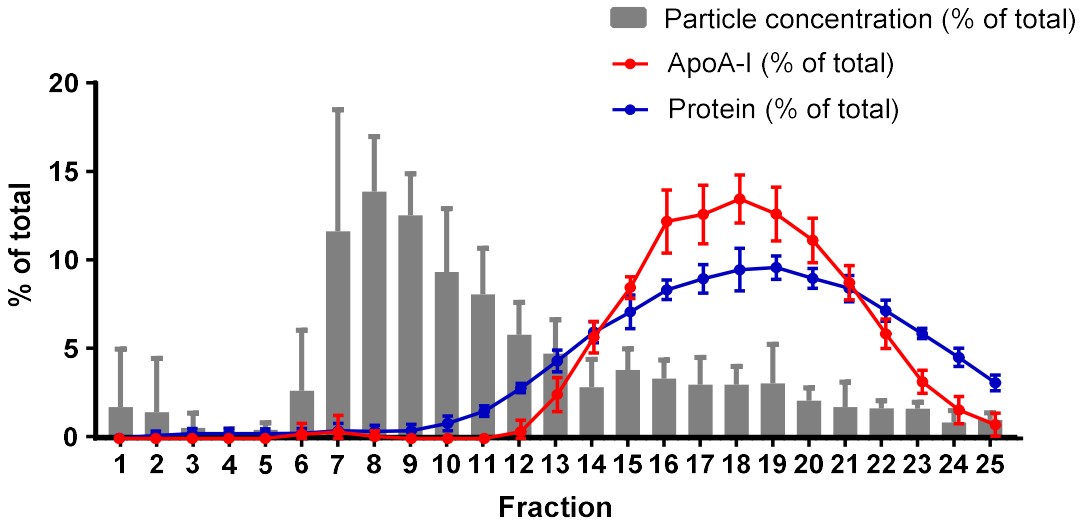

Figure 7-6 Distribution of particle concentration, apoA-I (HDL marker) and protein. Data is expressed as mean±SD. n=6.

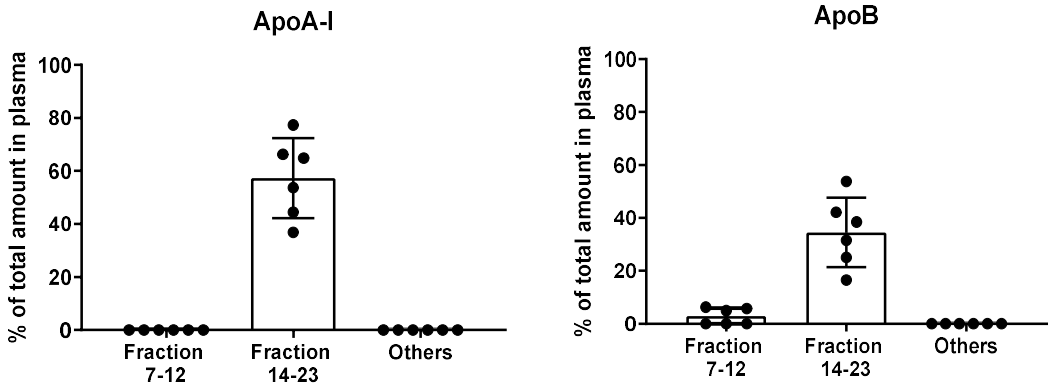

Figure 7-7 Percentage of apoA-I and apoB amount in pooled fractions 7-12, 14-23 and the rest (1-6, 13, 24-25) after SEC, compared to plasma concentration. Data is expressed as mean±SD. n=6.

Intra-individual difference was also assessed in 2 samples. Both samples showed similar distribution of particles, total protein and apoA-I in 25 fractions between SEC at 2 different times (Figure 7-8).

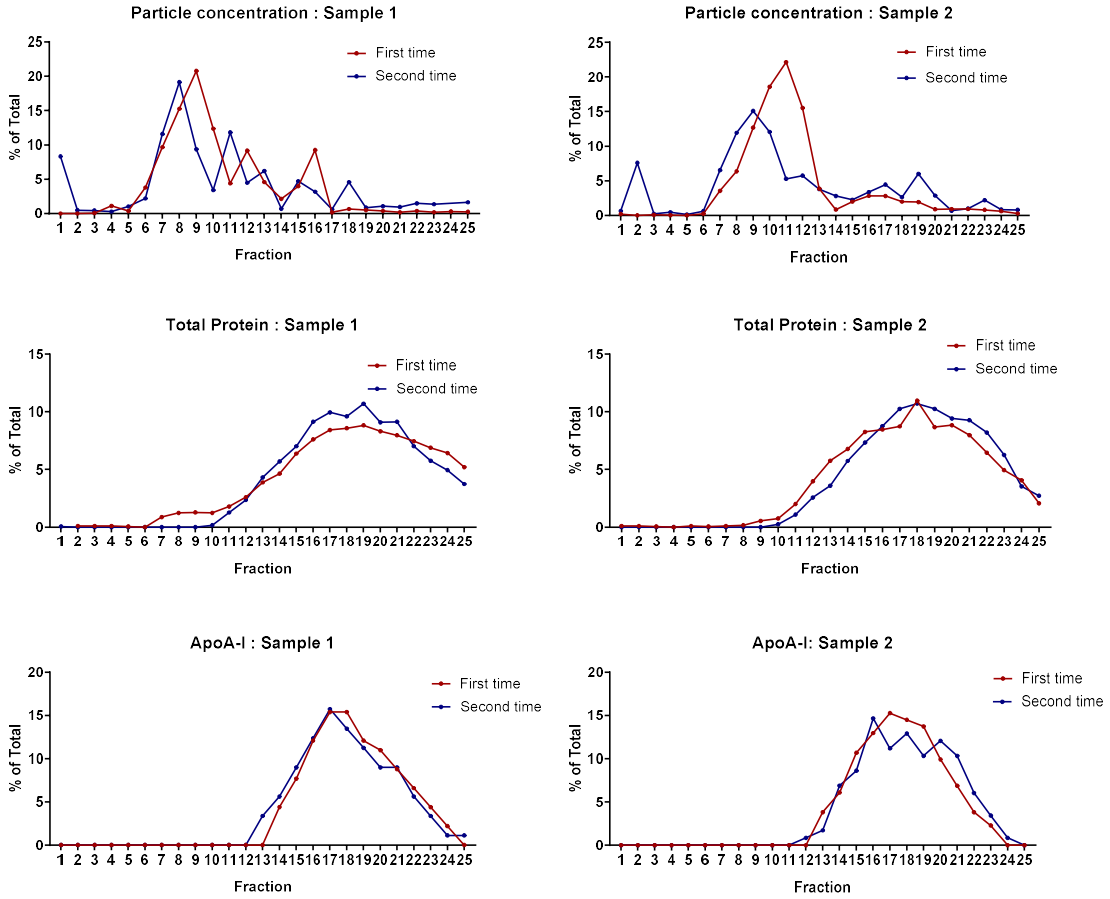

Figure 7-8: Intra-individual assessment of SEC Distribution of particles, total protein and apoA-I in 25 fractions between SEC at two different times of the same plasma sample were assessed in two samples (sample 1 and 2). Red and blue line represent two different times of SEC. Both samples showed similar distribution of particles, total protein and apoA-I in 25 fractions between SEC at 2 different times.

7.3.1.2 Pooled fraction concentration

Fractions 14-23 were pooled and concentrated to a volume of 500 µL (original plasma volume) in preparation for HDL isolation. To test whether there was any HDL or other lipoproteins eluted through the filter into the eluate after a single centrifugation the eluate from the first centrifugation was transferred from below the filter to above the filter in the same centrifugal filter column and the concentration step was repeated. ApoA-I and apoB concentration was measured in retentate and eluate from both the first and second concentration steps.

There was 99.8% of total apoA-I and 86.2% of total apoB appeared in the retentate from the first concentration and these proteins rarely appeared in the eluate after the first concentration or the retentate and eluate after the second concentration (Figure 7-9).

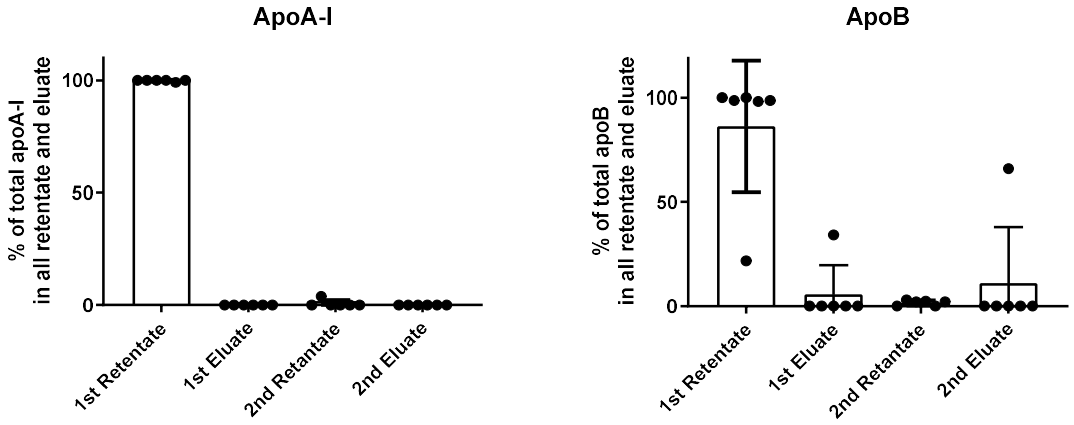

Figure 7-9 Percentage of apoA-I and apoB in retentate and eluate from serial concentration steps Data is expressed as mean±SD. n=6.

7.3.1.3 Density ultracentrifugation

HDL was isolated from concentrated pooled fractions 14-23 in 2 ways; single step and two-step density ultracentrifugation to determined which protocol provided higher HDL recovery and lower VLDL/LDL contamination. Firstly, single step ultracentrifugation was performed with 250 µL final volume of total lipoprotein fraction. ApoA-I recovery in the lipoprotein fraction was 9.4% of the total amount in plasma, while LpDF showed a higher percent recovery of apoA-I with 14.4% of total plasma (Figure 7-10). Collection of 500 µL final volume gave 9.0% recovery of apoA-I in total lipoprotein fraction with 1.6% in LpDF (Figure 7-10). On the other hand, two-step ultracentrifugation provided 20.5% recovery of apoA-I in the HDL fraction and 12.6% in the LpDF fraction (Figure 7-10). The total lipoprotein fraction from the single step ultracentrifugation with a final volume of 250 and 500 µL showed apoB recovery of 3.1% and 2.1%, respectively (Figure 7-11). ApoB recovery in the HDL fraction after a two-step ultracentrifugation was 0.5% (Figure 7-11).

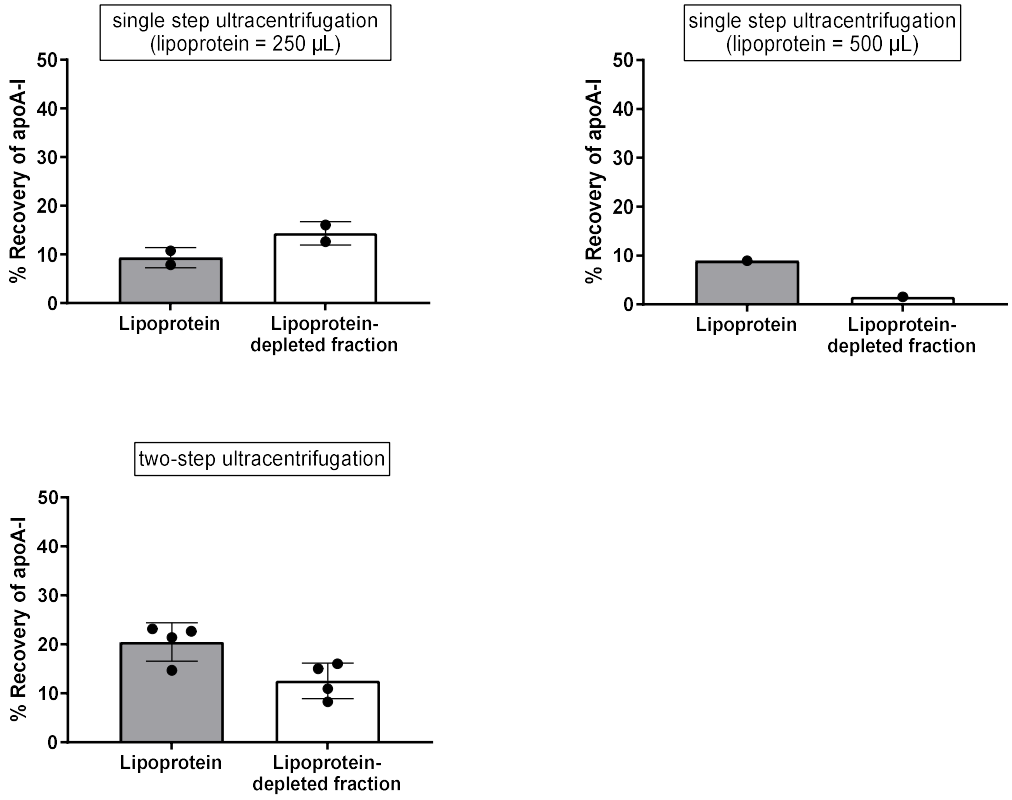

Figure 7-10 Percent recovery of apoA-I in total lipoprotein of HDL fraction and lipoprotein-depleted fraction after ultracentrifugation Data is expressed as mean±SD. n=2 for single step ultracentrifugation with final volume of 250 µL, n=1 for single step ultracentrifugation with final volume of 500 µL and n=4 for two-step ultracentrifugation.

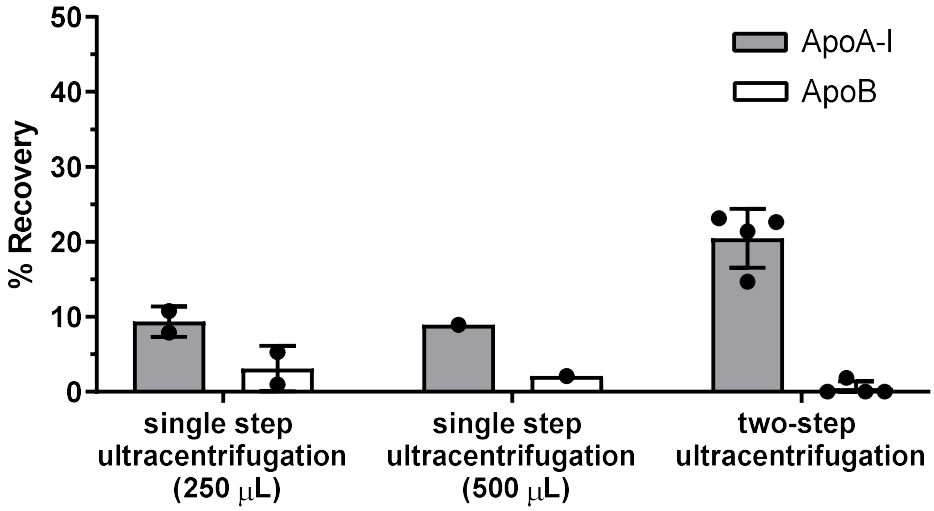

Figure 7-11 Percent recovery of apoA-I and apoB in lipoprotein or HDL fraction after ultracentrifugation Data is expressed as mean±SD. n=2 for single step ultracentrifugation with final volume of 250 µL, n=1 for single step ultracentrifugation with final volume of 500 µL and n=4 for two-step ultracentrifugation.

Overall apoA-I recovery from each step when isolating EV-free HDL, i.e. SEC, single concentrated pooled fractions 14-23 and two-step ultracentrifugation, is shown in Figure 7-12. After SEC, 70.1% of apoA-I remained in fractions 1-25. Fractions 14-23 showed 65.6% recovery of apoA-I and no significant loss of apoA-I after a concentration step with 67.2% recovery. ApoB recovery in fractions 14-23 was 44.7% after SEC and concentration. After two-step ultracentrifugation, there was 20.5% apoA-I recovery and 0.5% apoB recovery.

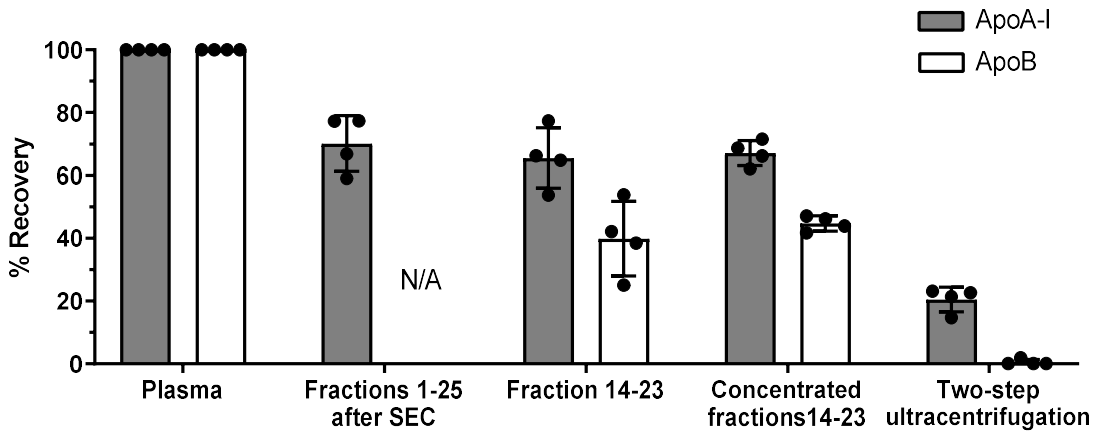

Figure 7-12 ApoA-I and apoB recovery along EV-free HDL isolation protocol. After SEC, 70.1% of apoA-I remained in fractions 1-25. Fractions 14-23 showed 65.6% recovery of apoA-I and no significant loss of apoA-I after a concentration step with 67.2% recovery. ApoB recovery in fractions 14-23 was 44.7% after SEC and concentration. After two-step ultracentrifugation, there was 20.5% apoA-I recovery and 0.5% apoB recovery. Data is expressed as mean±SD. n=4.

7.3.1.4 Development of optimal HDL and EV isolation protocol

Firstly, the two-step ultracentrifugation was modified whereby centrifugation at 73,000 rpm (232,174 g for maximum radius and 146,228 g for minimum radius), 23ºC for 16 hours was carried out instead of the second step of ultracentrifugation at 100,000 rpm, 23ºC for 5 hours to make this protocol more practical with day-time work. Centrifugation at 73,000 rpm for 16 hours was calculated to create the equivalent centrifugal force (gmin) to the original HDL isolation protocol from Lindgren et al. which centrifuged plasma at 40,000 rpm, 18ºC for 26 hours and gave 222,250,000 gmin for maximum radius and 136,700,9828 gmin for minimum radius (Lindgren et al. 1972). The modified technique showed similar apoA-I recovery with 17.0% apoA-I recovery and 0% apoB recovery in HDL fraction. Therefore, two-step ultracentrifugation with

100,000 rpm, 23ºC for 2.5 hours followed by at 73,000 rpm, 23ºC for 16 hours was chosen for this protocol.

Comparison between HDL isolation methods with and without pre-centrifugation to remove apoptotic bodies and microvesicles before SEC revealed 48.4% of apoA-I and 13.5% of apoB recovery in HDL fraction from the protocol without pre-spin compared to 17.0% of apoA-I and 0% of apoB recovery with pre-spin protocol (Figure 7-13).

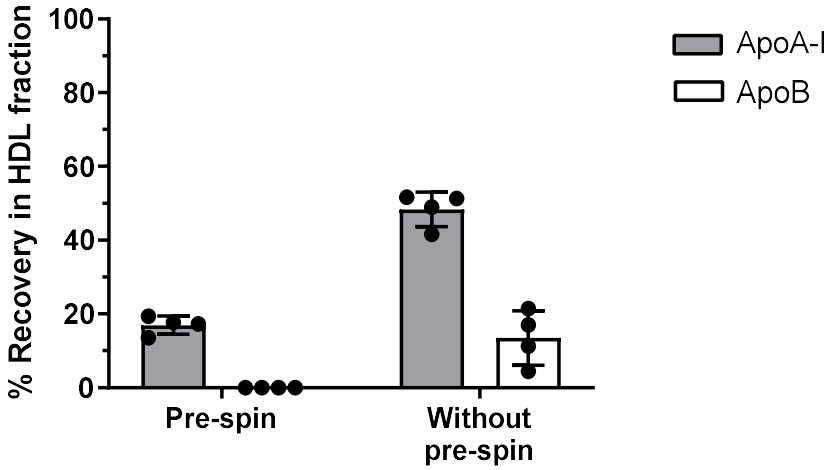

Figure 7-13 Percent recovery of apoA-I and apoB in HDL fraction between HDL isolation protocol with and without pre-centrifugation before SEC Data is expressed as mean±SD. n=4

The starting volume of plasma was also tested in this whole process. Plasma volumes 0.5 mL and 1.5 mL (n=4) were added to the SEC column. Pooled fractions 14-23 were concentrated, ultracentrifuged and desalted. After SEC, apoA-I in fractions 14-23 show a higher recovery from 1.5 mL plasma with 86.5% than from 0.5 mL plasma with 61.1% (Figure 7-14). However, after concentration and ultracentrifugation, a similar apoA-I recovery was achieved with 48.4% and 42.0% for 0.5 mL and 1.5 mL plasma, respectively. The final step with desalting shows the opposite result in that there was higher percent apoA-I recovery in 0.5 mL plasma (39.8%) than for 1.5 mL plasma (25.1%).

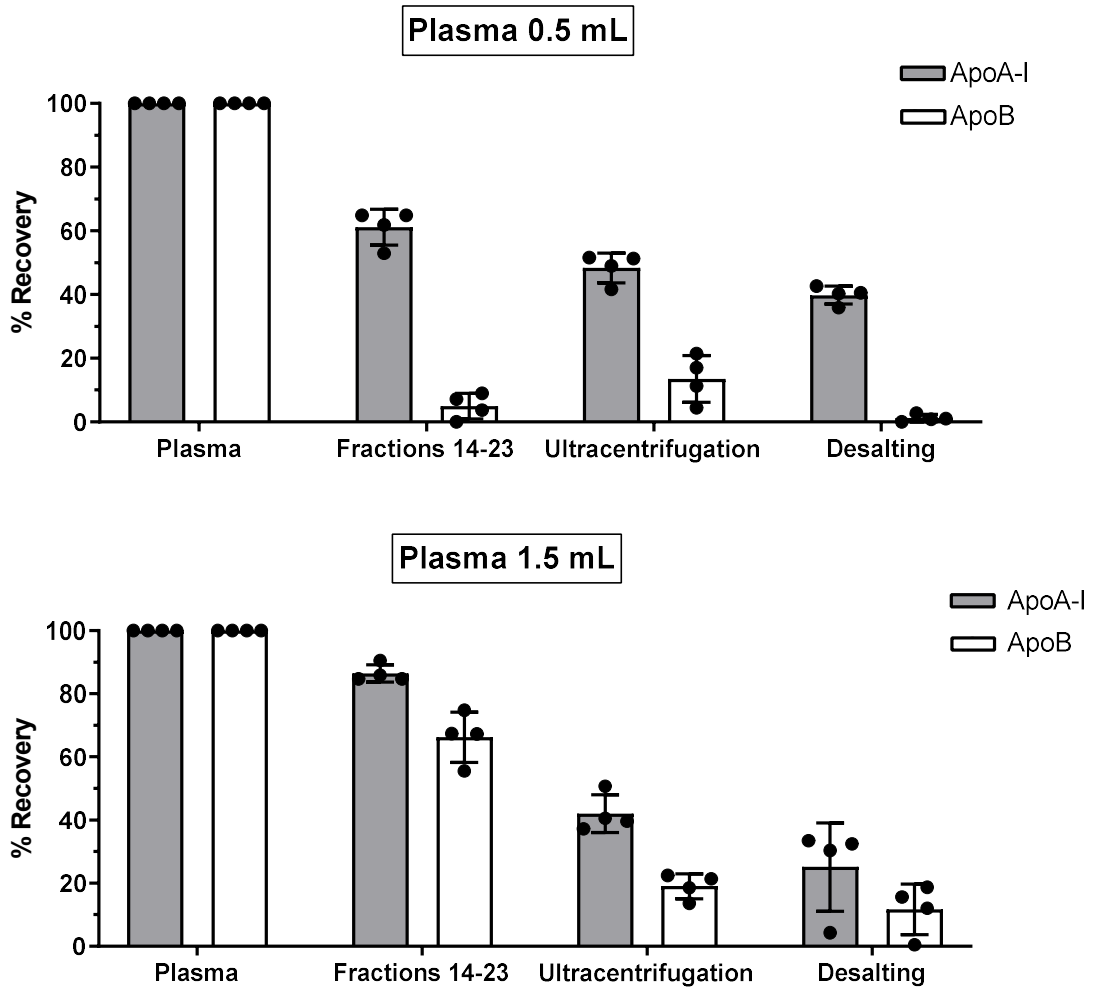

Figure 7-14 Percent recovery of apoA-I and apoB in each step of HDL isolation from 0.5 mL or 1.5 mL plasma After SEC, apoA-I in fractions 14-23 show a higher recovery from 1.5 mL plasma with 86.5% than from 0.5 mL plasma with 61.1%. After concentration and ultracentrifugation, a similar apoA-I recovery was achieved with 48.4% and 42.0% for 0.5 mL and 1.5 mL plasma, respectively. The final step with desalting shows the opposite result in that there was higher percent apoA-I recovery in 0.5 mL plasma (39.8%) than for 1.5 mL plasma (25.1%). Data is expressed as mean±SD. n=4

Finally, the reverse protocol was carried out to compare HDL recovery with the original protocol. HDL was isolated from plasma (n=4) by two-step ultracentrifugation following by SEC, concentrating and desalting. Final apoA-I and apoB recovery in HDL fraction were 30.7% and 5.0%, respectively.

7.3.2 Comparison of proteomic analysis of HDL, EV-free HDL and EV

Comparison of the proteomic composition of HDL (n=10), EV-free HDL (n=10) and EV (n=10) was performed. EV and EV-free HDL were isolated from SEC followed by two-step ultracentrifugation. EV was from pooling fractions 7-12 after SEC

and EV-free HDL was collected after two-step ultracentrifugation and desalting. HDL was also isolated from plasma of the same set of participants using density ultracentrifugation only.

7.3.2.1 Distribution of proteins among HDL, EV-free HDL and EV fraction

There were 156 types of protein found in HDL, EV-free HDL and EV. The distribution of the number of proteins identified among these three groups of samples is shown in Figure 7-15. There were 84, 74, 124 proteins in HDL, EV-free HDL and EV samples, respectively.

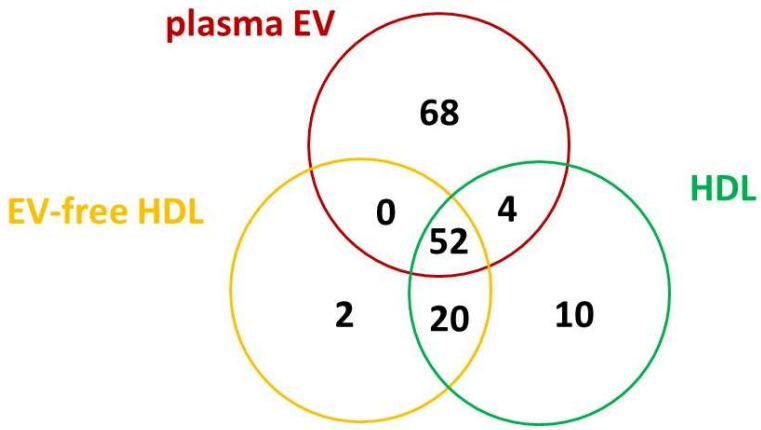

Figure 7-15 Venn diagram to illustrate the distribution of protein among EV, EV-free HDL and HDL samples

7.3.2.2 Proteins found uniquely in HDL, EV-free HDL or EV

There were 10, 2 and 68 proteins that were found only in HDL, EV-free HDL and EV samples, respectively. The list of 10 proteins found only in HDL is shown in Table 7.1. The 2 proteins found in EV-free HDL only were ATP-binding cassette sub-family A member 5 and corticosteroid-binding globulin. The list of 68 proteins found only in EV is shown in Table 7.2. Out of 68 proteins found only in EV, there were 30 immunoglobulins and 9 proteins involved in complement system (Table 7.2).

Table 7.1 List of proteins found in HDL only

BPI fold-containing family B member 1
Chorionic somatomammotropin hormone 2
Hornerin
Insulin-like growth factor-binding protein 3
L-selectin
Lipopolysaccharide-binding protein
N-acetylmuramoyl-L-alanine amidase
Serum amyloid A 2
Thymosin ß4
Thyroxine-binding globulin

Table 7.2 List of proteins found in EV only

Absent in melanoma 1 protein
Actin, cytoplasmic 2
α-2-macroglobulin
ß-actin-like protein 2
C4b-binding protein α chain
C4b-binding protein ß chain
Carboxypeptidase N subunit 2
CD5 antigen-like
Ceruloplasmin
Complement C1q subunit B
Complement C1q subunit C
Complement C1r
Complement C5
Complement C7
Complement C8 α chain
Complement factor B
Complement factor H
Complement factor H-related protein 1
Fibronectin
Fibulin-1
Ficolin-3
Galectin-3-binding protein
Hemoglobin subunit α
Hemoglobin subunit delta

Histidine-rich glycoprotein
Ig delta chain C region
Ig gamma-2 chain C region
Ig gamma-3 chain C region
Ig gamma-4 chain C region
Ig heavy chain V-II region NEWM
Ig heavy chain V-III region BRO
Ig heavy chain V-III region CAM
Ig heavy chain V-III region JON
Ig heavy chain V-III region WEA
Ig kappa chain V-I region HK102
Ig kappa chain V-II region FR
Ig kappa chain V-II region RPMI 6410
Ig kappa chain V-III region B6
Ig kappa chain V-III region POM
Ig kappa chain V-III region VG
Ig kappa chain V-IV region
Ig lambda-7 chain C region
Ig lambda chain V-I region HA
Ig lambda chain V-III region LOI
Ig mu chain C region
IgGFc-binding protein
Immunoglobulin alpha-2 heavy chain
Immunoglobulin heavy variable 3-15
Immunoglobulin heavy variable 3-49
Immunoglobulin heavy variable 5-10-1
Immunoglobulin J chain
Immunoglobulin kappa light chain
Immunoglobulin kappa variable 2-24
Immunoglobulin kappa variable 3D-20
Immunoglobulin lambda constant 3
Immunoglobulin mu heavy chain
Inter-alpha-trypsin inhibitor heavy chain H1
Inter-alpha-trypsin inhibitor heavy chain H2
Pappalysin-1
Plasma kallikrein
Plasminogen
Pregnancy zone protein
Properdin
Proteoglycan 4
Prothrombin
Serum amyloid P-component
Vitamin K-dependent protein S
von Willebrand factor

7.3.2.3 Overlapping proteins among HDL, EV-free HDL and EV

The list of 52 proteins found in all three groups of samples is shown in Table 7.3. Out of the 52 proteins, 14 were apolipoproteins. There were 43 proteins showing significant differences in LFQ intensity among HDL, EV-free HDL and EV. LFQ intensity of α-2-antiplasmin, α-1-acid glycoprotein 1, apoC-IV, apolipoprotein(a), ß-2-glycoprotein 1, apoA-IV, apoF, apoL-I, SAA4, PON1, apoB-100, vitronectin, clusterin, complement C4-A, protein AMBP, complement C3, fibrinogen α and ß chain, haptoglobin, hemopexin, immunoglobulin λ-like polypeptide 5 and serotransferrin were higher in HDL than EV-free HDL (Figure 7-16 to 7-21). LFQ intensity of α-2-antiplasmin showed no significant difference between HDL and EV (Figure 7-16). While LFQ intensity of α-1-acid glycoprotein 1, apoC-IV, apolipoprotein(a) and ß-2-glycoprotein 1 in HDL were higher than those in both EV-free HDL and EV (Figure 7-17). LFQ intensity of apoA-IV, apoF, apoL-I, SAA4 and PON1 were higher in HDL than those in in EV-free HDL and EV, and also higher in EV-free-HDL than those in EV (Figure 7-18). ApoB-100, vitronectin, clusterin, complement C4-A and protein AMBP showed significantly lower LFQ intensity in EV-free HDL than those in HDL and EV (Figure 7-19 and 7-20). Additionally, LFQ intensity of clusterin, complement C4-A and protein AMBP were the highest in plasma EV compared to HDL and EV-free HDL (Figure 7-20). LFQ intensity of complement C3, fibrinogen α and ß chain, haptoglobin, hemopexin, immunoglobulin λ-like polypeptide 5 and serotransferrin were significantly higher in HDL than EV-free HDL and were the highest in EV (Figure 7-21).

ApoA-I, apoA-II and inter-α-trypsin inhibitor heavy chain H4 had lower LFQ intensity in HDL than those in EV-free HDL (Figure 7-22 and 7-23). LFQ intensity of apoA-I and apoA-II were higher in HDL and EV-free HDL than in EV and were the highest in EV-free HDL (Figure 7-22). LFQ intensity of inter-α-trypsin inhibitor heavy chain H4 in HDL was lower than those in EV-free HDL and EV (Figure 7-23).

LFQ intensity of α-1-acid glycoprotein 2, α-1-antitrypsin, α-2-HS-glycoprotein and vitamin D-binding protein were higher in HDL than EV but showed no significant difference between HDL and EV-free HDL (Figure 7-24). Angiotensinogen, apoC-I, apoC-II, apoC-III, apoD, apoM, retinal-binding protein

4, sorting nexin 29 and transthyretin in HDL and EV-free HDL had higher LFQ intensity than in EV (Figure 7-25). Complement C4-B, Ig α-1 chain C region, Ig γ-1 chain C region, Ig κ chain C region and kininogen 1 had the highest LFQ intensity in plasma EV, compared to HDL and EV-free HDL (Figure 7-26).

Table 7.3 List of proteins found in HDL, EV-free HDL and EV

α-1-acid glycoprotein 1
α -1-acid glycoprotein 2
α -1-antichymotrypsin
α -1-antitrypsin
α -1B-glycoprotein
α -2-antiplasmin
α -2-HS-glycoprotein
Angiotensinogen
Antithrombin-III
Apolipoprotein A-I
Apolipoprotein A-II
Apolipoprotein A-IV
Apolipoprotein B-100
Apolipoprotein C-I
Apolipoprotein C-II
Apolipoprotein C-III
Apolipoprotein C-IV
Apolipoprotein D
Apolipoprotein E
Apolipoprotein F
Apolipoprotein L1
Apolipoprotein M
Apolipoprotein(a)
ß-2-glycoprotein 1
Clusterin
Complement C3
Complement C4-A
Complement C4-B
Fibrinogen α chain
Fibrinogen ß chain
Haptoglobin
Haptoglobin-related protein
Hemopexin
Heparin cofactor 2
Hyaluronan-binding protein 2
Ig α -1 chain C region
Ig γ-1 chain C region

Ig κ chain C region
Immunoglobulin lambda-like polypeptide 5
Inter-alpha-trypsin inhibitor heavy chain H4
Kininogen-1
Protein AMBP
Retinol-binding protein 4
Serotransferrin
Serum albumin
Serum amyloid A-4 protein
Serum paraoxonase/arylesterase 1
Sorting nexin-29
Transthyretin
Vitamin D-binding protein
Vitronectin
Sex hormone-binding globulin

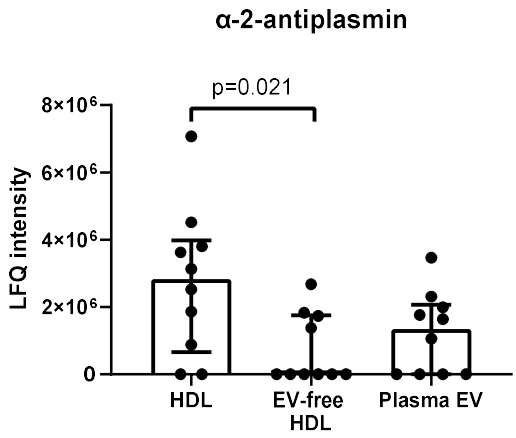

Figure 7-16 LFQ intensity of α-2-antiplasmin in HDL, EV-free HDL and EV: Data is expressed as median±interquartile range. Friedman tests followed by post hoc Wilcoxon signed rank tests were carried out to compare LFQ intensity among HDL, EV-free HDL and EV. $p<0.05$ was taken as statistically significant.

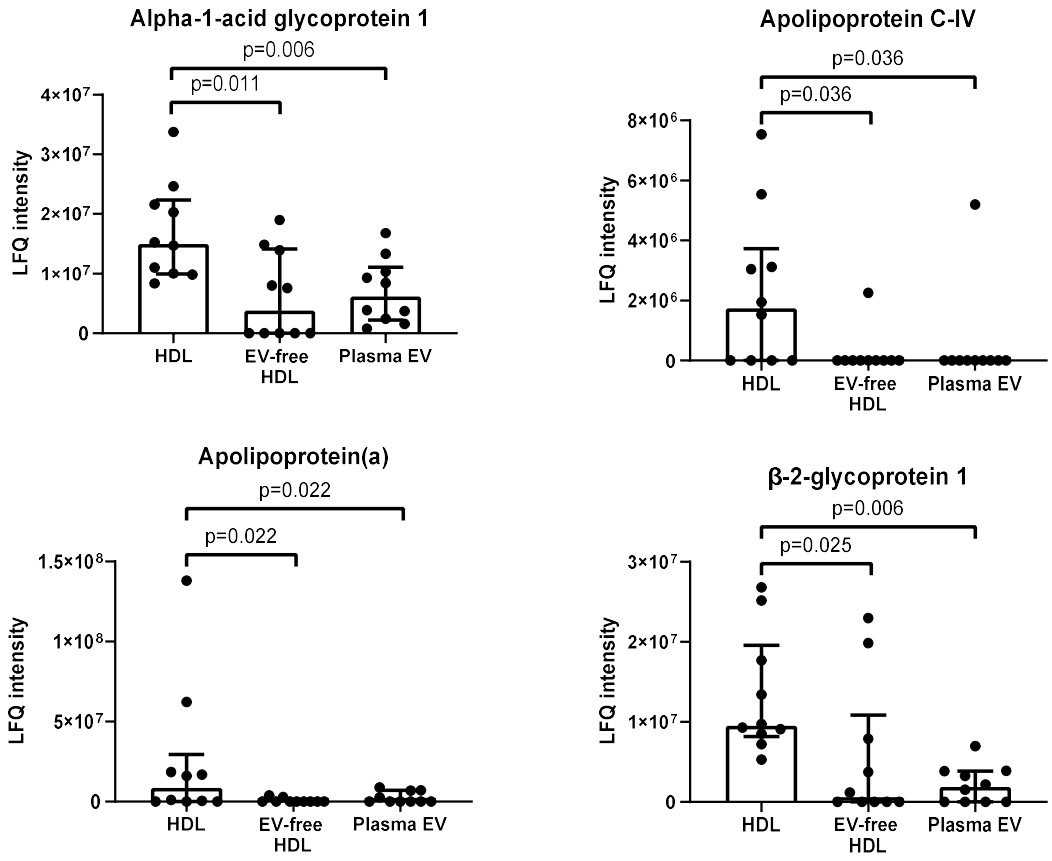

Figure 7-17 LFQ intensity α-1-acid glycoprotein 1, apoC-IV, apolipoprotein(a) and β-2-glycoprotein 1 in HDL, EV-free HDL and EV: Data is expressed as median±interquartile range. Friedman tests followed by post hoc Wilcoxon signed rank tests were carried out to compare LFQ intensity among HDL, EV-free HDL and EV. $p<0.05$ was taken as statistically significant.

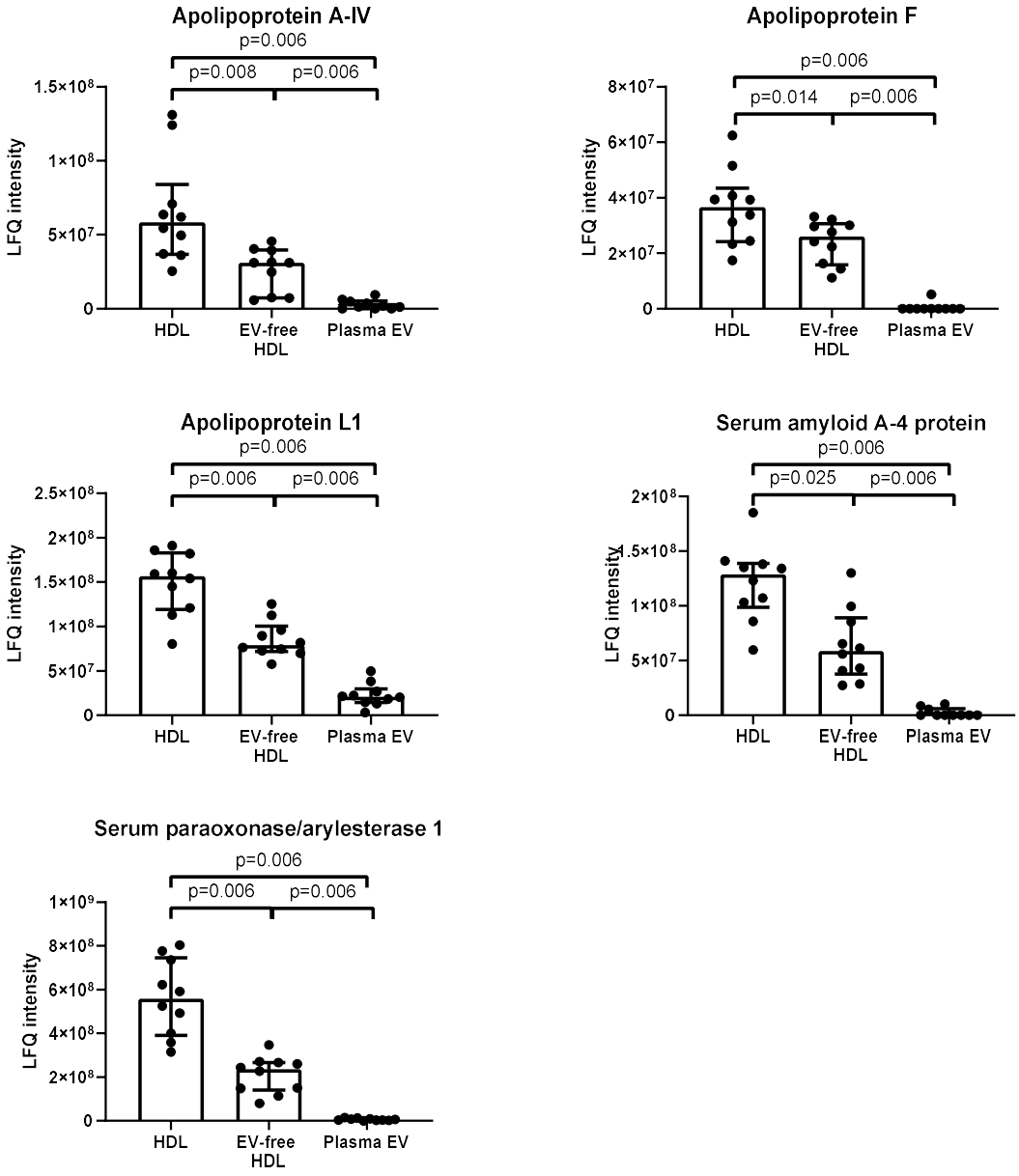

Figure 7-18 LFQ intensity of apoA-IV, apoF, apoL-I, SAA4 and PON1 in HDL, EV-free HDL and EV: Data is expressed as median±interquartile range. Friedman tests followed by post hoc Wilcoxon signed rank tests were carried out to compare LFQ intensity among HDL, EV-free HDL and EV. $p<0.05$ was taken as statistically significant.

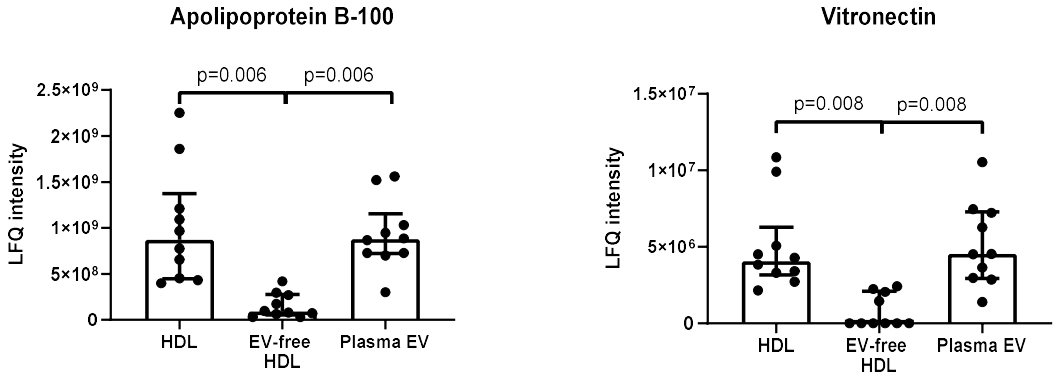

Figure 7-19 LFQ intensity of apoB-100 and vitronectin in HDL, EV-free HDL and EV: Data is expressed as median±interquartile range. Friedman tests followed by post hoc Wilcoxon signed rank tests were carried out to compare LFQ intensity among HDL, EV-free HDL and EV. $p<0.05$ was taken as statistically significant.

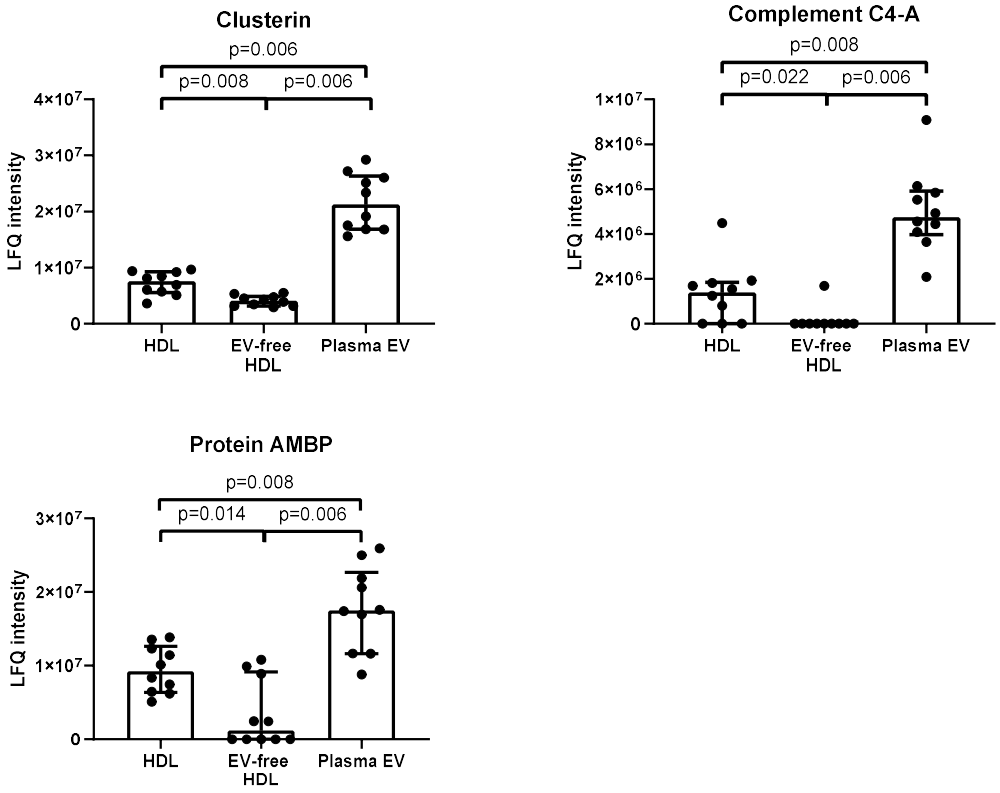

Figure 7-20 LFQ intensity of clusterin, complement C4-A and protein AMBP in HDL, EV-free HDL and EV: Data is expressed as median±interquartile range. Friedman tests followed by post hoc Wilcoxon signed rank tests were carried out to compare LFQ intensity among HDL, EV-free HDL and EV. $p<0.05$ was taken as statistically significant.

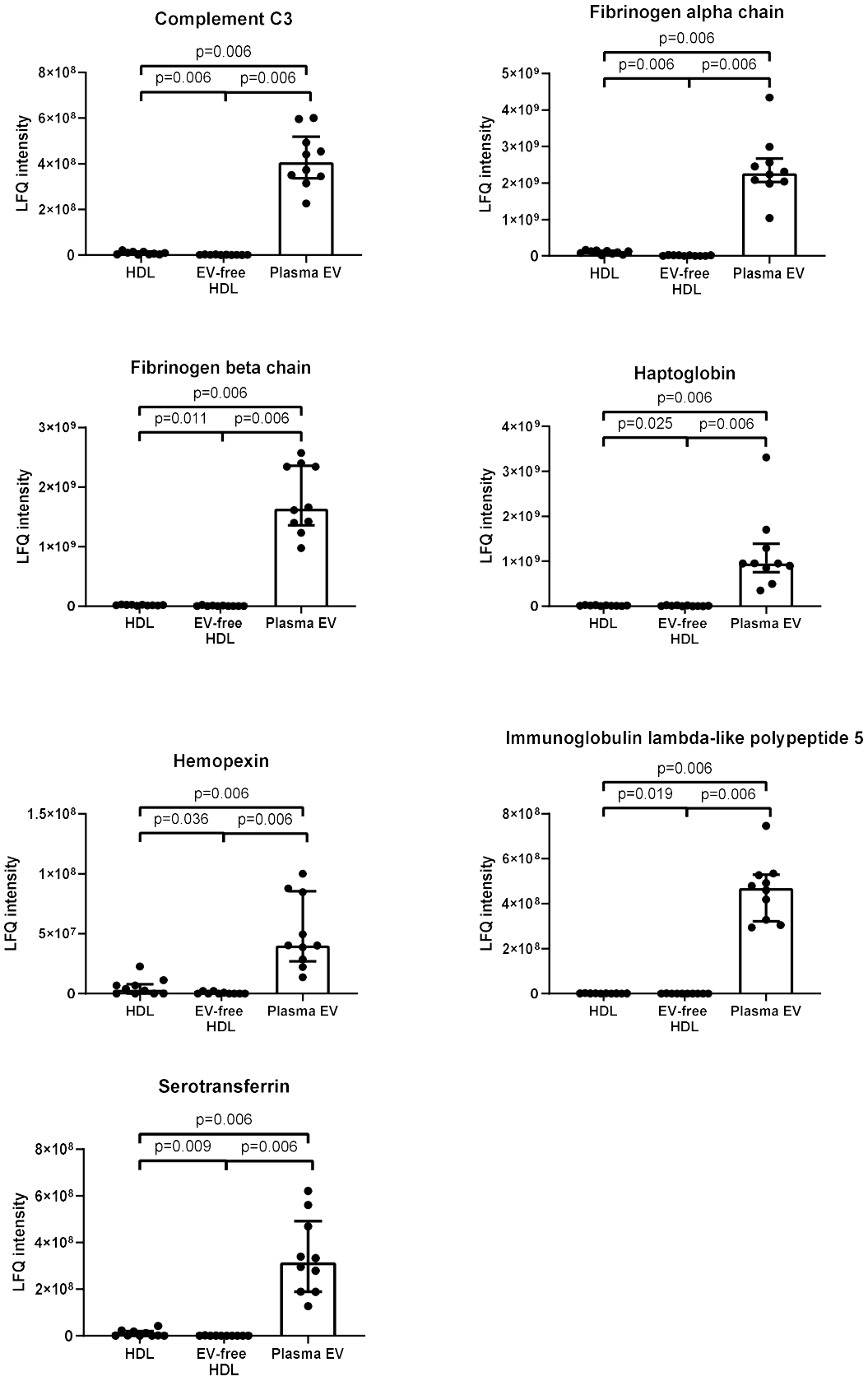

Figure 7-21 LFQ intensity of complement C3, fibrinogen α and β chain, haptoglobin, hemopexin, immunoglobulin λ-like polypeptide 5 and serotransferrin in HDL, EV-free HDL and EV: Data is expressed as median±interquartile range. Friedman tests followed by post hoc Wilcoxon signed rank tests were carried out to compare LFQ intensity among HDL, EV-free HDL and EV. $p<0.05$ was taken as statistically significant.

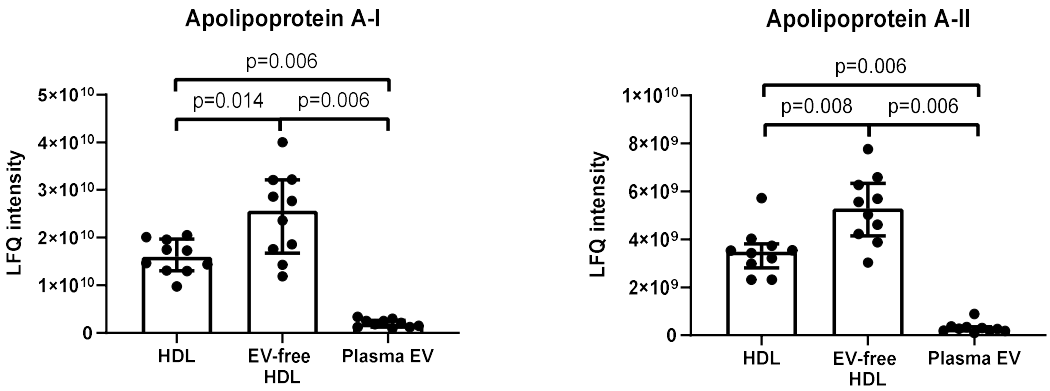

Figure 7-22 LFQ intensity of apoA-I and apoA-II in HDL, EV-free HDL and EV: Data is expressed as median±interquartile range. Friedman tests followed by post hoc Wilcoxon signed rank tests were carried out to compare LFQ intensity among HDL, EV-free HDL and EV. $p<0.05$ was taken as statistically significant.

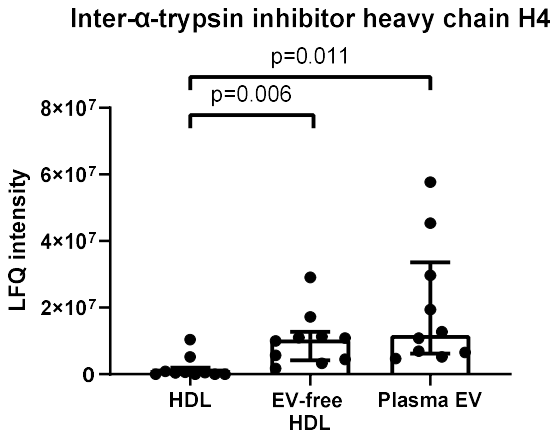

Figure 7-23 LFQ intensity of inter-α-trypsin inhibitor heavy chain H4 in HDL, EV-free HDL and EV: Data is expressed as median±interquartile range. Friedman tests followed by post hoc Wilcoxon signed rank tests were carried out to compare LFQ intensity among HDL, EV-free HDL and EV. $p<0.05$ was taken as statistically significant.

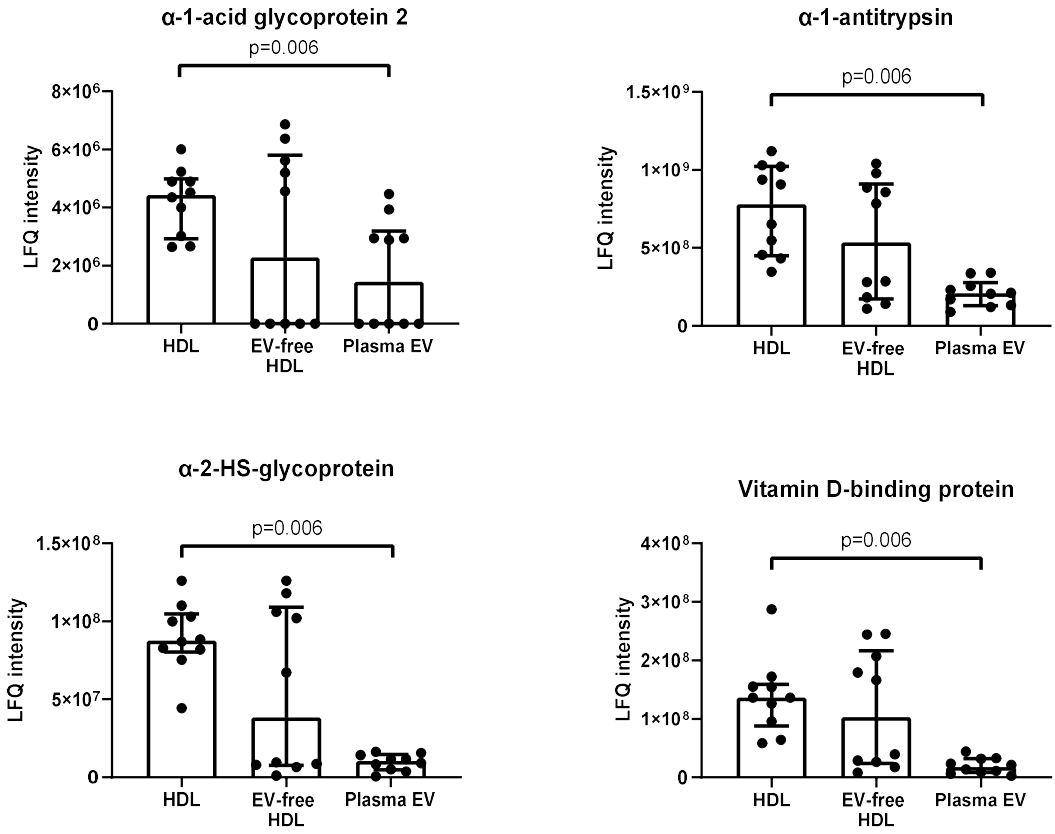

Figure 7-24 LFQ intensity of α-1-acid glycoprotein 2, α-1-antitrypsin, α-2-HS-glycoprotein and vitamin D-binding protein in HDL, EV-free HDL and EV: Data is expressed as median±interquartile range. Friedman tests followed by post hoc Wilcoxon signed rank tests were carried out to compare LFQ intensity among HDL, EV-free HDL and EV. $p<0.05$ was taken as statistically significant.

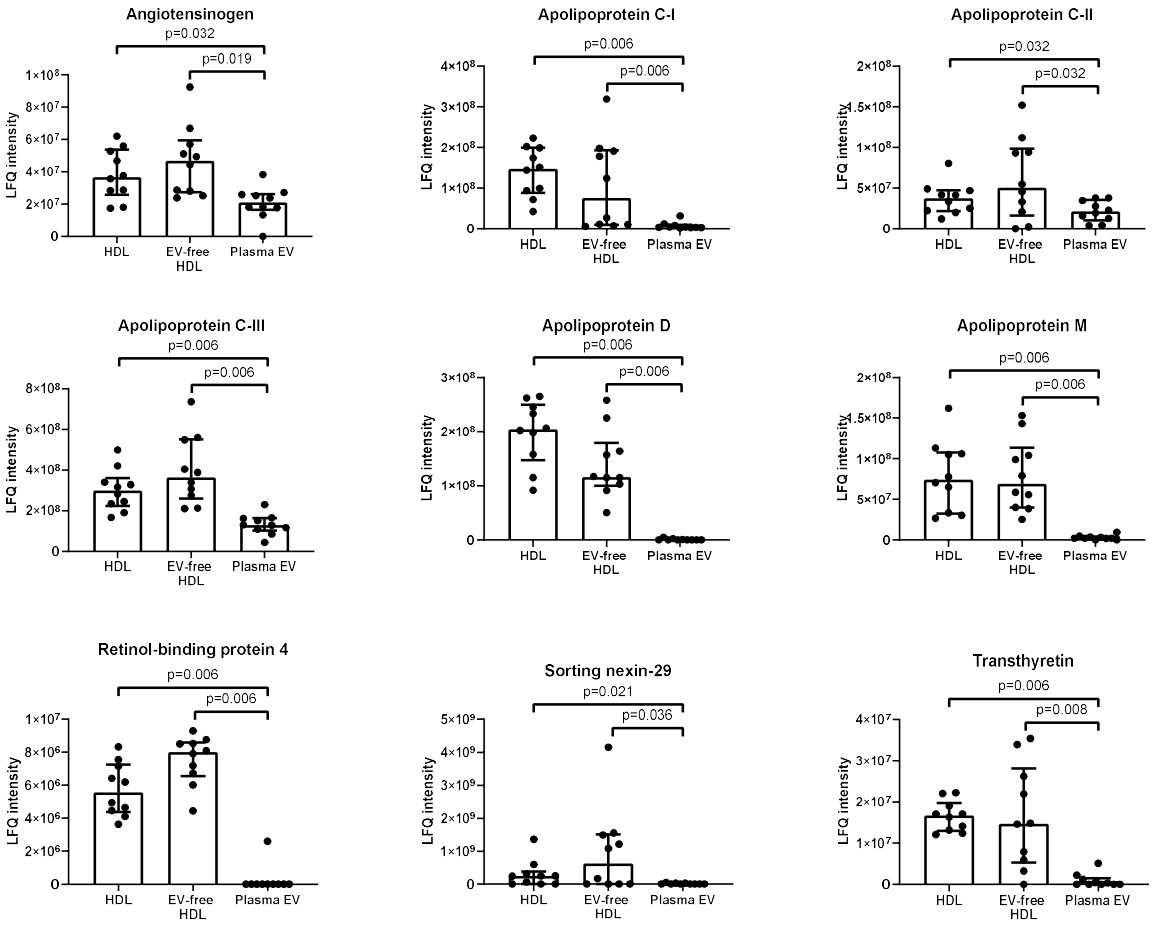

Figure 7-25 LFQ intensity of angiotensinogen, apoC-I, apoC-II, apoC-III, apoD, apoM, retinal-binding protein 4, sorting nexin 29 and transthyretin in HDL, EV-free HDL and EV: Data is expressed as median±interquartile range. Friedman tests followed by post hoc Wilcoxon signed rank tests were carried out to compare LFQ intensity among HDL, EV-free HDL and EV. $p<0.05$ was taken as statistically significant.

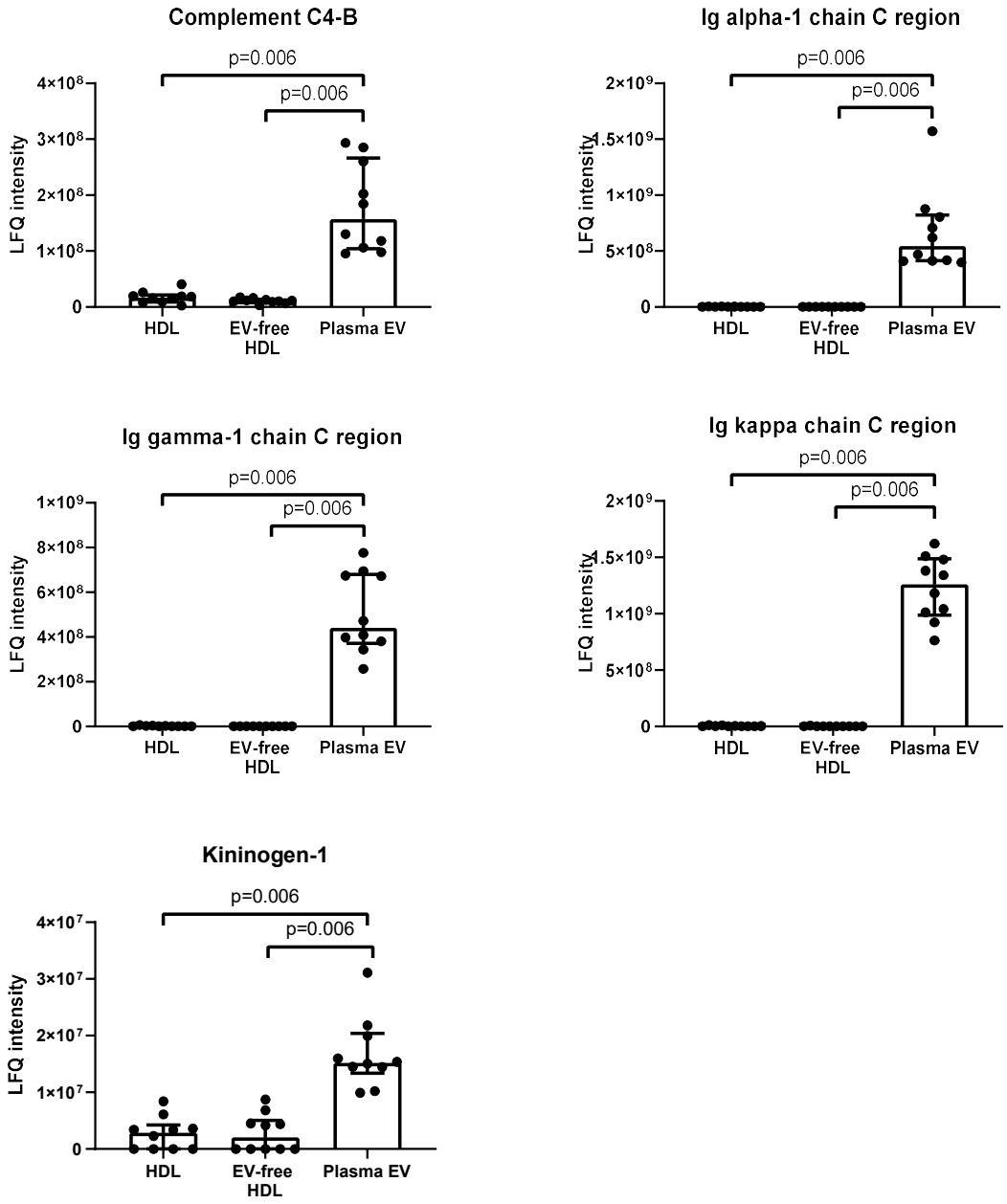

Figure 7-26 LFQ intensity of complement C4-B, Ig α-1 chain C region, Ig γ-1 chain C region, Ig κ chain C region and kininogen 1 in HDL, EV-free HDL and EV: Data is expressed as median±interquartile range. Friedman tests followed by post hoc Wilcoxon signed rank tests were carried out to compare LFQ intensity among HDL, EV-free HDL and EV. $p<0.05$ was taken as statistically significant.

HDL and EV-free HDL had 72 common proteins in which 52 proteins were common in all three groups of samples and the remaining 20 proteins were found in HDL and EV-free HDL, but not in EV. The list of 20 proteins found in HDL and EV-free HDL, but not in EV, are shown in Table 7.4. Out of these 20 proteins, 14 proteins showed significantly different LFQ intensity among the 3 groups of

samples. LFQ intensity of leucine-rich α-2-glycoprotein, pigment epithelium-derived factor, protein MENT and zinc-α-2-glycoprotein in HDL were higher than those in EV (Figure 7-27). LFQ intensity of ß-2-microglobulin, cathelicidin antimicrobial peptide, CETP, PLTP, platelet basic protein, platelet factor 4, prenylcysteine oxidase 1 and PON3 were higher in HDL than those in EV-free HDL and EV (Figure 7-28). LCAT had the highest LFQ intensity in HDL, followed by EV-free HDL and EV, respectively (Figure 7-29). Lastly, LFQ intensity of SAA1 was the lowest in EV compared to those in HDL and EV-free HDL (Figure 7-30).

Table 7.4 List of proteins found in both HDL and EV-free HDL, but not in EV

ß-2-microglobulin
Cathelicidin antimicrobial peptide
Cholesteryl ester transfer protein
Complement component C9
Leucine-rich alpha-2-glycoprotein
Phosphatidylcholine-sterol acyltransferase (LCAT)
Phospholipid transfer protein
Pigment epithelium-derived factor
Platelet basic protein
Platelet factor 4
Prenylcysteine oxidase 1
Protein MENT
Serum amyloid A-1 protein
Serum paraoxonase/lactonase 3
Zinc-alpha-2-glycoprotein
Afamin
Gelsolin
HLA class I histocompatibility antigen, A-23 α chain
Insulin-like growth factor II
Vacuolar protein sorting-associated protein 13D

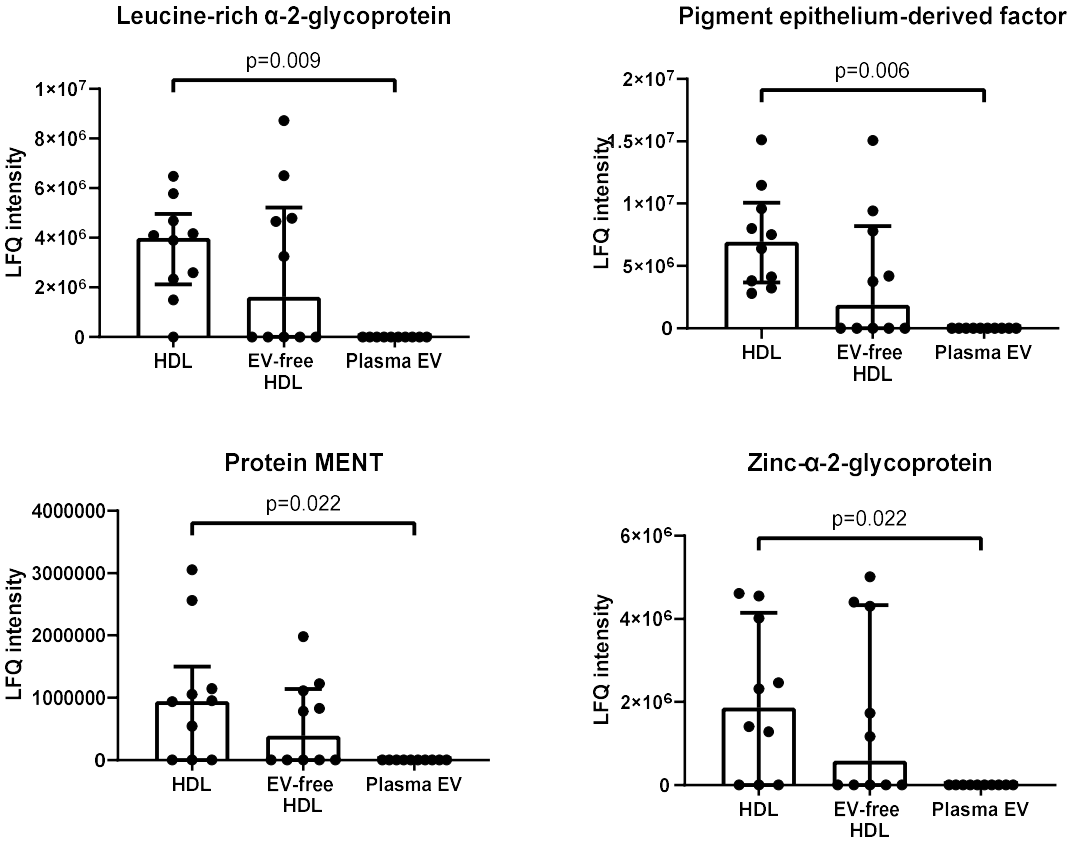

Figure 7-27 LFQ intensity of leucine-rich α-2-glycoprotein, pigment epithelium-derived factor, protein MENT and zinc-α-2-glycoprotein in HDL, EV-free HDL and EV: Data is expressed as median±interquartile range. Friedman tests followed by post hoc Wilcoxon signed rank tests were carried out to compare LFQ intensity among HDL, EV-free HDL and EV. $p<0.05$ was taken as statistically significant.

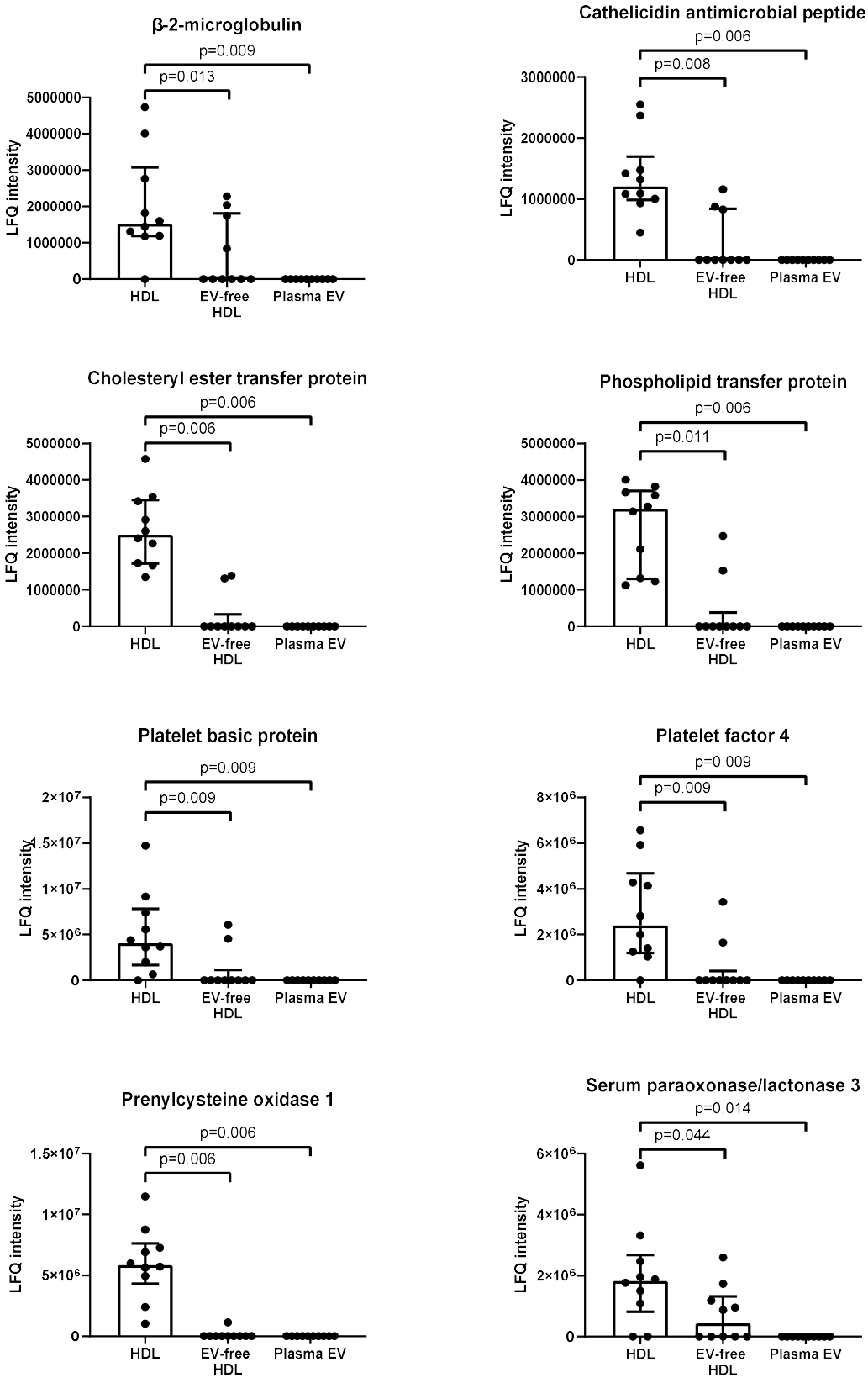

Figure 7-28 LFQ intensity of β-2-microglobulin, cathelicidin antimicrobial peptide, CETP, PLTP, platelet basic protein, platelet factor 4, prenylcysteine oxidase 1 and PON3 in HDL, EV-free HDL and EV: Data is expressed as median±interquartile range. Friedman tests followed by post hoc Wilcoxon signed rank tests were carried out to compare LFQ intensity among HDL, EV-free HDL and EV. $p<0.05$ was taken as statistically significant.

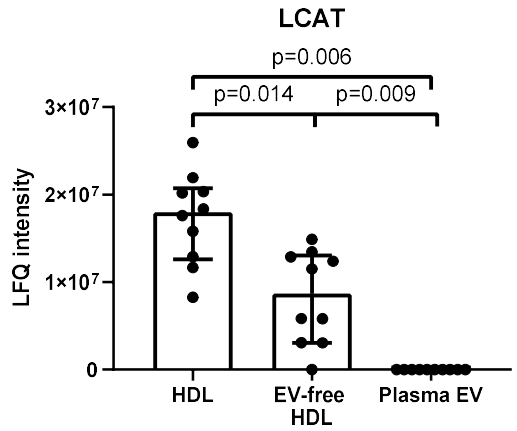

Figure 7-29 LFQ intensity of LCAT in HDL, EV-free HDL and EV: Data is expressed as median±interquartile range. Friedman tests followed by post hoc Wilcoxon signed rank tests were carried out to compare LFQ intensity among HDL, EV-free HDL and EV. p<0.05 was taken as statistically significant.

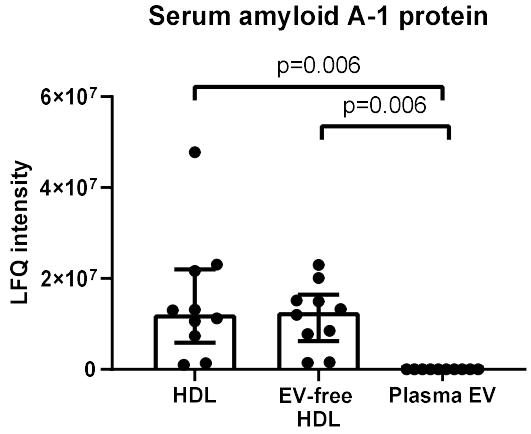

Figure 7-30 LFQ intensity of SAA1 in HDL, EV-free HDL and EV: Data is expressed as median±interquartile range. Friedman tests followed by post hoc Wilcoxon signed rank tests were carried out to compare LFQ intensity among HDL, EV-free HDL and EV. p<0.05 was taken as statistically significant.

There were 56 proteins found in both HDL and EV. Out of 56 proteins, 52 were proteins that were found in all three sample groups, while 4 proteins were found in HDL and EV, but not EV-free HDL. Proteins found in both HDL and EV, but not in EV-free HDL were adenylate cyclase type 1, fibrinogen γ chain, hemoglobin subunit ß and plasma protease C1 inhibitor. Fibrinogen γ chain, hemoglobin subunit ß and plasma protease C1 inhibitor had higher LFQ intensity in EV than those in HDL (Figure 7-31). There were no proteins found in EV-free HDL and EV, but not HDL (Figure 7-15).

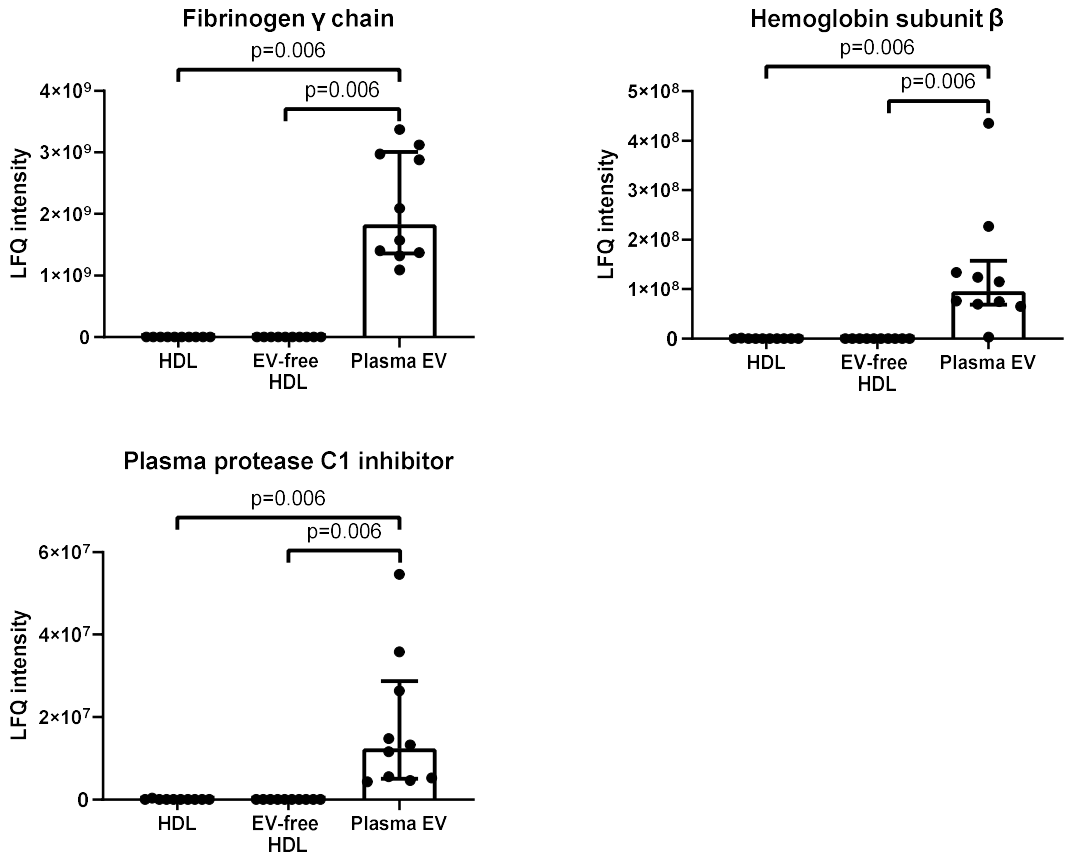

Figure 7-31 LFQ intensity of fibrinogen γ chain, hemoglobin subunit β and plasma protease C1 inhibitor in HDL, EV-free HDL and EV: Data is expressed as median±interquartile range. Friedman tests followed by post hoc Wilcoxon signed rank tests were carried out to compare LFQ intensity among HDL, EV-free HDL and EV. $p<0.05$ was taken as statistically significant.

7.3.3 Comparison of SAA1 concentration and PON1 activity in HDL, EV-free HDL and EV

SAA1 concentration and PON1 activity were determined in HDL (n=5), EV-free HDL (n=5) and EV (n=5). Mean SAA1 concentration in HDL, EV-free HDL and EV were 2936.88, 854.89 and 63.20 ng/mg HDL protein, respectively. SAA1 concentration in HDL was the highest, followed by those in EV-free HDL and EV (Figure 7-32). Mean PON1 activity in HDL samples was 7.23 U/mg HDL protein whereas PON1 activity in EV-free HDL and EV samples were below detectable range.

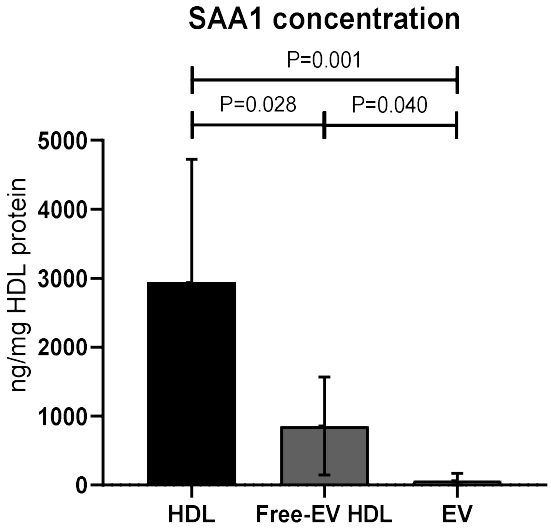

Figure 7-32 SAA1 concentration in HDL, EV-free HDL and EV: Data is expressed as mean±SD. Repeated measures ANOVA followed by *post hoc* Tukey test were carried out in square root transformed SAA1 concentration to compare SAA1 concentration among HDL, EV-free HDL and EV. $p<0.05$ was taken as statistically significant.

7.4 Discussion

In this chapter, the protocol to isolate HDL and EV separately from plasma was developed using the combination of SEC and density ultracentrifugation. The first step of isolating EV-free HDL was SEC. Particle size in 25 fractions of samples after SEC showed the largest particle size value in the first 3 fractions, gradually decreasing toward fraction 10 and remaining at plateau until the last fraction. This finding confirms the ability of the protocol to separate particles by size in which larger particles elute earlier than smaller particles. In the SEC protocol, Sepharose CL-2B was used as a stationary phase in chromatography. Sepharose CL-2B contains beads with approximately 75-nm pore (Böing et al. 2014). Therefore, theoretically, particles larger than 75 nm (EV) that cannot enter the pores elute earlier than particles smaller than 75 nm (HDL) that can enter the pores resulting in longer path length. The plateau line from fraction 10-25 may be due to limitation of nanoparticle tracking analysis that can only detect a particle larger than 70 nm.

Regarding the particle concentration distribution across all 25 fractions, the small proportion of particles observed in the first 6 fractions may be because

large particles such as apoptotic bodies (50 nm-2 μm) and microvesicle (100-1000 nm) that should be present in the early fraction were removed by centrifugation before adding samples to the SEC column. The largest amount of particles was in fractions 7-12. Measurement of particle concentration by nanoparticle tracking analysis detects any particles which are larger than 70 nm and therefore may include not only EV, but also chylomicron (100-500 nm), VLDL (30-80 nm) and protein aggregates. Together with protein concentration that is mostly present after fraction 12, the particles detected in fractions 7-12 are likely to be EV. On the other hand, apoA-I which is a marker of HDL particles was present mostly in fractions 14-23. This result is consistent with previous research by (Böing et al. 2014) who isolated EV by SEC using the same stationary phase (Sepharose CL-2B). In that study they confirmed the presence of EV in early SEC fractions by detection of EV markers such as CD9 and CD63 and visualisation by electron microscopy, and the bulk of protein and apoA-I appeared after fraction 10 (Böing et al. 2014; Karimi et al. 2018). Therefore, fractions 7-12 were chosen for EV collection and fractions 14-23 were chosen to collect HDL since this allowed high recovery of HDL with little contamination by EV.

When preparing fractions 14-23 for HDL isolation, the fractions were pooled and concentrated to decrease the volume to 500 μL. Almost all of apoA-I remained in the retentate after the concentrating step, illustrating the efficacy of this protocol to decrease the volume without losing apoA-I. Also, there was no benefit to conducting a second concentration step since no more apoA-1 was recovered. Therefore, a single concentration step with the centrifugal filter column was selected to reduce the volume of the pooled fraction, whilst recovering a high percentage of HDL. After SEC and the concentrating step, there was still a remarkable amount of apoB in pooled fractions 14-23. ApoB was further removed by ultracentrifugation. A two-step ultracentrifugation showed higher recovery of apoA-I and lower apoB contamination than the single step ultracentrifugation and was therefore chosen for the protocol.

The initial protocol of pre-centrifugation, SEC, single step concentration of the pooled fractions 14-23 and two-step ultracentrifugation showed a successful isolation of EV-free HDL with around 20% HDL recovery, however, percent recovery of HDL could be further improved. Comparison between HDL isolation

with and without centrifugation before SEC revealed a dramatic increase in apoA-I recovery of the HDL fraction using the protocol without a pre-spin compared to the protocol with a pre-spin. The reason for this difference may be that HDL particle was trapped in large apoptotic body and microvesicle pellets. Also, as the largest particles (apoptotic bodies and microvesicle) should elute in early fractions after SEC and not be carried through to fractions 14-23 used to collect HDL, this step is theoretically unnecessary. Therefore, centrifugation before SEC to remove apoptotic bodies and microvesicle was abolished from our protocol. Different initial volumes of plasma and the order of SEC and ultracentrifugation were also assessed. A starting volume of plasma (0.5 mL) and the use of SEC before ultracentrifugation showed the highest HDL recovery and were chosen to remain in the protocol.

After EV and EV-free HDL isolation protocol development and optimisation, the maximum apoA-I recovery was 39.8% with only 1.2% apoB contamination. This was achieved when 0.5 mL plasma was added to size-exclusion column without pre-centrifugation, followed by 1-time concentration, two-step ultracentrifugation and desalting. Thus, this protocol was chosen to isolate EV and EV-free HDL for further analysis of protein composition and comparison with HDL isolated by the gold standard method, sequential ultracentrifugation.

From the proteomic analysis, proteins found in EV only are likely to be EV-associated proteins. Most of proteins found in EV only were immune-related proteins such as immunoglobulin and complement proteins. This is reasonable since immunoglobulin and complement proteins are abundance in plasma. Even though these proteins have been found in HDL in many research including our study as shown in Chapter 3 and 4, contribution of these proteins to HDL function is still debatable. However, only four proteins were identified from the top 100 human EV proteins listed on EVpedia (Kim et al. 2015). These four proteins were α-2-macroglobulin, fibronectin, hemoglobin subunit α and galectin-3-binding protein. This finding suggests that although fractions 7-12 contained the highest particle concentration which are likely to be EV, a large proportion of other plasma proteins could also be identified in these fractions. This is consistent with a previous study of single-step SEC when using the same stationary phase as our experiment. This previous study showed the purest EV

resided in fraction 9. Adding fractions 10, 11 and 12 to fraction 9 increased EV recovery but may have decreased the purity (EV to protein ratio) (Böing et al. 2014).

Similarly, proteins found in the HDL fraction only are the most likely to be HDL-associated proteins and not contaminating EV proteins. These proteins were BPI fold-containing family B member 1, chorionic somatomammotropin hormone 2, hornerin, insulin-like growth factor-binding protein 3, L-selectin, lipopolysaccharide-binding protein, N-acetylmuramoyl-L-alanine amidase, SAA2, thymosin β4 and thyroxine-binding globulin. Most of these proteins, apart from chorionic somatomammotropin hormone 2 and insulin-like growth factor-binding protein 3, have been identified in at least three separate HDL proteomic studies, and are thus identified as HDL-associated proteins according to the HDL proteome watch database by the Davidson/Shah lab (Davidson S.). The two proteins that are not listed in the HDL proteome watch database could possibly be unique HDL protein components of pregnant women. Out of 45 articles in HDL proteome watch, there is only one study reporting HDL proteomic analysis of pregnant women. Some proteins may appear exclusively in HDL from pregnant women but not in HDL from non-pregnant population, thus do not meet the criterion of HDL-associated proteins by HDL proteome watch. For example, chorionic somatomammotropin hormone 2 is a hormone that is synthesized and secreted by the placenta so it is uniquely found in pregnant population and serum level of insulin-like growth factor-binding protein 3 has been found increased in pregnancy (Baxter and Martin 1986; Suikkari and Baxter 1991).

EV-free HDL and HDL had a similar protein composition with 72 out of 88 proteins overlapping. Among these 72 proteins, 38 proteins showed similar amounts between EV-free HDL and HDL. This illustrates the similarity of protein components of EV-free HDL and HDL. There were 34 out of 72 proteins distributed unevenly between EV-free HDL and HDL. Around 90% of these 34 proteins were significantly lower in EV-free HDL than those in HDL samples. Thus, these proteins could be more loosely attached to HDL than other proteins and thus loss from EV-free HDL isolated according to our protocol of SEC and ultracentrifugation, compared to HDL isolated by the gold standard.

There were 22 proteins found in all three fraction groups (HDL, EV-free HDL and EV) and were less abundant in EV-free HDL compared to HDL. These proteins were α-2-antiplasmin, α-1-acid glycoprotein 1, apoC-IV, apolipoprotein(a), ß-2-glycoprotein 1, apoA-IV, apoF, apoL-I, SAA4, PON1, apoB-100, vitronectin, clusterin, complement C4a, protein AMBP, complement C3, fibrinogen α and ß chain, haptoglobin, hemopexin, immunoglobulin λ-like polypeptide 5 and serotransferrin. These 22 proteins could be EV proteins contaminating HDL samples and were removed from EV-free HDL by the isolation protocol or they could be HDL proteins that are more loosely associated with the HDL particle and are lost during the isolation process of EV-free HDL. ApoB-100, vitronectin, clusterin, complement C4a, protein AMBP, complement C3, fibrinogen α and ß chain, haptoglobin, hemopexin, immunoglobulin λ-like polypeptide 5 and serotransferrin were significantly higher in the EV fraction than those in EV-free HDL. Moreover, clusterin and complement C3 were listed in the top 100 human EV proteins on EVpedia (Kim et al. 2015). This result suggests that these 12 proteins could be EV-associated proteins contaminating the HDL samples and could be subsequently removed from EV-free HDL by the isolation protocol. The rest of proteins, including α-2-antiplasmin, α-1-acid glycoprotein 1, apoC-IV, apolipoprotein(a), ß-2-glycoprotein 1, apoA-IV, apoF, apoL-I, SAA4 and PON1, were markedly lower or similar in EV compared to those in EV-free HDL. They have all been identified in at least three separate HDL proteomic studies, and are thus identified as HDL-associated proteins according to the HDL proteome watch database by the Davidson/Shah lab (Davidson S.). Decreased LFQ intensity of PON1 in EV-free HDL and EV compared to HDL was also confirmed by reduced PON1 activity in EV-free HDL and EV relative to that in HDL. These proteins are likely to be HDL-associated proteins that were lost during the isolation process of EV-free HDL.

There were only three proteins found in all three fraction groups (HDL, EV-free HDL and EV) and were less abundant in HDL compared to EV-free HDL: apoA-I, apoA-II and inter-α-trypsin inhibitor heavy chain H4. Inter-α-trypsin inhibitor heavy chain H4 was similarly abundant in EV-free HDL and EV, so it is undecidable whether it would be HDL or EV proteins. ApoA-I and apoA-II were markedly higher in HDL and EV-free HDL than those in EV thus these two proteins are most likely HDL-associated proteins. The more abundance apoA-I and apoA-II

in EV-free HDL compared to HDL may be due to EV-free HDL isolation protocol which was able to remove more of contaminating apoB and may improve recovery of apoA-I and apoA-II, the first and second abundant proteins in HDL.

There were 27 proteins found in all three fraction groups (HDL, EV-free HDL and EV) and were similarly abundant in HDL and EV-free HDL. Among these proteins, α-1-acid glycoprotein 2, α-1-antitrypsin, α-2-HS-glycoprotein, vitamin D-binding protein, angiotensinogen, apoC-I, apoC-II, apoC-III, apoD, apoM, retinal-binding protein 4, sorting nexin 29 and transthyretin were more abundant in HDL or EV-free HDL than EV. These proteins may be HDL-associated proteins. Most of these proteins, apart from retinal-binding protein 4 and sorting nexin 29, have been identified in at least three separate HDL proteomic studies, and are thus identified as HDL-associated proteins according to the HDL proteome watch (Davidson S.). Proteins that are not listed in the HDL proteome watch database could possibly be unique HDL protein components of pregnant women such as retinal-binding protein 4 in which its serum concentration increased from early to late pregnancy and was associated with a decrease in insulin sensitivity (Ueland et al. 2008). On the other hand, complement C4-B, Ig α-1 chain C region, Ig γ-1 chain C region, Ig κ chain C region and kininogen 1 were significantly more abundant in EV than HDL and EV-free HDL. Thus, these proteins may be EV proteins that were contaminated in HDL and EV-free HDL. Even though these proteins have all been identified in at least three separate HDL proteomic studies, and are thus identified as HDL-associated proteins according to the HDL proteome watch (Davidson S.), they were also identified in more than 100 EV high-throughput studies according to EVpedia (Kim et al. 2015).

Additionally, nine proteins were found in both EV-free HDL and HDL, but not EV, and were less abundant in EV-free HDL compared to HDL. These proteins were ß-2-microglobulin, cathelicidin antimicrobial peptide, CETP, PLTP, platelet basic protein, platelet factor 4, prenylcysteine oxidase 1, PON3 and LCAT. SAA1 was also found in both EV-free HDL and HDL, but not EV, according to proteomic analysis. Concentration of SAA1 was lower in EV-free HDL than that in HDL. These proteins reflect HDL proteins that are lost during the isolation process of EV-free HDL and are unlikely to be EV proteins. On the other hand, there were

fewer overlapping proteins of EV-free HDL and EV than those of HDL and EV (52 and 56 proteins). There were four proteins found in HDL and EV, but not EV-free HDL: adenylate cyclase type 1, fibrinogen γ chain, hemoglobin subunit ß and plasma protease C1 inhibitor. Fibrinogen γ chain, hemoglobin subunit ß and plasma protease C1 inhibitor were significant higher in EV than those in HDL. This suggests that these proteins may be EV proteins that were subsequently removed from EV-free HDL during processing. Even though these proteins have all been identified in at least three separate HDL proteomic studies, and are thus identified as HDL-associated proteins according to the HDL proteome watch (Davidson S.), they would also be identified as EV-associated proteins with the same criteria (Kim et al. 2015).

The strength of this study was the use of proteomic approach to identify potential EV or HDL protein contamination in each other fractions by comparing proteomic analysis of HDL and EV isolated by SEC and sequential ultracentrifugation with HDL isolated by the gold standard. Another strength was that HDL and EV isolated by SEC and sequential ultracentrifugation, and HDL isolated by the gold standard were from the same set of plasma sample. This developing HDL isolation protocol was able to remove some EV proteins from HDL sample. However, its weakness was that a number of essential HDL proteins lost from HDL during processing as well as HDL function such as PON1 activity. In summary, isolation of HDL by SEC followed by sequential ultracentrifugation was able to reduce EV protein contamination, but there was also a loss of HDL proteins. The result suggests that EV protein contamination in HDL which was removed by this isolation protocol were mostly immune-related proteins such as complement proteins and immunoglobulins, and other plasma proteins such as hemoglobin and fibrinogen. Whereas a lot of essential HDL proteins were lost from HDL particle during the isolation process of EV-free HDL, for example, apoC-IV, apoA-IV, PON1 and LCAT. It was decided for the samples in Chapter 3 and 4 of this thesis to use the gold standard of HDL isolation, used previously for proteomic analyses, instead of the method in this chapter due to this limitation of lost essential HDL proteins and limited availability of samples. The isolation method presented here requires to be developed to standardize/reduce the loss of essential HDL proteins before further use in future research. A focused analysis using ELISA and western blotting could be applied to determine where

these HDL proteins are lost during the isolation process. Another reason is that there is still a lack of evidence whether contaminated EV contributes to HDL properties and interferes with the outcome of other HDL's functional studies. Functional studies can be a crucial approach to determine quality of HDL isolated by different protocols, especially anti-inflammatory and immunomodulatory properties of HDL which could be changed or unchanged after removing contaminating EV proteins.

8 General Discussion

Preeclampsia is a vascular complication of pregnancy defined as the new onset of hypertension with proteinuria or end-organ dysfunction such as liver impairment, renal insufficiency or pulmonary edema which usually occurs after 20 weeks of gestation. Preeclampsia affects 2-8% of all pregnancies and contributes to 12% of maternal deaths. Various complications are associated with preeclampsia including preterm delivery, hemolysis, elevated liver enzymes, low platelet count (HELLP) syndrome, eclampsia and various organ dysfunctions. To date, there is still no definitive treatment for preeclampsia except to deliver the baby and placenta. Thus, it is important to understand the mechanisms underlying the pathophysiology of preeclampsia. Preeclampsia is thought to be mediated by abnormal placental development or placental malperfusion leading to enhanced oxidative stress and the release of antiangiogenic factors that disturb maternal endothelial function. There is also an atherogenic pattern of lipoproteins with decreased HDL concentration in preeclampsia. HDL is well-known for its ability to protect vascular function. In healthy pregnancy, there is an increase in plasma HDL concentration throughout gestation. Healthy pregnant women go through a physiological adaptation including increased insulin resistance and lipolysis, leading to high plasma glucose and lipid levels. There is also enhanced inflammation, coagulation and oxidative stress in late pregnancy. This unfavourable environment is known to lead to endothelial dysfunction in the non-pregnant population, however vascular function in healthy pregnant women appears to be enhanced. Based on the observation of increased HDL concentration in healthy pregnancy but a lack of an increase in HDL concentration in preeclampsia, it can be hypothesised that HDL could be a protective factor for vascular function in healthy pregnancy that fails in preeclampsia resulting in endothelial dysfunction.

The hypothesis of this thesis was that HDL in healthy pregnancy had a different protein and S1P/ceramide composition when compared to non-pregnant HDL and that the composition would suggest better HDL function in healthy pregnancy. The work presented in this thesis determined HDL composition throughout healthy pregnancy from before pregnancy to postpartum. Multivariate principal component analysis of proteins in HDL throughout gestation showed a continuous

change in HDL protein composition, from before pregnancy to the third trimester which reverted to the pre-pregnancy composition postpartum. The return to pre-pregnancy composition in the postpartum reflects that the compositional change of HDL is gestation-associated i.e., when no longer pregnant, they return to pre-pregnancy composition. There were 16 out of 63 HDL-associated proteins that showed significantly different concentration throughout pregnancy. These include changes that might confer enhanced core function of HDL in lipid metabolism, improved or reduced specific vasoprotective function of HDL, and changes that do not have much evidence on the impact on HDL function and possibly reflect contamination of plasma/EV proteins.

Changes in concentration of HDL proteins involved in lipid metabolism including apoC-II, apoC-III, apoC-IV and apoF are consistent with maternal lipid metabolism throughout gestation. Reduced apoC-III in the first trimester suggests reduced LPL inhibition and TRL uptake in adipose tissue, leading to enhanced triglyceride accumulation in maternal peripheral tissue in the first trimester. Later in pregnancy, the amount of HDL apoC-II, apoC-IV and the apoC-II/apoC-III ratio increased at 35 weeks of gestation which could promote maternal hyperlipidemia in late pregnancy. Reduced apoF during the second and third trimester could reduce plasma HDL concentration which was found in pregnant women after the peak of HDL concentration at around 20 weeks of gestation. ApoF is a CETP inhibitor. Reduced apoF may reduce the inhibition of CETP activity, leading to increased percent triglyceride content in HDL which facilitate HDL degradation and a decline in plasma HDL concentration. This proteomics data suggests a role for HDL in handling maternal adaptation of lipid metabolism. In early pregnancy, HDL might have reduced apoC-III to promote lipid accumulation, whereas in later pregnancy HDL apoC-II, apoC-IV and the apoC-II/apoC-III ratio increased to promote hyperlipidemia in order to provide sufficient lipid transport to fetus. ApoF may regulation CETP activity and triglyceride enrichment of HDL to regulate plasma HDL concentration in the third trimester.

Analysis of the proteomic dataset also revealed HDL composition in healthy pregnancy that might be associated with improved vascular protective function. This was indicated by increased HDL protein, S1P and ceramide content that has

previously been shown to be associated with better HDL function. Increased A1AT observed in the first trimester may protect the RCT function of HDL from protease-induced deterioration. During Th1 inflammatory state in the first trimester, serine proteases such as neutrophil elastase are released in response to inflammatory stimuli. They have been shown to impair RCT. Incubation of macrophages isolated from neutrophil elastase-deficient mice with exogenous neutrophil elastase resulted in reduced cholesterol efflux from macrophages to apoA-I (Wen et al. 2018). A1AT has an anti-elastase activity and binding of A1AT to HDL protected anti-elastase activity of A1AT from oxidative deterioration *in vitro* (Gordon et al. 2015). Thus, increased HDL-A1AT content could contribute to enhanced anti-elastase activity and protect HDL's RCT function from protease-induced deterioration in theTh1 inflammatory state in early pregnancy. The increase in HDL-A1AT occurred at 8.4 weeks of gestation before the establishment of the placental circulation which is inconsistent with my hypothesis that HDL protein composition begins to change at around 10-13 weeks of gestation when the maternal-fetal circulation is fully established. A1AT is synthesized by hepatocytes, and it could be that the liver is responsible for HDL protein changes during the first trimester.

Direct apoA-I quantification showed increased apoA-I concentration during the second and third trimester of pregnancy. Whereas LFQ intensity of apoA-I which represents the quantity of apoA-I in the specific amount of total HDL protein did not differ throughout gestation. Direct quantification of apoA-I may be more accurate than proteomics data as it provided an exact concentration. Nonetheless, it remains uncertain whether increased apoA-I concentration in the second and third trimester suggests improved efficacy of HDL function (RCT, vasodilation and antioxidant activity). HDL is a heterogenous collection of various proteins, lipids and physiochemical compositions i.e., particle size, particle density and function [reviewed in (Kunitake, O'Connor, and Naya-Vigne 1996)]. All HDL particles are not identical and have various abundance of apoA-I per HDL particle. Thus, apoA-I measurement does not directly represent HDL particle number. It may be implied from increased apoA-I concentration that overall HDL function increased during pregnancy, but it could result from either increased HDL particle number or improved efficacy of HDL particle. Increased apoA-I synthesis in the liver can be the effect of estrogen which continuously

increases during gestation and is related to hepatic production of nascent HDL. Also, the time plasma HDL and apoA-I concentration begins to increase, which is around 10-13 weeks of gestation, is the time when the placental circulation is fully established. It was previously shown by Melhem et al. in 2019 that there were significant amounts of apoA-I secreted from the maternal side of placenta estimated in human perfused placenta and primary trophoblast cell culture (Melhem et al. 2019). Thus, it is also possible that, in addition to the liver, fully formed placenta contributes to HDL concentration in healthy pregnancy.

S1P content in HDL which has an established vasodilatory and anti-inflammatory function increased during the second and third trimester. Moreover, the majority of ceramide species including ceramide C18:0, C20:0, C22:0, C24:1 which promote HDL-mediated RCT and are involved in the vasodilatory function of HDL, increased in HDL of pregnant women in the second and third trimester. Changes of S1P and ceramide in HDL suggest improved RCT, vasodilatory and anti-inflammatory function in the second and third trimester. The source of HDL-S1P could be hepatocytes where HDL synthesis mainly occurs, and blood cells and endothelial cells where HDL may acquire S1P during circulation. ApoM also promotes S1P efflux from erythrocytes. It was shown here that apoM concentration and the S1P to apoM ratio did not differ throughout gestation, even though S1P concentration increased. This may indicate a trend towards higher apoM concentration during pregnancy which could promote S1P abundance in HDL. While ceramide is secreted from the liver with VLDL and LDL, and may be acquired by HDL in the circulation [reviewed in (Patanapirunhakit et al. 2021)]. Ideally, examination of S1P and ceramide content as well as sphingolipid synthesis enzyme gene expression in the liver of pregnant women would be useful to understand the source of S1P and ceramide in HDL in healthy pregnancy. However, liver biopsy is considered a high-risk intervention, particularly in pregnant women. It has been shown that the gene expression of long chain polyunsaturated fatty acid (LC-PUFA) synthesis enzyme in SAT reflects that in the liver (Mackay et al. 2012). Erythrocyte LC-PUFA concentration was lower in preeclampsia compared to healthy pregnancy. There was no difference in LC-PUFA content in SAT between preeclampsia and healthy pregnancy that could explain lower erythrocyte LC-PUFA concentration. However, there was lower expression of the LC-PUFA synthesis enzyme gene in SAT of preeclampsia.

SAT may not be a major site for LC-PUFA synthesis, but the gene expression in SAT may reflect other potential sites of synthesis i.e., the liver. Therefore, SAT which is more accessible in pregnant women undergoing caesarean section was chosen as a surrogate for the liver in this thesis. The gene expression of sphingolipid synthesis enzymes in SAT of pregnant women favoured reduced ceramide production in adipose tissue but SAT may be a poor surrogate of the liver for this species of lipid, therefore, it is still undetermined whether the liver is the source of sphingolipid in HDL of pregnant women or not. It is also unlikely for placenta to be the main source of sphingolipid in HDL in pregnancy as there was no significance difference between sphingolipid synthesis gene expression in placenta of preeclampsia and healthy pregnancy as presented in this thesis in the presence of a known increase in plasma ceramide concentration in preeclampsia, compared to healthy pregnancy (Melland-Smith et al. 2015; Charkiewicz et al. 2017; Dobierzewska et al. 2017).

There were also protein changes that might suggest reduced HDL function during pregnancy. Decreased PON3, an antioxidant enzyme, in the second and third trimester suggests reduced antioxidant properties of HDL, which could enhance oxidative stress in late pregnancy. Oxidative stress was reflected in an increased ratio of oxidised to non-oxidised Met136 of apoA-I at postpartum, as HDL uses the methionine residues of apoA-I to redox-inactivate ROS which increases in late pregnancy. Reduced anti-oxidative activity of HDL could then be compensated by decreased prenylcysteine oxidase 1, a pro-oxidant enzyme, at postpartum. Proteomic data showed increased SAA1 and decreased apoA-IV at 8.4 weeks of gestation which are consistent with the Th1 inflammatory state in the first trimester. However, HDL proteomic analysis is a semi-quantitative measurement and the quantitative study of SAA1 in HDL by ELISA showed no significant change of SAA1 concentration throughout gestation. It can be interpreted that SAA1 protein level relative to all HDL proteins increased, but not the actual SAA1 concentration. Considering that HDL SAA1 concentration did not change throughout gestation, it may not have a role in enhancing Th1 dominance in the first trimester. Decreased secretion of apoA-IV which is a negative acute-phase-response protein from the liver could be induced by inflammatory stimuli increasing during the first trimester. Decreased apoA-IV can be a bystander from enhanced inflammation or its decrease can suggest

reduced anti-inflammatory function of HDL and role of HDL in enhancing inflammatory status in the first trimester.

Some of the observed changes in HDL protein composition may reflect bystander proteins, since HDL has a scavenger role and may pick up proteins that were prevalent in plasma during pregnancy (Kontush et al. 2015). Increased HDL angiotensinogen during pregnancy may be due to this role of HDL. Angiotensinogen is a precursor of angiotensin which causes vasoconstriction. There was no evidence suggesting a role for angiotensinogen in HDL function and angiotensin was not found in pregnant HDL proteome. There was increased plasma angiotensinogen concentration in pregnant women (Baker, Broughton Pipkin, and Symonds 1990). It may be that HDL acquired angiotensinogen because angiotensinogen was prevalent in plasma during pregnancy. Moreover, fibrinogen α and ß chain and vitronectin might be considered as EV proteins since these proteins were prominent in the EV fraction rather than EV-free HDL fraction isolated by SEC and sequential ultracentrifugation. These proteins may be contaminated in the HDL fractions of this pregnancy study which was isolated from plasma by sequential ultracentrifugation only.

After looking at the changes in HDL composition during healthy pregnancy, I then went on to compare HDL protein composition between early- or late-onset preeclampsia with gestational-age-matched healthy pregnancy controls. HDL proteins that showed differences in concentration between early-onset preeclampsia and their matched control, and late-onset preeclampsia and its matched control, were completely separate groups. ApoA-IV and L-selectin specifically decreased in HDL of early-onset preeclampsia. ApoA-IV is a negative acute-phase-response protein, thus apoA-IV synthesis by the liver could be reduced by increasing inflammatory stimuli in preeclampsia. Reduced apoA-IV may suggests reduced anti-inflammatory function of HDL in early-onset preeclampsia. L-selectin may be in less abundance in the circulation of women with early-onset preeclampsia as there were reduced L-selectin in HDL. Another study found lower surface L-selectin on neutrophils in preeclampsia (Sacks et al. 1998). However, increased L-selectin expression has previously been identified in placenta of early-onset preeclampsia (Mistry et al. 2020). These findings

suggest a role for L-selectin in inducing inflammation in early-onset preeclampsia through its placental expression rather than in HDL.

There was a change in only a small number of HDL proteins specific to early-onset preeclampsia, but the change is consistent with current understanding of the pathophysiology of early-onset preeclampsia which tends to associate with placental impairment. Both early- and late-onset preeclampsia are associated with maternal systemic inflammation, but it seems that only early-onset preeclampsia is associated with altered placental immune system and inflammation. There were reduced gene expression of complement, mast cells and macrophages in early-onset preeclampsia compared to healthy placentas while late-onset preeclampsia placentas did not show any immune-related gene expression differences compared to healthy controls (Broekhuizen et al. 2021). There was increased gasdermin D expression, a marker of inflammatory cell death pathway, in early-onset preeclampsia placenta as well as in autophagy-deficient human trophoblasts treated with serum from early-onset preeclampsia (Cheng et al. 2019). In contrast, there was no difference in placental gasdermin D expression between late-onset preeclampsia and healthy control (Cheng et al. 2019). Placental inflammation in early-onset preeclampsia may contribute to systemic inflammation. It should be noted that comparison of early-onset preeclampsia with gestational-age-matched controls was carried out to avoid the confounding factor of gestational age which has an impact on HDL protein composition. The gestation-matched control cohort of early-onset preeclampsia may not be strictly healthy as it included pregnant women with preterm delivery (before 37 weeks of gestation). Preterm delivery is also associated with placental inflammation. Chorioamnionitis, a clinical equivalent of placental inflammation, was more frequent in preterm labor than in term labor (Khong et al. 2016; Lee et al. 2013). Placental inflammation demonstrated in early-onset preeclampsia study may reflect the pathology of preterm delivery as well as early-onset preeclampsia.

HDL proteins that showed differences in concentration specifically between late-onset preeclampsia and their controls were BPI fold-containing family B member 1, protease C1 inhibitor and myosin-9. These are proteins involved in the innate immune response or complement activation but there is no evidence of the

impact of these proteins on HDL function. These proteins may be plasma proteins that HDL acquires in the circulation. Also, protease C1 inhibitor was more abundant in plasma EV than EV-free HDL and is likely to be EV protein. HDL in this preeclampsia study was isolated by ultracentrifugation and may include EV protein i.e., protease C1 inhibitor in HDL fraction. This work showed no evidence, from the protein composition, of improved or reduced HDL function in pathophysiology of late-onset preeclampsia. Late-onset preeclampsia tends to result from maternal underlying diseases that predispose to vascular insufficiency and leans toward a normal placenta size and function. It may be that the pathophysiology of late-onset preeclampsia is heterogenous. If reduced HDL function is one of the maternal pre-disposing factors that causes vascular insufficiency and preeclampsia, larger sample size would be needed to detect significant differences among the various underlying conditions that impair vascular function.

There were proteins that differed in their concentration in HDL in both early- or late-onset preeclampsia compared to controls and also when the data were analysed as a combined preeclampsia group compared to their combined healthy pregnancy controls. There is less confidence in identifying whether these proteins might be associated specifically with the pathophysiology of early- or late-onset preeclampsia. Rather, they could be affected by preeclampsia *per se*. Among these proteins, it is likely that Rap-1b, complement factor D, complement C9 and prothrombin are EV-associated proteins which contaminate the HDL sample. Reduced antithrombin-III and ß-2-glycoprotein 1 suggest both pro- and anti-thrombotic effect of HDL in preeclampsia. These changes may reflect a generalised influence of preeclampsia on the coagulation cascade and blood clotting.

Having established that there are gestational and early onset pre-eclampsia associated changes in HDL composition, the next step would be to assess HDL function. In the current study, this was done to a limited extent using the PON1 and SAA1 assay. It was shown that HDL PON1 arylesterase activity did not change throughout gestation and between early- or late-onset preeclampsia with controls. This is consistent with PON1 content (LFQ intensity) observed here which did not differ throughout gestation and in preeclampsia, suggesting

unaltered PON1 activity in hydrolysing phenyl acetate in pregnancy and preeclampsia. Other research showed similar results that PON1 activity in plasma measured by paraoxon hydrolysis rates did not change during pregnancy (Stefanović et al. 2012). Whereas a longitudinal study of plasma PON1 activity measured by diazoxon hydrolysis rates, showed significantly decreased activity in the third trimester compared to the first and second trimester (Stefanović et al. 2012). Other studies in preeclampsia showed lower PON1 activity in serum of preeclampsia than in healthy pregnancy (Genc et al. 2011; Al-Kuraishy, Al-Gareeb, and Al-Maiahy 2018). This heterogeneity in findings may be due to different PON1 enzyme activities towards different substrates measured in the studies. Phenyl acetate used to assay PON1 activity in this thesis has higher rate of hydrolysis than paraoxon. When store at -80ºC, PON1 activity toward phenyl acetate are more stable than paraoxon but less stable than diazoxon [reviewed in (Ceron, Tecles, and Tvarijonaviciute 2014)]. It would be difficult to compare data from different laboratory settings and to interpret overall PON1 activity. I further determined SAA1 concentration to PON1 activity ratio which is proposed to be a marker of dysfunctional HDL. This ratio increased at postpartum and could suggest dysfunctional HDL (reduced anti-inflammatory and antioxidant properties) after delivery relative to functional HDL during healthy pregnancy. Currently, clinical studies have shown a promising role of this ratio in clinical practice. Patients with morbid obesity showed higher SAA1 to PON1 ratio than non-obese controls, and the ratio decreased after life-style modification and bariatric surgery (Kjellmo et al. 2018). More research is required to verify the use of this ratio as a biomarker. This ratio did not differ in preeclampsia and may not be a good marker for diagnosis or clinical evaluation of preeclampsia. It would be better to directly measure HDL function in healthy pregnancy and preeclampsia.

It would be important to examine the vasodilatory, anti-thrombotic, RCT, anti-inflammatory and antioxidant functions of HDL in healthy pregnancy and preeclampsia using additional assays as composition analysis suggested changes in these HDL functions. Accordingly, in this thesis, I developed an HDL functional assay in vascular reactivity of human pregnant arteries using wire myography and an assay to determine anti-clotting potential of HDL. The wire myography protocol presented in this thesis was able to examine HDL effects on the

vasoconstriction of pregnant VAT arteries. However, because vessels contracted to the maximum dose of noradrenaline did not maintain contraction, the vasodilatory response could not be assessed. This wire myography protocol should be further developed since the changes of HDL protein and S1P observed here suggest improved vasodilatory effect of HDL in pregnancy. Wire myography could provide an insight into a direct HDL effect on arteries as an *ex vivo* assay. There should be systematic optimisation of wire myography protocol from tissue collection, vascular dissection, HDL incubation, and types of vasoconstrictors and vasodilators. Histological analysis of isolated arteries should also be carried out to confirm the presence of endothelial cells. It would be ideal to test pregnant HDL effects on pregnant vessels since such vessels will have undergone vascular adaptation to pregnancy and therefore will differ in structure and function from vessels from non-pregnant individual. Non-pregnant human vessels could also be assessed using this protocol to examine the effect of pregnant HDL on them. Access to non-pregnant human tissue could be achieved through general surgery.

An anti-thrombotic functional assay of HDL was also developed in this thesis. However, it was demonstrated that trace NaBr carried over from the HDL isolation process inhibited thrombin production in the assay, which reduces confidence in the results generated. Changes of HDL proteins (antithrombin-III and ß-2-glycoprotein 1) observed in this thesis suggest altered anti-clotting effect of HDL in preeclampsia. It would be worth finding an alternative protocol to isolate HDL for this assay. Iodixanol may be useful as an alternative to create a step density for HDL isolation protocol since it produces iso-osmotic solution at all densities, is non-toxic to cells and non-inhibitory to enzymes (Ford, Graham, and Rickwood 1994; Harman, Griffin, and Davies 2013).

Increased HDL-mediated RCT in pregnancy has already been demonstrated. Previous studies show there was increased cholesterol efflux from primary human trophoblasts to apoA-I obtained from pregnant women with supraphysiological hypercholesterolemia (total cholesterol≥280 mg/dL) relative to those with physiological hypercholesterolemia (total cholesterol<280 mg/dL), despite similar ABCA1 expression on the trophoblasts (Fuenzalida et al. 2020). There was also increased cholesterol efflux to apoA-I from endothelial cells

obtained from human term placenta compared to cholesterol efflux from HUVEC (Stefulj et al. 2009). HDL-mediated RCT is further enhanced in preeclampsia as demonstrated by increased cholesterol efflux from macrophage to apoB-depleted plasma obtained from preeclampsia compared to the efflux to apoB-depleted plasma from healthy pregnancy (Mistry et al. 2017). These findings suggest enhanced RCT function of HDL in pregnancy and preeclampsia to counter increased cholesterol availability and prevent excessive lipid peroxidation. It would be useful to set up HDL-mediated cholesterol efflux assay from macrophage and endothelial cells that represent maternal systemic vessels such as SAT arteries. These two cell types are essential in regulating cholesterol metabolism through RCT and affecting maternal endothelial function.

An anti-inflammatory assay could be developed in a cell culture assay. HDL exerts its anti-inflammatory effect by inhibiting TNFα-induced endothelial expression of VCAM-1 via apoA-I-SR-B1 interaction and S1P-S1PR1 interaction [reviewed in (Beazer et al. 2020)]. Also, HDL reduces secretion of VCAM-1 through apoA-I and apoA-IV, as demonstrated by reduced VCAM-1 concentration in conditioned medium of TNFα-treated HUVEC after incubation with synthetic HDL containing apoA-I or apoA-IV (Gomaraschi et al. 2010). By pre-incubating endothelial cells with HDL and then incubating this cell culture with TNFα to stimulate VCAM-1 expression, endothelial expression of VCAM-1 can be measured in cell lysate by western blot or flow cytometry, and soluble VCAM-1 levels can be measured in cell medium by ELISA to determine HDL ability in inhibiting TNFα-induced VCAM-1 expression (Lemmers et al. 2021; Gomaraschi et al. 2010). This assay could be used to compare the effect of HDL from pregnant versus non-pregnant women and HDL from preeclampsia versus healthy pregnancy in inhibiting TNFα-induced VCAM-1 expression. It could provide an insight into how increased apoA-I and S1P in pregnant HDL and reduced apoA-IV in early-onset preeclampsia affect HDL anti-inflammatory function.

It was observed in HDL protein composition analysis here that antioxidant effect of HDL may reduce in late pregnancy, so it would be interesting to determine this HDL function in pregnancy. Antioxidant property of HDL includes the ability of HDL to remove oxidants from cells and to inactivate them. The ability of HDL from pregnant women in removing ROS from cells could be tested by incubation

of oxidative-induced endothelial cells with HDL and measurement of ROS such as lipid hydroperoxides in cells, culture media and HDL (Ferretti et al. 2003). Copper ions are commonly used to induce ROS formation and stimulate oxidation in cells. Copper-induced oxidation of endothelial cells will then be incubated with HDL to exert antioxidant effect of HDL on the cells. The ability of HDL in removing ROS from cells will be reflected in ROS level in which the decrease in cells, increase in HDL and unchange in culture media suggest ROS transfer from cells to HDL. In part of HDL ability to inactivate ROS, I found unchanged PON1 activity throughout gestation, reduced HDL PON3 content in late pregnancy and increased oxidised Met136 at postpartum which suggest reduced HDL ability to inactivate ROS during late pregnancy to postpartum. Total ROS content in the co-incubation of oxidative-induced cells/LDL and HDL over time can reflect antioxidant effect of HDL when compared to the incubation in the absence of HDL (Mackness, Arrol, and Durrington 1991). Antioxidant function of HDL from pregnant and non-pregnant HDL can be compared using this model.

It is also important to determine the effect of HDL from healthy pregnancy and preeclampsia on NO production as NO is the center of HDL function. The ability of HDL in promoting NO production contributes to vasodilatory and anti-inflammatory effect and NO bioavailability can be reduced by enhanced oxidative stress. By incubation of endothelial cells with HDL from healthy pregnancy or preeclampsia, the impact of HDL on NOS enzymatic activity and NO production can be examined. NOS activity could be determined by measuring the conversion of L-arginine to L-citrulline in cell lysates (Kimura et al. 2006). NO production in endothelial cells could be evaluated using a fluorescent marker to indicate NO in cells and then cell imaging techniques i.e., confocal microscopy to collect cell images in which NO-sensitive fluorescence can be quantified (Morrow et al. 2003). NO release from endothelial cells could also be examined by quantifying NO content in cell media using NO-specific chemiluminescence (Morrow et al. 2003).

This thesis is the first longitudinal proteomic analysis of HDL in healthy pregnancy from pre-pregnancy to postpartum and also the first HDL proteomic study in preeclampsia. The longitudinal study throughout healthy pregnancy allowed the investigation of how and when HDL composition changes throughout

gestation. Moreover, HDL data of early- or late-onset preeclampsia relative to gestational-age-matched healthy pregnancy provides insights into how HDL composition changes differently between early- and late-onset preeclampsia. The proteomic approach is a semi-quantitative measurement that gave a relative level of protein to all proteins in the samples in term of LFQ intensity. The data should be analysed and interpreted with caution as the identification and quantification of minor proteins can be interfered by the presence of higher abundance proteins (such as apoA-1 which is 70% of HDL protein), so some minor protein may not have been detected by the proteomic approach [reviewed in (Chandramouli and Qian 2009)]. Any HDL protein of interest identified from proteomic data i.e., apoA-IV should be quantified using quantitative techniques such as western blot and ELISA.

My observations provide evidence for a potentially improved HDL function in healthy pregnancy and reduced HDL function in preeclampsia. Confirmation of dysfunctional HDL in preeclampsia may suggest potential novel curative treatments for preeclampsia. The rHDL has been developed to replicate HDL function and could be used to improve and prevent vascular impairment in preeclampsia. Various types of rHDL formed by apoA-I complexed with phospholipids have altered biological activities, for example, wild type apoA-I-containing rHDL has been shown to has increased efficacy of RCT and anti-inflammatory functions [reviewed in (Vucic and Rosenson 2011)]. Several apoA-I derived rHDL are being developed as promising novel treatment of cardiovascular disease in human. For example, infusion of ETC-216, a complex of apoA-I milano (a mutant form of human apoA-I) and 1-palmitoyl-2-oleoyl-sn-glycero-3-phosphocholine, in patients with acute coronary syndrome resulted in reduced atheroma volume (Nissen et al. 2003). Single intravenous infusion of the rHDL CSL-111 (human apoA-I-phosphatidylcholine complex) in patients with peripheral artery disease led to reduced plaque lipid content and VCAM-1 expression (Shaw et al. 2008). CSL-111 may be suitable to counteract potential reduced anti-inflammatory function of HDL in early-onset preeclampsia by given in high-risk pregnant women to prevent the development of preeclampsia or given in preeclampsia to improve endothelial function. However, adverse effects are a concerned as high dose CSL-111 (40 mg/kg) administration was associated with liver function test abnormality (transaminase elevation) (Tardif et al.

2007). Further clinical trials are required to confirm this clinical impact. The clinical endpoint of mortality, morbidity and adverse effect of rHDL are yet to be elucidated in order to establish rHDL therapy in humans [reviewed in (Cao et al. 2017)].

In summary, preeclampsia is a serious complication of pregnancy which contributes to 12% of maternal deaths worldwide and is associated with many maternal and fetal complications. Presently, there is no curative treatment for preeclampsia apart from delivery of the baby. Thus, it is essential to understand the underlying causes of preeclampsia and develop new treatments for this condition or prevent it developing in the first place.

Appendices

Chapter 5:

Included and Excluded artery segments in study of pregnant and non-pregnant HDL effect on vascular tone using wire myograph

Sample ID	Incubation media	VAT artery (segments)		
		Total	Excluded	Included
PP02	Pregnant HDL	4	1 (ΔP<2.1 kPa) 1 (ΔP<2.1 kPa, ΔT<0.4 mN/mm)	2
	Non-pregnant HDL	4	2 (ΔP<2.1 kPa, ΔT<0.4 mN/mm)	2
	PSS	-	-	-
PP03	Pregnant HDL	3	-	3
	Non-pregnant HDL	3	-	3
	PSS	2	-	2
PP04	Pregnant HDL	2	2 (not response to KPSS)	-
	Non-pregnant HDL	1	1 (not response to KPSS)	-
	PSS	-	-	-
PP05	Pregnant HDL	3	1 (ΔP<2.1 kPa, ΔT<0.4 mN/mm)	2
	Non-pregnant HDL	3	-	3
	PSS	2	1 (not response to KPSS) 1 (ΔP<2.1 kPa, ΔT<0.4 mN/mm)	-
PP06	Pregnant HDL	3	-	3
	Non-pregnant HDL	3	-	3

	PSS	2	-	2
PP07	**Pregnant HDL**	2	-	2
	Non-pregnant HDL	2	-	2
	PSS	-	-	-
PP09	**Pregnant HDL**	1	-	1
	Non-pregnant HDL	2	-	2
	PSS	1	-	1
PP12	**Pregnant HDL**	3	-	3
	Non-pregnant HDL	3	2 ($\Delta P<2.1$ kPa, $\Delta T<0.4$ mN/mm)	1
	PSS	2	-	2
PP13	**Pregnant HDL**	3	1 ($\Delta P<2.1$ kPa) 2 ($\Delta P<2.1$ kPa, $\Delta T<0.4$ mN/mm)	-
	Non-pregnant HDL	3	-	3
	PSS	2	-	2
Total		**59**		**44**

List of References

Aalkjaer, C., and M. J. Mulvany. 1981. 'Functional and morphological properties of human omental resistance vessels', *Blood Vessels*, 18: 233-44.

Acton, Susan, Attilio Rigotti, Katherine T. Landschulz, Shangzhe Xu, Helen H. Hobbs, and Monty Krieger. 1996. 'Identification of Scavenger Receptor SR-BI as a High Density Lipoprotein Receptor', *Science*, 271: 518-20.

Actor, Jeffrey K. 2019. 'Chapter 1 - A Functional Overview of the Immune System and Immune Components.' in Jeffrey K. Actor (ed.), *Introductory Immunology (Second Edition)* (Academic Press).

Ahmed, A, DJ Williams, V Cheed, LJ Middleton, S Ahmad, K Wang, AT Vince, P Hewett, K Spencer, KS Khan, JP Daniels, and the StAmP trial Collaborative Group. 2020. 'Pravastatin for early-onset pre-eclampsia: a randomised, blinded, placebo-controlled trial', *BJOG: An International Journal of Obstetrics & Gynaecology*, 127: 478-88.

Al-Kuraishy, Hayder M., Ali I. Al-Gareeb, and Thabat J. Al-Maiahy. 2018. 'Concept and connotation of oxidative stress in preeclampsia', *J Lab Physicians*, 10: 276-82.

Alam, J., and A. Smith. 1992. 'Heme-hemopexin-mediated induction of metallothionein gene expression', *Journal of Biological Chemistry*, 267: 16379-84.

Allan, C. M., and J. M. Taylor. 1996. 'Expression of a novel human apolipoprotein (apoC-IV) causes hypertriglyceridemia in transgenic mice', *J Lipid Res*, 37: 1510-8.

Altmäe, Signe, Mariann Koel, Urmo Võsa, Priit Adler, Marina Suhorutšenko, Triin Laisk-Podar, Viktorija Kukushkina, Merli Saare, Agne Velthut-Meikas, Kaarel Krjutškov, Lusine Aghajanova, Parameswaran G. Lalitkumar, Kristina Gemzell-Danielsson, Linda Giudice, Carlos Simón, and Andres Salumets. 2017. 'Meta-signature of human endometrial receptivity: a meta-analysis and validation study of transcriptomic biomarkers', *Scientific Reports*, 7: 10077.

Altruda, F., V. Poli, G. Restagno, P. Argos, R. Cortese, and L. Silengo. 1985. 'The primary structure of human hemopexin deduced from cDNA sequence: evidence for internal, repeating homology', *Nucleic Acids Res*, 13: 3841-59.

Alvarez, J. J., A. Montelongo, A. Iglesias, M. A. Lasunción, and E. Herrera. 1996. 'Longitudinal study on lipoprotein profile, high density lipoprotein subclass, and postheparin lipases during gestation in women', *Journal of Lipid Research*, 37: 299-308.

American College of Obstetricians and Gynecologists, Task force on hypertension in pregnancy 2013. "Hypertension in pregnancy, pregnancy-induced hypertension practice guideline." In.

Anagnostis, P., J. C. Stevenson, D. Crook, D. G. Johnston, and I. F. Godsland. 2015. 'Effects of menopause, gender and age on lipids and high-density lipoprotein cholesterol subfractions', *Maturitas*, 81: 62-8.

And, K. Dalaker, and H. Prydz. 1984. 'The coagulation factor VII in pregnancy', *Br J Haematol*, 56: 233-41.

Argraves, K. M., P. J. Gazzolo, E. M. Groh, B. A. Wilkerson, B. S. Matsuura, W. O. Twal, S. M. Hammad, and W. S. Argraves. 2008. 'High density lipoprotein-associated sphingosine 1-phosphate promotes endothelial barrier function', *J Biol Chem*, 283: 25074-81.

Argraves, Kelley M., Amar A. Sethi, Patrick J. Gazzolo, Brent A. Wilkerson, Alan T. Remaley, Anne Tybjaerg-Hansen, Børge G. Nordestgaard, Sharon D. Yeatts, Katherine S. Nicholas, Jeremy L. Barth, and W. Scott Argraves. 2011. 'S1P, dihydro-S1P and C24:1-ceramide levels in the HDL-containing fraction of serum inversely correlate with occurrence of ischemic heart disease', *Lipids in Health and Disease*, 10: 70-70.

Arnhold, Jürgen. 2020. 'Chapter 7 - Acute-Phase Proteins and Additional Protective Systems.' in Jürgen Arnhold (ed.), *Cell and Tissue Destruction* (Academic Press).

Ashby, Dale T., Kerry-Anne Rye, Moira A. Clay, Mathew A. Vadas, Jennifer R. Gamble, and Philip J. Barter. 1998. 'Factors Influencing the Ability of HDL to Inhibit Expression of Vascular Cell Adhesion Molecule-1 in Endothelial Cells', *Arteriosclerosis, Thrombosis, and Vascular Biology*, 18: 1450-55.

Ashworth, J. R., A. Y. Warren, P. N. Baker, and I. R. Johnson. 1996. 'A comparison of endothelium-dependent relaxation in omental and myometrial resistance arteries in pregnant and nonpregnant women', *Am J Obstet Gynecol*, 175: 1307-12.

Asselbergs, F. W., S. M. Williams, P. R. Hebert, C. S. Coffey, H. L. Hillege, G. Navis, D. E. Vaughan, W. H. van Gilst, and J. H. Moore. 2007. 'Gender-specific correlations of plasminogen activator inhibitor-1 and tissue plasminogen activator levels with cardiovascular disease-related traits', *J Thromb Haemost*, 5: 313-20.

Atkins, A. F., J. M. Watt, P. Milan, P. Davies, and J. S. Crawford. 1981. 'A longitudinal study of cardiovascular dynamic changes throughout pregnancy', *Eur J Obstet Gynecol Reprod Biol*, 12: 215-24.

Aviram, M., E. Hardak, J. Vaya, S. Mahmood, S. Milo, A. Hoffman, S. Billicke, D. Draganov, and M. Rosenblat. 2000. 'Human serum paraoxonases (PON1) Q and R selectively decrease lipid peroxides in human coronary and carotid atherosclerotic lesions: PON1 esterase and peroxidase-like activities', *Circulation*, 101: 2510-7.

Axler, O., J. Ahnström, and B. Dahlbäck. 2007. 'An ELISA for apolipoprotein M reveals a strong correlation to total cholesterol in human plasma', *J Lipid Res*, 48: 1772-80.

Aydın, Seval, Ali Benian, Riza Madazli, Seyfettin Uludağ, Hafize Uzun, and Safiye Kaya. 2004. 'Plasma malondialdehyde, superoxide dismutase, sE-selectin, fibronectin, endothelin-1 and nitric oxide levels in women with preeclampsia', *European Journal of Obstetrics & Gynecology and Reproductive Biology*, 113: 21-25.

Bagot, C. N., E. Leishman, C. C. Onyiaodike, F. Jordan, and D. J. Freeman. 2017. 'Normal pregnancy is associated with an increase in thrombin generation from the very early stages of the first trimester', *Thromb Res*, 157: 49-54.

Bagot, C. N., E. Leishman, C. C. Onyiaodike, F. Jordan, V. B. Gibson, and D. J. Freeman. 2019. 'Changes in laboratory markers of thrombotic risk early in the first trimester of pregnancy may be linked to an increase in estradiol and progesterone', *Thromb Res*, 178: 47-53.

Bailey, Liane Jennifer, Sruthi Alahari, Andrea Tagliaferro, Martin Post, and Isabella Caniggia. 2017. 'Augmented trophoblast cell death in preeclampsia can proceed via ceramide-mediated necroptosis', *Cell Death & Disease*, 8: e2590-e90.

Baker, P. N., F. Broughton Pipkin, and E. M. Symonds. 1990. 'Platelet angiotensin II binding and plasma renin concentration, plasma renin substrate and plasma angiotensin II in human pregnancy', *Clin Sci (Lond)*, 79: 403-8.

Bamberger, M., J. M. Glick, and G. H. Rothblat. 1983. 'Hepatic lipase stimulates the uptake of high density lipoprotein cholesterol by hepatoma cells', *J Lipid Res*, 24: 869-76.

Banka, C. L., T. Yuan, M. C. de Beer, M. Kindy, L. K. Curtiss, and F. C. de Beer. 1995. 'Serum amyloid A (SAA): influence on HDL-mediated cellular cholesterol efflux', *J Lipid Res*, 36: 1058-65.

Bartels, Susanne, Angelica Ruiz Franco, and Tatjana Rundek. 2012. 'Carotid intima-media thickness (cIMT) and plaque from risk assessment and clinical use to genetic discoveries', *Perspectives in Medicine*, 1: 139-45.

Basford, J. E., L. Wancata, S. M. Hofmann, R. A. Silva, W. S. Davidson, P. N. Howles, and D. Y. Hui. 2011. 'Hepatic deficiency of low density lipoprotein receptor-related protein-1 reduces high density lipoprotein secretion and plasma levels in mice', *J Biol Chem*, 286: 13079-87.

Bavendiek, Udo, Peter Libby, Meagan Kilbride, Rebecca Reynolds, Nigel Mackman, and Uwe Schönbeck. 2002. 'Induction of Tissue Factor Expression in Human Endothelial Cells by CD40 Ligand Is Mediated via Activator Protein 1, Nuclear Factor κB, and Egr-1*', *Journal of Biological Chemistry*, 277: 25032-39.

Baxter, R. C., and J. L. Martin. 1986. 'Radioimmunoassay of growth hormone-dependent insulinlike growth factor binding protein in human plasma', *The Journal of Clinical Investigation*, 78: 1504-12.

Bayly, Graham R. 2014. 'CHAPTER 37 - Lipids and disorders of lipoprotein metabolism.' in William J. Marshall, Marta Lapsley, Andrew P. Day and Ruth M. Ayling (eds.), *Clinical Biochemistry: Metabolic and Clinical Aspects (Third Edition)* (Churchill Livingstone).

Beazer, Jack D., Patamat Patanapirunhakit, Jason M.R. Gill, Delyth Graham, Helen Karlsson, Stefan Ljunggren, Monique T. Mulder, and Dilys J. Freeman. 2020. 'High-density lipoprotein's vascular protective functions in metabolic and cardiovascular disease – could extracellular vesicles be at play?', *Clinical Science*, 134: 2977-86.

Bello, J., D. Haas, and H. R. Bello. 1966. 'Interactions of protein-denaturing salts with model amides', *Biochemistry*, 5: 2539-48.

Belo, L., M. Caslake, D. Gaffney, A. Santos-Silva, L. Pereira-Leite, A. Quintanilha, and I. Rebelo. 2002. 'Changes in LDL size and HDL concentration in normal and preeclamptic pregnancies', *Atherosclerosis*, 162: 425-32.

Bennett, S. A., C. N. Bagot, A. Appiah, J. Johns, J. Ross, L. N. Roberts, R. K. Patel, and R. Arya. 2014. 'Women with unexplained recurrent pregnancy loss do not have evidence of an underlying prothrombotic state: experience with calibrated automated thrombography and rotational thromboelastometry', *Thromb Res*, 133: 892-9.

Berliner, Judith A., and Nima M. Gharavi. 2008. 'Endothelial cell regulation by phospholipid oxidation products', *Free Radic Biol Med*, 45: 119-23.

Bernardo, A., C. Ball, L. Nolasco, J. F. Moake, and J. F. Dong. 2004. 'Effects of inflammatory cytokines on the release and cleavage of the endothelial cell-derived ultralarge von Willebrand factor multimers under flow', *Blood*, 104: 100-6.

Bernier, George M. 1980. 'Beta-2-Microglobulin: Structure, Function and Significance', *Vox Sang*, 38: 323-27.

Bharadwaj, Shruthi K., B. Vishnu Bhat, V. Vickneswaran, B. Adhisivam, Zachariah Bobby, and S. Habeebullah. 2018. 'Oxidative Stress, Antioxidant Status and Neurodevelopmental Outcome in Neonates Born to Pre-eclamptic Mothers', *The Indian Journal of Pediatrics*, 85: 351-57.

Bikle, D. D., E. Gee, B. Halloran, and J. G. Haddad. 1984. 'Free 1,25-dihydroxyvitamin D levels in serum from normal subjects, pregnant subjects, and subjects with liver disease', *The Journal of Clinical Investigation*, 74: 1966-71.

Blair, Alison, Philip W. Shaul, Ivan S. Yuhanna, Patricia A. Conrad, and Eric J. Smart. 1999. 'Oxidized Low Density Lipoprotein Displaces Endothelial Nitric-oxide Synthase (eNOS) from Plasmalemmal Caveolae and Impairs eNOS Activation*', *Journal of Biological Chemistry*, 274: 32512-19.

Boden, W. E., J. L. Probstfield, T. Anderson, B. R. Chaitman, P. Desvignes-Nickens, K. Koprowicz, R. McBride, K. Teo, and W. Weintraub. 2011. 'Niacin in patients with low HDL cholesterol levels receiving intensive statin therapy', *N Engl J Med*, 365: 2255-67.

Bodnar, L. M., J. M. Catov, H. N. Simhan, M. F. Holick, R. W. Powers, and J. M. Roberts. 2007. 'Maternal vitamin D deficiency increases the risk of preeclampsia', *J Clin Endocrinol Metab*, 92: 3517-22.

Boehlen, Françoise, Patrick Hohlfeld, Philippe Extermann, Thomas V. Perneger, and Philippe De Moerloose. 2000. 'Platelet count at term pregnancy: a reappraisal of the threshold', *Obstetrics & Gynecology*, 95: 29-33.

Boghossian, N. S., P. Mendola, A. Liu, C. Robledo, and E. H. Yeung. 2017. 'Maternal serum markers of lipid metabolism in relation to neonatal anthropometry', *Journal of Perinatology*, 37: 629-35.

Böing, Anita N., Edwin van der Pol, Anita E. Grootemaat, Frank A. W. Coumans, Auguste Sturk, and Rienk Nieuwland. 2014. 'Single-step isolation of extracellular vesicles by size-exclusion chromatography', *Journal of extracellular vesicles*, 3: 10.3402/jev.v3.23430.

Boisramé-Helms, J., F. Meziani, N. Sananès, T. Boisramé, B. Langer, F. Schneider, T. Ragot, R. Andriantsitohaina, and A. Tesse. 2015. 'Detrimental arterial inflammatory effect of microparticles circulating in preeclamptic women: ex vivo evaluation in human arteries', *Fundam Clin Pharmacol*, 29: 450-61.

Boon, James, Andrew J. Hoy, Romana Stark, Russell D. Brown, Ruth C. Meex, Darren C. Henstridge, Simon Schenk, Peter J. Meikle, Jeffrey F. Horowitz, Bronwyn A. Kingwell, Clinton R. Bruce, and Matthew J. Watt. 2013. 'Ceramides contained in LDL are elevated in type 2 diabetes and promote inflammation and skeletal muscle insulin resistance', *Diabetes*, 62: 401-10.

Bradford, Marion M. 1976. 'A rapid and sensitive method for the quantitation of microgram quantities of protein utilizing the principle of protein-dye binding', *Analytical Biochemistry*, 72: 248-54.

Braschi, S., N. Couture, A. Gambarotta, B. R. Gauthier, C. R. Coffill, D. L. Sparks, N. Maeda, and J. R. Schultz. 1998. 'Hepatic lipase affects both HDL and ApoB-containing lipoprotein levels in the mouse', *Biochim Biophys Acta*, 1392: 276-90.

Brewster, L. M., Z. Taherzadeh, S. Volger, J. F. Clark, T. Rolf, H. Wolf, E. Vanbavel, and G. A. van Montfrans. 2010. 'Ethnic differences in resistance artery contractility of normotensive pregnant women', *Am J Physiol Heart Circ Physiol*, 299: H431-6.

Brinton, E. A., S. Eisenberg, and J. L. Breslow. 1994. 'Human HDL cholesterol levels are determined by apoA-I fractional catabolic rate, which correlates inversely with estimates of HDL particle size. Effects of gender, hepatic and lipoprotein lipases, triglyceride and insulin levels, and body fat distribution', *Arterioscler Thromb*, 14: 707-20.

Brinton, Eliot A., Uma Kher, Sukrut Shah, Christopher P. Cannon, Michael Davidson, Antonio M. Gotto, Tanya B. Ashraf, Christine McCrary Sisk, Hayes Dansky, Yale Mitchel, Philip Barter, M. Gerstman, L. Howes, K. Kostner, P. Nestel, D. Sullivan, H. Brath, J. Patsch, B. Paulweber, H. Toplak, C. M. Constance, E. Howlett, D. Mymin, L. Pliamm, K. K. Saunders, J. C. Tardif, R. Tytus, P. Aschner, S. Keinänen-Klukaanniemi, T. Strandberg, M. R. Taskinen, G. Luc, D. Richter, J. L. Schlienger, Y. Zaïr, K. F. Appel, M. Baar, C. Luley, U. Overhoff, T. Pomykaj, T. Schaefer, S. T. Lau, K. L. F. Lee, K. Tan, B. Tomlinson, M. W. Tsang, K. Badacsonyi, Á Kalina, N. Kanakaridisz, L. Márk, É Péterfai, L. Regos, I. Reiber, J. Takács, A. Vértes, A. Elis, D. Gavish, D. Harats, O. Hussein, T. Hayek, E. Leitersdorf, A. K. Bin Abdul Ghapar, K. H. Chee, S. B. Ismail, K. H. Ling, G. R. L. Ramanathan, K. H. Sim, R. Alvarado, M. Benavides, G. E. Cardona, G. Gonzalez, J. Verdejo, D. C. G. Basart, B. P. M. Imholz, J. J. C. Jonker, P. R. Nierop, J. L. Posma, Th B. Twickler, E. Barrington-Ward, R. Cutfield, D. H. Friedlander, R. S. Scott, H. Istad, G. Langslet, G. K. Skjelvan, S. J. Campodónico Hoyos, R. Coloma Araniya, A. Gallegos C, C. A. Pino Morales, L. Watanabe, G. P. Arutyunov, A. B. Blokhin, M. G. Bubnova, S. Y. Marcevich, C. Álvarez Sánchez, L. A. Álvarez-Sala Walther, B. Gil Extremera, F. Perez Jimenez, L. de Teresa Parreño, C. P. Anderberg, U. Hedin, A. Hellberg, P. Höök, T. Kjellström, P. Nilsson, A. G. Olsson, U. Rosenqvist, K. Tolagen, T. Wolff, A. Baskin, H. E. Bays, R. I. Bernstein, N. Bittar, E. A. Brinton, L. H. K. Chee, R. A. Cottiero, R. D. D'Agostino, M. H. Davidson, P. S. Denker, R. K. Garcia, R. K. Hippert, T. Isakov, S. R. Kaster, B. Kerzner, E. J. Klein, M. J. Koren, M. E. Kutner, D. Liljenquist, D. G. Lorch, R. Lorraine, B. C. Lubin, N. M. Lunde, T. J. Majchrzak, J. M. McKenney, S. Mukherjee, D. D. Muse, M. S. Otruba, J. E. Pappas, K. Patrick, S. J. Powell, E. Riffer, L. D. Rink, J. L. Rohlf, J. B. Rosen, P. D. Rosenbilt, E. M. Roth, C. J. Rubenstein, J. Rubino, L. A. Rudolph, A. Schneider, W. G. Short, J. C. Silverfield, D. P. Suresh, G. A. Tarshis, P. D. Toth, R. W. Townsend, and T. O. Wahl. 2015. 'Effects of anacetrapib on plasma lipids in specific patient subgroups in the DEFINE (Determining the Efficacy and Tolerability of CETP INhibition with AnacEtrapib) trial', *Journal of Clinical Lipidology*, 9: 65-71.

Brodde, M. F., S. J. Korporaal, G. Herminghaus, M. Fobker, T. J. Van Berkel, U. J. Tietge, H. Robenek, M. Van Eck, B. E. Kehrel, and J. R. Nofer. 2011. 'Native high-density lipoproteins inhibit platelet activation via scavenger receptor BI: role of negatively charged phospholipids', *Atherosclerosis*, 215: 374-82.

Broekhuizen, Michelle, Emilie Hitzerd, Thierry P. P. van den Bosch, Jasper Dumas, Robert M. Verdijk, Bas B. van Rijn, A. H. Jan Danser, Casper H. J. van Eijck, Irwin K. M. Reiss, and Dana A. M. Mustafa. 2021. 'The Placental Innate Immune System Is Altered in Early-Onset Preeclampsia, but Not in Late-Onset Preeclampsia', *Frontiers in Immunology*, 12: 780043-43.

Brown, M. A., M. D. Lindheimer, M. de Swiet, A. Van Assche, and J. M. Moutquin. 2001. 'The classification and diagnosis of the hypertensive disorders of

pregnancy: statement from the International Society for the Study of Hypertension in Pregnancy (ISSHP)', *Hypertens Pregnancy*, 20: Ix-xiv.

Brown, Mark A., Laura A. Magee, Louise C. Kenny, S. Ananth Karumanchi, Fergus P. McCarthy, Shigeru Saito, David R. Hall, Charlotte E. Warren, Gloria Adoyi, and Salisu Ishaku. 2018. 'The hypertensive disorders of pregnancy: ISSHP classification, diagnosis & management recommendations for international practice', *Pregnancy Hypertens*, 13: 291-310.

Brown, Simon H. J., Samuel R. Eather, Dilys J. Freeman, Barbara J. Meyer, and Todd W. Mitchell. 2016. 'A Lipidomic Analysis of Placenta in Preeclampsia: Evidence for Lipid Storage', *PLoS One*, 11: e0163972.

Brownfoot, Fiona C., Stephen Tong, Natalie J. Hannan, Natalie K. Binder, Susan P. Walker, Ping Cannon, Roxanne Hastie, Kenji Onda, and Tu'uhevaha J. Kaitu'u-Lino. 2015. 'Effects of Pravastatin on Human Placenta, Endothelium, and Women With Severe Preeclampsia', *Hypertension*, 66: 687-97.

Brünnert, D., M. Sztachelska, F. Bornkessel, N. Treder, S. Wolczynski, P. Goyal, and M. Zygmunt. 2014. 'Lysophosphatidic acid and sphingosine 1-phosphate metabolic pathways and their receptors are differentially regulated during decidualization of human endometrial stromal cells', *Mol Hum Reprod*, 20: 1016-25.

Cai, Hua, and David G. Harrison. 2000. 'Endothelial Dysfunction in Cardiovascular Diseases: The Role of Oxidant Stress', *Circulation Research*, 87: 840-44.

Campos, H., J. J. Genest, Jr., E. Blijlevens, J. R. McNamara, J. L. Jenner, J. M. Ordovas, P. W. Wilson, and E. J. Schaefer. 1992. 'Low density lipoprotein particle size and coronary artery disease', *Arterioscler Thromb*, 12: 187-95.

Cao, Yi-ni, Lu Xu, Ying-chun Han, Yu-nan Wang, George Liu, and Rong Qi. 2017. 'Recombinant high-density lipoproteins and their use in cardiovascular diseases', *Drug Discovery Today*, 22: 180-85.

Castellani, L. W., M. Navab, B. J. Van Lenten, C. C. Hedrick, S. Y. Hama, A. M. Goto, A. M. Fogelman, and A. J. Lusis. 1997. 'Overexpression of apolipoprotein AII in transgenic mice converts high density lipoproteins to proinflammatory particles', *The Journal of Clinical Investigation*, 100: 464-74.

Catalano, P. M., N. M. Roman-Drago, S. B. Amini, and E. A. Sims. 1998. 'Longitudinal changes in body composition and energy balance in lean women with normal and abnormal glucose tolerance during pregnancy', *Am J Obstet Gynecol*, 179: 156-65.

Catalano, P. M., E. D. Tyzbir, N. M. Roman, S. B. Amini, and E. A. Sims. 1991. 'Longitudinal changes in insulin release and insulin resistance in nonobese pregnant women', *Am J Obstet Gynecol*, 165: 1667-72.

Catalano, P. M., E. D. Tyzbir, R. R. Wolfe, J. Calles, N. M. Roman, S. B. Amini, and E. A. Sims. 1993. 'Carbohydrate metabolism during pregnancy in control subjects and women with gestational diabetes', *Am J Physiol*, 264: E60-7.

Catalano, P. M., E. D. Tyzbir, R. R. Wolfe, N. M. Roman, S. B. Amini, and E. A. Sims. 1992. 'Longitudinal changes in basal hepatic glucose production and suppression during insulin infusion in normal pregnant women', *Am J Obstet Gynecol*, 167: 913-9.

Ceron, J. J., F. Tecles, and A. Tvarijonaviciute. 2014. 'Serum paraoxonase 1 (PON1) measurement: an update', *BMC Vet Res*, 10: 74.

Chambliss, K. L., and P. W. Shaul. 2002. 'Estrogen modulation of endothelial nitric oxide synthase', *Endocr Rev*, 23: 665-86.

Chandramouli, Kondethimmanahalli, and Pei-Yuan Qian. 2009. 'Proteomics: challenges, techniques and possibilities to overcome biological sample complexity', *Human genomics and proteomics : HGP*, 2009: 239204.

Chapman, Arlene B., William T. Abraham, Stacy Zamudio, Carolyn Coffin, Aicha Merouani, David Young, Ann Johnson, Fritz Osorio, Carol Goldberg, Lorna G. Moore, Thomas Dahms, and Robert W. Schrier. 1998. 'Temporal relationships between hormonal and hemodynamic changes in early human pregnancy', *Kidney International*, 54: 2056-63.

Chapman, M. J., S. Goldstein, D. Lagrange, and P. M. Laplaud. 1981. 'A density gradient ultracentrifugal procedure for the isolation of the major lipoprotein classes from human serum', *J Lipid Res*, 22: 339-58.

Charkiewicz, K., J. Goscik, A. Blachnio-Zabielska, G. Raba, A. Sakowicz, J. Kalinka, A. Chabowski, and P. Laudanski. 2017. 'Sphingolipids as a new factor in the pathomechanism of preeclampsia - Mass spectrometry analysis', *PLoS One*, 12: e0177601.

Chau, K., A. Hennessy, and A. Makris. 2017. 'Placental growth factor and pre-eclampsia', *Journal of Human Hypertension*, 31: 782-86.

Chaurasia, B., and S. A. Summers. 2015. 'Ceramides - Lipotoxic Inducers of Metabolic Disorders', *Trends Endocrinol Metab*, 26: 538-50.

Cheng, A. M., P. Handa, S. Tateya, J. Schwartz, C. Tang, P. Mitra, J. F. Oram, A. Chait, and F. Kim. 2012. 'Apolipoprotein A-I attenuates palmitate-mediated NF-κB activation by reducing Toll-like receptor-4 recruitment into lipid rafts', *PLoS One*, 7: e33917.

Cheng, Shi-Bin, Akitoshi Nakashima, Warren J. Huber, Sarah Davis, Sayani Banerjee, Zheping Huang, Shigeru Saito, Yoel Sadovsky, and Surendra Sharma. 2019. 'Pyroptosis is a critical inflammatory pathway in the placenta from early onset preeclampsia and in human trophoblasts exposed to hypoxia and endoplasmic reticulum stressors', *Cell Death & Disease*, 10: 927-27.

Cheung, M. C., and J. J. Albers. 1984. 'Characterization of lipoprotein particles isolated by immunoaffinity chromatography. Particles containing A-I and A-II and particles containing A-I but no A-II', *J Biol Chem*, 259: 12201-9.

Cheung, M. C., G. Wolfbauer, and J. J. Albers. 1996. 'Plasma phospholipid mass transfer rate: relationship to plasma phospholipid and cholesteryl ester transfer activities and lipid parameters', *Biochim Biophys Acta*, 1303: 103-10.

Cheung, W. Y. 1980. 'Calmodulin plays a pivotal role in cellular regulation', *Science*, 207: 19-27.

Choi, J. W., M. W. Im, and S. H. Pai. 2002. 'Nitric oxide production increases during normal pregnancy and decreases in preeclampsia', *Ann Clin Lab Sci*, 32: 257-63.

Chow, Wang-Ngai, Yin-Lau Lee, Po-Chau Wong, Man-Kin Chung, Kai-Fai Lee, and William Shu-Biu Yeung. 2009. 'Complement 3 deficiency impairs early pregnancy in mice', *Molecular Reproduction and Development*, 76: 647-55.

Christensen, Pernille M., Markus H. Bosteen, Stefan Hajny, Lars B. Nielsen, and Christina Christoffersen. 2017. 'Apolipoprotein M mediates sphingosine-1-phosphate efflux from erythrocytes', *Scientific Reports*, 7: 14983.

Christison, J. K., K. A. Rye, and R. Stocker. 1995. 'Exchange of oxidized cholesteryl linoleate between LDL and HDL mediated by cholesteryl ester transfer protein', *J Lipid Res*, 36: 2017-26.

Christison, J., A. Karjalainen, J. Brauman, F. Bygrave, and R. Stocker. 1996. 'Rapid reduction and removal of HDL- but not LDL-associated cholesteryl ester hydroperoxides by rat liver perfused in situ', *Biochemical Journal*, 314: 739-42.

Christoffersen, Christina, Hideru Obinata, Sunil B. Kumaraswamy, Sylvain Galvani, Josefin Ahnström, Madhumati Sevvana, Claudia Egerer-Sieber, Yves A. Muller, Timothy Hla, Lars B. Nielsen, and Björn Dahlbäck. 2011. 'Endothelium-protective sphingosine-1-phosphate provided by HDL-associated apolipoprotein M', *Proceedings of the National Academy of Sciences of the United States of America*, 108: 9613-18.

Chroni, A., A. Duka, H. Y. Kan, T. Liu, and V. I. Zannis. 2005. 'Point mutations in apolipoprotein A-I mimic the phenotype observed in patients with classical lecithin:cholesterol acyltransferase deficiency', *Biochemistry*, 44: 14353-66.

Clapp, James F., Brian L. Seaward, Robert H. Sleamaker, and John Hiser. 1988. 'Maternal physiologic adaptations to early human pregnancy', *American Journal of Obstetrics and Gynecology*, 159: 1456-60.

Coetzee, G. A., A. F. Strachan, D. R. van der Westhuyzen, H. C. Hoppe, M. S. Jeenah, and F. C. de Beer. 1986. 'Serum amyloid A-containing human high density lipoprotein 3. Density, size, and apolipoprotein composition', *J Biol Chem*, 261: 9644-51.

Collier, Timothy S., Zhicheng Jin, Celalettin Topbas, and Cory Bystrom. 2018. 'Rapid Affinity Enrichment of Human Apolipoprotein A-I Associated Lipoproteins for Proteome Analysis', *Journal of Proteome Research*, 17: 1183-93.

Collins, L. A., S. P. Mirza, A. H. Kissebah, and M. Olivier. 2010. 'Integrated approach for the comprehensive characterization of lipoproteins from human plasma using FPLC and nano-HPLC-tandem mass spectrometry', *Physiol Genomics*, 40: 208-15.

Collins, L. A., and M. Olivier. 2010. 'Quantitative comparison of lipoprotein fractions derived from human plasma and serum by liquid chromatography-tandem mass spectrometry', *Proteome Sci*, 8: 42.

Cominacini, L., U. Garbin, A. F. Pasini, A. Davoli, M. Campagnola, G. B. Contessi, A. M. Pastorino, and V. Lo Cascio. 1997. 'Antioxidants inhibit the expression of intercellular cell adhesion molecule-1 and vascular cell adhesion molecule-1 induced by oxidized LDL on human umbilical vein endothelial cells', *Free Radic Biol Med*, 22: 117-27.

Consortium, The UniProt. 2020. 'UniProt: the universal protein knowledgebase in 2021', *Nucleic Acids Research*, 49: D480-D89.

Coresh, J., P. O. Kwiterovich, Jr., H. H. Smith, and P. S. Bachorik. 1993. 'Association of plasma triglyceride concentration and LDL particle diameter, density, and chemical composition with premature coronary artery disease in men and women', *J Lipid Res*, 34: 1687-97.

Costantine, Maged M., Kirsten Cleary, Mary F. Hebert, Mahmoud S. Ahmed, Linda M. Brown, Zhaoxia Ren, Thomas R. Easterling, David M. Haas, Laura S. Haneline, Steve N. Caritis, Raman Venkataramanan, Holly West, Mary D'Alton, and Gary Hankins. 2016. 'Safety and pharmacokinetics of pravastatin used for the prevention of preeclampsia in high-risk pregnant

women: a pilot randomized controlled trial', *American Journal of Obstetrics and Gynecology*, 214: 720.e1-20.e17.

Coumans, F. A. W., A. R. Brisson, E. I. Buzas, F. Dignat-George, E. E. E. Drees, S. El-Andaloussi, C. Emanueli, A. Gasecka, A. Hendrix, A. F. Hill, R. Lacroix, Y. Lee, T. G. van Leeuwen, N. Mackman, I. Mäger, J. P. Nolan, E. van der Pol, D. M. Pegtel, S. Sahoo, P. R. M. Siljander, G. Sturk, O. de Wever, and R. Nieuwland. 2017. 'Methodological Guidelines to Study Extracellular Vesicles', *Circ Res*, 120: 1632-48.

Couture, Patrick, James D. Otvos, L. Adrienne Cupples, Carlos Lahoz, Peter W. F. Wilson, Ernst J. Schaefer, and Jose M. Ordovas. 2000. 'Association of the C-514T Polymorphism in the Hepatic Lipase Gene With Variations in Lipoprotein Subclass Profiles', *Arteriosclerosis, Thrombosis, and Vascular Biology*, 20: 815-22.

Cravatt, Benjamin F., Gabriel M. Simon, and John R. Yates Iii. 2007. 'The biological impact of mass-spectrometry-based proteomics', *Nature*, 450: 991-1000.

Cué, J. I., J. T. DiPiro, L. J. Brunner, J. E. Doran, M. E. Blankenship, A. R. Mansberger, and M. L. Hawkins. 1994. 'Reconstituted high density lipoprotein inhibits physiologic and tumor necrosis factor alpha responses to lipopolysaccharide in rabbits', *Arch Surg*, 129: 193-7.

Cukier, A. M. O., P. Therond, S. A. Didichenko, I. Guillas, M. J. Chapman, S. D. Wright, and A. Kontush. 2017. 'Structure-function relationships in reconstituted HDL: Focus on antioxidative activity and cholesterol efflux capacity', *Biochim Biophys Acta Mol Cell Biol Lipids*, 1862: 890-900.

Cunningham, F. Gary, Kenneth J. Leveno, Steven L. Bloom, Jodi S. Dashe, Barbara L. Hoffman, Brian M. Casey, and Catherine Y. Spong. 2018. 'Implantation and Placental Development.' in, *Williams Obstetrics, 25e* (McGraw-Hill Education: New York, NY).

Daiger, S. P., M. S. Schanfield, and L. L. Cavalli-Sforza. 1975. 'Group-specific component (Gc) proteins bind vitamin D and 25-hydroxyvitamin D', *Proceedings of the National Academy of Sciences of the United States of America*, 72: 2076-80.

Davidson S., Shah AS. "HDL Proteome Watch." In. https://homepages.uc.edu/~davidswm/HDLproteome.html.

Davis, E. F., A. J. Lewandowski, C. Aye, W. Williamson, H. Boardman, R. C. Huang, T. A. Mori, J. Newnham, L. J. Beilin, and P. Leeson. 2015. 'Clinical cardiovascular risk during young adulthood in offspring of hypertensive pregnancies: insights from a 20-year prospective follow-up birth cohort', *BMJ Open*, 5: e008136.

de Villiers, W. J., J. P. Louw, A. F. Strachan, S. M. Etsebeth, E. G. Shephard, and F. C. de Beer. 1990. 'C-reactive protein and serum amyloid A protein in pregnancy and labour', *Br J Obstet Gynaecol*, 97: 725-30.

Del Turco, S., G. Basta, G. Lazzerini, L. Chancharme, L. Lerond, and R. De Caterina. 2014. 'Involvement of the TP receptor in TNF-α-induced endothelial tissue factor expression', *Vascul Pharmacol*, 62: 49-56.

Delves, Peter J. 2020. 'Chapter 4 - Innate and Adaptive Systems of Immunity.' in Noel R. Rose and Ian R. Mackay (eds.), *The Autoimmune Diseases (Sixth Edition)* (Academic Press).

den Hoedt, S., S. M. Crivelli, F. P. J. Leijten, M. Losen, J. A. A. Stevens, M. Mané-Damas, H. E. de Vries, J. Walter, M. Mirzaian, E. J. G. Sijbrands, Jmfg Aerts, A. J. M. Verhoeven, P. Martinez-Martinez, and M. T. Mulder. 2021. 'Effects of Sex, Age, and Apolipoprotein E Genotype on Brain

Ceramides and Sphingosine-1-Phosphate in Alzheimer's Disease and Control Mice', *Front Aging Neurosci*, 13: 765252.

Denimal, D., J. P. Pais de Barros, J. M. Petit, B. Bouillet, B. Verges, and L. Duvillard. 2015. 'Significant abnormalities of the HDL phosphosphingolipidome in type 1 diabetes despite normal HDL cholesterol concentration', *Atherosclerosis*, 241: 752-60.

Desai, K., K. R. Bruckdorfer, R. A. Hutton, and J. S. Owen. 1989. 'Binding of apoE-rich high density lipoprotein particles by saturable sites on human blood platelets inhibits agonist-induced platelet aggregation', *J Lipid Res*, 30: 831-40.

Dhanesha, N., P. Prakash, P. Doddapattar, I. Khanna, M. J. Pollpeter, M. K. Nayak, J. M. Staber, and A. K. Chauhan. 2016. 'Endothelial Cell-Derived von Willebrand Factor Is the Major Determinant That Mediates von Willebrand Factor-Dependent Acute Ischemic Stroke by Promoting Postischemic Thrombo-Inflammation', *Arterioscler Thromb Vasc Biol*, 36: 1829-37.

Diderholm, B, M Stridsberg, S Nordén-Lindeberg, and J Gustafsson. 2006. 'Decreased maternal lipolysis in intrauterine growth restriction in the third trimester', *BJOG: An International Journal of Obstetrics & Gynaecology*, 113: 159-64.

Diffenderfer, M. R., and E. J. Schaefer. 2014. 'The composition and metabolism of large and small LDL', *Curr Opin Lipidol*, 25: 221-6.

Dobierzewska, A., M. Palominos, M. Sanchez, M. Dyhr, K. Helgert, P. Venegas-Araneda, S. Tong, and S. E. Illanes. 2016. 'Impairment of Angiogenic Sphingosine Kinase-1/Sphingosine-1-Phosphate Receptors Pathway in Preeclampsia', *PLoS One*, 11: e0157221.

Dobierzewska, A., S. Soman, S. E. Illanes, and A. J. Morris. 2017. 'Plasma cross-gestational sphingolipidomic analyses reveal potential first trimester biomarkers of preeclampsia', *PLoS One*, 12: e0175118.

Doddapattar, Prakash, Nirav Dhanesha, Mehul R. Chorawala, Chandler Tinsman, Manish Jain, Manasa K. Nayak, Janice M. Staber, and Anil K. Chauhan. 2018. 'Endothelial Cell–Derived Von Willebrand Factor, But Not Platelet-Derived, Promotes Atherosclerosis in Apolipoprotein E–Deficient Mice', *Arteriosclerosis, Thrombosis, and Vascular Biology*, 38: 520-28.

Domingo-Espin, J., O. Nilsson, K. Bernfur, R. Del Giudice, and J. O. Lagerstedt. 2018. 'Site-specific glycations of apolipoprotein A-I lead to differentiated functional effects on lipid-binding and on glucose metabolism', *Biochim Biophys Acta Mol Basis Dis*, 1864: 2822-34.

Domingo-Espín, Joan, Oktawia Nilsson, Katja Bernfur, Rita Del Giudice, and Jens O. Lagerstedt. 2018. 'Site-specific glycations of apolipoprotein A-I lead to differentiated functional effects on lipid-binding and on glucose metabolism', *Biochimica et Biophysica Acta (BBA) - Molecular Basis of Disease*, 1864: 2822-34.

Dørup, Inge, Kristjar Skajaa, and Keld E. Sørensen. 1999. 'Normal pregnancy is associated with enhanced endothelium-dependent flow-mediated vasodilation', *American Journal of Physiology-Heart and Circulatory Physiology*, 276: H821-H25.

Draganov, D. I., P. L. Stetson, C. E. Watson, S. S. Billecke, and B. N. La Du. 2000. 'Rabbit serum paraoxonase 3 (PON3) is a high density lipoprotein-associated lactonase and protects low density lipoprotein against oxidation', *J Biol Chem*, 275: 33435-42.

Drury-Stewart, D. N., K. W. Lannert, D. W. Chung, G. T. Teramura, J. C. Zimring, B. A. Konkle, H. S. Gammill, and J. M. Johnsen. 2014. 'Complex changes in von Willebrand factor-associated parameters are acquired during uncomplicated pregnancy', *PLoS One*, 9: e112935.

Duckitt, Kirsten, and Deborah Harrington. 2005. 'Risk factors for pre-eclampsia at antenatal booking: systematic review of controlled studies', *BMJ*, 330: 565.

Duka, A., P. Fotakis, D. Georgiadou, A. Kateifides, K. Tzavlaki, L. von Eckardstein, E. Stratikos, D. Kardassis, and V. I. Zannis. 2013. 'ApoA-IV promotes the biogenesis of apoA-IV-containing HDL particles with the participation of ABCA1 and LCAT', *J Lipid Res*, 54: 107-15.

Duparc, Thibaut, Jean-Bernard Ruidavets, Annelise Genoux, Cécile Ingueneau, Souad Najib, Jean Ferrières, Bertrand Perret, and Laurent O. Martinez. 2020. 'Serum level of HDL particles are independently associated with long-term prognosis in patients with coronary artery disease: The GENES study', *Scientific Reports*, 10: 8138.

Dürr, U. H., U. S. Sudheendra, and A. Ramamoorthy. 2006. 'LL-37, the only human member of the cathelicidin family of antimicrobial peptides', *Biochim Biophys Acta*, 1758: 1408-25.

Ehrnthaller, Christian, Anita Ignatius, Florian Gebhard, and Markus Huber-Lang. 2011. 'New Insights of an Old Defense System: Structure, Function, and Clinical Relevance of the Complement System', *Molecular Medicine*, 17: 317-29.

Einbinder, Y., T. Biron-Shental, M. Agassi-Zaitler, K. Tzadikevitch-Geffen, J. Vaya, S. Khatib, M. Ohana, S. Benchetrit, and T. Zitman-Gal. 2018. 'High-density lipoproteins (HDL) composition and function in preeclampsia', *Arch Gynecol Obstet*, 298: 405-13.

Eiselein, Larissa, Dennis W. Wilson, Michael W. Lamé, and John C. Rutledge. 2007. 'Lipolysis products from triglyceride-rich lipoproteins increase endothelial permeability, perturb zonula occludens-1 and F-actin, and induce apoptosis', *American Journal of Physiology-Heart and Circulatory Physiology*, 292: H2745-H53.

Engin-Ustün, Y., Y. Ustün, A. B. Karabulut, E. Ozkaplan, M. M. Meydanli, and A. Kafkasli. 2007. 'Serum amyloid A levels are increased in pre-eclampsia', *Gynecol Obstet Invest*, 64: 117-20.

Esmon, C. T., and W. G. Owen. 1981. 'Identification of an endothelial cell cofactor for thrombin-catalyzed activation of protein C', *Proc Natl Acad Sci U S A*, 78: 2249-52.

Esmon, N. L., W. G. Owen, and C. T. Esmon. 1982. 'Isolation of a membrane-bound cofactor for thrombin-catalyzed activation of protein C', *J Biol Chem*, 257: 859-64.

Fahraeus, L., U. Larsson-Cohn, and L. Wallentin. 1985. 'Plasma lipoproteins including high density lipoprotein subfractions during normal pregnancy', *Obstet Gynecol*, 66: 468-72.

Fan, J., J. Wang, A. Bensadoun, S. J. Lauer, Q. Dang, R. W. Mahley, and J. M. Taylor. 1994. 'Overexpression of hepatic lipase in transgenic rabbits leads to a marked reduction of plasma high density lipoproteins and intermediate density lipoproteins', *Proc Natl Acad Sci U S A*, 91: 8724-8.

Fay, R. A., A. O. Hughes, and N. T. Farron. 1983. 'Platelets in pregnancy: hyperdestruction in pregnancy', *Obstet Gynecol*, 61: 238-40.

Ferretti, Gianna, Tiziana Bacchetti, Cinzia Moroni, Arianna Vignini, and Giovanna Curatola. 2003. 'Copper-induced oxidative damage on astrocytes:

protective effect exerted by human high density lipoproteins', *Biochimica et Biophysica Acta (BBA) - Molecular and Cell Biology of Lipids*, 1635: 48-54.

Fielding, C. J., V. G. Shore, and P. E. Fielding. 1972. 'A protein cofactor of lecithin:cholesterol acyltransferase', *Biochem Biophys Res Commun*, 46: 1493-8.

Fisslthaler, B., S. Dimmeler, C. Hermann, R. Busse, and I. Fleming. 2000. 'Phosphorylation and activation of the endothelial nitric oxide synthase by fluid shear stress', *Acta Physiol Scand*, 168: 81-8.

Fleming, I, M Hecker, and R Busse. 1994. 'Intracellular alkalinization induced by bradykinin sustains activation of the constitutive nitric oxide synthase in endothelial cells', *Circulation Research*, 74: 1220-26.

Ford, T., J. Graham, and D. Rickwood. 1994. 'Iodixanol: a nonionic iso-osmotic centrifugation medium for the formation of self-generated gradients', *Anal Biochem*, 220: 360-6.

Frej, Cecilia, Armando J. Mendez, Mario Ruiz, Melanie Castillo, Thomas A. Hughes, Björn Dahlbäck, and Ronald B. Goldberg. 2017. 'A Shift in ApoM/S1P Between HDL-Particles in Women With Type 1 Diabetes Mellitus Is Associated With Impaired Anti-Inflammatory Effects of the ApoM/S1P Complex', *Arteriosclerosis, Thrombosis, and Vascular Biology*, 37: 1194-205.

Fuenzalida, Bárbara, Claudette Cantin, Sampada Kallol, Lorena Carvajal, Valentina Pastén, Susana Contreras-Duarte, Christiane Albrecht, Jaime Gutierrez, and Andrea Leiva. 2020. 'Cholesterol uptake and efflux are impaired in human trophoblast cells from pregnancies with maternal supraphysiological hypercholesterolemia', *Scientific Reports*, 10: 5264-64.

Furchgott, Robert F., and John V. Zawadzki. 1980. 'The obligatory role of endothelial cells in the relaxation of arterial smooth muscle by acetylcholine', *Nature*, 288: 373-76.

Galvani, S., M. Sanson, V. A. Blaho, S. L. Swendeman, H. Obinata, H. Conger, B. Dahlbäck, M. Kono, R. L. Proia, J. D. Smith, and T. Hla. 2015. 'HDL-bound sphingosine 1-phosphate acts as a biased agonist for the endothelial cell receptor S1P1 to limit vascular inflammation', *Sci Signal*, 8: ra79.

Gant, N. F., R. J. Worley, R. B. Everett, and P. C. MacDonald. 1980. 'Control of vascular responsiveness during human pregnancy', *Kidney Int*, 18: 253-8.

Garner, B., A. R. Waldeck, P. K. Witting, K. A. Rye, and R. Stocker. 1998. 'Oxidation of high density lipoproteins. II. Evidence for direct reduction of lipid hydroperoxides by methionine residues of apolipoproteins AI and AII', *J Biol Chem*, 273: 6088-95.

Garrido-Gomez, Tamara, Francisco Dominguez, Alicia Quiñonero, Patricia Diaz-Gimeno, Mirhan Kapidzic, Matthew Gormley, Katherine Ona, Pablo Padilla-Iserte, Michael McMaster, Olga Genbacev, Alfredo Perales, Susan J. Fisher, and Carlos Simón. 2017. 'Defective decidualization during and after severe preeclampsia reveals a possible maternal contribution to the etiology', *Proceedings of the National Academy of Sciences*, 114: E8468-E77.

Gault, C. R., L. M. Obeid, and Y. A. Hannun. 2010. 'An overview of sphingolipid metabolism: from synthesis to breakdown', *Adv Exp Med Biol*, 688: 1-23.

Ge, P., C. Dong, X. Ren, E. Weiderpass, C. Zhang, H. Fan, J. Zhang, Y. Zhang, and J. Xi. 2015. 'The High Prevalence of Low HDL-Cholesterol Levels and Dyslipidemia in Rural Populations in Northwestern China', *PLoS One*, 10: e0144104.

Gellersen, Birgit, and Jan J. Brosens. 2014. 'Cyclic Decidualization of the Human Endometrium in Reproductive Health and Failure', *Endocrine Reviews*, 35: 851-905.

Genc, Habibe, Hafize Uzun, Ali Benian, Gönül Simsek, Remise Gelisgen, Rıza Madazli, and Onur Güralp. 2011. 'Evaluation of oxidative stress markers in first trimester for assessment of preeclampsia risk', *Arch Gynecol Obstet*, 284: 1367-73.

Ghering, A. B., and W. S. Davidson. 2006. 'Ceramide structural features required to stimulate ABCA1-mediated cholesterol efflux to apolipoprotein A-I', *J Lipid Res*, 47: 2781-8.

Glueck, C. J., R. W. Fallat, and D. Scheel. 1975. 'Effects of estrogenic compounds on triglyceride kinetics', *Metabolism*, 24: 537-45.

Goldstein, J. L., R. G. Anderson, and M. S. Brown. 1982. 'Receptor-mediated endocytosis and the cellular uptake of low density lipoprotein', *Ciba Found Symp*: 77-95.

Gomaraschi, Monica, Wendy E. Putt, Silvia Pozzi, Stefania Iametti, Alberto Barbiroli, Francesco Bonomi, Elda Favari, Franco Bernini, Guido Franceschini, Philippa J. Talmud, and Laura Calabresi. 2010. 'Structure and function of the apoA-IV T347S and Q360H common variants', *Biochemical and Biophysical Research Communications*, 393: 126-30.

González-Díez, María, Cristina Rodríguez, Lina Badimon, and José Martínez-González. 2008. 'Prostacyclin induction by high-density lipoprotein (HDL) in vascular smooth muscle cells depends on sphingosine 1-phosphate receptors: Effect of simvastatin', *Thromb Haemost*, 100: 119-26.

Gonzalez, Juan M., Silvia M. A. Pedroni, and Guillermina Girardi. 2014. 'Statins prevent cervical remodeling, myometrial contractions and preterm labor through a mechanism that involves hemoxygenase-1 and complement inhibition', *Mol Hum Reprod*, 20: 579-89.

Gordon, Scott M., Benjamin McKenzie, Georgina Kemeh, Maureen Sampson, Shira Perl, Neal S. Young, Michael B. Fessler, and Alan T. Remaley. 2015. 'Rosuvastatin Alters the Proteome of High Density Lipoproteins: Generation of alpha-1-antitrypsin Enriched Particles with Anti-inflammatory Properties', *Molecular & cellular proteomics : MCP*, 14: 3247-57.

Gordon, T., W. P. Castelli, M. C. Hjortland, W. B. Kannel, and T. R. Dawber. 1977. 'High density lipoprotein as a protective factor against coronary heart disease. The Framingham Study', *Am J Med*, 62: 707-14.

Grammatikos, G., N. Ferreiros, O. Waidmann, D. Bon, S. Schroeter, A. Koch, E. Herrmann, S. Zeuzem, B. Kronenberger, and J. Pfeilschifter. 2015. 'Serum Sphingolipid Variations Associate with Hepatic Decompensation and Survival in Patients with Cirrhosis', *PLoS One*, 10: e0138130.

Grant, L. K., M. A. St Hilaire, G. C. Brainard, C. A. Czeisler, S. W. Lockley, and S. A. Rahman. 2021. 'Endogenous circadian regulation and phase resetting of clinical metabolic biomarkers', *J Pineal Res*, 71: e12752.

Grantz, K. L., S. Kim, W. A. Grobman, R. Newman, J. Owen, D. Skupski, J. Grewal, E. K. Chien, D. A. Wing, R. J. Wapner, A. C. Ranzini, M. P. Nageotte, S. N. Hinkle, S. Pugh, H. Li, K. Fuchs, M. Hediger, G. M. Buck Louis, and P. S. Albert. 2018. 'Fetal growth velocity: the NICHD fetal growth studies', *Am J Obstet Gynecol*, 219: 285 e1-85 e36.

Greene, D. J., J. W. Skeggs, and R. E. Morton. 2001. 'Elevated triglyceride content diminishes the capacity of high density lipoprotein to deliver

cholesteryl esters via the scavenger receptor class B type I (SR-BI)', *J Biol Chem*, 276: 4804-11.

Griffin, J. H., K. Kojima, C. L. Banka, L. K. Curtiss, and J. A. Fernández. 1999. 'High-density lipoprotein enhancement of anticoagulant activities of plasma protein S and activated protein C', *J Clin Invest*, 103: 219-27.

Grummer, Mary A., Jeremy A. Sullivan, Ronald R. Magness, and Ian M. Bird. 2008. 'Vascular endothelial growth factor acts through novel, pregnancy-enhanced receptor signalling pathways to stimulate endothelial nitric oxide synthase activity in uterine artery endothelial cells', *Biochemical Journal*, 417: 501-11.

Grunfeld, C., M. Marshall, J. K. Shigenaga, A. H. Moser, P. Tobias, and K. R. Feingold. 1999. 'Lipoproteins inhibit macrophage activation by lipoteichoic acid', *J Lipid Res*, 40: 245-52.

Hafiane, A., and J. Genest. 2015. 'High density lipoproteins: Measurement techniques and potential biomarkers of cardiovascular risk', *BBA Clin*, 3: 175-88.

Haidar, B., R. S. Kiss, L. Sarov-Blat, R. Brunet, C. Harder, R. McPherson, and Y. L. Marcel. 2006. 'Cathepsin D, a lysosomal protease, regulates ABCA1-mediated lipid efflux', *J Biol Chem*, 281: 39971-81.

Haiyan Chu, Aradhana Awasthi, Gilbert C. White II, Magdalena Chrzanowska-Wodnicka, and Subramaniam Malarkannan. 2008. 'Rap1b Regulates B Cell Development, Homing, and T CellDependent Humoral Immunity', *J Immunol*: 3373-83.

Hammad, S. M., J. S. Pierce, F. Soodavar, K. J. Smith, M. M. Al Gadban, B. Rembiesa, R. L. Klein, Y. A. Hannun, J. Bielawski, and A. Bielawska. 2010. 'Blood sphingolipidomics in healthy humans: impact of sample collection methodology', *J Lipid Res*, 51: 3074-87.

Han, L., X. Liu, H. Li, J. Zou, Z. Yang, J. Han, W. Huang, L. Yu, Y. Zheng, and L. Li. 2014. 'Blood coagulation parameters and platelet indices: changes in normal and preeclamptic pregnancies and predictive values for preeclampsia', *PLoS One*, 9: e114488.

Harman, N. L., B. A. Griffin, and I. G. Davies. 2013. 'Separation of the principal HDL subclasses by iodixanol ultracentrifugation', *J Lipid Res*, 54: 2273-81.

Hartley, Adam, Dorian Haskard, and Ramzi Khamis. 2019. 'Oxidized LDL and anti-oxidized LDL antibodies in atherosclerosis – Novel insights and future directions in diagnosis and therapy', *Trends in Cardiovascular Medicine*, 29: 22-26.

Hassan, M. I., A. Waheed, S. Yadav, T. P. Singh, and F. Ahmad. 2008. 'Zinc alpha 2-glycoprotein: a multidisciplinary protein', *Mol Cancer Res*, 6: 892-906.

Hauth, J. C., R. G. Clifton, J. M. Roberts, L. Myatt, C. Y. Spong, K. J. Leveno, M. W. Varner, R. J. Wapner, J. M. Thorp, Jr., B. M. Mercer, A. M. Peaceman, S. M. Ramin, M. W. Carpenter, P. Samuels, A. Sciscione, J. E. Tolosa, G. Saade, Y. Sorokin, and G. D. Anderson. 2011. 'Maternal insulin resistance and preeclampsia', *Am J Obstet Gynecol*, 204: 327.e1-6.

Hayman, R. G., N. Sattar, A. Y. Warren, I. Greer, I. R. Johnson, and P. N. Baker. 1999. 'Relationship between myometrial resistance artery behavior and circulating lipid composition', *Am J Obstet Gynecol*, 180: 381-6.

Hayman, R., A. Warren, J. Brockelsby, I. Johnson, and P. Baker. 2000. 'Plasma from women with pre-eclampsia induces an in vitro alteration in the endothelium-dependent behaviour of myometrial resistance arteries', *BJOG*, 107: 108-15.

Heilmann, L., W. Rath, and K. Pollow. 2007. 'Hemostatic abnormalities in patients with severe preeclampsia', *Clin Appl Thromb Hemost*, 13: 285-91.

Hemmings, Denise G., Nicola K. Hudson, Deborah Halliday, Maureen O'Hara, Philip N. Baker, Sandra T. Davidge, and Michael J. Taggart. 2006. 'Sphingosine-1-Phosphate Acts via Rho-Associated Kinase and Nitric Oxide to Regulate Human Placental Vascular Tone1', *Biology of Reproduction*, 74: 88-94.

Henderson, C. M., T. Vaisar, and A. N. Hoofnagle. 2016. 'Isolating and Quantifying Plasma HDL Proteins by Sequential Density Gradient Ultracentrifugation and Targeted Proteomics', *Methods Mol Biol*, 1410: 105-20.

Hidalgo, J., L. Campmany, M. Borras, J. S. Garvey, and A. Armario. 1988. 'Metallothionein response to stress in rats: role in free radical scavenging', *American Journal of Physiology-Endocrinology and Metabolism*, 255: E518-E24.

Hill, J. S., D. Yang, J. Nikazy, L. K. Curtiss, J. T. Sparrow, and H. Wong. 1998. 'Subdomain chimeras of hepatic lipase and lipoprotein lipase. Localization of heparin and cofactor binding', *J Biol Chem*, 273: 30979-84.

Hoang, A., A. J. Murphy, M. T. Coughlan, M. C. Thomas, J. M. Forbes, R. O'Brien, M. E. Cooper, J. P. Chin-Dusting, and D. Sviridov. 2007. 'Advanced glycation of apolipoprotein A-I impairs its anti-atherogenic properties', *Diabetologia*, 50: 1770-9.

Hochepied, T., F. G. Berger, H. Baumann, and C. Libert. 2003. 'Alpha(1)-acid glycoprotein: an acute phase protein with inflammatory and immunomodulating properties', *Cytokine Growth Factor Rev*, 14: 25-34.

Hogan, J. C., M. J. Lewis, and A. H. Henderson. 1988. 'In vivo EDRF activity influences platelet function', *Br J Pharmacol*, 94: 1020-2.

Högberg, U. 2005. 'The World Health Report 2005: "make every mother and child count" - including Africans', *Scand J Public Health*, 33: 409-11.

Hoofnagle, Andrew N., and Jay W. Heinecke. 2009. 'Lipoproteomics: using mass spectrometry-based proteomics to explore the assembly, structure, and function of lipoproteins: Thematic Review Series: Proteomics', *Journal of Lipid Research*, 50: 1967-75.

Hoppe, B. 2014. 'Fibrinogen and factor XIII at the intersection of coagulation, fibrinolysis and inflammation', *Thromb Haemost*, 112: 649-58.

Horowitz, B. S., I. J. Goldberg, J. Merab, T. M. Vanni, R. Ramakrishnan, and H. N. Ginsberg. 1993. 'Increased plasma and renal clearance of an exchangeable pool of apolipoprotein A-I in subjects with low levels of high density lipoprotein cholesterol', *J Clin Invest*, 91: 1743-52.

Hosseinkhani, Baharak, Sören Kuypers, Nynke M. S. van den Akker, Daniel G. M. Molin, and Luc Michiels. 2018. 'Extracellular Vesicles Work as a Functional Inflammatory Mediator Between Vascular Endothelial Cells and Immune Cells', *Frontiers in Immunology*, 9.

Hubel, Carl A., Margaret K. McLaughlin, Rhobert W. Evans, Beth A. Hauth, Cynthia J. Sims, and James M. Roberts. 1996. 'Fasting serum triglycerides, free fatty acids, and malondialdehyde are increased in preeclampsia, are positively correlated, and decrease within 48 hours post partum', *American Journal of Obstetrics and Gynecology*, 174: 975-82.

Huda, Shahzya S., Naveed Sattar, and Dilys J. Freeman. 2009. 'Lipoprotein metabolism and vascular complications in pregnancy', *Clinical Lipidology*, 4: 91-102.

Hudson, Nicola K., Maureen O'Hara, Helen A. Lacey, Jemma Corcoran, Denise G. Hemmings, Mark Wareing, Philip Baker, and Michael J. Taggart. 2007. 'Modulation of Human Arterial Tone During Pregnancy: The Effect of the Bioactive Metabolite Sphingosine-1-Phosphate1', *Biology of Reproduction*, 77: 45-52.

Hung, Tai-Ho, and Graham J. Burton. 2006. 'Hypoxia and Reoxygenation: a Possible Mechanism for Placental Oxidative Stress in Preeclampsia', *Taiwanese Journal of Obstetrics and Gynecology*, 45: 189-200.

Iglesias, Angel, Adela Montelongo, Emilio Herrera, and Miguel A. Lasunción. 1994. 'Changes in cholesteryl ester transfer protein activity during normal gestation and postpartum', *Clin Biochem*, 27: 63-68.

Ignarro, L. J., G. M. Buga, K. S. Wood, R. E. Byrns, and G. Chaudhuri. 1987. 'Endothelium-derived relaxing factor produced and released from artery and vein is nitric oxide', *Proceedings of the National Academy of Sciences of the United States of America*, 84: 9265-69.

Inazu, Akihiro, Maryanne L. Brown, Charles B. Hesler, Luis B. Agellon, Junji Koizumi, Koki Takata, Yoshisuke Maruhama, Hiroshi Mabuchi, and Alan R. Tall. 1990. 'Increased High-Density Lipoprotein Levels Caused by a Common Cholesteryl-Ester Transfer Protein Gene Mutation', *New England Journal of Medicine*, 323: 1234-38.

Ishida, T., S. Choi, R. K. Kundu, K. Hirata, E. M. Rubin, A. D. Cooper, and T. Quertermous. 2003. 'Endothelial lipase is a major determinant of HDL level', *J Clin Invest*, 111: 347-55.

Iwamoto, N., R. Lu, N. Tanaka, S. Abe-Dohmae, and S. Yokoyama. 2010. 'Calmodulin interacts with ATP binding cassette transporter A1 to protect from calpain-mediated degradation and upregulates high-density lipoprotein generation', *Arterioscler Thromb Vasc Biol*, 30: 1446-52.

Jansen, Felix, Xiaoyan Yang, Katharina Baumann, David Przybilla, Theresa Schmitz, Anna Flender, Kathrin Paul, Adil Alhusseiny, Georg Nickenig, and Nikos Werner. 2015. 'Endothelial microparticles reduce ICAM-1 expression in a microRNA-222-dependent mechanism', *J Cell Mol Med*, 19: 2202-14.

Jauniaux, E., A. L. Watson, J. Hempstock, Y. P. Bao, J. N. Skepper, and G. J. Burton. 2000. 'Onset of maternal arterial blood flow and placental oxidative stress. A possible factor in human early pregnancy failure', *The American journal of pathology*, 157: 2111-22.

Jaye, M., K. J. Lynch, J. Krawiec, D. Marchadier, C. Maugeais, K. Doan, V. South, D. Amin, M. Perrone, and D. J. Rader. 1999. 'A novel endothelial-derived lipase that modulates HDL metabolism', *Nat Genet*, 21: 424-8.

Jeffrey T. Kuvin, MD, Maria E. Rämet, MD, Ayan R. Patel, MD, Natesa G. Pandian, MD, Michael E. Mendelsohn, MD,, and MD Richard H. Karas, PhD. 2002. 'A Novel Mechanism for the Beneficial Vascular Effects of High-Density Lipoprotein Cholesterol: Enhanced Vasorelaxation and Increased Endothelial Nitric Oxide Synthase Expression', *Am Heart J*, 144: 165-72.

Jensen, M. K., E. B. Rimm, J. D. Furtado, and F. M. Sacks. 2012. 'Apolipoprotein C-III as a Potential Modulator of the Association Between HDL-Cholesterol and Incident Coronary Heart Disease', *J Am Heart Assoc*, 1.

Jeyabalan, A. 2013. 'Epidemiology of preeclampsia: impact of obesity', *Nutr Rev*, 71 Suppl 1: S18-25.

Jiang, X. C., C. Bruce, J. Mar, M. Lin, Y. Ji, O. L. Francone, and A. R. Tall. 1999. 'Targeted mutation of plasma phospholipid transfer protein gene markedly reduces high-density lipoprotein levels', *J Clin Invest*, 103: 907-14.

Johnstone, E. D., G. Chan, C. P. Sibley, S. T. Davidge, B. Lowen, and L. J. Guilbert. 2005. 'Sphingosine-1-phosphate inhibition of placental trophoblast differentiation through a G(i)-coupled receptor response', *J Lipid Res*, 46: 1833-9.

Kaitu'u-Lino, T. J., R. Hastie, P. Cannon, S. Lee, O. Stock, N. J. Hannan, R. Hiscock, and S. Tong. 2014. 'Stability of absolute copy number of housekeeping genes in preeclamptic and normal placentas, as measured by digital PCR', *Placenta*, 35: 1106-9.

Kalogirou, Mihalis, Vasilis Tsimihodimos, Irene Gazi, Theodosios Filippatos, Vasilis Saougos, Alexandros D. Tselepis, Dimitri P. Mikhailidis, and Moses Elisaf. 2007. 'Effect of ezetimibe monotherapy on the concentration of lipoprotein subfractions in patients with primary dyslipidaemia', *Current Medical Research and Opinion*, 23: 1169-76.

Karimi, N., A. Cvjetkovic, S. C. Jang, R. Crescitelli, M. A. Hosseinpour Feizi, R. Nieuwland, J. Lötvall, and C. Lässer. 2018. 'Detailed analysis of the plasma extracellular vesicle proteome after separation from lipoproteins', *Cell Mol Life Sci*, 75: 2873-86.

Karlsson, H., A. Kontush, and R. W. James. 2015. 'Functionality of HDL: antioxidation and detoxifying effects', *Handb Exp Pharmacol*, 224: 207-28.

Karlsson, H., P. Leanderson, C. Tagesson, and M. Lindahl. 2005. 'Lipoproteomics II: mapping of proteins in high-density lipoprotein using two-dimensional gel electrophoresis and mass spectrometry', *Proteomics*, 5: 1431-45.

Kasumov, T., L. Li, M. Li, K. Gulshan, J. P. Kirwan, X. Liu, S. Previs, B. Willard, J. D. Smith, and A. McCullough. 2015. 'Ceramide as a mediator of non-alcoholic Fatty liver disease and associated atherosclerosis', *PLoS One*, 10: e0126910.

Kathiresan, S., A. K. Manning, S. Demissie, R. B. D'Agostino, A. Surti, C. Guiducci, L. Gianniny, N. P. Burtt, O. Melander, M. Orho-Melander, D. K. Arnett, G. M. Peloso, J. M. Ordovas, and L. A. Cupples. 2007. 'A genome-wide association study for blood lipid phenotypes in the Framingham Heart Study', *BMC Med Genet*, 8 Suppl 1: S17.

Keelan, J. A., M. Blumenstein, R. J. A. Helliwell, T. A. Sato, K. W. Marvin, and M. D. Mitchell. 2003. 'Cytokines, Prostaglandins and Parturition—A Review', *Placenta*, 24: S33-S46.

Khan, Anmar A., Piyushkumar A. Mundra, Nora E. Straznicky, Paul J. Nestel, Gerard Wong, Ricardo Tan, Kevin Huynh, Theodore W. Ng, Natalie A. Mellett, Jacquelyn M. Weir, Christopher K. Barlow, Zahir H. Alshehry, Gavin W. Lambert, Bronwyn A. Kingwell, and Peter J. Meikle. 2018. 'Weight Loss and Exercise Alter the High-Density Lipoprotein Lipidome and Improve High-Density Lipoprotein Functionality in Metabolic Syndrome', *Arteriosclerosis, Thrombosis, and Vascular Biology*, 38: 438-47.

Khera, Amit V., Marina Cuchel, Margarita de la Llera-Moya, Amrith Rodrigues, Megan F. Burke, Kashif Jafri, Benjamin C. French, Julie A. Phillips, Megan L. Mucksavage, Robert L. Wilensky, Emile R. Mohler, George H. Rothblat, and Daniel J. Rader. 2011. 'Cholesterol Efflux Capacity, High-Density Lipoprotein Function, and Atherosclerosis', *New England Journal of Medicine*, 364: 127-35.

Khong, T. Yee, Eoghan E Mooney, Ilana Ariel, Nathalie C. M. Balmus, Theonia K. Boyd, Marie-Anne Brundler, Hayley Derricott, Margaret J. Evans, Ona M. Faye-Petersen, John E. Gillan, Alex E. P. Heazell, Debra S. Heller, Suzanne M. Jacques, Sarah Keating, Peter Kelehan, Ann Maes, Eileen M. McKay, Terry K. Morgan, Peter G. J. Nikkels, W. Tony Parks, Raymond W.

Redline, Irene Scheimberg, Mirthe H. Schoots, Neil J. Sebire, Albert Timmer, Gitta Turowski, J. Patrick van der Voorn, Ineke van Lijnschoten, and Sanne J. Gordijn. 2016. 'Sampling and Definitions of Placental Lesions: Amsterdam Placental Workshop Group Consensus Statement', *Archives of Pathology & Laboratory Medicine*, 140: 698-713.

Kielar, D., W. Dietmaier, T. Langmann, C. Aslanidis, M. Probst, M. Naruszewicz, and G. Schmitz. 2001. 'Rapid quantification of human ABCA1 mRNA in various cell types and tissues by real-time reverse transcription-PCR', *Clin Chem*, 47: 2089-97.

Kim, D. K., J. Lee, S. R. Kim, D. S. Choi, Y. J. Yoon, J. H. Kim, G. Go, D. Nhung, K. Hong, S. C. Jang, S. H. Kim, K. S. Park, O. Y. Kim, H. T. Park, J. H. Seo, E. Aikawa, M. Baj-Krzyworzeka, B. W. van Balkom, M. Belting, L. Blanc, V. Bond, A. Bongiovanni, F. E. Borràs, L. Buée, E. I. Buzás, L. Cheng, A. Clayton, E. Cocucci, C. S. Dela Cruz, D. M. Desiderio, D. Di Vizio, K. Ekström, J. M. Falcon-Perez, C. Gardiner, B. Giebel, D. W. Greening, J. C. Gross, D. Gupta, A. Hendrix, A. F. Hill, M. M. Hill, E. Nolte-'t Hoen, D. W. Hwang, J. Inal, M. V. Jagannadham, M. Jayachandran, Y. K. Jee, M. Jørgensen, K. P. Kim, Y. K. Kim, T. Kislinger, C. Lässer, D. S. Lee, H. Lee, J. van Leeuwen, T. Lener, M. L. Liu, J. Lötvall, A. Marcilla, S. Mathivanan, A. Möller, J. Morhayim, F. Mullier, I. Nazarenko, R. Nieuwland, D. N. Nunes, K. Pang, J. Park, T. Patel, G. Pocsfalvi, H. Del Portillo, U. Putz, M. I. Ramirez, M. L. Rodrigues, T. Y. Roh, F. Royo, S. Sahoo, R. Schiffelers, S. Sharma, P. Siljander, R. J. Simpson, C. Soekmadji, P. Stahl, A. Stensballe, E. Stępień, H. Tahara, A. Trummer, H. Valadi, L. J. Vella, S. N. Wai, K. Witwer, M. Yáñez-Mó, H. Youn, R. Zeidler, and Y. S. Gho. 2015. 'EVpedia: a community web portal for extracellular vesicles research', *Bioinformatics*, 31: 933-9.

Kimura, T., H. Tomura, C. Mogi, A. Kuwabara, A. Damirin, T. Ishizuka, A. Sekiguchi, M. Ishiwara, D. S. Im, K. Sato, M. Murakami, and F. Okajima. 2006. 'Role of scavenger receptor class B type I and sphingosine 1-phosphate receptors in high density lipoprotein-induced inhibition of adhesion molecule expression in endothelial cells', *J Biol Chem*, 281: 37457-67.

King, A., Y. W. Loke, and G. Chaouat. 1997. 'NK cells and reproduction', *Immunol Today*, 18: 64-6.

Kinoshita, T., and M. Itoh. 2006. 'Longitudinal variance of fat mass deposition during pregnancy evaluated by ultrasonography: the ratio of visceral fat to subcutaneous fat in the abdomen', *Gynecol Obstet Invest*, 61: 115-8.

Kjellmo, C. A., H. Karlsson, T. K. Nestvold, S. Ljunggren, K. Cederbrant, M. Marcusson-Ståhl, M. Mathisen, K. T. Lappegård, and A. Hovland. 2018. 'Bariatric surgery improves lipoprotein profile in morbidly obese patients by reducing LDL cholesterol, apoB, and SAA/PON1 ratio, increasing HDL cholesterol, but has no effect on cholesterol efflux capacity', *J Clin Lipidol*, 12: 193-202.

Klimov, A. N., K. A. Kozhevnikova, A. A. Kuzmin, A. S. Kuznetsov, and E. V. Belova. 2001. 'On the ability of high density lipoproteins to remove phospholipid peroxidation products from erythrocyte membranes', *Biochemistry (Mosc)*, 66: 300-4.

Klimov, Anatoly N., Victor S. Gurevich, Aida A. Nikiforova, Larisa V. Shatilina, Alexander A. Kuzmin, Swjatoslaw L. Plavinsky, and Nataly P. Teryukova. 1993. 'Antioxidative activity of high density lipoproteins in vivo', *Atherosclerosis*, 100: 13-18.

Kontush, Anatol. 2014. 'HDL-mediated mechanisms of protection in cardiovascular disease', *Cardiovascular Research*, 103: 341-49.
Kontush, Anatol, Mats Lindahl, Marie Lhomme, Laura Calabresi, M. John Chapman, and W. Sean Davidson. 2015. 'Structure of HDL: Particle Subclasses and Molecular Components.' in Arnold von Eckardstein and Dimitris Kardassis (eds.), *High Density Lipoproteins: From Biological Understanding to Clinical Exploitation* (Springer International Publishing: Cham).
Kotani, Kazuhiko, Toshiyuki Yamada, and Alejandro Gugliucci. 2013. 'Paired measurements of paraoxonase 1 and serum amyloid A as useful disease markers', *BioMed research international*, 2013: 481437-37.
Kozyraki, R., J. Fyfe, M. Kristiansen, C. Gerdes, C. Jacobsen, S. Cui, E. I. Christensen, M. Aminoff, A. de la Chapelle, R. Krahe, P. J. Verroust, and S. K. Moestrup. 1999. 'The intrinsic factor-vitamin B12 receptor, cubilin, is a high-affinity apolipoprotein A-I receptor facilitating endocytosis of high-density lipoprotein', *Nat Med*, 5: 656-61.
Krishnaswamy, G., J. K. Smith, R. Mukkamala, K. Hall, W. Joyner, L. Yerra, and D. S. Chi. 1998. 'Multifunctional cytokine expression by human coronary endothelium and regulation by monokines and glucocorticoids', *Microvasc Res*, 55: 189-200.
Kristensen, K., D. Wide-Swensson, V. Lindstrom, C. Schmidt, A. Grubb, and H. Strevens. 2009. 'Serum amyloid a protein and C-reactive protein in normal pregnancy and preeclampsia', *Gynecol Obstet Invest*, 67: 275-80.
Kristoffersen, A. H., P. H. Petersen, T. Røraas, and S. Sandberg. 2017. 'Estimates of Within-Subject Biological Variation of Protein C, Antithrombin, Protein S Free, Protein S Activity, and Activated Protein C Resistance in Pregnant Women', *Clin Chem*, 63: 898-907.
Kubes, P., M. Suzuki, and D. N. Granger. 1991. 'Nitric oxide: an endogenous modulator of leukocyte adhesion', *Proc Natl Acad Sci U S A*, 88: 4651-5.
Kuchan, M. J., and J. A. Frangos. 1994. 'Role of calcium and calmodulin in flow-induced nitric oxide production in endothelial cells', *Am J Physiol*, 266: C628-36.
Kumar, C. A., and U. N. Das. 2000. 'Lipid peroxides, anti-oxidants and nitric oxide in patients with pre-eclampsia and essential hypertension', *Medical science monitor : international medical journal of experimental and clinical research*, 6: 901-07.
Kunitake, S. T., and J. P. Kane. 1982. 'Factors affecting the integrity of high density lipoproteins in the ultracentrifuge', *J Lipid Res*, 23: 936-40.
Kunitake, Steven T., Patricia O'Connor, and Josefina Naya-Vigne. 1996. '[16] Heterogeneity of high-density lipoproteins and apolipoprotein A-I as related to quantification of apolipoprotein A-I.' in, *Methods in Enzymology* (Academic Press).
Kurano, M., K. Tsukamoto, M. Hara, K. Tsuneyama, T. Nishikawa, H. Ikeda, and Y. Yatomi. 2020. 'Modulation of sphingosine 1-phosphate by hepatobiliary cholesterol handling', *FASEB J*, 34: 14655-70.
Laaksonen, R., K. Ekroos, M. Sysi-Aho, M. Hilvo, T. Vihervaara, D. Kauhanen, M. Suoniemi, R. Hurme, W. Marz, H. Scharnagl, T. Stojakovic, E. Vlachopoulou, M. L. Lokki, M. S. Nieminen, R. Klingenberg, C. M. Matter, T. Hornemann, P. Juni, N. Rodondi, L. Raber, S. Windecker, B. Gencer, E. R. Pedersen, G. S. Tell, O. Nygard, F. Mach, J. Sinisalo, and T. F. Luscher. 2016. 'Plasma ceramides predict cardiovascular death in patients with

stable coronary artery disease and acute coronary syndromes beyond LDL-cholesterol', *Eur Heart J*, 37: 1967-76.

Landray, M. J., R. Haynes, J. C. Hopewell, S. Parish, T. Aung, J. Tomson, K. Wallendszus, M. Craig, L. Jiang, R. Collins, and J. Armitage. 2014. 'Effects of extended-release niacin with laropiprant in high-risk patients', *N Engl J Med*, 371: 203-12.

Langmann, T., J. Klucken, M. Reil, G. Liebisch, M. F. Luciani, G. Chimini, W. E. Kaminski, and G. Schmitz. 1999. 'Molecular cloning of the human ATP-binding cassette transporter 1 (hABC1): evidence for sterol-dependent regulation in macrophages', *Biochem Biophys Res Commun*, 257: 29-33.

LaRosa, J. C., R. I. Levy, P. Herbert, S. E. Lux, and D. S. Fredrickson. 1970. 'A specific apoprotein activator for lipoprotein lipase', *Biochem Biophys Res Commun*, 41: 57-62.

Lecarpentier, E., O. Morel, T. Fournier, E. Elefant, P. Chavatte-Palmer, and V. Tsatsaris. 2012. 'Statins and pregnancy: between supposed risks and theoretical benefits', *Drugs*, 72: 773-88.

Lee-Rueckert, Miriam, Jani Lappalainen, Petri T. Kovanen, and Joan Carles Escola-Gil. 2022. 'Lipid-Laden Macrophages and Inflammation in Atherosclerosis and Cancer: An Integrative View', *Frontiers in Cardiovascular Medicine*, 9.

Lee, J., J. S. Kim, J. W. Park, C. W. Park, J. S. Park, J. K. Jun, and B. H. Yoon. 2013. 'Chronic chorioamnionitis is the most common placental lesion in late preterm birth', *Placenta*, 34: 681-9.

Lee, Yin-Lau, Kai-Fai Lee, Jia-Sen Xu, Qing-Yu He, Jen-Fu Chiu, Will M Lee, John M Luk, and William SB Yeung. 2004. 'The embryotrophic activity of oviductal cell-derived complement C3b and iC3b, a novel function of complement protein in reproduction', *Journal of Biological Chemistry*, 279: 12763-68.

Lemmers, R. F. H., N. E. M. A. Martens, A. H. Maas, L. C. van Vark-van der Zee, F. P. J. Leijten, C. M. Groot-van Ruijven, M. van Hoek, A. G. Lieverse, E. J. G. Sijbrands, H. R. Haak, P. J. M. Leenen, A. J. M. Verhoeven, W. A. Dik, and M. T. Mulder. 2021. 'Breakfast partly restores the anti-inflammatory function of high-density lipoproteins from patients with type 2 diabetes mellitus', *Atherosclerosis Plus*, 44: 43-50.

Lepedda, A. J., G. Nieddu, E. Zinellu, P. De Muro, F. Piredda, A. Guarino, R. Spirito, F. Carta, F. Turrini, and M. Formato. 2013. 'Proteomic analysis of plasma-purified VLDL, LDL, and HDL fractions from atherosclerotic patients undergoing carotid endarterectomy: identification of serum amyloid A as a potential marker', *Oxid Med Cell Longev*, 2013: 385214.

Levels, Johannes Hm, Pierre Geurts, Helen Karlsson, Raphaël Marée, Stefan Ljunggren, Louise Fornander, Louis Wehenkel, Mats Lindahl, Erik Sg Stroes, Jan A. Kuivenhoven, and Joost Cm Meijers. 2011. 'High-density lipoprotein proteome dynamics in human endotoxemia', *Proteome Sci*, 9: 34-34.

Levine, Richard J., Sharon E. Maynard, Cong Qian, Kee-Hak Lim, Lucinda J. England, Kai F. Yu, Enrique F. Schisterman, Ravi Thadhani, Benjamin P. Sachs, Franklin H. Epstein, Baha M. Sibai, Vikas P. Sukhatme, and S. Ananth Karumanchi. 2004. 'Circulating Angiogenic Factors and the Risk of Preeclampsia', *New England Journal of Medicine*, 350: 672-83.

Li, X. A., W. B. Titlow, B. A. Jackson, N. Giltiay, M. Nikolova-Karakashian, A. Uittenbogaard, and E. J. Smart. 2002. 'High density lipoprotein binding to

scavenger receptor, Class B, type I activates endothelial nitric-oxide synthase in a ceramide-dependent manner', *J Biol Chem*, 277: 11058-63.

Lindberger, E., A. K. Wikström, E. Bergman, K. Eurenius, A. Mulic-Lutvica, L. Lindström, I. Sundström Poromaa, and F. Ahlsson. 2021. 'Associations of ultrasound estimated early mid pregnancy visceral and subcutaneous fat depths and early pregnancy BMI with adverse neonatal outcomes', *Sci Rep*, 11: 4612.

Lindgren, F. T., L. C. Jensen, R. D. Wills, and G. R. Stevens. 1972. 'Subfractionation of S f 4-10 5 , S f 4-20 and high density lipoproteins', *Lipids*, 7: 194-201.

Liu, D., L. Ji, M. Zhao, Y. Wang, Y. Guo, L. Li, D. Zhang, L. Xu, B. Pan, J. Su, S. Xiang, S. Pennathur, J. Li, J. Gao, P. Liu, B. Willard, and L. Zheng. 2018. 'Lysine glycation of apolipoprotein A-I impairs its anti-inflammatory function in type 2 diabetes mellitus', *J Mol Cell Cardiol*, 122: 47-57.

Ljunggren, Stefan A., Ingela Helmfrid, Ulf Norinder, Mats Fredriksson, Gun Wingren, Helen Karlsson, and Mats Lindahl. 2017. 'Alterations in high-density lipoprotein proteome and function associated with persistent organic pollutants', *Environment International*, 98: 204-11.

Ljunggren, Stefan A., Ingela Helmfrid, Samira Salihovic, Bert van Bavel, Gun Wingren, Mats Lindahl, and Helen Karlsson. 2014. 'Persistent organic pollutants distribution in lipoprotein fractions in relation to cardiovascular disease and cancer', *Environment International*, 65: 93-99.

Lobmaier, S. M., F. Figueras, I. Mercade, F. Crovetto, A. Peguero, M. Parra-Saavedra, J. U. Ortiz, F. Crispi, and E. Gratacós. 2014. 'Levels of Maternal Serum Angiogenic Factors in Third-Trimester Normal Pregnancies: Reference Ranges, Influence of Maternal and Pregnancy Factors and Fetoplacental Doppler Indices', *Fetal Diagnosis and Therapy*, 36: 38-43.

Loeber, J. G., M. A. Franken, and F. X. van Leeuwen. 1983. 'Effect of sodium bromide on endocrine parameters in the rat as studied by immunocytochemistry and radioimmunoassay', *Food Chem Toxicol*, 21: 391-404.

Lorentzen, Bjosrg, Mark J. Endresen, Torun Clausen, and Tore Henriksen. 1994. 'Fasting Serum Free Fatty Acids and Triglycerides are Increased Before 20 Weeks of Gestation in Women who Later Develop Preeclampsia', *Hypertens Pregnancy*, 13: 103-09.

Lu, R., T. Ishikawa, M. Tanaka, T. Tsuboi, and S. Yokoyama. 2021. 'Zinc Increases ABCA1 by Attenuating Its Clearance Through the Modulation of Calmodulin Activity', *J Atheroscler Thromb*, 28: 261-70.

Luo, M., A. Liu, S. Wang, T. Wang, D. Hu, S. Wu, and D. Peng. 2017. 'ApoCIII enrichment in HDL impairs HDL-mediated cholesterol efflux capacity', *Sci Rep*, 7: 2312.

Lusa, S., M. Jauhiainen, J. Metso, P. Somerharju, and C. Ehnholm. 1996. 'The mechanism of human plasma phospholipid transfer protein-induced enlargement of high-density lipoprotein particles: evidence for particle fusion', *Biochem J*, 313 (Pt 1): 275-82.

Ma, Rong, Yang Gu, Shuang Zhao, Jingxia Sun, Lynn J. Groome, and Yuping Wang. 2012. 'Expressions of vitamin D metabolic components VDBP, CYP2R1, CYP27B1, CYP24A1, and VDR in placentas from normal and preeclamptic pregnancies', *Am J Physiol Endocrinol Metab*, 303: E928-E35.

MacCallum, P. K., J. A. Cooper, J. Martin, D. J. Howarth, T. W. Meade, and G. J. Miller. 2000. 'Haemostatic and lipid determinants of prothrombin fragment F1.2 and D-dimer in plasma', *Thromb Haemost*, 83: 421-6.

Mackay, Vanessa A., Shahzya S. Huda, Frances M. Stewart, Kahmeng Tham, Louise A. McKenna, Iain Martin, Fiona Jordan, E. Ann Brown, Leanne Hodson, Ian A. Greer, Barbara J. Meyer, and Dilys J. Freeman. 2012. 'Preeclampsia is associated with compromised maternal synthesis of long-chain polyunsaturated fatty acids, leading to offspring deficiency', *Hypertension (Dallas, Tex. : 1979)*, 60: 1078-85.

Mackness, B., R. Beltran-Debon, G. Aragones, J. Joven, J. Camps, and M. Mackness. 2010. 'Human tissue distribution of paraoxonases 1 and 2 mRNA', *IUBMB Life*, 62: 480-2.

Mackness, Bharti, Paul Durrington, Patrick McElduff, John Yarnell, Naheed Azam, Michael Watt, and Michael Mackness. 2003. 'Low Paraoxonase Activity Predicts Coronary Events in the Caerphilly Prospective Study', *Circulation*, 107: 2775-79.

Mackness, M. I., S. Arrol, C. Abbott, and P. N. Durrington. 1993. 'Protection of low-density lipoprotein against oxidative modification by high-density lipoprotein associated paraoxonase', *Atherosclerosis*, 104: 129-35.

Mackness, M. I., S. Arrol, and P. N. Durrington. 1991. 'Paraoxonase prevents accumulation of lipoperoxides in low-density lipoprotein', *FEBS Lett*, 286: 152-4.

Mahendru, Amita A., Thomas R. Everett, Ian B. Wilkinson, Christoph C. Lees, and Carmel M. McEniery. 2014. 'A longitudinal study of maternal cardiovascular function from preconception to the postpartum period', *Journal of Hypertension*, 32: 849-56.

Mahmoud, Ayman M., Fiona L. Wilkinson, Eoghan M. McCarthy, Daniel M. Moreno-Martinez, Alexander Langford-Smith, Miguel Romero, Juan Duarte, and M. Yvonne Alexander. 2017. 'Endothelial microparticles prevent lipid-induced endothelial damage via Akt/eNOS signaling and reduced oxidative stress', *The FASEB Journal*, 31: 4636-48.

Mai, J., A. Virtue, J. Shen, H. Wang, and X. F. Yang. 2013. 'An evolving new paradigm: endothelial cells--conditional innate immune cells', *J Hematol Oncol*, 6: 61.

Mannaerts, D., E. Faes, P. Cos, J. J. Briedé, W. Gyselaers, J. Cornette, Y. Gorbanev, A. Bogaerts, M. Spaanderman, E. Van Craenenbroeck, and Y. Jacquemyn. 2018. 'Oxidative stress in healthy pregnancy and preeclampsia is linked to chronic inflammation, iron status and vascular function', *PLoS One*, 13: e0202919.

Manten, G. T., A. Franx, J. M. Sikkema, T. M. Hameeteman, G. H. Visser, P. G. de Groot, and H. A. Voorbij. 2004. 'Fibrinogen and high molecular weight fibrinogen during and after normal pregnancy', *Thromb Res*, 114: 19-23.

Mardones, P., V. Quiñones, L. Amigo, M. Moreno, J. F. Miquel, M. Schwarz, H. E. Miettinen, B. Trigatti, M. Krieger, S. VanPatten, D. E. Cohen, and A. Rigotti. 2001. 'Hepatic cholesterol and bile acid metabolism and intestinal cholesterol absorption in scavenger receptor class B type I-deficient mice', *J Lipid Res*, 42: 170-80.

Maron, D. J. 2000. 'The epidemiology of low levels of high-density lipoprotein cholesterol in patients with and without coronary artery disease', *Am J Cardiol*, 86: 11l-14l.

Martinez Abundis, Esperanza, Manuel Gonzalez Ortiz, Alfredo Quiñones Galvan, and Ele Ferrannini. 1996. 'Hyperinsulinemia in glucose-tolerant women with preeclampsia A controlled study', *American Journal of Hypertension*, 9: 610-14.

Maruyama, I., C. E. Bell, and P. W. Majerus. 1985. 'Thrombomodulin is found on endothelium of arteries, veins, capillaries, and lymphatics, and on syncytiotrophoblast of human placenta', *J Cell Biol*, 101: 363-71.

Maruyama, T., N. Sakai, M. Ishigami, K. Hirano, T. Arai, S. Okada, E. Okuda, A. Ohya, N. Nakajima, K. Kadowaki, E. Fushimi, S. Yamashita, and Y. Matsuzawa. 2003. 'Prevalence and phenotypic spectrum of cholesteryl ester transfer protein gene mutations in Japanese hyperalphalipoproteinemia', *Atherosclerosis*, 166: 177-85.

Matsuura, F., N. Wang, W. Chen, X. C. Jiang, and A. R. Tall. 2006. 'HDL from CETP-deficient subjects shows enhanced ability to promote cholesterol efflux from macrophages in an apoE- and ABCG1-dependent pathway', *J Clin Invest*, 116: 1435-42.

Maugeais, Cyrille, Uwe J.F. Tietge, Uli C. Broedl, Dawn Marchadier, William Cain, Mary G. McCoy, Sissel Lund-Katz, Jane M. Glick, and Daniel J. Rader. 2003. 'Dose-Dependent Acceleration of High-Density Lipoprotein Catabolism by Endothelial Lipase', *Circulation*, 108: 2121-26.

Maynard, Sharon E., Jiang-Yong Min, Jaime Merchan, Kee-Hak Lim, Jianyi Li, Susanta Mondal, Towia A. Libermann, James P. Morgan, Frank W. Sellke, Isaac E. Stillman, Franklin H. Epstein, Vikas P. Sukhatme, and S. Ananth Karumanchi. 2003. 'Excess placental soluble fms-like tyrosine kinase 1 (sFlt1) may contribute to endothelial dysfunction, hypertension, and proteinuria in preeclampsia', *The Journal of Clinical Investigation*, 111: 649-58.

Mazer, Norman A., Franco Giulianini, Nina P. Paynter, Paul Jordan, and Samia Mora. 2013. 'A comparison of the theoretical relationship between HDL size and the ratio of HDL cholesterol to apolipoprotein A-I with experimental results from the Women's Health Study', *Clin Chem*, 59: 949-58.

McDonnell, Thomas, Chris Wincup, Ina Buchholz, Charis Pericleous, Ian Giles, Vera Ripoll, Hannah Cohen, Mihaela Delcea, and Anisur Rahman. 2020. 'The role of beta-2-glycoprotein I in health and disease associating structure with function: More than just APS', *Blood Reviews*, 39: 100610.

McVicar, J. P., S. T. Kunitake, R. L. Hamilton, and J. P. Kane. 1984. 'Characteristics of human lipoproteins isolated by selected-affinity immunosorption of apolipoprotein A-I', *Proc Natl Acad Sci U S A*, 81: 1356-60.

Mehta, Niyati U., Victor Grijalva, Susan Hama, Alan Wagner, Mohamad Navab, Alan M. Fogelman, and Srinivasa T. Reddy. 2016. 'Apolipoprotein E-/- Mice Lacking Hemopexin Develop Increased Atherosclerosis via Mechanisms That Include Oxidative Stress and Altered Macrophage Function', *Arteriosclerosis, Thrombosis, and Vascular Biology*, 36: 1152-63.

Melchior, J. T., D. K. Swertfeger, J. Morris, S. E. Street, C. R. Warshak, J. A. Welge, A. T. Remaley, J. M. Catov, W. S. Davidson, and L. A. Woollett. 2021. 'Pregnancy is accompanied by larger high density lipoprotein particles and compositionally distinct subspecies', *J Lipid Res*, 62: 100107.

Melhem, H., S. Kallol, X. Huang, M. Luthi, C. E. Ontsouka, A. Keogh, D. Stroka, W. Thormann, H. Schneider, and C. Albrecht. 2019. 'Placental secretion of apolipoprotein A1 and E: the anti-atherogenic impact of the placenta', *Sci Rep*, 9: 6225.

Melland-Smith, M., L. Ermini, S. Chauvin, H. Craig-Barnes, A. Tagliaferro, T. Todros, M. Post, and I. Caniggia. 2015. 'Disruption of sphingolipid

metabolism augments ceramide-induced autophagy in preeclampsia', *Autophagy*, 11: 653-69.

Memon, R. A., W. M. Holleran, A. H. Moser, T. Seki, Y. Uchida, J. Fuller, J. K. Shigenaga, C. Grunfeld, and K. R. Feingold. 1998. 'Endotoxin and cytokines increase hepatic sphingolipid biosynthesis and produce lipoproteins enriched in ceramides and sphingomyelin', *Arterioscler Thromb Vasc Biol*, 18: 1257-65.

Memon, R. A., W. M. Holleran, Y. Uchida, A. H. Moser, S. Ichikawa, Y. Hirabayashi, C. Grunfeld, and K. R. Feingold. 1999. 'Regulation of glycosphingolipid metabolism in liver during the acute phase response', *J Biol Chem*, 274: 19707-13.

Meraji, S., C. E. Moore, V. O. Skinner, and K. R. Bruckdorfer. 1992. 'The Importance of Oxidation or Glycosylation of Low-density Lipoproteins in Relation to Platelet Activation', *Platelets*, 3: 155-62.

Merrill, A. H., Jr., S. Lingrell, E. Wang, M. Nikolova-Karakashian, T. R. Vales, and D. E. Vance. 1995. 'Sphingolipid biosynthesis de novo by rat hepatocytes in culture. Ceramide and sphingomyelin are associated with, but not required for, very low density lipoprotein secretion', *J Biol Chem*, 270: 13834-41.

Miao, L., R. X. Yin, S. L. Pan, S. Yang, D. Z. Yang, and W. X. Lin. 2019. 'Circulating miR-3659 may be a potential biomarker of dyslipidemia in patients with obesity', *J Transl Med*, 17: 25.

Miller, G. J., and N. E. Miller. 1975. 'Plasma-high-density-lipoprotein concentration and development of ischaemic heart-disease', *Lancet*, 1: 16-9.

Mills, J. L., L. Jovanovic, R. Knopp, J. Aarons, M. Conley, E. Park, Y. J. Lee, L. Holmes, J. L. Simpson, and B. Metzger. 1998. 'Physiological reduction in fasting plasma glucose concentration in the first trimester of normal pregnancy: the diabetes in early pregnancy study', *Metabolism*, 47: 1140-4.

Mishra, N., W. H. Nugent, S. Mahavadi, and S. W. Walsh. 2011. 'Mechanisms of enhanced vascular reactivity in preeclampsia', *Hypertension*, 58: 867-73.

Mistry, H. D., M. V. H. Ogalde, F. Broughton Pipkin, G. Escher, and L. O. Kurlak. 2020. 'Maternal, Fetal, and Placental Selectins in Women With Pre-eclampsia; Association With the Renin-Angiotensin-System', *Front Med (Lausanne)*, 7: 270.

Mistry, Hiten D., Lesia O. Kurlak, Yosef T. Mansour, Line Zurkinden, Markus G. Mohaupt, and Geneviève Escher. 2017. 'Increased maternal and fetal cholesterol efflux capacity and placental CYP27A1 expression in preeclampsia', *Journal of Lipid Research*, 58: 1186-95.

Mistry, Hiten D., Vicky Wilson, Margaret M. Ramsay, Michael E. Symonds, and Fiona Broughton Pipkin. 2008. 'Reduced Selenium Concentrations and Glutathione Peroxidase Activity in Preeclamptic Pregnancies', *Hypertension*, 52: 881-88.

Mokkala, K., O. Pellonpera, H. Roytio, P. Pussinen, T. Ronnemaa, and K. Laitinen. 2017. 'Increased intestinal permeability, measured by serum zonulin, is associated with metabolic risk markers in overweight pregnant women', *Metabolism*, 69: 43-50.

Mor, G., S. L. Straszewski-Chavez, and V. M. Abrahams. 2006. 'Macrophage-trophoblast interactions', *Methods Mol Med*, 122: 149-63.

Mor, Gil, Ingrid Cardenas, Vikki Abrahams, and Seth Guller. 2011. 'Inflammation and pregnancy: the role of the immune system at the implantation site', *Annals of the New York Academy of Sciences*, 1221: 80-87.

Moreno-Navarrete, J. M., M. Sabater, F. Ortega, W. Ricart, and J. M. Fernandez-Real. 2012. 'Circulating zonulin, a marker of intestinal permeability, is increased in association with obesity-associated insulin resistance', *PLoS One*, 7: e37160.

Morrow, V. A., F. Foufelle, J. M. Connell, J. R. Petrie, G. W. Gould, and I. P. Salt. 2003. 'Direct activation of AMP-activated protein kinase stimulates nitric-oxide synthesis in human aortic endothelial cells', *J Biol Chem*, 278: 31629-39.

Morton, R. E., Y. Liu, and L. Izem. 2019. 'ApoF knockdown increases cholesteryl ester transfer to LDL and impairs cholesterol clearance in fat-fed hamsters', *J Lipid Res*, 60: 1868-79.

Morton, R. E., and D. B. Zilversmit. 1983. 'Inter-relationship of lipids transferred by the lipid-transfer protein isolated from human lipoprotein-deficient plasma', *J Biol Chem*, 258: 11751-7.

Mulvany, M. J., and W. Halpern. 1977. 'Contractile properties of small arterial resistance vessels in spontaneously hypertensive and normotensive rats', *Circ Res*, 41: 19-26.

Munroe, W. H., M. L. Phillips, and V. N. Schumaker. 2015. 'Excessive centrifugal fields damage high density lipoprotein', *J Lipid Res*, 56: 1172-81.

Murphy, A. J., N. Bijl, L. Yvan-Charvet, C. B. Welch, N. Bhagwat, A. Reheman, Y. Wang, J. A. Shaw, R. L. Levine, H. Ni, A. R. Tall, and N. Wang. 2013. 'Cholesterol efflux in megakaryocyte progenitors suppresses platelet production and thrombocytosis', *Nat Med*, 19: 586-94.

Muzakova, V., P. K. Beekhof, and Ehjm Jansen. 2020. 'Very long-term stability of lipid biomarkers in human serum', *Anal Biochem*, 597: 113695.

Nagamatsu, Takeshi, Tomoyuki Fujii, Maki Kusumi, Li Zou, Takahiro Yamashita, Yutaka Osuga, Mikio Momoeda, Shirou Kozuma, and Yuji Taketani. 2004. 'Cytotrophoblasts Up-Regulate Soluble Fms-Like Tyrosine Kinase-1 Expression under Reduced Oxygen: An Implication for the Placental Vascular Development and the Pathophysiology of Preeclampsia', *Endocrinology*, 145: 4838-45.

Nair, Akhila, Roshin U. Thankachen, Jithin Raj, and Sreeraj Gopi. 2021. '1 - Inflammation, symptoms, benefits, reaction, and biochemistry.' in Sreeraj Gopi, Augustine Amalraj, Ajaikumar Kunnumakkara and Sabu Thomas (eds.), *Inflammation and Natural Products* (Academic Press).

Nam, B. H., J. Y. Moon, E. H. Park, Y. O. Kim, D. G. Kim, H. J. Kong, W. J. Kim, Y. J. Jee, C. M. An, N. G. Park, and J. K. Seo. 2014. 'Antimicrobial activity of peptides derived from olive flounder lipopolysaccharide binding protein/bactericidal permeability-increasing protein (LBP/BPI)', *Mar Drugs*, 12: 5240-57.

Nan, B., H. Yang, S. Yan, P. H. Lin, A. B. Lumsden, Q. Yao, and C. Chen. 2005. 'C-reactive protein decreases expression of thrombomodulin and endothelial protein C receptor in human endothelial cells', *Surgery*, 138: 212-22.

Navab, M., S. S. Imes, S. Y. Hama, G. P. Hough, L. A. Ross, R. W. Bork, A. J. Valente, J. A. Berliner, D. C. Drinkwater, H. Laks, and et al. 1991. 'Monocyte transmigration induced by modification of low density lipoprotein in cocultures of human aortic wall cells is due to induction of

monocyte chemotactic protein 1 synthesis and is abolished by high density lipoprotein', *The Journal of Clinical Investigation*, 88: 2039-46.

Nestel, P. J., and N. E. Miller. 1980. 'Cholesterol kinetics and faecal steroid excretion in subjects with primary hyperalphalipoproteinaemia', *Atherosclerosis*, 36: 127-34.

Neville, Matt J., Jenny M. Collins, Anna L. Gloyn, Mark I. McCarthy, and Fredrik Karpe. 2011. 'Comprehensive human adipose tissue mRNA and microRNA endogenous control selection for quantitative real-time-PCR normalization', *Obesity (Silver Spring, Md.)*, 19: 888-92.

Newbern, Dorothee, and Michael Freemark. 2011. 'Placental hormones and the control of maternal metabolism and fetal growth', *Current Opinion in Endocrinology, Diabetes and Obesity*, 18: 409-16.

Ng, Qiu Ju, Jonathan Youxiang Han, Seyed Ehsan Saffari, George Seow-Heong Yeo, Bernard Su Min Chern, and Kok Hian Tan. 2019. 'Longitudinal circulating placental growth factor (PlGF) and soluble FMS-like tyrosine kinase-1 (sFlt-1) concentrations during pregnancy in Asian women: a prospective cohort study', *BMJ Open*, 9: e028321.

Ngene, N. C., and J. Moodley. 2018. 'Role of angiogenic factors in the pathogenesis and management of pre-eclampsia', *Int J Gynaecol Obstet*, 141: 5-13.

Nijstad, N., H. Wiersma, T. Gautier, M. van der Giet, C. Maugeais, and U. J. Tietge. 2009. 'Scavenger receptor BI-mediated selective uptake is required for the remodeling of high density lipoprotein by endothelial lipase', *J Biol Chem*, 284: 6093-100.

Nishida, Hiro I., and Toshiro Nishida. 1997. 'Phospholipid Transfer Protein Mediates Transfer of not Only Phosphatidylcholine but Also Cholesterol from Phosphatidylcholine-Cholesterol Vesicles to High Density Lipoproteins*', *Journal of Biological Chemistry*, 272: 6959-64.

Nissen, Steven E., Taro Tsunoda, E. Murat Tuzcu, Paul Schoenhagen, Christopher J. Cooper, Muhammad Yasin, Gregory M. Eaton, Michael A. Lauer, W. Scott Sheldon, Cindy L. Grines, Stephen Halpern, Tim Crowe, James C. Blankenship, and Richard Kerensky. 2003. 'Effect of Recombinant ApoA-I Milano on Coronary Atherosclerosis in Patients With Acute Coronary Syndromes: A Randomized Controlled Trial', *JAMA*, 290: 2292-300.

Njock, Makon-Sébastien, Henry S. Cheng, Lan T. Dang, Maliheh Nazari-Jahantigh, Andrew C. Lau, Emilie Boudreau, Mark Roufaiel, Myron I. Cybulsky, Andreas Schober, and Jason E. Fish. 2015. 'Endothelial cells suppress monocyte activation through secretion of extracellular vesicles containing antiinflammatory microRNAs', *Blood*, 125: 3202-12.

Nofer, Jerzy-Roch, Markus van der Giet, Markus Tölle, Iza Wolinska, Karin von Wnuck Lipinski, Hideo A. Baba, Uwe J. Tietge, Axel Gödecke, Isao Ishii, Burkhard Kleuser, Michael Schäfers, Manfred Fobker, Walter Zidek, Gerd Assmann, Jerold Chun, and Bodo Levkau. 2004. 'HDL induces NO-dependent vasorelaxation via the lysophospholipid receptor S1P3', *The Journal of Clinical Investigation*, 113: 569-81.

Okajima, F. 2002. 'Plasma lipoproteins behave as carriers of extracellular sphingosine 1-phosphate: is this an atherogenic mediator or an anti-atherogenic mediator?', *Biochim Biophys Acta*, 1582: 132-7.

Onyiaodike, Christopher C., Heather M. Murray, Ruiqi Zhang, Barbara J. Meyer, Fiona Jordan, E. Ann Brown, Robert J. B. Nibbs, Helen Lyall, Naveed Sattar, Scott M. Nelson, and Dilys J. Freeman. 2018. 'Pre-conception maternal erythrocyte saturated to unsaturated fatty acid ratio predicts

pregnancy after natural cycle frozen embryo transfer', *Scientific Reports*, 8: 1216.

Ooi, E. M., P. H. Barrett, D. C. Chan, and G. F. Watts. 2008. 'Apolipoprotein C-III: understanding an emerging cardiovascular risk factor', *Clin Sci (Lond)*, 114: 611-24.

Oslakovic, C., E. Norstrøm, and B. Dahlbäck. 2010. 'Reevaluation of the role of HDL in the anticoagulant activated protein C system in humans', *J Clin Invest*, 120: 1396-9.

Oslakovic, Cecilia, Michael J. Krisinger, Astra Andersson, Matti Jauhiainen, Christian Ehnholm, and Björn Dahlbäck. 2009. 'Anionic Phospholipids Lose Their Procoagulant Properties When Incorporated into High Density Lipoproteins*', *Journal of Biological Chemistry*, 284: 5896-904.

Owen, W. G., and C. T. Esmon. 1981. 'Functional properties of an endothelial cell cofactor for thrombin-catalyzed activation of protein C', *J Biol Chem*, 256: 5532-5.

Pankhurst, Greg, Xing Li Wang, David E. Wilcken, Georg Baernthaler, Ute Panzenböck, Mark Raftery, and Roland Stocker. 2003. 'Characterization of specifically oxidized apolipoproteins in mildly oxidized high density lipoprotein', *Journal of Lipid Research*, 44: 349-55.

Pankiewicz, K., E. Szczerba, T. Maciejewski, and A. Fijałkowska. 2019. 'Non-obstetric complications in preeclampsia', *Prz Menopauzalny*, 18: 99-109.

Panzenböck, U., L. Kritharides, M. Raftery, K. A. Rye, and R. Stocker. 2000. 'Oxidation of methionine residues to methionine sulfoxides does not decrease potential antiatherogenic properties of apolipoprotein A-I', *J Biol Chem*, 275: 19536-44.

Pascoal, I. F., M. D. Lindheimer, C. Nalbantian-Brandt, and J. G. Umans. 1998. 'Preeclampsia selectively impairs endothelium-dependent relaxation and leads to oscillatory activity in small omental arteries', *J Clin Invest*, 101: 464-70.

Patanapirunhakit, Patamat, Helen Karlsson, Monique Mulder, Stefan Ljunggren, Delyth Graham, and Dilys Freeman. 2021. 'Sphingolipids in HDL – Potential markers for adaptation to pregnancy?', *Biochimica et Biophysica Acta (BBA) - Molecular and Cell Biology of Lipids*, 1866: 158955.

Peng, J., and X. P. Li. 2018. 'Apolipoprotein A-IV: A potential therapeutic target for atherosclerosis', *Prostaglandins Other Lipid Mediat*, 139: 87-92.

Pérez-Morga, D., B. Vanhollebeke, F. Paturiaux-Hanocq, D. P. Nolan, L. Lins, F. Homblé, L. Vanhamme, P. Tebabi, A. Pays, P. Poelvoorde, A. Jacquet, R. Brasseur, and E. Pays. 2005. 'Apolipoprotein L-I promotes trypanosome lysis by forming pores in lysosomal membranes', *Science*, 309: 469-72.

Perneger, T. V. 1998. 'What's wrong with Bonferroni adjustments', *Bmj*, 316: 1236-8.

Perségol, L., B. Vergès, M. Foissac, P. Gambert, and L. Duvillard. 2006. 'Inability of HDL from type 2 diabetic patients to counteract the inhibitory effect of oxidised LDL on endothelium-dependent vasorelaxation', *Diabetologia*, 49: 1380.

Pillay, J., V. M. Kamp, M. Pennings, E. J. Oudijk, L. P. Leenen, L. H. Ulfman, and L. Koenderman. 2013. 'Acute-phase concentrations of soluble fibrinogen inhibit neutrophil adhesion under flow conditions in vitro through interactions with ICAM-1 and MAC-1 (CD11b/CD18)', *J Thromb Haemost*, 11: 1172-82.

Pipe, N. G. J., T. Smith, D. Halliday, C. J. Edmonds, C. Williams, and T. M. Coltart. 1979. 'CHANGES IN FAT, FAT-FREE MASS AND BODY WATER IN

HUMAN NORMAL PREGNANCY', *BJOG: An International Journal of Obstetrics & Gynaecology*, 86: 929-40.

Poppas, Athena, Sanjeev G. Shroff, Claudia E. Korcarz, Judith U. Hibbard, David S. Berger, Marshall D. Lindheimer, and Roberto M. Lang. 1997. 'Serial Assessment of the Cardiovascular System in Normal Pregnancy', *Circulation*, 95: 2407-15.

Potter, Julia M., and Paul J. Nestel. 1979. 'The hyperlipidemia of pregnancy in normal and complicated pregnancies', *American Journal of Obstetrics and Gynecology*, 133: 165-70.

Puppo, A., and B. Halliwell. 1988. 'Formation of hydroxyl radicals from hydrogen peroxide in the presence of iron. Is haemoglobin a biological Fenton reagent?', *Biochem J*, 249: 185-90.

Raichur, Suryaprakash, Siew Tein Wang, Puck Wee Chan, Ying Li, Jianhong Ching, Bhagirath Chaurasia, Shaillay Dogra, Miina K Öhman, Kosuke Takeda, Shigeki Sugii, Yael Pewzner-Jung, Anthony H Futerman, and Scott A Summers. 2014. 'CerS2 Haploinsufficiency Inhibits β-Oxidation and Confers Susceptibility to Diet-Induced Steatohepatitis and Insulin Resistance', *Cell Metabolism*, 20: 687-95.

Ramos, M. P., M. D. Crespo-Solans, S. del Campo, J. Cacho, and E. Herrera. 2003. 'Fat accumulation in the rat during early pregnancy is modulated by enhanced insulin responsiveness', *American Journal of Physiology-Endocrinology and Metabolism*, 285: E318-E28.

Rani, Neerja, Renu Dhingra, Dharamveer Singh Arya, Mani Kalaivani, Neerja Bhatla, and Rani Kumar. 2010. 'Role of oxidative stress markers and antioxidants in the placenta of preeclamptic patients', *Journal of Obstetrics and Gynaecology Research*, 36: 1189-94.

Rao, Rohini, John J. Albers, Gertrud Wolfbauer, and Henry J. Pownall. 1997. 'Molecular and Macromolecular Specificity of Human Plasma Phospholipid Transfer Protein', *Biochemistry*, 36: 3645-53.

Rapoport, R. M., and F. Murad. 1983. 'Agonist-induced endothelium-dependent relaxation in rat thoracic aorta may be mediated through cGMP', *Circ Res*, 52: 352-7.

Raymond, D., and E. Peterson. 2011. 'A critical review of early-onset and late-onset preeclampsia', *Obstet Gynecol Surv*, 66: 497-506.

Rico, J. E., V. V. Bandaru, J. M. Dorskind, N. J. Haughey, and J. W. McFadden. 2015. 'Plasma ceramides are elevated in overweight Holstein dairy cows experiencing greater lipolysis and insulin resistance during the transition from late pregnancy to early lactation', *J Dairy Sci*, 98: 7757-70.

Rico, J. E., S. Saed Samii, A. T. Mathews, J. Lovett, N. J. Haughey, and J. W. McFadden. 2017. 'Temporal changes in sphingolipids and systemic insulin sensitivity during the transition from gestation to lactation', *PLoS One*, 12: e0176787.

Rigotti, Attilio, Bernardo L. Trigatti, Marsha Penman, Helen Rayburn, Joachim Herz, and Monty Krieger. 1997. 'A targeted mutation in the murine gene encoding the high density lipoprotein (HDL) receptor scavenger receptor class B type I reveals its key role in HDL metabolism', *Proceedings of the National Academy of Sciences*, 94: 12610-15.

Riwanto, M., L. Rohrer, B. Roschitzki, C. Besler, P. Mocharla, M. Mueller, D. Perisa, K. Heinrich, L. Altwegg, A. von Eckardstein, T. F. Luscher, and U. Landmesser. 2013. 'Altered activation of endothelial anti- and proapoptotic pathways by high-density lipoprotein from patients with

coronary artery disease: role of high-density lipoprotein-proteome remodeling', *Circulation*, 127: 891-904.

Roberts, James M., and Augustine Rajakumar. 2009. 'Preeclampsia and Soluble fms-Like Tyrosine Kinase 1', *The Journal of Clinical Endocrinology & Metabolism*, 94: 2252-54.

Robertson, M. D., C. Pedersen, P. J. Hinton, Asjr Mendis, P. D. Cani, and B. A. Griffin. 2018. 'Elevated high density lipoprotein cholesterol and low grade systemic inflammation is associated with increased gut permeability in normoglycemic men', *Nutr Metab Cardiovasc Dis*, 28: 1296-303.

Rodie, V. A., M. J. Caslake, F. Stewart, N. Sattar, J. E. Ramsay, I. A. Greer, and D. J. Freeman. 2004. 'Fetal cord plasma lipoprotein status in uncomplicated human pregnancies and in pregnancies complicated by pre-eclampsia and intrauterine growth restriction', *Atherosclerosis*, 176: 181-87.

Rohatgi, A., A. Khera, J. D. Berry, E. G. Givens, C. R. Ayers, K. E. Wedin, I. J. Neeland, I. S. Yuhanna, D. R. Rader, J. A. de Lemos, and P. W. Shaul. 2014. 'HDL cholesterol efflux capacity and incident cardiovascular events', *N Engl J Med*, 371: 2383-93.

Rubanyi, G. M., and P. M. Vanhoutte. 1986a. 'Oxygen-derived free radicals, endothelium, and responsiveness of vascular smooth muscle', *American Journal of Physiology-Heart and Circulatory Physiology*, 250: H815-H21.

———. 1986b. 'Superoxide anions and hyperoxia inactivate endothelium-derived relaxing factor', *Am J Physiol*, 250: H822-7.

S. Handwerger, and M. Freemark. 2000. 'The Roles of Placental Growth Hormone and Placental Lactogen in the Regulation of Human Fetal Growth and Development', *Journal of Pediatric Endocrinology and Metabolism*, 13: 343-56.

Sacks, G. P., K. Studena, K. Sargent, and C. W. Redman. 1998. 'Normal pregnancy and preeclampsia both produce inflammatory changes in peripheral blood leukocytes akin to those of sepsis', *Am J Obstet Gynecol*, 179: 80-6.

Saito, S., H. Umekage, Y. Sakamoto, M. Sakai, K. Tanebe, Y. Sasaki, and H. Morikawa. 1999. 'Increased T-helper-1-type immunity and decreased T-helper-2-type immunity in patients with preeclampsia', *Am J Reprod Immunol*, 41: 297-306.

Saleheen, D., R. Scott, S. Javad, W. Zhao, A. Rodrigues, A. Picataggi, D. Lukmanova, M. L. Mucksavage, R. Luben, J. Billheimer, J. J. Kastelein, S. M. Boekholdt, K. T. Khaw, N. Wareham, and D. J. Rader. 2015. 'Association of HDL cholesterol efflux capacity with incident coronary heart disease events: a prospective case-control study', *Lancet Diabetes Endocrinol*, 3: 507-13.

Sandhoff, K., and T. Kolter. 2003. 'Biosynthesis and degradation of mammalian glycosphingolipids', *Philos Trans R Soc Lond B Biol Sci*, 358: 847-61.

Sanghavi, Monika, and John D. Rutherford. 2014. 'Cardiovascular Physiology of Pregnancy', *Circulation*, 130: 1003-08.

Sasson, Isaac E., Alexa P. Vitins, Monica A. Mainigi, Kelle H. Moley, and Rebecca A. Simmons. 2015. 'Pre-gestational vs gestational exposure to maternal obesity differentially programs the offspring in mice', *Diabetologia*, 58: 615-24.

Sattar, N., and I. A. Greer. 1999. 'Lipids and the pathogenesis of pre-eclampsia', *Current Obstetrics & Gynaecology*, 9: 190-95.

Sattar, N., I. A. Greer, J. Louden, G. Lindsay, M. McConnell, J. Shepherd, and C. J. Packard. 1997. 'Lipoprotein subfraction changes in normal pregnancy: threshold effect of plasma triglyceride on appearance of small, dense low density lipoprotein', *J Clin Endocrinol Metab*, 82: 2483-91.

Sattar, Naveed, Astrid Bendomir, Colin Berry, James Shepherd, Ian A. Greer, and Chris J. Packard. 1997. 'Lipoprotein subfraction concentrations in preeclampsia: Pathogenic parallels to atherosclerosis', *Obstetrics & Gynecology*, 89: 403-08.

Scaife, P. J., A. Simpson, L. O. Kurlak, L. V. Briggs, D. S. Gardner, F. Broughton Pipkin, C. J. P. Jones, and H. D. Mistry. 2021. 'Increased Placental Cell Senescence and Oxidative Stress in Women with Pre-Eclampsia and Normotensive Post-Term Pregnancies', *Int J Mol Sci*, 22.

Schaefer, E. J., D. M. Foster, L. A. Zech, F. T. Lindgren, H. B. Brewer, Jr., and R. I. Levy. 1983. 'The effects of estrogen administration on plasma lipoprotein metabolism in premenopausal females', *J Clin Endocrinol Metab*, 57: 262-7.

Schoots, M. H., S. J. Gordijn, S. A. Scherjon, H. van Goor, and J. L. Hillebrands. 2018. 'Oxidative stress in placental pathology', *Placenta*, 69: 153-61.

Schultz, Joshua R., Judy G. Verstuyft, Elaine L. Gong, Alex V. Nichols, and Edward M. Rubin. 1993. 'Protein composition determines the anti-atherogenic properties of HDL in transgenic mice', *Nature*, 365: 762-64.

Schwartz, G. G., A. G. Olsson, M. Abt, C. M. Ballantyne, P. J. Barter, J. Brumm, B. R. Chaitman, I. M. Holme, D. Kallend, L. A. Leiter, E. Leitersdorf, J. J. McMurray, H. Mundl, S. J. Nicholls, P. K. Shah, J. C. Tardif, and R. S. Wright. 2012. 'Effects of dalcetrapib in patients with a recent acute coronary syndrome', *N Engl J Med*, 367: 2089-99.

Seamon, K., L. O. Kurlak, M. Warthan, E. Stratikos, J. F. Strauss, 3rd, H. D. Mistry, and E. D. Lee. 2020. 'The Differential Expression of ERAP1/ERAP2 and Immune Cell Activation in Pre-eclampsia', *Front Immunol*, 11: 396.

Segrest, J. P., M. K. Jones, H. De Loof, C. G. Brouillette, Y. V. Venkatachalapathi, and G. M. Anantharamaiah. 1992. 'The amphipathic helix in the exchangeable apolipoproteins: a review of secondary structure and function', *J Lipid Res*, 33: 141-66.

Sela, S., A. Itin, S. Natanson-Yaron, C. Greenfield, D. Goldman-Wohl, S. Yagel, and E. Keshet. 2008. 'A novel human-specific soluble vascular endothelial growth factor receptor 1: cell-type-specific splicing and implications to vascular endothelial growth factor homeostasis and preeclampsia', *Circ Res*, 102: 1566-74.

Settasatian, N., M. Duong, L. K. Curtiss, C. Ehnholm, M. Jauhiainen, J. Huuskonen, and K. A. Rye. 2001. 'The mechanism of the remodeling of high density lipoproteins by phospholipid transfer protein', *J Biol Chem*, 276: 26898-905.

Shamshirsaz, A. A., K. A. Fox, H. Erfani, K. Bruzdoski, V. Kostousov, S. L. Clark, L. Hensch, S. R. Hui, and J. Teruya. 2021a. 'Trimester-specific thromboelastic values and coagulation activation markers in pregnancy compared across trimesters and compared to the nonpregnant state', *Int J Lab Hematol*, 43: 1216-24.

Shamshirsaz, Amir A., Karin A. Fox, Hadi Erfani, Karen Bruzdoski, Vadim Kostousov, Steven L. Clark, Lisa Hensch, Shiu-Ki Hui, and Jun Teruya. 2021b. 'Trimester-specific thromboelastic values and coagulation activation markers in pregnancy compared across trimesters and

compared to the nonpregnant state', *International Journal of Laboratory Hematology*, n/a.

Shao, B., G. Cavigiolio, N. Brot, M. N. Oda, and J. W. Heinecke. 2008. 'Methionine oxidation impairs reverse cholesterol transport by apolipoprotein A-I', *Proc Natl Acad Sci U S A*, 105: 12224-9.

Shao, B., M. N. Oda, J. F. Oram, and J. W. Heinecke. 2010. 'Myeloperoxidase: an oxidative pathway for generating dysfunctional high-density lipoprotein', *Chem Res Toxicol*, 23: 447-54.

Shao, B., C. Tang, A. Sinha, P. S. Mayer, G. D. Davenport, N. Brot, M. N. Oda, X. Q. Zhao, and J. W. Heinecke. 2014. 'Humans with atherosclerosis have impaired ABCA1 cholesterol efflux and enhanced high-density lipoprotein oxidation by myeloperoxidase', *Circ Res*, 114: 1733-42.

Shao, Baohai, and Jay W. Heinecke. 2018. 'Quantifying HDL proteins by mass spectrometry: how many proteins are there and what are their functions?', *Expert review of proteomics*, 15: 31-40.

Shao, Y., C. Li, Z. Che, P. Zhang, W. Zhang, X. Duan, and Y. Li. 2015. 'Cloning and characterization of two lipopolysaccharide-binding protein/bactericidal permeability-increasing protein (LBP/BPI) genes from the sea cucumber Apostichopus japonicus with diversified function in modulating ROS production', *Dev Comp Immunol*, 52: 88-97.

Shaw, J. A., A. Bobik, A. Murphy, P. Kanellakis, P. Blombery, N. Mukhamedova, K. Woollard, S. Lyon, D. Sviridov, and A. M. Dart. 2008. 'Infusion of reconstituted high-density lipoprotein leads to acute changes in human atherosclerotic plaque', *Circ Res*, 103: 1084-91.

Shen, Y., F. H. Ding, J. T. Sun, L. J. Pu, R. Y. Zhang, Q. Zhang, Q. J. Chen, W. F. Shen, and L. Lu. 2015. 'Association of elevated apoA-I glycation and reduced HDL-associated paraoxonase1, 3 activity, and their interaction with angiographic severity of coronary artery disease in patients with type 2 diabetes mellitus', *Cardiovasc Diabetol*, 14: 52.

Shore, V. H., T. H. Wang, C. L. Wang, R. J. Torry, M. R. Caudle, and D. S. Torry. 1997. 'Vascular endothelial growth factor, placenta growth factor and their receptors in isolated human trophoblast', *Placenta*, 18: 657-65.

Sies, H. 1997. 'Oxidative stress: oxidants and antioxidants', *Experimental Physiology*, 82: 291-95.

Simoncini, T., X. D. Fu, A. Caruso, S. Garibaldi, C. Baldacci, M. S. Giretti, P. Mannella, M. I. Flamini, A. M. Sanchez, and A. R. Genazzani. 2007. 'Drospirenone increases endothelial nitric oxide synthesis via a combined action on progesterone and mineralocorticoid receptors', *Hum Reprod*, 22: 2325-34.

Singh, A. T., A. Dharmarajan, I. L. Aye, and J. A. Keelan. 2012. 'Sphingosine-sphingosine-1-phosphate pathway regulates trophoblast differentiation and syncytialization', *Reprod Biomed Online*, 24: 224-34.

Sivan, E., X. Chen, C. J. Homko, E. A. Reece, and G. Boden. 1997. 'Longitudinal study of carbohydrate metabolism in healthy obese pregnant women', *Diabetes Care*, 20: 1470-5.

Skoura, A., J. Michaud, D. S. Im, S. Thangada, Y. Xiong, J. D. Smith, and T. Hla. 2011. 'Sphingosine-1-phosphate receptor-2 function in myeloid cells regulates vascular inflammation and atherosclerosis', *Arterioscler Thromb Vasc Biol*, 31: 81-5.

Smith, A., and W. T. Morgan. 1981. 'Hemopexin-mediated transport of heme into isolated rat hepatocytes', *J Biol Chem*, 256: 10902-9.

Sneddon, J. M., and J. R. Vane. 1988. 'Endothelium-derived relaxing factor reduces platelet adhesion to bovine endothelial cells', *Proc Natl Acad Sci U S A*, 85: 2800-4.

Sódar, Barbara W., Ágnes Kittel, Krisztina Pálóczi, Krisztina V. Vukman, Xabier Osteikoetxea, Katalin Szabó-Taylor, Andrea Németh, Beáta Sperlágh, Tamás Baranyai, Zoltán Giricz, Zoltán Wiener, Lilla Turiák, László Drahos, Éva Pállinger, Károly Vékey, Péter Ferdinandy, András Falus, and Edit Irén Buzás. 2016. 'Low-density lipoprotein mimics blood plasma-derived exosomes and microvesicles during isolation and detection', *Scientific Reports*, 6: 24316.

Soran, H., J. D. Schofield, and P. N. Durrington. 2015. 'Antioxidant properties of HDL', *Front Pharmacol*, 6: 222.

Sorrentino, Sajoscha A., Christian Besler, Lucia Rohrer, Martin Meyer, Kathrin Heinrich, Ferdinand H. Bahlmann, Maja Mueller, Tibor Horváth, Carola Doerries, Mariko Heinemann, Stella Flemmer, Andrea Markowski, Costantina Manes, Matthias J. Bahr, Hermann Haller, Arnold von Eckardstein, Helmut Drexler, and Ulf Landmesser. 2010. 'Endothelial-Vasoprotective Effects of High-Density Lipoprotein Are Impaired in Patients With Type 2 Diabetes Mellitus but Are Improved After Extended-Release Niacin Therapy', *Circulation*, 121: 110-22.

Speeckaert, M., G. Huang, J. R. Delanghe, and Y. E. Taes. 2006. 'Biological and clinical aspects of the vitamin D binding protein (Gc-globulin) and its polymorphism', *Clin Chim Acta*, 372: 33-42.

Sreckovic, I., R. Birner-Gruenberger, B. Obrist, T. Stojakovic, H. Scharnagl, M. Holzer, M. Scholler, S. Philipose, G. Marsche, U. Lang, G. Desoye, and C. Wadsack. 2013. 'Distinct composition of human fetal HDL attenuates its anti-oxidative capacity', *Biochim Biophys Acta*, 1831: 737-46.

Staff, A. C. 2019. 'The two-stage placental model of preeclampsia: An update', *J Reprod Immunol*, 134-135: 1-10.

Stefanini, L., and W. Bergmeier. 2019. 'RAP GTPases and platelet integrin signaling', *Platelets*, 30: 41-47.

Stefanović, Aleksandra, Daniela Ardalic, Jelena Kotur-Stevuljević, Ana Vujović, Slavica Spasic, Vesna Spasojević-Kalimanovska, Zorana Jelic-Ivanovic, Vesna Mandic-Markovic, Zeljko Mikovic, and Nikola Cerovic. 2012. 'Longitudinal changes in PON1 activities, PON1 phenotype distribution and oxidative status throughout normal pregnancy', *Reproductive Toxicology*, 33: 20-26.

Stefulj, Jasminka, Ute Panzenboeck, Tatjana Becker, Birgit Hirschmugl, Cornelia Schweinzer, Ingrid Lang, Gunther Marsche, Anton Sadjak, Uwe Lang, Gernot Desoye, and Christian Wadsack. 2009. 'Human Endothelial Cells of the Placental Barrier Efficiently Deliver Cholesterol to the Fetal Circulation via ABCA1 and ABCG1', *Circulation Research*, 104: 600-08.

Stepan, H., A. Philipp, I. Roth, S. Kralisch, A. Jank, W. Schaarschmidt, U. Lossner, J. Kratzsch, M. Bluher, M. Stumvoll, and M. Fasshauer. 2012. 'Serum levels of the adipokine zinc-alpha2-glycoprotein are increased in preeclampsia', *J Endocrinol Invest*, 35: 562-5.

Suikkari, Anne-Maria, and Robert C. Baxter. 1991. 'INSULIN-LIKE GROWTH FACTOR (IGF) BINDING PROTEIN-3 IN PREGNANCY SERUM BINDS NATIVE IGF-I BUT NOT IODO-IGF-L', *The Journal of Clinical Endocrinology & Metabolism*, 73: 1377-79.

Sulaiman, W. N., M. J. Caslake, C. Delles, H. Karlsson, M. T. Mulder, D. Graham, and D. J. Freeman. 2016. 'Does high-density lipoprotein protect vascular function in healthy pregnancy?', *Clin Sci (Lond)*, 130: 491-7.

Tailleux, Anne, Muriel Bouly, Gérald Luc, Graciela Castro, Jean-Michel Caillaud, Nathalie Hennuyer, Philippe Poulain, Jean-Charles Fruchart, Nicolas Duverger, and Catherine Fiévet. 2000. 'Decreased Susceptibility to Diet-Induced Atherosclerosis in Human Apolipoprotein A-II Transgenic Mice', *Arteriosclerosis, Thrombosis, and Vascular Biology*, 20: 2453-58.

Takahashi, C., M. Kurano, M. Nishikawa, K. Kano, T. Dohi, K. Miyauchi, H. Daida, T. Shimizu, J. Aoki, and Y. Yatomi. 2017. 'Vehicle-dependent Effects of Sphingosine 1-phosphate on Plasminogen Activator Inhibitor-1 Expression', *J Atheroscler Thromb*, 24: 954-69.

Tall, A. R., L. R. Forester, and G. L. Bongiovanni. 1983. 'Facilitation of phosphatidylcholine transfer into high density lipoproteins by an apolipoprotein in the density 1.20-1.26 g/ml fraction of plasma', *J Lipid Res*, 24: 277-89.

Tang, Norina, Bing Sun, Archana Gupta, Hans Rempel, and Lynn Pulliam. 2016. 'Monocyte exosomes induce adhesion molecules and cytokines via activation of NF-κB in endothelial cells', *The FASEB Journal*, 30: 3097-106.

Tang, W. H., J. Hartiala, Y. Fan, Y. Wu, A. F. Stewart, J. Erdmann, S. Kathiresan, R. Roberts, R. McPherson, H. Allayee, and S. L. Hazen. 2012. 'Clinical and genetic association of serum paraoxonase and arylesterase activities with cardiovascular risk', *Arterioscler Thromb Vasc Biol*, 32: 2803-12.

Tannetta, Dionne S., Christopher W. Redman, and Ian L. Sargent. 2014. 'Investigation of the actin scavenging system in pre-eclampsia', *Eur J Obstet Gynecol Reprod Biol*, 172: 32-35.

Tardif, J. C., J. Grégoire, P. L. L'Allier, R. Ibrahim, J. Lespérance, T. M. Heinonen, S. Kouz, C. Berry, R. Basser, M. A. Lavoie, M. C. Guertin, and J. Rodés-Cabau. 2007. 'Effects of reconstituted high-density lipoprotein infusions on coronary atherosclerosis: a randomized controlled trial', *JAMA*, 297: 1675-82.

Théry, C., S. Amigorena, G. Raposo, and A. Clayton. 2006. 'Isolation and characterization of exosomes from cell culture supernatants and biological fluids', *Curr Protoc Cell Biol*, Chapter 3: Unit 3.22.

Thomas, Christie P., Janet I. Andrews, Nandita S. Raikwar, Elizabeth A. Kelley, Florian Herse, Ralf Dechend, Thaddeus G. Golos, and Kang Z. Liu. 2009. 'A recently evolved novel trophoblast-enriched secreted form of fms-like tyrosine kinase-1 variant is up-regulated in hypoxia and preeclampsia', *The Journal of clinical endocrinology and metabolism*, 94: 2524-30.

Thornalley, P. J., and M. Vasák. 1985. 'Possible role for metallothionein in protection against radiation-induced oxidative stress. Kinetics and mechanism of its reaction with superoxide and hydroxyl radicals', *Biochim Biophys Acta*, 827: 36-44.

Thornton, Patrick, and Joanne Douglas. 2010. 'Coagulation in pregnancy', *Best Practice & Research Clinical Obstetrics & Gynaecology*, 24: 339-52.

Thuahnai, S. T., S. Lund-Katz, D. L. Williams, and M. C. Phillips. 2001. 'Scavenger receptor class B, type I-mediated uptake of various lipids into cells. Influence of the nature of the donor particle interaction with the receptor', *J Biol Chem*, 276: 43801-8.

Tranquilli, A. L., M. A. Brown, G. G. Zeeman, G. Dekker, and B. M. Sibai. 2013. 'The definition of severe and early-onset preeclampsia. Statements from

the International Society for the Study of Hypertension in Pregnancy (ISSHP)', *Pregnancy Hypertens*, 3: 44-7.

Tsai, J. C., Y. W. Lin, C. Y. Huang, C. Y. Lin, Y. T. Tsai, C. M. Shih, C. Y. Lee, Y. H. Chen, C. Y. Li, N. C. Chang, F. Y. Lin, and C. S. Tsai. 2014. 'The role of calpain-myosin 9-Rab7b pathway in mediating the expression of Toll-like receptor 4 in platelets: a novel mechanism involved in alpha-granules trafficking', *PLoS One*, 9: e85833.

Tsatsaris, V., F. Goffin, C. Munaut, J. F. Brichant, M. R. Pignon, A. Noel, J. P. Schaaps, D. Cabrol, F. Frankenne, and J. M. Foidart. 2003. 'Overexpression of the soluble vascular endothelial growth factor receptor in preeclamptic patients: pathophysiological consequences', *J Clin Endocrinol Metab*, 88: 5555-63.

Turpin, Sarah M, Hayley T Nicholls, Diana M Willmes, Arnaud Mourier, Susanne Brodesser, Claudia M Wunderlich, Jan Mauer, Elaine Xu, Philipp Hammerschmidt, Hella S Brönneke, Aleksandra Trifunovic, Giuseppe LoSasso, F. Thomas Wunderlich, Jan-Wilhelm Kornfeld, Matthias Blüher, Martin Krönke, and Jens C Brüning. 2014. 'Obesity-Induced CerS6-Dependent C_{16:0} Ceramide Production Promotes Weight Gain and Glucose Intolerance', *Cell Metabolism*, 20: 678-86.

Ueland, T, T Dalsoren, N Voldner, K Godang, T Henriksen, and J Bollerslev. 2008. 'Retinol-binding protein-4 is not strongly associated with insulin sensitivity in normal pregnancies', *European Journal of Endocrinology*, 159: 49-54.

Ulevitch, R. J., A. R. Johnston, and D. B. Weinstein. 1979. 'New function for high density lipoproteins. Their participation in intravascular reactions of bacterial lipopolysaccharides', *J Clin Invest*, 64: 1516-24.

van der Steeg, W. A., I. Holme, S. M. Boekholdt, M. L. Larsen, C. Lindahl, E. S. Stroes, M. J. Tikkanen, N. J. Wareham, O. Faergeman, A. G. Olsson, T. R. Pedersen, K. T. Khaw, and J. J. Kastelein. 2008. 'High-density lipoprotein cholesterol, high-density lipoprotein particle size, and apolipoprotein A-I: significance for cardiovascular risk: the IDEAL and EPIC-Norfolk studies', *J Am Coll Cardiol*, 51: 634-42.

van Himbergen, Thomas M., Yvonne T. van der Schouw, Hieronymus A. M. Voorbij, Lambertus J. H. van Tits, Anton F. H. Stalenhoef, Petra H. M. Peeters, and Mark Roest. 2008. 'Paraoxonase (PON1) and the risk for coronary heart disease and myocardial infarction in a general population of Dutch women', *Atherosclerosis*, 199: 408-14.

van Logten, M. J., M. Wolthuis, A. G. Rauws, R. Kroes, E. M. den Tonkelaar, H. Berkvens, and G. J. van Esch. 1974. 'Semichronic toxicity study of sodium bromide in rats', *Toxicology*, 2: 257-67.

VanderWeele, T. J., and M. B. Mathur. 2019. 'SOME DESIRABLE PROPERTIES OF THE BONFERRONI CORRECTION: IS THE BONFERRONI CORRECTION REALLY SO BAD?', *Am J Epidemiol*, 188: 617-18.

Vikstedt, R., J. Metso, J. Hakala, V. M. Olkkonen, C. Ehnholm, and M. Jauhiainen. 2007. 'Cholesterol efflux from macrophage foam cells is enhanced by active phospholipid transfer protein through generation of two types of acceptor particles', *Biochemistry*, 46: 11979-86.

Voight, B. F., G. M. Peloso, M. Orho-Melander, R. Frikke-Schmidt, M. Barbalic, M. K. Jensen, G. Hindy, H. Hólm, E. L. Ding, T. Johnson, H. Schunkert, N. J. Samani, R. Clarke, J. C. Hopewell, J. F. Thompson, M. Li, G. Thorleifsson, C. Newton-Cheh, K. Musunuru, J. P. Pirruccello, D. Saleheen, L. Chen, A. Stewart, A. Schillert, U. Thorsteinsdottir, G. Thorgeirsson, S. Anand, J. C. Engert, T. Morgan, J. Spertus, M. Stoll, K.

Berger, N. Martinelli, D. Girelli, P. P. McKeown, C. C. Patterson, S. E. Epstein, J. Devaney, M. S. Burnett, V. Mooser, S. Ripatti, I. Surakka, M. S. Nieminen, J. Sinisalo, M. L. Lokki, M. Perola, A. Havulinna, U. de Faire, B. Gigante, E. Ingelsson, T. Zeller, P. Wild, P. I. de Bakker, O. H. Klungel, A. H. Maitland-van der Zee, B. J. Peters, A. de Boer, D. E. Grobbee, P. W. Kamphuisen, V. H. Deneer, C. C. Elbers, N. C. Onland-Moret, M. H. Hofker, C. Wijmenga, W. M. Verschuren, J. M. Boer, Y. T. van der Schouw, A. Rasheed, P. Frossard, S. Demissie, C. Willer, R. Do, J. M. Ordovas, G. R. Abecasis, M. Boehnke, K. L. Mohlke, M. J. Daly, C. Guiducci, N. P. Burtt, A. Surti, E. Gonzalez, S. Purcell, S. Gabriel, J. Marrugat, J. Peden, J. Erdmann, P. Diemert, C. Willenborg, I. R. König, M. Fischer, C. Hengstenberg, A. Ziegler, I. Buysschaert, D. Lambrechts, F. Van de Werf, K. A. Fox, N. E. El Mokhtari, D. Rubin, J. Schrezenmeir, S. Schreiber, A. Schäfer, J. Danesh, S. Blankenberg, R. Roberts, R. McPherson, H. Watkins, A. S. Hall, K. Overvad, E. Rimm, E. Boerwinkle, A. Tybjaerg-Hansen, L. A. Cupples, M. P. Reilly, O. Melander, P. M. Mannucci, D. Ardissino, D. Siscovick, R. Elosua, K. Stefansson, C. J. O'Donnell, V. Salomaa, D. J. Rader, L. Peltonen, S. M. Schwartz, D. Altshuler, and S. Kathiresan. 2012. 'Plasma HDL cholesterol and risk of myocardial infarction: a mendelian randomisation study', *Lancet*, 380: 572-80.

von Asmuth, E. J., J. F. Leeuwenberg, M. Ceska, and W. A. Buurman. 1991. 'LPS and cytokine-induced endothelial cell IL-6 release and ELAM-1 expression; involvement of serum', *Eur Cytokine Netw*, 2: 291-7.

Vucic, Esad, and Robert S. Rosenson. 2011. 'Recombinant High-Density Lipoprotein Formulations', *Current Atherosclerosis Reports*, 13: 81-87.

Walker, R. K., and S. Krishnaswamy. 1994. 'The activation of prothrombin by the prothrombinase complex. The contribution of the substrate-membrane interaction to catalysis', *Journal of Biological Chemistry*, 269: 27441-50.

Walsh, Brian W., Isaac Schiff, Bernard Rosner, Louise Greenberg, Veronica Ravnikar, and Frank M. Sacks. 1991. 'Effects of Postmenopausal Estrogen Replacement on the Concentrations and Metabolism of Plasma Lipoproteins', *New England Journal of Medicine*, 325: 1196-204.

Wang, Hongliang, Qinyu Dang, Haiyan Zhu, Ning Liang, Zhiyin Le, Dongxu Huang, Rong Xiao, and Huanling Yu. 2020. 'Associations between maternal serum HDL-c concentrations during pregnancy and neonatal birth weight: a population-based cohort study', *Lipids in Health and Disease*, 19: 93.

Wang, N., D. L. Silver, P. Costet, and A. R. Tall. 2000. 'Specific binding of ApoA-I, enhanced cholesterol efflux, and altered plasma membrane morphology in cells expressing ABC1', *J Biol Chem*, 275: 33053-8.

Wang, Nan, Laurent Yvan-Charvet, Dieter Lütjohann, Monique Mulder, Tim Vanmierlo, Tae-Wan Kim, and Alan R. Tall. 2008. 'ATP-binding cassette transporters G1 and G4 mediate cholesterol and desmosterol efflux to HDL and regulate sterol accumulation in the brain', *The FASEB Journal*, 22: 1073-82.

Wang, S. H., S. G. Yuan, D. Q. Peng, and S. P. Zhao. 2012. 'HDL and ApoA-I inhibit antigen presentation-mediated T cell activation by disrupting lipid rafts in antigen presenting cells', *Atherosclerosis*, 225: 105-14.

Wang, X., D. M. Driscoll, and R. E. Morton. 1999. 'Molecular cloning and expression of lipid transfer inhibitor protein reveals its identity with apolipoprotein F', *J Biol Chem*, 274: 1814-20.

Wasenius, A., M. Stugaard, J. E. Otterstad, and D. Frøyshov. 1990. 'Diurnal and monthly intra-individual variability of the concentration of lipids, lipoproteins and apoproteins', *Scand J Clin Lab Invest*, 50: 635-42.

Watson, A. L., J. N. Skepper, E. Jauniaux, and G. J. Burton. 1998. 'Susceptibility of human placental syncytiotrophoblastic mitochondria to oxygen-mediated damage in relation to gestational age', *J Clin Endocrinol Metab*, 83: 1697-705.

Weissgerber, T. L., and L. M. Mudd. 2015. 'Preeclampsia and diabetes', *Curr Diab Rep*, 15: 9.

Wen, G., W. An, J. Chen, E. M. Maguire, Q. Chen, F. Yang, S. W. A. Pearce, M. Kyriakides, L. Zhang, S. Ye, S. Nourshargh, and Q. Xiao. 2018. 'Genetic and Pharmacologic Inhibition of the Neutrophil Elastase Inhibits Experimental Atherosclerosis', *J Am Heart Assoc*, 7.

Westwood, M., K. Al-Saghir, S. Finn-Sell, C. Tan, E. Cowley, S. Berneau, D. Adlam, and E. D. Johnstone. 2017. 'Vitamin D attenuates sphingosine-1-phosphate (S1P)-mediated inhibition of extravillous trophoblast migration', *Placenta*, 60: 1-8.

'WHO recommendations for prevention and treatment of pre-eclampsia and eclampsia'. 2011. *World Health Organization*

Wilcox, R. R., and H. J. Keselman. 2003. 'Modern robust data analysis methods: measures of central tendency', *Psychol Methods*, 8: 254-74.

Williams, C., and T. M. Coltart. 1978. 'Adipose tissue metabolism in pregnancy: the lipolytic effect of human placental lactogen', *Br J Obstet Gynaecol*, 85: 43-6.

Wilson, Peter W. F., James B. Meigs, Lisa Sullivan, Caroline S. Fox, David M. Nathan, and Ralph B. D'Agostino, Sr. 2007. 'Prediction of Incident Diabetes Mellitus in Middle-aged Adults: The Framingham Offspring Study', *Archives of Internal Medicine*, 167: 1068-74.

Witkowski, A., S. Carta, R. Lu, S. Yokoyama, A. Rubartelli, and G. Cavigiolio. 2019. 'Oxidation of methionine residues in human apolipoprotein A-I generates a potent pro-inflammatory molecule', *J Biol Chem*, 294: 3634-46.

Witting, S. R., J. N. Maiorano, and W. S. Davidson. 2003. 'Ceramide enhances cholesterol efflux to apolipoprotein A-I by increasing the cell surface presence of ATP-binding cassette transporter A1', *J Biol Chem*, 278: 40121-7.

Wolfrum, C., M. N. Poy, and M. Stoffel. 2005. 'Apolipoprotein M is required for prebeta-HDL formation and cholesterol efflux to HDL and protects against atherosclerosis', *Nat Med*, 11: 418-22.

Woollett, L. A., and D. K. Spady. 1997. 'Kinetic parameters for high density lipoprotein apoprotein AI and cholesteryl ester transport in the hamster', *The Journal of Clinical Investigation*, 99: 1704-13.

Wu, P., R. Haththotuwa, C. S. Kwok, A. Babu, R. A. Kotronias, C. Rushton, A. Zaman, A. A. Fryer, U. Kadam, C. A. Chew-Graham, and M. A. Mamas. 2017. 'Preeclampsia and Future Cardiovascular Health: A Systematic Review and Meta-Analysis', *Circ Cardiovasc Qual Outcomes*, 10.

Xiong, Sheng-Lin, Xing Liu, and Guang-Hui Yi. 2014. 'High-density lipoprotein induces cyclooxygenase-2 expression and prostaglandin I-2 release in endothelial cells through sphingosine kinase-2', *Molecular and Cellular Biochemistry*, 389: 197-207.

Xu, Chang, YunHui Li, Wen Zhang, and QiuShi Wang. 2021. 'Analysis of perinatal coagulation function in preeclampsia', *Medicine*, 100: e26482-e82.

Xu, S., M. Laccotripe, X. Huang, A. Rigotti, V. I. Zannis, and M. Krieger. 1997. 'Apolipoproteins of HDL can directly mediate binding to the scavenger receptor SR-BI, an HDL receptor that mediates selective lipid uptake', *J Lipid Res*, 38: 1289-98.

Yamamoto, Y., D. M. Olson, M. van Bennekom, D. N. Brindley, and D. G. Hemmings. 2010. 'Increased expression of enzymes for sphingosine 1-phosphate turnover and signaling in human decidua during late pregnancy', *Biol Reprod*, 82: 628-35.

Yang, W., Q. Li, and Z. Pan. 2014. 'Sphingosine-1-phosphate promotes extravillous trophoblast cell invasion by activating MEK/ERK/MMP-2 signaling pathways via S1P/S1PR1 axis activation', *PLoS One*, 9: e106725.

Yoshinaga, Koji. 2008. 'Review of factors essential for blastocyst implantation for their modulating effects on the maternal immune system', *Seminars in Cell & Developmental Biology*, 19: 161-69.

Yoshino, G., T. Hirano, and T. Kazumi. 2002. 'Treatment of small dense LDL', *J Atheroscler Thromb*, 9: 266-75.

Yu, R., Y. Dan, X. Xiang, Y. Zhou, X. Kuang, G. Yang, Y. Tang, M. Liu, W. Kong, W. Tan, and G. Deng. 2017. 'Stability of Chronic Hepatitis-Related Parameters in Serum Samples After Long-Term Storage', *Biopreserv Biobank*, 15: 211-19.

Yuana, Y., J. Levels, A. Grootemaat, A. Sturk, and R. Nieuwland. 2014. 'Co-isolation of extracellular vesicles and high-density lipoproteins using density gradient ultracentrifugation', *J Extracell Vesicles*, 3.

Yuhanna, I. S., Y. Zhu, B. E. Cox, L. D. Hahner, S. Osborne-Lawrence, P. Lu, Y. L. Marcel, R. G. Anderson, M. E. Mendelsohn, H. H. Hobbs, and P. W. Shaul. 2001. 'High-density lipoprotein binding to scavenger receptor-BI activates endothelial nitric oxide synthase', *Nat Med*, 7: 853-7.

Yvan-Charvet, Laurent, Jelena Kling, Tamara Pagler, Hongna Li, Brian Hubbard, Tim Fisher, Carl P. Sparrow, Andrew K. Taggart, and Alan R. Tall. 2010. 'Cholesterol Efflux Potential and Antiinflammatory Properties of High-Density Lipoprotein After Treatment With Niacin or Anacetrapib', *Arteriosclerosis, Thrombosis, and Vascular Biology*, 30: 1430-38.

Yvan-Charvet, Laurent, Fumihiko Matsuura, Nan Wang, Mark J. Bamberger, Tu Nguyen, Franz Rinninger, Xian-Cheng Jiang, Charles L. Shear, and Alan R. Tall. 2007. 'Inhibition of Cholesteryl Ester Transfer Protein by Torcetrapib Modestly Increases Macrophage Cholesterol Efflux to HDL', *Arteriosclerosis, Thrombosis, and Vascular Biology*, 27: 1132-38.

Zamai, N., C. H. Cortie, E. M. Jarvie, C. C. Onyiaodike, A. Alrehaili, M. Francois, D. J. Freeman, and B. J. Meyer. 2020. 'In pregnancy, maternal HDL is specifically enriched in, and carries the highest proportion of, DHA in plasma', *Prostaglandins Leukot Essent Fatty Acids*, 163: 102209.

Zambon, Alberto, Samir S. Deeb, John E. Hokanson, B. Greg Brown, and John D. Brunzell. 1998. 'Common Variants in the Promoter of the Hepatic Lipase Gene Are Associated With Lower Levels of Hepatic Lipase Activity, Buoyant LDL, and Higher HDL₂Cholesterol', *Arteriosclerosis, Thrombosis, and Vascular Biology*, 18: 1723-29.

Zannis, V. I., F. S. Cole, C. L. Jackson, D. M. Kurnit, and S. K. Karathanasis. 1985. 'Distribution of apolipoprotein A-I, C-II, C-III, and E mRNA in fetal human tissues. Time-dependent induction of apolipoprotein E mRNA by cultures of human monocyte-macrophages', *Biochemistry*, 24: 4450-5.

Zerrad-Saadi, A., P. Therond, S. Chantepie, M. Couturier, K. A. Rye, M. J. Chapman, and A. Kontush. 2009. 'HDL3-mediated inactivation of LDL-associated phospholipid hydroperoxides is determined by the redox status of apolipoprotein A-I and HDL particle surface lipid rigidity: relevance to inflammation and atherogenesis', *Arterioscler Thromb Vasc Biol*, 29: 2169-75.

Zeuke, Stefanie, Artur J Ulmer, Shoichi Kusumoto, Hugo A Katus, and Holger Heine. 2002. 'TLR4-mediated inflammatory activation of human coronary artery endothelial cells by LPS', *Cardiovascular Research*, 56: 126-34.

Zewinger, S., C. Drechsler, M. E. Kleber, A. Dressel, J. Riffel, S. Triem, M. Lehmann, C. Kopecky, M. D. Saemann, P. M. Lepper, G. Silbernagel, H. Scharnagl, A. Ritsch, B. Thorand, T. de las Heras Gala, S. Wagenpfeil, W. Koenig, A. Peters, U. Laufs, C. Wanner, D. Fliser, T. Speer, and W. Marz. 2015. 'Serum amyloid A: high-density lipoproteins interaction and cardiovascular risk', *Eur Heart J*, 36: 3007-16.

Zhang, J., C. E. Dunk, and S. J. Lye. 2013. 'Sphingosine signalling regulates decidual NK cell angiogenic phenotype and trophoblast migration', *Hum Reprod*, 28: 3026-37.